Particle Dynamics in Cosmological Spacetime

by

Nathan Michael Herring

B.A. in Philosophy and Physics, Central College, 2013

M.S. in Physics, University of Pittsburgh, 2019

Submitted to the Graduate Faculty of

the Kenneth P. Dietrich School of Arts and Sciences in partial fulfillment

of the requirements for the degree of

Doctor of Philosophy

University of Pittsburgh

2020

UNIVERSITY OF PITTSBURGH

KENNETH P. DIETRICH SCHOOL OF ARTS AND SCIENCES

This dissertation was presented

by

Nathan Michael Herring

It was defended on

July 22nd 2020

and approved by

Andrew Zentner, Professor, Dept. of Physics and Astronomy, University of Pittsburgh

Daniel Boyanovsky, Professor, Dept. of Physics and Astronomy, University of Pittsburgh

Brian Batell, Asst. Professor, Dept. of Physics and Astronomy, University of Pittsburgh

Vladimir Savinov, Professor, Dept. of Physics and Astronomy, University of Pittsburgh

Matthew Walker, Assoc. Professor, Dept. of Physics and Astronomy, Carnegie Mellon University

Particle Dynamics in Cosmological Spacetime

Nathan Michael Herring, PhD

University of Pittsburgh, 2020

This thesis studies the evolution of quantum fields in the curved spacetime of the expanding early universe, focusing on applications to open questions in cosmology, with special concentration on particle theories of dark matter. Particularly, the processes of particle production and decay are analyzed in detail.

The usual calculation of particle decay rates proceeds by a perturbative approach which supposes global energy conservation, a property not manifest for expanding universes. We demonstrate how the decay law of scalar particles decaying during the radiation dominated epoch of the standard cosmology can be obtained by introducing an adiabatic approximation valid for degrees of freedom with sub-particle horizon wavelengths. The cosmological expansion is treated consistently, through non-perturbative methods borrowed from quantum optics and adapted for cosmology. Both scalar to scalar and scalar to fermion (with Yukawa couplings) decays are studied. The effects of cosmic expansion, leading to salient differences from the usual static spacetime results, are highlighted. We suggest implications for very long-lived particles (such as DM) and baryogenesis.

We also present our study of non-adiabatic cosmological production of dark matter. By stipulating that the dark matter be a spectator field in its vacuum state during inflation and concentrating on super-particle horizon modes immediately after inflation, the particle production for scalar and fermionic dark matter is analytically computed. In both cases, the distribution of produced particles is peaked at low comoving momentum. We obtain the full energy momentum tensor, show explicitly its equivalence with the fluid-kinetic one in the adiabatic regime, and extract the abundance, equation of state and free streaming length for the dark matter. We show how this mechanism yields a cold dark matter particle consistent with astronomical observations, without any coupling to Standard Model species, and with solely gravitational interactions. Thus, these models represent theories of the *darkest* of dark matter. We argue that this abundance yields a lower bound on generic scalar (ULDM) and

axion-like particles (ALP) to be included in any assessment of (ULDM)/(ALP) dark matter candidates. For fermions, this production surprisingly leads to a nearly thermal distribution with an emergent temperature, which warrants further analysis.

Table of Contents

List of Tables

List of Figures

Preface

A modern dissertation in physics is an unusual document. Very often all of the important results have already been published in refereed journals. This raises the question, who is the target audience for such a document? Given that experts can already obtain and study the published works, reproducing the results for themselves, merely compiling the articles into a single document seems redundant at best and superfluous at worst. To that end, perhaps selfishly, I have decided to write this dissertation in a way that will be useful to myself, at the very least, but I hope it will also be useful to other graduate students. To achieve this goal I have included a rather large chapter, titled background physics, which is an independent set of notes on the topics of cosmology and quantum field theory, focusing on the aspects most necessary to understand/reproduce the original content of this document. This chapter is not a textbook. However, it should be sufficient for an intermediate graduate student to get "up to speed" with the conceptual toolkit and physics language used in particle cosmology. It has been sequestered after the introductory first chapter so as to not inundate the more expert (or only marginally curious) readers with too much review.

One of the customary functions of a preface is to provide space for the author to acknowledge the many persons who have been invaluable to the completion of this dissertation process. I am truly elated to have such space to thank my mentors, friends, and family.

Firstly, I am greatly indebted to my thesis advisors Andrew Zentner and Daniel Boyanovsky. Andrew, thank you for permitting me to pursue research in the aspects of physics that I found most intriguing, for being a tireless source of optimism and advice, and for genuinely showing interest in my interests, within physics and beyond. Dan, I am indebted to your patience and masterful pedagogical skill; it is a rare gift to be able to answer a student's questions in a manner that makes him feel intelligent and capable while learning something novel, a gift you possess. Your lifelong passion for learning, undaunted after years of scholarship, is truly inspiring. My long conversations with these two men are among my fondest memories in education and my gratitude towards them cannot be overstated.

Secondly, I would like to thank my high school physics teacher Daniel McGrail, a former

electrical engineer who left industry to dedicate his life to teaching physics. Thank you Mr. McGrail for igniting my interest in physics through your penetrating questions and zealous passion. Thirdly, I give thanks to my undergraduate advisor Alexey Pronin, who encouraged me to study broadly and deeply, and who always made time to chat about physics topics beyond the textbook curriculum. I would also like to thank the members of dissertation committee: Brian Batell, Matthew Walker, and Vladimir Savinov for valuable feedback, constructive criticism, and stimulating discussions throughout my graduate career. I also extend a heartfelt thanks to Rachel Bezanson, Arthur Kosowsky, Chandralekha Singh, and Michael Wood-Vasey for providing guidance and insight about physics, academia, and life in general. To Leyla Hirschfeld I give special thanks for handling the bureaucratic nightmares of the graduate school process.

To my coauthor, colleague, and friend Brian Pardo, thank you for passionately engaging with me in spirited yet friendly debate; I am a better physicist for it. To my oldest of friends, Talbot Hook and Quincey Smail, thank you for supporting me with humor, games, and most importantly conversation; you are truly candles in the darkest of nights. I am also delighted to acknowledge my friends Cat Fielder, Brian Flores, Olivia Lanes, Justin Stickel, and Kevin Wilk; your stalwart friendship in the toughest of times and happiest of moments has been a necessary, vitalizing force in these long years, and I look forward to continued friendship. I must particularly thank Cat, Brian, and Olivia for enduring the early years of graduate school with me. Our late nights of study with algebra-filled white boards are treasured memories, and I would do it all again with you guys.

Lastly, I am honored to thank my family, starting from oldest to newest. Debra and Michael Herring, thank you for being amazing parents with only love in your hearts and encouragement towards following my passions. Thank you for taking me to Iowa State University to watch a chemistry lecture, an unusual request for an elementary student. To my younger brother Brandon, thank you for always supporting me and sharing in my enthusiasms; you are the best brother I could have. Finally, to my love Natália Tenório Maia, it's impossible to put into words what your companionship has meant to me, especially during the thesis writing process. You are truly the best discovery I have made at the University of Pittsburgh.

1.0 Introduction

In this first chapter, the current open questions in theoretical cosmology, which motivate the research content of this thesis, are introduced. Subsequently, a brief summary of the main results of the work is provided. A pedagogical review of the relevant background physics, which further contextualizes this work, is reserved for chapter 2, and the interested reader is directed there. Chapters 3-6 provide the original research content of this thesis. Each is associated with a published journal article as indicated in Table 1. They are written to function self-sufficiently, so each begins with a brief introduction and ends with a summary, while the technical details are discussed in between and in the appendices. Readers uninterested in the technicalities are encouraged to read the introduction and summary of each of these chapters to glean the salient aspects. Of course, highly curious readers should delve into the body and the detailed discussion section for each chapter of interest. The final chapter provides an executive summary of the main outcomes, focusing on both technical results and broader conclusions.

1.1 Open Questions in Theoretical Cosmology

The end of the 20th century and beginning of the 21st have witnessed incredible accomplishments in the fields of cosmology and particle physics. Our understanding of the evolution of the Universe, from an initial uniform singularity to a vast, expanding void, populated with myriad clusters of galaxies has been crystallized in the concordance ΛCDM cosmological model bulwarked by tremendous observational data. In high energy physics, we now have a complete, experimentally vindicated, theory of elementary particle interactions: the Standard Model. Furthermore, these two pillars of physics both rest on the remarkable power of gauge field theories to describe the interactions of the natural world. However, important and confounding challenges remain. Observations of distant galaxies and analysis of the cosmic microwave background radiation (CMB) strongly suggest the presence of a

previously unknown, dark material in astrophysical environments referred to as dark matter [121, 46]. Moreover, the relatively recent observation that the universe is undergoing an *accelerated* expansion defies the expectation the we inhabit a cosmology whose energy is dominated by matter and radiation [167, 71]. Accounting for this increasingly rapid expansion is relatively straightforward by introducing an additional substance, with a pressure equal to negative its energy density, and which pervades all of space. However, no empirically confirmed precise theory of this dark energy, with its aberrant equation of state, exists. Finally, the observed asymmetry between matter and anti-matter, evinced by the fact that our ordinary macroscopic world is composed entirely out of the former and not the latter, requires explanation. The ordinary interactions of the Standard Model provide no mechanism for producing unequal abundances, to the degree required, of matter and anti-matter, and thus the correct mechanism for baryogenesis remains an open question [121, 122, 79].

1.1.1 Dark Matter

Cold dark matter (CDM) is presently believed to constitute $\sim$25% of the energy density of the Universe [5, 71]. This statement is based on a number of independent observations: the rotation curves of galaxies, gravitational lensing, the existence of large scale structure in the universe and its formation history, and the cosmic microwave background power spectrum.

Spiral galaxies have a flat, rotating disk composed of interstellar gas, dust, and of course star systems. This rotation is driven by the gravitational attraction of the mass interior to the orbit. As a star in the disk completes its orbit, it sweeps out an approximately elliptical trajectory. According to basic Newtonian mechanics, increasing the radius of the orbit will decrease the orbital velocity of the star *unless* such an increase results in more mass inside the orbit's circumference. By measuring the velocity of stars at different orbital radii, astronomers can construct a galactic rotation curve. However, these empirically constructed rotation curves do not agree with theoretical predictions if only the luminous mass of the galaxy is considered [171, 179, 121]. Yet, by including additional *dark* mass which extends beyond the visible component, forming a so-called halo, agreement between theory and observation can be reestablished.

The presence of dark matter can also be gleaned from gravitational lensing wherein the trajectories of light rays are distorted when passing by a gravitational source which curves spacetime in accordance with General Relativity. Most famously this technique was used in mapping the mass distribution of the Bullet Cluster [146]. The Bullet Cluster refers to an extragalactic structure formed from the collision of two galaxy clusters. The system gravitationally lenses the light from distant galaxies behind the merging clusters. A combination of visible light and x-ray astronomy confirmed that the stars of the colliding galaxies passed by each other unimpeded, while the interstellar gas and dust, having been slowed by ordinary electromagnetic interactions, became concentrated at the center of the collision. Yet, the lensing effect is strongest on the exterior poles of the merger, away from the visible material. Thus, a large amount of invisible matter must be sourcing the gravitational lensing, and moreover must comprise the majority of each galaxy clusters' mass. These clouds of dark matter, one from each colliding cluster, appear spatially separated from the radiating ordinary (baryonic) material, indicating that they bypassed each other, and the gas and dust, during the collision. This outcome suggests that if the dark matter possesses any interactions beyond gravitation, they are very weak.

The growth of galactic structures is itself further evidence of the existence of dark matter. In large N-body simulations of galaxy formation, with only the requisite amount of baryonic matter, interacting gravitationally, structure growth proceeds far too slowly for our own Milky Way galaxy to have formed by the present day [66]. However, in simulations with non-relativistic (cold) dark matter, the CDM acts as form of gravitational soil, collapsing under its own gravitational attraction to form large scale structures with deep gravitational potential wells upon which galaxies can form.

Finally, the CMB itself contains an imprint of dark matter. Temperature fluctuations in the cosmic microwave background are a remnant of acoustical oscillations in the plasma at the time when the photons decoupled. Precision analysis of these fluctuations as a function of angular size on the night sky (the so-called CMB power spectrum) connects them to the energy content of the universe [5]. In order to reproduce the correct power spectrum, our universe must contain nearly five times as much dark matter as ordinary, baryonic matter.

DM candidates can largely be separated into two categories: macroscopic and micro-

scopic. Macroscopic candidates for dark matter, known as Massive Compact Halo Objects (MACHOs) are brown dwarfs, neutron stars, black holes, and planets disassociated from a star system. These objects are ultimately comprised of baryonic matter and are merely referred to as "dark" since they may not be included in the observed luminous mass of their host galaxy. MACHO dark matter can be detected through gravitational microlensing where the compact object acts a gravitational lens as it passes in front of a star, bending the star's light rays and giving an apparent enhancement to its luminosity. MACHOs have been heavily constrained due to the vastly insufficient number of gravitational microlensing events [184, 7].

Elementary particle candidates for dark matter are numerous. A plausible particle dark matter candidate most have three properties [46, 121]: 1.) *Stability*: the particle cannot decay on time scales shorter than the age of the universe. Stability ensures that the dark matter can survive throughout the period of galactic structure growth. 2.) *Darkness*: the particle must have negligible interactions with electromagnetic radiation; otherwise its presence would be detected directly by astronomical observations. 3.) *Collsionless*: If the particle interacts beyond mere gravitation, these interactions must be sufficiently weak as to not inhibit to formation of the extended dark matter halo. No particle within the Standard Model has all three of these necessary properties. Thus, particle dark matter necessarily represents Beyond the Standard Model (BSM) physics. The most popular forms of BSM, particle dark matter are axions, sterile neutrinos, and weakly interacting massive particles (WIMPs). Axions/axion-like particles, are sub-eV mass scalar or pseudoscalar degrees of freedom [147]. They are naturally occurring in string theories and were originally proposed to solve the Strong CP problem. Sterile neutrinos are a fourth, heavier flavor of neutrino which does not couple directly to the other particles of the Standard Model, and is thus inert, but can mix with the three SM neutrino flavors [72]. It emerges naturally in mechanisms which provide the conventional neutrinos their small masses. Finally WIMPs are any BSM dark matter particle which participates in the weak nuclear force (or any novel force of weaker strength) and are motivated by models of supersymmetry [121].

Particle theories of dark matter necessarily require some production mechanism to generate the required energy density/abundance. Such production mechanisms usually require

adding interactions between the dark matter candidate(s) and the Standard Model or other degrees of freedom. In this way, interactions between these coupled degrees of freedom in the early universe then provide a channel for producing a relic abundance of dark matter. Thermal freeze-out is an example of such a production mechanism [121]; in the early universe the interactions between the dark matter and the degrees of freedom to which it couples are in local thermodynamic equilibrium (LTE). However, as the universe expands and the coupled sector cools, these interactions eventually become energetically prohibitive in one direction (if there is a difference in total invariant rest mass between the two sides of the reaction). As the expansion continues, the coupled sector becomes too dilute for even energetically allowed reactions to proceed, and a relic abundance is obtained. As an alternative example, one may consider a thermal freeze-in [100] wherein the dark matter does not begin in LTE. Rather, the dark matter is periodically, gradually produced (perhaps as a decay product or through feeble interactions) by the degrees of freedom to which it couples. In this scenario, eventually the universe cools, and there is insufficient energy for the production to continue generating a relic abundance.

Model parameters of particle theories of dark matter can therefore be constrained by their effect on the production of a relic abundance. Additionally, if the interactions required to produce the dark matter involve Standard Model particles, then in principle it may be detected either directly or indirectly [26]. Direct detection experiments seek to either produce the dark matter in a particle physics collider, thereby observing its presence as missing energy, or detect the particle scattering off a nucleon (as the Earth moves through ambient CDM), therefore causing observable nuclear recoil. In indirect detection, the DM particle annihilates or decays into SM particles (e.g. charged leptons) which are then observed.

In summary, the dark matter hypothesis rests on observational evidence from sub-galactic to extra-galactic distance scales and from early universe to late universe time scales. While, modifications to our theory of gravity may explain each of these phenomena independently, no such unique modification has been proposed which can account for all of them simultaneously [46]. Particle theories of dark matter, therefore, remain the most promising explanation, and determining the identity of the elusive dark matter, a significant task in contemporary physics.

1.1.2 Dark Energy

In the concordance ΛCDM cosmology, approximately 70% of the Universe's energy density is contained within a mysterious form, perhaps associated with empty space itself, known as dark energy [71, 46, 5]. In the concordance model, dark energy is characterized by a negative equation of state ($P = -\rho$). Consequently, the dark energy has a repulsive effect on the cosmology, driving an accelerating expansion of the Universe.

This expansion can be detected by studying the cosmic redshift and luminosity relation of distant astronomical sources whose rest frame brightness and spectral features are reliably predictable and ergo standardizable. Such objects are known as "standard candles" of which the stellar explosions of white dwarf stars, called Type Ia supernovae, are the prime example [167]. By creating a plot of redshift versus luminosity, populated by observations of standard candles, one can glean the expansion rate of the Universe, since higher redshift objects are recessing away from us more rapidly, and dimmer standard candles are farther away. By fitting these data with a model cosmology one can infer the amount of dark energy in the Universe.

Precision analysis of the temperature fluctuations in the cosmic microwave background are also sufficient for measuring the amount of dark energy. As discussed above with regards to dark matter, the CMB anisotropies can be decomposed into a power spectrum: fluctuation plotted versus angular scale. The resulting spectrum has multiple peaks. The position of the first and largest of these peaks is determined by the total energy density in the Universe which consequently determines its spatial geometry. Detailed measurement and analysis of this spectrum strongly suggest that the Universe is spatially flat, but the amount baryonic matter, dark matter, and radiation sum to only $\sim$ 30% of the energy required for such negligible spatial curvature [5, 180]. Consequently, the remaining energy density must exist in a different form.

The temperature fluctuations in the CMB are sourced by density inhomogenities in the baryon-photon plasma and the dark matter [121, 71]. The overdensities cause local gravitational attraction while the scattering interactions in the plasma produce a large amount of pressure. These countervailing effects generate acoustical oscillations which propagate

through the plasma as spherical waves with a finite wave speed. By the time the photons decouple from the plasma, these acoustical waves have traveled a finite distance known as the sound horizon. After decoupling, the oscillations cease due to the absence of pressure. Because there are many such overdensities in the primordial plasma, multiple spherical waves are produced akin to the pattern of ripples produced on the surface of a pond when stones are dropped in a different positions. The resulting density pattern in the plasma persists both in the CMB, but also, naturally, in the baryons themselves after decoupling. As the baryons collapse to form galaxies, the clustering of galaxies is framed by this density pattern. Accordingly, large voids, the size of the sound horizon, are expected between galaxy clusters since the density waves only had time to travel this finite distance, displacing material along the way.

Astronomical observations of the large scale clustering of galaxies can measure the present day sound horizon of the Universe. In an expanding Universe, the physical distance of the sound horizon increases. Thus, by comparing the present size of the sound horizon to its predicted size at the time of recombination (when the photons decouple from the plasma), the expansion rate of the Universe can be measured and the amount of dark energy inferred [75].

Our theoretical descriptions of the expansion of the Universe are based on solutions of the Einstein-Hilbert action of General Relativity. Accommodating an accelerated expansion is straightforward since the action need only be invariant under general coordinate transformations. Thus the action freely admits the addition of an overall constant:

$$\mathcal{A} = \mathcal{A}_{EH} + \int d^4x\sqrt{-g}\Big[\frac{-\Lambda}{8\pi G_N}\Big] \tag{1}$$

where $\mathcal{A}_{EH}$ is the usual Einstein-Hilbert action, G_N is Newton's gravitational constant, and Λ is the cosmological constant. By extremizing the action we derive the equations of motion. Examining the variation of the new addition:

$$\delta\mathcal{A}_\lambda = +\int d^4x\Big[\frac{-\Lambda}{8\pi G_N}\Big]\delta\sqrt{-g} = \int d^4x\sqrt{-g}\Big[\frac{+\Lambda}{16\pi G_N}g_{\mu\nu}\Big]\delta g^{\mu\nu} \tag{2}$$

We see that a new contribution is added to the Einstein-Field equations:

$$\frac{1}{8\pi G_N}R_{\mu\nu} - \frac{1}{32\pi G_N}Rg_{\mu\nu} + \frac{\Lambda}{16\pi G_N}g_{\mu\nu} - \frac{1}{2}T_{\mu\nu} = 0 \rightarrow R_{\mu\nu} - \frac{R}{2}g_{\mu\nu} = 8\pi G_N(T_{\mu\nu} - \frac{\Lambda}{8\pi G_N}g_{\mu\nu}) \tag{3}$$

Recalling that the left-hand side of the Einstein equations is the geometry of the spacetime while the right-hand side is the energy-momentum tensor of the material in spacetime, it is apparent, from this form of the equations, that adding an overall constant effectively supplies an additional contribution the effective energy-momentum tensor. The inclusion of this term, referred to as the *cosmological constant*, supplies the requisite energy density (with the correct equation of state) to drive the accelerated expansion, acting as the dark energy.

While the inclusion of a cosmological constant in General Relativity is simple enough, providing the correct, dynamical explanation for its presence is more challenging. The cosmological constant can be interpreted as the energy density of the vacuum. The amount of this vacuum energy required to be consistent with the observation of the accelerated expansion is $\rho_{vac} \simeq (10^{-3}\text{eV})^4$ [46]. In quantum field theory, our fundamental framework for describing elementary particle interactions, particles are described as excitations of underlying quantum fields. These fields, even in their ground/vacuum states, contribute non-vanishing energy. We can compute this energy:

$$\langle\rho\rangle \sim \int d^3k\ \omega(k) \sim \int_0^\infty dk\ k^2\sqrt{k^2+m^2} \tag{4}$$

Where $\omega(k)$ is the frequency of the quantum field mode, k is the momentum which must be integrated over, and m is the mass of the particle described by the field. This integral is of course formally divergent, but one can introduce a cutoff M, integrating up to a certain energy/momentum scale beyond which we suspect BSM physics to activate and modify the result. For instance, we can integrate up to 1 TeV, an energy scale regularly probed by the Large Hadron Collider giving the result: $\langle\rho\rangle \sim \int_0^M dk\ k^3 \sim M^4 = (10^{12}\text{eV})^4$. Clearly the resulting vacuum contribution is enormous compared to the amount required for dark energy.

We can attempt to make the result more palatable by renormalizing the bare parameter of the cosmological constant:

$$\rho_{vac} = \rho_{vac}^{bare} + \langle \rho \rangle \tag{5}$$

$$10^{-12}\,\mathrm{eV}^4 = (-10^{48}\,\mathrm{eV}^4 + 10^{-12}\,\mathrm{eV}^4) + 10^{48}\,\mathrm{eV}^4 \tag{6}$$

While this does give the correct result for the dark energy, it requires the value of the bare parameter of the theory to be finely tuned to *at least* 60 decimal places. As the cutoff is placed at higher scales, the fine-tuning worsens, thus giving rise to the cosmological constant problem and motivating alternative explanations for the dark energy [46, 191].

1.1.3 Baryogenesis

Antiparticles are a natural prediction of the Dirac equation which describes the behavior of fermions like the electron and neutrino. However, despite the natural presence of antiparticles in the Standard Model, the presence of antiparticles on Earth is all but constrained to the particle physics laboratories where they are actively created. At the level of our solar system, antimatter is also prohibitively rare, a fact most trivially established by the ability for our various space probes (composed of matter) to interact with the many asteroids, moons, and planets without annihilating instantly.

The study of cosmic rays incident on the Earth's atmosphere reveals that our galaxy is also composed entirely of matter. Only $\sim .01\%$ of incident cosmic rays are antiparticles (namely antiprotons) which is perfectly consistent with such antimatter being the secondary product of high energy cosmic ray collisions in the upper atmosphere [31]. Noting that there are cosmic ray sources throughout the Milky Way, we have strong evidence of a maximal asymmetry between matter and antimatter at galactic scales [121]. At extragalactic scales, x-ray astronomy provides evidence of a continued asymmetry. The intracluster gasses within galaxy clusters are a source of x-ray emissions, with a negligible gamma-ray component; if galaxy clusters contained both matter and anti-matter galaxies, one would expect a detectable gamma-ray flux from pair annihilation reactions in the intracluster material, and thus the matter/antimatter asymmetry exists *at least* on nearby, galaxy cluster scales (a few

Mpc) [49]. These observations motivate the baryon asymmetry problem: why and how is our observable Universe dominated by matter over antimatter?

In order to resolve the problem, it must first be quantified. In cosmology, the useful quantity for discussing particle populations is the ratio of $Y = \frac{n}{s}$, where n is the number of some species of particle per comoving volume (number density) and s is the amount of entropy per comoving volume (entropy density). Since the Universe undergoes isentropic expansion, Y can only change if the number of some species of particles in a comoving volume changes (i.e. particle creation or annihilation). Moreover, since n and s are both with respect to a comoving volume, Y is a dimensionless quantity which effectively counts the number of particles in the comoving volume. The utility of this expression is apparent after introducing the following [121]:

$$n_\gamma \simeq \frac{2.4}{\pi^2} T^3 \tag{7}$$

$$s = \frac{2\pi^2}{45} g_{*s} T^3 \tag{8}$$

Where n_γ is the number density of photons (computed from the Bose-Einstein distribution), s is the entropy density of relativistic degrees of freedom in the Universe, g_{*s} is the effective number of relativistic degrees of freedom, and T is the temperature of the photons. The relativistic species overwhelmingly contribute to the entropy density (since the non-relativistic species are exponentially suppressed.) Using these quantities:

$$\frac{s}{n_\gamma} = 1.8 g_{*s} \tag{9}$$

$$\frac{n_B}{n_\gamma} \equiv \eta = 1.8 g_{*s} \frac{n_B}{s} = 1.8 g_{*s} Y_B \tag{10}$$

Consequently the number density of baryons, n_B (and therefore Y_B) can be related to the baryon to photon ratio, η. During the early universe, g_{*s} decreases as particle species become non-relativistic and/or decouple from the photon/baryon plasma due to the expansion of space. After the decoupling of neutrinos (at $T < 1$ MeV), $\eta \simeq 7 Y_B$. The value of η is constrained by successful calculations of the primordial atomic abundances (big bang nucleosynthesis) so that $\eta \simeq 6 \times 10^{-10}$ [71, 159, 160]. Thus to be consistent with nucleosynthesis,

the effective number of baryons in a comoving volume must be, $Y_B \simeq 10^{-11}$. It is out of these baryons that our visible galaxies are composed.

The first natural question to ask is, can this baryon abundance be produced from a universe with initially equal amounts of matter and antimatter, i.e. a symmetric universe, through the ordinary interactions of the Standard Model? In the hot, early phases of such a universe, baryons and antibaryons interact with each other through pion exchange. This pion mediator has a mass of 135 MeV, and as the universe expands and cools below several MeV, these interactions effectively freeze-out. Consequently, a relic abundance of baryons (and antibaryons) is left over. Through the Boltzmann equation, this abundance can be computed yielding $Y_B \simeq 7 \times 10^{-20}$ [121, 160]. After these interactions cease, Y_B should be conserved, and thus the resulting abundance is roughly 9 orders of magnitude smaller than allowed by nucleosynthesis. One possible solution to this crisis is the introduction of a novel physical mechanism which acts before baryon/antibaryon freeze-out to segregate the particle populations. However, the size of the particle horizon (the causally connected region of space) of the Universe when temperatures were $\sim$ 20 MeV was $\sim 10^6$ meters, meaning causality would only permit segregation on these distance scales. Such a partitioning scale is far below the at least 1 Mpc scale at which maximal baryon asymmetry is observed. Therefore, the Universe, as we observe it must have a matter/antimatter asymmetry manifest at early times.

The physics mechanism which can provide the required baryon abundance is known as baryogenesis. The ingredients required for a physics model to provide the necessary baryon/antibaryon asymmetry are threefold [71, 121, 160]: 1. *Baryon number violation:* This condition is the most obvious as without the existence of some interactions which do not conserve baryon number, only baroque initial conditions can provide the required asymmetry. The ordinary, perturbative interactions of the Standard Model do not violate baryon number and no laboratory observations confirm the existence of baryon number violation [160]. 2. *Non-LTE physics:* In local thermodynamic equilibrium (LTE) between particle/antiparticles, the establishment of a chemical equilibrium causes the chemical potentials to vanish (since the sum of the chemical potentials on both sides of the reaction must be equivalent $\mu_1 + \bar{\mu_1} = 2\mu_\gamma = 0$.) Consequently, the thermal distribution functions depend only

on mass and temperature. Since particles and their antiparticle partners have the same mass, LTE guarantees that the number density of each species will be equal (reactions producing baryon number will be counteracted by those that deplete it). Therefore, a significant departure from LTE is required to produce an asymmetric number of baryons and antibaryons.
3. *C and CP violation*: The physical charges of a particle are inverted under the charge (C) operator. Thus, the charge operator conjugates particles to antiparticles. The parity (P) operator inverts spatial direction, thus $x \rightarrow -x$, left $\rightarrow$ right. In the Standard Model, the electromagnetic and strong nuclear forces are invariant under both C, P and CP (simultaneous charge and parity) operators; exchanging the sign of all the particles' charges, inverting left/right, or both does not alter the particle interactions [183]. On the contrary, C and P are both, separately, maximally violated by the weak nuclear force (e.g. only left chirality neutrinos and right chirality antineutrinos participate in weak interactions) [183]. Small CP violation is also present in the weak force, namely in the decay behavior of the neutral kaon meson [160]. Since the CP odd, neutral kaon eigenstate preferentially decays to positrons over electrons, the CP operator provides an unambiguous distinction between electrons and antielectrons and consequently matter/antimatter. The baryogenesis mechanism must also violate CP, otherwise baryon production and antibaryon production will occur at the same rate preventing the accumulation of a baryon asymmetry.

Taken together the above criteria are known as the Sakharov conditions, and any physics mechanism which aims to generate a baryon asymmetry from an initially symmetric universe must meet them. None of the perturbative interactions of the Standard Model sufficiently satisfy all three conditions. However, there exist non-perturbative interactions which can, in principle, violate conservation of baryon number and which then leverage the small CP violation endemic to the weak sector, and the departure from LTE during the electroweak phase transition, to simultaneously satisfy all three criteria. Known as electroweak baryogenesis, this model is heavily constrained by the apparently insufficient departure from equilibrium during the phase transition, and thus extensions to the Standard Model are required to salvage the mechanism [148]. In going beyond the Standard Model, so-called grand unified theories (GUTs), attempt to describe the quarks and leptons of the SM as all participating in the interaction of a single force (thereby unifying the strong force with the electroweak

force.) These GUTs generically predict baryon number violations through perturbative interactions and can easily admit CP violation; therefore, they are attractive theories for studying baryogenesis, using out of equilibrium decays as a means to evade LTE [160, 121]. Unfortunately, GUT models generically predict proton decay, and are consequently constrained by its experimentally validated long lifetime; moreover, there are theoretical reasons to worry about GUT baryogenesis as the resulting asymmetry can be destroyed by the known non-perturbative effects present during the electroweak phase transition.

Out of equilibrium decays in the early universe are a widely used method of meeting the 2nd Sakharov condition, and rely on a heavy particle decaying to significantly lighter states in the early universe [122, 79]. They are also used in leptogenesis models, where a lepton asymmetry is first established with particle decay and then subsequently transferred to the baryons through non-perturbative interactions [69]. These decay rates are typically calculated using the traditional methods of quantum field theory as defined in the static, Minkowski spacetime. Given that out of equilibrium decays occur deep in the rapidly expanding, radiation dominated epoch of the Universe, computing the proper decay rate, while consistently treating the expanding cosmology, is vital to properly understanding this mechanism as a model building tool for baryogenesis.

1.2 Thesis Goals and Summary of Main Results

The nature of dark matter, dark energy, and baryogenesis are not the only open questions in theoretical cosmology. However, these topics share a commonality in that they all admit of particle physics solutions. Specifically, they can in principle be addressed in the language of quantum field theory via the introduction of novel interactions and/or particles. Many of these new interactions/fields are motivated as Standard Model extensions which simultaneously address technical problems present in particle physics. Thus these questions lie at the intersection between cosmology and particle physics. Yet, despite multi-decade, theoretical developments and experimental probes of solutions of this kind, no empirically validated answers have emerged to any of these problems. This simultaneously motivates

the considering of new approaches and the reconsidering of old assumptions.

The research content of this thesis proceeds in light of this motivation. In particular, I focus primarily on the question of dark matter, although applications to baryogenesis are also highlighted. Phenomenological models of dark matter and baryogenesis generally compute interaction processes in static (Minkowski) spacetime (using an S-matrix inspired approach) despite the fact that our cosmology is most properly described by an expanding Friedmann-Robertson-Walker (FRW) spacetime. Moreover, the free field solutions for the quantum fields used in these models, are taken to be positive-frequency plane waves:

$$e^{\pm ik^a x_a} \;\; ; \; k^a x_a = \omega_k \, t - \vec{k} \cdot \vec{x} \tag{11}$$

where ω_k and k are the mode's energy and momentum respectively. Such solutions have the advantage of being naturally interpreted as free particle states with an associated vacuum (zero-particle) state which is invariant under Lorentz transformations. In Minkowski spacetime, these solutions represent a natural choice since the spacetime is completely flat, and the spacetime interval is invariant under Lorentz transformations and space/time translations. Therefore, the appropriate choice of solutions (and therefore vacuum) is one that reflects these symmetries. However, in an expanding spacetime not all of these symmetries are present since the metric depends explicitly on time, rendering the use of such states dubious.

The use of Minkowski spacetime descriptions for quantum effects in cosmology is also evident in the Boltzmann equation which describes the out of equilibrium evolution of populations of interacting particles,

$$\hat{L} f(\vec{p}, t) = C[f(\vec{p}, t)] \tag{12}$$

where $\vec{p}$ is the particle's momentum, f is their distribution, and t is time [24, 71, 121]. The left-hand side of the equation features a differential operator $\hat{L}$ known as the Liouville operator which is obtained purely from general relativity and *FRW spacetime*. Meanwhile, the right-hand side is known as the collision term which is a complicated functional of the distribution functions (those of the particle population and all populations with which it is interacting). The collision term accounts for all relevant interaction processes and is obtained

using quantum field theory techniques in *Minkowski spacetime*. Clearly the spacetime is not treated consistently.

There are multiple arguments given for why the flat, Minkowksi spacetime intuition can be be used in the curved, FRW spacetime with regards to quantum processes:

- 1. The equivalence principle of general relativity states that a local inertial frame (with Minkowski spacetime properties) can always be found at each point in spacetime, on sufficiently small scales. Particle physics processes happen on such scales.
- 2. There is a wide separation in scales between the characteristic timescale of cosmic expansion and the characteristic timescale for particle dynamics.
- 3. Minkowski spacetime intuition in cosmology has been enormously successful when used in the theories of big bang nucleosynthesis and recombination both of which are part of the contemporary cosmological paradigm.

However, while ostensibly valid, each of these arguments has important caveats and rebuttals

- 1. Particles are states of quantum fields. Quantum fields are extended objects defined on the entire spacetime manifold. Therefore, their evolution is sensitive to the entire spacetime structure/history [28]. The identification of "particles" (and how many there are) is a frame-dependent statement.
- 2. This is precisely a statement of the adiabatic approximation [28, 158]. If one wishes to operationalize this intuition, they must carefully treat the problem under this approximation. The adiabatic approximation description is not equivalent to a Minkowski spacetime description.
- 3. This is true, but these results may be special cases since they both involve particles which are at non-relativistic energies, and the relevant processes occur when the expansion rate is much smaller than the typical timescale for field oscillation ($H \ll E \simeq m$).

These responses highlight the vulnerabilities of Minkowksi spacetime intuition with regards to early universe particle cosmology. In this thesis, the assumed veracity of this intuition is revisited.

The central goal of this thesis can be tersely stated: rather than using Minkowksi spacetime reasoning, treat the expansion of spacetime consistently in the calculation of particle

dynamics; this requires the development of novel and interdisciplinary methods of quantum field theory (QFT). Subsequently, employ these methods to provide new solutions to the aforementioned open questions of cosmology. In adopting this strategy, a two-point approach is followed: (1) study the evolution of quantum fields in Friedmann-Robertson-Walker (FRW) spacetime, computing the salient effects of an expanding background cosmology on the dynamics of particle states and understand where these effects lead to significant departures from the usual Minkowski results. (2) Leverage these differences to further understand and constrain new physics, with a particular emphasis on phenomenological models of dark matter.

As an application of point (1), the process of particle decay in cosmological settings is studied. Next, the uniquely, curved spacetime phenomenon of gravitational/cosmological particle production is investigated as means of producing light dark matter, representing an application of point (2). This work has resulted in four articles [105, 36, 104, 103] each of which comprises a chapter and whose primary results I briefly summarize in the following sections. Table 1 indicates the connection between chapters and published results.

Chapter	Article	Arxiv
3	Phys. Rev. D 98, 083503 (2018)	arXiv:1808.02539
4	Phys. Rev. D 100, 023531 (2019)	arXiv:1904.12343
5	Phys. Rev. D 101, 083516 (2020)	arXiv:1912.10859
6	Phys. Rev. D 101, 123522 (2020)	arXiv:2005.00391

Table 1: Thesis Chapters and Associated Articles. Each of these chapters is based on an associated journal article. The chapters are written to function self-sufficiently from the rest of the thesis, so that they may be read in any order according to the reader's interest.

1.2.1 Cosmological Particle Decay Laws

Particle decay is a ubiquitous process wherein one type of particle spontaneously transmutes into particles of a different species (e.g. a neutron $\rightarrow$ proton + electron + anti-

neutrino) and is vital to understanding the production and depletion of particle populations. In early universe cosmology, leptogenesis and baryogenesis (the processes which produce the fundamental constituents of matter) invoke this process [122, 79]. Particle theories of dark matter (DM) also typically require understanding decay, since stable DM must have a production mechanism and is constrained to have long-lifetimes [196].

Particle decay is a quantum mechanical process whose occurrence rate is typically calculated using the framework of QFT. These decay rates are normally obtained through the perturbative, QFT S-matrix by constructing a unitary time evolution operator out of the interacting Hamiltonian of the theory, taking the infinite time limit, and computing the element of this matrix using the initial and final states of the system (which are defined in the asymptotic past and future respectively). By defining the transition probability as this S-Matrix element *squared*, the energy conserving delta function ensures that the transition amplitude is linear in total elapsed time. Dividing by the total elapsed time and summing over the final state momenta gives the decay rate.

While such an approach is highly effective for terrestrial particle physics analysis, it fails, in general, when performing calculations in dynamic spacetimes since the S-matrix necessitates global energy conservation which is *not present* in an expanding universe, like ours. Historically, physicists have ignored the effect of cosmic expansion in astro-particle calculations, and have recycled techniques like the S-matrix.

Not only are such approaches inconsistent, they are explicitly blind to the surprising consequences of an expanding universe. One such effect is cosmological particle production, where particle/anti-particle states spontaneously erupt from the vacuum as the spacetime expands [153, 154, 155]. Furthermore, in rapidly expanding spacetimes, normally prohibited phenomena have been encountered such as the "self-decay" of massive particles (i.e. a particle decaying into copies of itself) [38, 33, 34]. Given the wide range of phenomenological consequences for particle decay in cosmology and the inability to consistently compute decay laws for such processes in expanding/curved spactimes, the ultimate goal of this first project was to construct and implement an original QFT framework, that consistently includes the effects of cosmic expansion, and can be applied to the gamut of known field theory interactions.

In chapter 3, we adapt the quantum optics technique known as the Wigner–Weisskopf framework and apply it for the first time in cosmology to study the decay of spinless particles in the post-inflationary epoch of the Universe. These calculations reveal new effects including the attenuation of particle decay rates by cosmic redshift and the peculiar capability of lighter particles to decay into more massive species through channels which close and open based on the expansion rate.

In chapter 4, we extend the methods of the previous chapter to the study of a more physical scenario which is present in the Standard Model: the decay of a Higgs like scalar with Yukawa couplings to fermions. Unlike the previous study, this model is a *renormalizable* theory (the self-energy is divergent), and the study of cosmic particle decay into fermionic channels introduces a novel physics phenomenon related to the renormalization: the formation and subsequent decay of a *quasiparticle* state (i.e. a state dressed by fermion/anti-fermion pairs.) We implement a renormalization procedure which permits one to separate the dynamics of dressed-state formation from the decay dynamics since these two processes are *separated by a large time scale*. The decay law and survival probability of the decaying probability are obtained. As in the scalar-to-scalar case, the decay rate is redshifted and the particle lives longer than generically predicted in a static spacetime. Unlike in the previous case, however, the confluence of a renormalizable theory with the redshifting of the decaying particle state's momentum (by cosmic expansion) allows "memory" of the transient dynamics associated with the formation of the dressed state to persist and imprint on the decay law.

1.2.2 Cosmological Particle Production

ΛCDM cosmology assumes a cold dark matter abundance which coalesces to form structures known as dark matter halos within which the luminous galaxies form from ordinary (baryonic) matter. While numerical simulations of cold dark matter models successfully reproduce the observed large scale structure of the universe, they fail to capture the observed features at the scale of galactic and sub-galactic structures [46]. Furthermore, the lack of direct confirmation, despite multi-decade searches, of the leading candidate CDM

particle, weakly interacting massive particles (WIMPs), has impelled theorists to consider more exotic models. These structural and direct detection problems suggest the need for a new DM paradigm. One possible solution is the introduction of ultra-light, spinless, dark matter known as fuzzy dark matter (FDM). These tiny scalar particles, $m = O(10^{-22}eV)$, form a halo-sized Bose-Einstein condensate and exhibit collective motion which matches the large scale behavior of CDM; while on smaller scales quantum effects, like pressure from the uncertainty principle, slow the formation of structure [136, 111].

Cosmological analysis of FDM physics usually treats the particles non-relativistically using modifications of the Schrödinger equation. However, given the extremely small masses of these particles, during early cosmological epochs the expansion rate of the universe is larger than the local energy of a non-relativistic FDM particle ($\frac{H}{E} > 1$). For such conditions, the adiabatic condition is violated, and one naively expects large amounts of cosmological particle production coming from the expansion of the universe. Such a production mechanism could yield the necessary abundance of DM particles for structure formation without requiring the dark matter to couple to other degrees of freedom or the addition of other terms to the Lagrangian as is typically done [111]. The goal of this second project was to study the cosmological particle production of an ultralight dark matter field *coupled only to gravity*. Such a generic and conservative model can, in a sense, be considered the simplest and *darkest* possible dark matter candidate; however, it is also akin to the various axion-like dark matter models proposed (such as FDM).

In chapter 5, we study the cosmological production of an ultralight scalar field in detail for both conformal and minimal coupling to gravity. We proceed under a modest set of assumptions: 1. Our dark matter field does not couple to the inflaton and does not drive inflation. 2. We consider our field to be in its vacuum state at the beginning of inflation, and we focus on field fluctuations with wavelengths longer than the particle horizon at the end of inflation. 3. By considering such long wavelength modes, we are able to assume a smooth but instantaneous transition from the end of inflation to the beginning of the post-inflationary epoch since these modes are outside of the causally connected region of the Universe during this time and insensitive to any dynamics transpiring inside. As a result, our conclusions are not reheating model-dependent. 4. We consider dark matter particle masses for which the

field evolution will be non-adiabatic, even during much of the post-inflationary, radiation-dominated epoch, and hence substantial particle production can occur. Our field does not drive the expansion of the Universe during this epoch. For the given masses of interest, the non-adiabatic evolution ends by the onset of matter-domination.

With these assumptions in place we solve the equations of motion for the field exactly during and post inflation considering solutions which asympotically approach the adiabatic evolution. We use these solutions to compute the energy-momentum tensor (EMT) and extract the energy density and pressure at the onset of matter-domination, when the modes are well-described by an adiabatic approximation. Our results demonstrate that a relic abundance of cold, ultralight, spinless dark matter, $m = O(10^{-5}eV)$, whose properties agree with astrophysical observations, can be produced purely through this previously unstudied, non-adiabatic channel. We argue that this production mechanism yields a generic lower bound on ultralight scalar dark matter, in principle applicable to any axion-like particle.

In chapter 6, we consider the cosmological particle production a dark fermion field under the same set of assumptions as the previous chapter. Following the same procedure we are able to compute the abundance and equation of state for the produced dark fermions. Our analysis shows that a dark fermion of $m = O(10^8$ GeV) can be produced in sufficient quantities to saturate the necessary dark matter abundance and has a cold equation of state. Again this production mechanism relies only on gravitational interactions; the field does not couple to any other degrees of freedom. Surprisingly, unlike in the bosonic case, these particles are produced with a *nearly thermal* distribution with an effective, emergent temperature $T \simeq 10^{-36}$ eV.

2.0 Background Physics

This second chapter provides a pedagogical overview of the background physics pertinent to understanding the original research content of the thesis. The level of presentation is aimed at an intermediate graduate student who has had some exposure to cosmology and quantum field theory. This section also serves to remind the more experienced reader of the relevant frameworks, concepts, and developments which are fundamental to a contemporary understanding of particle cosmology. A note to the reader, natural units, $\hbar = c = 1$ are used unless otherwise stated.

2.1 Cosmology

The field of cosmology is the branch of physics concerned with the origins and evolution of the Universe. In the last century this discipline has developed from a speculative field to a rigorous science. The material presented here outlines the theoretical framework undergirding modern research in cosmology. A conventional treatment of this material is presented following the standard literature [71, 121, 160].

2.1.1 FLRW Spacetime

The General Theory of Relativity describes how the structure of spacetime is determined by the energy contained within it, giving rise to the gravitational interaction. This statement is codified in the Einstein field equations:

$$R_{\mu\nu} - \frac{R}{2} g_{\mu\nu} = 8\pi G_N (T_{\mu\nu} - \frac{\Lambda}{8\pi G_N} g_{\mu\nu}) \tag{13}$$

Here, $g_{\mu\nu}$, $R_{\mu\nu}$, and R are the spacetime metric, Ricci curvature tensor, and Ricci scalar respectively. Together they describe the geometric structure of spacetime. $T_{\mu\nu}$ is the energy-momentum tensor, encapsulating the energy-momentum contained within the spacetime.

G_N is Newton's universal gravitational constant. These equations can be derived via the variational principle applied to the Einstein-Hilbert action, which admits the addition of a constant scalar; thus I have included this cosmological constant, Λ.

The Universe is represented as a solution to these non-linear equations: a particular form of energy-momentum tensor generates an associated spacetime metric. On the largest scales, the Universe appears statistically homogeneous and isotropic. We can thus describe the energy-momentum tensor as a perfect fluid:

$$T_{\mu\nu} = (\rho + P)u_\mu u_\nu + P g_{\mu\nu} \tag{14}$$

Where ρ, P, and u_μ are the energy density, pressure, and relative 4-velocity (3 space + 1 time) between the fluid and the observer. In the frame at rest with fluid (the comoving frame), $u_\mu = (1, \vec{0})$. The spacetime metric for a homogeneous and isotropic universe is described by the Friedmann-Lemaître-Robertson-Walker metric, which when expressed in comoving, spherical coordinates gives the following invariant spacetime interval:

$$ds^2 = g_{\mu\nu}dx^\mu dx^\nu = dt^2 - a^2(t)\Big[\frac{dr^2}{1-kr^2} + r^2 d\theta^2 + r^2 \sin^2\theta d\phi^2\Big] \tag{15}$$

The FLRW metric features a parameter, $k = -1, 0, +1$ which describes an open, flat, or closed spatial curvature as well as the dimensionless scale factor, $a(t)$, which, as it increases, uniformly increases physical distances in the space. Consequently, the functional form of $a(t)$ determines the expansion history of the Universe. From this metric, we can compute the Ricci scalar and non-vanishing elements of the Ricci tensor:

$$R_{00} = -3\frac{\ddot{a}}{a} \tag{16}$$

$$R_{ij} = \Big(\frac{\ddot{a}}{a} + 2\frac{\dot{a}^2}{a^2} + 2\frac{k}{a^2}\Big)g_{ij} \tag{17}$$

$$R = 6\Big(\frac{\ddot{a}}{a} + \frac{\dot{a}^2}{a^2} + \frac{k}{a^2}\Big) \tag{18}$$

Where the Latin indices run over $1-3$, the spatial dimensions. Inserting equations 14, 16, 17, and 18 into the Einstein equations gives the constraint conditions for which the FLRW metric is a solution for a Universe filed with a homogeneous and isotropic energy-momentum; these constraint equations are known as the Friedmann equations.

2.1.1.1 The Friedmann Equations Upon the insertion of the perfect fluid energy-momentum tensor and FLRW metric, both in comoving coordinates, the Einstein equations reduce to a pair of differential equations determining the scale factor's evolution:

$$H^2 \equiv \Big(\frac{\dot{a}}{a}\Big)^2 = \frac{8\pi G_N}{3}\rho - \frac{k}{a^2} \tag{19}$$

$$\frac{\ddot{a}}{a} = \frac{-4\pi G_N}{3}\Big(\rho + 3P\Big) \tag{20}$$

Where Λ has been absorbed into the energy density and pressure, and H is defined as the Hubble parameter which characterizes the expansion *rate*. Additionally, covariant conservation of the energy momentum tensor, $\nabla_\mu T^\mu_\nu = 0$, supplies a third constraining equation:

$$\dot{\rho} + 3\frac{\dot{a}}{a}\Big(\rho + P\Big) = 0 \tag{21}$$

Equations 19-21 constitute the equations of motion for the scale factor (note, however, that they are not a set of linearly independent equations). Solutions to these equations describe different cosmologies, which are determined by the energy density and pressure.

We recall from thermodynamics that the energy density and pressure of a perfect fluid can be related through an equation of state, $P = w\rho$, where w is known as the equation of state parameter. In cosmology we are concerned with three fluid types comprising the energy-momentum of the Universe: radiation (relativistic material), matter (non-relativistic material), and vacuum energy. Here I present a heuristic argument for the equation of state parameter for each type.

Consider a finite volume cube, of side length L, containing a perfect fluid, e.g. an ideal gas of particles, each with mass m. We place a barometer on the right wall of the container. An individual particle travels from the left edge of the container to right edge and elastically collides with the wall of the container, supplying a pressure: $P^i = \frac{F_1}{L^2} = \frac{2p_1}{\Delta t\, L^2}$, where the subscript 1 refers to the horizontal direction, p_1 is the particle's horizontal momentum, and superscript i indicates the contribution from a single particle. If the particle has a horizontal velocity component, β_1, then these collisions occur at a rate, $\Delta t = \frac{2L}{\beta_1}$. Thus, if there are N such particles then,

$$P = \sum_i^N P^i = \sum_i^N \frac{2p_1^i}{\Delta t\, L^2} = \sum_i^N \frac{m\,\gamma_1^i\,(\beta_1^i)^2}{L^3} = nm\langle\gamma\beta_1^2\rangle = n\,m\,\frac{1}{3}\langle\gamma|\vec{\beta}|^2\rangle \tag{22}$$

where γ is the Lorentz factor. In the last step we have introduced the number density n and averaged over all 3 spatial dimensions, $\langle\gamma|\vec{\beta}|^2\rangle = \sum_{j=1}^{3}\langle\gamma\beta_j^2\rangle = 3\langle\gamma|\beta_1|^2\rangle$ since the gas is isotropic. For non-relativistic species, $\gamma \simeq 1$ and $\langle|\vec{\beta}|\rangle| \ll 1$. Meanwhile for the relativistic case, $\langle m\,\gamma\,|\vec{\beta}|^2\rangle = \langle|\vec{p}||\vec{\beta}|\rangle \simeq \langle|\vec{p}|\rangle = \langle E\rangle$. Consequently,

$$P = 0\,\rho_m \quad \textbf{Matter} \tag{23}$$

$$P = \frac{1}{3}\rho_R \quad \textbf{Radiation} \tag{24}$$

The above relations can be verified from the statistical mechanics of ideal gases.

For the vacuum energy, we consider an empty version of the same cube and replace the barometer with a movable piston. The energy of the vacuum is proportional to the amount of vacuum in the container, namely $E \propto V$. However, if an agent adiabatically increases the volume of the container, by moving the piston, they must supply energy $\Delta E = P\Delta V$. Therefore by energy conservation:

$$\Delta E = 0 = \rho\Delta V + P\Delta V \tag{25}$$

$$P = -\rho_\Lambda \quad \textbf{Vacuum Energy} \tag{26}$$

Alternatively, by noting that the vacuum energy must be a frame-independent quantity, we see its energy-momentum tensor cannot depend on the relative 4-velocity, u_μ, and so equation 14 gives the same equation of state.

Inserting the equation of state for a particular energy density into equation 21 yields a linear, first order differential equation the solution of which gives the functional dependence of that energy density on the scale factor, $\rho(a)$. Equation 19 can then be used with $\rho(a)$ to determine $a(t)$ and $H(t)$ thus determining how the Universe evolves when driven by a particular form of energy density. Table 2 (below) summarizes these results, where the factor of k in the Friedmann equations was neglected.

Notice in all cases, the scale factor increases in time. However, it is only in the case of a Universe driven by vacuum energy that the Hubble rate is not decreasing with time; rather the Universe exponentially increases in size while the Hubble parameter remains constant. Additionally the energy density of matter decreases as the scale factor increases, purely due

	Radiation	Matter	Vacuum
w	$1/3$	0	-1
$\rho(a)$	$\propto a^{-4}$	$\propto a^{-3}$	Constant
$a(t)$	$\propto t^{1/2}$	$\propto t^{2/3}$	$\propto e^{H\,t}$
$H(t)$	$1/2t$	$2/3t$	Constant

Table 2: Cosmological Solutions. The equation of state parameter, energy density, scale factor, and Hubble parameter are show for each type cosmological solution. Spatial curvature has been neglected.

to volumetric dilution, while the energy density of radiation decreases by an extra power of the scale factor, a consequence of cosmic redshift.

Of course the actual Universe contains all three sources of energy density. In order to describe a multi-component Universe, it is useful to introduce the *critical density*, $\rho_c = \frac{3H^2}{8\pi\,G_N}$, in terms of which Friedmann equation 19 becomes

$$1 = \Omega_R + \Omega_m + \Omega_\Lambda + \Omega_k \tag{27}$$

Where $\Omega_k \equiv -\frac{k}{(aH)^2}$ is defined as the curvature density parameter and $\Omega_{j=R,m,\Lambda} \equiv \frac{\rho_j}{\rho_c}$ are the density parameters of each of the three sources of energy density. When expressed in this form, the Friedmann equation naturally reveals the connection between the total energy density in the Universe and its spatial curvature:

$$\sum_j \Omega_j < 1 \rightarrow \Omega_k > 0 \rightarrow k = -1 \;\; \textbf{Open} \tag{28}$$

$$\sum_j \Omega_j = 0 \rightarrow \Omega_k = 0 \rightarrow k = 0 \;\; \textbf{Flat} \tag{29}$$

$$\sum_j \Omega_j > 1 \rightarrow \Omega_k < 0 \rightarrow k = +1 \;\; \textbf{Closed} \tag{30}$$

Finally, by leveraging the relationship between energy density and scale factor, $\rho(a)$, for each form of energy density and setting the present day scale factor to unity ($a_0 = 1$), the

same Friedmann equation (19) can also be written in terms of the present day values of each density parameter ($\Omega_{0,j=R,m,\Lambda} \equiv \frac{\rho_{0,j}}{\rho_{0,c}}$, $\rho_{0,c} = \frac{3H_0^2}{8\pi G_N}$):

$$H^2(a) = H_0^2\Big[\frac{\Omega_{R,0}}{a^4} + \frac{\Omega_{m,0}}{a^3} + \Omega_{\Lambda,0} + \frac{\Omega_{k,0}}{a^2}\Big] \tag{31}$$

2.1.1.2 Cosmological Epochs In view of equation 31, one of the central projects for observational cosmology is to determine the value of each of the present day density parameters thereby determining the evolution of the Universe. Detailed probes of the cosmic microwave background, galaxy clustering and distribution surveys, analysis of nucleosynthesis, and studies of gravitational lensing have allowed cosmologists to constrain the values of the density parameters. Table 3 (below) gives the present day values for each of these parameters as inferred from observation. Note for the rest of this thesis we will drop the "0" from the density parameters thereby defining Ω_j as the present day value.

Component	Parameter	Present Value
Curvature	Ω_k	0.0008 ± 0.0013
Radiation	Ω_R	$9.17 \pm 1.90 \times 10^{-6}$
Baryonic Matter	Ω_B	0.0486 ± 0.0010
Dark Matter	Ω_{DM}	0.2589 ± 0.0057
Dark Energy	Ω_Λ	0.6911 ± 0.0062

Table 3: Cosmological Parameters as Determined by the Planck Collaboration [5].

Examining Table 3, reveals that our observable Universe has negligible spatial curvature (effectively flat), and is dominated by matter (specifically dark matter) and dark energy which differ in contribution by a roughly a factor of 3. This incarnation of the FLRW model is consequently referred to as the ΛCDM cosmology (Λ, dark energy; CDM, cold dark matter).

Inserting the ΛCDM values into the Friedmann equation 31 gives an equation with no closed form, analytic solution. However, the relative values of the density parameters allow partitioning of the expansion history into *cosmological epochs*, as the various energy density components scale with $a(t)$ differently, implying that for certain ranges of the scale factor the expansion is effectively driven primarily by a single component. These ranges can be straightforwardly computed by solving for the scale factor at which the various terms are equivalent:

$$\textbf{Radiation Domination (RD)} \quad a \ll a_{eq} = \frac{\Omega_R}{\Omega_m} \simeq 10^{-5} \tag{32}$$

$$\textbf{Matter Domination (MD)} \quad a \ll a_{de} = \left(\frac{\Omega_m}{\Omega_\Lambda}\right)^{1/3} \simeq 0.76 \tag{33}$$

Evidently, at early times the expansion of the Universe was driven by Ω_R until the energy density in radiation was sufficiently redshifted, and the the non-relativistic matter became the dominant contribution to the total energy density. This period of matter domination continued until the Universe was roughly 76% its present size corresponding to a time of ~ 9 Gyrs at which point the dilution of energy density in baryons and cold dark matter rendered their contribution subdominant to the dark energy, initiating the current Λ domination era.

2.1.1.3 Conformal Time and Particle Horizons The FLRW metric admits of a simple coordinate transformation,

$$d\eta \equiv \frac{dt}{a(t)} \tag{34}$$

in terms of which the spacetime interval of the *spatially flat* FLRW metric 15 becomes

$$ds^2 = g_{\mu\nu}dx^\mu dx^\nu = a^2(\eta)\Big[d\eta^2 - d\vec{x}^2\Big] = a^2(\eta)\eta_{\mu\nu}dx^\mu dx^\nu \tag{35}$$

In terms of these new comoving variables, the metric is revealed to be conformal to the Minkowski spacetime metric, $\eta_{\mu\nu} \equiv \text{diag}\Big[1, -1, -1, -1\Big]$, thus $d\eta$ is referred to as *conformal time*. Working in conformal time is often convenient for complex calculations in FLRW

spacetime. By rewriting the Friedmann equation 31 in conformal time and considering specific cosmic epochs, one can determine $a(\eta)$:

$$a(\eta) = H_0\sqrt{\Omega_R}\,\eta \quad \mathbf{RD} \tag{36}$$

$$a(\eta) = H_0^2\,\Omega_m\,\frac{\eta^2}{4} \quad \mathbf{MD} \tag{37}$$

$$a(\eta) = \frac{-1}{H_0\sqrt{\Omega_\Lambda}\,\eta} \quad \Lambda\mathbf{D} \tag{38}$$

One immediate advantage of conformal time concerns causality. In either Special or General Relativity, events in spacetime are characterized by the interval, ds^2, separating them. For space-like intervals, $ds^2 < 0$, it is possible to transform to a coordinate system where two events are simultaneous ($dt^2 = 0$) since the spacetime interval is invariant under general coordinate transformations. However, such events would necessarily be separated by a non-zero distance and as such $(\frac{d\vec{x}}{dt})^2 \gg 1$, and thus outside the light-cone defined by $\frac{d\vec{x}}{dt} = 1$ (in natural units). Consequently, no signal traveling at the speed of light could connect any two such events, so they are said to be causally disconnected. As a corollary, the boundary of causally connected regions of spacetime is determined null/light-like intervals, $ds^2 = 0$, since causally connected events may, at maximum, have such separation. Considering, a null interval traversed by a light ray in the FLRW metric,

$$ds^2 = 0 \rightarrow \int dr = \int d\eta \rightarrow r_H(\eta(t)) = \eta(t) = \int \frac{dt}{a(t)} \tag{39}$$

we therefore see that the size of causally connected regions of the Universe, known as the comoving particle horizon, r_H, is a function of (comoving) time and is equivalent to the conformal time. Therefore, finding $\eta(t)$ is tantamount to computing the particle horizon. As an example consider radiation domination:

$$r_H(t) = \eta(t) = \frac{a(t)}{H_0\sqrt{\Omega_R}} = \sqrt{\frac{2t}{H_0\sqrt{\Omega_R}}} \tag{40}$$

where the last line follows from computing a change of variables ($\dot{a} = \frac{a^{'}}{a}$). Equation 40 demonstrates that the size of the causally connected Universe also grows with time. Expressing the comoving particle horizon as a *proper distance* is straightforward, $d_H(t) = a(t)\,r_H(t)$. During RD, the proper distance particle horizon is therefore, $d_H(t) = 2t = 1/H(t)$, and consequently is determined by the Hubble rate (and of finite size).

2.1.2 The Standard Cosmological Picture

The ΛCDM cosmological model represents a particular FLRW solution to the Einstein equations for a homogeneous and isotropic universe. As a description of the observable Universe, ΛCDM makes a number of precise predictions regarding phenomena throughout the expansion history. These predictions have been tested through astronomical observations which provide empirical support for the cosmic history implied by the model.

In this history, the hot early Universe is characterized by a primordial plasma of fundamental particles which cools to form nucleons and ultimately trace amounts of the lightest elements as space expands in a process known as *big bang nucleosynthesis*. This expansion is driven primarily by the energy density in relativistic species which comprises the dominant contribution to the total energy density of the Universe. At a scale factor $a \sim 10^{-4}$, the matter dominated phase of cosmic expansion begins as the energy density in non-relativistic matter becomes dominant. During this phase, the opaque baryon-photon plasma sufficiently cools for neutral hydrogen to form while the photons fall out of equilibrium with matter, decoupling from the plasma. Thus, the Universe becomes transparent to electromagnetic radiation through this process referred to as *recombination*. The radiation produced during the recombination event, which occurs at $t \simeq 300$ kyrs, is presently detectable as the *cosmic microwave background radiation*. As the expansion continues, the growth of extragalactic structure, seeded by the gravitational collapse of the dark matter, proceeds and the matter dominated era concludes with the formation of the first generation of stars and quasars. At $t \simeq 9Gyrs$, the matter energy density is sufficiently diluted by expansion such that dark energy becomes the dominant contribution to the expansion, initiating the present era of accelerated expansion detectable through the *cosmic redshifting* of distant light sources.

In this section the evidence for this cosmological picture, painted by ΛCDM, is reviewed by studying the major astrophysical phenomenology associated with the model.

2.1.2.1 Cosmological Redshift As the scale factor increases physical distances between objects on in the Universe also increase uniformly on extragalactic scales. To an observer in the Universe, this expansion causes distant objects, in all directions, to appear to be

recessing away. Astronomical observations of this recession constitute an important probe of our cosmological model. To understand the origin of this effect, consider the trajectory taken by a light ray emitted from a distant source at a comoving time $t = t_0$ and which arrives here on Earth at $t = t_1$:

$$ds^2 = 0 \rightarrow \int_{t_0}^{t_1} \frac{dt}{a(t)} = \int_0^{r_1} dr \tag{41}$$

where we have considered a FLRW spacetime with negligible spatial curvature. If a second light signal is emitted at a time $t = t_0 + \delta t_0$, it will arrive at the *same* comoving position r_1 at $t = t_1 + \delta t_1$. Therefore,

$$\int_{t_0+\delta t_0}^{t_1+\delta t_1} \frac{dt}{a(t)} = r_1 = \int_{t_0}^{t_1} \frac{dt}{a(t)} \tag{42}$$

and by writing both sides of eqn. 42 as a sum of two integrals we find

$$\int_{t_1}^{t_1+\delta t_1} \frac{dt}{a(t)} = \int_{t_0}^{t_0+\delta t_0} \frac{dt}{a(t)} \tag{43}$$

$$\frac{\delta t_1}{a(t_1)} = \frac{\delta t_0}{a(t_0)} \tag{44}$$

where the last line follows from $\delta t_j \ll t_j$. Given that $\delta t_0[\delta t_1]$ is the time between the emission [detection] of successive light pulses, it follows that

$$\frac{a(t_1)}{a(t_0)} = \frac{\delta t_1}{\delta t_0} = \frac{\nu_0}{\nu_1} = \frac{\lambda_1}{\lambda_0} \equiv 1 + z \tag{45}$$

where ν and λ are the frequency and wavelength of the signal. The identity of z as the Doppler shift, becomes apparent by solving eqn. 45

$$z = \frac{\lambda_1 - \lambda_0}{\lambda_0} = \frac{\Delta a}{a(t_0)} \tag{46}$$

Since the scale factor increases with time in an expanding universe, $z > 1$, and so z is known as the cosmic redshift. Notice that since the present day scale factor is set to unity ($a(t_1) = 1$), the redshift can be computed as $z = \frac{1}{a} - 1$. Thus redshift can be used in place of the scale factor for describing the expansion history of the Universe.

Incidentally, since $\frac{da}{dt}\frac{1}{a} = H$, the age of the Universe can be computed using redshift:

$$\int_{t_*}^{t_0} dt' = \int_{a_*}^{a_0} \frac{da}{aH(a)} = \int_{z(a_0)}^{z(a_*)} \frac{dz}{(1+z)H(z)} \tag{47}$$

where a_* is the scale factor at the beginning of the Universe (typically taken to be 0 with $t_* = 0$) and a_0 is the present day scale factor (typicall set to unity). $H(z)$ is given by the Friedmann equation (eqn. 31). Consequently, cosmic redshift can also be used as a proxy for the age of the Universe.

Having introduced the cosmic redshift endemic to an expanding universe, we can now construct the relationship between the redshift of an extragalactic light source and its distance from Earth. Consider an astrophysical, light-emitting source. In a static universe, if such an object emits light isotropically, with a luminosity L, then the apparent luminosity l as seen by an observer a distance d away is given by

$$l = \frac{L}{4\pi d^2} \tag{48}$$

since the light is spread out over a spherical surface area. In astronomy, one typically uses absolute magnitude M and apparent magnitude m as measures of luminosity:

$$L = 10^{\frac{-2M}{5}} \times 3.02 \times 10^{35} \text{erg s}^{-1} \tag{49}$$

$$l = 10^{\frac{-2m}{5}} \times 2.52 \times 10^{-5} \text{erg cm}^{-2}\text{s}^{-1} \tag{50}$$

From these relations, the distance measure d in eqn. 48 becomes

$$d = \Big[\frac{L}{4\pi l}\Big]^{1/2} = 10^{[1+(m-M)/5]} \text{pc} \tag{51}$$

which is referred to as the *luminosity distance*. Astronomical observation directly probe $m - M$ known as the *distance modulus* thus measuring the luminosity distance indirectly:

$$m - M = 5(\log \frac{d}{1\,\text{pc}} - 1) \tag{52}$$

Including the effects of cosmic expansion will modify the luminosity distance in three ways:

- The spherical surface area over which the light dissipates must computed as a proper distance, $d = a(t)\, r$

- The absolute luminosity is energy per unit time ($\frac{\Delta E}{\Delta t}$). Cosmic expansion redshifts the energy of the emitted light, $\Delta E_1 = \frac{\Delta E_0}{1+z}$ (see eqn. 45).
- The absolute luminosity is energy per unit time ($\frac{\Delta E}{\Delta t}$). The rate of arrival of the photons is also attenuated by the same cosmic redshift factor, $\Delta t_1 = \Delta t_0(1+z)$ (see eqn. 45).

The confluence of these effects modifies eqn. 48 yielding

$$l = \frac{L}{4\pi r_1^2 a(t_1)^2\,(1+z)^2} \quad \rightarrow d_L \equiv r_1 a(t_1)\,(1+z) \tag{53}$$

Where d_L is the analogously defined luminosity distance in an expanding universe. What is immediately apparent from eqn. 53 is the prediction that in such an expanding cosmology higher redshift light sources should be farther away. We can recast this relationship into a more useful form by considering light sources at relatively low redshift ($z \ll 1$):

$$a(t_0) \simeq a(t_1) + (t_0 - t_1)\dot{a}(t_1) + \frac{1}{2}(t_0 - t_1)^2\ddot{a}(t_1) + \ldots \tag{54}$$

$$a(t_0) \simeq a(t_1)\Big[1 + (t_0 - t_1)H(t_1) - \frac{1}{2}(t_0 - t_1)^2 H^2(t_1) q(t_1) \ldots\Big] \tag{55}$$

$$1 + z = \frac{a(t_1)}{a(t_0)} \simeq 1 - (t_0 - t_1)H(t_1) + \frac{1}{2}(t_0 - t_1)^2 H^2(t_1) q(t_1) + (t_0 - t_1)^2 H^2(t_1) + \ldots \tag{56}$$

$$z \simeq (t_1 - t_0)H(t_1) + \frac{1}{2}(t_1 - t_0)^2 H^2(t_1)[q(t_1) + 2] + \ldots \tag{57}$$

$$\text{where} \quad q(t) \equiv -\frac{\ddot{a}(t)}{H(t)a(t)} \tag{58}$$

where we have treated $(t_1 - t_0)H(t_1)$ as the small parameter and defined the deceleration parameter $q(t)$. Next we compute r_1 by considering the light ray trajectory (eqn. 41) and leveraging eqn. 56

$$r_1 = \int_{t_0}^{t_1} \frac{dt}{a(t)} \simeq \frac{1}{a(t_1)} \int_{t_0}^{t_1} dt\Big[1 + (t_0 - t_1)H(t_1)\Big] \tag{59}$$

$$r_1 = \frac{1}{a(t_1)}\Big[(t_1 - t_0) + \frac{1}{2}(t_1 - t_0)^2 H(t_1)\Big]. \tag{60}$$

The combination $(t_1 - t_0)H(t_1)$ can be expressed in terms of $q(t)$ and z by inverting the series in eqn. 57, giving $(t_1 - t_0)H(t_1) = z - \frac{1}{2}[q(t_1) + 2]z^2$. Now the luminosity distance d_L can be expressed in terms of z, $H(t_1)$, and $q(t_1)$ by plugging eqn. 60 into eqn. 53:

$$d_L = (1+z)\Big(\Big[(t_1 - t_0) + \frac{1}{2}(t_1 - t_0)^2 H(t_1)\Big]\Big)\frac{H(t_1)}{H(t_1)} \tag{61}$$

$$= \frac{(1+z)}{H(t_1)}\Big(z - \frac{1}{2}[q(t_1) + 2]z^2 + \frac{1}{2}z^2 + \dots\Big) \tag{62}$$

$$d_L = \frac{1}{H(t_1)}\Big(z + \frac{1}{2}(1 - q(t_1))z^2 + \dots\Big) \tag{63}$$

Recall t_1 is the time when the light signal arrives at the location of the observer. Calling this the present time, and introducing the recessional velocity $v \equiv zc$, where $c = 1$ is the spend of light, gives the familiar Hubble's law:

$$d_L = \frac{1}{H_0}\Big(v + \frac{1}{2}(1 - q_0)v^2 + \mathcal{O}(v^3)\Big) \tag{64}$$

where H_0 and q_0 are the present day Hubble parameter and deceleration parameter respectively. To leading order in the recessional velocity (and redshift), one obtains the canonical form $H_0 d_L = v$ for Hubble's law. The eqn. 64 is a valid approximation for the luminosity distance at low redshift $z \ll 1$. Notice the z^2 term is sensitive to the radiation, matter, and dark energy density parameters of the cosmological model through the deceleration parameter, $q \propto \ddot{a}$. Consequently to constrain the model parameters, observations must probe distance scales at higher redshift. This requires extending the calculation of the luminosity distance d_L beyond the asymptotic form given above. Making no assumptions on the spatial curvature and using eqns. 41, 47, and 31, this procedure is straightforward:

$$\int_0^r \frac{dr'}{\sqrt{1 - kr'^2}} = \int_0^z \frac{1}{a(z')}\frac{dz'}{(1+z')H(z')} = \int_0^z \frac{dz'}{H(z')} \tag{65}$$

$$r(z) = \mathcal{S}\left(\int_0^z \frac{dz'}{H_0}\Big[\Omega_\Lambda + \Omega_k(1+z)^2 + \Omega_M(1+z)^3 + \Omega_R(1+z)^4\Big]^{-1/2}\right) \tag{66}$$

$$\text{Where } \mathcal{S}(y) = (\sin y, y, \sinh y) \text{ for } k = (1, 0, -1) \tag{67}$$

$$r(z) = \frac{\sqrt{-k}}{H_0\sqrt{\Omega_k}}\mathcal{S}\left(\frac{\sqrt{\Omega_k}}{\sqrt{-k}}\ I[z]\right) = \frac{1}{H_0\sqrt{\Omega_k}}\sinh\sqrt{\Omega_k}\ I[z] \tag{68}$$

where the last line follows from using the present day curvature density parameter $\sqrt{\Omega_k} = \frac{\sqrt{-k}}{H_0}$ and the properties $i \sin -iy = \sinh y$ and $\sinh \alpha y \simeq \alpha y$ for $\alpha \ll 1$. The integral over redshift, $I[z]$ does not have a closed, analytic form and must be evaluated numerically. With the comoving distance computed, the luminosity distance becomes (see eqn. 53)

$$d_L = a_0 r(z)(1+z) = \frac{1+z}{H_0\sqrt{\Omega_k}} \sinh \sqrt{\Omega_k}\ I[z] \tag{69}$$

$$I[z] = \int_0^z dz' \Big[\Omega_\Lambda + \Omega_k(1+z)^2 + \Omega_M(1+z)^3 + \Omega_R(1+z)^4\Big]^{-1/2} \tag{70}$$

By inserting eqn. 69 into eqn. 52 one obtains the *magnitude-redshift relation* which in principle can constrain the model parameters of the cosmology each of which enters into the equation with different powers of redshift. This constraining is done by fitting a distance modulus versus redshift plot populated by astronomical observations of astrophysical "standard candles"(objects with known absolute magnitude). Such a plot is known as a Hubble diagram.

Type Ia Supernovae (SNIa) are known to be reliable standard candles given that their intrinsic brightness is correlated with their dimming timescale [175]. The Supernova Cosmology Project and High-z Supernovae Search Team have both utilized the magnitude-redshift relation with observations of SNIa to constrain the density parameters of the Universe. Figure 1 (below) shows their data along with multiple theoretical projections based on model cosmologies. It is worth mentioning that since at low redshift, $z \ll 1$, the luminosity distance is well approximated by eqn. 64, and the linear term of this equation is only sensitive to the Hubble constant, the magnitude-redshift relation also provides an empirical probe of the present day Hubble parameter, insensitive to the cosmological density parameters [169].

2.1.2.2 Nucleosynthesis Big bang nucleosynthesis (BBN) provides one of the earliest probes of the big bang cosmology and ΛCDM in particular. Using Standard Model particle interactions in conjunction with the expanding FLRW framework, one is able to predict the primordial abundances of the lightest chemical elements; predictions which can then be compared with astronomical observations. The process of nucleosynthesis proceeds through multiple stages, but let us first consider initial conditions.

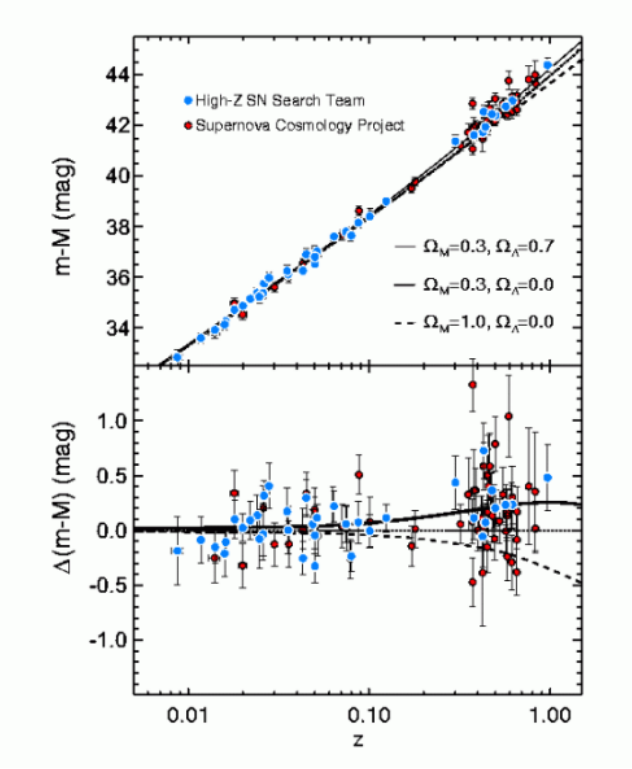

Figure 1: The Magnitude-redshift relation using type Ia supernovae as standard candles produced by High-z SN Search Team with data from the SCP [168]. Different black lines represent distinct model cosmologies. While all are consistent in the low redshift range, ΛCDM cosmology provides the best fit for high redshift behavior.

Once the early Universe has cooled, through expansion, below $T \lesssim 20$ MeV (baryon freeze-out [121]), a plasma of coupled nucleons, leptons, and photons persists in (very nearly) local thermodynamic equilibrium (LTE). This equilibrium is maintained by the following weak interactions:

$$\nu_e + n \leftrightarrow e^- + p \tag{71}$$

$$\bar{\nu}_e + p \leftrightarrow e^+ + n \tag{72}$$

$$n \rightarrow p + e^- + \bar{\nu}_e \tag{73}$$

At MeV scale temperatures, the nucleons (n, p) in the above reactions are non-relativistic ($m \gg T$) while the leptons are ultra-relativistic ($m \ll T$). Consequently, the number density of each type of nucleon will be given by

$$n_{nuc} \simeq 2\Big(\frac{m_{nuc}T}{2\pi}\Big)^{3/2} e^{-(m_{nuc}-\mu_{nuc})/T} \tag{74}$$

where μ_{nuc} is the chemical potential of the nucleon. The ratio of neutrons to protons is therefore

$$\frac{n_n}{n_p} = \Big(\frac{m_n}{m_p}\Big)^{3/2} e^{-(m_n-m_p)/T}\, e^{(\mu_n-\mu_p)/T} \simeq e^{-Q/T}\, e^{(\mu_e-\mu_\nu)/T} \;\; ; \; Q \equiv m_n - m_p = 1.293\text{MeV} \tag{75}$$

where we have used the fact that $\frac{m_n}{m_p} \sim 1$ and the relationship between chemical potentials implied by eqn. 71. Incidentally, the charge neutrality of the Universe implies that $n_e - \bar{n}_e = n_p - \bar{n}_p \simeq \eta\, n_\gamma$, where η is the present day baryon to photon ratio (since most baryons today are protons). Moreover, for ultra-relativistic particles, the combination, $n - \bar{n}$ is proportional to $T^3(\frac{\mu}{T})$. Using these two facts and recalling the photon number density leads to the following relation,

$$\eta\, n_\gamma = \eta \frac{2.4}{\pi^2} T^3 = n_e - \bar{n}_e \propto T^3\Big(\frac{\mu_e}{T}\Big) \rightarrow \eta \simeq \frac{\mu_e}{T}. \tag{76}$$

As we will soon see nucleosynthesis constrains $\eta \ll 1$, a result also confirmed by analysis of the cosmic microwave background power spectrum [23]. Therefore, the result of eqn. 76 along with a similar argument for $\frac{\mu_\nu}{T}$ justify dropping the chemical potential dependence from eqn. 75, thus giving a simple temperature dependence for the neutron-proton ratio while the species are in LTE. This ratio plays a key role in determining the BBN abundances. We now consider it's value at the onset of BBN after neutron freeze-out.

As the Universe continues expanding and cooling, the reactions 71 and 72 become inefficient at maintaining equilibrium between protons and neutrons. The temperature (T_f) at which this thermal freeze-out occurs is properly computed through the Boltzmann equation; however, it can be reliably estimated using the decoupling criterion ($H(T_f) \simeq W(T_f)$)

where H and W are the Hubble parameter and interaction rate (of the process decoupling) respectively. First the interaction rate for the process 71 can be estimated [121]:

$$W = n_e \langle \sigma[pe \to n\nu] \cdot (v \simeq c = 1) \rangle \tag{77}$$

$$\sigma \simeq 5.76 \, (G_F)^2 \, p_f^2 \;\; ; \;\; n_e \simeq \frac{1}{\pi^2} T^3 \, , (T > Q) \tag{78}$$

$$W \simeq (G_F)^2 T^5 \tag{79}$$

where G_F is Fermi's constant, v is the velocity of the relativistic electron flux, σ is the scattering cross section typical of a weak force interaction when the center of mass energy is below the mass of the W-boson mediator. p_f is the magnitude of the outgoing momentum in the center of mass frame, and the number 5.76 comes from the axial vector coupling of nucleons. The number density of the electrons comes from the Fermi-Dirac distribution. In the above estimate, $p_f^2 \sim T^2$, and consequently, the interaction rate scales with T^5. Meanwhile, the Hubble rate comes from noting that BBN occurs during the radiation dominated epoch:

$$H^2 = \frac{8\pi G_N}{3} \rho_R \;\; ; \;\; \rho_R = \frac{\pi^2}{30} g_* T^4 \tag{80}$$

$$H = \frac{1.66 T^2}{M_{pl}} \sqrt{g_*} \tag{81}$$

where g_* is the effective number of relativistic degrees of freedom and M_{pl} is the Planck mass. Setting eqns. 79 and 81 equal to each other gives as a freeze out temperature $T_f \simeq 1$MeV. This result is approximate however, and when all of the relevant effects are properly included in the evaluation of the scattering cross-section, the freeze-out temperature is found to be $T_f = 0.8$MeV [160, 121]. Evaluating the neutron-proton ratio at this temperature (see eqn. 75, dropping the chemical potentials) yields

$$r_0 \equiv \frac{n_n}{n_p}(T = 0.8\text{MeV}) = 0.2 \tag{82}$$

which is the initial condition for the onset of BBN. After freeze-out, the neutron-proton ratio still decreases since the beta decay process 73 continues. The lifetime of the neutron is

$\tau_n \simeq 880\,\mathrm{s}$ [183, 159]; therefore at time t after neutron freeze-out, the neutron-proton ratio is

$$\frac{n_n}{n_p}(t) \equiv r(t) = \frac{r_0 e^{-t/\tau_n}}{1 + r_0(1 - e^{-t/\tau_n})}. \tag{83}$$

While the neutron abundance is slowly depleting due to beta decay, other nuclear processes involving neutrons can proceed. Of particular importance is the production of deuterium:

$$n + p \leftrightarrow {}^2H + \gamma \;\; ; \;\; E_\gamma \simeq 2.2\mathrm{MeV} \tag{84}$$

where 2.2 MeV is the deuterium binding energy. The deuterium abundance is of vital importance to nucleosynthesis since the nuclear production of all other elements proceed through a deuterium channel. Thus deuterium production is known as stage one of BBN. A relic abundance of deuterium will accumulate once the reaction decouples. The temperature at which the deuterium freeze-out occurs can again be estimated through the decoupling criterion ($H(T_f) \simeq W(T_f)$). However, this reaction proceeds via an electromagnetic interaction and consequently has a much larger scattering cross section, $\sigma[\gamma\, {}^2H \to np] \simeq 2.57 \times 10^{-7}$ MeV^{-2} [160]. Additionally, since the binding energy is larger than the temperature of the plasma (2.2 Mev $>$ 0.8 MeV), only photons in the tail of Bose-Einstein distribution will be able to photodisintegrate the deuterium nucleus; accordingly the relevant n_γ must be computed by integrating the distribution over the relevant domain. Accounting for these factors, the decoupling criterion gives an approximate freeze-out temperature of $T_f \simeq 0.06$ MeV.

The time at which the Universe reaches this temperature can be computed via eqn. 81 and Table 2

$$\frac{\dot{a}}{a} = \frac{1}{2t} = H = \frac{1.66 T^2}{M_{pl}} \sqrt{g_*} \tag{85}$$

which for $T = 0.06$ MeV gives $t_{dec} \sim 300$ seconds, for the age of the Universe in comoving time. Computing the neutron-proton ratio, $r(t)$, at this time yields

$$r(t_{dec}) \simeq 0.14. \tag{86}$$

After the synthesis of a deuterium abundance, stage two and three of nucleosynthesis can rapidly proceed through a cascade of fusions, leading to the production of helium-4, beryllium, and lithium. Helium-4 has the largest binding energy of all the primordial nuclei

produced through BBN and consequently the majority of the frozen-out neutron abundance ends up in this isotope. The ^{4}He mass fraction can be estimated,

$$Y_p \equiv \frac{\rho_{He}}{\rho_{He} + \rho_p} \tag{87}$$

$$Y_p \simeq \frac{4n_{He}}{4n_{He} + n_p} = \frac{2n_n(t_{dec})}{2n_n(t_{dec}) + n_p} \tag{88}$$

$$n_p = n_p(t_{dec}) - 2n_{He} = n_p(t_{dec}) - n_n(t_{dec}) \tag{89}$$

where we have noted that the species are all non-relativistic and treated their mass as $m = m_n \times N$, where N is the number of nucleons in the species. Finally, we have assumed $\frac{1}{2}n_n(t_{dec}) \simeq n_{He}$), namely that nearly all the neutrons become helium-4. Finally, combining eqns. 88, 89, and 86 we obtain

$$Y_p = \frac{2n_n(t_{dec})}{n_n(t_{dec}) + n_p(t_{dec})} = \frac{2r(t_{dec})}{2r(t_{dec}) + 1} \tag{90}$$

$$Y_p \simeq 0.245 \tag{91}$$

The Helium-4 mass fraction can be measured astronomically by observing low metallicity environments such as globular clusters, extragalactic dust clouds, and planetary nebulae [121, 159, 160]. Although helium-4 is produced in stellar cores of main sequence stars, the amount synthesized increases the helium-4 abundance only at $\sim 1\%$ level [160]. Thus, given the stability of the isotope, the helium-4 abundance represents a stringent test of BBN and by extension our cosmological model.

As previously mentioned, nucleosynthesis also accounts for the primordial production of deuterium, helium-3, and lithium. A rigorous computation of these primordial abundances, requires numerically solving the coupled Boltzmann equations for the various particle species' distribution functions, tracking their evolution through time. Figure 2 below shows the results of such an analysis and a comparison with observations. Two important points remain in our discussion of nucleosynthesis. First, BBN represents the only real means of producing deuterium in the Universe since it functions only as an intermediate stage in the nuclear reactions of stellar interiors [160, 159]. Therefore any detection of deuterium translates into a lower bound on its primordial abundance. Second, of particular importance is the strong sensitivity of all the abundances save for ^{4}He on the baryon to photon ratio η

(see fig. 2). Assuming the three standard model flavors of neutrino (which effects the value of g_*), η represents the only true independent variable in the nucleosynthesis analysis [159].

The success of BBN calculations at predicting the primordial abundances, whose mass fractions span nearly 9 orders of magnitude, is an important achievement in the physics of the early Universe. Using equation 85 and $T_f \simeq 1$ MeV for the neutron freeze-out temperature gives an age of the Universe of ~ 1 s. The ability to accurately describe the physics of such an extraordinarily young, Universe motivates the extrapolation to even earlier times.

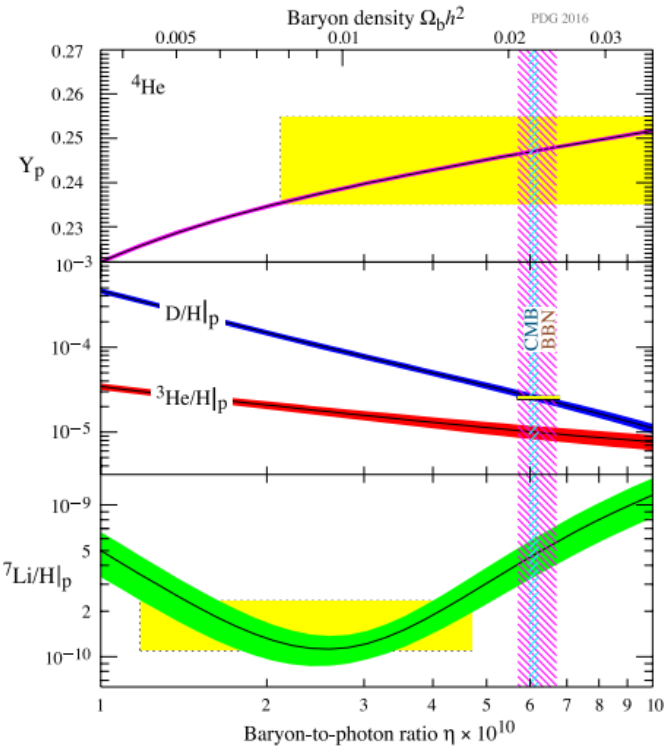

Figure 2: The primordial abundances for ^{4}He, D, ^{3}He, and ^{7}Li as predicted by Standard Model nucleosynthesis [159]. The bands show 95% CL range. Boxes indicate regions consistent with astronomical observation. Narrow vertical band indicates CMB observations of baryon-photon ratio. The wider vertical band is the BBN concordance region. The major source of discrepancy is the lithium abundance which prefers an η range differing by roughly a factor of 2.

2.1.2.3 The Cosmic Microwave Background: Recombination The Cosmic Microwave Background radiation (CMB) refers to the isotropic electromagnetic radiation which is detectable in the microwave frequency range, and permeates the Universe. The CMB is the result of the rapid transition of the early Universe's state from an opaque plasma of tightly coupled baryons, electrons, and photons to a gas of mostly neutral hydrogen and freely propagating photons. To an observer inhabiting this Universe, the transition from opaque to transparent, appears as a gradual enlarging of a transparent spherical volume, centered on the observer, and whose comoving radius is determined by the speed of light times amount of time elapsed since the transition. At the edge of this visible volume is an opaque, radiating surface. This so-called *surface of last scattering* looks like how the Universe appeared at the time of this opacity transition (albeit cosmically redshifted), since those photons are just now reaching the observer. The "glow" of this surface is the CMB. In this section we discuss its formation through the confluence of recombination and photon decoupling, its redshifted thermal spectrum, and the significance of the anisotropies in that spectrum.

Recombination and photon decoupling:

Photons are held in equilibrium with the early Universe plasma through electromagnetic scattering interactions which have much larger cross sections than the weak nuclear interactions that lead to neutron freeze-out. Therefore, photon decoupling happens after nucleosynthesis. At this phase of the cosmic evolution, the Universe consists of a baryon-electron-photon plasma and ostensibly an abundance of dark matter which has negligible interactions with the plasma. Note that we are neglecting the products of nucleosynthesis (^{4} He, etc.) which are still subdominant compared to the number of free protons. By this time, the temperature of this plasma is much lower than even the electron mass $T \ll 0.5$ MeV. Consequently, all of the species comprising the coupled plasma may be treated non-relativistically with number densities given by

$$n_i = g_i \left(\frac{m_i T}{2\pi}\right)^{\frac{3}{2}} \exp\left(\frac{\mu_i - m_i}{T}\right) \quad ; \quad i = \mathrm{e, p, H} \tag{92}$$

where e, p, and H refer to free electrons, free protons, and neutral hydrogen respectively each with a mass m_i, chemical potential μ_i, and internal degrees of freedom g_i. Hydrogen

atoms are kept in equilibrium by the process

$$p + e \leftrightarrow \mathrm{H} + \gamma \tag{93}$$

and consequently, $\mu_p + \mu_e = \mu_H$ (photons have zero chemical potential). Moreover since we are discounting the small abundances yielded by nucleosynthesis, the number of hydrogen atoms and free protons essentially determine the number of baryons: $n_B \simeq n_p + n_H$. Using these relations along with the number densities given by eqn. 92, the number density of neutral hydrogen can be expressed as

$$n_H = \frac{g_H}{g_e g_p} n_p n_e \Big(\frac{m_e T}{2\pi}\Big)^{-3/2} \exp\Big(B/T\Big) \;\; ; \;\; B \equiv m_p + m_e - m_H \tag{94}$$

where we have treated the hydrogen and proton mass as equal everywhere *except* for in the exponential function, and $B = 13.6$ eV is the binding energy of hydrogen. Given the low binding energy of hydrogen, one should not expect a significant abundance of H atoms to form until the plasma cools significantly, $T \sim 1$ eV. To find the temperature of recombination, it is convenient to introduce the ionization fraction $\chi_e \equiv \frac{n_p}{n_B}$. Eqn. 94 can then be rewritten in terms of this new variable

$$\frac{n_H}{n_B} = \frac{n_B - n_p}{n_B} = \chi_e^0 \, \chi_e^0 n_B \Big(\frac{m_e T}{2\pi}\Big)^{-3/2} \exp\Big(B/T\Big) \tag{95}$$

$$\frac{1 - \chi_e^0}{(\chi_e^0)^2} = \eta \, n_\gamma \Big(\frac{m_e T}{2\pi}\Big)^{-3/2} \exp\Big(B/T\Big) \tag{96}$$

$$\frac{1 - \chi_e^0}{(\chi_e^0)^2} = \frac{4\sqrt{2}\zeta(3)}{\sqrt{\pi}} \eta \Big(\frac{T}{m_e}\Big)^{3/2} \exp\Big(B/T\Big) \tag{97}$$

where charge neutrality $n_e = n_p = \chi_e n_B$ has been used along side the baryon-photon ratio, $\eta = \frac{n_B}{n_\gamma}$. Additionally we have noted that $g_e = g_p = 2$ and $g_H = 4$. Finally in the last line the photon number density coming from the Bose-Einstein distribution has been inserted with $\zeta(3)$ referring to the Riemann zeta function. The derived eqn. 97 is known as the Saha equation for the thermal equilibrium ionization fraction (to which the superscript 0 refers). The Saha equation describes the change in the fractional ionization of the coupled plasma, and thus ultimately the amount of free charge carriers.

Recombination refers to the point in the cosmic evolution where virtually all free electrons have been captured by the protons in the plasma thereby forming an abundance of hydrogen

gas. By convention, this is defined to correspond to the equilibrium ionization fraction falling to $\chi_e^0 = 0.1$, namely 90% of electrons have been captured. Inserting this value into eqn. 97 along with a baryon-photon ratio $\eta \simeq 10^{-10}$, consistent with nucleosynthesis, yields the temperature at which recombination occurs:

$$T_{rec} = 0.3\,\mathrm{eV}. \tag{98}$$

Since the Universe undergoes an isentropic expansion, and the entropy density scales with the photon temperature $s \propto T^3$ [121], we can relate the temperature and scale factor

$$S = s \cdot a^3 \propto T^3 \quad \rightarrow T \propto a^{-1} \tag{99}$$

and therefore noting the present day temperature photon temperature is $T_0 = 2.35 \times 10^{-4}\,\mathrm{eV}$ [71], the scale factor of recombination is

$$a_{rec} = T_0/T_{rec} \simeq 7.8 \times 10^{-4} \tag{100}$$

which in accordance with eqn. 32 indicates that recombination occurs during the matter dominated epoch.

In order to propagate freely and thus source an isotropic background radiation, the photons must decouple from the early Universe thermal plasma. The most significant scattering process maintaining their equilibrium with the other coupled degrees of freedom is

$$e + \gamma \rightarrow e + \gamma \tag{101}$$

namely Thomson scattering. As previously stated, this is an electromagnetic interaction with a large scattering cross section $\sigma[e\gamma \rightarrow e\gamma] \simeq 1.7 \times 10^{-3}\mathrm{MeV}^{-2}$ [121, 183]. Given their small mass, electrons remain relativistic throughout most of the early Universe meaning their number density is not Boltzmann factor suppressed. Accordingly, the large scattering cross section and large electron number density make Thomson scattering very efficient at maintaining local thermodynamic equilibrium (LTE), and thus photon decoupling will only begin to happen after the free electron number density begins to decrease, i.e. during recombination. The decoupling temperature can be estimated by comparing the Hubble rate

and interaction via the decoupling criterion, $H(T) \simeq W(T)$. First, we can consider the Saha eqn. (97) under $\chi_e^0 \ll 1$,

$$\chi_e^d \simeq \left[\frac{4\sqrt{2}\,\zeta(3)}{\sqrt{\pi}}\eta\left(\frac{T}{m_e}\right)^{3/2}\exp\Big(B/T\Big)\right]^{-1/2} \tag{102}$$

where χ_e^d refers to the equilibrium ionization fraction during decoupling. Next the interaction rate is estimated,

$$W = W = n_e\,\langle\sigma[e\gamma \to e\gamma]\cdot(v \simeq c = 1)\rangle \tag{103}$$

$$\sigma \simeq \left(\frac{\alpha_{em}}{m_e}\right)^2 \;\;;\;\; n_e = n_p = \chi_e^d n_B = \chi_e^d n_\gamma\,\eta \tag{104}$$

$$W \simeq \chi_e^d\,\eta\left(\frac{\alpha_{em}}{m_e}\right)^2\frac{2\zeta(3)}{\pi^2}T^3 = \left(\frac{\alpha_{em}}{m_e}\right)^2\left[4\frac{\zeta(3)}{\pi^2}T^3\Big(\frac{m_e T}{2\pi}\Big)^{3/2}e^{-B/T}\right]^{1/2} \tag{105}$$

where α_{em} is the electromagnetic fine structure constant, and we have again used the ionization fraction. Also note that here I have *estimated* the scattering cross section by noting that Thomson scattering is a non-relativistic quantum electrodynamics process. The exact value for this cross section, from the limit of the Klein-Nishina formula, is quoted on the previous page.

Turning our attention to the Hubble rate, since we anticipate photon decoupling to occur during the matter dominated epoch using eqns. 31, 32, and 99 we find

$$H^2(a) \simeq H_0^2\frac{\Omega_M}{a^3}\Big[1 + \frac{\Omega_R}{\Omega_M}\frac{1}{a}\Big] \tag{106}$$

$$H(T) = \left(H_0^2\Omega_M\Big(\frac{T}{T_0}\Big)^3\Big[1 + a_{eq}\Big(\frac{T}{T_0}\Big)\Big]\right)^{1/2} \tag{107}$$

$$H(T) \simeq H_0\sqrt{\Omega_M}\Big(\frac{T}{T_0}\Big)^{3/2} \tag{108}$$

where in the last line we have expanded ($a_{eq}\,\frac{T}{T_0} \ll 1$) and kept the leading order term. Now setting eqns. 105 and 108 equal to each other, and solving for T gives the decoupling temperature and scale factor

$$T_{dec} \simeq 0.28\,\mathrm{eV} \;\;\rightarrow\;\; a_{dec} \simeq 8.3\times 10^{-4}. \tag{109}$$

The above calculation was an estimate, since it utilized the equilibrium ionization fraction coming from the Saha equation. In reality, after the onset of recombination, the electrons rapidly fall out of equilibrium, and thus the ionization fraction must be tracked by solving the Boltzmann equation for the electron number density which changes under the process 93 [71]. Computing the evolution of the ionization fraction in this manner and using it in place of χ_e^d in eqn. 105 modifies the result of the decoupling criterion and yields [121]

$$T_{dec} = 0.26\,\text{eV} \quad \rightarrow \quad a_{dec} \simeq 9.09 \times 10^{-4}. \tag{110}$$

Comparing results 100 and 110 indicates, as expected, that recombination and photon decoupling occur sequentially and at nearly the same moment in the expansion history, specifically at comoving times (using eqn 108 and 3) $t_{rec} \sim 3.8 \times 10^5$ yrs and $t_{dec} \sim 4.1 \times 10^5$ yrs.

Redshifted thermal spectrum:

The photon spectrum observed on the surface of last scattering still exhibits a nearly thermal blackbody spectrum despite photons decoupling billions of years ago. This relic, thermal nature can be explained as follows: prior to decoupling, the photons were in LTE with the plasma, and thus with an associated number density,

$$n(\nu, T)\, d\nu = \frac{8\pi\nu^2\, d\nu}{\exp(\frac{\nu}{T}) - 1} \tag{111}$$

namely a Planck distribution (Bose-Einstein distribution with zero chemical potential), where ν is the frequency and T is the temperature of the plasma (the integral over all frequencies is implied). If the photon decoupling is abrupt, then the form of the distribution is preserved. After this process the Universe becomes transparent, with the transparent volume as seen by an observer increasing yet always bounded by the last scattering surface. The photons traveling from the last scattering surface, to the observer's detector experience cosmic redshift, and accordingly the distribution redshifts with the change in the scale factor. Consequently, for a photon observed with frequency ν_0 and arriving at the detector at time t_0,

$$n_0(\nu_0, T)\, d\nu_0 = \Big(\frac{a(t_{dec})}{a(t_0)}\Big)^3 n_{dec}\Big(\nu_0\, \frac{a(t_0)}{a_{dec}}, T\Big)\, \frac{a(t_0)}{a_{dec}} d\nu_0 \tag{112}$$

$$n_0(\nu_0, T)\, d\nu_0 = \frac{8\pi\nu_0^2\, d\nu_0}{\exp(\frac{\nu_0\, a(t_0)}{T\, a(t_{dec})}) - 1} = \frac{8\pi\nu_0^2\, d\nu_0}{\exp(\frac{\nu_0}{T(t_0)}) - 1} \tag{113}$$

where a combination of two effects has resulted in the last line: the number density decreases as the scale factor enlarges the comoving volume, and the emitted frequency (ν_{dec}) is larger than the observed frequency (ν_0) as specified in eqn. 45. The external ratios of the scale factor mutually cancel, leaving only the ratio inside the argument of the exponential which in turn can be absorbed into the temperature leading to

$$T(t_0) = T\,\frac{a(t_{dec})}{a(t_0)} \tag{114}$$

which is the same temperature scaling as seen in eqn. 99. Evidently, the photons observed from the last scattering surface will have a thermal distribution with redshifted temperature. Normalizing the present day scale factor to unity, and using the results of eqn. 110 this yields an observed blackbody spectrum with

$$T(t_0) \equiv T_0 = 2.4 \times 10^{-4}\,\mathrm{eV} \tag{115}$$

and consequently peaked in the microwave frequency range as advertised before [71]. Given it's present day, nearly thermal distribution function, measurements of the CMB spectrum allow one to compute the present day photon energy density by integrating the distribution, yielding

$$\int_0^\infty \frac{\nu_0}{(2\pi)^3} n(\nu_0) d\nu_0 \;= \rho_{0,\gamma} = \frac{2\pi^2}{30} T_0^4 \rightarrow \Omega_\gamma = 5.04 \times 10^{-5}\,. \tag{116}$$

Figure 3 (below) shows the observations of the last scattering surface, and therefore the CMB, as detected by the Planck satellite and expressed as a map of temperature anisotropies. These observations confirm the presence of an exceedingly isotropic thermal spectrum, with tiny temperature fluctuations ($\delta T/T \sim \mathcal{O}(10^{-5})$).

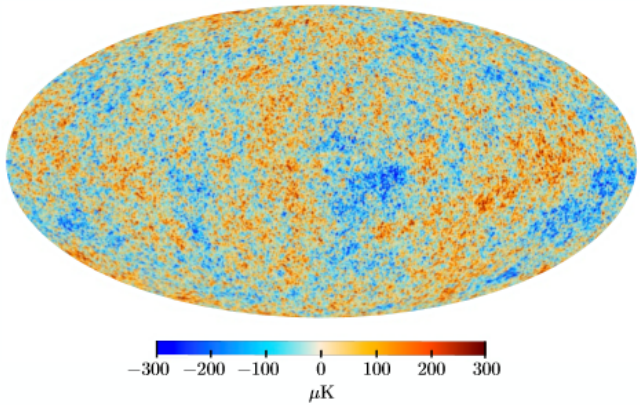

Figure 3: The CMB temperature anisotropy map produced by the Planck collaboration [3]. The different colors correspond to temperature fluctuations (about 1 part in 10^5) around the mean temperature of $T \simeq 2.72\,\mathrm{K}$. In ΛCDM during matter domination, points with an angular separation $\theta \leq 2^\circ$ are contained within the particle horizon and are therefore causally connected. These observations show that the entire CMB is highly isotropic, across scales much larger than this, indicating that the entire surface must have been somehow causally connected in the past.

2.1.2.4 The Cosmic Microwave Background: Anisotropies While the CMB spectrum displays a large degree of homogeneity and isotropy, and can be well characterized by a thermal, Planck spectrum, the small anisotropies present must be explained. The theory of cosmological perturbations offers a precise, dynamical explanation of these anisotropies and connects these fluctuations to the cosmological parameters of our FLRW model. Cosmological perturbation theory, as applied to the analysis of the CMB, is thoroughly and pedagogically explained in [139]; in this section I provide a qualitative overview of the subject following the treatment discussed therein.

Observational analysis of the CMB anisotropies is carried out by studying the the *angular temperature anisotropy power spectrum*. To introduce this object, we begin by defining the

spectrum of temperature fluctuations

$$\frac{\delta T}{\overline{T}} \equiv \Theta(\eta_0, \vec{x_0}, \hat{\eta}) = \sum_{l,m} a_{lm} Y_{lm}(\hat{\eta}) \tag{117}$$

where η_0 is the present day conformal time, $\vec{x_0}$ describes the observer's location, and looking in a direction $-\hat{\eta}$ such that the CMB photons are traveling in direction $\hat{\eta}$. This function is expanded in spherical harmonics, (Y_{lm}) which form a complete set of functions in spherical coordinates, a natural choice when studying the last scattering surface as viewed from Earth. In practice it is easier to work with the spatial Fourier transform of the temperature fluctuation

$$\Theta(\eta_0, \vec{x_0}, \hat{\eta}) = \int \frac{d^3k}{(2\pi)^3} \Theta(\eta_0, \vec{k}, \theta)\, e^{i\vec{k}\cdot\vec{x_0}} \tag{118}$$

where we have used the fact that statistical isotropy guarantees that the equation of motion for Θ will only depend on the combination $\vec{k} \cdot \hat{\eta} = k\cos(\theta)$, and so we have opted to use the relative angle, θ, between the line of sight and wave vector instead of $\hat{\eta}$. Incidentally, this exact form of angular dependence allows one to perform a multipole expansion of the temperature anisotropy

$$\Theta(\eta_0, \vec{k}, \theta) = \sum_l (-i)^l (2l+1) \Theta_l(\eta_0, \vec{k})\, \mathcal{P}_l(\cos\theta) \tag{119}$$

where $\mathcal{P}_l(\cos\theta)$ are the associated Legendre polynomials. Insert equations 118 and 119 into equation 117, and using the relations between the associated Legendre polynomials and the spherical harmonics yields (choosing the detector to be at $\vec{x}_0 = 0$)

$$a_{lm} = (-i)^l \int \frac{d^3k}{2\pi^2} Y_{lm}(\hat{k}) \Theta_l(\eta_0, \vec{k}) \;\; ; \frac{\vec{k}}{k} = \hat{k} \tag{120}$$

which can then be used to compute the two-point correlation function

$$\langle a_{lm}\, a^*_{l'm'} \rangle = \delta_{mm'} \delta_{ll'} \frac{1}{2\pi^2} \int \frac{dk}{k}\, \Theta_l^2(\eta_0, k)\, \mathcal{P}_{\mathcal{R}}(k) \tag{121}$$

$$C_l \equiv = \frac{1}{2\pi^2} \int \frac{dk}{k} \Theta_l^2(\eta_0, k)\, \mathcal{P}_{\mathcal{R}}(k) \tag{122}$$

where the Kronecker deltas arise from the orthogonality of the spherical harmonics and are encoding the statistical homogeneity. The resulting correlation function has been written in terms of a dimensionless power spectrum $\mathcal{P}_{\mathcal{A}}(k)$ which is defined as

$$\int \frac{d^3k}{(2\pi)^3} P_A(k)\, f(k) \equiv \int \frac{dk}{k} \mathcal{P}_{\mathcal{A}}(k) f(k). \tag{123}$$

A number of comments should be made about the equation 122, which is the angular temperature anisotropy power spectrum we were seeking to derive. First, the result does not depend on the subscript m. This is unsurprising given the form of the polynomial expansion in eqn. 119; however, on physical grounds this is expected as a consequence of the Universe being statistically isotropic. Second, because of statistical isotropy the temperature anisotropy power spectrum only depends on the magnitude $k = |\vec{k}|$. Third, the dimensionless power spectrum used to write the correlation function in this form is the primordial curvature power spectrum $\mathcal{P}_{\mathcal{R}}(k)$ which represents the initial spatial curvature of spacetime. This particular quantity is chosen because its conserved on super-horizon scales under adiabatic initial conditions (see below) [71]. Finally, in this form the function $\Theta_l^2(\eta_0, k)$ is known as the transfer function for a given mode, l, and it describes the linear evolution of the probability distribution for that particular mode.

The reason for the introduction of probablities into this discussion owes to the theory of cosmological perturbations being stochastic. Consequently, each temperature fluctuation at a point in spacetime is given by a probability distribution. Since we will restrict ourselves to linear perturbations, the evolution of the initial probability distribution will also linear, hence the role of the transfer function. The brackets in equation 121 represent an averaging over many identically prepared initial states, i.e. "universes". However, since we only have a single Universe and ergo CMB to study, one may question the validity of this approach. However, because of the lack of azimuthal dependence (m) in the temperature power spectrum, one can measure many a_{lm}'s with the same multipole moment l but different m's resulting in many outcomes for the same random variable (see [139]).

In light of equation 122, the remaining theoretical task becomes clear: 1.) a primordial power spectrum must postulated or derived from a model of even earlier Universe physics, 2.) the transfer functions for all multipole moments must be computed. The former may be

provided by the theory of inflation. The latter is an involved process which requires solving the Einstein-Boltzmann hierarchy of equations. Here I summarize the procedure, which is explained in detail in [139]:

- Perturb the Einstein Equations: The anisotropies in the CMB represent small departures from the homogeneity and isotropy of the FLRW metric. Accordingly we consider perturbations $g_{\mu\nu} = \bar{g}_{\mu\nu} + \delta g_{\mu\nu}$ and $T_{\mu\nu} = \bar{T}_{\mu\nu} + \delta T_{\mu\nu}$, the bar being the spatially averaged result, namely the usual FLRW metric and perfect fluid EMT. The perturbations can be decomposed into scalar, vector, and tensor perturbations. The vectors represent the response of the metric to vorticity in the fluid material, and thus rapidly decay in FLRW. The tensors represent gravitational wave disturbances and decouple (at first order) from the scalars which themselves represent local changes in the gravitational potential due to inhomogeneities in the fluid material distribution. Since temperature is a scalar quantity, it is the scalar perturbations are the most significant for studying the CMB fluctuations. There are four scalar perturbation quantities from the EMT: energy density perturbations ($\delta\rho$), pressure perturbations (δp), velocity potential (v), and anisotrpoic stress (σ). Additionally there are four quantities from perturbing the metric: the gravitational potential ψ, local distortions in the average scale factor ϕ, and finally δg_{0i} and the traceless piece of δg_{ij}.
- Choose a Gauge: Since General Relativity is invariant under general coordinate transformations, there is gauge freedom in how the metric perturbations are written. While one may compute gauge invariant quantities, in general it is easier to work in a particular gauge. In the Newtonian gauge only ϕ and ψ are non-vanishing quantities, and the perturbed metric becomes

$$g_{\mu\nu} = \text{diag}\Big[(1+2\psi)a^2, -(1-2\phi)a^2, -(1-2\phi)a^2, -(1-2\phi)a^2)\Big] \tag{124}$$

  working with the spatially flat FLRW metric in conformal time as the unperturbed background. For this perturbative scheme, to first order, one obtains four Einstein equations relating the geometric and energy momentum perturbations. Because of the

gauge choice, only two are needed ($' \equiv \frac{\partial}{\partial \eta}$):

$$\frac{2}{3}\Big(\frac{k}{a}\Big)^2(\phi - \psi) = 8\pi G_N \sum_x (\bar{\rho_x} + \bar{p_x})\sigma_x \tag{125}$$

$$2a^{-2}\left[(k)^2\phi + 3\frac{a'}{a}\Big(\phi' + \frac{a'}{a}\psi\Big)\right] = -8\pi G_N \sum_x \delta\rho_x \tag{126}$$

where the sum over x is the sum over each species contributing to the EMT (baryons, photons, etc.) and k is the wave number.

- Specific Equations of Motion: The energy momentum tensor of this system is comprised of several components which can be classified generically as relativistic versus non-relativistic, and coupled versus uncoupled. Cold dark matter (CDM) is treated as both non-relativistic and uncoupled. Neutrinos are relativistic, and in this stage in the cosmic history uncoupled. Baryons and electrons are non-relativistic and interpolate between coupled and uncoupled regimes. Finally, the photons are relativistic and also transition from the coupled to the uncoupled regime. Given that each component is described by four parameters $(\delta\rho, \delta p, v, \sigma)$ a total of four equations of motion are required, for each component, to close the system. For each uncoupled component, there is covariant conservation of that species' EMT: $\nabla_\mu T^\mu_{\nu,x} = 0$. While for coupled species, the previous relation must be modified with a source term accounting for the change in energy-momentum from interactions. Either way, this relation provides two scalar equations of motion for each individual component. For strongly coupled components, an ideal fluid description can be used on account of the rapid microphysical interactions imposing thermodynamic equilibrium. Consequently, they exhibit no anistropic stress $\sigma_x = 0$ and have a sound speed c_x such that $\delta p_x = c_x^2 \delta\rho_x$ which provide the missing two equations. CDM is modeled as completely collisionless with negligible anisotropic stress, and so may treated effectively as a perfect fluid with $\delta p_{CDM} = 0 \rightarrow c_{CDM} = 0$. Meanwhile for decoupled species, a fluid description is insufficient, and the Boltzmann equation must be solved instead.
- Adiabatic Initial Conditions: We specify initial conditions during the time when all Fourier modes of interest (those actually observable in the CMB) have physical wavelengths outside the particle horizon $\frac{2\pi}{k}a \gg \frac{1}{H}$. Such modes are causally disconnected from

small scale interactions, and therefore only reflect whatever mechanism initally seeds the inhomogeneities. Additionally, for superhorizon modes, the EMT is necessarily diagonal and has the fluid-kinetic form $\mathrm{diag}(\delta\rho, -\delta p, -\delta p, -\delta p)$, which can be demonstrated by expanding the EMT in powers of $k/(aH)$. This means the initial conditions are specified solely in terms of the energy density and pressure. Adiabatic initial conditions are chosen by the following ansatz:

$$\rho_x(\eta, \vec{x}) = \bar{\rho}_x(\eta) + \bar{\rho}'_x(\eta)\delta\eta(\vec{x}) \tag{127}$$

$$p_x(\eta, \vec{x}) = \bar{p}_x(\eta) + \bar{p}'_x(\eta)\delta\eta(\vec{x}) \tag{128}$$

which is appropriate if we imagine the perturbations arise from a single inhomogeneous degree of freedom perturbing all others at some moment in conformal time. Combining this ansatz with $\nabla_\mu T^\mu_{\nu,x} = 0$ which holds for super-horizon modes (since they are effectively uncoupled by causality) yields:

$$\bar{\rho}'_x = -3\frac{a'}{a}(\bar{\rho}_x + \bar{p}_x) \tag{129}$$

$$\frac{\delta\rho_x}{(\bar{\rho}_x + \bar{p}_x)} = -3\frac{a'}{a}\delta\eta \tag{130}$$

Notice the right-hand side of equation 130 does not depend on the species label. The consequence of this statement is that the left-hand sides of eqn. 130 *for each species are equal*. Therefore, using eqns. 23 and 24

$$\frac{\delta\rho_b}{\bar{\rho}_b} = \frac{\delta\rho_{cdm}}{\bar{\rho_{cdm}}} = \frac{3}{4}\frac{\delta\rho_\nu}{\bar{\rho}_\nu} = \frac{3}{4}\frac{\delta\rho_\gamma}{\bar{\rho}_\gamma} \tag{131}$$

where we made use of the fact that baryons and CDM are non-relativistic while neutrinos and photons are ultra-relativistic. The consequence of this result is that the initial conditions for all of the species can be set by a single parameter. As a final note, since under these conditions the initial anisotropic stress $\sigma = 0$, eqn. 125 then guarantees that $\phi = \psi$ initially. When the perturbed Einstein equations are solved under this constraint, in radiation domination (with the assistance of 19), one obtains the solution $\phi = \text{const.}$ [71]. Subsequently, as a result of 126, the relation $-2\psi = \frac{\delta\bar{\rho}_{tot}}{\rho_{tot}}$ is manifest. Consequently, only one parameter is needed to fix the metric perturbations as well. This is the power of adiabatic initial conditions: they lead to static super-horizon metric and density fluctuations, and all initial conditions can be related to one parameter.

- Integrate the Boltzmann Equation: We are now able to compute the temperature fluctuation, $\Theta(\eta, \vec{x}, \hat{\eta})$ and ultimately the transfer function. First, the Boltzmann equation (in Newtonian gauge) for the fluctuation is written

$$\Theta' + \hat{\eta} \cdot \vec{\nabla}\Theta - \phi' + \hat{\eta} \cdot \vec{\nabla}\psi = -W \times (\Theta - \Theta_0 - \hat{\eta} \cdot \vec{v}_e) \tag{132}$$

where the collision term is determined by the Thomson scattering interaction rate W, the bulk velocity of the electrons, $\vec{v}_e$, and Θ_0 is the temperature fluctuation monopole. Notice the terms on the left-hand side of the equation correspond to free streaming, local dilation of the scale factor, and gravitational redshift respectively. Next we introduce the combination $B = e^{-\tau}\Theta(\eta, \vec{x}, \hat{\eta})$, where $\tau = \int_{\eta_0}^{\eta} W \, d\eta$ is the optical depth, which represents the opacity of the Universe at a particular time when viewed today. Computing the total derivative of B with respect to η along the trajectory of CMB photons yields:

$$\frac{d}{d\eta}B = e^{-\tau}\Theta' + e^{-\tau}\hat{\eta} \cdot \vec{\nabla}\Theta - \tau' e^{-\tau} \tag{133}$$

with the gradient coming from the chain rule. Fourier transforming equation 132 and inserting it into the Fourier transformed eqn. 133 gives an equation, which when integrated over conformal time (from initial conditions η_i to the present η_0), produces an integral expression for the Fourier transformed temperature fluctuation,

$$\Theta(\eta_0, \vec{k}) = \int_{\eta_i}^{\eta_0} d\eta \, e^{i\vec{k}\cdot\hat{\eta}(\eta_i - \eta_0)} \left[e^{-\tau}\Big(\phi' + \psi'\Big) + W e^{-\tau}\Big(\Theta_0 + \psi - \frac{1}{k}v_e'\Big) \right] \tag{134}$$

since the optical depth at the time of initial conditions η_i is zero, while today $\tau(\eta_0) = 1$. Note, that to obtain the prior result, an integration by parts was done for any terms proportional to $\vec{k} \cdot \hat{\eta}$ with the surface terms vanishing at the limits. Finally, in order to formally compute the the transfer function, the result 134 must be written in terms of spherical harmonics [177]

$$\Theta(\eta_0, \vec{k})_l = \int_{\eta_i}^{\eta_0} d\eta \left[g\Big(\Theta_0 + \psi\Big) - g\frac{1}{k}v_e' + e^{-\tau}\Big(\phi' + \psi'\Big) \right] j_l(k\eta_0 - k\eta) \tag{135}$$

where $g = We^{-\tau}$ is defined as the visibility function and j_l are the spherical Bessel functions.

The result 135 is the formal solution for the multipole transfer functions which was obtained from a line of sight type calculation. However, in practice, eqn. 132 can be solved numerically. Yet the integral form of the solution is of conceptual value since by inspection we see the transfer function depends on three terms (shown in the square brackets). In order these contributions are known as the Sachs-Wolfe, Doppler, and Integrated Sachs-Wolfe effects. The Doppler contribution is a correction to the observed anisotropies due to the bulk motion of the baryon-photon fluid, hence the dependence on v_e. Note $v_e = v_b$ due to the tight coupling between baryons and electrons via Coulomb scattering. The other two effects are the result of gravitational perturbations, namely the changes to the gravitational potential that the photons encounter on their path to the observer. If one assumes that photon decoupling is almost instant $g \simeq \delta(\eta - \eta_{dec})$ the transfer function simplifies,

$$\Theta(\eta_0, \vec{k})_l \simeq \Big(\Theta_0(\eta_{dec}, k) + \psi(\eta_{dec}, k)\Big) j_l(\eta_0 - \eta_{dec}) + v_b(\eta_{dec}) \dot{j}_l(k\eta_0 - k\eta_{dec}) + \int_{\eta_{dec}}^{\eta_0} \Big(\phi' + \psi'\Big) j_l(\eta_0 - \eta)\, d\eta \qquad (136)$$

where the dot over j_l indicates a derivative with respect to its argument, a consequence of integrating that term by parts. In this form the difference between the Sachs-Wolfe and Integrated Sachs-Wolfe effects is made clear: the former is associated with the gravitational potential well an incident CMB photon must overcome at the last scattering surface; the latter encodes the blue/redshifting the traveling photon experiences as it traverses through the metric inhomogeneities on its journey to the detector.

In order to get a sense of how the various terms in the transfer function impact the temperature anisotropy power spectrum 122, consider just the Sachs-Wolfe contribution. First note the function $j_l(x)$ and $)\dot{j}_l(x)$ are both peaked, for large l, as $x \to l$. In this case $x = k(\eta_0 - \eta_{dec}) = k\Delta\eta$, meaning the Bessel function is peaked for $k = l/(\Delta\eta)$. This result also has a geometric interpretation. The C_l's describe the correlation structure of temperature fluctuations as seen on the last scattering surface, under an angle $\theta = \pi/l$ (since for spherical harmonics this is the angle between a maxima and a minima). Given a proper distance, d_A (known as the *angular diamater distance*) from the observer to the last scattering surface, the product $\theta \cdot d_A$ gives the arc length between a maximum and minimum. This maxima/minima pattern is seeded by Fourier modes which have a physical

wavelength $\lambda = 2\pi\frac{a(\eta_{dec})}{k}$ and distance between maxima and minima, $\lambda/2$. Computing the aforementioned proper distance d_A using eqns. 41 and 39, and combining these geometric arguments gives,

$$d_A = a(\eta_{dec})(\eta_0 - \eta_{dec}) \tag{137}$$

$$\frac{\lambda}{2} = \frac{\pi a(\eta_{dec})}{k} = \theta d_A = \frac{\pi}{l} a(\eta_{dec})(\eta_0 - \eta_{dec}) \tag{138}$$

$$k = l/(\Delta\eta) \tag{139}$$

which is the same result before. The result is that for large multipole moments (and consequently small angular scales), the Fourier modes have simple relationship with l. Additionally, since in this regime the Bessel function is approximately maximal, the temperature power spectrum (from solely the Sachs-Wolfe contribution) is

$$C_{l\simeq k\Delta\eta} \sim \Big(\Theta_0(\eta_{dec}, k) + \psi(\eta_{dec}, k)\Big)^2 \mathcal{P}_{\mathcal{R}}(k) \tag{140}$$

where $\Theta_0(\eta_{dec}, k)$ and $\psi(\eta_{dec}, k)$ are determined by the adiabatic initial conditions (see eqn. 131)

$$\left.\frac{\delta\rho_\gamma}{\bar{\rho}_\gamma}\right|_{\eta_{dec}} = 4\frac{\delta T}{T} = 4\Theta_0(\eta_{dec}, k) \tag{141}$$

$$-2\psi(\eta_{dec}, k) = \frac{\delta\rho_{tot}}{\bar{\rho}_{tot}} \simeq \frac{\delta\rho_{CDM}}{\bar{\rho}_{CDM}} = \frac{3}{4}\left.\frac{\delta\rho_\gamma}{\bar{\rho}_\gamma}\right|_{\eta_{dec}} \tag{142}$$

$$\Theta(\eta_0, \vec{k})_l \simeq -\frac{1}{8}\left.\frac{\delta\rho_\gamma}{\bar{\rho}_\gamma}\right|_{\eta_{dec}} \tag{143}$$

where we have made use of the fact that decoupling occurrs during matter domination and the last line is in reference to eqn. 136. Notice these results imply that for large multipoles the Sachs-Wolfe contribution is set by the photon energy fluctuations at the time of decoupling. Additionally, the relative minus sign between the density fluctuation and the temperature fluctuation indicates that over densities cause local decreases in the temperature while for under densities the opposite occurs. An analysis of the this type, for the Sachs-Wolfe contribution, can be extended to the Doppler and Integrated Sachs-Wolfe contributions as well (see [139] for details). However, ultimately the composite angular temperature power

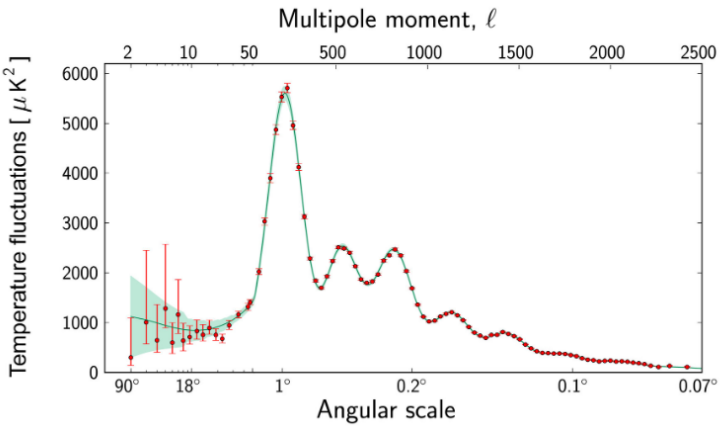

Figure 4: The CMB temperature anisotropy power spectrum measured by the Planck collaboration [74]. This graph displays the temperature fluctuations in the Cosmic Microwave Background detected by Planck at different angular scales on the sky. The multipole moments associated with various angular scales are indicated at the top of the graph. The red dots are measurements made with Planck shown with measurement and estimated uncertainty error bars. The green curve represents the best fit of λCDM cosmology. The pale green area around the curve shows the predictions of all the variations of this standard model that best agree with the data. Observations on small and intermediate angular scales are extremely consistent with model predictions. However on angular scales between 90° and 6° the agreement is about 10% weaker. These may represent challenges to ΛCDM.

spectrum is the result of each of the three terms squared and three cross terms, since the power spectrum depends on the transfer function squared.

The observed angular CMB temperature anisotropy power spectrum as measured by Planck is shown in Figure 4. Recall that this analysis studies the anisotropies through Fourier modes which start outside the particle horizon (and therefore with trivial time evolution) but then cross into the horizon, one after another, as the Universe expands. Accordingly, smaller scale modes correspond to scales that crossed the horizon earlier. As a particular

mode enters, its evolution is determined by the transfer function 135 which encodes the effect of metric perturbations which are sourced by density inhomogeneities. These initial density inhomogeneities are encapsulated in the primordial power spectrum, $\mathcal{P}_{\mathcal{R}}(k)$. As the Universe evolves, these primordial overdensities propagate as acoustic waves originating from oscillations in the plasma material. The oscillations are the result of the opposing forces of local increases in the attractive, gravitational potential and repulsive pressure (generated by electromagnetic scattering processes). This process can continue until recombination and photon decoupling at which point the CMB power spectrum is fixed. Consequently there is a physically relevant distance scale, namely how far an acoustical wave front can travel before decoupling,

$$d_s \equiv a(\eta_{dec}) \int_{\eta_i}^{\eta_{dec}} c_s d\eta \tag{144}$$

known as the sound horizon, with c_s referred to as the sound speed in the baryon-photon fluid. η_i is the conformal time when initial conditions are set. We expect points separated by this distance to be at least partially correlated since density waves will have traveled from one point to another. This correlation is reflected in the angular power spectrum (constructed in spherical harmonics) as correlation features at scales $\pi/l \sim d_s(\eta_{dec})/d_A(\eta_{dec})$ (where d_A is defined in eqn. 137). Additionally, since we are working in Fourier space, the harmonics of this scale should also exhibit correlation features. To see this effect consider the effect of the fluid oscillations on $\Theta_0(\eta, \vec{x})$ the temperature fluctuation monopole [71],

$$c_s^2 = \frac{\delta p_\gamma + \delta p_b}{\delta \rho_\gamma + \delta \rho_b} \simeq \frac{1}{3(1+R)} \;\; ; \; R \equiv \frac{4\bar{\rho}_b}{3\bar{\rho}_\gamma} \tag{145}$$

$$\Theta_0'' + \frac{R'}{1+R}\Theta_0' + k^2 c_s^2 \Theta_0 = -\frac{k^2}{3}\psi + \frac{R'}{1+R}\phi' + \phi'' \tag{146}$$

where eqns. 131 and the equations of state for non-relativistic and relativistic particles was used to derive the sound speed. Considering $R' = 0$ and neglecting the metric perturbations, this equation of motion is that of an harmonic oscillator with solutions $\Theta_0 = \Theta_i \cos(kc_s\eta + \alpha)$. Recall that super-horizon modes ($k\eta \ll 1$) are static, which mandates that the phase $\alpha = 0$ and also indicates that $kc_s\eta \ll 1 \rightarrow \lambda \gg d_s$ is the limit of no oscillations. Consequently, *only modes with wavelength less than the sound horizon oscillate.*

Returning to Figure 4, we see the temperature anisotropy power spectrum features multiple peaks. The first of these peaks corresponds to modes just crossing the sound horizon at the time of decoupling. Consequently they experience a resonant enhancement, a consequence of forced oscillation by the metric perturbations (which now begin to decay due to horizon crossing). We can see this effect by inspecting eqn. 146 in which the term proportional to ψ acts as a driving term. Keeping only this gravitational term in the equation and setting all derivatives of the monopole to zero, yields

$$\Theta_0^{eq} = \frac{-1}{3c_s^2}\psi = -(1+R)\psi \tag{147}$$

consequently the zero-point of oscillations is shifted. For the smaller modes we observe the aforementioned acoustic oscillations, alternating rarefaction and compression. Each mode that is either at a moment of maximum compression or minimum compression (rarefaction) at the moment of decoupling provides a peak since the power spectrum involves the square of the transfer function. The second oscillatory pattern is damped due to the friction term in equation 146, which becomes more significant during matter domination as it grows with baryon energy density. These modes have been within the horizon for longer during matter domination and are consequently more significantly impacted.

Precise analysis of the shape of the temperature anisotropy power spectrum can constrain cosmology parameters in a number of ways [139]. Here, I briefly discuss four important effects. **1. Position of the First Peak:** All the peaks are harmonics of a single distance scale in coordinate (physical) space, the sound horizon. The location of the first peak is determined by the ratio of the sound horizon at decoupling $d_s(\eta_{dec})$ and the angular diameter distance at decoupling $d_A(\eta_{dec})$. The first distance is a function of the matter energy density Ω_m since it is determined by when matter/radiation equality occurs, and also a function of the baryon energy density Ω_b which determines the baryon-photon sound speed. The second distance is determined by the expansion history and geometry of the Universe and thus probes the Hubble constant H_0 and curvature density parameter Ω_k. **2. Overall Peak Amplitude:** The amplitude of the peaks is determined by the time when matter/radiation equality occurs since during matter domination, but before decoupling, the baryon sourced friction term damps oscillations. If equality happens earlier in the cosmic history, then the

damping will be increased and the amplitude of all peaks will decrease. Consequently peak amplitude probes the matter energy density Ω_m. **3. Odd/Even Peak Ratio:** The first peak is enhanced relative to the second due to the displacing of the zero-point of oscillations (eqn. 147) for those modes which are crossing the sound horizon at decoupling. The ratio of these two peaks therefore probes the strength of this enhancement which is governed by $R \propto \Omega_b$, the baryon density. **4. Global Amplitude:** Finally, the overall amplitude of the entire spectrum is an obvious measure of the scalar primordial power spectrum $\mathcal{P}_\mathcal{R}(k)$ since the transfer function evolves the distribution from this initial function. This represents a probe of pre-ΛCDM cosmological evolution, e.g. inflation.

2.1.3 Inflation

The notion of an early phase of exponential cosmic expansion, known as inflation, was originally introduced as a means of diluting and sequestering unobserved relic particles such as magnetic monopoles; however, this phase was soon realized to provide a natural resolution to perennial problems with the ΛCDM cosmology [98]. These are known as the Horizon and Flatness problems. Additionally, inflation driven by scalar field dynamics provides a mechanism for producing the fundamental density inhomogeneities, namely the primordial power spectrum. This quantity is an input into the calculation of the cosmic microwave background (CMB) temperature anisotropies by the theory of cosmological perturbations (see eqn. 122). In this section we review the Horizon and Flatness problems, their solution by a period of inflationary expansion, how that expansion can be generated by a primordial scalar field, and finally how in turn that scalar field can generate a primordial power spectrum. This review is primarily qualitative following the treatment of [71, 120]. For the more curious reader, a detailed pedagogical overview of inflation is provided in [170].

2.1.3.1 Horizon and Flatness Problems Previously the concept of the particle horizon was introduced in order to describe the size of the causally connected region of spacetime in an FLRW cosmology, in comoving coordinates. Using eqns. 39 and 37, one can compute

the proper distance particle horizon (d_H) during the matter dominated epoch

$$r_H^{MD}(t) = \eta^{MD}(t) = \Big(\frac{4a(t)}{H_0^2\,\Omega_m}\Big)^{1/2} \equiv \frac{\sqrt{a(t)}}{H_m} \tag{148}$$

$$d_H^{MD}(a) = a\,r_H(a) = a\,\eta(a) = \frac{a^{3/2}}{H_m}\,. \tag{149}$$

This distance scale will be visible on the last scattering surface of the CMB. Using the angular diameter distance given by eqn. 137, one can compute the angle subtended by a patch, of particle horizon size, on the last scattering surface

$$d_A(a_{dec}) = a_{dec}(\eta(a_0) - \eta(a_{dec})) = a_{dec}\Big(\frac{1-\sqrt{a_{dec}}}{H_m}\Big) \tag{150}$$

$$\delta\theta = \frac{d_H^{MD}(a_{dec})}{d_A(a_{dec})} = \frac{a_{dec}^{1/2}}{1-(a_{dec})^{1/2}}\,. \tag{151}$$

Recalling that the scale factor at decoupling is $a_{dec} \simeq 9.09\times10^{-4}$ (see eqn. 110), the angular size of horizon-sized patches on the CMB is

$$\delta\theta \simeq 0.31\,\mathrm{rad} \simeq 2^\circ \tag{152}$$

which is far smaller than the scale of homogeneity and isotropy manifest on the last scattering surface (see Figure 3). This is the statement of the *Horizon problem*: how does the early Universe exhibit homogeneity and isotropy on scales far larger than the particle horizon (as evinced by the CMB) since such regions would have been causally disconnected?

One possibility is that the initial conditions of the universe were homogeneous to one part in a million. However, this raises an issue of fine-tuning. A dynamical explanation for this widespread homogeneity can be achieved if the particle horizon is in fact significantly larger than suggested by matter (or radiation) dominated expansion. The idea is to consider a period of exponential expansion wherein the scale factor obeys

$$a(t) = a(t_*)e^{H_I(t-t_*)} \tag{153}$$

where t_* is defined to be the beginning of the exponentially expanding phase, and H_I is the Hubble rate during this phase, which is constant. It is more convenient to express this in terms of the time when this phase ends, t_I

$$a(t_I) = a(t_*)e^{H_I(t_I-t_*)} \to a(t_*) = a(t_I)e^{-H_I(t_I-t_*)} \to a(t) = a(t_I)e^{H_I(t-t_I)}\,. \tag{154}$$

Now computing the particle horizon by the time of photon decoupling

$$d_H(t_{dec}) = a(t_{dec})\left[\int_{t_*}^{t_I}\frac{dt'}{a(t')} + \int_{t_I}^{t_{dec}}\frac{dt'}{a(t')}\right] \tag{155}$$

$$\simeq a(t_{dec})\int_{t_*}^{t_I} dt'\,\frac{e^{-H_I(t-t_I)}}{a(t_I)} = \frac{a(t_{dec})}{a(t_I)\,H_I}\Big(e^{H_I(t_I-t_*)}-1\Big) \tag{156}$$

$$d_H(t_{dec}) \simeq \frac{a(t_{dec})}{a(t_I)\,H_I}\Big(e^{N_e}-1\Big) \tag{157}$$

where we have assumed that the exponential phase is the dominant contribution to the particle horizon. $N_e \equiv H_I(t_I - t_*)$ is the number of e-folds of exponential expansion. Thus the angle subtended by the inflated particle horizon is

$$\delta\theta = \frac{d_H(t_{dec})}{d_A(a(t_{dec}))} \simeq d_H(t_{dec})\,\frac{H_m}{a(t_{dec})} \simeq d_H(t_{dec})\,\frac{H_0}{a(t_{dec})} \tag{158}$$

$$\rightarrow \delta\theta \simeq \frac{H_0}{a(t_I)\,H_I}\Big(e^{N_e}-1\Big) \tag{159}$$

$$\delta\theta \gg 1 \rightarrow e^{N_e} \gg \frac{a(t_I)\,H_I}{H_0} \tag{160}$$

where in the first line eqn. 150 has been used in conjunction with the fact that $a(t_{dec}) \ll 1$ and $H_m = \frac{H_0\sqrt{\Omega_m}}{2} \simeq H_0$. The last line gives the condition on the number of e-folds needed to resolve the Horizon problem. We will return to this condition later.

As seen in Table 3, the ΛCDM cosmology sets the value of the present day curvature density, $\Omega_k \ll 1$; accordingly the Universe can be regarded as spatially flat. Recall the definition of this parameter

$$\Omega_k(a) = -\frac{k}{(H(a)\,a)^2} = \Omega_k(a_0=1)\frac{H_0^2}{a^2H^2(a)} = \left\{\begin{matrix}\Omega_k(a_0=1)\Omega_R\,a^2 & RD\\ \Omega_k(a_0=1)\Omega_m\,a & MD\end{matrix}\right\}\ ;\ k=-1,0,+1 \tag{161}$$

where in the final equality the Friedmann eqn. 31 has been used to study the dependence of the parameter on the scale factor during both radiation and matter domination. Inspecting this result reveals that however small the present day curvature density parameter is, it would have had to be even smaller in the past. To make explicit this concern consider what the value of the curvature density parameter would have been at the time of nucleosynthesis ($a_{nuc} \sim 10^{-10}$)

$$\Omega_k(a_{nuc}) = \Omega_k(a_0=1)\Omega_R\,a_{nuc}^2 \sim 10^{-28} \tag{162}$$

using values from Table 3. Evidently any small deviation from flatness will be amplified as the Universe grows to its present size. Consequently, a spatially flat Universe represents an unstable solution. This is the statement of Flatness problem: why is the spatial curvature so small initially?

In order to avoid fine-tuning, a phase of exponential expansion can be invoked. This is because such an expansion the dilutes curvature density parameter

$$\Omega_k^I(a) = \frac{k}{H_I^2\, a^2(t_I)} e^{-2H_I(t-t_I)} \tag{163}$$

where eqn. 154 has been used. Suppose that initially the parameter is $\Omega_{a(t_*)} \simeq \mathcal{O}(1)$ at the onset of the exponential expansion. Then by the end of the expansion,

$$\Omega_k(a(t_I)) = \Omega_k(a(t_*)) e^{-2H_I(t_I - t_*)} \simeq e^{-2N_e} \tag{164}$$

where the previous result has been used. However, this value can also be obtained using eqn. 161 yielding,

$$\Omega_k(a(t_I)) = \Omega_k(a_0 = 1)\, \frac{H_0^2}{a_I^2 H_I^2}\,. \tag{165}$$

Equating these two expressions gives

$$e^{-2N_e} = \Omega_k(a_0 = 1)\, \frac{H_0^2}{a_I^2 H_I^2} \rightarrow \Omega_k(a_0 = 1) = \frac{H_0^2}{a_I^2 H_I^2}\, e^{2N_e} \tag{166}$$

$$\Omega_k(a_0 = 1) \ll 1 \rightarrow e^{N_e} \gg \frac{a(t_I)\, H_I}{H_0} \tag{167}$$

and we see that the condition for the number of e-folds needed to solve the Flatness problem is the same as in the Horizon problem case (see eqn. 160). Thus the same period of exponential expansion can simultaneously solve both problems.

Investigating this constraint on the required number of e-folds, consider an instantaneous, smooth, continuous transition from the exponential phase to the radiation dominated epoch. Namely,

$$a(t_I) H_I = a^{RD}(t_I)\, H(a^{RD}(t_I)) \equiv a_R\, H(a_R) \tag{168}$$

which is known as the instantaneous reheating approximation. During the RD epoch the Friedmann eqn. 31 gives

$$H(a_R) = H_0 \Big(\frac{\Omega_R}{a_R^4}\Big)^{1/2} \rightarrow a_R = \Big(\frac{H_0}{H(a_R)}\Big)^{1/2} (\Omega_R)^{1/4}\,. \tag{169}$$

Inserting this result into the e-fold condition yields,

$$e^{N_e} \gg (\Omega_R)^{1/4} \left(\frac{H(a_R)}{H_0}\right)^{1/2} = \left(\Omega_R \frac{\rho(a_R)}{\rho_{0,c}}\right)^{1/4} \simeq \frac{(\rho(a_R))^{1/4}}{0.03\,\mathrm{eV}} \tag{170}$$

where eqn. 19 and the critical density, $\rho_{0,c} = \frac{3H_0^2}{8\pi G_N}$ have been used. In the final equality the values from Table 3 have been used. The quantity $\rho(a_R)$ is the energy density at the end of the exponential expansion.

The value of this quantity is uncertain although it certainly scales as $\rho \propto T^4$ since the subsequent epoch is radiation dominated, and we are considering the instantaneous reheating approximation. Given the success of nucleosynthesis, $\rho(T = 1\,\mathrm{MeV}) \lesssim \rho(a_R)$. However, the energy scale could in principle be substantially higher. A rough upper bound is the Planck scale $\rho(a_R) \lesssim \rho(T = 10^{19}\,\mathrm{GeV})$ since beyond the scale quantum gravitational effects certainly cannot be ignored. This gives the range on the necessary number of e-folds (under the instantaneous reheating assumption)

$$17 < N_e < 68 \tag{171}$$

thus, provided sufficiently long period of exponential expansion, the Horizon and Flatness problems can be solved, and then the Universe can transition into the hot, primordial RD phase of the big bang. This period of exponential expansion is known as inflation.

2.1.3.2 Single-field Inflation Having seen that an initial period of inflation can resolve problems with ΛCDM, the natural question to ask is what mechanism can achieve this exponential expansion. Consulting Table 2 reveals that an exponentially growing scale factor is obtained when the Universe's energy density is dominated by vacuum energy (with negative pressure equal to the energy density, $(P = -\rho)$. Using eqns. 19 and 20, under vacuum energy domination yields

$$\dot{\rho}_{vac} = 0 \rightarrow H^2 = \left(\frac{\dot{a}}{a}\right)^2 = \text{const.} \equiv H_I^2 \tag{172}$$

$$\ln\left[\frac{a}{a(t_*)}\right] = H_I(t - t_*) = N_e \tag{173}$$

which is precisely the functional form of the scale factor required (see eqn. 150) for inflationary expansion.

The simplest, and canonical, model for realizing an early epoch of vacuum energy domination is through the introduction of classical scalar field, suffusing spacetime, and known as the inflaton (Φ). The inflaton action, in comoving coordinates, is given by[1],

$$S = \int d^4x\sqrt{(-g)}\ \frac{1}{2}\Big(g^{\mu\nu}\partial_\mu\Phi\partial_\nu\Phi - V(\Phi)\Big) \tag{174}$$

where $(-g) \equiv -\det(g_{\mu\nu})$ and $V(\Phi)$ is the inflaton potential. Extremizing the above action with respect to variations of the inflaton and the metric gives the inflaton equations of motion and energy-momentum tensor respectively,

$$\frac{\delta S}{\delta\Phi} = 0 \rightarrow \frac{1}{\sqrt{-g}}\partial_\nu\sqrt{-g}\, g^{\mu\nu}\partial_\mu\Phi - \frac{dV}{d\Phi} = 0 \tag{175}$$

$$T_{\mu\nu} = \frac{-2}{\sqrt{-g}}\frac{\delta S}{\delta g^{\mu\nu}} = \partial_\mu\Phi\partial_\nu\Phi - g_{\mu\nu}\Big(\frac{1}{2}g^{\alpha\beta}\partial_\alpha\Phi\partial_\beta\Phi - V(\Phi)\Big)\,. \tag{176}$$

Reflecting the properties of the FLRW spacetime, the inflaton is treated as a spatially homogeneous field such that $\Phi(t,\vec{x}) = \Phi(t)$. Inserting the spatially flat FLRW metric (eqn. 15 with $k = 0$) and this ansatz for the inflaton into the energy-momentum tensor gives

$$T_{00} = \frac{1}{2}\dot{\Phi}^2 + V(\Phi) = \rho\ \ ;\ T_{0j} = 0\ \ ;\ T_{ji} = a^2\delta_{ji}\Big(\frac{1}{2}\dot{\Phi}^2 - V(\Phi)\Big) = P\delta_{ji} \tag{177}$$

showing that the energy-momentum tensor is diagonal and has the structure of a perfect fluid (fluid kinetic form). Using these results, the equation of state parameter w for the inflaton can be computed

$$w \equiv \frac{P}{\rho} = \frac{\frac{1}{2}\dot{\Phi}^2 - V(\Phi)}{\frac{1}{2}\dot{\Phi}^2 + V(\Phi)} \rightarrow w \simeq -1\ \ \text{for}\, V(\Phi) \gg \frac{1}{2}\dot{\Phi}^2 \tag{178}$$

and consequently if the inflaton potential dominates over the kinetic energy of the field, the correct equation of state for exponential expansion is obtained. Inserting the inflaton energy density into the Friedmann equation 19 gives the evolution of the Hubble parameter

$$H^2 = \Big(\frac{\dot{a}}{a}\Big)^2 = \frac{8\pi G_N}{3}\Big(\frac{1}{2}\dot{\Phi}^2 + V(\Phi)\Big) \simeq \frac{8\pi G_N}{3}\,V \tag{179}$$

[1]The topic of scalar fields in curved spacetimes is discussed in detail in section 2.2.2; in this section some of the results therein will be used.

where the last equality assumes potential energy domination. Meanwhile, the equations of motion for a spatially homogeneous inflaton field on the spatially flat FLRW metric become

$$\ddot{\Phi} + 3H\dot{\Phi} + \frac{dV}{d\Phi} = 0\,. \tag{180}$$

The introduction of the above inflaton model provides a dynamical schematic for how a period of exponential expansion can be generated. However if the field configuration lies at at the global minimum of its potential, $V(\Phi_0)$ and if this potential is positive $V(\Phi_0) > 0$, then the stipulation of $V(\Phi_0) \gg \dot{\Phi}_0^2$ implies that the field will trapped in this minimum configuration indefinitely. Accordingly, inflation will never end.

In order to avoid infinite inflation, the field must be allowed to evolve towards its true ground state, for which $V(\Phi_0) = 0$. The canonical class of single field models which achieve this outcome are known as *single field slow-roll inflation* [141]. In these models, the inflaton field is initially displaced from its global potential minimum, and slowly "rolls" down its potential gradient towards the zero-energy ground state. These models are characterized by two slow-roll parameters (ϵ_V, η_V) which together constrain the necessary features of the inflaton potential.

The first parameter ϵ_V ensures that inflationary phase is exponential and can be introduced as follows:

$$\dot{H} = \frac{\ddot{a}}{a} - H^2 \rightarrow \frac{\ddot{a}}{a} = H^2(1 - \epsilon_V) \;\; ; \;\; \epsilon_V \equiv -\frac{\dot{H}}{H^2} \tag{181}$$

where we have merely differentiated the definition of the Hubble parameter with respect to time. Note if $\epsilon_V \ll 1$, then the above equation for the scale factor yields an exponential solution. Incidentally, the definition of ϵ_V can also be expressed in terms of the inflaton and its potential by using the Friedmann equations 19 and 20,

$$\dot{H} = \frac{\ddot{a}}{a} - H^2 = -\frac{4\pi G_N}{3}\Big(2\dot{\Phi}^2 - 2V(\Phi)\Big) - \frac{8\pi G_N}{3}\Big(\frac{1}{2}\dot{\Phi}^2 + V(\Phi)\Big) = -4\pi G_N \dot{\Phi}^2 \tag{182}$$

$$\epsilon_V \equiv -\frac{\dot{H}}{H^2} = \frac{3\dot{\Phi}^2}{\dot{\Phi}^2 + 2V(\Phi)} \rightarrow \epsilon_V \ll 1 \rightarrow \dot{\Phi}^2 \ll V(\Phi) \tag{183}$$

and so the slow roll parameter enforces potential energy domination. Therefore under this limit, differentiating eqn. 179 gives

$$\dot{H} = \frac{4\pi G_N}{3H}\frac{dV}{d\Phi}\dot{\Phi} \tag{184}$$

and so the first slow roll parameter can also be expressed as

$$\epsilon_V = -\frac{4\pi G_N}{3H^3} V'\dot{\Phi} \;\; ; \; ' \equiv \frac{d}{d\Phi} \, . \tag{185}$$

The second parameter η_V ensures that the inflationary epoch is sufficiently prolonged, namely that the fractional change in the inflaton velocity is small over the age of the Universe $\Delta t \sim \frac{1}{H}$

$$\frac{|\Delta\dot{\Phi}|}{|\dot{\Phi}|} = \frac{|\ddot{\Phi}| \, \Delta t}{|\dot{\Phi}|} \simeq \frac{|\ddot{\Phi}|}{H \, |\dot{\Phi}|} \equiv \eta_V \ll 1 \tag{186}$$

which ultimately guarantees that the inflaton does not evolve towards its potential minimum too quickly, hence the name slow roll. Enforcing this second parameter simplifies the inflaton equation of motion eqn. 180

$$\dot{\Phi} \simeq -V' \, \frac{1}{3H} \tag{187}$$

which can then be inserted into eqn. 185 for the first slow roll parameter giving

$$\epsilon_V = \frac{4\pi G_N}{9H^4}(V')^2 = \frac{M_{pl}^2}{16\pi} \left(\frac{V'}{V}\right)^2 \ll 1 \tag{188}$$

where eqn. 179 has been used in the final equality, and $M_{pl}^2 = \frac{1}{G_N}$ is the Planck mass. Meanwhile the approximate equation of motion 187 can be differentiated

$$\ddot{\Phi} = -\frac{V''\dot{\Phi}}{3H} + \frac{V'}{3}\frac{\dot{H}}{H^2} \simeq -\frac{V''\dot{\Phi}}{3H} \tag{189}$$

which when inserted into the equation for the second slow roll parameter (eqn. 186) produces the constraint

$$\eta_V = \frac{V''}{3H^2} = \frac{M_{pl}^2}{8\pi}\frac{V''}{V} \ll 1 \tag{190}$$

where again eqn. 179 has been used.

The equations for the slow roll parameters (eqns. 188,190) provide the conditions for a nearly exponential expansion of the Universe. Once the condition $\epsilon_V = 1$ is satisfied, the slow roll criteria are violated, and the inflationary phase ends. The number of e-folds of expansion produced by slow roll inflation can be computed using the first slow roll parameter,

$$dN_e = \frac{da}{a} = H \, dt = \frac{H}{\dot{\Phi}} \, d\Phi = -\frac{3H^2}{V'} \, d\Phi = -\frac{8\pi}{M_{pl}^2} \, \frac{V}{V'} \, d\Phi \tag{191}$$

$$N_e(\Phi) = \frac{2\sqrt{\pi}}{M_{pl}} \int_{\Phi_e}^{\Phi} \frac{d\Phi}{\sqrt{\epsilon_V(\Phi)}} \tag{192}$$

where eqns. 187, 179, and 188 have been used.

2.1.3.3 Perturbations In the previous section a single scalar field, with particular constraints on the form of its potential, was shown to be able to drive a period of inflationary expansion. However, this field was treated as classical and homogeneous. A complete picture of inflation must include inhomogeneous fluctuations, and the theory must be quantized. Remarkably, instantiating this more complete description leads to a natural explanation for the initial density inhomogeneities of the early universe which evolve into the observed anistropies in the CMB and the present locally overdense regions of matter in space, namely galaxies. Below we discuss the emergence of these primordial fluctuations.

To begin with the inflaton field is written as

$$\phi(t, \vec{x}) = \Phi(t) + \delta\phi(t, \vec{x}) \tag{193}$$

where Φ is the homogeneous background inflaton field, whose properties were discussed in the last section, and $\delta\phi(t, \vec{x})$ is the fluctuation. Inserting this field decomposition into the inflaton equations of motion (see eqn. 175 with the spatially flat FLRW metric) yields the equations

$$\ddot{\Phi} + 3H\dot{\Phi} + V'(\Phi) = 0 \tag{194}$$

$$\ddot{\delta\phi} + 3H\dot{\delta\phi} - \frac{\nabla^2 \delta\phi}{a^2} + \delta\phi V''(\Phi) \;\; ; \, ' \equiv \frac{d}{d\phi} \tag{195}$$

where we have expanded the derivative of potential ($V'(\phi)$) and only kept terms linear in the fluctuation $\delta\phi$. The first of these equations is just the previously encountered equation of motion for the homogeneous background (eqn. 180). Meanwhile the second equation describes the behavior of the fluctuation. In seeking to understand its behavior, it is convenient to work in conformal time $d\eta \equiv \frac{dt}{a}$ and to introduce the conformally rescaled field $\chi(\eta, \vec{x}) \equiv a(\eta)\, \delta\phi$. In terms of this new variable eqn. 195 becomes

$$\frac{1}{a^3}\Big(\frac{\partial^2 \chi}{\partial \eta^2} - \nabla^2 \chi - \frac{2\chi}{\eta^2} + \frac{V''}{H^2\eta^2}\chi\Big) = 0 \tag{196}$$

where we have used the fact that during exponential expansion the scale factor in conformal time obeys

$$a(\eta) = -\frac{1}{H\eta} \;\; ; \, H = H_I \;\; ; \, -\infty < \eta < 0\,. \tag{197}$$

Because the spacetime is spatially flat the equations of motion for the fluctation can be solved via Fourier transform yielding,

$$\frac{\partial^2 \chi_k}{\partial \eta^2} + \Big[k^2 - \frac{1}{\eta^2}\Big(\nu_\chi^2 - \frac{1}{4}\Big)\Big]\chi_k = 0 \;\; ; \;\; \nu_\chi^2 \equiv \frac{9}{4} - \frac{V''}{H^2} \tag{198}$$

where χ_k is the Fourier transform of χ. The resulting equation, written in this form, is readily identified as a Bessel differential equation. Since the field fluctuation is real-valued, and the differential equation is second order, the solutions will be $g_k(\eta)$ and it's complex conjugate. These solutions must satisfy the Wronksian condition

$$\frac{dg_k}{d\eta} g_k^* - g_k \frac{dg_k^*}{d\eta} = -i \, . \tag{199}$$

so that the Fourier expansion coefficients, once promoted to quantum mechanical operators in the quantized theory, obey canonical commutation relations [28]. In particular, one set of solutions are Hankel functions, $H_{\nu_\chi}^{(1)}(-k\eta)$. The Hankel functions have the following asymptotic form [170]

$$\lim_{-k\eta\to\infty} H_{\nu_\chi}^{(1)}(-k\eta) = \frac{e^{-ik\eta}}{\sqrt{-k\eta}} \cdot e^{-i\frac{\pi}{2}(\nu_x + 1/2)} \cdot \sqrt{\frac{2}{\pi}} \tag{200}$$

and so it is customary to write the solutions as

$$g_k(\eta) = \frac{1}{2} e^{+i\frac{\pi}{2}(\nu_x+1/2)} \sqrt{-\pi\,\eta} H_{\nu_\chi}^{(1)}(-k\eta) \tag{201}$$

$$\lim_{-k\eta\to\infty} g_k(\eta) \to \frac{e^{-ik\eta}}{\sqrt{2k}} \tag{202}$$

which under this limit have the behavior of plane waves in Minkowski spacetime. Notice what the above limit physically entails,

$$-k\eta = \frac{-k\eta a}{a} = \frac{2\pi}{\lambda_{phys}} \cdot d_H \to \infty \longrightarrow d_H \gg \lambda_{phys} \tag{203}$$

where $\lambda_{phys} = -a\lambda$ is the physical/proper wavelength and $d_H = a\eta$ is the proper distance particle horizon. Therefore, the limit $-k\eta \to \infty$ corresponds to Fourier modes whose physical wavelengths are deep inside the particle horizon of the expanding universe. Hence the Minkowski behavior is a consequence of the Einstein equivalence principle.

Recalling eqn. 186, we see that $V''/H^2 = 3\eta_V$. Therefore assuming the second slow roll parameter is small, then in the Fourier transformed equation of motion (eqn. 196) $\nu_\chi \simeq 3/2$, and upon inserting the corresponding Hankel function, the solution becomes

$$g_k(\eta) = \frac{e^{-k\eta}}{\sqrt{2k}}\Big[1 - \frac{i}{k\eta}\Big]. \tag{204}$$

Notice that in the limit $-k\eta \to \infty$, the same Minkowski plane wave behavior emerges as it must. However, in the opposite limit, namely $-k\eta \to 0$, the solution rapidly grows. Thus, this solution features an infrared enhancement. Writing the full solution for the fluctuation field, one obtains

$$\hat{\chi}(\vec{x},\eta) = \frac{1}{\sqrt{V}}\sum_k \Big[\hat{a}_k\, g_k(\eta) e^{i\vec{k}\cdot\vec{x}} + \hat{a}_k^\dagger\, g_k^*(\eta) e^{-i\vec{k}\cdot\vec{x}}\Big] \tag{205}$$

where the field has been quantized by promoting the expansion coefficients to creation and annihilation operators. Note, the discrete volume/box normalization (with comoving volume V) has been introduced for the Fourier transform. The vacuum state annihilated by these operators (which in turn are directly associated with the solutions $g_k(\eta)$)

$$\hat{a}_k|0\rangle = 0 \tag{206}$$

is known as the Bunch-Davies vacuum, which is the state observed by an observer comoving with the cosmic expansion. It is this vacuum state which is used with both the homogeneous field and the fluctuation field operators, which have the following vacuum expectation values

$$\langle 0|\hat{\phi}(t,\vec{x})|0\rangle = \langle 0|\hat{\Phi}(t)|0\rangle + \langle 0|\hat{\delta\phi}(t,\vec{x})|0\rangle = \Phi(t) + 0 \tag{207}$$

namely, only the homogeneous piece has a non-zero vacuum expectation value (VEV). In the nearly vacuum energy dominated epoch of inflationary expansion, the spacetime is approximately de Sitter, hence the exponential expansion[2]. The use of the Bunch-Davies vacuum allows for a correspondence between the inflationary mode solutions $g_k(\eta)$ and the positive

[2]A de Sitter spacetime is a type of FLRW spacetime which expands exactly exponentially, driven by a positive constant energy density. Slow roll inflationary models source a nearly de Sitter spacetime, but are not exactly de Sitter because of the kinetic energy contribution of the inflaton field.

frequency plane waves of Minkowski spacetime. It is for this reason, that we have chosen the Hankel function solution to the equations of motion since they in turn select the Bunch-Davies vacuum.

Having solved for the behavior of the fluctuation, we now must connect these inhomogeneities in the inflaton (which source inhomogeneities in the energy-momentum tensor) to inhomogeneities in the spacetime. Assuming the perturbations are small, the perturbed FLRW metric is

$$g_{\mu\nu} = \text{diag}\Big[(1+2\psi)a^2, -(1-2\psi)a^2, -(1-2\phi)a^2, -(1-2\phi)a^2)\Big] \tag{208}$$

working in the Newtonian gauge in conformal time (also note there is no anisotropic stress since the spacetime is nearly de Sitter). These small perturbations distort the scale factor locally such that $\delta a(t,\vec{x}) = a(t)\psi(t,\vec{x})$. The perturbations of the geometry tensor $\delta G^{\mu\nu}$ are connected to the perturbations of the energy-momentum tensor $\delta T^{\mu\nu}$ through the perturbed Einstein equations

$$\delta G^{\mu\nu} = 8\pi G_N \delta T^{\mu\nu} \tag{209}$$

which is a daunting proposal. The approximate scheme is to treat the homogeneous background inflaton as the quantity which sources the FRW spacetime, thereby establishing a set of global comoving coordinates (most importantly comoving time). Then $\delta\phi(t,\vec{x})$ sources local gravitational potentials which vary the time coordinate:

$$t \to t + \delta t(\vec{x}) \tag{210}$$

$$\phi(t+\delta t,\vec{x}) \simeq \Phi(t) + \dot{\Phi}\delta t = \Phi(t) + \delta\phi(t,\vec{x}) \tag{211}$$

$$\delta t(\vec{x}) = \frac{\delta\phi(t,\vec{x})}{\Phi(t)} \tag{212}$$

where in the second line we have used the field decomposition eqn. 193. These perturbations in the time coordinate adjust the scale factor accordingly

$$a(t+\delta t) = a(t) + \dot{a}\delta t = a(t) + \delta a(t,\vec{x}) = a(t) + a(t)\psi(t,\vec{x}) \tag{213}$$

$$\psi(t,\vec{x}) = \frac{\delta a}{a} = \frac{\dot{a}}{a}\delta t \tag{214}$$

and so combining this result with the expression for the local time variation we obtain

$$\psi(t,\vec{x}) = H\frac{\delta\phi(t,\vec{x})}{\Phi(t)} \tag{215}$$

which exhibits the connection between the local gravitational distortions and the inflaton fluctuations.

The spectrum of these inhomogeneities can be obtained by computing the two-point correlation function of the inflaton fluctuations

$$\langle 0|\delta\phi(t,\vec{x})\,\delta\phi(t,\vec{y})|0\rangle \equiv C(\vec{x},\vec{y},t) \tag{216}$$

which, since the Bunch-Davies vacuum state is rotationally and translationally invariant, can be expressed in the form of a power spectrum. Namely,

$$C(\vec{x},\vec{y},t) = \int \frac{d^3k}{(2\pi)^3}\,P(k,t)\,e^{i\vec{k}\cdot(\vec{x}-\vec{y})} = \int \frac{k^2\,dk}{2\pi^2}\,P(k,t)\,\frac{\sin kr}{kr} \equiv \int \frac{dk}{k}\,\mathcal{P}(k,t)\,\frac{\sin kr}{kr} \tag{217}$$

where $\vec{r}\equiv\vec{x}-\vec{y}$ and in the final equality the result has been written in terms of a dimensionless power spectrum (see eqn. 123). Using the field expansion for the conformally rescaled fields (eqn. 205) the two-point function can be straightforwardly computed

$$\langle 0|\delta\phi(t,\vec{x})\,\delta\phi(t,\vec{y})|0\rangle = \frac{1}{a^2}\langle 0|\chi(t,\vec{x})\,\chi(t,\vec{y})|0\rangle = \int \frac{d^3k}{(2\pi)^3}|g_k(\eta)|^2\,e^{i\vec{k}\cdot(\vec{x}-\vec{y})} \tag{218}$$

and therefore the dimensionless power spectrum can be directly read off

$$\mathcal{P}(k,\eta) = \frac{k^3}{2\pi^2\,a^2}|g_k(\eta)|^2 = \frac{H^2}{4\pi^2}\,k^2\eta^2\Big[1+\frac{1}{k^2\eta^2}\Big] \tag{219}$$

where eqns. 204 and 197 have been used. Notice that for the superhorizon limit ($\lambda_{phys} \gg d_H$) the power spectrum becomes

$$\lim_{-k\eta\to 0}\mathcal{P}(k,\eta) = \Big(\frac{H}{2\pi}\Big)^2. \tag{220}$$

Accordingly, the power spectrum for modes outside the particle horizon is "frozen" and *scale invariant*. We can use this quantity to compute the superhorizon mode power spectrum for the curvature perturbations ψ. Using eqn. 215

$$\lim_{-k\eta\to 0}\mathcal{P}_\psi(k) = \frac{H^2}{\dot{\Phi}^2}\Big(\frac{H}{2\pi}\Big)^2 = \frac{H^2}{\pi M_{pl}^2\,\epsilon_V} \tag{221}$$

where for the last equality eqns. 187 and 188 have been used.

The resulting picture of each inflationary perturbation mode is thus: 1. Each mode begins inside the particle horizon and oscillates. 2. As the scale factor exponentially expands, the physical wavelengths of the modes become larger than particle horizon. These modes become acausal, unable to effect microphysics within the horizon, and their power spectrum becomes frozen. 3. After inflation ends, the Universe continues to expand, and the modes begin to re-enter the particle horizon producing local gravitational disturbances that cause density fluctuations in the now present baryon-photon plasma. Therefore the curvature power spectrum acts as the primordial power spectrum ($\mathcal{P}_\psi = \mathcal{P}_\mathcal{R}$) which is used in the analysis of CMB temperature anisotropies (see eqn. 122). Bluntly speaking, it is the therefore inflaton fluctuations which are the source of primordial inhomogeneities. A key result of the above analysis is that the superhorizon modes are scale invariant. As a result, the temperature anisotropy power spectrum should reflect this scale invariance on the largest scales, since these correspond to modes which had not yet re-entered the particle horizon by the time of recombination. In examining Figure 4, the nearly flat tail at the far left of the spectrum is consistent with this analysis.

Measurements of the primordial power spectrum serve to constrain models of inflation. For the purposes of comparing with observations it is useful to work with the following form of the primordial curvature power spectrum [71, 170]

$$\mathcal{P}_\psi(k) = \left(\frac{H}{2\pi}\right)^2 = \frac{H^2}{\pi M_{pl}^2\, \epsilon_V} \left[\frac{k}{k_0}\right]^{n_s - 1} \tag{222}$$

where n_s is known scalar spectral index and is a function of the slow roll parameters, and k_0 is a so-called pivot scale (which is a reference scale used to define n_s). The above equation can be derived if one carries out the calculation of the power spectrum keeping all powers of the slow roll parameters.

When the metric tensor is perturbed, the perturbations can be decomposed into scalar, vector and tensor perturbations [71]. As was discussed in section 2.1.2.4, vector perturbations represent the response of the metric to vorticity in the energy momentum tensor, and are thus insignificant in conventional inflaton models which have small perturbations about a homogeneous and isotropic field sourcing a de Sitter spacetime. Thus far we have focused

exclusively on the scalar perturbations sourced by the inflaton fluctuations. Given that scalar perturbations are of principle interest in the analysis of the CMB temperature power spectrum, since temperature is a scalar quantity, this is appropriate. However, tensor perturbations, which represent primordial gravitational waves, can induce subtle anisotropies in the polarization of the CMB. The measuring of these so-called B-modes, therefore, represents another important probe of inflation.

The calculation of the power spectrum of tensor metric perturbations is discussed at length in [71, 170]. As with the scalar metric perturbations, the power spectrum is proportional to the square of the mode functions (eqn. 204) and thus under the superhorizon limit ($-k\eta \to 0$), power spectrum becomes scale invariant,

$$\lim_{-k\eta\to 0} \mathcal{P}_h(k) = \frac{16}{\pi}\frac{H^2}{M_{pl}^2} \tag{223}$$

to leading order in the slow roll parameters. Notice, unlike for the scalar curvature power spectrum, this result depends only on the Hubble parameter during inflation (which is essentially constant) and the Planck mass. Consequently, a measurement of primordial gravitational waves, from inflation, would represent a direct probe of the scale of inflation. Additionally, when comparing to observations, it is customary to introduce the tensor index n_T and associated pivot scale k_0

$$\mathcal{P}_h(k) = \frac{16}{\pi}\frac{H^2}{M_{pl}^2}\Big[\frac{k}{k_0}\Big]^{n_T}. \tag{224}$$

Incidentally, computing the tensor to scalar power spectra ratio yields the first slow roll parameter,

$$\frac{\mathcal{P}_h(k)}{\mathcal{P}_\psi(k)} \equiv r \simeq 16\epsilon_V \tag{225}$$

and so a measurement of both power spectra would allow one to constrain the shape of the inflaton potential. Recent observations of the CMB temperature and polarization anisotropies place constraints on the model parameters of inflation. These results are summarized in Table 4 below. The parameters suggest a very nearly scale invariant scalar curvature power spectrum and place an upper bound on the tensor to scalar ratio. The combination of these values in conjunction with eqns. 221 and 225 place an upper bound on scale of inflation at $H_I \leq 10^{14}\,\mathrm{GeV}$. The only reasonable lower bound comes from nucleosynthesis which as

we have seen occurs at $T \simeq 1\,\mathrm{MeV}$. Thus the scale of inflation and the precise inflationary model remain open questions. Despite these concerns, the success of inflation in simultaneously resolving the Horizon and Flatness problems while elegantly providing a source of the primordial inhomogeneities, has made the theory a reasonable extension to the ΛCDM cosmological paradigm.

Parameter	Measured Value
$\mathcal{P}_\psi$	$2.141 \pm 0.049 \times 10^{-9}$
n_s	0.9667 ± 0.0040
r	< 0.07 (95%)

Table 4: Primordial Power Spectra Parameters. The parameters of the primordial power spectrum as measured by Planck and BICEP/Keck [4]. The observations indicate the scalar power spectrum is very nearly scale invariant, and place an upper bound on the tensor to scalar ratio. These values consider a pivot scale $k_0 = 0.05\,\mathrm{Mpc}^{-1}$.

2.2 Quantum Field Theory

Quantum field theory (QFT) is a theoretical physics framework which synthesizes relativistic dynamics, quantum mechanics, and the field concept into a single structure and which sees ubiquitous usage in contemporary physics. In QFT, the dynamics of particles are governed by the interactions of extended objects known as fields which are quantized in a particular spacetime. The fields have specific equations of motion which govern their time evolution. The particles are then excited states of these underlying fields. Within the QFT framework, one can construct myriad theories, each with different numbers of fields and interactions between them. The Standard Model of particle physics represents a particular instantiation of QFT; one which has been enormously successful in explaining particle physics experiments. In this section a pedagogical review of QFT in general is presented

following conventional textbooks[161] and [95], and in the later sections, [28] and [158]. We begin by studying QFT in the limit where gravitational effects can be neglected (i.e. considering only special relativity) before discussing gravitational effects, later on. This section is only meant to review the concepts that are pertinent to understanding the original research content of the later chapters.

2.2.1 QFT in Minkowski Spacetime

The spacetime geometry implied by the Special Theory of Relativity is known as Minkowski spacetime and is characterized by the following metric, here shown via the invariant spacetime interval written in Cartesian coordinates:

$$ds^2 = \eta_{\mu\nu} dx^\mu dx^\nu = dt^2 - dx^2 - dy^2 - dz^2 \tag{226}$$

The Minkowski metric, $\eta_{\mu\nu}$ ensures, by construction, that the interval is invariant under Lorentz transformations, Λ^ν_μ (velocity boosts and rotations) such that

$$\eta_{\mu\nu} dx'^\mu dx'^\nu = \eta_{\mu\nu} \Lambda^\mu_\alpha \Lambda^\nu_\beta dx^\alpha dx^\beta \tag{227}$$

and moreover

$$\eta_{\alpha\beta} = \Lambda^\mu_\alpha \Lambda^\nu_\beta \eta_{\mu\nu} \tag{228}$$

One may consider infinitesimal Lorentz transformations which can be written in the form of a generalized rotation

$$x'^\mu = x^\mu + \omega^{\mu\nu} x_\nu \tag{229}$$

$$\Lambda^\nu_\mu = \eta^\nu_\mu + \omega^\nu_\mu \tag{230}$$

where the matrix $\omega^{\mu\nu}$ depends on the rotation angles. Note condition 228 requires that this matrix be anti-symmetric. The equation 230 can be parameterized in terms of 6, 4×4, anti-symmetric matrices ($I^{\alpha\beta}$) (where the two indices collectively define each of the 6 matrices)

known as the infinitesimal generators of the transformation. Using these generators we obtain [95]

$$\Lambda^{\nu}_{\mu} = \eta^{\nu}_{\mu} + \frac{1}{2}\omega_{\alpha\beta}(I^{\alpha\beta})^{\nu}_{\mu} \tag{231}$$

$$[I^{\mu\nu}, I^{\sigma\tau}] = \eta^{\nu\sigma}I^{\mu\tau} - \eta^{\mu\sigma}I^{\nu\tau} + \eta^{\nu\tau}I^{\mu\sigma} - \eta^{\mu\tau}I^{\nu\sigma} \tag{232}$$

where the last line defines the Lie algebraic relations of the generators which any matrix representation must satisfy [**?**]. In QFT, physical fields $\phi_r(x)$ are functions of spacetime coordinate, x, and are classified based on their transformation under Lorentz transformations. Using eqn. 231 leads to the infinitesimal Lorentz transformation of such a field,

$$\phi'_r(x') = \phi_r(x) + \frac{1}{2}\omega_{\mu\nu}(I^{\mu\nu})_{rs}\phi_s(x) \tag{233}$$

where we see that the matrices $(I^{\mu\nu})_{rs}$ mix the various components (referred to with Latin indices for clarity) of the multi-component physical field. As we will see later on, the above result is deeply connected to the angular momentum/spin of a field. For scalars (spin-0), fermions (spin-1/2), vectors (spin-1), etc. the infinitesimal Lorentz transformation law will look very different as each type of field will have a different representation of the generators. The Standard Model contains fields of the scalar, fermion, and vector types. In this section we will restrict ourselves to the scalar and fermion cases, as these are the field types studied in the later chapters.

2.2.1.1 Scalar Field Quantization The procedure for developing a quantum field theoretic description of a system begins with a classical field theory. Let us first consider a real, scalar field $\phi(x)$ which is defined at all points of Minkowski spacetime. The field is considered scalar because of its behavior under Lorentz transformations,

$$\phi'(x') = \phi'(\Lambda\, x) = \phi(x) \tag{234}$$

where the Lorentz indices have been suppressed for brevity. Notice by eqn. 233, the above result implies that the generators are trivially null for the scalar field. The action for this scalar field is given by

$$S = \int \mathcal{L}\, d^4x = \int \frac{1}{2}\Big(\eta^{\mu\nu}\partial_\mu\phi\partial_\nu\phi - m^2\phi^2\Big)\, d^4x \tag{235}$$

where $\partial_\mu \equiv (\partial_t, \nabla)$ is the 4-gradient, and m is to be interpreted as the mass of the associated field quanta, once the field is quantized. The equations of motion are found by demanding that variations of the action with respect of ϕ vanish, leading to the Euler-Lagrange equation, which for the scalar field is

$$\Big(\Box + m^2\Big)\phi = 0 \;\; ; \; \Box \equiv \eta^{\mu\nu}\partial_\mu\partial_\nu \tag{236}$$

and is known as the Klein-Gordon equation. This is a second order partial differential equation akin to the wave equation. Since the Minkowski spacetime upon which this field is defined is spatially flat, one may solve the spatial part of the differential equation through a Fourier transform

$$\phi(t, \vec{x}) = \frac{1}{\sqrt{V}} \sum_k \phi_k(t) e^{i\vec{k}\cdot\vec{x}} \equiv \sum_k \phi_k(t) u_k \tag{237}$$

where for the time being we are considering the field to be bounded by a large box/cube of volume, $V = L^3$ and are considering periodic boundary conditions $e^{ikL} = 1$ (consequently k takes on discrete integer values). Note the factor of $\sqrt{V}$ is introduced for normalization purposes:

$$\int d^3x \, u_k \, u^*_{k'} = \delta_{kk'} \, . \tag{238}$$

Inserting this Fourier form into eqn. 236 gives the second order, linear differential equation

$$\Big(\partial_t^2 + \omega_k^2\Big)\phi_k(t) = 0 \;\; ; \; \omega_k^2 \equiv k^2 + m^2 \tag{239}$$

which because the field ϕ is real must have a general solution of the form

$$\phi_k(t) = b_k \, g_k(t) + b_k^* \, g_k^*(t) \tag{240}$$

where the g_k's are known as *mode functions*. Because the frequencies, ω_k are time-independent, eqn. 239 can be straightforwardly solved with complex exponential mode functions. Thus, the solution for the classical, real scalar field is

$$\phi(t, \vec{x}) = \frac{1}{\sqrt{V}} \sum_k \, b_k e^{-i(\omega t - \vec{k}\cdot\vec{x})} + \text{C.C.} \tag{241}$$

where C.C. refers to the complex conjugate. Associated with this field is the canonical conjugate momentum field

$$\pi(t,\vec{x}) = \frac{\partial \mathcal{L}}{\partial \dot{\phi}} = \dot{\phi}(t,x) \tag{242}$$

where the dot refers to a time derivative. In conjunction with Lagrangian density in eqn. 235 one can obtain the Hamiltonian,

$$H = \int d^3x\, \mathcal{H} = \int d^3x\, \pi\, \dot{\phi} - \mathcal{L} = \int \frac{1}{2}\Big(\pi^2 + (\nabla\phi)^2 + m^2\phi^2\Big)\, d^3x\,. \tag{243}$$

So far this discussion has concerned classical fields. In order to move to a quantum mechanical discussion, field ϕ must be quantized. This can be done by following the canonical quantization procedure. First the coefficients b_k (b_k^*) are isolated using the orthogonality of the terms in the Fourier series

$$b_k\, g_k(t) = \frac{1}{2}\int d^3x\, u_k^*\Big(\phi(t,\vec{x}) + \frac{i}{\omega_k}\pi(t,\vec{x})\Big) \tag{244}$$

$$b_k^*\, g_k^*(t) = \frac{1}{2}\int d^3x\, u_k\Big(\phi(t,\vec{x}) - \frac{i}{\omega_k}\pi(t,\vec{x})\Big)\,. \tag{245}$$

Next, the Poisson brackets

$$\{a,b\}_{PB} \equiv \partial_\phi a\, \partial_\pi b - \partial_\pi a\, \partial_\phi b \tag{246}$$

are computed for the coefficients,

$$\{b_k\, g_k(t), b_{k'}^*\, g_{k'}^*(t)\}_{PB} \to \{b_k\,, b_{k'}^*\}_{PB} = \frac{i}{4}\int d^3x\, u_k^* u_{k'}\left\{(\phi + \pi/\omega_k), (\phi - \pi/\omega_k')\right\}_{PB} = -\frac{i\delta_{kk'}}{2\omega_k}\,. \tag{247}$$

Similarly in can be shown that

$$\{b_k, b_k\}_{PB} = \{b_k^*, b_k^*\}_{PB} = 0 \tag{248}$$

Finally, canonical quantization requires that the *coefficients* be promoted to *operators* with equal time commutation relations equal to i times the value of the Poisson brackets of the coefficients ($i\{a,b\}_{PB} = [\hat{a},\hat{b}]$). Therefore,

$$b_k \to \hat{a}_k/\sqrt{2\omega_k}\ \ ;\ \ b_k^* \to \hat{a}_k^\dagger/\sqrt{2\omega_k} \tag{249}$$

$$[\hat{a}_k, \hat{a}_{k'}^\dagger] = 2\omega_k \cdot i\{b_k\,, b_{k'}^*\}_{PB} = \delta_{kk'} \tag{250}$$

$$[\hat{a}_k, \hat{a}_{k'}] = [\hat{a}_k^\dagger, \hat{a}_{k'}^\dagger] = 0 \tag{251}$$

where we have elected to make the operators dimensionless and have normalized their commutator by splitting off the factor $\sqrt{2\omega_k}$. These operators $(\hat{a}_k^\dagger, \hat{a}_k)$ are referred to as creation and annihilation operators for reasons which will become apparent below. Using these operators, the solution for the quantized real, scalar field takes the form

$$\hat{\phi}(t,\vec{x}) = \frac{1}{\sqrt{2\omega_k V}} \sum_k \hat{a}_k e^{-i(\omega t - \vec{k}\cdot\vec{x})} + \text{h.c.} \tag{252}$$

where h.c. stands for Hermitian conjugate. Note the field is now a time-evolving operator consistent with the Heisenberg picture of quantum mechanics. In this picture, the quantum states of the operator are time-independent, and span a Hilbert space. In QFT, the most convenient basis of states to work in is the so-called Fock representation which is the sum of Hilbert spaces representing one particle states, two particle states, etc. whereby particles we strictly mean *identical particles*. Beginning with the vacuum state, (henceforth, I will suppress the hats over operators)

$$a_k|0\rangle = 0 \; \forall k \tag{253}$$

which is annihilated by all a_k operators, the many particle states of the Fock representation may be constructed from the vacuum

$$|1_{k_1}, 1_{k_2}, 1_{k_3}, ..., 1_{k_j}\rangle = a_{k_1}^\dagger \, a_{k_2}^\dagger \, a_{k_3}^\dagger ... \, a_{k_j}^\dagger |0\rangle \tag{254}$$

where the state on the left is interpreted as containing one particle of momentum $\vec{k}_1$, one particle of momentum $\vec{k_2}$, etc. Since scalar particles are bosons, creation operators for the same momentum may be applied repeatedly yielding,

$$a_k^\dagger|n_k\rangle = (n+1)^{1/2}|(n+1)_k\rangle \tag{255}$$

$$a_k|n_k\rangle = (n)^{1/2}|(n-1)_k\rangle \tag{256}$$

where the prefactors in front of the states follow from the commutation relations. One may also count the number of particles in a state by introducing the number operator, $N_k \equiv a_k a_k^\dagger$ whose expectation value is given by,

$$\langle n_k|N_k|n_k\rangle = n_k \, . \tag{257}$$

Thus, the Fock states are eignestates of the number operator, and we may interpret n_k as counting the number of quanta with momentum k. Using the field solution eqn. 252, and the creation/annihilation operator commutation relations leads to the following commutation relations

$$[\phi(t,\vec{x}),\phi(t,\vec{x}')] = 0 \tag{258}$$

$$[\pi(t,\vec{x}),\pi(t,\vec{x}')] = 0 \tag{259}$$

$$[\phi(t,\vec{x}),\pi(t,\vec{x}')] = i\delta^3(\vec{x}-\vec{x'})\,. \tag{260}$$

Finally inserting the field solution into the Hamiltonian eqn. 243 yields

$$H = \sum_k (a_k^\dagger a_k + \frac{1}{2})\omega_k \tag{261}$$

which reveals that the energy in a particular state is proportional to the number particles in the state (though importantly, the zero particle/vacuum state does *not* have zero energy). Hence the the reason for names creation and annihilation operators becomes apparent: the application $a_k^\dagger$ to the vacuum state changes the state and increases the energy stored in the field by an amount ω_k which is precisely the energy of a quanta of mass m with momentum k. Meanwhile the operator a_k has the opposite effect when acting on a state $|n_k\rangle$.

2.2.1.2 Fermion Field Quantization Quantum fields of half-integer spin are used in the Standard Model to describe the elementary, matter particles (e.g. electrons, quarks). These fermion fields are also the second type of quantum field considered at length in this thesis. Here I provide a brief review of only the most salient aspects of the quantum field theory of fermions; standard texts such as [95], [161] provide much greater detail for the curious reader. As with scalar bosons, we proceed by specifying a classical field theory and then performing a canonical quantization. Fermion fields, $\psi(t,\vec{x})$ are described by the Dirac action

$$S = \int \mathcal{L}\, d^4x = \int d^4x\, \bar{\psi}\Big(i\gamma^\mu\partial_\mu - m\Big)\psi \tag{262}$$

where the $\bar{\psi} = \psi^\dagger \gamma^0$ is known as the Dirac adjoint. Additionally, the matrices $\gamma^\mu\,;\, \mu = 0, 1, 2, 3$ are known as the Dirac matrices. They satisfy the *anti-commutation* relations:

$$\gamma^\mu \gamma^\nu + \gamma^\nu \gamma^\mu = 2\eta^{\mu\nu}\,. \tag{263}$$

The simplest possible matrix representation of this algebra is a set of 4×4 matrices. The standard Dirac representation uses block diagonal matrices composed of the Pauli matrices σ^i,

$$\gamma^0 = \begin{pmatrix} 1 & 0 \\ 0 & -1 \end{pmatrix} \quad , \quad \gamma^j = \begin{pmatrix} 0 & \sigma^j \\ -\sigma^j & 0 \end{pmatrix} \tag{264}$$

$$\sigma^1 \equiv \begin{pmatrix} 0 & 1 \\ 1 & 0 \end{pmatrix} \ , \ \sigma^2 \equiv \begin{pmatrix} 0 & -i \\ i & 0 \end{pmatrix} \ , \ \sigma^3 \equiv \begin{pmatrix} 1 & 0 \\ 0 & -1 \end{pmatrix}\,. \tag{265}$$

Using eqn. 263, it is possible to prove the following commutation relations:

$$S^{\mu\nu} \equiv= \frac{1}{4}[\gamma^\mu, \gamma^\nu] = \begin{Bmatrix} 0 & \mu = \nu \\ \frac{1}{2}\gamma^\mu\gamma^\nu & \mu \neq \nu \end{Bmatrix} \tag{266}$$

$$[S^{\mu\nu}, \gamma^\rho] = \gamma^\mu \eta^{\nu\rho} - \gamma^\nu \eta^{\rho\mu} \tag{267}$$

$$[S^{\mu\nu}, S^{\rho\tau}] = \eta^{\nu\rho} S^{\mu\tau} - \eta^{\mu\rho} S^{\nu\tau} + \eta^{\nu\tau} S^{\mu\rho} - \eta^{\mu\tau} S^{\nu\rho} \tag{268}$$

where the result of each line follows directly from the one proceeding it. Notice that the last line has the exact same form as the relation 232. Consequently, $S^{\mu\nu}$ are the representation of the generators of Lorentz transformations for fermion fields, and therefore eqn. 233 proscribes the transformation of ψ under infinitesimal Lorentz transformations; ψ must be a 4-component spinor (a fact also immediately evinced by the form of the Dirac Lagrangian).

By varying the action 262 with respect to $\bar{\psi}$ (or ψ), the equations of motion for ψ (or $\bar{\psi}$) are obtained

$$(i\gamma^\mu \partial_\mu - m)\psi = 0 \tag{269}$$

$$i\partial_\mu \bar{\psi}\gamma^\mu + m\bar{\psi} = 0\,. \tag{270}$$

Unsurprisingly, the first and second lines are known as the Dirac equation and adjoint Dirac equation respectively. There is no immediately obvious argument for why this first order,

partial differential equation, of unusual form, is the necessary one for describing spin-1/2 particles. The historical motivation and development of the equation is discussed at length in [183]. Regardless, once properly understood, the Dirac equation has elegant and profound implications. For now we begin by deriving the associated conjugate momentum fields

$$\pi_\psi = \frac{\partial \mathcal{L}}{\partial \dot{\psi}} = i\psi^\dagger \tag{271}$$

which interestingly is not proportional to a derivative of the fermion field, but rather it's conjugate. Accordingly, the phase space for a Dirac spinor field is fully parameterized by ψ and it's Hermitian conjugate meaning it is 8 dimensional (2 sets of 4 components). Since the number of degrees of freedom of a system is one half the dimensionality of the associated phase space, the fermion field has 4 real degrees of freedom (of course fields are extended objects with infinite degrees of freedom, here we are specifically counting degrees of freedom *at each spacetime point*). Using the conjugate momentum allows one to obtain the Hamiltonian

$$H = \int d^3x\, \mathcal{H} = \int d^3x\, \pi_\psi\, \dot{\psi} - \mathcal{L} = \int d^3x\, \bar{\psi}(-i\gamma^j\partial_j + m)\psi = \int d^3x\, i\bar{\psi}\gamma^0\dot{\psi} \tag{272}$$

where the Dirac equation was used for the last equality. One can solve the Dirac equation by making an ansatz similar to the solution of the Klein-Gordon equation, namely using a Fourier transform:

$$\psi(t,\vec{x}) = \frac{1}{\sqrt{V}} \sum_p U_s(p,t) e^{i\vec{p}\cdot\vec{x}} \tag{273}$$

where we again are considering the field to be bound by a large box/cube of volume V and periodic boundary conditions. Note the object $U_{p,s}(t)$ is a time-dependent, 4-component spinor (the subscript $s = 1, 2, 3, 4$ labels the components). Inserting this expression into eqn. 269 yields

$$(i\gamma^0\partial_t - \vec{\gamma}\cdot\vec{p} - m)U_s(p,t) = 0 \tag{274}$$

$$U_s(p,t) \equiv (i\gamma^0\partial_t - \vec{\gamma}\cdot\vec{p} + m) f_p(t)\, u_s = 0 \tag{275}$$

$$(\partial_t^2 + (p^2 + m^2)) f_p(t) = 0 \tag{276}$$

where in the second line, the spinor has been written in terms of the product of a mode function $f_p(t)$ and a *time-independent* spinor u_s. The third line then follows from inserting

the second into the first. Notice the resulting equation for the time-dependence is the same second order, linear differential equation encountered for the scalar case (see eqn. 239), and thus the solution will be the same. Note, there are two solutions to this equation:

$$f_p^{(1)}(t) = e^{-i\omega_p t} \;\; ; \;\; f_p^{(2)}(t) = e^{+i\omega_p t} \tag{277}$$

with $\omega_p^2 \equiv p^2 + m^2$. Meanwhile, for the time-independent spinors, we are free to choose the form:

$$u_1^\dagger = (\chi_1, 0) \; , \; u_2^\dagger = (\chi_2, 0); \; , \; u_3^\dagger = (0, \phi_1) \; , \; u_4^\dagger = (0, \phi_2) \tag{278}$$

where χ_j and ϕ_j are 2-spinors

$$\chi_1 = \begin{pmatrix} 1 \\ 0 \end{pmatrix} \; , \; \chi_2 = \begin{pmatrix} 0 \\ 1 \end{pmatrix} \; ; \; \phi_1 = \chi_2 \; , \; \phi_2 = \chi_1 \tag{279}$$

and so u_1 and u_4 describe spin-up states while u_2 and u_3 describe spin-down states. Now, eqn. 275 can be used to determine the form of the full U spinors. Inserting the u_s spinors, mode functions, and Dirac matrices into this equation yields

$$U_\lambda(p) = \begin{bmatrix} (\omega_p + m)\chi_\lambda \\ (\vec{\sigma} \cdot p)\chi_\lambda \end{bmatrix} \cdot f_p^{(1)}(t) \;\; , \; \lambda = 1, 2 \tag{280}$$

where for the moment we have restriced ourselves to $s = \lambda = 1, 2$ and have matched those solutions with the first mode function solution. Incidentally these spinors can be normalized since

$$U_\lambda^\dagger(p) U_{\lambda'}(p) = 2\omega_p(\omega_p + m)\delta_{\lambda\lambda'} \tag{281}$$

and therefore the normalized spinor takes the form,

$$U_\lambda(p) = \begin{bmatrix} \chi_\lambda \\ \frac{(\vec{\sigma}\cdot p)}{\omega_p + m}\chi_\lambda \end{bmatrix} \cdot \frac{f_p^{(1)}(t)}{\sqrt{2\omega_p}} \;\; , \; \lambda = 1, 2 \, . \tag{282}$$

The result 282 represents one of two solutions to the Dirac equation. Insertion of this result into eqn. 272 for the Hamiltonian leads to $H \propto \omega_p$. Evidently this is a positive energy solution since $\omega_p > 0$.

Turning our attention to other solution, eqn. 275 can be used, while considering $s = 3, 4$, with the second mode function to obtain

$$V_\lambda(p) = \begin{bmatrix} \frac{(\vec{\sigma}\cdot p)}{(\omega_p + m)}\phi_\lambda \\ \phi_\lambda \end{bmatrix} \cdot f_p^{(2)}(t) \ \ , \ \lambda = 1, 2 \tag{283}$$

where the symbol $V_\lambda(p)$ is used to distinguish these spinors from the previous solution, and the normalization has already been imposed. One can also readily verify that these two types of spinor solutions are orthogonal

$$U_{\lambda'}^\dagger(p)V_\lambda(p) = V_{\lambda'}^\dagger(p)U_\lambda(p) = 0 \tag{284}$$

Superfically this second solution, $V_\lambda(p)$ seems parsimonious. However, once inserted into the Hamiltonian (see eqn. 272) we discover $H \propto -\omega_p$; these spinors correspond to *negative* energy solutions. Given that were are solving the equations of motion for a completely free field, the negative energy solutions are problematic since excitations of this field (once quantized) ought correspond to freely propagating particles. The problem of negative energy solutions becomes even more exacerbated when considering the Hamiltonian including both solutions. First we write the general free field solution:

$$\psi = \frac{1}{\sqrt{V}} \sum_{p,\lambda} \frac{1}{\sqrt{2\omega_p}} \Big(c_{p,\lambda}^+ u_\lambda(p)\, e^{-i\omega_p t} + c_{p,\lambda}^- v_\lambda(p)\, e^{+i\omega_p t} \Big) e^{i\vec{p}\cdot\vec{x}} \tag{285}$$

where the lower case spinors $u_\lambda(p)$ and $v_\lambda(p)$ refer to the capital case spinors $U_\lambda(p)$ and $V_\lambda(p)$ without the mode function and $\sqrt{2\omega_p}$ factors, since these have been written explicitly. Moreover, the $c^{+/-}$ are the coefficients for the positive/negative energy solutions. Upon inserting this solution and the associated expression for $\psi^\dagger$ into eqn. 272, and using the orthonormality relations of the spinors, one finds

$$H = \sum_{p,\lambda} \Big(\omega_p\, c_{p,\lambda}^{\dagger +} c_{p,\lambda}^+ - \omega_p\, c_{p,\lambda}^{\dagger -} c_{p,\lambda}^- \Big) \tag{286}$$

which makes the problem of negative energies manifest: if the coefficients are promoted to creation and annihilation operators in order to quantize the theory, the energy of the system is not bounded from below. Namely as the number of negative energy particles ($N^- = c^{\dagger -} c^-$) increases, the energy of the field plunges towards negative infinity. Fortunately

this conundrum can be solved. First, the coefficients are promoted to operators using the following convention

$$c^{+}_{p,\lambda} \to b_{p,\lambda} \;\; ; \;\; c^{\dagger -}_{p,\lambda} \to d_{p,\lambda} \tag{287}$$

where $b_{p,\lambda}$ and $d_{p,\lambda}$ are referred to as particle and antiparticle annihilation operators respectively (hats are suppressed). Second, these operators are made to obey canonical *anti-commutation* relations

$$\{b_{p,\lambda}, b^{\dagger}_{p',\lambda'}\} = \{d_{p,\lambda}, d^{\dagger}_{p',\lambda'}\} = \delta^3(\vec{p} - \vec{p}')\, \delta_{\lambda\lambda'} \tag{288}$$

$$\{b_{p,\lambda}, b_{p',\lambda'}\} = \{d_{p,\lambda}, d_{p',\lambda'}\} = 0\,. \tag{289}$$

Using these new results, the free field Hamiltonian becomes

$$H = \sum_{p,\lambda} \omega_p \left(b^{\dagger}_{p,\lambda} b_{p,\lambda} + d^{\dagger}_{p,\lambda} d_{p,\lambda} \right) + E_0 \tag{290}$$

where the anti-commutation relations have permitted us to flip the sign of the antiparticle contribution (albeit at the expense of introducing a positive zero-point energy, E_0). Thus, the Hamiltonian is a positive definite operator. The free field general solution for the fermion field operator is also recast as

$$\psi = \frac{1}{\sqrt{V}} \sum_{p,\lambda} \frac{1}{\sqrt{2\omega_p}} \Big(b_{p,\lambda} u_\lambda(p)\, e^{-ip^\mu x_\mu} + d^{\dagger}_{-p,\lambda} v_\lambda(-p)\, e^{+ip^\mu x_\mu} \Big) \tag{291}$$

where we have introduced the antiparticle spinors, $v_\lambda(p) = v_\lambda(p), \vec{p} \to -\vec{p}$, namely antiparticles of positive energy are described as particles propagating backwards in time [183]. Concluding our discussion of Fermion fields, through the anti-commutation relations of the creation and annihilation operators it is possible to prove the following relations

$$\{\psi(t,\vec{x}), \bar{\psi}(t,\vec{x}')\} = \delta^3(\vec{x} - \vec{x}') \tag{292}$$

$$\{\psi(t,\vec{x}), \psi(t,\vec{x}')\} = \{\bar{\psi}(t,\vec{x}), \bar{\psi}(t,\vec{x}')\} \tag{293}$$

which hold for equal time t. Additionally, since

$$b_{p,\lambda} b_{p,\lambda} = -b_{p,\lambda} b_{p,\lambda} \tag{294}$$

by anti-commutation, evidently $(b_{p,\lambda})^2 = (b^\dagger_{p,\lambda})^2 = 0$, and the same holds for antiparticle operators. This result necessarily prevents two fermions from being in the same Fock state, and hence the Pauli exclusion principle emerges naturally. Mindful of this critical difference from the bosonic case, the Fock basis is still a convenient choice of states to use when working with fermionic field operators. Finally, we note that it is often expedient to choose the 2-spinors χ_j and ϕ_j (see eqn. 279) to be eigenstates of the helicity operator $\vec{\sigma} \cdot \vec{p}$ such that

$$\vec{\sigma} \cdot \vec{p}\xi_\pm = \pm p\xi_\pm \ , \ \lambda = (1,2) \rightarrow (\xi_+, \xi_-) \tag{295}$$

which simplifies algebraic manipulations involving Dirac spinors and is convenient for most particle physics calculations. Earlier we noted that fermion fields have 4 real degrees of freedom per spacetime point. We can now clearly see these are the result of 2 spin states (spin-up/spin-down) plus two charge states (particle/antiparticle).

2.2.1.3 The S-Matrix Thus far we have described the time evolution of non-interacting quantum fields using the Heisenberg picture of quantum mechanics, where the states are time-independent, and the operators are time-dependent, obeying the Heisenberg equation of motion

$$\partial_t A(t, \vec{x}) = -i[A, H] \tag{296}$$

where A is a quantum field operator, and H is the field Hamiltonian. While in the previous sections we choose to derive the equations of motion for the fields through a Lagrangian formalism, one can readily show that for real scalar fields ($A = \phi$), and with the Hamiltonian given in equation 243, the Heisenberg equation yields the Klein-Gordon equation (eqn. 236). Similarly one can obtain the Dirac equation (6.2.11) through the Hamiltonian defined in equation 272 and the Heisenberg equation of motion.

In practice, however, one is concerned not merely with free fields, but those which interact since such couplings lead to the rich dynamics we observe in nature. In the Standard Model (SM), the matter fields feature specific gauge symmetries which, when described as *local gauge symmetries*, proscribe the exact mathematical form of these interactions (see [161]). In general, however, one may consider interactions between fields which are motivated on phenomenological grounds.

Regardless of the motivation for considering a particular form of interaction, the task at hand is to understand the time evolution of a field operator when interactions are included. Mathematically, this is tantamount to including more complicated terms in the Lagrangian. Generically, this leads to a non-linear field theory which is difficult to solve (and often cannot be solved exactly). However, if the interactions are small, namely their coupling is weak ($\lambda \ll 1$), then a perturbative approach can be used to obtain reliable, approximate solutions. This is exactly the situation for the SM interactions (under most, but not all of the scenarios of calculational interest), and it is generally true of new physics extensions. Consequently, in this section, we shall consider exclusively this perturbative approach to interactions, made possible via the *scattering matrix* (or S-matrix for short).

To begin with, we write the Hamiltonian of each interacting field divided into two parts:

$$H = H_0 + H_I \tag{297}$$

where H_0 is the free field Hamiltonian (i.e. the Hamiltonian of the non-interacting theory) and H_I is the interacting Hamiltonian (i.e. the perturbation term). We then define operators and states in the interaction picture as:

$$O^I(t) \equiv e^{iH_0 t}\, O^S\, e^{-iH_0 t} \tag{298}$$

$$|\alpha, t\rangle^I \equiv e^{iH_0 t}|\alpha\rangle^S = e^{iH_0 t}\, e^{-iHt}|\alpha\rangle^H \tag{299}$$

where the superscripts I, H, S refer to the interaction, Heisenberg, and Schrodinger pictures respectively. Recall, that in the Schrodinger picture, the operators are time-independent while states evolve according to the Schrodinger equation $\left(i\partial_t|\psi(x,t)\rangle^S = H|\psi(x,t)\rangle^S\right)$. If one computes an operator matrix element:

$${}^I\langle\alpha, t|O^I(t)|\beta, t\rangle^I = {}^H\langle\alpha|e^{iHt}\, O^S\, e^{-iHt}|\beta\rangle^H \tag{300}$$

$${}^I\langle\alpha, t|O^I(t)|\beta, t\rangle^I = {}^H\langle\alpha|O^H(t)|\beta\rangle^H = {}^S\langle\alpha, t|O^S|\beta, t\rangle^S \tag{301}$$

we see that the result is equivalent in all three pictures. This is naturally expected since the Hamiltonian is an Hermitian operator and these transformations from picture to picture are therefore unitary. Differentiating equation 298 respect to time yields

$$\partial_t O^I(t) = iH_0\, O^I(t) - iO^I(t)\, H_0 = -i[O^I(t), H_0] \tag{302}$$

and so evidently the operators in the interaction picture obey the Heisenberg equation of motion with the free field Hamiltonian (compare with eqn. 296). Thus, in the interaction picture *the fields obey their free field equations of motion*, and we do not need to solve any new equations of motion. Meanwhile, differentiating the interaction picture states (eqn. 299) produces

$$\partial_t |\alpha, t\rangle^I = -iH_I |\alpha, t\rangle^I \tag{303}$$

implying these states evolve according to the Schrodinger equation albeit exclusively in terms of the interacting Hamiltonian. Thus, the states of the interacting theory will feature a non-trivial time-evolution since H_I is in principle time-dependent. In order to formally solve for this time-evolution, one may construct a unitary time-evolution operator

$$|\alpha, t\rangle^I = U_I(t, t_0)|\alpha, t_0\rangle^I \tag{304}$$

which when inserted into the interaction picture Schrodinger equation yields

$$\partial_t |\alpha, t\rangle^I = -iH_I |\alpha, t\rangle^I \rightarrow \partial_t U_I(t, t_0)|\alpha, t_0\rangle^I = -iH_I\, U_I(t, t_0)|\alpha, t_0\rangle^I \tag{305}$$

$$\partial_t U_I(t, t_0) = -iH_I\, U_I(t, t_0)\,. \tag{306}$$

The resulting differential equation can be unfolded into integral form

$$U_I(t, t_0) = 1 - i\int_{t_0}^{t} dt'\, H_I(t')\, U(t', t_0) \tag{307}$$

which can solved iteratively, by successive reinsertion of the left-hand side, giving rise to the Neumann series

$$U_I(t, t_0) = 1 + (-i)\int_{t_0}^{t} dt_1\, H_I(t_1) + (-i)^2 \int_{t_0}^{t} dt_1 \int_{t_0}^{t_1} dt_2\, H_I(t_1)\, H_I(t_2) + \ldots \tag{308}$$

The resulting series involves a ever increasing products of H_I with each successive factor evaluated at a prior time ($t_1 > t_2 > t_3$ etc.) Accordingly, the domains of integration are over ever smaller intervals in time and with the upper limit of one integral serving as the

integration variable for the next integral. These successive integrations can be simplified via the introduction of the time ordered product ($\mathcal{T}\{A(x_1)A(x_2)\} \equiv A(x_1)A(x_2) + A(x_2)A(x_1)$):

$$U_I(t,t_0) = 1 + (-i)\int_{t_0}^{t} dt_1\, H_I(t_1) + \frac{(-i)^2}{2!}\int_{t_0}^{t} dt_1 \int_{t_0}^{t} dt_2\, \mathcal{T}\{H_I(t_1)\, H_I(t_2)\} + \frac{(-i)^3}{3!}\int_{t_0}^{t} dt_1 \int_{t_0}^{t} dt_2 \int_{t_0}^{t} dt_3\, \mathcal{T}\{H_I(t_1)\, H_I(t_2)\, H_I(t_3)\} + \ldots \tag{309}$$

$$U_I(t,t_0) = \sum_{n=0}^{\infty} \frac{(-i)^n}{n!}\int_{t_0}^{t} dt_1 \cdots \int_{t_0}^{t} dt_n\, \mathcal{T}\{H_I(t_1)\ldots H_I(t_n)\} \tag{310}$$

leading to a perturbation series for the time evolution operator.

Armed with a perturbative expansion for the time evolution operator one can construct the scattering matrix, which describes the probability amplitude for a quantum mechanical transition from an initial state (prepared in the asymptotic past) to a final state (observed in the asymptotic future) under the influence of an interaction,

$$S_{fi} = \lim_{t_0\to-\infty}\lim_{t\to\infty}\langle f|U_I(t,t_0)|i\rangle = \langle f|U_I(\infty,-\infty)|i\rangle \tag{311}$$

where $|i\rangle$ and $\langle f|$ are Fock states of the quantum field theory. Naturally, the S-matrix can be used to compute the probability amplitudes for a variety of transition processes. Of particular interest to this thesis is particle decay, whereby one particle transmutes into multiple quanta of a different species. Incidentally such a process represents the simplest, non-trivial S-matrix calculation wherein one can obtain the decay rate of the process as follows:

$$S_{fi} = \langle f|U_I(\infty,-\infty)|i\rangle \simeq \mathcal{M}_{fi}\,\delta(\sum_{f=1}^{2}\vec{p}_f - \vec{p}_i)\,\delta(\sum_{f=1}^{2}E_f - E_i) \tag{312}$$

where here we are considering a two-particle final state. $\mathcal{M}_{fi}$ refers to a matrix element whose form is dependent on the nature of the interacting Hamiltonian. The momentum conserving delta functions arise naturally from integrating the Hamiltonian density over 3-spatial dimensions to obtain the Hamiltonian and are a direct consequence of the Fourier series in the free field operator solution. The energy conserving delta function is a distinct consequence of the infinite time limit and the complex exponential mode functions. By

defining the transition probability as this S-Matrix *squared*, the energy conserving delta function ensures that the transition amplitude is linear in total elapsed time,

$$T_{fi} \equiv |S_{fi}|^2 \simeq |\mathcal{M}_{fi}|^2 \, \delta(\sum_{f=1}^{2} \vec{p}_f - \vec{p}_i) \, \delta(\sum_{f=1}^{2} E_f - E_i) \, T \ . \tag{313}$$

Finally, dividing by the total elapsed time and summing over the final state momenta gives the decay rate:

$$\Gamma = \sum_{p_1} \sum_{p_2} \frac{T_{fi}}{T} \, . \tag{314}$$

As an example of this formalism, consider the decay of a massive, real scalar boson into two, real, massless scalars through the interaction Hamiltonian density $\mathcal{H}_I = \lambda \phi_1 (\phi_2)^2$ where λ is the coupling constant. The Fock states of interest are

$$|i\rangle = |1^{\phi_1}_{p_1}\rangle \ \ ; \ |f\rangle = |1^{\phi_2}_{p_2} \, 1^{\phi_2}_{p_3}\rangle \, . \tag{315}$$

Based on these states and the form of the interacting Hamiltonian, the lowest order contribution to the perturbative S-matrix is

$$S_{fi} = (-i) \int_{-\infty}^{\infty} dt_1 \int d^3x \, \lambda \langle 1^{\phi_2}_{p_2} \, 1^{\phi_2}_{p_3} | \phi_1 (\phi_2)^2 | 1^{\phi_1}_{p_1} \rangle \tag{316}$$

The free field solution for these fields is given by eqn. 252. Inserting those expressions into the above equation yields

$$S_{fi} = \frac{-2i\lambda}{\sqrt{2E_1 \, 2E_2 \, 2E_3}} \frac{(2\pi)^4}{\sqrt{V^3}} \, \delta(\vec{p_1} - \vec{p_2} - \vec{p_3}) \, \delta(E_1 - E_2 - E_3) \tag{317}$$

and squaring the S-matrix gives the transition probability,

$$T_{fi} = |S_{fi}|^2 = \frac{4\lambda^2}{2E_1 \, 2E_2 \, 2E_3} \frac{(2\pi)^4 \, VT}{V^3} \, \delta(\vec{p_1} - \vec{p_2} - \vec{p_3}) \, \delta(E_1 - E_2 - E_3) \, . \tag{318}$$

and subsequently inserting the result into eqn. 314 gives the decay rate

$$\Gamma = \frac{(2\pi)^4}{2E_1} \int \frac{d^3p_2}{(2\pi)^3 2E_2} \int \frac{d^3p_3}{(2\pi)^3 2E_3} 4\lambda^2 \, \delta(\vec{p_1} - \vec{p_2} - \vec{p_3}) \, \delta(E_1 - E_2 - E_3) \tag{319}$$

where we have passed from box normalization to the continuum description via $\frac{1}{V} \sum_k \rightarrow \int \frac{d^3p}{2\pi^3}$. This integral is over the Lorentz invariant phase space (see [183]), and thus one is free

to evaluate the result in any frame connected by a Lorentz transformation. A convenient choice is the rest frame of parent particle $\vec{p}_1 = 0, E_1 = m_1$ which gives

$$\Gamma = \frac{2\lambda^2}{32\pi^2 m_1} \int \delta\Big(m_1 - \sqrt{m_2^2 + p_2^2} - \sqrt{m_3^2 + p_2^2}\Big) \frac{p_2^2 \, dp_2 d\Omega}{E_2 E_3} \, . \tag{320}$$

where we have integrated over the momentum conserving delta function, and passed to spherical coordinates hence the solid angle $d\Omega$. Additionally the result has been multiplied by $1/2$ since the outgoing particles are indistinguishable. Finally, integrating over the remaining delta function and the solid angle yields

$$\Gamma = 2\lambda^2 \frac{|\vec{p}^*|}{8\pi m_1^2} \;\; ; \;\; |\vec{p}^*| = \frac{1}{2m_1} \sqrt{[m_1^2 - (m_2 + m_3)^2][m_1^2 - (m_2 - m_3)^2]} \tag{321}$$

and taking the massless limit for the daughter particles $m_{2,3} \to 0$,

$$\Gamma = \frac{\lambda^2}{8\pi m_1} \tag{322}$$

which is the final result for the decay rate of a massive scalar to two massless scalars, computed in the rest frame of the decaying particle in the Minkowski spacetime. Although this was a specific example, the phase space integral result is very generic and will hold for any two-body decay.

While the perturbative S-matrix is a powerful tool for computing transition amplitudes, notice that its effectiveness is predicated on the both the *infinite time limit* and *global energy conservation*. These properties are a manifest result of the time translational symmetry of Minkowski spacetime. In chapters 3 and 4 we will develop and utilize an alternative framework, which is not dependent on these properties, for general use in cosmological settings.

2.2.2 QFT in Curved Spacetime

The theory of fields quantized in the flat Minkowski spacetime of special relativity describes a special case: the study of relativistic quantum systems in regimes with negligible gravitational effects. At first glance this may seem to be a restrictive consideration since essentially all particle physics experiments occur in the gravitational field of the Earth. However, a simple argument of scales can readily convince one of the insignificance of the local gravitational field in terrestrial particle dynamics. In general relativity, an approximately spherical mass like the Earth sources a warped spacetime described by the Schwarzschild metric. This metric features a departure from the, flat, Minkowski spacetime determined by the Schwarzschild radius, $R_S = \frac{2G_N M}{c^2}$ (G_N is the Newton's gravitational constant, M is the mass of the spherical body, and c is the speed of light). For the Earth, $R_S^E \simeq 1$cm. Accordingly, only quantum modes with very long wavelengths ($\lambda \geq R_S^E$) will "see" the spatial curvature and experience relevant gravitational effects. Even for a non-relativistic free electron, with kinetic energy E_{kin}, $\lambda = \frac{2\pi}{p} \simeq \frac{2\pi}{\sqrt{2m\,E_{Kin}}} \sim 1.2 \times 10^{-7} (\frac{1\text{eV}}{E_{kin}})^{1/2}$ cm, so local gravitational effects can be safely neglected.

One may, however, be concerned about treating the gravitational field classically, through general relativity, rather than quantum mechanically. After all, QFT aims to provide a quantum description of all the classical fields of nature, and this ought extend to gravity. However, if one treats the gravitational field as small, quantum excitations (called gravitons) on a flat spacetime background, then the gravitational coupling constant is $\frac{G_N \hbar}{c^3} = G_N$ in natural units [28]. The resulting coupling constant therefore has units of GeV^{-2}, and so it is customary to write it as $\frac{1}{M_{pl}^2}$ where $M_{pl} \equiv \sqrt{\frac{\hbar c}{G_N}} = 1.22 \times 10^{19}$ GeV in natural units, and is known as the *Planck mass*. Consequently, unlike in the case of the Standard Model interactions (which have dimensionless coupling constants [183],[160]), the gravitational interaction has a minuscule, dimension-full coupling, and therefore quantum gravitational effects become important only as the energy scales of quantum processes approach the Planck mass. Below this large energy scale, gravity can be treated semiclassically[3].

[3]Strictly speaking there are two problems with this reasoning. Firstly, the strong equivalence principle requires that gravity couple to gravitons as it does to photons, matter, etc. Therefore strong gravity effects on matter/radiation also effect gravitons which then in principle backreact on the curvature. One can avoid this complication by linearizing the perturbed metric and including it in the energy-momentum piece of the

Even in the regime where quantum effects of gravity are ostensibly unimportant, there exist scenarios where the macroscopic, general relativistic form of gravitation leads to important effects for microscopic, quantum physics. The rapidly expanding early Universe is precisely such a place. The quantifying of these effects on particle dynamics (and the implications of those effects) associated with cosmic expansion is the primary concern of the subsequent chapters of this thesis. Therefore, in order to study these phenomena one must understand how to quantize field theories in the general spacetimes of general relativity.

2.2.2.1 Field Quantization Previously, we defined the spin of a quantum field based on its infinitesimal Lorentz transformation properties, namely the representation of its generators (see eqn. 232). This poses a problem in moving to curved spacetime since in general relativity the action is invariant under *general coordinate transformations* and not Lorentz transformations. This is the principle of general covariance. By general coordinate transformations we mean

$$d\tilde{x}^{\mu} = \frac{\partial \tilde{x}^{\mu}}{\partial x^{\nu}} dx^{\nu} \tag{323}$$

$$\tilde{g}_{\mu\nu} = \frac{\partial x^{\alpha}}{\partial \tilde{x}^{\mu}} \frac{\partial x^{\beta}}{\partial \tilde{x}^{\nu}} g_{\alpha\beta} \tag{324}$$

where the tilde refers to a different arbitrary set of coordinates, and $g_{\mu\nu}$ is a general spacetime metric. The problem then is how to maintain contact with the group of Lorentz transformations used to define the spin-type of quantum fields while obeying the principle of general covariance. To resolve this conundrum, we recall that the equivalence principle permits any observer to describe their frame as locally inertial, and therefore described by the Minkowski metric. Operationally this is done by introducing *tetrads*, e^{a}_{μ}, which are a set of four spacetime basis vectors which connect the local inertial frame to a more general coordinate system via

$$g_{\mu\nu} = e^{a}_{\mu} e^{b}_{\nu} \eta_{ab} \;\; ; \;\; e^{a}_{\mu} \equiv \frac{\partial y^{a}}{\partial x^{\mu}} \tag{325}$$

Einstein equations. Therefore, gravitons are treated as sources and not curvature. Secondly, since GR is a non-renormalizable theory, one must truncate the perturbation series (see S-matrix section) at a particular order. Both of these problems are discussed at length in chapter 1 of [28].

where the Latin indices are associated with the Minkowski metric indices and the Greek indices refer to the general spacetime. y^a are a set of normal coordinates which transform under Lorentz transformations in the usual fashion. Accordingly, each observer in spacetime carries a set of tetrads used to define their local inertial frame. The transformation properties of the tetrads are

$$\tilde{e}^a_\mu = \frac{\partial \tilde{x}^\mu}{\partial x^\nu} e^a_\nu \tag{326}$$

$$e'^a_\mu = \Lambda^a_b e^b_\mu \tag{327}$$

and thus the tetrad transforms as a covariant vector under general coordinate transformations and a contravariant vector under local Lorentz transformations. Finally, a generally contravariant vector A^μ contracted with a tetrad yields

$$A^a = e^a_\mu A^\mu \tag{328}$$

and thus transforms as a *scalar* under general coordinate transformations, but as a *vector* under local Lorentz transformations. The power of tetrads is there ability to convert general tensors into local, Lorentz-transforming tensors, by passing the remaining spacetime dependence into the tetrad. In order to use these objects in field theory, we promote the tetrad into a field known as a vierbein

$$e^a_\mu \to e^a_\mu(x) \tag{329}$$

such that at every spacetime point x there exists a set of normal coordinates defining a local inertial reference frame. Recall that the Lagrangian densities of field theory depend on the fields (ϕ) themselves as well as their derivatives ($\partial_a \phi$) both of which have defined transformations under Lorentz transformations. In order to maintain the local Lorentz transformation properties of the fields and their derivatives while moving to curved spacetime the general covariant derivative is introduced

$$\mathcal{D}_a \equiv e^\mu_a(x)(\partial_\mu + \Gamma_\mu) \tag{330}$$

$$\Gamma_\mu \equiv \frac{1}{2} I^{ab} e^\nu_a(x) \Big(\partial_\mu e_{b\nu}(x) - \Gamma^\lambda_{\mu\nu} e_{b\nu}(x) \Big) \tag{331}$$

where Γ_μ is known as the spin-connection [191, 28]. The spin-connection is defined in terms of the Lorentz transformation generators I^{ab} (see 232) associated with each field's representation (scalar, spinor, vector, etc.). Note, $\Gamma^\lambda_{\mu\nu}$ are the associated Christoffel symbols for the spacetime on which the field is defined. Also notice that in defining the general covariant derivative we have used the corollaries of eqn. 325

$$g^{\mu\nu} = e^\mu_a e^\nu_b \eta^{ab} \;\; ; \;\; e_{b\nu} = g_{\mu\nu} e^\mu_b \, . \tag{332}$$

By introducing the general covariant derivative $\mathcal{D}_a$, any field which transforms as a tensor under Lorentz transformations will necessarily transform as a tensor of the same rank under general coordinate transformations. Thus, a scalar field in Minkowski spacetime under Lorentz transformations remains a scalar field in a general spacetime under general coordinate transformations. So, the Lagrangian density of the field can be generalized to curved spacetime by replacing the derivative with the general covariant derivative ($\partial_a \to \mathcal{D}_a$) and by contracting all field vectors and higher rank tensors into vierbiens (e.g. $A_a \to e^\mu_a A_\mu$). Table 5 below shows the spin connections and general covariant derivatives for scalar and fermion fields defined on a generic, curved spacetime (recall that the generator representations were discussed in the previous sections).

Field	Generators (I^{ab})	Spin Connection (Γ_μ)	Covariant Derivative ($\mathcal{D}_a$)
Scalar	0	0	$e^\mu_a(x)\partial_\mu$
Fermion	$\frac{1}{4}[\gamma^b, \gamma^c]$	$\frac{1}{8}[\gamma^b, \gamma^c] e^\nu_b (\partial_\mu e_{c\nu} - \Gamma^\lambda_{\mu\nu} e_{c\lambda})$	$e^\mu_a(x)(\partial_\mu + \frac{1}{8}[\gamma^b, \gamma^c] e^\nu_b (\partial_\mu e_{c\nu} - \Gamma^\lambda_{\mu\nu} e_{c\lambda}))$

Table 5: General Covariant Derivatives for Fields.

To see concretely how this works, we write the real, scalar field action (from eqn. 235) in curved spacetime using the results of Table 5:

$$\begin{aligned} S = \int \mathcal{L} \, d^4x &= \int d^4x \sqrt{(-g)} \, \frac{1}{2}\Big(\eta^{ab} e^\mu_a \partial_\mu \phi e^\nu_b \partial_\nu \phi - m^2 \phi^2\Big) \\ &= \int d^4x \sqrt{(-g)} \, \frac{1}{2}\Big(g^{\mu\nu} \partial_\mu \phi \partial_\nu \phi - m^2 \phi^2 - \epsilon R \phi^2\Big) \end{aligned} \tag{333}$$

where in the final expression we have used eqn. 325 to simplify the expression and have included the only additional geometric scalar that can be added to the Lagrangian ϵR, where R is the Ricci scalar. Additionally the factor $\sqrt{(-g)} \equiv \sqrt{-\det(g_{\mu\nu})} = \det(e^a_\mu)$ is the Jacobian included to ensure the action is a scalar under general coordinate transformations.

Having formally developed the language necessary to construct field theories in curved spacetimes out of their Minkowski analogs, the next steps are to 1.) obtain the classical equations of motion by the variation principle (or through Hamilton's equations), 2.) solve the classical equations of motion through an expansion in a complete set of mode functions, 3.) promote the expansion coefficients to quantum mechanical annihilation and creation operators which obey canonical commutation relations (or anti-commutation relations for fermions), and 4.) work in the Fock basis states which are eigenstates of the number operator. Considering the case of a real, scalar field $\phi(x)$ the result has the generic form

$$\phi(x) = \sum_j \left(a_j \, u_j(x) + a_j^\dagger \, u_j^* \right) \tag{334}$$

$$[a_j, a_{j'}^\dagger] = \delta_{jj'} \;\; ; \;\; 0 = a_j|0\rangle, \forall j \;\; ; \;\; |1_j\rangle = a_j^\dagger|0\rangle \tag{335}$$

however, in the curved spacetime case there are two challenges, one conceptual and the other technical.

The essence of the conceptual challenge lies in the connection between the extra symmetries of Minkowski spacetime and the identification of free particle mode functions [28, 158]. Recall that in Minkowski spacetime we always obtained free field mode functions of the form

$$e^{\pm i k^a x_a} \;\; ; \;\; k^a x_a = \omega_k \, t - \vec{k} \cdot \vec{x} \tag{336}$$

namely plane waves in Cartesian coordinates. The spatial mode function was a result of expanding in Fourier series, a step allowed by the spatially flat nature of the metric. The temporal mode function has a more nuanced origin. Since the Minkowksi metric does not depend on time t, there is a Killing vector associated with the operator ∂_t and an associated conserved quantity given by the eigenvalue of that operator $(-i\omega_k)$ specifically the energy $(E_k = \omega_k \;, \; \omega_k > 0)$ [191, 28]. Therefore the complex exponential temporal mode functions

are the eigenfunctions of this operator. Thus, the mode functions 336 emerge as the natural choice in Minkowski spacetime *precisely* because the spacetime interval in Minkowski spacetime is invariant under Lorentz transformations and space/time translations. Since the mode functions determine the expansion coefficients (a_j) and these coefficients (once promoted to operators) determine the vacuum state, the mode functions dictate the vacuum. Consequently, the natural vacuum state is also invariant under Lorentz transformations and space/time translations [4].

Yet, for general metrics one cannot make general statements about Killing vectors or special symmetries, and so there are in principle no natural mode functions to expand the free field in since there are no privileged coordinates. This is precisely in accordance with the central claim of general relativity (i.e. the principle of covariance): physics phenomena are independent of coordinate systems. In light of this insight, we expect that in general a different complete set of mode functions exists for the field ϕ

$$\phi(x) = \sum_k \left(\tilde{a}_k \, \tilde{u}_k(x) + \tilde{a}_k^\dagger \, \tilde{u}_k^*(x) \right) \tag{337}$$

which specify a new vacuum and Fock space

$$0 = \tilde{a}_k |\tilde{0}\rangle, \forall k \;\; ; \;\; |\tilde{1}_k\rangle = \tilde{a}_k^\dagger |\tilde{0}\rangle \, . \tag{338}$$

Since both sets of mode functions are complete, they can be expanded in terms of each other

$$\tilde{u}_k(x) = \sum_j \left(A_{kj} u_j(x) + B_{kj} u_j^*(x) \right) \tag{339}$$

which is known as the Bogoliubov transformation, and A, B are known as Bogoliubov coefficients. Since, as a complete set, the mode functions feature orthonormality relations when integrated appropriately over the spacetime. Consequently by equating eqns. 334 and 337, inserting the Bogoliubov transformation, and noting the orthonormality of the modes one obtains

$$a_j = \sum_k \left(\tilde{a}_k A_{kj} + \tilde{a}_k^\dagger B_{kj}^* \right) \tag{340}$$

[4] To be clear, Minkowksi spacetime does not feature a unique vacuum. Rather, the mode functions of eqn. 336 define a vacuum state that all inertial observers will measure (since it is invariant under Lorentz transformations and space/time translations). Thus it is the *natural* vacuum choice.

and of course taking the Hermitian conjugate gives the expansion for the operator $a_j^\dagger$. Since all of the creation and annihilation operators obey their own canonical commutation relations, evidently

$$[a_j, a_j^\dagger] = 1 = \sum_k \left(|A_{kj}|^2 - |B_{kj}|^2 \right) \tag{341}$$

$$[a_j, a_{j'}] = 0 = \sum_k \left(A_{jk} B^*_{j'k} - B^*_{jk} A_{j'k} \right). \tag{342}$$

The result of eqn. 340 has profound and subtle implications. So long as $|B_{jk}| \neq 0$,

$$a_j |\tilde{0}\rangle = \sum_k B^*_{jk} |\tilde{1}_k\rangle \neq 0 \tag{343}$$

which means the vacuum of the $\tilde{u}_k$ modes is *not annihilated* by the operator a_j meaning it must contain quanta associated with the u_j modes. To reiterate, if the Bogoliubov coefficient $|B_{jk}| \neq 0$, the vacuum state of one Fock space contains particles associated with another. If one has physical reasons for regarding one set of modes as the proper description in a region of spacetime, but in another region of spacetime a second set of modes constitutes the correct physical description, then an observer in either region will measure the appropriate vacuum state to be populated by quanta (if the Bogoliubov coefficient connecting these modes does not vanish). This result is known as gravitational particle production and is the principle subject of chapters 5 and 6 of this thesis.

Returning to the aformentioned technical problem, the spacetime mode functions $u_j(x)$ (or $\tilde{u}_k(x)$) can be extremely complicated objects based on the nature of the spacetime on which the field is defined. In many cases of interest the modes cannot be written down in a closed form. Even in the cases where they can be analytically obtained, computing quantities with the mode functions is often a daunting proposition unless simplifying assumptions can be made. Thus one often resorts to obtaining the mode functions approximately.

2.2.2.2 The Adiabatic Approximation Approximate mode function solutions are often desired either because the equations of motion do not have a closed-form analytic solution or the resulting solutions are far too difficult to manipulate. Additionally, there are physical situations where the spacetime appears exceeingly close to Minkowski, suggesting that the mode functions should also approach the Minkowski form. Moreover, the Minkowski spacetime mode functions have the advantage of an unambiguous definition of particle number since their associated vacuum is agreed upon by all inertial observers. The question is therefore, are there approximate mode function solutions, valid for certain spacetime configurations, which are approximately Minkowksi? The answer is yes, and in the case where the only non-trivial dependence of the spacetime metric is on time (such as in an expanding universe), or at the very least the spatial part is homogeneous/isotropic, they are known as *adiabatic mode functions* and constitute the adiabatic approximation.

The adiabatic approximation can be introduced by considering the metric of an FLRW spacetime. Working in conformal time (η), the spacetime metric for a spatially flat, homogeneous, and isotropic universe is given by eqn. 35

$$ds^2 = g_{\mu\nu}dx^\mu dx^\nu = a^2(\eta)\,\eta_{\mu\nu}dx^\mu dx^\nu \tag{344}$$

and because of the spatial homogeneity of this metric one can again employ the Fourier transform as a means of isolating and obtaining the spatial dependence of the modes. In the case of a real, scalar field, this then leads to second order, ordinary differential equation for the time-dependence

$$\phi_k''(\eta) + \omega_k^2(\eta)\phi_k(\eta) = 0 \;\; ; \; \omega_k^2 \equiv k^2 + M^2(\eta) \tag{345}$$

where $' \equiv \partial_\eta$. Notice the resulting equation is highly similar to the one encountered in Minkowski spacetime (see eqn. 239), albeit with a time-dependent frequency originating from the effective mass term $M^2(\eta)$. The derivation of this equation has not been presented here, but is presented in full in chapter 3. Suffice it to say this equation arises directly from working with the real, conformally-coupled ($\epsilon = 1/6$) scalar field action defined on the FLRW metric in conformal time, and the time-dependence of the effective mass term is due to the scalar factor. However, for present purposes, the point of introducing eqn. 345 is

to provide an example of a situation where the equation of motion for the temporal mode functions is almost identical to the Minkowksi spacetime result, but for the time-dependent frequency. Since ϕ is a real-valued field, we seek mode functions $g_k(\eta)$ such that

$$\phi_k(\eta) = a_k\, g_k(\eta) + a_k^\dagger\, g_k^*(\eta) \tag{346}$$

$$g_k''(\eta) + \omega_k^2(\eta) g_k(\eta) = 0 \tag{347}$$

where I've anticipated that the coefficients will become quantum mechanical operators. The above differential equation for the mode functions can be solved with a WKB ansatz [28]

$$g_k(\eta) = \frac{1}{\sqrt{2W_k}} e^{-i\int^\eta W_k(\eta')\, d\eta'} \tag{348}$$

which when inserted into the differential equation yields a contraint equation for the $W_k(\eta)$

$$W_k^2(\eta) = \omega_k^2(\eta) - \frac{1}{2}\left(\frac{W_k''}{W_k} - \frac{3}{2}\Big(\frac{W_k'}{W_k}\Big)^2\right). \tag{349}$$

This equation can then be solved iteratively, first taking $W_k(\eta) \simeq \omega_k(\eta)$ and inserting back into the equation, which generates a series expansion

$$W_k^2(\eta) = \omega_k^2(\eta)\left[1 - \frac{1}{2}\frac{\omega_k''(\eta)}{\omega_k^3(\eta)} + \frac{3}{4}\left(\frac{\omega_k'(\eta)}{\omega_k^2(\eta)}\right)^2 + \cdots\right] \tag{350}$$

which is known as the adiabatic expansion. Notice that if $\omega_k^2 \gg \omega_k'$, then the higher order terms are small, and this expansion will be effective. Thus this condition defines the adiabatic criterion

$$\frac{\omega_k'}{\omega_k^2} \equiv \delta \ll 1 \tag{351}$$

which is a statement about the rate of change of the mode frequencies. δ also defines the adiabatic order, ergo two derivatives of the frequency is a second-order contribution. If the spacetime is varying sufficiently slowly so that the derivative of the frequency satisfies the above criterion, then the modes are well described by adiabatic modes. Taking the zeroth order solution for example

$$\phi_k(\eta) = a_k \frac{e^{-i\int^\eta \omega_k(\eta)\, d\eta'}}{\sqrt{2\omega_k(\eta)}} + h.c. \tag{352}$$

and clearly the approximate solution bears a striking similarity to the Minkowski mode functions. In fact if the time interval is small enough, then the time-dependent frequency can be pulled outside of the integral and the mode function has the usual complex exponential form of $\sim e^{-i\omega_k \Delta\eta}$. Note however, that this result will not hold over all times, and in general even the zeroth order adiabatic mode function is not identical to the Minkowksi mode functions since the frequencies are time-dependent. The important consequences of this statement are explored in chapters 3 and 4.

In closing the discussion of the adiabatic approximation there are three important points to make. 1.) The adiabatic approximation operationalizes the intuition that if there is a wide separation between the particle physics time scale and the gravitational time scale, namely if the spacetime is changing slowly compared to the particle frequency, then the quantum modes should not be very sensitive to the gravitational effects and should approach the Minkowski modes. 2.) Although, this derivation was motivated by the spacetime of an expanding cosmology, the adiabatic approximation can be implemented whenever the mode functions are separable into spatial and temporal pieces, and the temporal mode functions obey an equation of motion for a harmonic oscillator with a time-dependent frequency (see eqn. 345) [28]. 3.) Whenever the spacetime configuration warrants an adiabatic approximation, one can parameterize the exact mode function solutions in terms of the adiabatic mode functions via time-dependent Bogoliubov coefficients α, β

$$g_k(\eta) = \alpha_k^{(\delta)}(\eta)\, g_k^{(\delta)}(\eta) + \beta_k^{(\delta)}(\eta)\, g_k^{(\delta)*}(\eta) \tag{353}$$

where $g_k^{(\delta)}(\eta)$ are the adiabatic mode functions at a particular adiabatic order δ. The vacuum state associated with these modes is referred to as the *adiabatic vacuum* which is *not* an approximate state, despite the adiabatic mode functions themselves being approximate, since it is the exact mode function g_k which will be quantized and hence define the vacuum. Rather, the adiabatic vacuum refers only to a particular choice of vacuum state identified by matching the exact mode functions with the adiabatic ones (at a particular adiabatic order) [28]. Yet, parameterizing the mode functions in this fashion does introduce a time-dependent number operator. The subtle issues of the adiabatic vacuum and time-dependent number operator are addressed in chapters 3 and 5.

2.3 Quantum Kinetics

In many physical situations one is concerned with following the dynamics of particle populations which have efficient interactions between them. These interactions allow for depletion and/or augmentation of each coupled species' number density. For example, in early universe cosmology, the primordial plasma is characterized by large numbers of the various Standard Model degrees of freedom which are interacting with each other (e.g. electron/positron pairs annihilating into photons, photons pair producing muons, etc.). The broad, quantum mechanical framework for studying the evolution of particle populations (which may evolve into and/or out of local thermodynamic equilibrium) is known as quantum kinetics. While quantum kinetics is a subject with myriad applications, in this section I aim to briefly highlight the most important features of the theory which are relevant for particle cosmology and the subsequent chapters of this thesis. To that end, the important result of *detailed balance* is first discussed, highlighting its natural emergence from perturbative quantum field theory in Minkowski spacetime. Subsequently, the ubiquitous Boltzmann equation is introduced, first in general, and then in its more specialized form as used in early universe cosmology to study the effect of particle number changing interactions on particle populations. Throughout this section I closely follow the treatments of [24, 71, 121] unless otherwise stated.

2.3.1 Detailed Balance in QFT

To demonstrate the efficacy of quantum kinetics and derive the principle of detailed balance, consider a toy model scenario where two real, scalar particles χ, ϕ of mass M, m respectively interact through the interaction Hamiltonian density

$$\mathcal{H}_I = \lambda \, \chi \phi^2 \, . \tag{354}$$

Assume the underlying fields for these quanta are quantized in Minkowski spacetime. Accordingly, these fields have free field solutions given by eqn. 252

$$\hat{\phi}(t,\vec{x}) = \frac{1}{\sqrt{2\omega_k V}} \sum_k \hat{a}_k e^{-i(\omega_k t - \vec{k}\cdot\vec{x})} + \text{h.c.} \tag{355}$$

$$\hat{\chi}(t,\vec{x}) = \frac{1}{\sqrt{2\omega_k V}} \sum_k \hat{b}_k e^{-i(\omega_k t - \vec{p}\cdot\vec{x})} + \text{h.c.} \tag{356}$$

Suppose we wish track the evolution of $n_\chi(k,t)$, the number density of quanta associated with the ϕ field. We anticipate the number of particles of each momentum k will vary, so $n_\chi(k,t)$ is a distribution. We begin the quantum kinetic treatment by considering an ordinary differential equation for the rate of change of this quantity,

$$\frac{dn_\chi(k,t)}{dt} = \Gamma_k^G - \Gamma_k^L \tag{357}$$

where Γ_k^G (Γ_k^L) is the gain (loss) term representing the effect of particle number changing processes that increases (decreases) the number of χ quanta. The above equation is a simple example of a quantum master equation. These equations constitute the equations of motion for particle populations in quantum kinetics. In order to solve this equation, we must compute the required gain and loss terms, which can be done via the S-matrix.

Beginning with the loss term, we wish to compute the transition amplitude for particle number changing processes which increase the n_χ. Based on the form of the interaction Hamiltonian, the lowest order, non-vanishing S-matrix contribution to the loss process is $\chi \to \phi\phi$, namely a decay process. In quantum kinetics one is usually working in conditions with large occupation numbers, so we will stipulate our initial and final state for the loss process as

$$|i\rangle = |n_k\,, n_p\,, n_q\rangle \;\; ; \;\; |f\rangle^L = |n_k - 1\,, n_p + 1\,, n_q + 1\rangle \tag{358}$$

where n_k refers to the number of χ particles with momentum k, while $n_{p,q}$ refers to the number of ϕ particles with momentum p and q respectively (remember the two daughter phi

particles in principle will not be produced with equal momentum). Computing the S-matrix element between these two states yields

$$\langle n_k - 1\,, n_p + 1\,, n_q + 1|U_I(\infty, -\infty)|n_k\,, n_p\,, n_q\rangle = S^L_{fi} \tag{359}$$

$$S^L_{fi} = \frac{-2i\lambda}{\sqrt{2E_k\,2E_p\,2E_q}}\frac{(2\pi)^4}{\sqrt{V^3}}\,\delta(\vec{k} - \vec{p} - \vec{q})\,\delta(E_k - E_p - E_q)\sqrt{n_k}\sqrt{1+n_p}\sqrt{1+n_q} \tag{360}$$

where we have made use of equation 310 to first order, and the square root factors are the result of the action of the creation/annihilation operators on the Fock state. Squaring the S-matrix element gives the transition amplitude, which once integrated over the outgoing momenta (p, q) yields

$$\Gamma^L_k = \frac{|S^L_{fi}|^2}{T} = \frac{\lambda^2}{8\pi^2}\int d^3p\,\frac{\delta(E_k - E_p - E_q)}{E_k E_p E_q} n_k(1+n_p)(1+n_q)\ \ ;\ \vec{q} = \vec{k} - \vec{p} \tag{361}$$

where the result has been multiplied by a factor of $1/2$ since the outgoing particles are indistinguishable, the result has been divided by the total time T in order to extract a rate. Notice, that in the limit $n_k \to 1$; $n_{p,q} \to 0$ the result is exactly a decay rate (compare with eqn. 319). Accordingly, the elementary process of particle decay plays a vital role in quantum kinetics.

The gain term can be computed similarly. The lowest order, non-vanishing S-matrix contribution to the gain process is $\phi\phi \to \chi$, namely an inverse decay rate. We consider the same initial state, but this process produces a different final state

$$|i\rangle = |n_k\,, n_p\,, n_q\rangle\ \ ;\ |f\rangle^G = |n_k + 1\,, n_p - 1\,, n_q - 1\rangle\,. \tag{362}$$

Computing the S-matrix element between these two states, squaring the element, dividing by the total elapsed time, and integrating over the outgoing momentum yields

$$\Gamma^G_k = \frac{|S^G_{fi}|^2}{T} = \frac{\lambda^2}{8\pi^2}\int d^3p\,\frac{\delta(E_k - E_p - E_q)}{E_k E_p E_q}(1+n_k)n_p n_q\ \ ;\ \vec{q} = \vec{k} - \vec{p} \tag{363}$$

where again the result has been multiplied by $1/2$ due to indistinguishable outgoing particles. Comparing equations 363 and 361 we see the first is proportional to $1 + n_k$ while the second is proportional to n_k. Therefore we define,

$$\Gamma^G_k = (1+n_k)\tilde{\Gamma}^G_k\ \ ;\ \Gamma^L_k = (n_k)\tilde{\Gamma}^L_k \tag{364}$$

and so eqn. 357 becomes (replacing $n_k \to n_\chi(k,t)$ for clarity)

$$\frac{dn_\chi(k,t)}{dt} = -\gamma_k\Big(n_\chi - \mathcal{N}_k\Big) \;\; ; \;\; \gamma_k \equiv \tilde{\Gamma}_k^L - \tilde{\Gamma}_k^G \;\; ; \;\; \mathcal{N}_k \equiv \frac{\tilde{\Gamma}_k^G}{\gamma_k} \tag{365}$$

where γ_k is known as the relaxation rate. In order to solve this master equation initial conditions must be specified. Consider that the ϕ particles are in local thermodynamic equilibrium such that their distributions are of the Bose-Einstein form

$$n_p = \frac{1}{e^{E_p/T} - 1} \tag{366}$$

$$e^{E_p/T}\, n_p = 1 + n_p \tag{367}$$

which when inserted into the expression for $\tilde{\Gamma}_k^L$ (for n_p and n_q) gives

$$\tilde{\Gamma}_k^L = \frac{\lambda^2}{8\pi^2}\int d^3p\, \frac{\delta(E_k - E_p - E_q)}{E_k E_p E_q} n_p n_q e^{(E_p+E_q)/T} \tag{368}$$

which by virtue of the energy conserving delta function ($e^{(E_p+E_q)/T} = e^{E_k/T}$) and comparison with the gain term (eqn. 363) leads to,

$$\tilde{\Gamma}_k^L = \tilde{\Gamma}_k^G\, e^{E_k/T}\,. \tag{369}$$

The resulting expression is known as the *detailed-balance relation*, and is a consequence of 1.) energy conservation and 2.) the local thermodynamic equilibrium (LTE) of the particles to which χ is coupled. Inserting this relation into the master equation for the χ particle number density (eqn. 365) results in

$$\mathcal{N}_k \equiv \frac{\tilde{\Gamma}_k^G}{\tilde{\Gamma}_k^G\, e^{E_k\, T} - \tilde{\Gamma}_k^G} = \frac{1}{e^{E_k/T} - 1} = n_\chi^{eq} \tag{370}$$

$$\frac{dn_\chi(k,t)}{dt} = -\gamma_k\Big(n_\chi - n_\chi^{eq}\Big) \tag{371}$$

where n_χ^{eq} is the LTE distribution for the χ particles. Solving the master equation is now straightforward and yields,

$$n_\chi(k,t) = n_\chi^{eq} + \Big(n_\chi(k,0) - n_\chi^{eq}\Big)e^{-\gamma_k\, t} \tag{372}$$

$$\text{where} \;\; \gamma_k = \tilde{\Gamma}_k^G\,(e^{E_k/T} - 1) \tag{373}$$

with $n_\chi(k,0)$ being the initial χ particle number density. Notice as $t \to \infty$ $n_\chi \simeq n_\chi^{eq}$. This final result illustrates the result of detailed balance; a population of particles that are coupled to degrees of freedom, which themselves are in local thermodynamic equilibrium, will asymptotically approach local thermodynamic equilibrium on a time scale $1/\gamma_k$. Thus, a process and its inverse (gain and loss) obtain a chemical equilibrium.

In early universe cosmology, the primordial plasma is composed of elementary particles whose interactions maintain LTE between all of the coupled species; the principle of detailed balance provides an analytic description of how a coupled species can rapidly evolve into LTE through its interactions with already thermalized degrees of freedom. It is paramount, however, to emphasize that *the detailed balance result only obtains under the conservation of energy.*

2.3.2 The General Boltzmann Equation

In physics, the set of all states, permitted by the equations of motion, in which a system may exist is known as phase space. In classical physics, the set of canonical coordinates (q_i) and their conjugate momenta (p_i) are sufficient to span this space. Thus, a the specific state of a system, is completely specified the value of these variables and therefore its position in phase space. As the system evolves in time, it traces out a trajectory in phase space as dictated by the equations of motion. In the case of an ensemble of identical systems (e.g. a swarm of identical particles) the many individual systems can have unique phase space positions each of which is consistent with the same value of a macroscopic observable (e.g. temperature). In this case, it becomes expedient to introduce a function which describes the distribution of the individual systems in phase space known as a phase space density function, $f(q,p,t)$. Once properly normalized, f maybe convolved with another physical quantity over phase space to give the average value of that function. As an example, in the case of an amalgam of identical particles in three spatial dimensions,

$$\langle g \rangle = \int g(\vec{q},\vec{p}) f(\vec{q},\vec{p},t)\, d^3q d^3p \tag{374}$$

where we are integrating over a *single particle* phase space. Through the Hamilton equations and the continuity equation, it is possible to prove

$$\frac{df}{dt} = \frac{\partial f}{\partial t} + \{f, H\}_{PB} = 0 \tag{375}$$

where H is the Hamiltonian of the system, and $\{\}_{PB}$ are the Poisson brackets. This result is known as Liouville's theorem, and it holds under the assumption that no members of the ensemble are being created or destroyed.

In the case of particle populations, the system is an individual particle and the ensemble is the particle amalgam. In order to generalize Liouville's theorem to the case where particles can be added or subtracted we first compute the total derivative of $f(\vec{q}, \vec{p}, t)$. Considering Newtonian mechanics,

$$df = \frac{\partial f}{\partial t} dt + (\nabla_q f) \cdot d\vec{q} + (\nabla_p f) \cdot d\vec{p} \tag{376}$$

$$\frac{df}{dt} = \left(\frac{\partial}{\partial_t} + \frac{\vec{p}}{m} \cdot \nabla_q + \vec{F} \cdot \nabla_p \right) f \equiv \hat{L}\, f \tag{377}$$

where $d\vec{q} = \frac{\vec{p}}{m} dt$ and $\vec{F} = \frac{d\vec{p}}{dt}$ have been used. In the final line, the resulting differential operator $\hat{L}$ is known as the Liouville operator which includes (in order) the effects of explicit time-dependence, diffusion, and external forces acting on the system. Inserting this expression into Liouville's theorem produces the collisionless Boltzmann equation,

$$\hat{L}\, f(\vec{q}, \vec{p}, t) = 0 \tag{378}$$

which describes the evolution of the distribution function. With an eye towards using the Boltzmann equation to describe particle populations in cosmology, we seek a covariant, relativistic generalization. Writing the distribution function in terms of general contravariant 4-vectors as $f(x^\mu, p^\mu)$

$$df = \frac{\partial f}{\partial x^\mu} dx^\mu + \frac{\partial f}{\partial p^\mu} dp^\mu \tag{379}$$

$$\frac{df}{d\lambda} = \frac{\partial f}{\partial x^\mu} p^\mu - \Gamma^\mu_{\alpha\beta} p^\alpha p^\beta \frac{\partial f}{\partial p^\mu} = \hat{L} f \tag{380}$$

where in the last line we have used an affine parameter λ and the geodesic equation hence the Christoffel symbols $\Gamma^\mu_{\alpha\beta}$ [71].

So far we have been considering the Boltzmann equation in the case of constant particle number. Further generalizing the Boltzmann equation to the case where interactions can add or subtract particles from the collection requires the introduction of the collision operator $\hat{C}$ resulting in the general, covariant Boltzmann equation

$$\frac{\partial f}{\partial x^\mu}p^\mu - \Gamma^\mu_{\alpha\beta}p^\alpha p^\beta \frac{\partial f}{\partial p^\mu} = \hat{C}\, f(x^\mu, p^\mu)\,. \tag{381}$$

The particular form of the collison term on the right-hand side will depend on the type of interaction. In general, it is the result of a quantum kinetics/master equation type calculation where one considers gain and loss terms which are computed via the perturbative S-matrix. This equation sees widespread use in early universe cosmology to study the evolution of particle distribution functions. In this case, a copy is written for every coupled species thus producing a system of coupled Boltzmann equations. It is also one half of the Einstein-Boltzmann hierarchy which is used to study inhomogeneities. In this case, one considers small perturbations in the spacetime metric which are connected with small perturbations in the energy momentum tensor of the Universe via the perturbed, linearized Einstein field equations. The energy momentum tensor perturbations are then directly associated with inhomogeneities in the energy/number densities of particles; the equations of motion for those densities are precisely the Boltzmann equation [71, 139]. In most cases the Boltzmann equations can only be solved numerically.

2.3.3 The Annihilation Boltzmann Equation

One particular form of the Boltzmann equation 381 is frequently used to study the evolution of particle number densities in the early universe. Specifically, the equation is used to compute the abundances of particles, formerly in local thermodynamic equilibrium, after they fallout of equilibrium (referred to as decoupling or freeze-out). Using the Christoffel symbols of the FLRW metric the covariant Boltzmann equation can be written [121],

$$E\frac{df}{dt} - \frac{\dot{a}}{a}|\vec{p}|^2\frac{\partial f}{\partial E} = \hat{C}f(E,t) \tag{382}$$

where E refers to the energy of the particle, p its momentum, and a is the scale factor. Note, $\dot{} \equiv \partial_t$. Notice that the distribution function does not depend on spatial coordinates or

momentum in a homogenous and isotropic universe. Next, we formally define the particle number density,

$$n(t) \equiv \frac{g}{(2\pi)^3} \int d^3p\, f(E,t) \tag{383}$$

where g is the number of internal degrees of freedom. This quantity corresponds to the number of particles per comoving volume. Changing variables $\frac{\partial f}{\partial E} \rightarrow \frac{\partial p}{\partial E}\frac{\partial f}{\partial p}$, dividing by E, and integrating over d^3p in equation 382 yields

$$\dot{n} + 3Hn = \frac{g}{(2\pi)^3} \int \frac{d^3p}{E}\, \hat{C} f(E,t) \tag{384}$$

where we have integrated by parts to the get the second term on the left hand side (dropping the vanishing surface term) and introduced the Hubble parameter $H = \dot{a}/a$. Next, we scale out the effect of cosmic expansion by defining

$$Y = \frac{n}{s} \tag{385}$$

where is s is the comoving entropy density $sa^3 = S$. Taking the time derivative

$$\dot{n} = \dot{s}Y + \dot{Y}s \;\rightarrow\; \dot{n} + 3Hn = s\dot{Y} \tag{386}$$

where we have used the fact that S is constant in a comoving volume even as the Universe expands. Then, we define the variable $x \equiv m/T$ where m and T are the mass of the particle associated with the number density, and the temperature of the primordial plasma respectively. This permits us to write,

$$\dot{Y} = \frac{1.66m^2}{M_{pl}x}\sqrt{g_*}\frac{dY}{dx} \equiv \frac{H(m)}{x}\frac{dY}{dx} \tag{387}$$

where we have used eqn. 85 (M_{pl} is the Planck mass and g_* is the effective number of relativistic degrees of freedom). Finally inserting eqns. 386 and 387 into the integrated Boltzmann equation 384 results in

$$\frac{dY}{dx} = \frac{x}{sH(m)}\frac{g}{(2\pi)^3}\int \frac{d^3p}{E}\, \hat{C} f(E,t)\,. \tag{388}$$

Now we focus on the collision term on the right hand side. As previously mentioned, this object is usually computed in a quantum kinetics framework using an S-matrix approach. To obtain the presently desired form of the Boltzmann equation, consider the interaction to

be a 2 to 2 process: $Z\bar{Z} \leftrightarrow X\bar{X}$ where X, Z are two different particles, and the bar refers to their anti-partner. Assuming the number density we are tracking is for the X particle, our initial state, final (gain) state, and final (loss) state are

$$|i\rangle = |n_X\,, n_{\bar{X}}\,, n_Z\,, n_{\bar{Z}}\rangle \tag{389}$$

$$|f\rangle^G = |n_X + 1\,, n_{\bar{X}} + 1\,, n_Z - 1\,, n_{\bar{Z}} - 1\rangle \;\;;\;\; |f\rangle^L = |n_X - 1\,, n_{\bar{X}} - 1\,, n_Z + 1\,, n_{\bar{Z}} + 1\rangle\,. \tag{390}$$

Therefore, the resulting collision term has the form

$$\frac{g}{(2\pi)^3}\int \frac{d^3p}{E}\,\hat{C}f(E,t) = -\int \frac{d^3p_X}{2E_X}\,\frac{d^3p_{\bar{X}}}{2E_{\bar{X}}}\,\frac{d^3p_Z}{2E_Z}\,\frac{d^3p_{\bar{Z}}}{2E_{\bar{Z}}}\,(2\pi)^4\delta^{(4)}(P_X + P_{\bar{X}} - P_Z - P_{\bar{Z}})\Big\{ \\ |\mathcal{M}|^2_L f_X f_{\bar{X}}(1 \pm f_Z)(1 \pm f_{\bar{Z}}) - |\mathcal{M}|^2_G f_Z f_{\bar{Z}}(1 \pm f_X)(1 \pm f_{\bar{X}})\Big\} \tag{391}$$

where the $1\pm$ is the refers to fermion/boson particles respectively, and $|M|^2$ is a matrix element coming from an S-matrix field theory calculation whose specific form will depend on the particular fields involved and their coupling. Four assumptions are then made to simplify the collision term: 1.) We assume very large occupation numbers so that we can drop the Pauli-blocking and condensation factors, $1 \pm f \simeq 1$. 2.) Any thermal distributions are Maxwell-Boltzmann ($f^{eq} = e^{\mu/T}e^{-E/T}$) since we are interested in scenarios where the temperature is much lower than the average particle energy (and chemical potential μ). 3.) CPT invariance implying the QFT matrix element for the gain and loss contributions are equivalent ($|\mathcal{M}|^2_L = |\mathcal{M}|^2_G = |\mathcal{M}|^2$). 4.) The Z particles are in thermal equilibrium (via other efficient scattering interactions), so that in combination with the energy conserving delta function detailed balance is achieved. These considerations lead to the following simplifications

$$f_Z f_{\bar{Z}} = e^{(\mu_Z + \mu_{\bar{Z}})/T}e^{-(E_Z + E_{\bar{Z}})/T} = e^{(\mu_Z + \mu_{\bar{Z}})/T}e^{-(E_X + E_{\bar{X}})/T} = e^{(\mu_Z + \mu_{\bar{Z}})/T} f^{eq}_X f^{eq}_{\bar{X}} \tag{392}$$

$$f_X f_{\bar{X}} - f_Z f_{\bar{Z}} = f^{eq}_X f^{eq}_{\bar{X}}\Big(\frac{f_X f_{\bar{X}}}{f^{eq}_X f^{eq}_{\bar{X}}} - \frac{f^{eq}_Z f^{eq}_{\bar{Z}}}{f^0_Z f^0_{\bar{Z}}}\Big) \;\;;\;\; f^0 \equiv e^{-E/T}\,. \tag{393}$$

Finally, the thermally averaged cross-section is introduced

$$\langle \sigma\, v \rangle \equiv (n_X^{eq})^{-2} \int \frac{d^3p_X}{2E_X}\frac{d^3p_{\bar{X}}}{2E_{\bar{X}}}\frac{d^3p_Z}{2E_Z}\frac{d^3p_{\bar{Z}}}{2E_{\bar{Z}}}(2\pi)^4\delta^{(4)}(P_X + P_{\bar{X}} - P_Z - P_{\bar{Z}})|\mathcal{M}|^2 e^{-(E_X+E_{\bar{X}})/T} \tag{394}$$

and thus using these simplifications, and the thermally averaged cross-section, we obtain the full, integrated Boltzmann equation

$$\dot{n} + 3Hn = -(n_X^{eq})(n_{\bar{X}}^{eq})\langle \sigma\, v\rangle \Big(\frac{n_X n_{\bar{X}}}{n_X^{eq} n_{\bar{X}}^{eq}} - \frac{n_Z^{eq} n_{\bar{Z}}^{eq}}{n_Z^0 n_{\bar{Z}}^0} \Big) \tag{395}$$

$$\frac{dY_X}{dx} = -\frac{x\, s}{H(m)}(Y_X^{eq})(Y_{\bar{X}}^{eq})\langle \sigma\, v\rangle \Big(\frac{Y_X Y_{\bar{X}}}{Y_X^{eq} Y_{\bar{X}}^{eq}} - \frac{Y_Z^{eq} Y_{\bar{Z}}^{eq}}{Y_Z^0 Y_{\bar{Z}}^0} \Big) \;\; ; \;\; x \equiv m_X/T \tag{396}$$

where in the second line we have simply written the equation in terms of the variables Y, x. The resulting equation is known as the integrated annihilation Boltzmann equation for a species X and is frequently used in early universe physics to understand the out of equilibrium dynamics of particle populations. For the sake of clarity, it should be mentioned that the second form of the equation above explicitly assumes the radation dominated epoch (hence the usage of 85 in defining dY/dx). This equation (or ones very similar to it) can be used to study dark matter relic abundances, neutrino decoupling, nucleosynthesis, and recombination/photon decoupling, etc. [71, 121]. In practice, this requires one to solve a system of such Boltzmann equations numerically as the above equation does not have a simple analytic solution. In many of these scenarios, one can argue that the chemical potential of the Z particles is negligible ($\mu_Z/T \ll 1$) (e.g. see eqn. 76). Under that extra assumption, $n_Z^{eq} \simeq n_Z^0$ and the equation can be further simplified,

$$\frac{x}{Y_{X,eq}}\frac{dY_X}{dx} = \frac{-W_X}{H(T)}\Big(\frac{Y_{X,eq}^2}{Y_X^2} - 1 \Big) \;\; ; \;\; W_X \equiv n_X^{eq}\langle \sigma\, v\rangle \;\; ; \;\; Y_X^2 \equiv Y_X Y_{\bar{X}} \tag{397}$$

where we have inserted the expression for $H(m)$ from eqn. 387 and again used eqn. 85. In writing eqn. 397, the annihilation interaction rate for the X particles, W_X has been introduced. This form of the integrated annihilation Boltzmann equation reveals a particularly salient piece of physics, if $W_X \gg H$, then the right-hand side terms will be much larger than the left-hand side. In this situation, only $n_X \simeq n_X^{eq}$ can maintain an equality between both sides. Meanwhile, if $W_X \ll H$ then the right-hand side of the equation becomes very small,

and consequently the rate of change in the abundance of X particles approaches zero. The conclusion then, is that while the interaction rate is large compared to the expansion rate, the X particles maintain local thermodynamic equilibrium (chemical and kinetic) with the Z particles. However, when the expansion rate becomes larger, the number of X particles stabilizes, becoming nearly constant, and they fall out of equilibrium. This result is known as thermal freeze-out or decoupling. This analysis consequently justifies the heuristic decoupling criteria, $W(T_{dec} \simeq H(T_{dec}))$ where T_{dec} defines the temperature of the plasma at which decoupling occurs.

As a final comment, we note that the Boltzmann equation analysis which is successfully employed in the study of early universe physics does *not* treat spacetime consistently. The left-hand side, relies on the generally covariant Liouville operator constructed in FLRW spacetime. Meanwhile, the right-hand side results from a quantum kinetic analysis in Minkowski spacetime. The nature of this inconsistency and its implications are discussed in chapters 3 and 4.

3.0 Particle Decay in Post-inflationary Cosmology

3.1 Introduction

Particle decay is an ubiquitous process that has profound implications in cosmology, for baryogenesis [122, 79], leptogenesis [43, 69], CP violating decays [127], big bang nucleosynthesis (BBN) [196, 116, 115, 118, 119, 82, 114, 112, 163, 164, 165, 172], and dark matter (DM) where large scale structure and supernova Ia luminosity distances constrain the lifetimes of potential, long-lived candidates [196, 189, 190, 188, 30, 166, 12]. Most analyses of particle decay in cosmology use decay rates obtained from S-matrix theory in Minkowski spacetime. In this formulation, the decay rate is obtained from the total transition probability from a state prepared in the infinite past (in) to final states in the infinite future (out). Dividing this probability by the total time elapsed enables one to extract a transition probability per unit time. Energy conservation emerging in the infinite time limit yields kinematic constraints (thresholds) for decay processes.

The decay rate so defined, and calculated, is an input in analyses of cosmological processes. In an expanding cosmology with a time-dependent gravitational background, there is no global time-like Killing vector; therefore, particle energy is not manifestly conserved, even in spatially flat Friedmann-Robertson-Walker (FRW) cosmologies, which do supply spatial momentum conservation. Early studies of quantum field theory in curved spacetime revealed a wealth of unexpected novel phenomena, such as particle production from cosmological expansion [153, 154, 155, 194, 195, 86, 29, 47, 28, 87, 149, 158, 157, 88] and the possibility of processes that are forbidden in Minkowski space time as a consequence of energy/momentum conservation. Pioneering investigations of interacting quantum fields in expanding cosmologies generalized the S-matrix formulation for in-out states in Minkowski spacetimes for model expansion histories. Self-interacting quantized fields were studied with a focus on renormalization aspects and contributions from pair production to the energy momentum tensor [29, 47]. The decay of a massive particle into two massless particles conformally coupled to gravity was studied in Ref. [15, 16, 14] within the context of in-out

S-matrix for simple cosmological space times. Particle decay in inflationary cosmology (near de Sitter space-time) was studied in Refs. [38, 33, 34, 40, 41], revealing surprising phenomena, such as a quantum of a massive field decaying into two (or more) quanta of the *same* field. The lack of a global, time-like Killing vector, and the concomitant absence of energy conservation, enables such remarkable processes that are forbidden in Minkowski spacetime. More recently, the methods introduced in Ref. [15] were adapted to study the decay of a massive particle into two conformally massless particles in radiation and "stiff" matter dominated cosmology, focusing on extracting a decay rate for *zero momentum* [133, 135]. The results of Ref. [133, 135] approach those of Minkowski spacetime asymptotically in the long-time limit.

Motivation, goals and summary of results:

The importance and wide range of phenomenological consequences of particle decay in cosmology motivate us to study this process within the realm of the standard post inflationary cosmology, during the radiation and matter dominated eras. Our goal is to obtain and implement a quantum field theory framework that includes consistently the cosmological expansion and that can be applied to the various interactions and fields of the standard model and beyond.

Brief summary of results:

We combine a physically motivated adiabatic expansion with a non-perturbative method that is the *quantum field theoretical* version of the Wigner-Weisskopf theory of atomic linewidths[192] ubiquitous in quantum optics [176]. This method is manifestly unitary, and has been implemented in both Minkowski spacetime and inflationary cosmology [138, 137, 37], and provides a systematic framework to obtain the *decay law* of the parent along with the production probability of the daughter particles. One of our main results, to leading order in this adiabatic expansion, is a *cosmological Fermi's Golden Rule* wherein the particle horizon (proportional to the Hubble time) determines an uncertainty in the (local) comoving energy. We find that the parent survival probability may be written in terms of an *effective time-dependent decay rate* which includes the effects of (local) time dilation and cosmological redshift, resulting in a delayed decay. This effective rate depends crucially on a transition time, t_{nr}, between the relativistic and non-relativistic regimes of the parent particle, and

is always *smaller* than that in Minkowski spacetime, becoming equal only in the limit of a parent particle always at rest in the comoving frame. An unexpected consequence of the cosmological expansion is that the uncertainty implied by the particle horizon opens new decay channels to particles *heavier* than the parent. As the expansion proceeds this channel closes and the usual kinematic thresholds constrain the phase space for the decay process. While in this study we focus on the radiation dominated (RD) era, our results can be simply extended to the subsequent matter dominated (MD) and dark energy dominated eras. In appendix (A.1) we implement the Wigner-Weisskopf method in Minkowski spacetime to provide a basis of comparison which will enable us to highlight the major differences with the cosmological setting.

3.2 The Standard Post-Inflationary Cosmology

We focus on the decay of particles in the post-inflationary universe, described by a spatially flat (FRW) cosmology with the metric in comoving coordinates given by

$$g_{\mu\nu} = \mathrm{diag}(1, -a^2, -a^2, -a^2)\,. \tag{3.2.1}$$

The standard cosmology post-inflation is described by three distinct stages: radiation (RD), matter (MD) and dark energy (DE) domination; we model the latter by a cosmological constant. Friedmann's equation is

$$\left(\frac{\dot{a}}{a}\right)^2 = H^2(t) = H_0^2\left[\frac{\Omega_M}{a^3(t)} + \frac{\Omega_R}{a^4(t)} + \Omega_\Lambda\right], \tag{3.2.2}$$

where the scale factor is normalized to $a_0 = a(t_0) = 1$ today. We take as representative the following values of the parameters [23, 181, 3]:

$$H_0 = 1.5\times 10^{-42}\,\mathrm{GeV} \;\;;\;\; \Omega_M = 0.308 \;\;;\;\; \Omega_R = 5\times 10^{-5} \;\;;\;\; \Omega_\Lambda = 0.692\,. \tag{3.2.3}$$

It is convenient to pass from "comoving time," t, to conformal time η with $d\eta = dt/a(t)$, in terms of which the metric becomes ($a \equiv a(\eta)$)

$$g_{\mu\nu} = \mathrm{diag}(a^2, -a^2, -a^2, -a^2)\,. \tag{3.2.4}$$

With ($' \equiv \frac{d}{d\eta}$) we find

$$a'(\eta) = H_0 \sqrt{\Omega_M} \left[r + a + s\, a^4 \right]^{1/2}, \tag{3.2.5}$$

with

$$r = \frac{\Omega_R}{\Omega_M} \simeq 1.66 \times 10^{-4} \;\; ; \;\; s = \frac{\Omega_\Lambda}{\Omega_M} \simeq 2.25\,. \tag{3.2.6}$$

Hence the different stages of cosmological evolution, namely radiation domination (RD), matter domination (MD), and dark energy domination (DE), are characterized by

$$a \ll r \Rightarrow \text{RD} \;\; ; \;\; r \ll a \lesssim 0.76 \Rightarrow \text{MD} \;\; ; \;\; a > 0.76 \Rightarrow \text{DE}\,. \tag{3.2.7}$$

In the standard cosmological picture and the majority of the most well-studied variants, most of the interesting particle physics processes occur during the RD era and so we focus most of our attention on this epoch; however, we also contemplate the possibility of long-lived dark matter particles that would decay on time scales of the order of $1/H_0$. The RD and MD epochs cover approximately half of the age of the Universe and during these stages the evolution of the scale factor can be written as

$$a(\eta) = H_R\, \eta + \frac{H_M^2}{4}\, \eta^2 \;\; ; \;\; H_R = H_0 \sqrt{\Omega_R}, \;\; ; \;\; H_M = H_0 \sqrt{\Omega_M}\,, \tag{3.2.8}$$

which facilitates the explicit analytical study of the decay laws. In turn, the conformal time at a given scale factor a is given by

$$\eta(a) = \frac{2\sqrt{r}}{H_M} \left[\sqrt{1 + \frac{a}{r}} - 1 \right]. \tag{3.2.9}$$

During the (RD) stage the relation between conformal and comoving time is given by

$$\eta = \left(\frac{2\,t}{H_R} \right)^{\frac{1}{2}} \Rightarrow a(t) = \left[2\, t H_R \right]^{\frac{1}{2}}, \tag{3.2.10}$$

a result that will prove useful in the study of the decay law during this stage.

3.3 The Model

We consider two interacting scalar fields ϕ_1, ϕ_2 in the FRW cosmology determined by the metric (3.2.1), with action given by

$$A = \int d^4x\sqrt{|g|}\left\{\frac{1}{2}g^{\mu\nu}\,\partial_\mu\phi_1\partial_\nu\phi_1 - \frac{1}{2}\big[m_1^2+\xi_1\,R\big]\phi_1^2 + \frac{1}{2}g^{\mu\nu}\,\partial_\mu\phi_2\partial_\nu\phi_2 - \frac{1}{2}\big[m_2^2+\xi_2\,R\big]\phi_2^2 - \lambda\phi_1 : \phi_2^2 :\right\} \tag{3.3.1}$$

where

$$R = 6\Big[\frac{\ddot{a}}{a} + \Big(\frac{\dot{a}}{a}\Big)^2\Big] \tag{3.3.2}$$

is the Ricci scalar, and $\xi_{1,2}$ are couplings to gravity, with $\xi = 0, 1/6$ corresponding to minimal or conformal coupling, respectively. We identify ϕ_1 as the field associated with the decaying ("parent") particle, and ϕ_2 as that of the decay product ("daughter") particles.

Expressing the action of Eq. (3.3.1) in terms of the usual spatial coordinates and the conformal time, while rescaling the fields as

$$\phi_{1,2}(t) = \frac{\chi_{1,2}(\eta)}{a(\eta)} \quad ; \quad a(\eta) = a(t(\eta))\,, \tag{3.3.3}$$

yields

$$A = \int d^3x\,d\eta\Big\{\sum_{j=1,2}\Big[\tfrac{1}{2}\Big(\frac{d\chi_j}{d\eta}\Big)^2 - \tfrac{1}{2}\big(\nabla\chi_j\big)^2 - \tfrac{1}{2}\chi_j^2\,\mathcal{M}_j^2(\eta)\Big] - \lambda\,a(\eta)\,\chi_1\ :\chi_2^2:\Big\} \tag{3.3.4}$$

neglecting surface terms as usual, where

$$\mathcal{M}_j^2(\eta) = m_j^2\,a^2(\eta) - \frac{a''}{a}\,(1-6\xi_j) \quad ; \quad j = 1,2\,. \tag{3.3.5}$$

For the standard cosmology, using (3.2.5)

$$\frac{a''}{a} = \frac{H_M^2}{2\,a(\eta)}\Big[1 + 4sa^3(\eta)\Big]\,. \tag{3.3.6}$$

Quantization:

We begin with the quantization of free fields [28, 87, 149, 158, 29] ($\lambda = 0$) as a prelude

to the interacting theory. The Heisenberg equations of motion for the conformally rescaled fields in conformal time are

$$\frac{d^2}{d\eta^2}\,\chi_j(\vec{x},\eta) - \nabla^2\chi_j(\vec{x},\eta) + \mathcal{M}_j^2(\eta)\,\chi_j(\vec{x},\eta) = 0 \;\;;\;\; j = 1,2\,. \tag{3.3.7}$$

It is convenient to consider the spatial Fourier transform in a comoving volume V, namely,

$$\chi(\vec{x},\eta) = \frac{1}{\sqrt{V}}\sum_{\vec{k}}\chi_{\vec{k}}(\eta)\,e^{-i\vec{k}\cdot\vec{x}}\,, \tag{3.3.8}$$

leading to

$$\frac{d^2}{d\eta^2}\,\chi_{\vec{k}}(\eta) + \left[\omega_k^2(\eta) - \frac{a''}{a}\,(1-6\xi_j)\right]\chi_{\vec{k}}(\vec{k},\eta) = 0 \;\;;\;\; \omega_k^2(\eta) = k^2 + m_j^2\,a^2(\eta)\,, \tag{3.3.9}$$

for either field, respectively.

Although solutions of (3.3.9) can be found for separate stages or model expansion histories[133, 135], solving for the exact mode functions for the standard cosmology with the different stages, even when neglecting the term with a''/a, is not feasible. Instead we focus on obtaining approximate solutions in an adiabatic expansion[28, 87, 149, 158, 29, 64, 65, 193] that relies on a separation of time scales between those of the particle physics process and that of the cosmological expansion. As an example, let us consider a physically motivated setting wherein the decaying particle has been produced ("born") early during the radiation dominated stage by the decay of heavier particle states at the Grand Unification (GUT) scale $\simeq 10^{15}\,\mathrm{GeV}$. Assuming that the mass of the (DM) particle is much smaller than this scale, the production process will endow the (DM) particle with a *physical* momentum $k_p(\eta) = k/a(\eta) \simeq 10^{15}\,\mathrm{GeV}$ with k being the *comoving* momentum. If the environmental temperature of the plasma is $T \simeq T_{\mathrm{GUT}} \simeq 10^{15}\,\mathrm{GeV}$ and neglecting the processes that reheat the photon bath by entropy injection from massive degrees of freedom, then $T_{\mathrm{GUT}} \simeq T_{\mathrm{CMB}}/a(\eta_i)$ implying that the scale factor at the GUT scale $a(\eta_i) \simeq 10^{-28}$. In turn this estimate implies that the *comoving* wavevector k with which the (DM) is produced is $k \simeq 10^{-13}\,\mathrm{GeV}$.

The result (3.3.6) suggests that when considering initial conditions at the GUT scale (or below) corresponding to $a(\eta_i) \geq 10^{-28}$ the term a''/a in (3.3.9) can be neglected for $\omega_k(\eta_i) \gg 10^{-30}\,\mathrm{GeV}$ for scalar fields minimally coupled to gravity (or for any $|\xi_j| \simeq \mathcal{O}(1)$),

since $\omega_k^2(\eta_i) \gg \frac{H_m^2}{2a(\eta_i)}$. This condition is most certainly realized for particles produced from processes at the GUT scale, since as argued above such processes would yield comoving wavectors $k \simeq 10^{-13}\,\mathrm{GeV}$, hence $\omega_k(\eta_i) \geq 10^{-13}\,\mathrm{GeV}$ for (DM) particles (or daughters) with masses below the GUT scale. Therefore under these conditions we can safely ignore the term with a''/a in (3.3.9). Below (see eqn. (3.3.26) and following comments) we show explicitly that this term is of second order in the adiabatic expansion and can be ignored to leading order. The mode equations (3.3.9) now become

$$\frac{d^2}{d\eta^2}\,\chi_{\vec{k}}(\eta) + \omega_k^2(\eta)\,\chi_{\vec{k}}(\eta) = 0\,. \tag{3.3.10}$$

Field quantization is achieved by writing

$$\chi_{\vec{k}} = a_{\vec{k}}\,g_k(\eta) + a^{\dagger}_{-\vec{k}}\,g_k^*(\eta)\,, \tag{3.3.11}$$

where the mode functions $g_k(\eta)$ obey the equation of motion

$$\frac{d^2}{d\eta^2}\,g_k(\eta) + \omega_k^2(\eta)\,g_k(\eta) = 0\,, \tag{3.3.12}$$

with the Wronskian condition

$$g_k^{'}(\eta)g_k^*(\eta) - g_k^{*\,'}(\eta)g_k(\eta) = -i \tag{3.3.13}$$

so that the annihilation $a_{\vec{k}}$ and creation $a^{\dagger}_{\vec{k}}$ operators are *time independent* and obey the canonical commutation relations $[a_{\vec{k}}, a^{\dagger}_{\vec{k}'}] = \delta_{\vec{k},\vec{k}'}$.

Writing the solution of this equation in the WKB form[28, 87, 149, 158, 29]

$$g_k(\eta) = \frac{e^{-i\int_{\eta_i}^{\eta} W_k(\eta')\,d\eta'}}{\sqrt{2\,W_k(\eta)}}\,, \tag{3.3.14}$$

and inserting this ansatz into (3.3.10) it follows that $W_k(\eta)$ must be a solution of the equation[28]

$$W_k^2(\eta) = \omega_k^2(\eta) - \frac{1}{2}\left[\frac{W_k^{''}(\eta)}{W_k(\eta)} - \frac{3}{2}\left(\frac{W_k^{'}(\eta)}{W_k(\eta)}\right)^2\right]. \tag{3.3.15}$$

This equation can be solved in an *adiabatic expansion*

$$W_k^2(\eta) = \omega_k^2(\eta)\left[1 - \frac{1}{2}\,\frac{\omega_k^{''}(\eta)}{\omega_k^3(\eta)} + \frac{3}{4}\left(\frac{\omega_k^{'}(\eta)}{\omega_k^2(\eta)}\right)^2 + \cdots\right]. \tag{3.3.16}$$

We refer to terms that feature n-derivatives of $\omega_k(\eta)$ as of n-th adiabatic order. The nature and reliability of the adiabatic expansion is revealed by considering the term of first adiabatic order for generic mass m:

$$\frac{\omega_k^{'}(\eta)}{\omega_k^2(\eta)} = \frac{m^2\, a(\eta) a^{'}(\eta)}{\Big[k^2 + m^2\, a^2(\eta)\Big]^{3/2}}\,, \tag{3.3.17}$$

this is most easily recognized in *comoving* time t, introducing the *local* energy $E_k(t)$ and Lorentz factor $\gamma_k(t)$ measured by a comoving observer in terms of the *physical* momentum $k_p(t) = k/a(t)$

$$E_k(t) = \sqrt{k_p^2(t) + m^2} \tag{3.3.18}$$

$$\gamma_k(t) = \frac{E_k(t)}{m}\,, \tag{3.3.19}$$

and the Hubble expansion rate $H(t) = \frac{\dot{a}(t)}{a(t)} = a^{'}/a^2$. In terms of these variables, the first order adiabatic ratio (3.3.17) becomes

$$\frac{\omega_k^{'}(\eta)}{\omega_k^2(\eta)} = \frac{H(t)}{\gamma_k^2(t)\, E_k(t)}\,. \tag{3.3.20}$$

In similar fashion the higher order terms in the adiabatic expansion can be constructed as well:

$$\begin{aligned}\frac{\omega_k^{''}(\eta)}{\omega_k^3(\eta)} &= \frac{m^2\big((a^{'}(\eta))^2 + a(\eta)a^{''}(\eta)\big)}{\omega_k^4(\eta)} - \frac{m^4 a^2(\eta)(a^{'}(\eta))^2}{\omega_k^6(\eta)} \\ &= \frac{1}{\gamma_k^2(t)}\Big(\frac{R(t)}{6E_k^2(t)} + \frac{H^2(t)}{E_k^2(t)}\Big) - \frac{H^2(t)}{\gamma_k^4(t) E_k^2(t)}\,,\end{aligned} \tag{3.3.21}$$

where $R(t)$ is the Ricci scalar (3.3.2). Consequently, (3.3.16) takes the form:

$$W_k^2(t) = a^2(t) E_k^2(t)\Big[1 - \frac{1}{2\gamma_k^2(t)}\Big(\frac{R(t)}{6E_k^2(t)} + \frac{H^2(t)}{E_k^2(t)}\Big) + \frac{5}{4}\frac{H^2(t)}{\gamma_k^4(t) E_k^2(t)} + \cdots\Big]\,. \tag{3.3.22}$$

Consider that the decaying (parent) particle is produced during the radiation dominated stage at the GUT scale with $T \simeq 10^{15}\,\mathrm{GeV}$, with $m \ll T$ and $k_p \simeq T$ corresponding to $E_k(t) \simeq T$ and $\gamma_k \gg 1$ (ultrarelativistic). With the number of ultrarelativistic degrees of freedom $g_{\rm eff} \simeq 100$ the expansion rate is

$$H(t) \simeq 1.66\sqrt{g_{\rm eff}}\,\frac{T^2(t)}{M_{\rm Pl}} \simeq 10^{-2}\, T(t)\,, \tag{3.3.23}$$

and it follows that

$$\frac{\omega_k^{'}(\eta)}{\omega_k^2(\eta)} \ll 1\,. \tag{3.3.24}$$

This analysis clarifies the separation of scales: the Hubble expansion rate $H(t) \ll E_k(t)$, namely there are many oscillations of the field during a Hubble time and the ratio is further suppressed by large local Lorentz factors. This ratio becomes smaller as the scale factor grows and the Hubble rate slows, thereby improving the reliability of the adiabatic expansion. For example, today $H(t_0) \simeq H_0 \simeq 10^{-42}\,\mathrm{GeV}$, which is much smaller than the typical particle physics scales even for very light axion-like (DM) candidates.

Therefore we adopt the ratio

$$\frac{H(t)}{E_k(t)} \ll 1\,, \tag{3.3.25}$$

as the small, dimensionless *adiabatic* expansion parameter. The physical interpretation of this (small) ratio is clear: typical particle physics degrees of freedom feature wavelengths that are much smaller than the particle horizon proportional to the Hubble radius at any given time (see discussion section below for caveats).

Consequently, when considering the term a''/a in the equation of motion (3.3.9), we find that

$$\frac{a''}{a\,\omega_k^2} = 2\Big(\frac{\dot{H}}{2\,E_k^2} + \frac{H^2}{E_k^2}\Big) = \alpha\,\frac{H^2}{E_k^2} \quad ; \quad \alpha \simeq 0 \quad (RD)\;;\; \alpha \simeq \frac{1}{2} \quad (MD)\,. \tag{3.3.26}$$

Therefore the ratio $a''/\omega_k^2 a$ is of second adiabatic order and can be safely neglected to the leading adiabatic order which we will pursue in this study, justifying the simplification of the mode equations to (3.3.10).

In this article we consider the zeroth-adiabatic order with the mode functions given by

$$g_k(\eta) = \frac{e^{-i\,\int_{\eta_i}^{\eta}\,\omega_k(\eta')\,d\eta'}}{\sqrt{2\,\omega_k(\eta)}} \tag{3.3.27}$$

postponing to future study higher adiabatic corrections (see discussion section below). The phase of the mode function has an immediate interpretation in terms of comoving time and the local comoving energy (3.3.18), namely

$$e^{-i\,\int_{\eta_i}^{\eta}\,\omega_k(\eta')\,d\eta'} = e^{-i\,\int_{t_i}^{t}\,E_k(t')\,dt'}\,, \tag{3.3.28}$$

which is a natural and straighforward generalization of the phase of *positive frequency particle states in Minkowski space-time*.

3.4 Particle interpretation: Adiabatic Hamiltonian

Unlike in Minkowski space-time where the full Lorentz group unambiguously leads to a description of particle states associated with Fock states that transform irreducibly and are characterized by mass and spin, the definition of particle states in an expanding cosmology without a global time-like Killing vector is more subtle[28, 87, 149, 158, 29, 153].

Our goal is to study particle decay implementing the adiabatic approximation described above, focusing on the leading, zeroth order contribution with the mode functions (3.3.27). Field quantization in terms of these modes entail that the creation and annihilation operators of the adiabatic particle states depend on time so that the quantum field obeys the (free field) Heisenberg equations of motion. Passing to the interaction picture to obtain the transition amplitudes and probabilities, we would need the explicit time dependence of the creation and annihilation operators. In this section we show explicitly that to leading adiabatic order the operators that create and annihilate the adiabatic states are *time independent*. This is an important simplification that allows the calculation of matrix elements in a straightforward manner.

In order to establish a clear identification of the zeroth order adiabatic modes with particles we analyze the free-field Hamiltonian, which in terms of the conformally rescaled field operators is given by

$$H(\eta) = \frac{1}{2}\int d^3x \left\{\pi^2 + (\nabla\chi)^2 + \mathcal{M}^2(\eta)\chi^2\right\}. \tag{3.4.1}$$

Writing the field operators in terms of their Fourier expansions, we have

$$\chi(\vec{x},\eta) = \frac{1}{\sqrt{V}}\sum_k [a_k g_k(\eta)e^{i\vec{k}\cdot\vec{x}} + a_k^\dagger g_k^*(\eta)e^{-i\vec{k}\cdot\vec{x}}], \tag{3.4.2}$$

$$\pi(\vec{x},\eta) = \chi'(\vec{x},\eta) = \frac{1}{\sqrt{V}}\sum_k [a_k g_k'(\eta)e^{i\vec{k}\cdot\vec{x}} + a_k^\dagger g_k^{*\prime}(\eta)e^{-i\vec{k}\cdot\vec{x}}]. \tag{3.4.3}$$

Integrating over d^3x, gathering terms and neglecting the term a''/a in (3.3.9) as discussed above, we find

$$H(\eta) = \frac{1}{2}\sum_k \Big\{ a_k^\dagger a_k \big(|g_k'|^2 + \omega_k^2(\eta)\,|g_k|^2\big) + a_k a_{-k}\big((g_k')^2 + \omega_k^2(\eta)(g_k)^2\big) + h.c.\Big\} \tag{3.4.4}$$

$$\equiv \frac{1}{2}\sum_k \Big\{ \Omega_k(\eta)a_k^\dagger a_k + \Delta_k(\eta)a_k a_{-k} + h.c.\Big\}. \tag{3.4.5}$$

We can now expand these coefficients $\Omega_k(\eta)$ and $\Delta_k(\eta)$ in terms of the functions $W_k(\eta)$ by using the explicit form of the mode functions

$$g_k(\eta) = \frac{e^{-i\int^\eta W_k(\eta')\,d\eta'}}{\sqrt{2W_k(\eta)}}\,;\; g_k'(\eta) = -iW_k(\eta)g_k(\eta)\Big[1 - i\frac{W_k'(\eta)}{2W_k^2(\eta)}\Big] \tag{3.4.6}$$

and using the relation (3.3.15) the frequencies $\Omega_k(\eta); \Delta_k(\eta)$ can be written as

$$\Omega_k(\eta) = |g_k|^2\Big(2W_k^2 + \frac{W_k''}{2W_k} - \frac{W_k'^2}{2W_k^2}\Big), \quad \Delta_k(\eta) = (g_k)^2\Big(\frac{W_k''}{2W_k} - \frac{W_k'^2}{2W_k^2} - iW_k'\Big). \tag{3.4.7}$$

It is convenient to introduce

$$\alpha_k(\eta) \equiv \frac{W_k''}{2W_k} - \frac{W_k'^2}{2W_k^2}\,, \tag{3.4.8}$$

which allows us to rewrite the Hamiltonian as

$$H(\eta) = \frac{1}{2}\sum_k \begin{pmatrix} a_k^\dagger & a_{-k}\end{pmatrix}\begin{pmatrix} |g_k|^2(\alpha_k + 2W_k^2) & (g_k^*)^2(\alpha_k + iW_k') \\ (g_k)^2(\alpha_k - iW_k') & |g_k|^2(\alpha_k + 2W_k^2)\end{pmatrix}\begin{pmatrix} a_k \\ a_{-k}^\dagger\end{pmatrix} \tag{3.4.9}$$

This Hamiltonian can be diagonalized by a time-dependent Bogoliubov transformation. We do this in two steps. First we write

$$\tilde{a}_k(\eta) = a_k\, e^{-i\int^\eta W_k(\eta')\,d\eta'}\, e^{-i\theta_k(\eta)/2}\,, \tag{3.4.10}$$

and choose $\theta_k(\eta)$ to absorb the phase of Δ_k, i.e., $\tan\theta_k(\eta) = W_k'(\eta)/\alpha_k(\eta)$. Then

$$H(\eta) = \frac{1}{2}\sum_k \begin{pmatrix} \tilde{a}_k^\dagger & \tilde{a}_{-k}\end{pmatrix}\begin{pmatrix} \Omega_k(\eta) & |\Delta_k|(\eta) \\ |\Delta_k|(\eta) & \Omega_k(\eta)\end{pmatrix}\begin{pmatrix} \tilde{a}_k \\ \tilde{a}_{-k}^\dagger\end{pmatrix}, \tag{3.4.11}$$

where

$$\Omega_k(\eta) = \frac{1}{2W_k}(\alpha_k(\eta) + 2W_k^2(\eta)) \;\;;\;\; |\Delta_k| = \frac{1}{2W_k}\sqrt{\alpha_k^2(\eta) + (W_k'(\eta))^2}\,. \tag{3.4.12}$$

We introduce the Bogoliubov transformation to a new set of creation and annihilation operators $\hat{b}_{\vec{k}}^\dagger$, $\hat{b}_{\vec{k}}$ as

$$\tilde{a}_{\vec{k}}^\dagger = u_k(\eta)\,\hat{b}_{\vec{k}}^\dagger + v_k\,(\eta)\hat{b}_{-\vec{k}} \;\;;\;\; \tilde{a}_{\vec{k}} = u_k(\eta)\,\hat{b}_{\vec{k}} + v_k(\eta)\,\hat{b}^\dagger{}_{-\vec{k}}\,, \tag{3.4.13}$$

noting that u_k, v_k are real functions of η and $|\vec{k}|$ only. For the $\hat{b}_{\vec{k}}$, $\hat{b}^\dagger_{\vec{k}}$ to obey the canonical commutation relations, it follows that $u_k^2 - v_k^2 = 1$. Then the Hamiltonian can be written

$$H(\eta) = \frac{1}{2}\sum_k \begin{pmatrix} \hat{b}^\dagger_{\vec{k}} & \hat{b}_{-\vec{k}} \end{pmatrix} \begin{pmatrix} u_k & v_k \\ v_k & u_k \end{pmatrix} \begin{pmatrix} \Omega_k & |\Delta_k| \\ |\Delta_k| & \Omega_k \end{pmatrix} \begin{pmatrix} u_k & v_k \\ v_k & u_k \end{pmatrix} \begin{pmatrix} \hat{b}_{\vec{k}} \\ \hat{b}^\dagger_{-\vec{k}} \end{pmatrix} \tag{3.4.14}$$

$$= \frac{1}{2}\sum_k \begin{pmatrix} \hat{b}^\dagger_{\vec{k}} & \hat{b}_{-\vec{k}} \end{pmatrix} \begin{pmatrix} (u_k^2+v_k^2)\Omega_k + 2u_kv_k|\Delta_k| & (u_k^2+v_k^2)|\Delta_k| + 2u_kv_k\Omega_k \\ (u_k^2+v_k^2)|\Delta_k| + 2u_kv_k\Omega_k & (u_k^2+v_k^2)\Omega_k + 2u_kv_k|\Delta_k| \end{pmatrix} \begin{pmatrix} \hat{b}_{\vec{k}} \\ \hat{b}^\dagger_{-\vec{k}} \end{pmatrix}, \tag{3.4.15}$$

and the u_k and v_k chosen to make off-diagonal terms vanish. Then writing $u_k = \cosh\phi_k$ and $v_k = \sinh\phi_k$, we find

$$\tanh 2\phi_k = -\frac{|\Delta_k|}{\Omega_k}. \tag{3.4.16}$$

In the second step we absorb the fast phases into the redefinition

$$\hat{b}_{\vec{k}} = e^{-i\int^\eta W_k(\eta')\,d\eta'}\, b_{\vec{k}} \;\;;\;\; \hat{b}^\dagger_{\vec{k}} = e^{i\int^\eta W_k(\eta')\,d\eta'}\, b^\dagger_{\vec{k}}, \tag{3.4.17}$$

in terms of which the Hamiltonian can be written as

$$H(\eta) = \sum_k \omega_k(\eta)\Big(b^\dagger_{\vec{k}}(\eta)_{\vec{k}}\, b_{\vec{k}}(\eta) + \tfrac{1}{2}\Big). \tag{3.4.18}$$

This is a remarkable result: the new operators $b^\dagger_{\vec{k}}, b_{\vec{k}}$ define a Fock Hilbert space of *adiabatic eigenstates*, the exact frequencies of which are the *zeroth order adiabatic frequencies* $\omega_k(\eta) = \sqrt{k^2 + m^2\,a^2(\eta)}$. We emphasize that $b^\dagger_{\vec{k}}(\eta), b_{\vec{k}}(\eta)$ depend explicitly on time because the Bogoliubov coefficients $u_k(\eta), v_k(\eta)$ depend on time, while the original operators $a_{\vec{k}}, a^\dagger_{\vec{k}}$ are time independent in the Heisenberg picture. This is also clear by inverting the relations (3.4.13), and using (3.4.10) the redefinition (3.4.17) along with $u_k^2 - v_k^2 = 1$, we find

$$b^\dagger_{\vec{k}}(\eta) = u_k(\eta)\, e^{-i\theta_k(\eta)/2}\, a^\dagger_{\vec{k}} + v_k(\eta)\, e^{i\theta_k(\eta)/2}\, e^{-2i\int^\eta W_k(\eta')\,d\eta'}\, a_{-\vec{k}} \tag{3.4.19}$$

$$b_{\vec{k}}(\eta) = u_k(\eta)\, e^{i\theta_k(\eta)/2}\, a_{\vec{k}} + v_k(\eta)\, e^{-i\theta_k(\eta)/2}\, e^{2i\int^\eta W_k(\eta')\,d\eta'}\, a^\dagger_{-\vec{k}}. \tag{3.4.20}$$

Using (3.3.15) and the adiabatic expansion (3.3.16) it is straightforward to find that

$$u_k(\eta) = 1 + \mathcal{O}\Big((\omega_k'(\eta))^2, \omega_k''(\eta)\Big) \;\;;\;\; v_k(\eta) \simeq \mathcal{O}\Big((\omega_k'(\eta))^2, \omega_k''(\eta)\Big). \tag{3.4.21}$$

Hence, *to zeroth order in the adiabatic expansion* $b_{\vec{k}} = a_{\vec{k}}$ and the annihilation and creation operators of *adiabatic particle* states are independent of time. Time dependence of the operators $b_{\vec{k}}, b^{\dagger}_{\vec{k}}$ emerges at *second order* in the adiabatic expansion.

Therefore, the study in this section justifies our identification of particle states to leading (zeroth) order in the adiabatic expansion, namely the *time independent* operators $a^{\dagger}, a$ create and annihilate zeroth order adiabatic particle states of time dependent frequency $\omega_k(\eta)$. This is important because below we cast the interaction picture in terms of these operators and the mode functions $g_k(\eta)$. The analysis above explicitly shows the consistency of this approach to leading order in the adiabatic approximation. In higher order the time evolution of the operators $b, b^{\dagger}$ entail particle production[153, 28, 87, 149, 158, 29, 64, 65, 193], an important aspect that will be relegated to future study (see discussion section below). In the analysis that follows we will consider the leading (zeroth) order adiabatic modes.

3.5 The Interaction Picture in Cosmology

The creation and annihilation operators $a_{\vec{k}}, a^{\dagger}_{\vec{k}}$ for each respective field define Fock states, with a vacuum state $|0\rangle$ defined by $a_{\vec{k}}|0\rangle = 0$. Since to leading order in the adiabatic approximation $a, a^{\dagger}$ coincide with $b, b^{\dagger}$ associated with single particle adiabatic states, it follows that $a^{\dagger}_{\vec{k}}|0\rangle$ are identified (to this order) with the single particle states associated with the mode functions(3.3.27).

In the Schrödinger picture, quantum states obey

$$i\frac{d}{d\eta}|\Psi(\eta)\rangle = H(\eta)|\Psi(\eta)\rangle\,, \tag{3.5.1}$$

where in general the Hamiltonian carries explicit η dependence. The solution of (3.5.1) is given in terms of the unitary time evolution operator $U(\eta, \eta_0)$, taking the particular form $|\Psi(\eta)\rangle = U(\eta, \eta_0)|\Psi(\eta_0)\rangle$. Therefore, $U(\eta, \eta_0)$ obeys

$$i\frac{d}{d\eta}U(\eta, \eta_0) = H(\eta)U(\eta, \eta_0) \;\;;\;\; U(\eta_0, \eta_0) = 1\,. \tag{3.5.2}$$

Consider a Hamiltonian that can be written as $H(\eta) = H_0(\eta) + H_i(\eta)$, where $H_0(\eta)$ is the free theory Hamiltonian and $H_i(\eta)$ the interaction Hamiltonian. In the absence of interactions with $H_i = 0$, the time evolution operator of the free theory $U_0(\eta, \eta_0)$ obeys

$$i\frac{d}{d\eta}U_0(\eta,\eta_0) = H_0(\eta)U_0(\eta,\eta_0), \quad -i\frac{d}{d\eta}U_0^{-1}(\eta,\eta_0) = U_0^{-1}(\eta,\eta_0)H_0(\eta), \quad U(\eta_0,\eta_0) = 1\,. \tag{3.5.3}$$

It is convenient to pass to the interaction picture, where the operators evolve with the free field Hamiltonian and the states carry the time dependence from the interaction, namely

$$|\Psi(\eta)\rangle_I = U_0^{-1}(\eta,\eta_0)\,|\Psi(\eta)\rangle\,, \tag{3.5.4}$$

and their time evolution is given by

$$|\Psi(\eta)\rangle_I = U_I(\eta,\eta_0)\,|\Psi(\eta_0)\rangle_I \;\;;\;\; U_I(\eta,\eta_0) = U_0^{-1}(\eta,\eta_0)\,U(\eta,\eta_0)\,. \tag{3.5.5}$$

The unitary time evolution operator in the interaction picture $U_I(\eta, \eta_0)$ obeys

$$i\frac{d}{d\eta}U_I(\eta,\eta_0) = H_I(\eta)U_I(\eta,\eta_0) \quad H_I(\eta) = U_0^{-1}(\eta,\eta_0)H_i(\eta)U_0(\eta,\eta_0) \;\;;\;\; U_I(\eta_0,\eta_0) = 1\,. \tag{3.5.6}$$

For the conformal action (3.3.4) it follows that

$$H_I(\eta) = \lambda\, a(\eta)\int d^3x\;\chi_1(\vec{x},\eta)\;:\chi_2^2(\vec{x},\eta):\,, \tag{3.5.7}$$

where the fields are given by the free field expansion (3.3.11) with the mode functions solutions of (3.3.12,3.3.13) and time independent creation and annihilation operators for the respective fields. The perturbative solution of eqn. (3.5.6) is

$$U_I(\eta,\eta_0) = 1 - i\int_{\eta_0}^{\eta} H_I(\eta_1)\,d\eta_1 + (-i)^2\int_{\eta_0}^{\eta}\int_{\eta_0}^{\eta_1} H_I(\eta_1)\,H_I(\eta_2)\,d\eta_1\,d\eta_2 + \cdots \tag{3.5.8}$$

Amplitudes and probabilities in perturbation theory:

Before we consider the *non-perturbative* Wigner-Weisskopf method, we study the transition amplitudes and probabilities in perturbation theory as this will yield a clear interpretation of the results.

Let us consider the amplitude for the decay process $\chi_1 \to 2\,\chi_2$ given by

$$\mathcal{A}_{1\to 22}(\eta,\eta_i) = \langle 1^{(2)}_{\vec{p}}, 1^{(2)}_{\vec{q}}|\, U_I(\eta,\eta_i)\,|1^{(1)}_{\vec{k}}\rangle\,, \tag{3.5.9}$$

where $|1^{(a)}_{\vec{p}}\rangle, a=1,2$ are the single particle states associated with the respective fields. With the expansion (3.5.8) we find to lowest order in perturbation theory,

$$\begin{aligned}\mathcal{A}_{1\to 22}(\eta,\eta_i) &= -i\lambda\int_{\eta_i}^{\eta} d\eta'\,a(\eta')\int d^3x\,\langle 1^{(2)}_{\vec{p}}, 1^{(2)}_{\vec{q}}|\chi_1(\vec{x},\eta')\,\chi_2^2(\vec{x},\eta')\,|1^{(1)}_{\vec{k}}\rangle \\ &= -2i\frac{\lambda}{V^{1/2}}\int_{\eta_i}^{\eta} d\eta'\,a(\eta')\,g^{(1)}_k(\eta')\,(g^{(2)}_p(\eta'))^*\,(g^{(2)}_q(\eta'))^*\,\delta_{\vec{k},\vec{p}+\vec{q}}\,. \end{aligned}\tag{3.5.10}$$

The total transition probability is given by

$$\mathcal{P}_{1\to 22}(\eta,\eta_i) = \frac{1}{2!}\sum_{\vec{p}}\sum_{\vec{q}}|\mathcal{A}_{1\to 22}(\eta,\eta_i)|^2\,, \tag{3.5.11}$$

and taking the continuum limit yields

$$\mathcal{P}_{1\to 22}(\eta,\eta_i) = \int_{\eta_i}^{\eta} d\eta_2\int_{\eta_i}^{\eta} d\eta_1\,\Sigma_k(\eta_2;\eta_1)\,, \tag{3.5.12}$$

where

$$\Sigma_k(\eta;\eta') = 2\lambda^2 a(\eta)\,a(\eta')\,(g^{(1)}_k(\eta))^*\,g^{(1)}_k(\eta')\int\tfrac{d^3p}{(2\pi)^3}\;g^{(2)}_p(\eta)\,g^{(2)}_q(\eta)\,(g^{(2)}_k(\eta'))^*\,(g^{(2)}_q(\eta'))^*\quad;$$
$$q = |\vec{k}-\vec{p}|\,. \tag{3.5.13}$$

Noting the property

$$(\Sigma_k(\eta;\eta'))^* = \Sigma_k(\eta';\eta)\,, \tag{3.5.14}$$

and introducing the identity $\Theta(\eta_2-\eta_1)+\Theta(\eta_1-\eta_2)=1$, relabelling terms and using the property (3.5.14), we find

$$\mathcal{P}_{1\to 22}(\eta,\eta_i) = 2\int_{\eta_i}^{\eta} d\eta_2\int_{\eta_i}^{\eta_2} d\eta_1\,\mathrm{Re}[\Sigma_k(\eta_2;\eta_1)]\,. \tag{3.5.15}$$

We define the *transition rate*

$$\Gamma(\eta) \equiv \frac{d}{d\eta}\mathcal{P}_{1\to 22}(\eta,\eta_i) = 2\int_{\eta_i}^{\eta} d\eta_1\,\mathrm{Re}[\Sigma_k(\eta;\eta_1)]\,. \tag{3.5.16}$$

We emphasize to the reader that in typical S-matrix calculations in Minkowski spacetime, the presence of a time-like Killing vector (and the implementation of the infinite time limit) lead to a *time independent transition rate* and subsequently a standard exponential decay law. In FRW spacetime, this approach is in general invalid. Rather, the transition rate introduced above will define the decay law obtained within the non-perturbative Wigner-Weisskopf framework described below.

3.6 Wigner–Weisskopf Theory in Cosmology

The quantum field theoretical Wigner-Weisskopf method has been introduced in refs.[138, 137, 37], where the reader is referred to for more details. As discussed in these references, this method is manifestly unitary and leads to a non-perturbative systematic description of transition amplitudes and probabilities directly in real time. Here we describe the main aspects of its implementation within the cosmological setting. Consider an interaction picture state $|\Psi(\eta)\rangle_I = \sum_n C_n(\eta)|n\rangle$, expanded in the Hilbert space of the free theory; these are the Fock states associated with the annihilation and creation operators $a_{\vec{k}}, a^\dagger_{\vec{k}}$ of the free field expansion (3.4.2) for each field. Inserting into (3.5.6) yields an *exact* set of coupled equations for the coefficients

$$i\frac{d}{d\eta}C_n(\eta) = \sum_m C_m(\eta)\langle n|H_I(\eta)|m\rangle. \tag{3.6.1}$$

In principle this is an infinite hierarchy of integro-differential equations for the coefficients $C_n(\eta)$; progress can be made, however, by considering states connected by the interaction Hamiltonian to a given order in the interaction. Consider that initially the state is $|A\rangle$ so that $C_A(\eta_i) = 1\,;\, C_\kappa(\eta_i) = 0$ for $|\kappa\rangle \neq |A\rangle$, and consider a first order transition process $|A\rangle \to |\kappa\rangle$ to intermediate multiparticle states $|\kappa\rangle$ with transition matrix elements $\langle\kappa|H_I(\eta)|A\rangle$. Obviously the state $|\kappa\rangle$ will be connected to other multiparticle states $|\kappa'\rangle$ different from $|A\rangle$ via $H_I(\eta)$. Hence for example up to second order in the interaction, the state $|A\rangle \to |\kappa\rangle \to |\kappa'\rangle$. Restricting the hierarchy to *first order transitions* from the initial state $|A\rangle \leftrightarrow |\kappa\rangle$ results in a coupled set of equations

$$i\frac{d}{d\eta}C_A(\eta) = \sum_\kappa C_\kappa(\eta)\langle A|H_I(\eta)|\kappa\rangle \tag{3.6.2}$$

$$i\frac{d}{d\eta}C_\kappa(\eta) = C_A(\eta)\langle\kappa|H_I(\eta)|A\rangle \;\;;\;\; C_A(\eta_i) = 1\,;\, C_\kappa(\eta_i) = 0\,. \tag{3.6.3}$$

These processes are depicted in fig. (5).

Equation (3.6.3) with $C_\kappa(\eta_i) = 0$ is formally solved by

$$C_\kappa(\eta) = -i\int_{\eta_i}^{\eta} \langle\kappa|H_I(\eta')|A\rangle\, C_A(\eta')\, d\eta'\,, \tag{3.6.4}$$

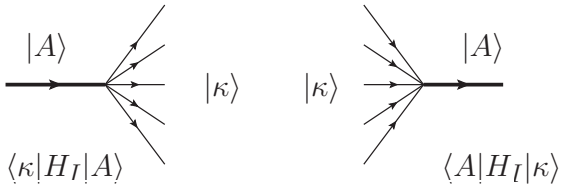

Figure 5: Transitions $|A\rangle \leftrightarrow |\kappa\rangle$ in first order in H_I.

and inserting this solution into equation (3.6.2) we find

$$\frac{d}{d\eta}C_A(\eta) = -\int_{\eta_i}^{\eta} d\eta'\, \Sigma_A(\eta,\eta')\; C_A(\eta')\,, \tag{3.6.5}$$

where we have introduced the *self-energy*

$$\Sigma_A(\eta;\eta') = \sum_{\kappa}\langle A|H_I(\eta)|\kappa\rangle\langle\kappa|H_I(\eta')|A\rangle\,. \tag{3.6.6}$$

This integro-differential equation with *memory* yields a non-perturbative solution for the time evolution of the amplitudes and probabilities. In Minkowski space-time and in frequency space, this is recognized as a Dyson resummation of self-energy diagrams, which upon Fourier transforming back to real time, yields the usual exponential decay law[138, 137, 37]. Introducing the solution for $C_A(\eta)$ back into (3.6.3) yields the build-up of the *population* of "daughter" particles.

The equation (3.6.5) is in general very difficult to solve, but progress can be made under the weak coupling assumption by invoking the *Markovian* approximation. A systematic implementation of this approximation begins by introducing

$$\mathcal{E}_A(\eta,\eta') \equiv \int_{\eta_i}^{\eta'} \Sigma_A(\eta,\eta'')\, d\eta''\,, \tag{3.6.7}$$

such that

$$\frac{d}{d\eta'}\,\mathcal{E}_A(\eta,\eta') = \Sigma_A(\eta,\eta')\,, \tag{3.6.8}$$

with the condition

$$\mathcal{E}_A(\eta,\eta_i) = 0\,. \tag{3.6.9}$$

Then (3.6.5) can be written as

$$\frac{d}{d\eta}C_A(\eta) = -\int_{\eta_i}^{\eta} d\eta' \, \frac{d}{d\eta'}\mathcal{E}_A(\eta,\eta')\, C_A(\eta') \tag{3.6.10}$$

which can be integrated by parts to yield

$$\frac{d}{d\eta}C_A(\eta) = -\mathcal{E}_A(\eta,\eta)C_A(\eta) + \int_{\eta_i}^{\eta} d\eta' \, \mathcal{E}_A(\eta,\eta')\frac{d}{d\eta'}C_A(\eta'). \tag{3.6.11}$$

Since $\mathcal{E}_A \propto \mathcal{O}(H_I^2)$ the first term on the right hand side is of order H_I^2, whereas the second is $\mathcal{O}(H_I^4)$ because $dC_A(\eta)/d\eta \propto \mathcal{O}(H_I^2)$. Therefore to leading order in the interaction, the evolution equation for the amplitude becomes

$$\frac{d}{d\eta}C_A(\eta) = -\mathcal{E}_A(\eta,\eta)C_A(\eta)\,, \tag{3.6.12}$$

with solution

$$C_A(\eta) = \exp\Big(-\int_{\eta_i}^{\eta} \mathcal{E}_A(\eta',\eta')\, d\eta'\Big)\, C_A(\eta_i)\,. \tag{3.6.13}$$

This expression clearly highlights the non-perturbative nature of the Wigner-Weisskopf approximation. The imaginary part of the self energy Σ_A yields a *renormalization* of the frequencies which we will not pursue here[37, 138, 137], whereas the real part gives the decay rate, with

$$|C_A(\eta)|^2 = e^{-\int_{\eta_i}^{\eta}\Gamma_A(\eta')d\eta'}\,|C_A(\eta_i)|^2 \quad ; \quad \Gamma_A(\eta) = 2\int_{\eta_i}^{\eta} d\eta_1\, \mathrm{Re}\,[\Sigma_A(\eta,\eta_1)]\,. \tag{3.6.14}$$

Finally, the amplitude for the decay product state $|\kappa\rangle$ is obtained by inserting the amplitude (3.6.13) into (3.6.4), and the *population* of the daughter particles is $|C_\kappa(\eta)|^2$.

In our study the state $|A\rangle$ is a single particle state of momentum $\vec{k}$ of the decaying parent particle.

3.6.1 Disconnected Vacuum Diagrams

Before we set out to obtain the self-energy and decay law for a single particle state of the field χ_1 into two particles of the field χ_2 we must clarify the nature of the vacuum diagrams. Consider the initial single particle state $|A\rangle = |1^{(1)}_{\vec{k}}\rangle$ and the set of intermediate states connected to this state by the interaction Hamiltonian to first order. There are *two different* contributions: a): the decay process $|1^{(1)}_{\vec{k}}\rangle \to |1^{(2)}_{\vec{p}}; 1^{(2)}_{\vec{k}-\vec{p}}\rangle$ in which the initial state is annihilated and the two particle state produced, and b): a *four particle state* in which the initial state evolves unperturbed and a *three particle state* $|1^{(2)}_{\vec{p}}; 1^{(2)}_{\vec{q}}; 1^{(1)}_{-\vec{p}-\vec{q}}\rangle$ is created out of the vacuum by the perturbation. These contributions are depicted in fig. (6).

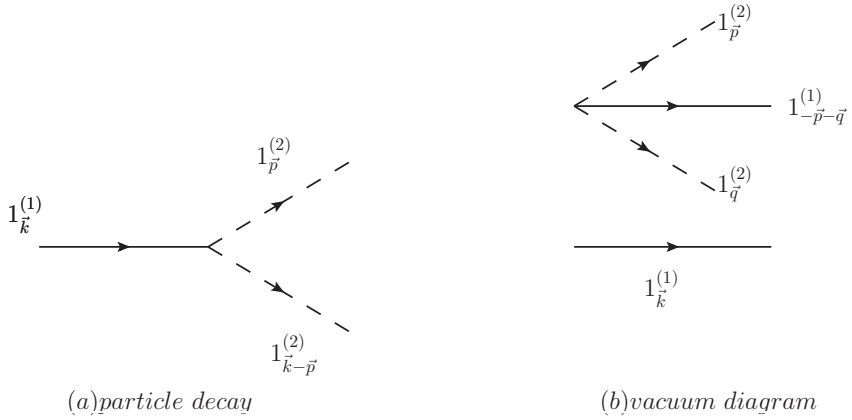

Figure 6: Decay and vacuum diagrams for $|A\rangle = |1^{(1)}_{k}\rangle$ to first order in H_I. Solid lines single particle states of the field χ_1, dashed lines are single particle states of the field χ_2.

These processes yield two different contributions to $\sum_\kappa \langle 1^{(1)}_{\vec{k}}|H_I(\eta)|\kappa\rangle\langle\kappa|H_I(\eta')|1^{(1)}_{\vec{k}}\rangle$, depicted in fig. (7).

The second disconnected diagram (b) corresponds to the "dressing" of the vacuum. This is clearly understood by considering the initial state to be the non-interacting vacuum state $|0\rangle$; it is straightforward to repeat the analysis above to obtain the closed set of leading order equations that describe the build-up of the full interacting vacuum state. One finds that diagram (b) without the non-interacting single particle state precisely describes the "dressing" of the vacuum state. Clearly, similar disconnected diagrams enter the evolution of *any* initial state. In the case under consideration, namely the decay of single particle

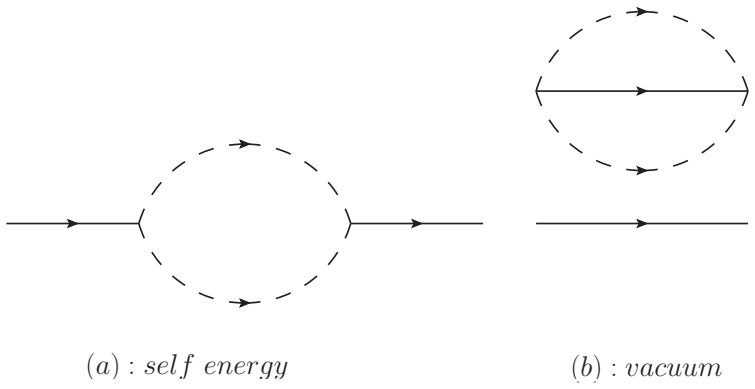

Figure 7: Contributions to the self-energy for decay (a) and vacuum diagram (b) for $|A\rangle = |1_k^{(1)}\rangle$ to first order in H_I with the same notation as in fig.(6).

states, the disconnected diagram (b) *does not* contribute to the decay but to the definition of a single particle state obtained out of the full vacuum state. In S-matrix theory these disconnected diagrams are cancelled by dividing *all transition matrix elements* by $\langle 0|S|0\rangle$. Within the Wigner-Weisskopf framework, we write the amplitude for the single particle state $|A\rangle = |1_{\vec{k}}^{(1)}\rangle$ as

$$C_A(\eta) = \tilde{C}_A(\eta)\, \tilde{C}_0(\eta) \tag{3.6.15}$$

where $\widetilde{C}_0(\eta)$ is the amplitude for the interacting vacuum state obeying

$$\frac{d}{d\eta}\tilde{C}_0(\eta) = -\mathcal{E}_0(\eta,\eta)\, \tilde{C}_0(\eta)\,, \tag{3.6.16}$$

where

$$\mathcal{E}_0(\eta,\eta') \equiv \int_{\eta_i}^{\eta'} \Sigma_A^{(b)}(\eta,\eta'')\, d\eta''\,, \tag{3.6.17}$$

and $\Sigma_A^{(b)}(\eta,\eta'')$ is the vacuum self-energy diagram (b) in figure (7). With the total self energy given by the sum of the decay (a) and vacuum (b) diagrams as in figure (7), it follows that the amplitude $\tilde{C}_A(\eta)$ obeys

$$\frac{d}{d\eta}\tilde{C}_A(\eta) = -\mathcal{E}_A^{(a)}(\eta,\eta)\tilde{C}_A(\eta)\,, \tag{3.6.18}$$

where $\mathcal{E}_A^{(a)}$ is determined *only* by the connected (decay) self energy diagram (a). This is precisely the same as dividing by the vacuum matrix element in S-matrix theory where similar diagrams arise in Minkowski space time with a similar interpretation[37, 138, 137]. This is tantamount to redefining the single particle states as built from the full vacuum state. Therefore we neglect diagram (b). We emphasize that this is in contrast with the method proposed in ref.[133, 135] wherein following ref.[15] the disconnected diagram (b) is kept in the calculation of the decay process.

Now we are able to calculate the general form of the decay law by considering the decay process $\chi_1 \to 2\chi_2$ in the interacting theory with $H_I(\eta)$ given by (3.5.7) to leading order in λ and keeping only the connected diagrams.

The initial state corresponds to single particle state of the χ_1 field $|A\rangle = |1_k^{(1)}\rangle$, and the decay process corresponds to a transition to the state $|\kappa\rangle = |1_{\vec{p}}^{(2)}; 1_{\vec{q}}^{(2)}\rangle$. Then

$$\begin{aligned}
\langle 1_{\vec{p}}^{(2)}; 1_{\vec{q}}^{(2)}|H_I(\eta')|1_k^{(1)}\rangle &= \frac{2\lambda\, a(\eta')}{V^{1/2}} g_k^{(1)}(\eta') g_p^{(2)*}(\eta') g_q^{(2)*}(\eta')\, \delta_{\vec{k},\vec{p}+\vec{q}}, \\
\langle 1_k^{(1)}|H_I(\eta)|1_{\vec{p}}^{(2)}; 1_{\vec{q}}^{(2)}\rangle &= \frac{2\lambda\, a(\eta)}{V^{1/2}} g_k^{(1)*}(\eta) g_p^{(2)}(\eta) g_q^{(2)}(\eta)\, \delta_{\vec{k},\vec{p}+\vec{q}}\,. \qquad (3.6.19)
\end{aligned}$$

Taking the continuum limit, summing over intermediate states, and accounting for the Bose symmetry factor in the final states yields

$$\begin{aligned}
\Sigma_k(\eta,\eta') &= \frac{1}{2!}\sum_{\vec{p},\vec{q}} \langle 1_k^{(1)}|H_I(\eta)|1_{\vec{p}}^{(2)}; 1_{\vec{q}}^{(2)}\rangle \langle 1_{\vec{p}}^{(2)}; 1_{\vec{q}}^{(2)}|H_I(\eta')|1_k^{(1)}\rangle \\
&= \frac{4\lambda^2}{2!} a(\eta)a(\eta') g_k^{(1)}(\eta')\, (g_k^{(1)}(\eta))^* \int \frac{d^3p}{(2\pi)^3}\, g_p^{(2)}(\eta)\, g_{|\vec{k}-\vec{p}|}^{(2)}(\eta)\, (g_p^{(2)}(\eta'))^*\, (g_{|\vec{k}-\vec{p}|}^{(2)}(\eta'))^* \qquad (3.6.20)
\end{aligned}$$

This is *precisely* the self-energy (3.5.13) obtained in the perturbative description of the transition probability and amplitude, equation (3.5.12), which enters in the evolution equation (3.6.5) for the single (parent) particle. Following the steps of the Markovian approximation leading up to the final result (7.1.1), we find

$$|C_A(\eta)|^2 = |C_A(\eta_i)|^2\, \exp\left(-\int_{\eta_i}^{\eta} \Gamma_k(\eta')d\eta'\right) \;\; ; \;\; \Gamma_k(\eta') = 2\int_{\eta_i}^{\eta'} d\eta''\, \mathrm{Re}\,\Sigma_k(\eta',\eta'')\,. \qquad (3.6.21)$$

This expression for the probability makes manifest the *non-perturbative* nature of the Wigner-Weisskopf method.

3.7 Decay Law in Leading Adiabatic Order

In this article we study the decay law in the theory described above to leading adiabatic order, namely zeroth order. The study of higher adiabatic order effects, primarily associated with the production of particles by the cosmological expansion, is relegated to a future article (see discussion section below).

In the leading (zeroth) order adiabatic approximation the mode functions are given by

$$g_k(\eta) = \frac{e^{-i\int_{\eta_i}^{\eta}\omega_k(\eta')d\eta'}}{\sqrt{2\omega_k(\eta)}}, \quad \omega_k(\eta') = \sqrt{k^2 + m^2a^2(\eta')}\,, \tag{3.7.1}$$

and Σ_k takes the following form

$$\Sigma_k(\eta,\eta') = \frac{2\lambda^2\, a(\eta)a(\eta')}{\sqrt{2\omega_k^{(1)}(\eta)2\omega_k^{(1)}(\eta')}} \int \frac{d^3p}{(2\pi)^3} \frac{e^{i\int_{\eta'}^{\eta}\left[\omega_k^{(1)}(\eta'')-\omega_p^{(2)}(\eta'')-\omega_q^{(2)}(\eta'')\right]d\eta''}}{\sqrt{2\omega_p^{(2)}(\eta)2\omega_p^{(2)}(\eta')2\omega_q^{(2)}(\eta)2\omega_q^{(2)}(\eta')}}\,, \tag{3.7.2}$$

where $q = |\vec{k} - \vec{p}|$. Obviously even to this order both the time and momentum integrals are daunting. However, progress is made by first considering the case of a massive parent particle decaying into two massless daughter particles. This study will reveal a path forward to the more general case of all massive particles.

3.7.1 Massive Parent, Massless Daughters in RD Cosmology

Setting $m_2 = 0$, the self energy becomes

$$\Sigma_k(\eta,\eta') = \frac{2\lambda^2\, a(\eta)a(\eta')\, e^{i\int_{\eta'}^{\eta}\omega_k(\eta'')d\eta''}}{\sqrt{2\omega_k^{(1)}(\eta)2\omega_k^{(1)}(\eta')}} \int \frac{d^3p}{(2\pi)^3} \frac{e^{-i(p+q)(\eta-\eta')}}{2p\,2q} \quad ; \quad q = |\vec{k} - \vec{p}|\,. \tag{3.7.3}$$

The momentum integral in (3.7.3) is carried out *exactly* by introducing a convergence factor after which it becomes

$$I = \frac{1}{16\pi^2}\int_0^\infty \frac{p^2\,dp}{p}\int_{-1}^{1}\frac{d(\cos(\theta))}{q}\, e^{-i(p+q)(s-i\epsilon)},\ \epsilon\to 0^+, \quad s \equiv \eta - \eta' \tag{3.7.4}$$

Changing integration variables from $d(\cos(\theta))$ to $q = |\vec{k} - \vec{p}|$ this integral becomes

$$I = \frac{1}{16\pi^2 k}\int_0^\infty dp\, e^{-ip(s-i\epsilon)}\int_{|k-p|}^{|k+p|} dq\, e^{-iq(s-i\epsilon)} \quad = \frac{-ie^{-ik\,(\eta-\eta')}}{16\pi^2(\eta-\eta'-i\epsilon)} \quad ; \quad \epsilon\to 0^+\,, \tag{3.7.5}$$

yielding

$$\Sigma_k(\eta,\eta') = \frac{\lambda^2\, a(\eta)\, a(\eta')\; e^{i\int_{\eta'}^{\eta}\omega_k(\eta'')\,d\eta''}\; e^{-ik(\eta-\eta')}}{16\pi^2\;\sqrt{\omega_k^{(1)}(\eta)\,\omega_k^{(1)}(\eta')}}\;\;\left[-iP\Big(\frac{1}{\eta-\eta'}\Big)+\pi\delta(\eta-\eta')\right], \tag{3.7.6}$$

where the Sokhotski-Plemelj theorem has been used in the last line. This expression is similar to that obtained in appendix (A.1) in Minkowski space-time, where the scale factor is set to one and the frequencies are time independent (see eqn. (A.1.3)). The explicit time dependence obtained in Minkowski space-time in appendix (A.1) *cannot* be gleaned in the usual calculations of decay rates via S-matrix theory where the initial and final times are taken to $\mp\infty$, respectively.

The decay width $\Gamma_k(\eta)$ is obtained from eqn. (3.6.21), and is given by

$$\Gamma_k(\eta) = \frac{\lambda^2\, a^2(\eta)}{8\pi\,\omega_k^{(1)}(\eta)}\;\frac{1}{2}\Big[1+\mathcal{S}(\eta)\Big]\,, \tag{3.7.7}$$

where a factor of $\frac{1}{2}$ originates from the integration of the delta function in η (the "prompt" term), and

$$\mathcal{S}(\eta) = \frac{2}{\pi}\int_0^{\eta} P[\eta,\eta']\;\frac{\sin\big[A(\eta,\eta')\big]}{\eta-\eta'}\,d\eta'\,, \tag{3.7.8}$$

where we set $\eta_i = 0$ and introduce

$$P[\eta,\eta'] \;=\; \frac{a(\eta')}{a(\eta)}\left[\frac{\omega_k^{(1)}(\eta)}{\omega_k^{(1)}(\eta')}\right]^{1/2}\,, \tag{3.7.9}$$

$$A(\eta,\eta') \;=\; \int_{\eta'}^{\eta}\omega_k(\eta'')\,d\eta'' - k(\eta-\eta')\,. \tag{3.7.10}$$

The expression for $\mathcal{S}$ can be simplified substantially, revealing a hierarchy of time scales associated with the adiabatic expansion in radiation domination, during which

$$a(\eta) = H_R\,\eta \;\;;\;\; H_R = H_0\,\sqrt{\Omega_R}\,. \tag{3.7.11}$$

First we address the integral

$$J_k[\eta,\eta'] = \int_{\eta'}^{\eta}\omega_k^{(1)}(\eta'')\,d\eta'' = \int_{\eta'}^{\eta}\sqrt{k^2+m_1^2\,a^2(\eta'')}\,d\eta''\,. \tag{3.7.12}$$

To begin with we introduce the dimensionless variable (in what follows we suppress the η dependence of z to simplify notation)

$$z = \omega_k(\eta)\,\eta = E_k(t)\,a(\eta)\,\eta = \frac{E_k(t)}{H(t)} \gg 1 \tag{3.7.13}$$

where $E_k(t) = \sqrt{k_p^2(t) + m^2}$ is the physical energy measured locally by a comoving observer with $k_p(t) = k/a(\eta)$ the physical momentum, and $H(t) = a'(\eta)/a^2(\eta) = 1/(\eta\, a(\eta))$ during radiation domination, while $H(t) = 2/(\eta\, a(\eta))$ during matter domination. The dimensionless ratio (3.7.13) is the *inverse* of the adiabatic ratio $H(t)/E_k(t)$ (we have suppressed the momentum and η dependence in z to simplify notation). The inequality in (3.7.13) is a consequence of the adiabatic approximation wherein the physical wavelengths are much smaller than the Hubble radius ($\propto$ the particle horizon). Next, we write $\eta'' = \eta\left[1 - (\eta - \eta'')/\eta\right]$ and introduce

$$\omega_k^{(1)}(\eta)\,(\eta - \eta'') = x \;\;;\;\; \omega_k^{(1)}(\eta)\,(\eta - \eta') = \tau\,, \tag{3.7.14}$$

in terms of which

$$a(\eta'') = a(\eta)\Big[1 - \frac{x}{z}\Big] \;\;;\;\; a(\eta') = a(\eta)\Big[1 - \frac{\tau}{z}\Big]\,. \tag{3.7.15}$$

This relation allows us to write

$$\big(\omega_k^{(1)}(\eta'')\big)^2 = \big(\omega_k^{(1)}(\eta)\big)^2 + m_1^2 a^2(\eta)\Big[\Big(1 - \frac{x}{z}\Big)^2 - 1\Big] = \big(\omega_k^{(1)}(\eta)\big)^2\, R^2[x]\,, \tag{3.7.16}$$

where we introduced

$$R[x;\eta] = \left[1 - \frac{2\,x}{\gamma_k^2(\eta)\,z}\left(1 - \frac{x}{2z}\right)\right]^{1/2}\,, \tag{3.7.17}$$

with the local Lorentz factor given by

$$\frac{1}{\gamma_k(\eta)} = \frac{m_1\,a(\eta)}{\omega_k^{(1)}(\eta)} = \frac{m_1}{E_k^{(1)}(t)}\,. \tag{3.7.18}$$

During (RD) the Lorentz factor can be written as

$$\gamma_k(\eta) = \left[\Big(\frac{a_{nr}}{a(\eta)}\Big)^2 + 1\right]^{1/2} = \left[\Big(\frac{\eta_{nr}}{\eta}\Big)^2 + 1\right]^{1/2} \;\;;\;\; \eta_{nr} = \frac{k}{m_1\,H_R} \equiv \frac{a_{nr}}{H_R}\,, \tag{3.7.19}$$

the conformal time η_{nr} determines the time scale at which the parent particle transitions from relativistic $\eta \ll \eta_{nr}$ to non-relativistic $\eta \gg \eta_{nr}$. In the following analysis we suppress the η-dependence of γ_k, z for simplicity.

We emphasize that the relations (3.7.15,3.7.16) are *exact* in a radiation dominated cosmology. Changing integration variables from η'' to x given by (3.7.14) and using the above variables we find that the integral (3.7.12) simplifies to the following expression

$$J_k[\eta, \eta'] \equiv J_k[\tau; \eta] = \int_0^\tau \left[1 - \frac{2\,x}{\gamma_k^2\, z}\left(1 - \frac{x}{2z}\right)\right]^{1/2} dx\,, \tag{3.7.20}$$

obtaining

$$J_k[\tau; \eta] = \tau + \delta_k(\tau; \eta)\,, \tag{3.7.21}$$

where $\delta_k(\tau)$ is of adiabatic order ≥ 1 and given by

$$\delta_k(\tau;\eta) = \frac{z}{2}\left\{\left(1-\frac{2\,\tau}{z}\right)-\left(1-\frac{\tau}{z}\right) R[\tau;\eta]\right\}-\frac{z}{2\gamma_k}\,(\gamma_k^2-1)\,\ln\left[\frac{\gamma_k\, R[\tau;\eta]+\left(1-\frac{\tau}{z}\right)}{1+\gamma_k}\right], \tag{3.7.22}$$

where we recall that both z and γ_k depend explicitly on η. Inserting these results into (3.7.8,3.7.9,3.7.10), and using the new variables z, τ given by eqns. (3.7.13,3.7.14) we find

$$\mathcal{S}(\eta) = \int_0^z P[\tau;\eta]\,\frac{\sin[A(\tau;\eta)]}{\tau}\,d\tau\,, \tag{3.7.23}$$

where

$$P[\tau;\eta] = \frac{\left[1-\frac{\tau}{z}\right]}{\sqrt{R[\tau;\eta]}}\,, \tag{3.7.24}$$

and

$$A[\tau;\eta] = \tau\left[1-\left(1-\frac{1}{\gamma_k^2}\right)^{1/2}\right] + \delta_k(\tau;\eta)\,, \tag{3.7.25}$$

where the term in the bracket follows from $k/\omega_k^{(1)}(\eta) = (1-1/\gamma_k^2)^{1/2}$. The expression (3.7.23) is amenable to straightforward numerical analysis. However, before we pursue such study, it is important to recognize several features that will yield to a simplification in the general case of massive daughters. The various factors above display a hierarchy of (dimensionless)

time scales widely separated by $1/z \ll 1$ in the adiabatic approximation: the "fast" scale τ, the "slow" scale τ/z etc. It is straightforward to find that

$$\delta_k(\tau;\eta) = -\frac{\tau^2}{2\gamma_k^2\, z} + \cdots , \tag{3.7.26}$$

confirming that δ_k is of first and higher adiabatic order. This has a simple, yet illuminating interpretation in terms of an adiabatic expansion of the integral (3.7.12). If the frequencies $\omega_k^{(1)}$ were independent of time, this integral would simply be $J_k(\eta,\eta') = \omega_k^{(1)}\,(\eta-\eta') \equiv \tau$. Therefore an expansion of $J_k[\eta,\eta']$ around $\eta' = \eta$ would necessarily entail derivatives of $\omega_k^{(1)}$, namely terms of higher adiabatic order. Consider such an expansion:

$$\begin{aligned} J_k[\eta,\eta'] &= 0 + \frac{d}{d\eta'}\, J_k[\eta,\eta']\bigg|_{\eta'=\eta} (\eta-\eta') + \frac{1}{2}\,\frac{d^2}{d\eta'^{\,2}}\, J_k[\eta,\eta']\bigg|_{\eta'=\eta} (\eta-\eta')^2 + \cdots \\ &= \omega_k^{(1)}(\eta)\,(\eta-\eta') - \frac{1}{2}\omega_k^{'(1)}(\eta)\,(\eta-\eta')^2 + \cdots \end{aligned} \tag{3.7.27}$$

In terms of $\tau = \omega_k^{(1)}(\eta)\,(\eta-\eta')$, this expansion becomes

$$J_k[\eta,\eta'] = \tau - \frac{\tau^2}{2\gamma_k^2\, z} + \cdots \tag{3.7.28}$$

where we used (3.3.20) and (3.7.13). The second term is precisely the leading contribution to δ_k (3.7.26). This analysis makes explicit that an expansion of the integral (3.7.12) in powers of $\eta-\eta'$ is precisely an adiabatic expansion in terms of derivatives of the frequencies. Since the n-th power of $\eta-\eta'$ in such expansion is multiplied by the $n-1$ derivative of the frequencies, and when $(\eta-\eta')$ is replaced by $\tau/\omega_k^{(1)}(\eta)$ the $n-1$ derivative of the frequencies is divided by $(\omega_k^{(1)}(\eta))^n$ yielding a dimensionless ratio of adiabatic order $n-1$.

Let us now consider the full integral expression for $\mathcal{S}(\eta)$ given by (3.7.23) with the corresponding expressions for $P[\tau]$ and $\delta_k(\tau)$. For $z \gg 1$ the terms of the form $\tau/z, \tau^2/z^2$ will be negligible in most of the integration region but for the region of $\tau \approx z$ where these terms become of $\mathcal{O}(1)$. However, because of the factor τ in the denominator of the integrand in (3.7.23), a consequence of the momentum integration, this region is suppressed by a factor $1/z \ll 1$ yielding effectively a contribution of first (and higher) adiabatic order. Therefore the contribution from adiabatic corrections, proportional to powers of τ/z are, in

fact, subleading. This argument suggests that the *zeroth order* adiabatic approximation to $\mathcal{S}(\eta)$, namely

$$\mathcal{S}_0(\eta) = \frac{2}{\pi}\int_0^z \frac{\sin[A_0(\tau;\eta)]}{\tau}\,d\tau \quad ; \quad A_0[\tau;\eta] = \tau\left[1-\left(1-\frac{1}{\gamma_k^2}\right)^{1/2}\right], \tag{3.7.29}$$

should be a very good approximation to the full function $\mathcal{S}(\eta)$ for $z \gg 1$ with closed form expression

$$\mathcal{S}_0(\eta) = \frac{2}{\pi}\,Si[A_0(z(\eta);\eta)]\,. \tag{3.7.30}$$

where $Si[x]$ is the sine-integral function with asymptotic behavior $Si[x] \to \pi/2 - \cos(x)/x + \cdots$ as $x \to \infty$. This function rises and begins to oscillate around its asymptotic value at $x \simeq \pi$. This behavior implies that the rise-time of $Si[A_0(z;\eta)]$ to its asymptotic value in the ultrarelativistic case $\gamma_k \gg 1$ increases $\propto \gamma_k^2$. In fact one finds that the full function $\mathcal{S}(\eta)$ and its first order adiabatic approximation $\mathcal{S}_0(\eta)$ *vanish* as $\gamma_k \to \infty$. Namely, the contribution from $\mathcal{S}_0$ (and similarly from $\mathcal{S}$) is negligible while the particle is ultrarelativistic. This expectation is verified numerically.

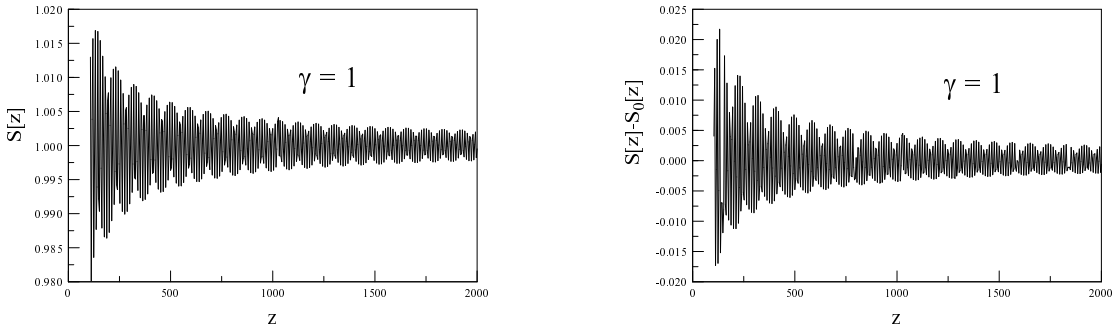

Figure 8: $S[z]$ and $S[z] - S_0[z]$ vs. z for $\gamma_k = 1$.

Figures (8,9) display $S(z)$ and $S(z) - S_0(z)$ vs. z for the non-relativistic limit $\gamma_k = 1$ and for the relativistic regime $\gamma_k = 10$. In both cases these figures confirm that the zeroth adiabatic approximation $S_0(z)$ is excellent for $z \gg 1$. They also confirm the slow rise of this

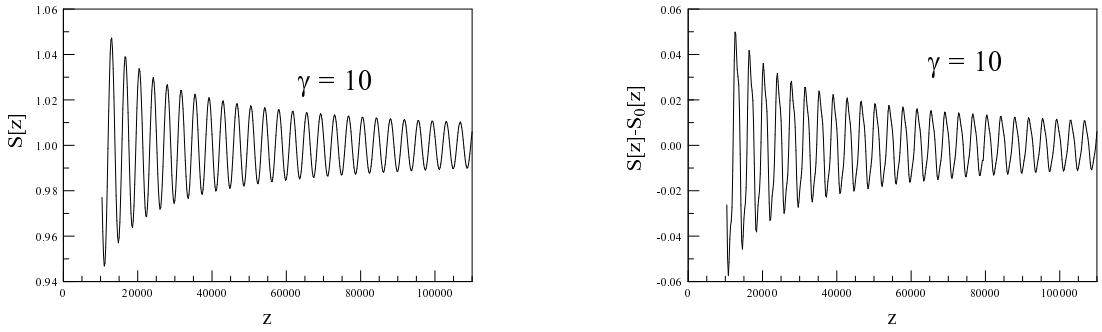

Figure 9: $S(z)$ and $S(z) - S_0(z)$ vs. z for $\gamma_k = 10$.

contribution in the ultrarelativistic case, note the scale on the horizontal axis for the case $\gamma_k = 10$ compared to that for $\gamma_k = 1$. For $\gamma_k > 1$ we have displayed the results for a fixed value of γ_k to illustrate the main behavior for the non-relativistic and relativistic limits and highlight that the relativistic case features a larger rise-time. Obviously a detailed numerical study including the η dependence of γ_k will depend on the particular values of k, m_1.

Replacing the function $\mathcal{S}(\eta)$ by the zeroth order approximation $S_0(\eta)$ is also consistent with our main approximation of keeping only the zeroth order adiabatic contribution in the mode functions. Therefore consistently with the zeroth adiabatic order, we find that the decay rate for the case of a massive parent decaying into two massless daughters is given by

$$\Gamma_k(\eta) = \frac{\lambda^2\, a^2(\eta)}{8\pi\, \omega_k^{(1)}(\eta)}\; \frac{1}{2}\left[1 + \frac{2}{\pi}\, Si[A_0(z(\eta);\eta)]\right] \quad ; \quad A_0(z(\eta);\eta) = z(\eta)\left[1 - \left(1 - \frac{1}{\gamma_k^2(\eta)}\right)^{1/2}\right]. \tag{3.7.31}$$

We emphasize that although in several derivations leading up to the results (3.7.23, 3.7.24,3.7.25) we have used the scale factor during the RD dominated era, for example in eqns. (3.7.15,3.7.16), only the explicit dependence of $\delta_k(\tau,\eta)$ and the prefactor $P[\tau;\eta]$ on τ, η depend on this choice. However, as shown above the leading adiabatic order corresponds to taking $\delta_k = 0$ and $P[\tau,\eta] = 1$, namely δ_k and the τ, η dependent terms in $P[\tau,\eta]$ yield

contributions of higher adiabatic order. Therefore, the leading (zeroth) adiabatic order given by (3.7.31) is valid either for the (RD) or (MD) dominated eras.

Remarkably, this result is similar to that in Minkowski space time obtained in appendix (A.1) with the *only* difference being the scale factor and explicit time dependence of the frequency.

The *decay law* of the probability, given by (3.6.21) requires the integral of the rate (3.7.31). It is now convenient to pass to comoving time in terms of which we find (again setting $\eta_i = 0$)

$$\int_0^\eta \Gamma_k(\eta)\, d\eta \equiv \Gamma_0 \int_0^t \frac{\mathcal{F}(t')}{\gamma_k(t')}\, dt' \,, \tag{3.7.32}$$

where

$$\Gamma_0 = \frac{\lambda^2}{8\pi m_1} \quad ; \quad \mathcal{F}(t') = \frac{1}{2}\Big[1 + \frac{2}{\pi}\, Si[A_0(t')]\Big] \,, \tag{3.7.33}$$

where Γ_0 is the decay rate of a particle at rest in Minkowski space-time and $\gamma_k(t)$ the time dilation factor, which depends explicitly on time as a consequence of the cosmological redshift of the physical momentum.

Up to the factor $\mathcal{F}(t')$, the decay rate in comoving time has a simple interpretation:

$$\Gamma_k(t) \simeq \frac{\Gamma_0}{\gamma_k(t)} \,, \tag{3.7.34}$$

namely a decay width at rest divided by the time dilation factor. During (RD) it follows that

$$\gamma_k(t) = \Big[1 + \frac{t_{nr}}{t}\Big]^{1/2} \quad ; \quad t_{nr} = \frac{k^2}{2m_1^2 H_R} \,, \tag{3.7.35}$$

where $t_{nr}(k)$ is the transition time scale between the ultrarelativistic ($t \ll t_{nr}$) and non-relativistic ($t \gg t_{nr}$) regimes, assuming that the transition occurs during the (RD) era, which is a suitable assumption for masses larger than a few eV.

In the (RD) era we find (using 3.7.13, 3.7.18, 3.7.19, and 3.7.31)

$$z(t) = \left[\frac{k^2}{m_1\, H_R}\right] \left[\frac{t}{t_{nr}}\Big(1 + \frac{t}{t_{nr}}\Big)\right]^{1/2} , \tag{3.7.36}$$

$$A_0(t) = \left[\frac{k^2}{m_1\, H_R}\right] \sqrt{\frac{t}{t_{nr}}} \left[\Big(1 + \frac{t}{t_{nr}}\Big)^{1/2} - 1\right] . \tag{3.7.37}$$

In Minkowski space time, the calculation of the decay rate in S-matrix theory takes the initial and final states at $t = \mp\infty$ respectively, in which case the Si function attains its asymptotic value and $\mathcal{F} = 1$. The derivation of the decay rate in Minkowski space-time but in real time implementing the Wigner-Weisskopf method is described in detail in appendix (A.1) and offers a direct comparison between the flat and curved space time results.

In general the integral in (3.7.32) must be obtained numerically. However, in order to understand the main differences resulting from the cosmological expansion we first focus on the non-relativistic and the ultra-relativistic limits respectively.

Non-relativistic limit:

In this limit we set $k = 0$ with $\gamma_k(t) = 1$ and for simplicity we take the Si function to have reached its asymptotic value, therefore replacing $\mathcal{F}(t') \simeq 1$ inside the integrand yielding[1]

$$\int_0^\eta \Gamma_{k=0}(\eta')\, d\eta' = \frac{\lambda^2}{8\pi m_1}\, t\,. \tag{3.7.38}$$

This is precisely the decay law in Minkowski space time and coincides with the results obtained in ref.[133, 135]. However this is the case *only* if the parent particle is "born" at rest in the comoving frame, otherwise the time dilation factor modifies (substantially, see below) the decay rate and law.

Ultra-relativistic limit:

In this limit we set $m_1 = 0$ corresponding to $\gamma_k \to \infty$ in the argument of the Si function, in which case its contribution vanishes identically, yielding $\mathcal{F}(t') = 1/2$ and

$$\int_0^\eta \Gamma_k(\eta)\, d\eta \equiv \frac{\lambda^2}{16\pi}\int_0^t \frac{1}{k_p(t')}\, dt'\,, \tag{3.7.39}$$

with *physical* wavevector $k_p(t) = k/a(\eta(t))$. During (RD) this result yields the following decay law of the probability

$$\left|C^{(1)}_{\vec{k}}(t)\right|^2 = e^{-(t/t^*)^{3/2}} \quad ; \quad t^* = \left[\frac{\lambda^2\ (2H_R)^{1/2}}{24\pi\, k}\right]^{-2/3}\,. \tag{3.7.40}$$

[1]Keeping the function $\mathcal{F}$ in the integrand yields a subdominant constant term in the long time limit. A similar term is found in ref.[133, 135].

This decay law is a *stretched exponential*, it is a distinct consequence of time dilation combined with the cosmological redshift of the physical momentum.

Although obtaining the decay law throughout the full range of time entails an intense numerical effort and depends in detail on the various parameters k, m_1, H_R etc. We can obtain an approximate but more clear understanding of the transition between the ultrarelativistic and non-relativistic regimes by focusing solely on the time integral of the inverse Lorentz factor, because the contribution from $\mathcal{F}$ is bound $1/2 \leq \mathcal{F} \leq 1$. Therefore, setting $\mathcal{F} = 1$ and during (RD) we find

$$\begin{aligned} \int_0^t \Gamma_k(t')\, dt' &= \Gamma_0\, t_{nr}\, G_k(t) \\ G_k(t) &= \left[\frac{t}{t_{nr}}\Big(1+\frac{t}{t_{nr}}\Big)\right]^{1/2} - \ln\left[\sqrt{1+\frac{t}{t_{nr}}} + \sqrt{\frac{t}{t_{nr}}}\right]. \end{aligned} \tag{3.7.41}$$

For the ultrarelativistic regime $t \ll t_{nr}$ we find the result (3.7.40) up to a factor $1/2$ because we have set $\mathcal{F} = 1$, whereas in the non-relativistic regime, for $t \gg t_{nr}$, we obtain the transition probability

$$\left|C^{(1)}_{\vec{k}}(t)\right|^2 = e^{-\Gamma_0\, t}\left(\frac{t}{t_{nr}}\right)^{\Gamma_0 t_{nr}/2}, \tag{3.7.42}$$

again, the extra power of time is a consequence of the cosmological redshift in the time dilation factor. For $k = 0$, namely $t_{nr} = 0$, we obtain the non-relativistic result (3.7.38).

The function $G_k(t)$ interpolates between the ultrarelativistic case $\propto t^{3/2}$ for $t \ll t_{nr}$ and the non-relativistic case $\propto t$ for $t \gg t_{nr}$ and encodes the time dependence of the time dilation factor through the cosmological redshift.

In Minkowski space time the result of the integral in (3.7.41) is simply $\Gamma_0 t$ which is conveniently written as as $\Gamma_0 t_{nr}\,(t/t_{nr})$. Because G_k is a function of t/t_{nr}, a measure of the *delay* in the cosmological decay compared to that of Minkowski space time is given by the ratio $G_k(x)/x$ with $x \equiv t/t_{nr}$. This ratio is displayed in fig. (10), it vanishes as $x \to 0$ as $x^{1/2}$ and $G_k(x)/x \to 1$ as $x \to \infty$, in particular $G_k(1) = \sqrt{2} - \ln[1+\sqrt{2}] = 0.533$.

This analysis suggests that the effect of the cosmological expansion can be formally included by defining a *time dependent effective decay rate*,

$$\widetilde{\Gamma}_k(t) = \Gamma_0\,(G_k(x)/x) \quad ; \quad x = t/t_{nr}\,, \tag{3.7.43}$$

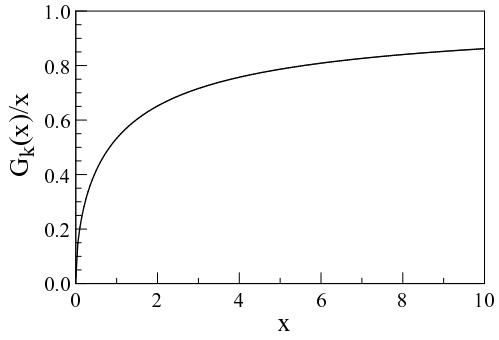

Figure 10: The ratio $G_k(x)/x$ for $x = t/t_{nr}$.

and t_{nr} depends on k (see (3.7.41)), so that the decay law for the survival probability of the parent particle becomes

$$P(t) = e^{-\widetilde{\Gamma}_k(t)\, t}\,. \tag{3.7.44}$$

This effective decay rate is *always* smaller than the Minkowski rate for $k \neq 0$ as a consequence of time dilation and its time dependence through the cosmological redshift, coinciding with the Minkowski rate at rest only for $k = 0$, namely particles born and decaying at rest in the comoving frame.

Finally, the effect of the function $\mathcal{F}$ must be studied numerically for a given set of parameters k, m_1. However, we can obtain an estimate during the (RD) era from the expression (3.7.37) for the argument of the Si-function. Writing

$$\left[\frac{k^2}{m_1\, H_R}\right] \equiv \beta \simeq 10^{16}\left[\frac{\Big(k/10^{-13}\,\mathrm{GeV}\Big)^2}{\Big(m_1/100\,\mathrm{GeV}\Big)}\right], \tag{3.7.45}$$

it follows that $A_0(t) \ll 1$ for $t/t_{nr} \ll 1/\beta^{2/3}$ and $A_0(t) > 1$ for $t/t_{nr} > 1/\beta^{2/3}$. Because $Si[x] \propto x$ as $x \to 0$ and approaches $\pi/2$ for $x \simeq \pi$ the large pre-factor in (3.7.45) for typical

values of k, m_1 entails that the transition between these regimes is fairly sharp, therefore we can approximate the function $\mathcal{F}(t')$ as

$$\mathcal{F}(t') \approx \frac{1}{2}\,\Theta\Big(\beta^{-2/3} - t'/t_{nr}\Big) + \Theta\Big(t'/t_{nr} - \beta^{-2/3}\Big)\,. \tag{3.7.46}$$

3.7.2 Massive Parent and Daughters

We now consider the self energy (3.7.2) for the case of massive daughters. Unlike the case of massless daughters, in this case neither the time nor the momentum integrals can be done analytically. However, the study of massless daughters revealed that the adiabatic approximation in the time integrals is excellent when the adiabatic conditions $H(t)/E_k(t) \ll 1$ are fulfilled for all species. The analysis of the previous section has shown that inside the time integrals we can replace $a(\eta') \to a(\eta)$; $\omega_k(\eta') \to \omega_k(\eta)$ since the difference is at least first order (and higher) in the adiabatic approximation (see the results for the factor $P(\tau)$ in eqn. (3.7.23)). Furthermore, carrying an adiabatic expansion of the time integrals of the frequencies is tantamount to expanding these in powers of $\eta - \eta'$, with the first term, proportional to $\eta - \eta'$ yielding the zeroth adiabatic order and the higher powers of $\eta - \eta'$ being of higher adiabatic order. Replacing $\eta - \eta' = \tau/\omega_k^{(1)}(\eta)$ associates the higher powers of τ with higher orders in the adiabatic expansion as discussed above. However, this argument by itself does not guarantee the reliability of the adiabatic expansion because for $\tau \simeq z = E_k/H$ each term in this expansion becomes of the same order. What guarantees the reliability of the adiabatic expansion is the momentum integral that suppresses the large $\eta - \eta'$ regions. This is manifest in the $1/\tau$ suppression of the integrand in the case of massless daughters (see eqn. (3.7.23)). This can be understood from a simple observation. Consider the momentum integral in the full expression (3.7.2), setting $\eta = \eta'$ in the exponent yields a linearly divergent momentum integral. This is the origin of the singularity as $\eta \to \eta'$ in (3.7.5). The contributions from regions with large $\eta - \eta'$ oscillate very fast and are suppressed. Therefore the momentum integral is dominated by the region of small $\eta - \eta'$. In appendix (A.2) we provide an analysis of the first adiabatic correction and confirm both analytically and numerically that it is indeed suppressed by the momentum integration also in the case of massive daughters.

Therefore we consider the leading adiabatic order that yields

$$\Gamma_k(\eta) = \frac{2\,\lambda^2\,a^2(\eta)}{\omega_k^{(1)}(\eta)} \int \frac{d^3p}{(2\pi)^3} \frac{1}{2\,\omega_p^{(2)}(\eta)\,2\,\omega_q^{(2)}(\eta)} \; \frac{\sin\left[\left(\omega_k^{(1)}(\eta)-\omega_p^{(2)}(\eta)-\omega_q^{(2)}(\eta)\right)\eta\right]}{\left(\omega_k^{(1)}(\eta)-\omega_p^{(2)}(\eta)-\omega_q^{(2)}(\eta)\right)} \tag{3.7.47}$$

$$q = |\vec{k}-\vec{p}|$$

It is convenient to recast this expression in terms of the physical (comoving) energy and momenta: $\omega_k(\eta) = a(\eta)E_k(t)$ absorbing the three powers of $a(\eta)$ in the denominator in the momentum integral in (3.7.47) into the measure $d^3p \to d^3p_{ph}$ where $p_{ph}(\eta) \equiv p/a(\eta)$ is the physical momentum, keeping the same notation for the integration variables (dropping the subscript "ph" from the momenta) to simplify notation, we obtain

$$\Gamma_k(\eta) = \frac{2\,\lambda^2\,a(\eta)}{E_k^{(1)}(\eta)} \int \frac{d^3p}{(2\pi)^3} \frac{1}{2\,E_p^{(2)}(\eta)\,2\,E_q^{(2)}(\eta)} \; \frac{\sin\left[\left(E_k^{(1)}(\eta)-E_p^{(2)}(\eta)-E_q^{(2)}(\eta)\right)\widetilde{T}\right]}{\left(E_k^{(1)}(\eta)-E_p^{(2)}(\eta)-E_q^{(2)}(\eta)\right)} \tag{3.7.48}$$

$$q = |\vec{k}-\vec{p}|$$

The variable

$$\widetilde{T} = a(\eta)\,\eta \equiv \frac{1}{\widetilde{H}} = \begin{cases} \frac{1}{H} & (RD) \\ \frac{2}{H} & (MD) \end{cases} , \tag{3.7.49}$$

corresponds to the physical particle horizon, proportional to the Hubble time. Obviously the momentum integrals cannot be done in closed form, however (3.7.48) becomes more familiar with a dispersive representation, namely

$$\Gamma_k(\eta) = \int_{-\infty}^{\infty} dk_0 \; \rho(k_0,k) \, \frac{\sin\left[\left(k_0 - E_k^{(1)}(\eta)\right)\widetilde{T}\right]}{\pi\left(k_0 - E_k^{(1)}(\eta)\right)} \, , \tag{3.7.50}$$

with the spectral density

$$\rho(k_0,k;\eta) = \frac{\lambda^2\,a(\eta)}{E_k^{(1)}(\eta)} \int \frac{d^3p}{(2\pi)^3} \frac{(2\pi)\,\delta\Big[k_0 - E_p^{(2)}(\eta) - E_q^{(2)}(\eta)\Big]}{2\,E_p^{(2)}(\eta)\,2\,E_q^{(2)}(\eta)} \, , \tag{3.7.51}$$

we refer to (3.7.50) the *cosmological Fermi's Golden Rule*. In the formal limit $\widetilde{T} \to \infty$

$$\frac{\sin\left[\left(k_0 - E_k^{(1)}(\eta)\right)\widetilde{T}\right]}{\pi\left(k_0 - E_k^{(1)}(\eta)\right)} \quad \longrightarrow \quad \delta(k_0 - E_k^{(1)}(\eta)) \, . \tag{3.7.52}$$

The density of states (3.7.51) is the familiar two body decay phase space in Minkowski space-time for a particle of energy k_0 into two particles of equal mass. It is given by (see appendix (A.1)),

$$\rho(k_0, k; \eta) = \frac{\lambda^2\, a(\eta)}{8\pi\, E_k^{(1)}(\eta)} \left[1 - \frac{4\, m_2^2}{k_0^2 - k^2}\right]^{1/2} \Theta(k_0^2 - k^2 - 4\, m_2^2)\, \Theta(k_0)\,, \tag{3.7.53}$$

where $k \equiv k_{ph}(\eta)$ is the the physical momentum, and the theta function describes the reaction threshold.

Before we proceed to the study of $\Gamma_k(\eta)$ for $m_2 \neq 0$, we establish a direct connection with the results of the previous section for $m_2 = 0$, where the momentum integration was carried out first. Setting $m_2 = 0$ in (3.7.53), inserting it into the dispersive integral (3.7.50) and changing variables $(k_0 - E_k^{(1)}(\eta))\, \widetilde{T} \to x$ we find

$$\Gamma_k(\eta) = \frac{\lambda^2\, a(\eta)}{8\pi\, E_k^{(1)}(\eta)} \int_{-\left(E_k^{(1)}(\eta) - k\right)\widetilde{T}}^{\infty} \frac{\sin(x)}{\pi\, x}\, dx = \frac{\lambda^2\, a(\eta)}{8\pi\, E_k^{(1)}(\eta)}\, \frac{1}{2}\left[1 + \frac{2}{\pi}\, Si\Big[\big(E_k^{(1)}(\eta) - k\big)\, \widetilde{T}\Big]\right], \tag{3.7.54}$$

which is precisely the result (3.7.31) displaying the "prompt" (1) and "raising" (Si) terms inside the bracket.

Restoring $m_2 \neq 0$, and taking formally the infinite time limit (3.7.52), the rate (3.7.50) becomes

$$\Gamma(\eta) = \frac{\lambda^2\, a(\eta)}{8\pi\, E_k^{(1)}(\eta)} \left[1 - \frac{4\, m_2^2}{m_1^2}\right]^{1/2} \Theta(m_1^2 - 4\, m_2^2)\,, \tag{3.7.55}$$

revealing the usual two particle threshold $m_1 \geq 2\, m_2$.

Threshold relaxation:

However, before taking the infinite time limit we recognize important physical consequences of the rate (3.7.50). The Hubble time $\widetilde{T}$ introduces an uncertainty in energy $\Delta E \simeq 1/\widetilde{T} \equiv \widetilde{H}$ which allows physical processes that *violate local energy conservation* on the scale of this uncertainty. In particular, this uncertainty allows a particle of mass m_1 to decay into *heavier* particles, as a consequence of the relaxation of the threshold condition via the uncertainty. This remarkable feature can be understood as follows. The sine function in (3.7.50) features a maximum at $k_0 = E_k^{(1)}(\eta)$ with half-width (in the variable k_0) $\approx \pi \widetilde{H}$, narrowing as $\widetilde{T}$ increases. The spectral density $\rho(k_0, k; \eta)$ has support above the threshold at

$k_0^* = \sqrt{k^2 + 4m_2^2}$, it is convenient to write this threshold as $k_0^* = \sqrt{(E_k^{(1)}(\eta))^2 + (4m_2^2 - m_1^2)}$. For $4m_2^2 - m_1^2 < 0$ the position of the peak of the sine function, at $k_0 = E_k^{(1)}(\eta)$ lies above the threshold, but for $4m_2^2 - m_1^2 > 0$ it lies below it. In this latter case, if the condition

$$\left(E_k^{(1)}(\eta) + \pi\widetilde{H}\right)^2 \gg (E_k^{(1)}(\eta))^2 + (4m_2^2 - m_1^2) \tag{3.7.56}$$

is fulfilled, the "wings" of the sine function beyond the peak feature a large overlap with the region of support of the spectral density. This is displayed in figs. (11,12). This phenomenon entails the opening of unexpected new channels for a particle to decay into two *heavier* particles as a consequence of the energy uncertainty determined by the Hubble time.

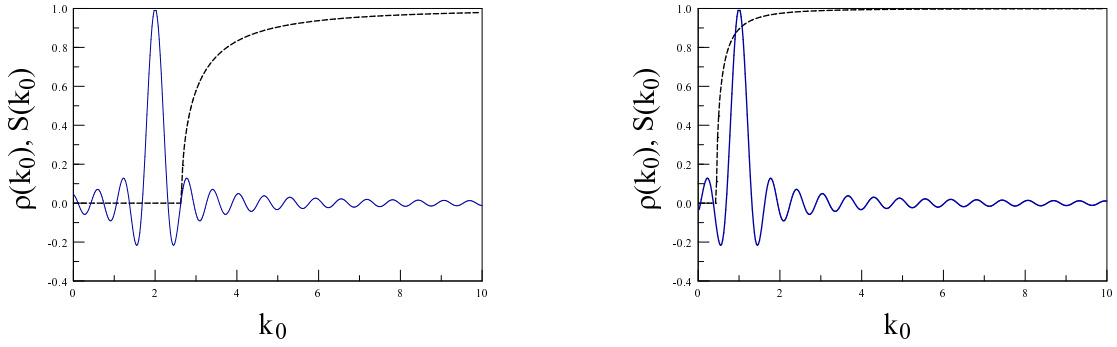

Figure 11: The functions $\rho(k_0, k)$ (dashed line) and $S(k_0) = \sin[(k_0 - E)T]/[(k_0 - E)T]$ in units of m_1. Left panel: $E = 2, 4m_2^2 = 4, T = 10$ corresponding to E below threshold. Right panel: $E = 1, 4m_2^2 = 0.2, T = 10$ corresponding to E above threshold.

In the adiabatic approximation with $E_k^{(1)}(\eta) \gg \widetilde{H}$ the overlap condition (3.7.56) reads

$$2\pi\, E_k^{(1)}(\eta)\, \widetilde{H}(\eta) \gg 4m_2^2 - m_1^2\,, \tag{3.7.57}$$

which shows that this condition becomes more easily fulfilled for a relativistic parent. This is clearly displayed in fig. (12).

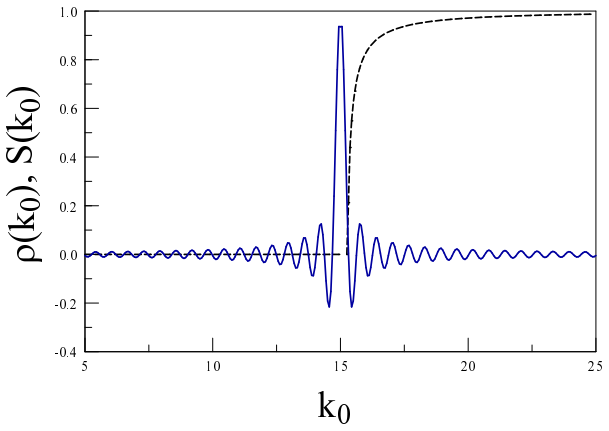

Figure 12: The functions $\rho(k_0, k)$ (dashed line) and $S(k_0) = \sin[(k_0 - E)T]/[(k_0 - E)T]$ in units of m_1 for $E = 15, 4m_2^2 = 10, T = 10$ corresponding to an ultrarelativistic parent with E below threshold.

To gain better understanding of this condition, let us consider the specific case of an ultrarelativistic parent with mass $m_1 \simeq 100\,\mathrm{GeV}$ with a GUT-scale comoving energy $E_k \simeq 10^{15}\,\mathrm{GeV}$ decaying into two daughters with mass $m_2 \simeq 1\,\mathrm{TeV}$ for illustration. We can then replace $E_k \simeq k/a(\eta)$ with $k \simeq 10^{-13}\,\mathrm{GeV}$ being the comoving momentum that yields a physical momentum $k_{ph} \simeq 10^{15}\,\mathrm{GeV}$ (with $a(\eta_i) \simeq 10^{-28}$), furthermore with $\widetilde{H} \simeq H_R/a^2(\eta)$ and $H_R = H_0\sqrt{\Omega_R} \simeq 10^{-44}\,\mathrm{GeV}$ one finds that the condition (3.7.57) implies that this decay channel will remain open within the window of scale factors

$$10^{-28} \leq a(\eta) \ll 10^{-21}\,, \tag{3.7.58}$$

corresponding to the temperature range $10^8\,\mathrm{GeV} < T(t) \leq 10^{15}\mathrm{GeV}$ during the (RD) dominated era. In this temperature regime, the heavier daughter particles in this example are also typically ultrarelativistic.

Under these circumstances the results from eqns. (3.7.39,3.7.40) are valid during the time interval in which this decay channel remains open, determined by the inequality (3.7.58). Eventually, however as the expansion proceeds both the local energy and expansion rate diminish and this channel closes. The detailed dynamics of this phenomenon must be studied numerically for a given range of parameters.

The integration of the convolution of the spectral density with the sine function and the further integration to obtain the decay law is extremely challenging and time consuming because of the wide separation of scales and the rapid oscillations. In a more realistic model with specific parameters such endeavor would be necessary for a detailed assessment of the contribution from the new open channels. Here we provide a "proof of principle" by displaying in fig. (13) the result of the integral (see 3.7.50 and 3.7.51)

$$R(E) = \int_{k_0^*}^{\infty} dk_0 \left[\frac{k_0^2 - E^2 - (4\,m_2^2 - m_1^2)}{k_0^2 - E^2 + m_1^2}\right]^{1/2} \frac{\sin\Big[\big(k_0 - E\big)T\Big]}{\big(k_0 - E\big)} \quad ; \quad k_0^* = \sqrt{E^2 + (4m_2^2 - m_1^2)} \tag{3.7.59}$$

for $4m_2^2 > m_1^2$ so that E is below threshold.

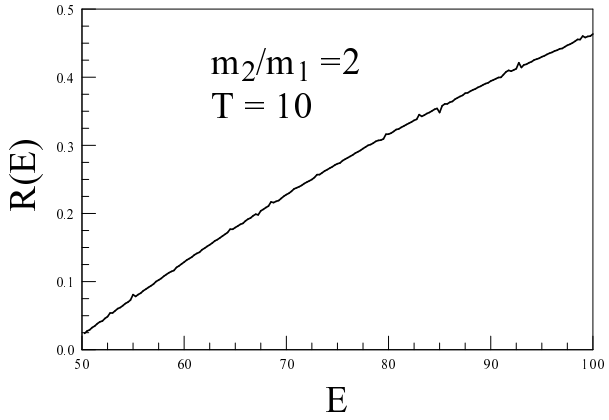

Figure 13: The integral R(E) vs. E, for $m_2/m_1 = 2$; $\widetilde{T} = 10$ in units of m_1.

The range of E, T are chosen to comply with the validity of the adiabatic condition $ET \gg 1$. This figure shows that the uncertainty "opens" the threshold to decaying into heavier particles, the example in the figure corresponds to $m_2 = 2m_1$. We have numerically confirmed that as T increases $R(E)$ diminishes as a consequence of a smaller overlap. As the scale factor increases these new decay channels close, allowing only the two body decay for $m_1 > 2m_2$ and the decay rate is given by the long time limit (3.7.55)

$$\Gamma(\eta) = \Gamma_0 \, \frac{a(\eta)}{\gamma_k(\eta)} \quad ; \quad \Gamma_0 = \frac{\lambda^2}{8\pi \, m_1} \left[1 - \frac{4\, m_2^2}{m_1^2}\right]^{1/2} \Theta(m_1^2 - 4\, m_2^2)\,, \tag{3.7.60}$$

where Γ_0 is the usual decay rate at rest in Minkowski space time. Following the analysis of the previous section, one now finds a decay law similar to that in eqn. (3.7.41) but with Γ_0 now given by (3.7.60).

Daughters pair probability:

With the solution for the amplitude of the single particle state, we can now address the amplitude for the decay products from the result (3.6.4) with $|\kappa\rangle = |1^{(2)}_{\vec{p}}, 1^{(2)}_{\vec{q}}\rangle$ and $|A\rangle = |1^{(1)}_{\vec{k}}\rangle$. The decay product is a *correlated pair of daughter particles*. The corresponding matrix element is given by (3.6.19) in terms of the zeroth order adiabatic mode functions (3.7.1). Writing the solution for the decaying amplitude

$$C^{(1)}_{\vec{k}}(\eta) = e^{-\int_{\eta_i}^{\eta} \mathcal{E}^{(1)}_k(\eta'')d\eta''} \tag{3.7.61}$$

where $\mathrm{Re}\big[\mathcal{E}^{(1)}_k(\eta)\big] = \Gamma_k(\eta)/2$, and neglecting the contribution from the imaginary part which amounts to a renormalization of the frequencies[138, 137, 37], we find (using 3.6.4)

$$C^{(2)}_{\vec{p},\vec{q}}(\eta) = -i\frac{2\lambda}{V^{1/2}} \int_{\eta_i}^{\eta} \frac{e^{\,i\int_{\eta_i}^{\eta'} \left[\omega^{(2)}_{\vec{p}}(\eta'')+\omega^{(2)}_{\vec{q}}(\eta'')-\omega^{(1)}_{\vec{k}}(\eta'')\right]d\eta''}}{\left[2\omega^{(2)}_{\vec{p}}(\eta')\, 2\omega^{(2)}_{\vec{q}}(\eta') 2\omega^{(1)}_{\vec{k}}(\eta')\right]^{1/2}} \; e^{-\int_{\eta_i}^{\eta'} \Gamma_k(\eta'')/2 \; d\eta''} \; d\eta' \quad ; \quad \vec{q} = \vec{k} - \vec{p}\,. \tag{3.7.62}$$

The time integral is extremely challenging and can only be studied numerically. We can make progress by implementing the same approximations discussed above. Since Γ_k depends on the slowly varying frequency, it itself varies slowly, therefore we will consider an interval in η so that the decay rate remains nearly constant, replacing the exponentials by their lowest

order expansion in $\eta' - \eta_i$. During this interval we find the following approximate form of the daughter pair probability,

$$|C_{\vec{p},\vec{k}}(\eta)|^2 \approx \frac{\lambda^2}{2\omega_k^{(1)}(\eta)\,\omega_p^{(2)}(\eta)\,\omega_q^{(2)}(\eta)\,V}\;\frac{\left|1-e^{-\Gamma_k(\eta)\eta/2}\,e^{-i\left(\omega_k^{(1)}(\eta)-\omega_p^{(2)}(\eta)-\omega_q^{(2)}(\eta)\right)\eta}\right|^2}{\left(\omega_k^{(1)}(\eta)-\omega_p^{(2)}(\eta)-\omega_q^{(2)}(\eta)\right)^2+\frac{\Gamma_k^2(\eta)}{4}}\;\;;\;\;\vec{q}=\vec{k}-\vec{p}, \tag{3.7.63}$$

where we set $\eta_i = 0$. This expression is only valid in restricted time interval, its main merit is that it agrees with the result in Minkowski space time (see appendix A.1) and describes the early build up of the daughters population from the decay of the parent particle. The occupation number of daughter particles is obtained by calculating the expectation value of the number operators $a^\dagger_{\vec{q}}a_{\vec{q}}\;;\;a^\dagger_{\vec{p}}a_{\vec{p}}$ in the time evolved state, it is straightforward to find

$$\langle a^\dagger_{\vec{q}}a_{\vec{q}}\rangle = \langle a^\dagger_{\vec{p}}a_{\vec{p}}\rangle = |C_{\vec{p},\vec{k}}(\eta)|^2\,, \tag{3.7.64}$$

the fact that these occupation numbers are the same is a consequence of the pair correlation.

A more detailed assessment of the population build up and asymptotic behavior requires a full numerical study for a range of parameters.

3.8 Discussion

There are several aspects and results of this study that merit further discussion.

Spontaneous vs. stimulated decay:

We have focused on the dynamics of decay from an initial state assuming that there is no established population of daughter particles in the plasma that describes an (RD) cosmology. If there is such population there is a contribution from *stimulated* decay in the form of extra factors $1 + n$ for each bosonic final state where n is the occupation of the particular state. These extra factors enhance the decay. On the other hand, if the particles in the final state are fermions (a case not considered in this study), the final state factors are $1 - n$ for each fermionic daughter species and the decay rate would decrease as a consequence of Pauli

blocking. The effect of an established population of daughter particles on the decay rate clearly merits further study.

Medium corrections:

In this study we focus on the corrections to the decay law arising solely from the cosmological expansion as a prelude to a more complete treatment of kinetic processes in the early Universe. In this preliminary study we have not included the effect of medium corrections to the interaction vertices or masses. Finite temperature effects, and in particular in the early radiation dominated stage, modify the effective couplings and masses, for example a Yukawa coupling to fermions or a bosonic quartic self interaction would yield finite temperature corrections to the masses $\propto T^2$. These modifications may yield important corrections to the spectral densities and may also modify threshold kinematics. However, the *dynamical* effects such as threshold relaxation, consequences of uncertainty and delayed decay (relaxation) as a consequence of cosmological redshift of time dilation are robust phenomena that do not depend on these aspects. Our formulation applies to the time evolution of (pure) states. In order to study the time evolution of distribution functions it must be extrapolated to the time evolution of a density matrix, from which one can extract the quantum kinetic equations including the effects of cosmological expansion described here. This program merits a deeper study beyond the scope of this article. We are currently pursuing several of these aspects.

Cosmological particle production:

Our study has focused on the zeroth adiabatic order as a prelude to a more comprehensive program. We have argued that at the level of the Hamiltonian, the creation and annihilation operators introduced in the quantization procedure create and destroy particles as identified at leading adiabatic order and diagonalize the Hamiltonian at leading (zero) order. Beyond the leading order, there emerge contributions that describe the creation (and annihilation) of *pairs* via the cosmological expansion. We have argued that these processes are of higher order in the adiabatic expansion, therefore can be consistently neglected to leading order. For weak coupling, including these higher order processes of cosmological particle production (and annihilation) in the calculation of the *decay rate* (and decay law) will result in higher order corrections to the rate of the form $\lambda^2 \times$ (higher order adiabatic). However, once these

processes are included *at tree level*, namely at the level of *free field* particle production, they may actually *compete* with the decay process. It is possible that for weak coupling, cosmological particle production (and annihilation) competes on similar time scales with decay, thereby perhaps "replenishing" the population of the decaying particle. The study of these competing effects requires the equivalent of a quantum kinetic description including the gain from particle production and the loss from decay (and absorption of particles into the vacuum). Such study will be the focus of a future report.

Validity of the adiabatic approximation:

The adiabatic approximation relies on the ratio $H(t)/E_k(t) \ll 1$ (3.3.25). In a radiation dominated cosmology the Hubble radius ($H^{-1}(t)$) grows as $a^2(t)$ and during matter domination it grows as $a^{3/2}(t)$ whereas physical wavelengths grow as $a(t)$, with $a(t)$ the scale factor. During these cosmological eras, physical wavelengths become deeper inside the Hubble radius and the ratio $H(t)/E_k(t)$ diminishes fast. Therefore if the condition $H(t)/E_k(t) \ll 1$ is satisfied at the very early stages during radiation domination, its validity *improves* as the cosmological expansion proceeds.

Modifications to BBN?

The results obtained in the previous sections show potentially important modifications to the decay law during the (RD) cosmological era. An important question is whether these corrections affect standard BBN. To answer this question we focus on neutron decay, which is an important ingredient in the primordial abundance of Helium and heavier elements. The neutron is "born" after the QCD confining phase transition at $T_{QCD} \simeq 150\,\mathrm{MeV}$ at a time $t_{QCD} \simeq 10^{-5}\,s$ hence neutrons are "born" non-relativistically. With a mass $M_N \simeq 1\,\mathrm{GeV}$ and a typical physical energy $\simeq T_{QCD}$ the transition time $t_{nr} \simeq 10^{-6}\,s \simeq t_{QCD}$. The neutron's lifetime $\simeq 900\,s$ implies that $\Gamma_0\, t_{nr}/2 \simeq 10^{-9}$ and the modifications from the decay law determined by the extra factor in (3.7.42) are clearly irrelevant. Therefore it is not expected that the modifications of the decay law found in the previous sections would affect the dynamics of BBN and the primordial abundance of light elements. There is, however, the possibility that *other* degrees of freedom, such as, sterile neutrinos for example, whose decay may inject energy into the plasma with potential implications for BBN. Such a possibility has been raised in refs.[116]-[172] with regard to the abundance of ^7Li. The decay law of

these other species of particles (such as sterile neutrinos beyond the standard model) *could* be modified and their efficiency for energy injection and potential impact on BBN may be affected by these modifications. Such possibility remains to be studied.

Wave packets:

We have studied the decay dynamics from an initial state corresponding to a single particle state with a given comoving wavector. However, it is possible that the decaying parent particle is not created ("born") as a single particle eigenstate of momentum, but in a wave packet superposition. Taking into account this possibility is straightforward within the Wigner-Weisskopf method, and it has been considered in Minkowski space time in ref.[138, 137]. Consider an initial wave packet as a linear superposition of single particle states of the parent field, namely $|\mathbf{1}^{(1)}\rangle = \sum_{\vec{k}} C^{(1)}_{\vec{k}}(\eta_i)|1^{(1)}_{\vec{k}}\rangle$, where $C^{(1)}_{\vec{k}}(\eta_i)$ are the Fourier coefficients of a wavepacket localized in space (for example a Gaussian wave-packet). Implementing the Wigner-Weisskopf method, the time evolution of this state leads to the solution (3.6.13) for the coefficients with $C_A(\eta_i) = C^{(1)}_{\vec{k}}(\eta_i)$, and by Fourier transform one obtaines the full space-time evolution of the wavepacket[138, 137]. Such an extension presents no conceptual difficulty, however, the major technical complication would be to extract the decay law: as pointed out in the previous section, the main difference with the result in Minkowski space time is that the time dilation factors depend explicitly on time through the cosmological redshift. In a wave packet description, each different wavector component features a different time dilation factor with a differential red-shift between the various components. This will modify the evolution dynamics in several important ways: there is spreading associated with dispersion, the different time dilation factors for each wavevector imply a superposition of different decay time scales, and finally, each different time dilation factor features a different time dependence through the cosmological redshift. All these aspects amount to important technical complexities that merit further study.

Caveats:

The main approximation invoked in this study, the adiabatic approximation, relies on the physical wavelength of the particle to be deep inside the physical particle horizon at any given time, namely, much smaller than the Hubble radius. If the decaying parent particle is produced ("born") satisfying this condition, this approximation becomes more reliable with

cosmological expansion as the Hubble radius grows faster than a physical wavelength during an (RD) or (MD) cosmology. However, it is possible that such particle has been produced during the inflationary, near de Sitter stage, in which case the Hubble radius remains nearly constant and the physical wavelength is stretched beyond it. In this situation, the adiabatic approximation as implemented in this study breaks down. While the physical wavelength remains outside the particle horizon, the evolution must be obtained by solving the equations of motion for the mode function. During the post inflationary evolution well after the physical wavelength of the parent particle re-enters the Hubble radius the adiabatic approximation becomes reliable. However, it is possible that while the physical wavelength is *outside* the particle horizon during (RD) (or (MD)) the parent particle has decayed substantially with the ensuing growth of the daughter population. The framework developed in this study would need to be modified to include this possibility, again a task beyond the scope and goals of this article.

3.9 Conclusions and Further Questions

Motivated by the phenomenological importance of particle decay in cosmology for physics within and beyond the standard model, in this article we initiate a program to provide a systematic framework to obtain the *decay law* in the standard post inflationary cosmology. Most of the treatments of phenomenological consequences of particle decay in cosmology describe these processes in terms of a decay rate obtained via usual S-matrix theory in Minkowski space time. Instead, recognizing that rapid cosmological expansion may modify this approach with potentially important phenomenological consequences, we study particle decay by combining a physically motivated adiabatic expansion and a *non-perturbative* quantum field theory method which is an extension of the ubiquitous Wigner-Weisskopf theory of atomic line widths in quantum optics[176]. The adiabatic expansion relies on a wide separation of scales: the typical wavelength of a particle is much smaller than the particle horizon (proportional to the Hubble radius) at any given time. Hence we introduce the *adiabatic* ratio $H(t)/E_k(t)$ where $H(t)$ is the Hubble rate and $E_k(t)$ the (local) energy measured by a

comoving observer. The validity of the adiabatic approximation relies on $H(t)/E_k(t) \ll 1$ and is fulfilled under *most* general circumstances of particle physics processes in cosmology.

The Wigner-Weisskopf framework allows to obtain the survival probability and *decay law* of a parent particle along with the probability of population build-up for the daughter particles (decay products). We implement this framework within a model quantum field theory to study the generic aspects of particle decay in an expanding cosmology, and compare the results of the cosmological setting with that of Minkowski space time.

One of our main results is a *cosmological Fermi's Golden Rule* which features an energy uncertainty determined by the particle horizon ($\propto 1/H(t)$) and yields the *time dependent decay rate*. In this study we obtain two main results: i) During the (RD) stage, the survival probability of the decaying (single particle) state may be written in terms of an *effective time dependent rate* $\widetilde{\Gamma}_k(t)$ as $P(t) = e^{-\widetilde{\Gamma}_k(t)\, t}$. The effective rate is characterized by a time scale t_{nr} (3.7.41) at which the particle transitions from the relativistic regime ($t \ll t_{nr}$) when $P(t) = e^{-(t/t^*)^{3/2}}$ to the non-relativistic regime ($t \gg t_{nr}$) when $P(t) = e^{-\Gamma_0\, t}\left(\frac{t}{t_{nr}}\right)^{\Gamma_0 t_{nr}/2}$ where Γ_0 is the Minkowski space-time decay width at rest. Generically the decay is *slower* in an expanding cosmology than in Minkowski space time. Only for a particle that has been produced ("born") at rest in the comoving frame is the decay law asymptotically the same as in Minkowski space-time. Physically the reason for the delayed decay is that for non-vanishing momentum the decay rate features the (local) time dilation factor, and in an expanding cosmology the (local) Lorentz factor depends on time through the cosmological redshift. Therefore lighter particles that are produced with a large Lorentz factor decay with an effective longer lifetime. ii) The second, unexpected result of our study is a *relaxation of thresholds* as a consequence of the energy uncertainty determined by the particle horizon. A distinct consequence of this uncertainty is the opening of new decay channels to decay products that are *heavier* than the parent particle. Under the validity of the adiabatic approximation, this possibility is available when $2\pi E_k(t) H(t) \gg 4m_2^2 - m_1^2$ where m_1, m_2 are the masses of the parent, daughter particles respectively. As the expansion proceeds this channel closes and the usual kinematic threshold constrains the phase space available for decay. Both these results *may* have important phenomenological consequences in baryogenesis, leptogenesis, and dark matter abundance and constraints which remain to be studied

further.

Further questions:

We have focused our study on a simple quantum field theory model that is not directly related to the standard model of particle physics or beyond. Yet, the results have a compelling and simple physical interpretation that is likely to transcend the particular model. However, the analysis of this study must be applied to other fields in particular fermionic degrees of freedom and vector bosons. Both present new and different technical challenges primarily from their couplings to gravity which will determine not only the scale factor dependence of vertices but also the nature of the mode functions (spinors in particular). As mentioned above, cosmological particle production is not included to leading order in the adiabatic approximation but must be consistently included beyond leading order. The results of this study point to interesting avenues to pursue further: in particular the relaxation of kinematic thresholds from the cosmological uncertainty opens the possibility for unexpected phenomena and possible modifications to processes, such as inverse decays, the dynamics of thermalization and detailed balance. These are all issues that merit a deeper study, and we expect to report on some of them currently in progress.

4.0 Cosmological Decay of Higgs-like Scalars into a Fermion Channel

4.1 Introduction

The decay and scattering of particles are some of the most fundamental processes in particle physics, within and beyond the Standard Model, with profound impact in cosmology. These processes are ultimately responsible for establishing a state of local thermodynamic and chemical equilibrium and are fundamental ingredients in kinetic processes in the early universe[123, 141, 24]. Particle decay is not only ubiquitous, but it plays an important role in big bang nucleosynthesis (BBN)[123, 182, 174, 83, 82, 112, 163, 116, 115], and the generation of the baryon and lepton asymmetries[185, 123, 44, 42]. The decay of long-lived dark matter particles is constrained by various cosmological and astrophysical probes[189, 188, 30, 166, 12], and recently it has been suggested that the two body decay of a long lived dark matter particle may relieve the tension between distance ladder and cosmic microwave background measurements of the Hubble constant[186].

Most treatments of particle decay (and/or inverse decay) in cosmology implement the S-matrix quantum field theory approach as in Minkowski space-time. In this framework, the unstable decaying state is prepared at a time far in the past ($t \to -\infty$), and one obtains the transition amplitude to a given final state far in the future ($t \to \infty$). Taking the infinite time limit in the transition amplitude yields a total energy conserving delta function. Squaring this delta function to obtain the transition probability yields a total energy conservation delta function multiplied by the total elapsed time. Dividing by this large time and summing over all the final states for a given decay channel gives the total transition probability per unit time, namely a decay rate. Energy conservation, *a consequence of the infinite time limit*, yields kinematic constraints (thresholds) for decay and scattering processes.

In an expanding cosmology such an approach is at best approximate and at worst unreliable when the Hubble expansion rate is large even during a post-inflationary early stage of a radiation dominated cosmology. In a spatially flat Friedmann-Robertson-Walker (FRW) cosmology there are three space-like Killing vectors associated with spatial translational in-

variance and spatial momentum conservation, however, as a consequence of cosmological expansion there is no global time-like Killing vector, therefore particle energy is not manifestly conserved in scattering or decay processes.

A consistent formulation of dynamic processes in an expanding cosmology requires implementing methods of quantum field theory in curved space time[154, 195, 86, 29, 47, 28, 87, 149, 158]. Early studies revealed a wealth of novel phenomena such as particle production[153, 154, 29, 47] and processes that are forbidden in Minkowski space time as consequence of strict energy conservation.

S-matrix theory was extended to simple cosmological space times to study the decay of a massive particle into two massless particles conformally coupled to gravity in ref.[15, 16, 14]. In references[133, 132] these methods were adapted to calculate the decay of a massive bosonic particle *at rest* into two massless bosonic particles conformally coupled to gravity and into massless fermions Yukawa coupled to a scalar.

More recently[105] the decay of bosonic particles into two other bosonic degrees of freedom during a radiation dominated era was studied by implementing a non-perturbative method. This method was adapted to quantum field theory from the study of linewidths in quantum optics[138, 37], combined with a physically motivated adiabatic expansion. While the results of this reference agreed with those obtained in ref.[133] for a particle decaying *at rest* in the comoving frame *in the long time limit*, they revealed new phenomena for highly relativistic decaying particles as a consequence of the cosmological redshift, and the *relaxation of kinematic thresholds* as a consequence of energy uncertainties determined by the Hubble scale.

Our study in this article is a natural extension of that in ref.[105] focusing on decay of a heavy bosonic particle into fermions, a more relevant case for standard model physics (and probably beyond) since most of the fermionic degrees of freedom in the standard model (with the possible exception of neutrinos) are Yukawa coupled to the Higgs boson.

Brief summary:

The study of fermionic degrees of freedom as decay products introduces several conceptually important distinctions with the bosonic case studied in refs.[133, 105] that results in novel aspects of cosmological decay. First, fermionic degrees of freedom couple to the back-

ground gravitational field via the spin connection[191, 153, 73, 50, 28, 158, 144, 18, 68, 67, 19, 81, 35, 17]. Secondly, fermions Yukawa coupled to a bosonic degree of freedom yield a renormalizable theory. Recently the decay of a bosonic particle Yukawa coupled to fermions was studied within a non-perturbative real time framework in Minkowski space-time[32]. This study revealed novel transient dynamics associated with the *dressing* of the decaying particle by fermion-antifermion pairs into a *quasiparticle* state, which decays on a longer time scale. Such "dressing" leads to the necessity of an ultraviolet divergent renormalization of the decaying state and a detailed understanding of the various time scales to separate the many-particle dynamics of renormalization and dressing from that of the actual decay of the *quasiparticle*. Such dynamical effects cannot be addressed within an S-matrix framework since these effects are not secular in time and their contribution vanishes when the transition probability is divided by the total time in the infinite time limit. The dynamics of dressing and quasiparticle formation have been recently addressed in ref.[61] for a consistent interpretation of the reduction formula in asymptotic quantum field theory.

We introduce a *dynamical renormalization* that absorbs the ultraviolet divergences associated with fermion pairs into a renormalized survival probability at a renormalization time scale t_b. The survival probability obeys a *dynamical renormalization group equation* with respect to t_b. The cosmological redshift encodes the memory of the transient dynamics of quasiparticle formation in the decay law not seen in Minkowski space-time. If the decaying particle is ultrarelativistic, the decay dynamics depends crucially on t_{nr}, the time scale at which it becomes non-relativistic as a consequence of the cosmological redshift. An S-matrix inspired, phenomenologically motivated, Minkowski-like decay law is shown to *under estimate* the lifetime of the decaying state. Section (II) introduces the model and the adiabatic approximation, section (III) summarizes the non-perturbative framework to obtain the time evolution of the survival probability. In section (IV) we obtain the decay function for massless fermions during radiation domination, section (V) describes the dynamical renormalization method, section (VI) analyzes the decay dynamics of the renormalized survival probability during radiation domination, compares the results to an S-matrix inspired decay function, and introduces an upper bound to the decay function for very long lived, very weakly coupled particles valid all throughout the expansion history. Section (VII) discusses

the various results analyzing their regime of validity and highlighting several implications. Section (VIII) presents our conclusions summarizing the main results. Various appendices contain technical details, in particular appendix (B.2) derives the decay law in Minkowski space time, highlighting the renormalization aspects to compare to the curved space-time case.

4.2 The Model

We consider a Higgs-like scalar field Yukawa coupled to one Dirac fermion in a spatially flat Friedmann-Robertson-Walker (FRW) cosmology with scale factor $a(t)$ in comoving time. Generalizing to include Majorana fermions and/or more fermionic species is straightforward.

In comoving coordinates, the action is given by

$$S = \int d^3x\, dt\, \sqrt{-g} \left\{ \frac{1}{2}\dot{\phi}^2 - \frac{(\nabla\phi)^2}{2a^2} - \frac{1}{2}\left[M^2 + \xi\, R\right]\phi^2 + \overline{\Psi}\Big[i\,\gamma^\mu\, \mathcal{D}_\mu - m_f - Y\phi\Big]\Psi \right\}, \quad (4.2.1)$$

where

$$R = 6\Big[\frac{\ddot{a}}{a} + \Big(\frac{\dot{a}}{a}\Big)^2\Big], \quad (4.2.2)$$

is the Ricci scalar, and ξ is the coupling to gravity, with $\xi = 0, 1/6$ corresponding to minimal or conformal coupling, respectively. Introducing the vierbein field $e^\mu_a(x)$ defined as

$$g^{\mu\,\nu}(x) = e^\mu_a(x)\; e^\nu_b(x)\; \eta^{ab}\;,$$

where η_{ab} is the Minkowski space-time metric, the curved space time Dirac gamma- matrices $\gamma^\mu(x)$ and the fermionic covariant derivative $\mathcal{D}_\mu$ are given by[191, 28, 73, 50]

$$\gamma^\mu(x) = \gamma^a e^\mu_a(x) \quad , \quad \{\gamma^\mu(x), \gamma^\nu(x)\} = 2\; g^{\mu\nu}(x)\;, \quad (4.2.3)$$

where the γ^a are the Minkowski space time Dirac matrices, chosen to be in the standard Dirac representation, and the covariant derivative $\mathcal{D}_\mu$ is given in terms of the spin connection by

$$\mathcal{D}_\mu = \partial_\mu + \frac{1}{8}\,[\gamma^c, \gamma^d]\; e^\nu_c\; \left(\partial_\mu e_{d\nu} - \Gamma^\lambda_{\mu\nu}\; e_{d\lambda}\right)\;, \quad (4.2.4)$$

where $\Gamma^{\lambda}_{\mu\nu}$ are the usual Christoffel symbols.

For an (FRW) in conformal time $d\eta = dt/a(t)$, the metric becomes

$$g_{\mu\nu} = C^2(\eta)\,\eta_{\mu\nu} \quad , \quad C(\eta) \equiv a(t(\eta))\,, \tag{4.2.5}$$

where $\eta_{\mu\nu} = \mathrm{diag}(1,-1,-1,-1)$ is the flat Minkowski space-time metric, and the vierbeins e^{μ}_{a} are given by

$$e^{\mu}_{a} = C^{-1}(\eta)\,\delta^{\mu}_{a} \;\; ; \;\; e^{a}_{\mu} = C(\eta)\,\delta^{a}_{\mu}\,. \tag{4.2.6}$$

The fermionic part of the action in conformal coordinates now becomes

$$S_f = \int d^3x\, d\eta\, C^4(\eta)\,\overline{\Psi}(\vec{x},\eta)\left[i\frac{\gamma^0}{C(\eta)}\left(\frac{d}{d\eta}+3\frac{C'(\eta)}{2C(\eta)}\right)+i\,\frac{\gamma^i}{C(\eta)}\nabla_i - m_f - Y\,\phi\right]\Psi(\vec{x},\eta)\,. \tag{4.2.7}$$

The Dirac Lagrangian density in conformal time simplifies to

$$\sqrt{-g}\;\overline{\Psi}\Big(i\,\gamma^{\mu}\,\mathcal{D}_{\mu}\Psi - m_f - Y\phi\Big)\Psi = \Big(C^{3/2}(\eta)\,\overline{\Psi}(\vec{x},\eta)\Big)\;\Big[i\;\partial\!\!\!/ - (m_f + Y\phi)\;C(\eta)\Big]\Big(C^{3/2}(\eta)\,\Psi(\vec{x},\eta)\Big)\,, \tag{4.2.8}$$

where $i\partial\!\!\!/ = \gamma^a\partial_a$ is the usual Dirac differential operator in Minkowski space-time in terms of flat space time γ^a matrices. Introducing the conformally rescaled fields

$$C(\eta)\,\phi(\vec{x},t) = \chi(\vec{x},\eta) \;\; ; \;\; C^{\frac{3}{2}}(\eta)\,\Psi(\vec{x},t) = \psi(\vec{x},\eta)\,, \tag{4.2.9}$$

and neglecting surface terms, the action becomes

$$S = \int d^3x\; d\eta\,\Big\{\mathcal{L}_0[\chi] + \mathcal{L}_0[\psi] + \mathcal{L}_I[\chi,\psi]\Big\}\,, \tag{4.2.10}$$

with

$$\mathcal{L}_0[\chi] = \frac{1}{2}\left[\chi'^2 - (\nabla\chi)^2 - \mathcal{M}^2(\eta)\,\chi^2\right]\,, \tag{4.2.11}$$

$$\mathcal{L}_0[\psi] = \overline{\psi}\,\Big[i\;\partial\!\!\!/ - M_f^2(\eta)\Big]\psi\,, \tag{4.2.12}$$

$$\mathcal{L}_I[\chi,\psi] = -Y\chi\overline{\psi}\,\psi\,. \tag{4.2.13}$$

The effective time dependent masses are given by

$$\mathcal{M}^2(\eta) = m^2_{\phi}\,C^2(\eta) - \frac{C''(\eta)}{C(\eta)}\,(1-6\xi)\,, \tag{4.2.14}$$

and

$$M_f(\eta) = m_f\, C(\eta)\,. \tag{4.2.15}$$

In the non-interacting case, $Y = 0$, the Heisenberg equations of motion for the spatial Fourier modes with comoving wavevector $\vec{k}$ for the conformally rescaled scalar field are

$$\chi''_{\vec{k}}(\eta) + \Big[k^2 + \mathcal{M}^2(\eta)\Big]\chi_{\vec{k}}(\eta) = 0\,. \tag{4.2.16}$$

The Heisenberg fields are quantized in a comoving volume V, the real scalar field χ is expanded as

$$\chi(\vec{x},\eta) = \frac{1}{\sqrt{V}}\sum_{\vec{k}}\Big[a_{\vec{k}}\, g_k(\eta)\, e^{i\vec{k}\cdot\vec{x}} + a^\dagger_{\vec{k}}\, g^*_k(\eta)\, e^{-i\vec{k}\cdot\vec{x}}\Big]\,, \tag{4.2.17}$$

where the mode functions $g_k(\eta)$ obey

$$\Big[\frac{d^2}{d\eta^2} + k^2 + \mathcal{M}^2(\eta)\Big]g_k(\eta) = 0\,. \tag{4.2.18}$$

The mode functions are chosen to obey the Wronskian condition

$$g_k^{'}(\eta)g^*_k(\eta) - g_k^{*'}(\eta)g_k(\eta) = -i\,, \tag{4.2.19}$$

and $a, a^\dagger$ obey the usual canonical commutation relations.

For Dirac fermions the field $\psi(\vec{x},\eta)$ is expanded as

$$\psi(\vec{x},\eta) = \frac{1}{\sqrt{V}}\sum_{\vec{k},\lambda=1,2}\Big[b_{\vec{k},\lambda}\, U_\lambda(\vec{k},\eta)\, e^{i\vec{k}\cdot\vec{x}} + d^\dagger_{\vec{k},\lambda}\, V_\lambda(\vec{k},\eta)\, e^{-i\vec{k}\cdot\vec{x}}\Big]\,, \tag{4.2.20}$$

where the spinor mode functions U, V obey the Dirac equations[144, 18, 68, 67, 19, 81, 35, 17]

$$\Big[i\,\gamma^0\,\partial_\eta - \vec{\gamma}\cdot\vec{k} - M_f(\eta)\Big]U_\lambda(\vec{k},\eta) = 0\,, \tag{4.2.21}$$

$$\Big[i\,\gamma^0\,\partial_\eta + \vec{\gamma}\cdot\vec{k} - M_f(\eta)\Big]V_\lambda(\vec{k},\eta) = 0\,. \tag{4.2.22}$$

These equations become simpler by writing

$$U_\lambda(\vec{k},\eta) = \Big[i\,\gamma^0\,\partial_\eta - \vec{\gamma}\cdot\vec{k} + M_f(\eta)\Big]f_k(\eta)\,\mathcal{U}_\lambda\,, \tag{4.2.23}$$

$$V_\lambda(\vec{k},\eta) = \Big[i\,\gamma^0\,\partial_\eta + \vec{\gamma}\cdot\vec{k} + M_f(\eta)\Big]h_k(\eta)\,\mathcal{V}_\lambda\,, \tag{4.2.24}$$

with $\mathcal{U}_\lambda; \mathcal{V}_\lambda$ being constant spinors[35, 17] obeying

$$\gamma^0 \, \mathcal{U}_\lambda = \mathcal{U}_\lambda \qquad , \qquad \gamma^0 \, \mathcal{V}_\lambda = -\mathcal{V}_\lambda \, . \tag{4.2.25}$$

Inserting (4.2.23,4.2.24) into the Dirac equations (4.2.21,4.2.22) and using (4.2.25), it follows that the mode functions $f_k(\eta); h_k(\eta)$ obey the equations

$$\left[\frac{d^2}{d\eta^2} + k^2 + M_f^2(\eta) - i \, M_f'(\eta) \right] f_k(\eta) \;\; = \;\; 0 \, , \tag{4.2.26}$$

$$\left[\frac{d^2}{d\eta^2} + k^2 + M_f^2(\eta) + i \, M_f'(\eta) \right] h_k(\eta) \;\; = \;\; 0 \, . \tag{4.2.27}$$

Multiplying the Dirac equations on the left by γ^0, it is straightforward to confirm that

$$\frac{d}{d\eta}(U_\lambda^\dagger(q,\eta) \, U_\lambda(q,\eta)) = 0 \;\; ; \;\; \frac{d}{d\eta}(V_\lambda^\dagger(q,\eta) \, V_\lambda(q,\eta)) = 0 \, . \tag{4.2.28}$$

We choose the normalizations

$$U_\lambda^\dagger(q,\eta) \, U_{\lambda'}(q,\eta) = V_\lambda^\dagger(q,\eta) \, V_{\lambda'}(q,\eta) = \delta_{\lambda,\lambda'} \, , \tag{4.2.29}$$

so that the operators $b, b^\dagger, d, d^\dagger$ obey the canonical anticommutation relations. Furthermore, we will choose particle-antiparticle boundary conditions so that $h_k(\eta) = f_k^*(\eta)$ (see below). We note that for $m_f = 0$ the conformally rescaled fermi fields obey the same equations as in Minkowski space-time but in terms of conformal time, whereas this only occurs for bosons if they are conformally coupled to gravity, namely with $\xi = 1/6$, or for a radiation dominated cosmology (see below). The equivalence of massless fermions to those in Minkowski space-time will allow a direct comparison with the case of decay in flat space time studied in ref.[32] and summarized in appendix (B.2), and to interpret the differences with the curved space-time case.

4.2.1 Adiabatic Approximation in Post-inflationary Cosmology

The standard (post-inflation) cosmology is described by radiation (RD), matter (MD) and dark energy (DE) dominated stages, we take the latter to be described by a cosmological constant. Friedmann's equation in comoving time is

$$\left(\frac{\dot{a}}{a}\right)^2 = H^2(t) = H_0^2 \left[\frac{\Omega_M}{a^3(t)} + \frac{\Omega_R}{a^4(t)} + \Omega_\Lambda\right], \tag{4.2.30}$$

where the scale factor is normalized to $a_0 = a(t_0) = 1$ today. We take as representative the following values of the parameters [23, 181, 3]:

$$H_0 = 1.5 \times 10^{-42}\,\text{GeV} \;\;;\;\; \Omega_M = 0.308 \;\;;\;\; \Omega_R = 5 \times 10^{-5} \;\;;\;\; \Omega_\Lambda = 0.692\,. \tag{4.2.31}$$

Passing to conformal time η with $d\eta = dt/a(t)$, where the metric is given by (4.2.5) and $C(\eta) \equiv a(t(\eta))$, it follows that

$$\frac{d\,C(\eta)}{d\eta} = H_0\,\sqrt{\Omega_M}\left[a_{eq} + C(\eta) + s\,C^4(\eta)\right]^{1/2}, \tag{4.2.32}$$

with

$$a_{eq} = \frac{\Omega_R}{\Omega_M} \simeq 1.66\;\times 10^{-4} \;\;;\;\; s = \frac{\Omega_\Lambda}{\Omega_M} \simeq 2.25\,, \tag{4.2.33}$$

a_{eq} is the scale factor at matter-radiation equality.

Hence the different stages of cosmological evolution, namely (RD), (MD), and (DE), are characterized by

$$C(\eta) \ll a_{eq} \Rightarrow \text{RD} \;\;;\;\; a_{eq} \ll C(\eta) \lesssim 0.76 \Rightarrow \text{MD} \;\;;\;\; C(\eta) > 0.76 \Rightarrow \text{DE}\,. \tag{4.2.34}$$

We will begin the study the dynamics of particle decay during the (RD) dominated era, generalizing afterwards to the case of a very long lived, very weakly coupled particle. During (RD) and (MD) we find,

$$C(\eta) = H_R\,\eta\left[1 + \frac{H_R\,\eta}{4\,a_{eq}}\right], \tag{4.2.35}$$

where

$$H_R = H_0\,\sqrt{\Omega_R} \simeq 10^{-44}\,\text{GeV}\,, \tag{4.2.36}$$

and conformal time in terms of the scale factor is given by

$$\eta(C) = \frac{2\,a_{eq}}{H_R}\left[\sqrt{1+\frac{C}{a_{eq}}}-1\right]. \tag{4.2.37}$$

During the (RD) stage

$$C(\eta) \simeq H_R\,\eta\,, \tag{4.2.38}$$

and the relation between conformal and comoving time is given by

$$\eta = \Big(\frac{2\,t}{H_R}\Big)^{\frac{1}{2}} \Rightarrow a(t) = \Big[2\,tH_R\Big]^{\frac{1}{2}}, \tag{4.2.39}$$

a result that will prove useful in the study of the decay law during this stage.

Bosonic fields:

Solving the mode equations (4.2.18,4.2.26,4.2.27) with the cosmological scale factor (4.2.35) is obviously very challenging, instead we implement a physically motivated adiabatic expansion. To highlight the nature of the expansion let us consider first the bosonic mode equation (4.2.18). The term proportional to C''/C in (4.2.18) vanishes identically in a radiation dominated cosmology or for conformally coupled bosonic fields for which $\xi = 1/6$. We argue below that we can consistently neglect this term to leading order in the adiabatic expansion all throughout the cosmological evolution during (RD) and (MD) (see eqn. (4.2.54)). Neglecting this term, the mode equation (4.2.18) becomes

$$\Big[\frac{d^2}{d\eta^2}+\omega_k^2(\eta)\Big]g_k(\eta) = 0 \;\;;\;\; \omega_k^2(\eta) = k^2 + m_\phi^2\,C^2(\eta)\,. \tag{4.2.40}$$

We recognize that

$$\omega_k(\eta) = C(\eta)\,E_k(t)\,, \tag{4.2.41}$$

where

$$E_k(t) = \sqrt{k_p^2(t)+m_\phi^2} \;\;;\;\; k_p(t) = k/a(t)\,, \tag{4.2.42}$$

is the local energy measured by a comoving observer, and $k_p(t)$ is the physical wavevector redshifting with the cosmological expansion.

Writing the solution of (4.2.40) in the WKB form[28, 87, 149, 158, 29]

$$g_k(\eta) = \frac{e^{-i\int_{\eta_i}^{\eta} W_k(\eta')\,d\eta'}}{\sqrt{2\,W_k(\eta)}}\,, \tag{4.2.43}$$

and inserting this ansatz into (4.2.40) it follows that $W_k(\eta)$ must be a solution of the equation[28]

$$W_k^2(\eta) = \omega_k^2(\eta) - \frac{1}{2}\left[\frac{W_k^{''}(\eta)}{W_k(\eta)} - \frac{3}{2}\left(\frac{W_k^{'}(\eta)}{W_k(\eta)}\right)^2\right]. \tag{4.2.44}$$

This equation can be solved in an *adiabatic expansion*

$$W_k^2(\eta) = \omega_k^2(\eta)\left[1 - \frac{1}{2}\frac{\omega_k^{''}(\eta)}{\omega_k^3(\eta)} + \frac{3}{4}\left(\frac{\omega_k^{'}(\eta)}{\omega_k^2(\eta)}\right)^2 + \cdots\right]. \tag{4.2.45}$$

We refer to terms that feature n-derivatives of $\omega_k(\eta)$ as of n-th adiabatic order. The nature and reliability of the adiabatic expansion is revealed by considering the term of first adiabatic order

$$\frac{\omega_k^{'}(\eta)}{\omega_k^2(\eta)} = \frac{m_\phi^2\, C(\eta)C^{'}(\eta)}{\left[k^2 + m_\phi^2\, C^2(\eta)\right]^{3/2}}, \tag{4.2.46}$$

this is most easily recognized in *comoving* time t in terms of the comoving local energy (4.2.41,4.2.42) and the Hubble expansion rate

$$H(t) = \frac{\dot{a}(t)}{a(t)} = \frac{C^{'}(\eta)}{C^2(\eta)}. \tag{4.2.47}$$

In terms of these variables, the first order adiabatic ratio (4.2.46) becomes[105]

$$\frac{\omega_k^{'}(\eta)}{\omega_k^2(\eta)} = \frac{H(t)}{\gamma_k^2(t)\, E_k(t)}. \tag{4.2.48}$$

where

$$\gamma_k(t) = \frac{E_k(t)}{m_\phi}, \tag{4.2.49}$$

is the local Lorentz factor.

The adiabatic approximation relies on the smallness of the (time dependent) adiabatic ratio

$$\frac{H(t)}{E_k(t)} \ll 1, \tag{4.2.50}$$

corresponding to the physical wavelength $\propto 1/k_p(t)$ and/or the Compton wavelength of the particle $1/m_\phi$ being *much smaller* than the size of the particle horizon $d_H(t) \propto 1/H(t)$ at a given time. During (RD) the particle horizon grows as $a^2(t)$ and during (MD) it grows as $a^{3/2}(t)$ whereas the physical wavelength grows as $a(t)$. Therefore, if at a given initial time the

adiabatic approximation is valid and $H(t) \ll E_k(t)$ the reliability of the adiabatic expansion *improves* with the cosmological expansion.

To understand the origin of this approximation consider that the decaying particle is produced in the (RD) stage during which

$$H(t) \simeq 1.66\sqrt{g_{\rm eff}}\,\frac{T^2(t)}{M_{\rm Pl}}\,, \tag{4.2.51}$$

where $g_{\rm eff} \lesssim 100$ is the number of ultrarelativistic degrees of freedom. Therefore,

$$\frac{H(t)}{E_k(t)} \lesssim \left[\frac{T(t)}{E_k(t)}\right]\left[\frac{T(t)}{\rm GeV}\right] \times 10^{-18}\,. \tag{4.2.52}$$

An *upper bound* on this ratio is obtained by considering that the decaying particle is produced at the scale of grand unification with $T \simeq 10^{15}\,{\rm GeV}$, assuming that this scale describes the onset of the (RD) era. Taking a typical comoving energy $E_k(t) \simeq T(t)$, one finds that $H(t)/E_k(t) \lesssim 10^{-3}$ and diminishes with cosmological expansion and diminishing temperature. This argument suggests that for typical particle physics processes the adiabatic ratio $H(t)/E_k(t) \ll 1$ throughout the post-inflation thermal history.

In terms of this adiabatic ratio, we find

$$\frac{\omega_k^{''}(\eta)}{\omega_k^3(\eta)} = \frac{1}{\gamma_k^2(t)}\Big(\frac{R(t)}{6E_k^2(t)} + \frac{H^2(t)}{E_k^2(t)}\Big) - \frac{H^2(t)}{\gamma_k^4(t)E_k^2(t)}\,, \tag{4.2.53}$$

where $R(t)$ is the Ricci scalar (3.3.2). Furthermore, it is straightforward to find that

$$\frac{C''}{C\,\omega_k^2} = 2\Big(\frac{\dot{H}}{2\,E_k^2} + \frac{H^2}{E_k^2}\Big) = \alpha\;\frac{H^2}{E_k^2}\;\;;\;\;\alpha \simeq 0\;\;\;(RD)\;;\;\alpha \simeq \frac{1}{2}\;\;\;(MD)\,, \tag{4.2.54}$$

therefore, this ratio is of second adiabatic order and can be safely neglected to the leading adiabatic order pursued in this study, justifying the simplification of the mode equations to (4.2.40) even for non-conformal coupling to gravity.

In this study we consider the zeroth-adiabatic order with the mode functions given by

$$g_k(\eta) = \frac{e^{-i\int_{\eta_i}^{\eta}\omega_k(\eta')\,d\eta'}}{\sqrt{2\,\omega_k(\eta)}}\,. \tag{4.2.55}$$

Since the decay function is $\propto Y^2$, keeping the zeroth adiabatic order yields the *leading contribution* to the decay law. Furthermore, as shown in detail in ref.[105] particle production

as a consequence of cosmological expansion is an effect of higher order in the adiabatic expansion, thus it can be safely neglected to leading order.

The phase of the mode function has an immediate interpretation in terms of comoving time and the local comoving energy (4.2.41,4.2.42), namely

$$e^{-i\int_{\eta_i}^{\eta}\omega_k(\eta')\,d\eta'} = e^{-i\int_{t_i}^{t}E_k(t')\,dt'}\,, \tag{4.2.56}$$

which is a natural generalization of the phase of *positive frequency particle states in Minkowski space-time.*

During the (RD) era with $C(\eta)$ given by (4.2.38) we find that the criterion (4.2.50) for the validity of the adiabatic approximation implies

$$\omega_k(\eta)\,\eta = \frac{E_k(t)}{H(t)} \gg 1\,. \tag{4.2.57}$$

Fermi fields:

The adiabatic expansion is straightforwardly applied to the fermionic case and has been discussed in the literature[18, 68, 67, 19, 81]. Beginning with the mode equations (4.2.26,4.2.27) with $M_f'(\eta) = m_f\,C'(\eta)$ and, now with $\omega_k^2(\eta) = k^2 + M_f^2(\eta)$, it follows that

$$\frac{M_f'(\eta)}{\omega_k^2(\eta)} = \frac{H(t)}{\gamma_k(t)\,E_k(t)}\,, \tag{4.2.58}$$

therefore the purely imaginary term in these mode equations are of first adiabatic order and will be neglected to leading (zeroth) adiabatic order. Hence, to leading order we find

$$f_k(\eta) = h_k^*(\eta) = \frac{e^{-i\int_{\eta_i}^{\eta}\omega_k(\eta')\,d\eta'}}{\sqrt{2\,\omega_k(\eta)}}\,. \tag{4.2.59}$$

In what follows we will refer to $\omega_k^2(\eta) = k^2 + M^2(\eta)$ for both bosonic and fermionic degrees of freedom with $M^2(\eta) = m^2C^2(\eta)$ for either case. To leading (zeroth) order in the adiabatic expansion the Dirac spinor solutions in the standard Dirac representation and with the normalization conditions (4.2.29) are found to be

$$U_\lambda(\vec{k},\eta) = \frac{e^{-i\int_{\eta_i}^{\eta}\omega_k(\eta')\,d\eta'}}{\sqrt{2\,\omega_k(\eta)}}\begin{pmatrix}\sqrt{\omega_k(\eta)+M_f(\eta)}\,\chi_\lambda\\ \frac{\vec{\sigma}\cdot\vec{k}}{\sqrt{\omega_k(\eta)+M_f(\eta)}}\,\chi_\lambda\end{pmatrix}\;\;;\;\;\chi_1 = \begin{pmatrix}1\\0\end{pmatrix}\;;\;\chi_2 = \begin{pmatrix}0\\1\end{pmatrix}, \tag{4.2.60}$$

and

$$V_\lambda(\vec{k},\eta) = \frac{e^{i\int_{\eta_i}^{\eta}\omega_k(\eta')\,d\eta'}}{\sqrt{2\,\omega_k(\eta)}} \begin{pmatrix} \frac{\vec{\sigma}\cdot\vec{k}}{\sqrt{\omega_k(\eta)+M_f(\eta)}}\,\varphi_\lambda \\ \sqrt{\omega_k(\eta)+M_f(\eta)}\,\varphi_\lambda \end{pmatrix} \;\; ; \;\; \varphi_1 = \begin{pmatrix} 0 \\ 1 \end{pmatrix} \; ; \; \varphi_2 = -\begin{pmatrix} 1 \\ 0 \end{pmatrix}. \tag{4.2.61}$$

To leading adiabatic order these spinors satisfy the completeness relations

$$\begin{aligned} \sum_{\lambda=1,2} U_{\lambda,a}(\vec{k},\eta)\,\overline{U}_{\lambda,b}(\vec{k},\eta') &= \frac{e^{-i\int_{\eta'}^{\eta}\omega_k(\eta_1)\,d\eta_1}}{2\sqrt{\omega_k(\eta)\omega_k(\eta')}}\;\Lambda^{+}_{\vec{k},ab}(\eta,\eta') \\ \sum_{\lambda=1,2} V_{\lambda,a}(\vec{k},\eta')\,\overline{V}_{\lambda,b}(\vec{k},\eta) &= \frac{e^{-i\int_{\eta'}^{\eta}\omega_k(\eta_1)\,d\eta_1}}{2\sqrt{\omega_k(\eta)\omega_k(\eta')}}\;\Lambda^{-}_{\vec{k},ab}(\eta',\eta)\,, \end{aligned} \tag{4.2.62}$$

where the projector operators at different times $\Lambda^{+}_{k}(\eta,\eta')\;;\;\Lambda^{-}_{k}(\eta',\eta)$ and their properties are given in appendix (B.1).

4.3 Non-Perturbative Approach to the Decay Law

In Minkowski space-time, the decay rate of a particle is typically computed via S-matrix theory by obtaining the transition probability per unit time from an in-state prepared in the infinite past to an out-state in the infinite future. Obviously, such an approach – taking the infinite time limit– is not suitable in a time dependent gravitational background. An alternative approach in Minkowski space-time considers the Dyson-resummed propagator in frequency space that includes radiative corrections through the self-energy. The imaginary part of the self-energy evaluated on the mass shell in frequency space is identified with the decay rate, and a Breit-Wigner approximation to the full propagator, namely approximating the self-energy near the (complex) pole yields the exponential decay law. Again such an approach is not available in an expanding cosmological background where the lack of a time-like Killing vector prevents Fourier transforms in time-frequency, and makes the self-energy explicitly dependent on two time arguments, not only on the difference.

Instead we implement a quantum field theory method that complements and extends the Wigner-Weisskopf theory of atomic linewidths, that is particularly suited to study time

evolution in time dependent situations. This method is manifestly unitary and yields a non-perturbative description of transition amplitudes and probabilities directly in real time. We summarize below the main aspects of the method as it applies to this study, referring the reader to[105, 138, 37] for details. The total Hamiltonian in conformal time is given by $H_0 + H_I$ where H_0 is the free field Hamiltonian and

$$H_I(\eta) = Y \int d^3x\, \chi(\vec{x},\eta)\, \overline{\psi}(\vec{x},\eta)\, \psi(\vec{x},\eta) \tag{4.3.1}$$

is the interaction Hamiltonian in the interaction picture. Passing to the interaction picture wherein a given state is expanded in the Fock states associated with the creation and annihilation operators $a, a^\dagger, b, d$, etc. of the free theory, namely $|\Phi(\eta)\rangle_I = \sum_n \mathcal{C}_n(\eta)|n\rangle$, the amplitudes obey the coupled equations

$$i\frac{d}{d\eta}\mathcal{C}_n(\eta) = \sum_m \mathcal{C}_m(\eta)\langle n|H_I(\eta)|m\rangle\,. \tag{4.3.2}$$

This is an infinite hierarchy of integro-differential equations for the coefficients $\mathcal{C}_n(\eta)$. Consider that initially the state is $|\Phi\rangle$ so that $\mathcal{C}_\Phi(\eta_i) = 1\,;\, \mathcal{C}_\kappa(\eta_i) = 0$ for $|\kappa\rangle \neq |\Phi\rangle$, and consider a first order transition process $|\Phi\rangle \to |\kappa\rangle$ to intermediate multiparticle states $|\kappa\rangle$ with transition matrix elements $\langle\kappa|H_I(\eta)|\Phi\rangle$. Obviously the state $|\kappa\rangle$ will be connected to other multiparticle states $|\kappa'\rangle$ different from $|\Phi\rangle$ via $H_I(\eta)$. Hence for example up to second order in the interaction, the state $|\Phi\rangle \to |\kappa\rangle \to |\kappa'\rangle$. Restricting the hierarchy to *first order transitions* from the initial state $|\Phi\rangle \leftrightarrow |\kappa\rangle$, and neglecting the contribution from vacuum diagrams which just yield a re-definition of the vacuum state[1] (see discussion in ref.[105]) results in the following coupled equations

$$i\frac{d}{d\eta}\mathcal{C}_\Phi(\eta) = \sum_\kappa \mathcal{C}_\kappa(\eta)\langle\Phi|H_I(\eta)|\kappa\rangle \tag{4.3.3}$$

$$i\frac{d}{d\eta}\mathcal{C}_\kappa(\eta) = \mathcal{C}_\Phi(\eta)\langle\kappa|H_I(\eta)|\Phi\rangle \;\;;\;\; \mathcal{C}_\Phi(\eta_i) = 1\,;\, \mathcal{C}_\kappa(\eta_i) = 0\,. \tag{4.3.4}$$

Equation (3.6.3) with $C_\kappa(\eta_i) = 0$ is formally solved by

$$\mathcal{C}_\kappa(\eta) = -i\int_{\eta_i}^{\eta} \langle\kappa|H_I(\eta')|\Phi\rangle\, C_\Phi(\eta')\, d\eta'\,, \tag{4.3.5}$$

[1] This is one of the main differences with the method used in references[15, 133, 132] where a disconnected vacuum diagram is *also* included in the transition amplitude.

and inserting this solution into equation (3.6.2) we find

$$\frac{d}{d\eta}\,\mathcal{C}_\Phi(\eta) = -\int_{\eta_i}^{\eta} d\eta'\,\Sigma_\Phi(\eta,\eta')\;\mathcal{C}_\Phi(\eta')\,, \tag{4.3.6}$$

where we have introduced the *self-energy*

$$\Sigma_\Phi(\eta;\eta') = \sum_\kappa \langle\Phi|H_I(\eta)|\kappa\rangle\langle\kappa|H_I(\eta')|\Phi\rangle\,. \tag{4.3.7}$$

We study the decay of a single particle bosonic state into a fermion-anti-fermion pair to leading order in the Yukawa coupling and the adiabatic approximation. Therefore the initial state is a single particle bosonic state with momentum $\vec{k}$, namely $|\Phi\rangle \equiv |1^\chi_{\vec{k}}\rangle$. The set of states $|\kappa\rangle$ with a non-vanishing matrix element of H_I with this single particle state are $|\kappa\rangle \equiv |1^f_{\vec{p},\lambda}, \overline{1^f}_{\vec{q},\lambda'}\rangle$ where λ,λ' are the polarization of the fermion and antifermion states. The matrix elements entering in the evolution of the amplitudes are

$$\begin{aligned}
\langle 1^\chi_{\vec{k}}|H_I(\eta)|1^f_{\vec{p},\lambda}, \overline{1^f}_{\vec{q},\lambda'}\rangle &= \frac{V\,\delta_{\vec{k},\vec{p}+\vec{q}}}{V^{3/2}}\sum_a U_{\lambda,a}(\vec{p},\eta)\,\overline{V}_{\lambda',a}(\vec{q},\eta)\,g^*_k(\eta)\\
\langle 1^f_{\vec{p},\lambda}, \overline{1^f}_{\vec{q},\lambda'}|H_I(\eta')|1^\chi_{\vec{k}}\rangle &= \frac{V\,\delta_{\vec{k},\vec{p}+\vec{q}}}{V^{3/2}}\sum_b V_{\lambda',b}(\vec{q},\eta')\,\overline{U}_{\lambda,b}(\vec{p},\eta')\,g_k(\eta')\,,
\end{aligned} \tag{4.3.8}$$

and the self-energy (4.3.7) to leading order in the adiabatic expansion becomes

$$\Sigma_\chi(k,\eta,\eta') = \sum_{\vec{p},\vec{q}}\sum_{\lambda,\lambda'}\Big[\langle 1^\chi_{\vec{k}}|H_I(\eta)|1^f_{\vec{p},\lambda}, \overline{1^f}_{\vec{q},\lambda'}\rangle\langle 1^f_{\vec{p},\lambda}, \overline{1^f}_{\vec{q},\lambda'}|H_I(\eta')|1^\chi_{\vec{k}}\rangle\Big] =$$

$$Y^2\,\frac{e^{i\int_{\eta'}^{\eta}\omega^\phi_k(\eta_1)d\eta_1}}{2\sqrt{\omega^\phi_k(\eta)\omega^\phi_k(\eta')}}\int\frac{d^3p}{(2\pi)^3}\,\frac{e^{-i\int_{\eta'}^{\eta}(\omega^\psi_p(\eta_1)+\omega^\psi_q(\eta_1))d\eta_1}}{4\sqrt{\omega^\psi_p(\eta)\omega^\psi_p(\eta')}\,\sqrt{\omega^\psi_q(\eta)\omega^\psi_q(\eta')}}\;\mathrm{Tr}\Big[\Lambda^+_{\vec{p}}(\eta,\eta')\Lambda^-_{\vec{q}}(\eta',\eta)\Big] \tag{4.3.9}$$

where $\vec{q} = \vec{k} - \vec{p}$. This is the fermionic one-loop self energy in curved space time to leading order in the adiabatic expansion.

Obviously the differential equation (4.3.6) cannot be solved exactly with the above self-energy. In Minkowski space time the self-energy is a function of the time difference allowing a solution via Laplace transform[138, 37]. However, in a time dependent expanding cosmology such an approach is not available. This is a consequence of the lack of a global time-like Killing vector. Instead for weak coupling we resort to a *Markov* approximation[105]. While

details are available in ref.[105, 37, 138] to which the reader is referred, we summarize here the main aspects of this approximation.

We begin by introducing

$$\mathcal{E}_\Phi(\eta,\eta') \equiv \int_{\eta_i}^{\eta'} \Sigma_\Phi(\eta,\eta'')\, d\eta'' \,, \tag{4.3.10}$$

such that

$$\frac{d}{d\eta'}\,\mathcal{E}_\Phi(\eta,\eta') = \Sigma_\Phi(\eta,\eta')\,, \tag{4.3.11}$$

with the condition

$$\mathcal{E}_\Phi(\eta,\eta_i) = 0\,. \tag{4.3.12}$$

Then (4.3.6) can be written as

$$\frac{d}{d\eta}\mathcal{C}_\Phi(\eta) = -\int_{\eta_i}^{\eta} d\eta'\,\frac{d}{d\eta'}\mathcal{E}_\Phi(\eta,\eta')\,\mathcal{C}_\Phi(\eta')\,, \tag{4.3.13}$$

which can be integrated by parts to yield

$$\frac{d}{d\eta}\mathcal{C}_\Phi(\eta) = -\mathcal{E}_\Phi(\eta,\eta)C_\Phi(\eta) + \int_{\eta_i}^{\eta} d\eta'\,\mathcal{E}_\Phi(\eta,\eta')\frac{d}{d\eta'}\mathcal{C}_\Phi(\eta')\,. \tag{4.3.14}$$

Since $\mathcal{E}_\Phi \propto \mathcal{O}(Y^2)$ the first term on the right hand side of (4.3.14) is of order Y^2, whereas the second is $\mathcal{O}(Y^4)$ because $d\,\mathcal{C}_\Phi(\eta)/d\eta \propto Y^2$. Therefore up to $\mathcal{O}(Y^2)$ the evolution equation for the amplitude $\mathcal{C}_\Phi$ becomes

$$\frac{d}{d\eta}\mathcal{C}_\Phi(\eta) = -\mathcal{E}_\Phi(\eta,\eta)\,\mathcal{C}_\Phi(\eta)\,, \tag{4.3.15}$$

with solution

$$\mathcal{C}_\Phi(\eta) = \exp\Big(-\int_{\eta_i}^{\eta} \mathcal{E}_\Phi(\eta',\eta')\,d\eta'\Big)\,\mathcal{C}_\Phi(\eta_i)\,. \tag{4.3.16}$$

This expression clearly highlights the non-perturbative nature of the Wigner-Weisskopf approximation. The imaginary part of the self energy Σ_Φ yields a *renormalization* of the adiabatic frequencies and will not be addressed here[37, 138], whereas the real part determines the decay law

$$\mathcal{P}_\Phi(\eta) \equiv |\mathcal{C}_\Phi(\eta)|^2 = e^{-\int_{\eta_i}^{\eta}\Gamma_\Phi(\eta')d\eta'}\,\mathcal{P}_\Phi(\eta_i) \;\;;\;\; \Gamma_\Phi(\eta) = 2\int_{\eta_i}^{\eta} d\eta_1\,\mathrm{Re}\left[\Sigma_\Phi(\eta,\eta_1)\right], \tag{4.3.17}$$

where we introduced the *survival probability* $\mathcal{P}_\Phi(\eta)$ with $\mathcal{P}_\Phi(\eta_i) = |C_\Phi(\eta_i)|^2$. This final expression for the survival probability directly exhibits the non-perturbative nature of the method. The self-energy is given by (4.3.9) to leading order in Yukawa coupling.

4.4 Massless Fermions

Our goal in this article is to study the decay of a heavy Higgs-like scalar field into much lighter fermions, neglecting the fermion masses. This is a suitable scenario for the standard model where the Higgs scalar can decay into all the charged leptons and quarks but for the top, and the quark and lepton masses may be safely neglected. Such scenario also includes the possibility of decay into neutrinos in the case that neutrino masses originate in Yukawa couplings to a Higgs-like scalar beyond the standard model. We postpone the study of decay into heavier fermionic degrees of freedom to a companion article. Focusing on the case of massless fermions allows a direct comparison with results in Minkowski space time, which are summarized in appendix (B.2). Furthermore, understanding this simpler case provides a pathway towards the more general case of massive fermions to be studied elsewhere.

For massless fermions $\omega^{\psi}_{k}(\eta) = k$, in this case the projector operators $\Lambda^{\pm}$ in (4.3.9) are given by eqn. (B.1.12) in appendix (B.1), and the self-energy (4.3.9) can be written in dispersive form as

$$\Sigma_{\chi}(k,\eta,\eta') = Y^2 \, \frac{e^{i\int_{\eta'}^{\eta}\omega^{\phi}_{k}(\eta_1)d\eta_1}}{2\sqrt{\omega^{\phi}_{k}(\eta)\omega^{\phi}_{k}(\eta')}} \int \rho(k_0,k)\, e^{-ik_0(\eta-\eta')}\, \frac{dk_0}{2\pi}\,, \tag{4.4.1}$$

where the spectral density is given by

$$\rho(k_0,k) = 8\pi \int \frac{d^3p}{(2\pi)^3}\, \frac{\delta(k_0 - p - |\vec{k}-\vec{p}|)}{4p\,|\vec{k}-\vec{p}|}\Big[p\,|\vec{k}-\vec{p}| - \vec{p}\cdot(\vec{k}-\vec{p})\Big]\,, \tag{4.4.2}$$

with the result

$$\rho(k_0,k) = \frac{1}{4\pi}\,(k_0^2 - k^2)\,\Theta(k_0 - k)\,. \tag{4.4.3}$$

We carry out the k_0 integral in (4.4.1) by introducing an upper (comoving) ultraviolet cutoff Λ *and* a short time convergence factor $\eta - \eta' \to \eta - \eta' - i\epsilon$ with $\epsilon \to 0^+$ and replacing $k_0^2 \to -d^2/d\eta^{'\,2}$ yielding the final result for the self-energy

$$\Sigma_{\chi}(k,\eta,\eta') = -i\frac{Y^2}{16\pi^2}\, \frac{e^{i\int_{\eta'}^{\eta}\omega^{\phi}_{k}(\eta_1)d\eta_1}}{\sqrt{\omega^{\phi}_{k}(\eta)\omega^{\phi}_{k}(\eta')}} \left[\frac{d^2}{d\eta^{'\,2}} + k^2\right]\left[\frac{e^{-i\Lambda(\eta-\eta'-i\epsilon)} - e^{-ik(\eta-\eta'-i\epsilon)}}{(\eta-\eta'-i\epsilon)}\right]. \tag{4.4.4}$$

In our analysis we will keep Λ fixed but large and take the limit $\epsilon \to 0^+$ first, clearly this is the correct limit when the theory is considered as an effective field theory valid below a cutoff Λ. We note that the flat space time limit is obtained by replacing $\eta \to t$, and the frequency ω_k^ϕ to be time independent (see appendix (B.2)).

It remains to perform the time integrals to obtain $\Gamma_\Phi(\eta)$ and $\int_{\eta_i}^{\eta} \Gamma_\Phi(\eta')\, d\eta'$ given by eqn. (4.3.17). The total time derivative in (4.4.4) is integrated by parts and consistently with keeping the leading order in the adiabatic expansion, terms of the form ω'/ω^2 are neglected since these yield higher order adiabatic corrections. In the limit $\epsilon \to 0^+$ for fixed Λ we find the *decay function*

$$\int_{\eta_i}^{\eta} \Gamma_\Phi(\eta')\, d\eta' = \frac{Y^2}{8\pi^2}\, I(\Lambda,k,\eta) \;\; ; \;\; I(\Lambda,k,\eta) \equiv \Big[I_1(\Lambda,k,\eta) + I_2(\Lambda,k,\eta) + I_3(\Lambda,k,\eta) \Big] \,, \tag{4.4.5}$$

where

$$I_1(\Lambda,k,\eta) = \frac{\Lambda - k}{\omega_k^\phi(\eta_i)} \left\{ 1 - \sqrt{\frac{\omega_k^\phi(\eta_i)}{\omega_k^\phi(\eta)}} \left[\frac{\sin\Big(\int_{\eta_i}^{\eta} \big(\Lambda - \omega_k^\phi(\eta')\big) d\eta' \Big)}{(\Lambda - k)(\eta - \eta_i)} + \frac{\sin\Big(\int_{\eta_i}^{\eta} \big(\omega_k^\phi(\eta') - k\big) d\eta' \Big)}{(\Lambda - k)(\eta - \eta_i)} \right] \right\} , \tag{4.4.6}$$

$$\begin{aligned} I_2(\Lambda,k,\eta) &= \int_{\eta_i}^{\eta} \left[\sqrt{\frac{\omega_k^\phi(\eta')}{\omega_k^\phi(\eta_i)}} + \sqrt{\frac{\omega_k^\phi(\eta_i)}{\omega_k^\phi(\eta')}} \right] \times \left[\frac{1 - \cos\Big(\int_{\eta_i}^{\eta'} \big(\omega_k^\phi(\eta_1) - \Lambda\big) d\eta_1 \Big)}{\eta' - \eta_i} \right. \\ &- \left. \frac{1 - \cos\Big(\int_{\eta_i}^{\eta'} \big(\omega_k^\phi(\eta_1) - k\big) d\eta_1 \Big)}{\eta' - \eta_i} \right] d\eta' \equiv I_{2a}(\Lambda,k,\eta) + I_{2b}(k,\eta) \,, \end{aligned} \tag{4.4.7}$$

$$\begin{aligned} I_3(\Lambda,k,\eta) &= m_\phi^2 \int_{\eta_i}^{\eta} \frac{1}{\sqrt{\omega_k^\phi(\eta')}} \left\{ \int_{\eta_i}^{\eta'} \frac{C^2(\eta_1)}{\sqrt{\omega_k^\phi(\eta_1)}} \left[\frac{\sin\Big(\int_{\eta_1}^{\eta'} \big(\Lambda - \omega_k^\phi(\eta_2)\big) d\eta_2 \Big)}{\eta' - \eta_1} \right. \right. \\ &+ \left. \left. \frac{\sin\Big(\int_{\eta_1}^{\eta'} \big(\omega_k^\phi(\eta_2) - k\big) d\eta_2 \Big)}{\eta' - \eta_1} \right] d\eta_1 \right\} d\eta' \equiv I_{3a}(\Lambda,k,\eta) + I_{3b}(k,\eta) \,. \end{aligned} \tag{4.4.8}$$

In obvious notation the contributions $I_{2b}(k,\eta), I_{3b}(k,\eta)$ are the Λ independent terms in $I_{2,3}$ respectively. These three contributions are studied separately below, analyzing their cutoff dependent and independent terms extracting the different physics of each term.

4.4.1 Analysis of $I_{1,2,3}$

In the following analysis we will take the cutoff Λ to be the largest of all scales, in particular $\Lambda \gg \omega_k(\eta)$ at all times.

I_1**:** I_1 vanishes identically as $\eta \to \eta_i$ and the oscillatory terms become negligibly small for $\Lambda(\eta - \eta_i) \gg 1$, therefore I_1 *grows* to its asymptotic value

$$I_1 = \frac{\Lambda - k}{\omega_k^\phi(\eta_i)} \tag{4.4.9}$$

very rapidly, on a time scale $\eta - \eta_i \simeq 1/\Lambda$. This divergent contribution corresponds to a renormalization of the amplitude and is similar to a linearly divergent renormalization in Minkowski space time[32] (see appendix (B.2)).

I_2**:** The technical details of the analysis of I_2 are relegated to appendix (B.4). The main result is that for $\Lambda\,(\eta - \eta_i) \gg 1$

$$I_2(\Lambda, k, \eta) = 2\Big[\,\ln\big[\Lambda\,(\eta - \eta_i)\big] + \gamma_E\Big] + I_{2b}(k, \eta) \tag{4.4.10}$$

where $\gamma_E = 0.577\cdots$ is Euler's constant and $I_{2b}(k,\eta)$ is given by equation (B.4.5) in appendix (B.4) where this contribution is analyzed in detail. We discuss this contribution in further detail in sections (4.5,4.6) below.

I_3**:** With $\Lambda \gg \omega_k$ the argument of the sine function in the first term in eqn. (4.4.8), namely in $I_{3a}(\Lambda, k, \eta)$, simplifies to $\Lambda\,(\eta' - \eta_1)$, therefore

$$I_{3a}(\Lambda, k, \eta) = m_\phi^2 \int_{\eta_i}^{\eta} \frac{1}{\sqrt{\omega_k^\phi(\eta')}} \left\{ \int_{\eta_i}^{\eta'} \frac{C^2(\eta_1)}{\sqrt{\omega_k^\phi(\eta_1)}}\, \frac{\sin\Big(\Lambda\,(\eta' - \eta_1)\Big)}{\eta' - \eta_1}\, d\eta_1 \right\} d\eta'\,. \tag{4.4.11}$$

Defining $\sigma = \Lambda\,(\eta' - \eta_1)$; $\sigma_f = \Lambda\,(\eta' - \eta_i)$, and taking the limits $\Lambda \to \infty$; $\sigma_f \to \infty$, the integral over η_1 in eqn. (4.4.11) becomes

$$\int_0^\infty \frac{C^2(\eta' - \sigma/\Lambda)}{\sqrt{\omega_k^\phi(\eta' - \sigma/\Lambda)}}\, \frac{\sin\sigma}{\sigma}\, d\sigma \quad \xrightarrow[\Lambda\to\infty]{} \quad \frac{\pi}{2}\, \frac{C^2(\eta')}{\sqrt{\omega_k^\phi(\eta')}}\,, \tag{4.4.12}$$

therefore in this limit we find

$$I_{3a}(k,\eta) = \frac{\pi}{2}\, m_\phi^2 \int_{\eta_i}^{\eta} \frac{C^2(\eta')}{\omega_k^\phi(\eta')}\, d\eta' = \frac{\pi}{2}\, m_\phi \int_{t_i}^{t} \frac{1}{\gamma_k(t')}\, dt' \tag{4.4.13}$$

where we used $\omega_k^\phi(\eta) = C(\eta)E_k^\phi(t) = m_\phi\, C(\eta)\,\gamma_k(t)$ and $C(\eta)d\eta' = dt'$, with $\gamma_k(t) = \sqrt{1+k_p^2(t)/m^2}$ being the Lorentz factor whose time dependence is a consequence of the cosmological redshift.

In appendix (B.5) we provide the analysis for I_{3b}, gathering both terms we find that

$$I_3(k,\eta) = \frac{\pi}{2}\, m_\phi^2 \int_{\eta_i}^{\eta} \frac{C^2(\eta')}{\omega_k^\phi(\eta')}\left[1+\mathcal{S}(k,\eta')\right] d\eta' \,, \tag{4.4.14}$$

where $\mathcal{S}(k,\eta')$ is given by (B.5.25) with asymptotic limit $\mathcal{S}(k,\eta') \to 1$ for large η'. Therefore $I_3 = I_{3a} + I_{3b}$ *does not* depend on Λ in the limit $\Lambda \to \infty$. This is similar to the case in Minkowski space time (see appendix (B.2) where the equivalent term is called $T_3(k,t)$, eqn. (B.2.7)).

4.5 Renormalization: Dynamics of "Dressing"

The final result for the decay function in (4.4.5), $I(\Lambda,k,\eta)$ is given by ,

$$I(\Lambda,k,\eta) = \frac{\Lambda-k}{\omega_k^\phi(\eta_i)} + 2\,\ln\left[\Lambda\,\eta_i\, e^{\gamma_E}\right] + I_{fin}(k,\eta)\,, \tag{4.5.1}$$

where $I_{fin}(k,\eta)$ is independent of the cutoff Λ in the limit $\Lambda \to \infty$, and for $(\eta-\eta_i) \gg 1/\Lambda$ it is given by

$$I_{fin}(k,\eta) = 2\,\ln\left[\frac{\eta}{\eta_i}-1\right] + I_{2b}(k,\eta) + I_3(k,\eta)\,. \tag{4.5.2}$$

The linear and logarithmic dependence on the cutoff Λ are *exactly* the same as in Minkowski space time[32], as obtained in the appendix (B.2). This similarity is expected as the cutoff dependence arises from the short distance behavior of the self-energy correction which should be insensitive to the curvature of space time. As discussed in ref.[32] the origin of this divergence is the "dressing" of the bare single particle state by a cloud of fermion-anti-fermion pairs into a renormalized *quasiparticle* state. In a renormalizable theory the growth of the density of states at high energy implies that this cloud of excitations contains high energy states. The dynamical build-up of the cloud of excitations occurs on a time scale $\eta-\eta_i \simeq 1/\Lambda$ at which the divergent contributions to $I_{1,2}$ saturate, see eqn. (4.4.6) and the discussion in appendix (B.4).

The "dressing" of the bare into the physical renormalized quasiparticle state is accounted for by the wave-function renormalization of the amplitude[32]. For large cutoff scale Λ and for a weakly coupled theory with $Y^2 \ll 1$ there is a wide separation betweeen the time scales of formation of the dressed renormalized state $\eta - \eta_i \simeq 1/\Lambda$, the time scale of typical oscillations $\eta - \eta_i \simeq 1/\omega_k^\phi(\eta)$ and finally the decay time scale $\eta - \eta_i \propto 1/Y^2\omega_k^\phi(\eta)$, which for weak coupling is the longest scale. Therefore, we can evolve the initial state in time up to an intermediate time scale η_b with $(\eta_b - \eta_i) \gg 1/\Lambda$, but much smaller than the typical decay time scale $\propto 1/Y^2\omega_k^\phi(\eta_i)$, so that the initial state had enough time to be "dressed" by fermion-antifermion pairs into the renormalized quasiparticle state, but did not have time to decay. For example, taking $\eta_b - \eta_i = 1/\omega_k^\phi(\eta_i)$ fulfills the conditions of time scale separation because $\omega_k^\phi \ll \Lambda$, and because for $Y^2 \ll 1$ there will be many oscillations of the field before it decays. Taking this renormalization scale is tantamount to an "on-shell" renormalization scheme. We identify η_b as the time of formation – or "birth" – of the "dressed" or quasiparticle state[32], which after formation decays on a much longer time scale.

The time evolution of the "bare" single particle state until it is renormalized or "dressed" is implemented by the following procedure. Writing

$$I(\Lambda, k, \eta) \equiv I(\Lambda, k, \eta_b) + I_S(k, \eta, \eta_b) \;\; ; \;\; I_S(k, \eta, \eta_b) = I(\Lambda, k, \eta) - I(\Lambda, k, \eta_b)\,, \tag{4.5.3}$$

where, taking $(\eta_b - \eta_i) \gg 1/\Lambda$, the subtracted quantity

$$I_S(k, \eta, \eta_b) = 2\,\ln\left[\frac{\eta - \eta_i}{\eta_b - \eta_i}\right] + I_{2b}(k, \eta, \eta_b) + I_{3S}(k, \eta, \eta_b)\,, \tag{4.5.4}$$

is independent of Λ for $\eta > \eta_b$ and $\Lambda(\eta_b - \eta_i) \gg 1$. The subtracted contributions $I_{2b}(k, \eta, \eta_b)$; $I_{3S}(k, \eta, \eta_b)$ are defined as follows

$$I_{2b}(k, \eta, \eta_b) \equiv I_{2b}(k, \eta) - I_{2b}(k, \eta_b) \;\; ; \;\; I_{3S}(k, \eta, \eta_b) \equiv I_3(k, \eta) - I_3(k, \eta_b)\,, \tag{4.5.5}$$

and are obtained explicitly in appendices (B.4, B.5) respectively. During (RD) we find (see appendix (B.4) for definitions and eqn. (B.4.12))

$$I_{2b}(k, \eta, \eta_b) = -\int_{\xi_b}^{\xi} \left[\sqrt{W[\xi']} + \frac{1}{\sqrt{W[\xi']}}\right] \left[1 - \cos[J(\xi')]\right] \frac{d\xi'}{\xi'}\,, \tag{4.5.6}$$

with

$$\begin{aligned} \xi &= (\eta-\eta_i)/\eta_i \;\;;\;\; \xi_b=(\eta_b-\eta_i)/\eta_i \\ W[\xi] &= \frac{1}{\gamma_i}\left[(\gamma_i^2-1)+(1+\xi)^2\right]^{\frac{1}{2}} \;\;;\;\; \gamma_i\equiv\gamma(\eta_i)\,, \end{aligned} \tag{4.5.7}$$

$J(\xi')$ is given by eqn. (B.4.9) in appendix (B.4), and

$$I_{3S}(k,\eta,\eta_b)=\frac{\pi}{2}\,m_\phi\int_{\eta_b}^{\eta}\frac{C(\eta')}{\gamma_k(\eta')}\Big[1+\mathcal{S}(\eta')\Big]\,d\eta'\,, \tag{4.5.8}$$

where $\mathcal{S}(\eta)$ is given by eqn. (B.5.25) in appendix (B.5). The contribution from $I(\Lambda,k,\eta_b)$ is absorbed into wave-function renormalization Z as follows. Writing equation (4.3.17) as

$$\mathcal{P}_\Phi(\eta)=e^{-\int_{\eta_i}^{\eta}\Gamma_\Phi(\eta')d\eta'}\,\mathcal{P}_\Phi(\eta_i)\equiv e^{-\int_{\eta_b}^{\eta}\Gamma_\Phi(\eta')d\eta'}\,\mathcal{P}_{\Phi,r}(\eta_b)\,, \tag{4.5.9}$$

where the renormalized probability is given by

$$\mathcal{P}_{\Phi,r}(\eta_b)=Z(\eta_b)\,\mathcal{P}_\Phi(\eta_i)\;\;;\;\; Z(\eta_b)=e^{-\int_{\eta_i}^{\eta_b}\Gamma_\Phi(\eta')d\eta'}\,. \tag{4.5.10}$$

The exponent in the wave function renormalization $Z(\eta_b)$ is given by

$$\int_{\eta_i}^{\eta_b}\Gamma_\Phi(\eta')d\eta'=\frac{Y^2}{8\pi^2}\,I(\Lambda,k,\eta_b)\,, \tag{4.5.11}$$

yielding an ultraviolet divergent wave function renormalization. The *renormalized* probability obeys

$$\mathcal{P}_{\Phi,r}(\eta)=e^{-\int_{\eta_b}^{\eta}\Gamma_\Phi(\eta')d\eta'}\,\mathcal{P}_{\Phi,r}(\eta_b)\,. \tag{4.5.12}$$

The decay function that describes the time evolution of the *renormalized* survival probability is given by

$$\int_{\eta_b}^{\eta}\Gamma_\Phi(\eta')d\eta'=\frac{Y^2}{8\pi^2}\,I_S(k,\eta,\eta_b)\,, \tag{4.5.13}$$

it is *finite* and independent of Λ in the large cutoff limit. The time scale η_b acts as a renormalization scale, obviously the survival probability $\mathcal{P}_{\Phi,r}(\eta)$ is *independent* of this renormalization scale, hence it obeys a *dynamical renormalization group* equation, namely

$$\frac{\partial}{\partial\eta_b}\,\mathcal{P}_{\Phi,r}(\eta)=0\,. \tag{4.5.14}$$

The solution of this equation is, obviously[2],

$$\mathcal{P}_{\Phi,r}(\eta_A) = e^{-\int_{\eta_B}^{\eta_A} \Gamma_\Phi(\eta')d\eta'}\, \mathcal{P}_{\Phi,r}(\eta_B)\,. \tag{4.5.15}$$

$\mathcal{P}_{\Phi,r}(\eta_b)$ describes the probability of the renormalized *quasiparticle* state. This "dressed" state decays with the finite and cutoff independent decay function $\int_{\eta_b}^{\eta} \Gamma_\Phi(\eta')d\eta'$ on time scales much longer than the "dressing" or renormalization scale η_b.

In the following analysis we will drop the subscript r from $\mathcal{P}_{\Phi,r}$ to simplify notation since we will be strictly dealing with the *renormalized* survival probability.

The decay function (4.5.13) depends explicitly on the initial time η_i (see explicit expressions in appendix (B.4)). However, $\mathcal{P}_{\Phi,r}(\eta_b)$ is defined at the renormalization scale η_b and it is taken to be the initial probability of the fully renormalized state after all the short time transient dynamics that result in the "dressing" of the bare into the renormalized quasiparticle state have subsided. Therefore, the dependence of the contributions (4.5.6,4.5.8) on η_i must be traded for a dependence on η_b.

Let us write

$$\eta_b - \eta_i = \frac{\beta}{\Lambda}\,, \tag{4.5.16}$$

with $\beta \gg 1$ so that the Λ dependent terms in $I_{1,2}$ reached their asymptotic behavior. For example, the "on-shell" renormalization scheme corresponds to $\beta \equiv \Lambda/\omega_k(\eta_i)$. Therefore, in terms of the Hubble rate and the physical cutoff $\Lambda_{ph}(\eta_i) = \Lambda/C(\eta_i)$ at the initial time $H(\eta_i)$ we find in (RD)

$$\frac{\eta_b}{\eta_i} = 1 + \beta\, \frac{H(\eta_i)}{\Lambda_{ph}(\eta_i)}\,. \tag{4.5.17}$$

Since the cutoff scale Λ is taken to be much larger than any of the energy scales and the adiabatic condition requires that $H(\eta)/E_k(\eta) \ll 1$ at all times, it follows that $H(\eta_i)/\Lambda_{ph}(\eta_i) \ll H(\eta)/E_k(\eta) \ll 1$. Furthermore, we find that

$$\omega_k(\eta_i) = \omega_k(\eta_b)\Big[1 - \beta\, \frac{\omega_k^{'}(\eta_b)}{\omega_k^2(\eta_b)}\, \frac{\omega_k(\eta_b)}{\Lambda} + \cdots\Big]\,, \tag{4.5.18}$$

the second term in the bracket is at most of first adiabatic order, this is the case for the "on-shell" renormalization scheme for which $\beta\, \omega_k(\eta_b)/\Lambda = 1$. Hence, to leading adiabatic

[2]Note the similarity with the usual renormalization group function associated with the running of the wave function renormalization that yields anomalous dimensions.

order we can safely replace $\omega_k(\eta_i) \to \omega_k(\eta_b)$ in the expressions. Using the results of appendix (B.4) we find that similar arguments justify the replacement $\gamma_k(\eta_i) \to \gamma_k(\eta_b)$ along with $\eta_i \to \eta_b$ in all the quantities that enter in the decay function. In the limit of large cutoff Λ the trade-off between the variables at the initial time and those at the renormalization scale η_b *does not* depend on the cutoff as it must be for a consistent effective field theory description well below the cutoff scale. We note that the adiabatic approximation plays an important role in this separation and is a necessary ingredient because the frequencies depend on time unlike in Minkowski space-time. In particular for the "on-shell" renormalization scheme

$$\frac{\eta_b}{\eta_i} - 1 = \frac{1}{\omega_k(\eta_i)\,\eta_i} \ll 1\,, \tag{4.5.19}$$

because the adiabatic condition (during (RD)) corresponds to $\omega_k(\eta_i)\,\eta_i \gg 1$ (see equation (4.2.57)).

4.6 Dynamics of Decay

Once we have absorbed the ultraviolet divergences into a renormalization of the amplitude, we now proceed to analyze the main physical aspects of the decay dynamics leveraging the adiabatic approximation.

4.6.1 Decay During Radiation Domination

We assume that the decaying particle has been produced early during the (RD) stage by some (unspecified) particle physics process at a high energy/temperature scale, focusing first on the dynamics of decay during this era. The subtracted decay function $I_S(k, \eta, \eta_b)$ (4.5.4) can be written in a compact manner amenable to a numerical study as

$$I_S(k, \eta, \eta_b) = I_S^R(k, \eta, \eta_b) + I_{3S}(k, \eta, \eta_b)\,, \tag{4.6.1}$$

with

$$I_S^R(k, \eta, \eta_b) = 2\,\ln\left[\frac{\xi}{\xi_b}\right] - \Big(F_1[\xi, \xi_b] - F_2[\xi, \xi_b]\Big)\,, \tag{4.6.2}$$

and

$$I_{3S}(k,\xi) = \frac{\pi}{2}\,\frac{\omega_i \eta_i}{\gamma_i}\,\int_{\xi_b}^{\xi} \frac{(1+\xi')^2\left[1+\mathcal{S}(\xi')\right]}{\sqrt{(\gamma_i^2-1)+(1+\xi')^2}}\,d\xi'\,, \tag{4.6.3}$$

where $\xi, W[\xi]$ are defined in eqn. (4.5.7), and we have introduced the following functions (see appendices B.4, B.5)

$$F_1[\xi,\xi_b] = \int_{\xi_b}^{\xi}\left[\sqrt{W[\xi']}+\frac{1}{\sqrt{W[\xi']}}\right]\,\frac{d\xi'}{\xi'}\,, \tag{4.6.4}$$

$$F_2[\xi,\xi_b] = \int_{\xi_b}^{\xi}\left[\sqrt{W[\xi']}+\frac{1}{\sqrt{W[\xi']}}\right]\,\cos[J(\xi')]\,\frac{d\xi'}{\xi'}\,, \tag{4.6.5}$$

where $J[\xi]$ is defined in eqn. (B.4.9) in appendix (B.4). To leading adiabatic order (see appendix (B.5))

$$\mathcal{S}(\xi') = \frac{2}{\pi}\,Si\big[\alpha(\xi')\big] \;\;;\;\; \alpha(\xi') = \frac{\omega_i\,\eta_i}{\gamma_i}\,\xi'\left[\sqrt{(\gamma_i^2-1)+(1+\xi')^2}-\sqrt{(\gamma_i^2-1)}\right], \tag{4.6.6}$$

where $Si[x]$ is the sine-integral function (see equation (B.5.26) and discussion in appendix (B.5)).

We highlight that the contribution I_S^R is a distinct feature of the renormalizable Yukawa interaction and of the fermionic density of states, whereas I_{3S} in (4.5.8) is very similar to the decay function found in the scalar case studied in ref.[105].

As discussed above, to leading adiabatic order we set $\eta_b = \eta_i$ in I_{3S} and obtain (see appendix (B.5))

$$I_{3S}(k,\eta,\eta_b) = \frac{\pi}{4}\,\omega_i\eta_i\left\{(1+\xi)\,W[\xi]-1-\frac{(\gamma_i^2-1)}{\gamma_i}\,\ln\left[\frac{\gamma_i\,W[\xi]+(1+\xi)}{1+\gamma_i}\right]\right\}+\widetilde{I}_{3S}(k,\eta,\eta_b)\,, \tag{4.6.7}$$

$$\widetilde{I}_{3S}(k,\eta,\eta_b) = \frac{\pi}{2}\,\frac{\omega_i\eta_i}{\gamma_i}\,\int_{\xi_b}^{\xi}\frac{(1+\xi')^2\,\mathcal{S}(\xi')}{\sqrt{(\gamma_i^2-1)+(1+\xi')^2}}\,d\xi'\,, \tag{4.6.8}$$

where $\widetilde{I}_{3S}(k,\eta,\eta_b)$ must be obtained numerically.

However, before we engage in a numerical study we analyze the different contributions to extract a physical picture of which terms dominate at different time scales. In order to analyze the behavior in the different regimes, we write the Lorentz factor both in terms of

the variable $\xi = \frac{\eta}{\eta_i} - 1$ (see appendix (B.3)) as well as in terms of comoving time with the equivalence $1 + \xi \equiv \sqrt{t/t_i}$ (see also appendix (B.3)),

$$\gamma(\xi) = \left[\frac{(\gamma_i^2 - 1)}{(1+\xi)^2} + 1\right]^{\frac{1}{2}} \equiv \left[\frac{(\gamma_i^2 - 1)}{\left(\frac{t}{t_i}\right)} + 1\right]^{\frac{1}{2}} = \left[\frac{t_{nr}}{t} + 1\right]^{\frac{1}{2}} \equiv \gamma(t)\,, \tag{4.6.9}$$

where t_{nr} is the comoving time scale at which the decaying particle becomes non-relativistic, given by

$$t_{nr} = t_i\,(\gamma_i^2 - 1) = \frac{k^2}{2m_\phi^2 H_R}\,. \tag{4.6.10}$$

Whence the limits

$$\begin{aligned}(\gamma_i^2 - 1) \ll (1+\xi)^2 \;\; &\Rightarrow \;\; \text{Non}-\text{relativistic} \;\; ; \;\; (\gamma_i^2 - 1) \gg (1+\xi)^2 \Rightarrow \; \text{Ultra}-\text{relativistic} \\ t_{nr} \ll t \;\; &\Rightarrow \;\; \text{Non}-\text{relativistic} \;\; ; \;\; t_{nr} \gg t \Rightarrow \; \text{Ultra}-\text{relativistic}\,.\end{aligned} \tag{4.6.11}$$

Let us focus first on the contribution $I_S^R(k,\eta,\eta_b)$ given by (4.6.2). In Minkowski space-time the frequencies are time independent, therefore $W[\xi'] = 1$ and $J(\xi') = (\omega_k - k)\eta_i\,\xi'$. The analysis of appendix (B.2) shows that in Minkowski space time for $\xi \gg 1$ the second term in (4.6.2), namely $F_1 - F_2$, yields $2\ln[\xi/\xi_b] + \text{constant}$, thereby cancelling the logarithmic time dependence of the first term (see appendix (B.2)). *Such cancellation only occurs during a limited interval in time in the expanding cosmology as a consequence of the time dependence of the frequencies*. This follows from the analysis of appendix (B.4) which shows that there are three distinct stages:

i) $\xi \lesssim \xi_m$**:** where ξ_m given by (B.4.15, B.4.16) is the time scale at which $F_2[\xi,\xi_b]$ reaches a maximum. During this interval $F_1 - F_2$ in (4.6.2) is negligible and $I_S^R \simeq 2\ln[\xi/\xi_b]$.

ii) $\xi_m < \xi \lesssim \gamma_i$: during this interval the function $F_1[\xi,\xi_b]$ continues to rise monotonically whereas $F_2[\xi,\xi_b]$ oscillates around its constant asymptotic value $F_2[\xi,\xi_b] \simeq F_2[\xi_m,\xi_b] \simeq 2\ln[\xi_m/\xi_b]$, a behavior summarized by figure (30) and equation (B.4.19) in appendix (B.4).

For $\omega_i\eta_i \gg 1$ the results (B.4.15, B.4.16) show that $\xi_m \ll \gamma_i$ for all values of $\gamma_i \geq 1$. Therefore, for $\gamma_i \gg 1$, during the interval $\xi_m \leq \xi < \gamma_i$ it follows that $W[\xi'] \simeq 1$ and $F_1 \simeq 2\,\ln[\xi/\xi_b]$ thereby (approximately) cancelling the logarithm from the first term in I_S^R, whereas $F_2 \simeq 2\ln[\xi_m/\xi_b]$ remains constant, yielding a plateau in I_S^R. This approximate

cancellation is effective during a time interval that increases for $\gamma_i \gg 1$ (see discussion in appendix (B.4)). According with eqn. (4.6.9) and the limits (4.6.11) during this interval, wherein I_S^R is approximately constant, the decaying particle is in the *ultrarelativistic regime*. In this stage the constancy of I_S^R is expected because in the ultrarelativistic regime the frequencies are nearly time independent since $\omega_k(\eta) \simeq k \simeq \omega_i$. Therefore $W[\xi] \simeq 1$ yielding $F_1 \simeq 2\ln[\xi/\xi_b]$ thereby cancelling the logarithmic time dependence of the first term in (4.6.2), similarly to Minkowski space-time.

If $\gamma_i \gg 1$ the decaying particle is "born" ultrarelativistically and there is a (long) time window $\xi_m < \xi < \gamma_i$ within which $\sqrt{W[\xi']} \simeq 1$ and $F_1[\xi, \xi_b] \simeq 2\ln[\xi/\xi_b]$ thereby approximately cancelling the first term in I_S^R whereas $F_2[\xi, \xi_b]$ remains nearly constant. Therefore for $\gamma_i \gg 1$ it follows that $I_S^R(k, \eta, \eta_b)$ rises rapidly on a time scale $\simeq \xi_m$ reaching a maximum and remaining nearly constant $I_S^R \simeq 2\ \ln[\xi_m/\xi_b]$ until $\xi \simeq \gamma_i$.

iii) $\xi \gg \gamma_i$: The cosmological redshift eventually makes the decaying particle to become non-relativistic when $\xi \gg \gamma_i \gg 1$. During this stage the particle is *non-relativistic* as a consequence of the cosmological redshift. The time dependence of the frequency now yields $\sqrt{W[\xi']} + 1/\sqrt{W[\xi']} \gg 2$, hence $F_1 > 2\ \ln[\xi]$. In this stage it follows that $W[\xi] \approx \xi/\gamma_i$, therefore for $\xi \gg \gamma_i \gg 1$ we find that $F_1[\xi] \simeq 2\sqrt{\xi/\gamma_i}$ and $F_2[\xi, \xi_b] \simeq 2\ln[\xi_m/\xi_b]$. For $\xi \gg \gamma_i$, the integral for $F_1[\xi, \xi_b]$ is estimated by splitting it into the stages $\xi_b \leq \xi \leq \gamma_i$ and $\xi > \gamma_i$. The first stage yields $2\ln[\gamma_i/\xi_b]$ since during this (ultrarelativistic) stage $W[\xi'] \simeq 1$, and the second yields (approximately) $2\sqrt{\xi/\gamma_i}$ since during this (non-relativistic) stage $W[\xi] \approx \xi/\gamma_i$.

In summary, for a particle that is "born" ultrarelativistically, namely with $\gamma_i \gg 1$, the contribution I_S^R rises rapidly up to a value $\simeq 2\ \ln[\xi_m/\xi_b]$ on a time scale $\xi_m \ll \gamma_i$ given by (B.4.16), remains nearly constant up to a time scale $\xi \simeq \gamma_i$ at which the particle becomes non-relativistic, and begins to fall-off as $-2\sqrt{\xi/\gamma_i}$ for $\xi \gg \gamma_i$.

In the opposite limit when $\gamma_i \simeq 1$ the decaying particle is non-relativistic already at the initial time and $\omega_k(\eta) \simeq m_\phi\, C(\eta)$. In this case $F_2[\eta, \eta_b]$ saturates rapidly, on a scale $\xi_m \simeq \pi/\omega_i\, \eta_i \ll 1$, and $F_1[\eta, \eta_b]$ grows *faster* than logarithmically, hence $F_1 - F_2$ becomes larger than the logarithm in the first term of I_S^R and *negative*. This behavior leads to an early *suppression* of decay.

This analysis is approximately summarized during the ultrarelativistic (UR) and non-

relativistic (NR) regimes, by (see eqn. (B.4.19) in appendix (B.4)),

$$I_S^R(k,\eta,\eta_b) \simeq \begin{cases} 2\ln\left[\frac{\xi}{\xi_b}\right]\Theta(\xi_m-\xi) + 2\ln\left[\frac{\xi_m}{\xi_b}\right]\Theta(\xi-\xi_m) \quad , \quad \text{for} \quad \gamma_i > \xi \quad (UR) \\ 2\ln\left[\frac{\xi_m}{\xi_b}\right] + 2\ln\left[\frac{\xi}{\gamma_i}\right] - 2\sqrt{\frac{\xi}{\gamma_i}} \quad , \quad \text{for} \quad \xi \gg \gamma_i > \xi_m \quad (NR)\,. \end{cases} \tag{4.6.12}$$

The main aspects of this analysis are confirmed by a numerical study summarized in figures (14) and (15) for $\gamma_i = 2, 10$ respectively. Notice the different scales in the figures highlighting the emergence of the plateau and the crossover to a diminishing (negative) square root behavior at a scale $\xi \simeq \gamma_i$.

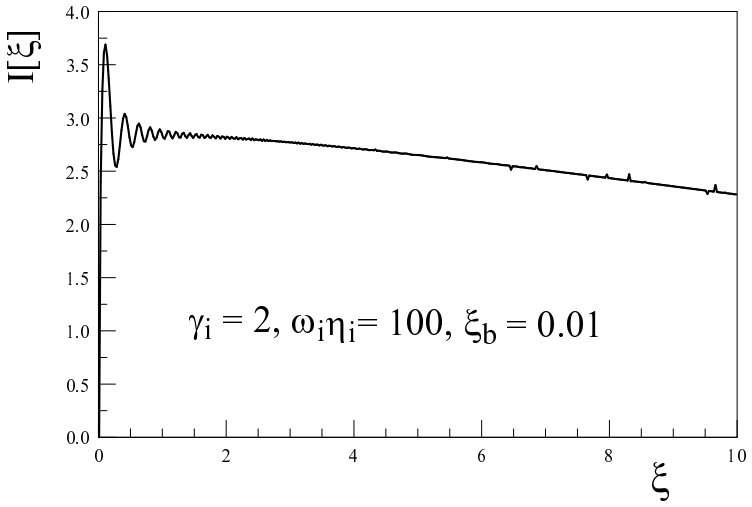

Figure 14: The contribution I_S^R, eqn. (4.6.2), for $\omega_i\eta_i = 100, \xi_b = 0.01, \gamma_i = 2$.

Decay at rest:

For a very massive particle "born" and decaying at rest in the comoving frame, namely for $\gamma_i = 1$, and $\omega_i\eta_i \gg 1$ we can provide an analytic form of the decay function for time scales $\xi \gg \xi_b \simeq 1/\omega_i\eta_i$ for on-shell renormalization. As discussed in appendices (B.4, B.5), $F_2[\eta,\eta_b]$ reaches its asymptotic limit on a time scale $\xi \simeq \pi/2\omega_i\eta_i \ll 1$ (see equation (B.4.15)

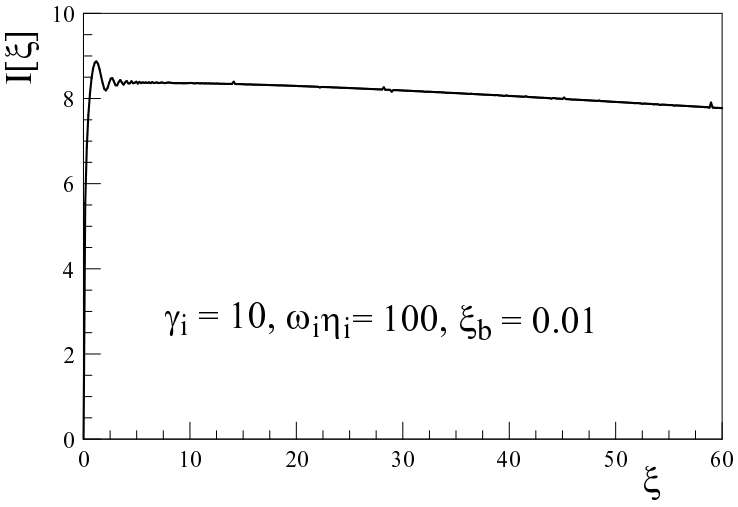

Figure 15: The contribution I_S^R, eqn. (4.6.2), for $\omega_i\eta_i = 100, \xi_b = 0.01, \gamma_i = 10$.

in appendix (B.4)). Furthermore, the function $\mathcal{S}(\xi')$ in (4.6.3) reaches its asymptotic value $\mathcal{S} \simeq 1$ at a time scale $\xi' \simeq \pi/\omega_i\eta_i \ll 1$. Therefore for $\xi' \gg 1/\omega_i\eta_i$ we can neglect the contribution from F_2 and set $\mathcal{S}(\xi') = 1$ in (4.6.3), hence $I_{3S}[k, \eta, \eta_b]$ is given by the first term in eqn. (4.6.7) with $\gamma_i = 1$ and multiplied by a factor 2 to account for $\mathcal{S} = 1$. Gathering all terms we find in this case ($\gamma_i = 1$; $\omega_i\eta_i \gg 1$; $\xi \gg 1/\omega_i\eta_i$),

$$I_S(0, \eta, \eta_b) = 2\left\{ \ln[\xi] - \ln\left[\frac{\sqrt{1+\xi}-1}{\sqrt{1+\xi}+1}\right] - \sqrt{1+\xi} \right\} + \frac{\pi}{2}\omega_i\eta_i\left[\left(1+\xi\right)^2\right] - 1\Big], \quad (4.6.13)$$

where we have neglected a constant term of $\mathcal{O}(1)$. This expression displays all the features described above. Note that for $\xi \ll 1$ the logarithmic time dependence cancels out, but for $\xi \gg 1$ the first logarithm in (4.6.13) continues to grow, however the *negative* square root eventually dominates the contribution of the first terms within brackets. These are precisely

the terms arising form the renormalization and their time dependence is a consequence of the time dependence of the frequencies.

To compare to the decay law in Minkowski space time it is convenient to cast the result (4.6.13) in terms of comoving time, using $1+\xi = \eta/\eta_i$, with $\eta = \sqrt{2t/H_R}$ (see eqn. (4.2.39) valid in (RD)), and the relation

$$\frac{\omega_i \eta_i}{\gamma_i} = m_\phi H_R \, \eta_i^2 = 2\, m_\phi \, t_i \,. \tag{4.6.14}$$

Setting $\eta_i = \eta_b$ to leading adiabatic order, we find for $\gamma_i = 1$ and $t \gg t_b$

$$I_S(0,t) \simeq \ln\left[\frac{t}{t_b}\right] - 2\left[\frac{t}{t_b}\right]^{\frac{1}{4}} + \pi\, m_\phi \,(t - t_b)\,, \tag{4.6.15}$$

leading to the survival probability for $t \gg t_b$

$$\mathcal{P}_\Phi(t) = \left[\frac{t}{t_b}\right]^{-\frac{Y^2}{8\pi^2}} \; e^{\frac{Y^2}{4\pi^2}\left(t/t_b\right)^{1/4}} \; e^{-\Gamma_0\,(t-t_b)} \; \mathcal{P}_\Phi(t_b) \quad ; \quad \Gamma_0 = \frac{Y^2}{8\pi}\, m_\phi \,. \tag{4.6.16}$$

This is one of the important results of this study. Remarkably Γ_0 is the same as the decay width at rest in Minkowski space time, however the power law with "anomalous dimension" $Y^2/8\pi^2$ and the *stretched exponential* with the power law $(t/t_b)^{1/4}$ are a consequence of the renormalization and the time dependence of the frequencies, manifestly a consequence of the expanding cosmology. The combined effect of these two terms yields a *slowing down* of the decay as compared with the case of Minkowski space time with a concomitant enhancement of the lifetime of the decaying particle as compared to Minkowski space-time. This is a noteworthy result: as a consequence of the cosmological expansion the contribution from the renormalization and quasiparticle formation *slows down the decay* leading to an enhancement of the lifetime of the initial state.

Decay of particles with $\gamma_i \gg 1$:

These are particles that are "born" ultrarelativistically. For $\gamma_i \gg 1$ the contribution from $I_S^R(k,\eta,\eta_b)$ has been summarized by eqn (4.6.12) and is displayed in fig. (15): a rapid rise on a time scale $\xi_m \ll \gamma_i$ given by (B.4.16) up to $I_S^R \simeq 2\,\ln[\xi_m/\xi_b]$ followed by a near plateau during the stage while $\xi \lesssim \gamma_i$. This contribution falls off slowly as $-\sqrt{\xi/\gamma_i}$ during the non-relativistic stage, $\xi \geq \gamma_i$ (see eqn. (4.6.12)). While a quantitative analysis of I_{3S} requires a

numerical study, we can obtain a fairly accurate estimate as follows. The contribution from $\mathcal{S}$ to I_{3S} (see equation (4.6.3)) is discussed in appendix (B.5), and can be approximately summarized as: $\mathcal{S} \approx 0$ for $\xi < \xi_s$ and $\mathcal{S}(\eta) \approx 1$ for $\xi > \xi_s$ with ξ_s given by (B.5.28, B.5.29).

With $\gamma_i \gg 1$, the ultrarelativistic stage corresponds to $\gamma_i \gg \xi$, during the stage $\gamma_i \gg \xi_s \gg \xi$ it follows that $\mathcal{S} \approx 0$, using $1 + \xi = \sqrt{t/t_i}$, and eqns. (4.6.10,4.6.14), during this stage I_{3S} is given in comoving time t by

$$I_{3S}(t) = \frac{\pi}{2}\, m_\phi\, t_{nr} \left[G\Big[\frac{t}{t_{nr}}\Big] - G\Big[\frac{t_b}{t_{nr}}\Big] \right], \tag{4.6.17}$$

where

$$G[x] = \Big[x(1+x)\Big]^{1/2} - \ln\Big[\sqrt{1+x} - \sqrt{x}\Big], \tag{4.6.18}$$

also describes the decay function in the case of a scalar field decaying into two massless scalars[105]. During this stage for $t \ll t_{nr}$ we find

$$I_{3S}(t) = \frac{\pi}{3}\, m_\phi\, t_{nr} \left(\frac{t}{t_{nr}}\right)^{\frac{3}{2}} \left[1 - \left(\frac{t_b}{t}\right)^{\frac{3}{2}} + \cdots\right]. \tag{4.6.19}$$

For $\gamma_i \gg \xi \gg \xi_s$ it follows that $\mathcal{S} \simeq 1$, therefore the above result is multiplied by a factor 2. Hence, during the ultrarelativistic stage with $\gamma(t) \gg 1$, or $t \ll t_{nr}$, and $\mathcal{S} = 1$ in (4.6.3), it follows that

$$I_{3S}(t) \simeq \frac{2\,\pi}{3}\, m_\phi\, t_{nr} \left(\frac{t}{t_{nr}}\right)^{3/2} \left[1 - \left(\frac{t_b}{t}\right)^{\frac{3}{2}} + \cdots\right], \tag{4.6.20}$$

which when combined with the result (4.6.12) yields in this ultrarelativistic regime, for $\gamma_i \gg \xi \gg \xi_s, \xi_m$

$$I_S(t) \simeq 2\ln\Big[\frac{\xi_m}{\xi_b}\Big] + \frac{2\,\pi}{3}\, m_\phi\, t_{nr} \left(\frac{t}{t_{nr}}\right)^{3/2} \left[1 - \left(\frac{t_b}{t}\right)^{\frac{3}{2}} + \cdots\right]. \tag{4.6.21}$$

Neglecting the perturbatively small non-secular constant in the decay function from the first term in (4.6.21)[3] , we find in the time interval for $t_{nr} \gg t \gg t_b$ during which the decaying particle is ultrarelativistic and the transient dynamics of quasiparticle formation has saturated

$$\mathcal{P}_\Phi(t) = e^{-\frac{2}{3}\Gamma_0\, t_{nr}\, (t/t_{nr})^{3/2}}\; \mathcal{P}_\Phi(t_b)\,. \tag{4.6.22}$$

[3]Or absorbing it in a *finite* perturbatively small time independent wave function renormalization of $\mathcal{P}_\Phi$.

We can now use the property (4.5.15) and write for $t > t_{nr}$

$$\mathcal{P}_\Phi(t) = e^{-\int_{\eta_{nr}}^{\eta} \Gamma_\Phi(\eta')\, d\eta'}\, \mathcal{P}_\Phi(t_{nr})\,, \tag{4.6.23}$$

where

$$\int_{\eta_{nr}}^{\eta} \Gamma_\Phi(\eta')\, d\eta' = \frac{Y^2}{8\pi^2}\left[I_S(k,\eta,\eta_b) - I_S(k,\eta_{nr},\eta_b)\right]. \tag{4.6.24}$$

After the decaying particle becomes non-relativistic for $\xi \gg \gamma_i$ or $t \gg t_{nr}$ when $\gamma(t) \simeq 1$, the contribution $\mathcal{S} \simeq 1$ and $I_{3S}(\xi) - I_{3S}(\xi_{nr})$ becomes

$$I_{3S}(t) - I_{3S}(t_{nr}) = \pi\, m_\phi\, t\left[1 - \frac{t_{nr}}{t} - \frac{t_{nr}}{2\,t}\,\ln\left[\frac{t}{t_{nr}}\right] + \cdots\right], \tag{4.6.25}$$

the dots in the above expression stand for terms of higher order in the ratio t_{nr}/t.

Finally, combining with the result given by eqn. (4.6.12), the total decay function after the particle has become non relativistic $\xi \gg \gamma_i$ (or $t \gg t_{nr} \gg t_b$) is given in comoving time by

$$I_S(t) - I_S(t_{nr}) \simeq \ln\left[\frac{t}{t_{nr}}\right] - 2\left[\frac{t}{t_{nr}}\right]^{\frac{1}{4}} + \pi\, m_\phi\, t\left[1 - \frac{t_{nr}}{t} - \frac{t_{nr}}{2\,t}\,\ln\left[\frac{t}{t_{nr}}\right] + \cdots\right], \tag{4.6.26}$$

where we have neglected a perturbatively small constant term and approximated $t_i\gamma_i^2 \simeq t_{nr}$ for $\gamma_i \gg 1$. Hence for $t \gg t_{nr} \gg t_b$ we find

$$\mathcal{P}_\Phi(t) = \left[\frac{t}{t_{nr}}\right]^{-\frac{Y^2}{8\pi^2}}\, e^{\frac{Y^2}{4\pi^2}\left(t/t_{nr}\right)^{1/4}}\, \left[\frac{t}{t_{nr}}\right]^{\Gamma_0 t_{nr}/2}\, e^{-\Gamma_0\,(t-t_{nr})}\, \mathcal{P}_\Phi(t_{nr})\,. \tag{4.6.27}$$

It would be expected that after t_{nr} when the particle has become non-relativistic as a consequence of the cosmological redshift, the time evolution of the survival probability would be similar to that of a particle born and decaying at rest. However, the result (4.6.27) features an extra power law with exponent $\Gamma_0 t_{nr}/2$ as compared to the decay function for the particle born at rest, eqn. (4.6.16). This difference reflects the memory of the past evolution in the form of the integral (4.6.24).

We can provide a measure of the impact of curved space time effects on the decay function by comparing the results above to a phenomenological, S-matrix inspired Minkowski decay

law allowing for a *local time dilation factor* to account for the cosmological redshift, namely

$$\mathcal{P}_{\Phi}^{(M)}(t) = e^{-\frac{\Gamma_0}{\gamma(t)}\,(t-t_i)}\,\mathcal{P}_{\Phi}^{(M)}(t_i)\,, \tag{4.6.28}$$

where $\Gamma_0 = \frac{Y^2\,m_\phi}{8\pi}$ is the decay width at rest in Minkowski space time, and $\gamma(t)$ the local Lorentz factor (4.6.9). The comparison to the cutoff independent subtracted decay function (4.6.1) is facilitated by introducing

$$I_M(t) = \frac{\pi\,m_\phi\,t}{\gamma(t)}\left[1 - \frac{t_i}{t}\right], \tag{4.6.29}$$

so that the Minkowski-like decay function is given by

$$\frac{\Gamma_0}{\gamma(t)}\,(t-t_i) \equiv \frac{Y^2}{8\pi^2}\,I_M(t)\,, \tag{4.6.30}$$

where a factor is included in (4.6.30) to ensure that $I_M(t_i = t_b) = 0$ consistently with the subtraction definining (4.6.1). For $t \gg t_i$ this *phenomenological* decay function is interpreted as that of Minkowski space-time but with the instantaneous Lorentz time dilation factor. For $t \gg t_i$ it provides a "benchmark" to compare the results obtained above for the decay function to an S-matrix inspired *instantaneous* Minkowski decay law.

Before we engage in a numerical comparison, it is illuminating to analyze the cases discussed above.

Non-relativistic: $\gamma(t) = 1$

For this case the $I_S(t)$ is given by (4.6.15), the last term of which is precisely $I_M(t)$ for $\gamma(t) = 1$. The first two terms in (4.6.15) yield a *negative* contribution for $t \gg t_b = t_i$, therefore the cosmological decay function is *smaller* in this case than the phenomenological Minkowski function, leading to a longer lifetime.

Ultra-relativistic: $\gamma_i \gg 1$

During the ultrarelativistic regime $\gamma(t) \gg 1$ ($t \ll t_{nr}$), taking the time large enough so that the transient build-up of $\mathcal{S}$ in eqn. (4.6.3) has saturated, the cosmological decay function is given by (4.6.21) whereas $I_M(t) \simeq \pi m_\phi t \left(t/t_{nr}\right)^{1/2}$. The logarithmic term in (4.6.21) could be fairly large for large γ_i thereby yielding $I_S(t) > I_M(t)$ during a time interval. This can be understood from the following argument.

As discussed above and in appendix (B.4), for $\gamma_i \gg 1$ the contribution I_S^R (see eqn. (4.6.2)) rises on a time scale $\xi_m \simeq (3\pi\gamma_i^2/\omega_i\eta_i)^{1/3}$ up to a maximum $\simeq 2\ln(\xi_m/\xi_b)$ after which it remains nearly constant up to $\xi \simeq \gamma_i$ yielding the logarithmic term in (4.6.21). For example, for $\gamma_i \simeq 200$, $\omega_i\eta_i \simeq 100$ and "on-shell" renormalization with $\xi_b = 1/\omega_i\eta_i$, the contribution from I_S^R rises up to a value $\simeq \frac{4}{3}\ln[\sqrt{3\pi}\gamma_i\omega_i\eta_i] \simeq 14.7$ on a comoving time scale $t_m/t_i \approx 240$. Since the Hubble time scale $1/H(t) = 2t$ during (RD), it follows that I_S^R rises up to the plateau over $\simeq 240$ Hubble times, with the possibility that during this time $I_S(t) > I_M(t)$. However, after the particle has become non-relativistic, namely for $t \gg t_{nr}$, the cosmological decay function $I_S(t)$ is given by (4.6.26) whereas

$$I_M(t) \simeq \pi m_\phi\, t\left[1 - \frac{t_{nr}}{2t} + \cdots\right], \tag{4.6.31}$$

showing that $I_S(t) \ll I_M(t)$ for $t \gg t_{nr}$. This suggests a crossover behavior for very large values of γ_i: there is an early time window during the ultrarelativistic stage wherein the cosmological decay function may be larger than the Minkowski one, however as the decaying particle eventually becomes non-relativistic the latter will ultimately dominate. This behavior is borne out by a detailed numerical study.

Figures (16,17,18) show a comparison between the phenomenological Minkowski decay function (4.6.29), the total contribution I_S (4.6.1) along with I_{3S} (4.6.3) for on-shell renormalization with $\omega_i\eta_i = 100$ and $\gamma_i = 10, 50, 200$ respectively. For these values the transition time to the non-relativistic behavior is $t_{nr}/t_i \simeq 10^2, 2.5\times 10^3, 4\times 10^4$ respectively. For $\gamma_i = 10, 50$ figs. (16,17) show that I_S and I_{3S} are nearly indistinguishable, namely I_S^R (4.6.2) is subleading in these cases, and that the phenomenological I_M is always *larger* than I_S.

However, for $\gamma_i = 200$ fig. (18) shows that the contribution from I_S^R dominates at early time, rising on a time scale $t/t_i \simeq 100$. In this case I_M is smaller than I_S during a substantial time window, ≈ 500 Hubble times from the "birth" of the quasiparticle, before crossing over to becoming the largest decay function.

Therefore we conclude that in the ultrarelativistic case, for very large values of γ_i, the decay function is *larger* than the phenomenological Minkowski one within a substantial time interval but eventually becomes smaller at a time scale that depends on the various parameters. In either case, at long time the decaying particle lives *longer* than predicted

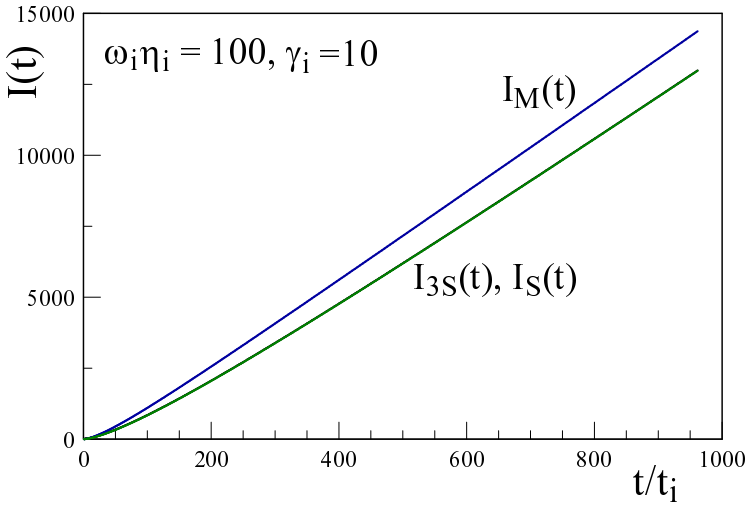

Figure 16: Comparison between I_M, I_S, I_{3S} for on-shell subtraction with $\omega_i\eta_i = 100, \gamma_i = 10$, $t_{nr}/t_i = 99$.

by a Minkowski decay law extrapolated to the expanding cosmology. This is a generic result: after an intermediate time scale that depends on γ_i, the cosmological decay function is *smaller* than the phenomenological Minkowski-like one. Therefore the S-matrix inspired phenomenological Minkowski decay law *under estimates* the lifetime of the decaying particle.

4.6.2 Long Lived Particles: Decay During Matter Domination or Beyond

The discussion above focused on decay during the radiation dominated era that lasts until $C(\eta) = a_{eq} \simeq 10^{-4}$ corresponding to an ambient temperature $T \simeq$ eV at a time $t_{eq} \approx 10^{12}$ secs. If the decaying particle is very long lived as would befit a dark matter candidate, it would continue to decay during the matter and perhaps dark energy dominated eras. This case corresponds to an extremely small Yukawa coupling, which allows to safely

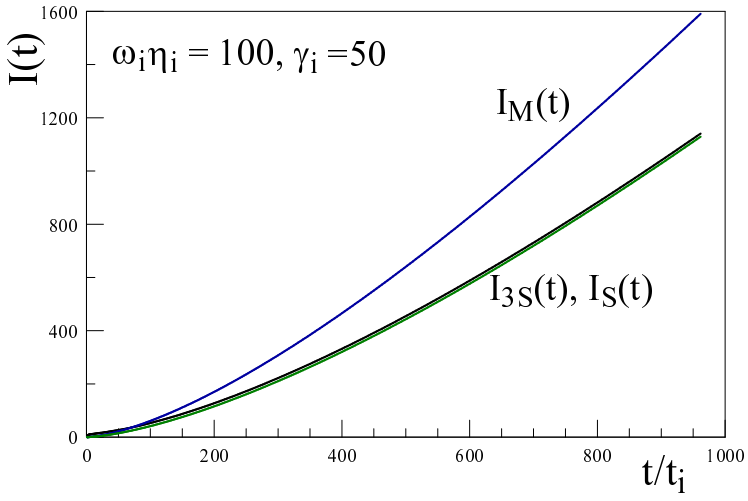

Figure 17: Comparison between I_M, I_S, I_{3S} for on-shell subtraction with $\omega_i\eta_i = 100, \gamma_i = 50$,$t_{nr}/t_i = 2499$.

neglect early transient effects that saturate at early times. The general form of the decay function after renormalization is given by eqns. (4.5.13,4.5.4). Under the assumption of very weak Yukawa coupling we can neglect the contribution from the cosine term in I_{2b}, eqn. (4.5.6) (the contribution F_2 in eqn. (4.6.5)) and we can set $\mathcal{S} = 1$ in eqn. (4.5.8). This is because both terms saturate on short time scales therefore they yield perturbatively small corrections to the decay function for very weak Yukawa coupling as compared to the terms that continue to grow in time. Hence, neglecting these perturbatively small transient contributions for very weak Yukawa couplings, the decay function simplifies to

$$\int_{\eta_b}^{\eta} \Gamma_\Phi(\eta')\, d\eta' = \frac{Y^2}{8\pi^2}\left[2\,\ln\left[\frac{\xi}{\xi_b}\right] - F_1[\xi,\xi_b] + \pi\, m_\phi \int_{\eta_b}^{\eta} \frac{C(\eta')}{\gamma_k(\eta')}\, d\eta'\right] + \cdots , \tag{4.6.32}$$

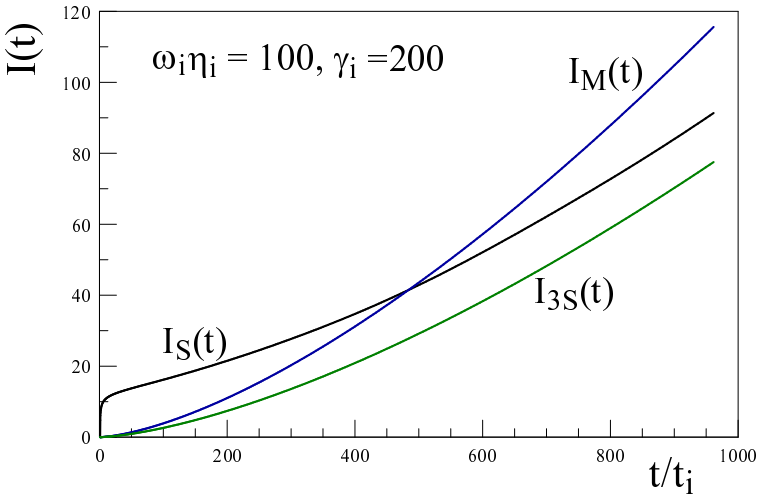

Figure 18: Comparison between I_M, I_S, I_{3S} for on-shell subtraction with $\omega_i\eta_i = 100, \gamma_i = 200$, $t_{nr}/t_i \simeq 4 \times 10^4$.

where $\xi = (\eta - \eta_i)/\eta_i$ and F_1 is given by (4.6.4) and the dots in (4.6.32) stand for constant terms that are of $\mathcal{O}(Y^2)$.

For general scale factor $W[\xi]$ is given by

$$W[\xi] = \frac{1}{\gamma_i}\left[(\gamma_i^2 - 1) + \frac{C^2(\eta)}{C^2(\eta_i)}\right]^{\frac{1}{2}}. \tag{4.6.33}$$

Let us analyze each term separately in order to understand their behavior at long time during the (MD) era, taking as an upper bound $C(\eta) \simeq \mathcal{O}(1)$, or, upon using eqn. (4.2.37) $\eta \simeq \sqrt{a_{eq}}/H_R$. With "on-shell" renormalization ($\xi_b = 1/\omega_i\eta_i$), we find

$$\ln\left[\frac{\xi}{\xi_b}\right] \simeq \ln\left[\frac{\omega_i\sqrt{a_{eq}}}{H_R}\right] \simeq \ln[10^{42}\, C(\eta_i)\Big] + \ln\left[\gamma_i\left(\frac{m_\phi}{\text{GeV}}\right)\right]. \tag{4.6.34}$$

Taking the initial time to correspond to an initial temperature $10^{15}\,\mathrm{GeV}$ yields $C(\eta_i) \simeq 10^{-28}$ therefore the logarithm contribution to the decay function for $\eta \simeq \sqrt{a_{eq}}/H_R$ yields

$$\frac{Y^2}{4\pi^2}\,\ln\left[\frac{\xi}{\xi_b}\right] \simeq 0.82\,Y^2 + \frac{Y^2}{4\pi^2}\,\ln\left[\gamma_i\left(\frac{m_\phi}{\mathrm{GeV}}\right)\right]. \tag{4.6.35}$$

Obtaining the contribution from F_1 over the whole history from early (RD) into (MD) can be done numerically, although this is a rather challenging task because of the enormous dynamic range with the scale factor varying over twenty four orders of magnitude. However, we can provide a simple estimate of the remaining two terms of the decay function at long time during the (MD) era and/or beyond. If the particle remains ultrarelativistic, then as discussed in the previous sections the contribution from F_1 cancels the logarithmic time dependence of the first term, hence the combination of the first two terms saturates (this is the plateau in fig. (15)) and yields a perturbatively small time independent contribution to the decay function. Hence during this ultrarelativistic stage the last term in (4.6.32) dominates the decay function.

After the particle has become non-relativistic then $W[\xi] \simeq C(\eta)/\gamma_i C(\eta_i) \gg 1$ and

$$F_1[\xi,\xi_b] \simeq \frac{1}{\sqrt{\gamma_i C(\eta_i)}}\int^{\eta}\frac{\sqrt{C(\eta')}}{\eta'}\,d\eta'\,, \tag{4.6.36}$$

during (MD) using eqn. (4.2.35) and taking as an upper bound $\eta \simeq \sqrt{a_{eq}}/H_R$ we find

$$F_1[\xi,\xi_b] \simeq \frac{1}{2\sqrt{\gamma_i C(\eta_i)}} \simeq \frac{10^{14}}{\sqrt{\gamma_i}}\,. \tag{4.6.37}$$

Finally, we can estimate the last term in (4.6.32) during the stage when the particle is non-relativistic and (MD) dominated, taking $\gamma(\eta') \simeq 1$ and taking $\eta \simeq \sqrt{a_{eq}}/H_R$, we find

$$m_\phi\int^{\eta}\frac{C(\eta')}{\gamma_k(\eta')}\,d\eta' \simeq 10^{42}\left(\frac{m_\phi}{\mathrm{GeV}}\right). \tag{4.6.38}$$

Since during the ultrarelativistic stage the time dependence of the first and second term cancel out and the last term dominates the decay dynamics, we conclude that the last term in (4.6.32) dominates the decay dynamics of a very long-lived particle with very weak Yukawa coupling, *all throughout the time evolution*. Since the first (logarithmic) term is always subdominant, and the second term is negative, larger in magnitude than the logarithmic

term but also subdominant at late time, the last term in (4.6.32) yields an *upper bound* to the decay function throughout all the expansion history. It can be written as a function of the redshift by recalling that $C(\eta)\, d\eta = dt$, and using $dt = da/(a\, H(a))$ with $H(a)$ the Hubble expansion rate given by eqn. (4.2.30). Writing the local Lorentz factor as $\gamma(a(t))) = \left[\frac{a^2_{nr}}{a^2(t)} + 1\right]^{1/2}$; $a_{nr} \equiv k/m_\phi$, we find that the upper bound to the decay function at redshift z is given by

$$\int_{\eta_b}^{\eta} \Gamma_\Phi(\eta')\, d\eta' \simeq \frac{\Gamma_0}{H_0}\, \Upsilon(z, z_b)\,, \tag{4.6.39}$$

where $\Gamma_0 = Y^2 m_\phi/8\pi$ is the decay rate at rest in Minkowski space time, and

$$\Upsilon(z, z_b) = \int_{1/z_b}^{1/(1+z)} \frac{da}{\sqrt{a^2_{nr} + a^2}\left[\frac{\Omega_M}{a^3} + \frac{\Omega_R}{a^4} + \Omega_\Lambda\right]^{1/2}}\,, \tag{4.6.40}$$

depends solely on the cosmological parameters and $a_{nr} = k/m_\phi$ the scale factor at which the decaying particle transitions from ultrarelativistic to non-relativistic, and we have taken $z_b \gg 1$.

The redshift evolution of the survival probability all throughout the expansion history is summarized concisely as

$$\mathcal{P}_\Phi(z) \gtrsim e^{-\frac{\Gamma_0}{H_0}\,\Upsilon(z,z_b)}\, \mathcal{P}_\Phi(z_b)\,. \tag{4.6.41}$$

The inequality in eqn. (4.6.41) reflects that eqn. (4.6.39) yields an *upper bound* to the decay function. For $a_{nr} = 0$, namely when the decaying particle is "born" at rest, it follows that $\Upsilon(z, z_b) = H_0(t - t_b)$ independently of the cosmology, and we can compare the result (4.6.39) for $a_{nr} = 0$ to the case of the particle decaying at rest given by eqn. (4.6.15) valid during the (RD) era. The discussion on dominant terms above clarifies that the last term in (4.6.15) dominates the decay dynamics, whereas the first two terms combine into a negative contribution which becomes subleading at long time for very weak Yukawa couplings. Hence it is clear that for very weak Yukawa coupling and long time (4.6.39) becomes the leading contribution and yields an upper bound to the decay function for long-lived particles decaying at rest. Furthermore, for $a \ll a_{nr}$, namely when the decaying particle is ultrarelativistic and taking this regime to be during the (RD) era with $a \propto t^{1/2}$ it follows that

$$\Upsilon(z, z_b) \propto t^{3/2}\,, \tag{4.6.42}$$

in agreement with the decay law (4.6.22) during the ultrarelativistic regime in (RD). This analysis confirms the validity of the decay law (4.6.41) with (4.6.40) as an upper bound to describe the evolution of the survival probability for very weakly coupled, long lived particles all throughout the cosmological evolution, under the assumption that the fermionic decay products can be considered massless in the decay process.

4.7 Discussion

The final form of the renormalized decay function, eqn. (4.6.1) describing the time evolution of the survival probability of the *quasiparticle* state is amenable to a straightforward numerical study. The analysis of section (4.6) reveals a very rich dynamical evolution with various different time scales. The shortest time scales describe the build-up of the quasiparticle; this early transient dynamics is absorbed into a wave function renormalization of the quasiparticle survival probability at a time scale t_b. After this short time transient there remain the time scales over which F_2 (4.6.5) saturates at a constant value and $\mathcal{S}$ (4.6.6) rapidly approaches $\mathcal{S} \simeq 1$. The detailed dynamics over these scales was studied analytically and numerically in appendices (B.4) and (B.5)) respectively. The evolution of the survival probability on the intermediate and long time scales becomes simpler and can be summarized succinctly. Furthermore, because the short time transients saturate to constant values, for weak Yukawa coupling the largest contributions to the decay dynamics arises from terms that are secular (grow in time) over the intermediate and long time scales.

Decay at rest in the comoving frame ($\gamma_i = 1$):

The time evolution of the survival probability is given by

$$\mathcal{P}_\Phi(t) = \left[\frac{t}{t_b}\right]^{-\frac{Y^2}{8\pi^2}} e^{\frac{Y^2}{4\pi^2}\left(t/t_b\right)^{1/4}} e^{-\Gamma_0\,(t-t_b)}\; \mathcal{P}_\Phi(t_b)\,, \tag{4.7.1}$$

where $\Gamma_0 = \frac{Y^2}{8\pi}\, m_\phi$ is the decay width of a particle at rest in Minkowski space-time. The power law and stretched exponentials are both a remnant of the renormalization, or "dressing" of the bare into the quasiparticle state and a distinct consequence of the cosmological redshift. Indeed, in Minkowski space-time the terms that give rise to these contribution

become time independent after the transient dynamics, whereas, in curved space-time, the origin of these contributions is the time dependence of the frequencies via the cosmological redshift.

The methods that we implemented in this study, a non-perturbative formulation combined with a physically motivated adiabatic expansion including a consistent treatment of renormalization, are very different from those implemented in ref.[132]. The decay law of a particle at rest (4.7.1) is also very different from that reported in ref.[132]. The origin of the discrepancy is not clear to us. However, since the power law and stretched exponentials originate precisely from the contributions to the renormalization of the survival probability, we suspect that the discrepancy originates in the treatment of the ultraviolet divergences. These are of the same form as in Minkowski space-time (see appendix (B.2) and ref.[32]) as expected since these are short distance divergences, but have not been discussed or addressed in ref.[132]. As explained above, the time dependence of the frequency yields an unexpected contribution to the decay law on longer time scales that originates in the dynamics of quasi-particle formation.

Born ultrarelativistically:

If the particle is "born" or produced ultrarelativistically, namely with $\gamma_i \gg 1$ during (RD), an important time scale is $t_{nr} = \frac{k^2}{2m_\phi^2 H_0\sqrt{\Omega_R}}$, which determines when the particle transitions from being ultrarelativistic ($\gamma(t) \gg 1$ or $t \ll t_{nr}$) to non-relativistic ($\gamma(t) \simeq 1$ or $t \gg t_{nr}$) as a consequence of the cosmological redshift. The dynamical evolution of the survival probability is different in these stages. **a)** ultrarelativistic stage: ($\gamma(t) \gg 1$, or $t_b \ll t \ll t_{nr}$)

$$\mathcal{P}_\Phi(t) = e^{-\frac{2}{3}\Gamma_0\, t_{nr}\,(t/t_{nr})^{3/2}}\; \mathcal{P}_\Phi(t_b)\,. \tag{4.7.2}$$

b) non-relativistic stage ($t \gg t_{nr}$ or $\gamma(t) \simeq 1$),

$$\mathcal{P}_\Phi(t) = \Big[\frac{t}{t_{nr}}\Big]^{-\frac{Y^2}{8\pi^2}}\; e^{\frac{Y^2}{4\pi^2}\left(t/t_{nr}\right)^{1/4}}\; \Big[\frac{t}{t_{nr}}\Big]^{\Gamma_0 t_{nr}/2}\, e^{-\Gamma_0\,(t-t_{nr})}\; \mathcal{P}_\Phi(t_{nr})\,. \tag{4.7.3}$$

Although for $t \gg t_{nr}$ the particle has become non-relativistic because of the cosmological redshift, as compared to the case of decay at rest (4.7.1), this decay law features a new power with exponent $\Gamma_0 t_{nr}/2$. Its origin is the *memory* of the decay function manifest in the form of the integral of the cosmological redshift in (4.5.8) over the whole history of the decay process.

Therefore, even well after the decaying particle has become non-relativistic, the survival probability features an *enhancement* factor that "knows" about the past history when the particle was ultrarelativistic. The dynamics during the transition from the ultrarelativistic to the non-relativistic behavior must be studied numerically, and the previous section shows such study for several values of the parameters.

Massless fermions vs massless bosons:

Ref.[105] studied the decay of a scalar into two massless scalars, therefore we can now compare the results of that study to those obtained here for the case of scalar decay into massless fermions. The main difference is in the contribution I_S^R in eqn.(4.6.1) which is given by eqn. (4.6.2). The contribution from I_{3S} to the decay function is the same for fermions and bosons, for example the function $G[x]$ is the same that enters in scalar decay[105]. The extra contribution, namely I_S^R has the same origin as the ultraviolet divergent contributions that are absorbed in wave function renormalization. This is also the case in Minkowski space-time[32] as shown in appendix (B.2). Whereas in Minkowski space time this contribution becomes time independent after a short time transient and is absorbed into wave function renormalization, in a FRW cosmology, it is time dependent as a consequence of the cosmological redshift and becomes important for non-relativistic particles. Namely, I_S^R is a *remnant* of the physical process of quasiparticle formation. There is no such contribution in the case of decay into two scalars because the theory in this case is superrenormalizable, hence there is no equivalent of the I_S^R term. This contribution *suppresses* the decay function at long time, thereby enhancing the lifetime of the decaying particle. This behavior is yet another source of discrepancy with the results of ref.[132], which finds a *larger* rate in the fermionic case. The source of this discrepancy are precisely the "anomalous" power and stretched exponential which are a consequence of the quasiparticle formation and wave function renormalization. Although the decay probability requires an ultraviolet divergent wave function renormalization even in Minkowski space-time, this seems to be an aspect missing in the treatment of ref.[132]. The cumulative effect of these differences results in that a meaningful comparison to our study has eluded us.

"Benchmarking" the decay law:

The decay laws obtained above are very different from the usual exponential decay fa-

miliar in Minkowski space time, one of the reasons for the difference being the cosmological redshift. Thus a natural question arises: would an S-matrix inspired, *phenomenologically* motivated exponential decay law with a time dependent Lorentz factor to account for the cosmological redshift describe even approximately the decay of the particle?. This motivates the comparison of the previous results to the following Minkowski-like decay law (in (RD))

$$\mathcal{P}_{\Phi}^{(M)}(t) = e^{-\frac{\Gamma_0}{\gamma(t)}\,(t-t_i)}\,\mathcal{P}_{\Phi}^{(M)}(t_i) \;\;;\;\; \gamma(t) = \Big[\frac{t_{nr}}{t}+1\Big]^{1/2}. \tag{4.7.4}$$

For decay at rest $\gamma(t) = 1$, this decay law misses the power with anomalous dimension and the stretched exponential, whose combination is *negative*. Therefore the Minkowski-like decay law *over-estimates* the suppression of the survival probability in the case of decay at rest. For a particle that is produced ultrarelativistically, during the stage wherein $\gamma(t) \gg 1$, namely $t \ll t_{nr}$ one finds

$$\mathcal{P}_{\Phi}^{(M)}(t) = e^{-\Gamma_0 t_{nr}(t/t_{nr})^{3/2}}\,\mathcal{P}_{\Phi}^{(M)}(t_i)\,, \tag{4.7.5}$$

which is *smaller* than (4.7.2). For $t \gg t_{nr}$ when the decaying particle has become non-relativistic

$$\mathcal{P}_{\Phi}^{(M)}(t) = e^{-\Gamma_0\left(t-t_{nr}/2\right)}\,\mathcal{P}_{\Phi}^{(M)}(t_i)\,. \tag{4.7.6}$$

Comparing this result with (4.7.3) clearly shows that the phenomenological Minkowski decay law including the instantaneous Lorentz factor over-estimates the suppression of the survival probability, namely *under estimates* the lifetime of the decaying state. The discrepancies with the cosmological decay law, both the factor 2/3 in (4.7.2) along with the powers and stretched exponential in (4.7.3) are traced to i) the memory of quasiparticle formation, ii) the memory of the past evolution in the integral of the time dilation factor. None of these can be captured by a phenomenological Minkowski-like decay law including an instantaneous Lorentz factor as such description has no memory of the past evolution. We draw two important conclusions from this comparison: i) a phenomenological, S-matrix inspired Minkowski decay law *under estimates* the lifetime of the decaying particle since it *over estimates* the suppression of the survival probability, ii) describing particle decay in cosmology in terms of a decay *rate*, even one that includes the cosmological redshift in the time dilation factor, is not only not useful

but is misleading insofar as missing important physical processes and yielding a substantial under estimate of the lifetime of the decaying particle.

Modifications to BBN?

Although the results obtained in this study do not apply directly to neutron decay, since we focused on scalar decay Yukawa coupled to massless fermions, and the small phase space available for three body neutron decay is a result of the small neutron-proton mass difference, let us explore the consequences of the results on this process, with all these caveats. First: the neutron is "born" after the QCD phase transition at $T_{QCD} \simeq 150\,\mathrm{MeV}$ at a time $t_b \simeq 10^{-5}\,\mathrm{secs}$, because the neutron mass $M_N \simeq \mathrm{GeV} \gg T_{QCD}$ it is "born" at rest in the plasma. Let us identify the dimensionless coupling $Y^2/8\pi \equiv \Gamma_N/M_N$ where $\Gamma_N \simeq 10^{-3}\,\mathrm{secs}^{-1}$ is the neutron's lifetime. Hence $Y^2/8\pi \simeq 10^{-21}$, and taking $t/t_b \simeq 1/\Gamma_N t_b \simeq 10^8$ we see that the power law with "anomalous" dimension and the stretched exponential correction to the usual exponential decay law in eqn. (4.6.16) for decay at rest are all but negligibly small and would *not* affect the dynamics of neutron decay during (BBN). Of course, there are the above mentioned caveats to this conclusion which should only be taken as an extrapolation and as a gross estimate of the effects. This analysis also suggests that the corrections to the decay law are more important for particles "born" very early during (RD) and very long lived a situation that befits most descriptions of a dark matter candidate.

Caveats:

We have focused on studying scalar decay into massless fermion pairs, a situation that approximates most of the fermionic decay channels of a Higgs scalar in the standard model. An important aspect of this decay process is that it does not feature thresholds. Including the mass for the decay products introduces kinematic thresholds, a consequence of strict energy-momentum conservation. In ref.[105] it was argued that the Hubble rate of expansion introduces a natural energy uncertainty leading to a relaxation of the kinematic thresholds, thereby allowing processes that are forbidden in Minkowski space-time by energy conservation. Furthermore, ref.[32] has shown that energy uncertainties associated with transient non-equilibrium aspects of the decay allow decay into heavier particles during a time interval. In an expanding cosmology these effects may combine with the energy uncertainty from Hubble expansion to *enhance* the decay by opening up novel channels that would be

otherwise forbidden by strict energy conservation. These aspects associated with the masses of the decay products will be the subject of further study.

The inclusion of masses for the decay products becomes a more pressing issue in the case of decay of very long lived particles studied in section (4.6.2) where we have extended the results obtained for the (RD) era to provide an *upper bound* on the decay function all throughout the expansion history. Therefore, the decay law (4.6.41) with the decay function (4.6.40) must be understood within the context of decay of a heavy particle into massless or nearly massless fermionic channels with the caveat that such an approximation may be of limited validity during the (MD) or (DE) eras and should be interpreted as indicative of the decay dynamics.

In this study we have neglected finite temperature corrections to decay vertices and masses, their inclusion requires studying the time evolution of an initial *density matrix*. Furthermore, if the decay products thermalize with the medium, their population build-up will lead to Pauli blocking factors thereby suppressing the decay of the parent particle. These effects remain to be studied but are beyond the scope and goals of this article.

Possible implications:

The time dependence of the decay function reveals non-equilibrium aspects that have not been previously recognized, not only from the transient build-up of the quasiparticle but also the memory effects that yield the unexpected power laws and stretched exponentials. These novel non-equilibrium effects may lead to interesting and perhaps important dynamics relevant to baryogenesis and leptogenesis. In particular, we envisage corrections to quantum kinetic processes for particle production and their inverse processes. Typically quantum kinetics inputs transition rates perhaps with finite temperature contributions but ultimately obtained from S-matrix theory. Namely, such transition rates are obtained in the infinite time limit and the forward and backward probabilities input strict energy conservation, and as a consequence, obey detailed balance . The richer time dependence of the decay function revealed by this study, with the hitherto unexplored novel non-equilibrium aspects, suggests that similar dynamical processes *may* enter in a modified quantum kinetic description in the early universe. We expect to report on these and other related issues in future studies.

4.8 Summary, Conclusions and Further Questions

In this article we studied the decay of a bosonic particle into massless fermions via a Yukawa coupling in post-inflation cosmology. The approximation of massless fermions is warranted for a heavy Higgs-like scalar within or beyond the standard model decaying into most charged leptons or quarks (but for the top) of the standard model. We implemented a non-perturbative method that yields the time evolution of the survival probability $\mathcal{P}_\Phi(t)$ combined with a physically motivated adiabatic expansion. This expansion is justified when $H(t)/E_k(t) \ll 1$ where $H(t)$ is the Hubble rate and $E_k(t)$ the local energy of the particle as measured by a comoving observer. We have argued that this approximation is valid for typical particle physics processes during the radiation dominated era and beyond. In a standard cosmology the reliability of this approximation improves with the cosmological expansion, therefore if the adiabatic condition is fulfilled at the initial time when the decaying particle is produced, its reliability improves along the expansion history.

Particle decay into fermionic channels introduces novel phenomena associated with ultraviolet divergences requiring renormalization that result into two different physical processes: i) the build-up of a *quasiparticle* state out of the bare initial state by dressing with fermion-antifermion pairs, ii) the decay of this quasiparticle state via the emission of fermion pairs. These two different processes occur on widely separated time scales. We introduced a dynamical renormalization method that allows to separate the dynamics of formation of the quasiparticle from its decay on longer time scales. It relies on introducing a renormalization time scale t_b to absorb the transient dynamics of formation into the wave function renormalization of the quasiparticle state. The survival probability obeys a *dynamical renormalization group equation* with respect to t_b. The decay function of this renormalized state is ultraviolet finite and cutoff independent.

We carried out a detailed analytic and numerical study of the decay function during the radiation dominated era. The dynamics of decay depends crucially on whether the particle is non-relativistic or relativistic. For a particle that is "born" at rest in the comoving frame

during (RD) we find that after short time transients, the survival probability is given by

$$\mathcal{P}_\Phi(t) = \left[\frac{t}{t_b}\right]^{-\frac{Y^2}{8\pi^2}} e^{\frac{Y^2}{4\pi^2}\left(t/t_b\right)^{1/4}} e^{-\Gamma_0\,(t-t_b)}\; \mathcal{P}_\Phi(t_b) \;\;;\;\; \Gamma_0 = \frac{Y^2}{8\pi}\, m_\phi\,. \tag{4.8.1}$$

where Y is the Yukawa coupling and Γ_0 is the decay rate at rest in Minkowski space-time. The scale t_b is an intermediate time scale that describes the build-up of the quasiparticle state, and $\mathcal{P}(t_b)$ is the renormalized probability of such state. The power of t/t_b with "anomalous" dimension and the stretched exponential with power $1/4$ are both a remnant of the formation of the quasiparticle on long time scales as a consequence of the *cosmological redshift*.

For the case in which the decaying particle is "born" ultrarelativistically the time evolution over the whole history during (RD) must be obtained numerically. Different regimes emerge depending on whether the particle is ultrarelativistic for $t \ll t_{nr}$ or non-relativistic for $t \gg t_{nr}$ where $t_{nr} = k^2/(2m_\phi^2 H_0\sqrt{\Omega_R})$ is the time scale at which the decaying particle of mass m_ϕ that is born ultrarelativistically with comoving momentum k transitions to being non-relativistic as a consequence of the cosmological redshift. During the ultrarelativistic regime ($t \ll t_{nr}$) we find for $t \gg t_b$ that the decay function is a stretched exponential

$$\mathcal{P}_\Phi(t) = e^{-\frac{2}{3}\Gamma_0\, t_{nr}\,(t/t_{nr})^{3/2}}\; \mathcal{P}_\Phi(t_b)$$

whereas for $t \gg t_b$ and after the particle has become non-relativistic ($t \gg t_{nr}$) we find

$$\mathcal{P}_\Phi(t) = \left[\frac{t}{t_{nr}}\right]^{-\frac{Y^2}{8\pi^2}} e^{\frac{Y^2}{4\pi^2}\left(t/t_{nr}\right)^{1/4}} \left[\frac{t}{t_{nr}}\right]^{\Gamma_0 t_{nr}/2} e^{-\Gamma_0\,(t-t_{nr})}\; \mathcal{P}_\Phi(t_{nr})\,.$$

The extra power of t/t_{nr} as compared to the case when the particle is born at rest (see eqn. (4.8.1)) is a consequence of the *memory* of the decay function on the past history during the ultrarelativistic stage.

The cosmological decay law is compared to a *phenomenological* Minkowski-like, S-matrix inspired decay law with an instantaneous Lorentz time dilation factor

$$\mathcal{P}^{(M)}_\Phi(t) = e^{-\frac{\Gamma_0}{\gamma(t)}\,(t-t_i)}\, \mathcal{P}^{(M)}_\Phi(t_i)\,, \tag{4.8.2}$$

we found that this phenomenological law describes at long times a *much faster decay* thereby *under estimating* the lifetime of the decaying particle.

The decay dynamics revealed by this study during (RD) allows us to extrapolate to the case of very long lived, i.e. very weakly coupled particles. We obtain a decay function that yields an *upper bound* to the survival probability *all throughout the expansion history* under the assumption of two body decay into a massless fermions, it is given by

$$\mathcal{P}_{\Phi}(z) \gtrsim e^{-\frac{\Gamma_0}{H_0}\,\Upsilon(z,z_b)}\,\mathcal{P}_{\Phi}(z_b)\,, \tag{4.8.3}$$

where $\Upsilon(z, z_b)$ is given by (4.6.39) and depends *only* on the cosmological parameters and the scale factor at which the particle transitions from ultrarelativistic to non-relativistic.

One important conclusion from these results is that using a *decay rate* as measure of the decay dynamics is not a useful concept and misses the correct dynamical evolution. An S-matrix calculation of transition amplitudes or probabilities, where the time interval is taken to infinity not only it does not capture the various different dynamical scales and temporal behaviour of the survival probability, but substantially *under estimates* the lifetime of the decaying state.

An important corollary of this study is that the S-matrix approach to describe quantum decay in the cosmological setting is in general inadequate, while it may yield a good approximation for processes of decay at rest for weakly coupled particles late in the cosmological history, it misses important non-equilibrium dynamics. The non-equilibrium effects revealed by our study, from the transient dynamics of the formation to the quasiparticle, to the memory of the decay function on the past history of the decaying particle *could* be relevant in the quantum kinetics of processes in the very early universe. These could have potential impact in CP-violating non-equilibrium dynamics, baryogenesis and leptogenesis and merit further study.

5.0 Non-adiabatic Cosmological Production of Ultra-light Dark Matter

5.1 Introduction

Despite a large effort on the direct detection of weakly interacting massive particles in the mass range of few to 100 GeV with weak interactions cross sections, no particle beyond the Standard Model with these properties has been found[25]-[60]. This lack of evidence is motivating the study of alternative *light* or *ultra-light* (DM) candidates, such as sterile neutrinos, axions or axion-like particles, "fuzzy" dark matter (FDM), light dark scalars and dark vector bosons[147]-[80]. An (FDM) candidate with mass $m \simeq 10^{-22}\,\mathrm{eV}$, and de-Broglie wavelength $\simeq$ kpc could be a cold-dark matter (CDM) candidate with the potential for solving some small scale aspects of galaxy formation[109]-[150]. All of these candidates are characterized by very small masses and couplings to Standard Model degrees of freedom. Lyman-α[113, 151] and pulsar timing[162] provide constraints on the mass range of (ultra) light dark matter (ULDM). Light dark matter (DM) candidates are not only probed by their gravitational properties[45] but there are various proposals for *direct* detection, from high energy colliders[62] to "table-top" experiments[187]-[11]. There are several proposed mechanisms of production of light or ultra-light dark matter[147, 178, 1, 70, 106, 22, 8, 80].

Particle production in a dynamical cosmological background was studied in pioneering work in refs.[153, 154, 155, 156, 28, 84, 87, 158, 149]. Gravitational production of (DM) candidates was studied for various candidates and within different settings: heavy (DM) particles[55, 52, 54, 124], production from inflaton oscillations or oscillatory backgrounds [173, 77, 76], for "stiff" equations of state in[134], or during reheating[102, 131]. These previous studies considered heavy (DM) candidates and often invoked the adiabatic approximation valid for large masses and/or wavevectors.

In this article we study the gravitational production of ultra-light (DM) with important differences from previous studies:

i) We study the *non-adiabatic* gravitational production of *ultra-light dark matter* (ULDM) as a consequence of cosmological expansion during the inflationary and post-inflationary ra-

diation dominated era until matter-radiation equality. We obtain the abundance, equation of state and free-streaming length (cutoff scale in the matter power spectrum) to assess whether this candidate describes cold, warm or hot (DM).

ii) We consider a real free scalar field describing the (ULDM) as a *spectator field* during inflation, namely it does *not* couple to the inflaton, it does *not* acquire an expectation value, hence it does not contribute to *linear* isocurvature perturbations that couple to long-wavelength metric perturbations[92, 48, 20]. We discuss the issue of *non-linear* entropy perturbations in section(5.6). This scalar field is in its (Bunch-Davies) vacuum state during inflation. A vanishing expectation value of the field precludes a "misalignement" type production mechanism.

iii) This field does not feature self-interactions or interactions with any other field, it only interacts gravitationally.

iv) We focus on scales that are well outside the horizon at the end of inflation, since these are the scales of cosmological relevance for structure formation, and we *assume* a rapid transition from the inflationary stage to a radiation dominated (RD) era.

v) We obtain the full energy momentum tensor; its expectation value in the "in" Bunch-Davies vacuum yields the energy density and pressure. We show that in the asymptotic regime when the evolution becomes adiabatic, the zeroth-order adiabatic energy momentum tensor coincides with the usual fluid-kinetic one. We obtain the abundance, equation of state and free-streaming length near matter-radiation equality to assess whether this candidate describes cold, warm or hot (DM). Imposing the observed (DM) abundance yields a bound on the mass of the (ULDM) particle which *only* depends on cosmological parameters.

We discuss (ULDM) minimally and conformally coupled to gravity. Although we expect negligible production of an (ULDM) particle conformally coupled to gravity, its detailed study provides an explicit quantitative confirmation of this expectation and highlights the main differences with the case of minimal coupling. The comparison between the minimally and conformally coupled cases allow us to conclude that in the minimal coupling scenario, substantial particle production occurs during inflation after the corresponding wavelengths become super-horizon.

Summary of main results:

For a minimally coupled light scalar field taken as *spectator* in its Bunch-Davies vacuum state during inflation, non-adiabatic particle production yields a *distribution function* peaked at small comoving momentum $\mathcal{N}_k \propto 1/k^3$. The low momentum enhancement is a distinct remnant of the infrared enhancement of light minimally coupled fields during inflation. Assuming the upper bound on the scale of inflation established by Planck[59], we find that a mass $\simeq 10^{-5}\,\mathrm{eV}$ yields the correct dark matter abundance. Furthermore, we find that this (DM) candidate, despite being very light is extremely cold; its equation of state parameter at matter-radiation equality is $w \simeq 10^{-14}$ and features a free streaming length (cutoff scale in the matter power spectrum) $\lambda_{fs} \simeq 70\,\mathrm{pc}$. Conformally coupled (ULDM) features a negligible abundance.

The results of this study apply also to axion-like particles, albeit with no other interactions but gravitational. The abundance, equation of state, and clustering properties only depend on cosmological parameters and the mass, therefore this study provides the simplest scenario for particle production of (ULDM), and for a long-lived (DM) candidate a *lower bound* on the abundance. This lower bound on the abundance from non-adiabatic cosmological production should enter in *any* assessment of (ULDM) candidates, even those with interactions.

The model of (ULDM) is introduced in section (5.2). Section (5.3) discusses the "in" states and define the "out" particle states, obtaining the number of asymptotic "out" particles produced non-adiabatically for minimal and conformal coupling to gravity. In section (5.4) we discuss the non-adiabatic nature of particle production. Section (5.5) analyzes the energy momentum tensor, discusses renormalization aspects, establishes the relation with the fluid-kinetic energy momentum tensor in the adiabatic regime and defines the energy density and pressure of the asymptotic particle states. In this section we obtain the relation between the dark matter abundance, the particle's mass and cosmological parameters. We also obtain the equation of state and free-streaming length and establish that non-adiabatic production of (ULDM) yields a *cold dark matter* candidate. In section (5.6) we discuss linear and non-linear entropy perturbations. Section (5.7) discusses various aspects and caveats suggesting further questions and avenues of study, and section (5.8) summarizes our

conclusions. Two appendices provide technical details.

5.2 The Model for the (ULDM) Scalar

We consider a free real ultra-light scalar degree of freedom as a dark matter candidate (ULDM) and invoke the following main assumptions:

i:) It is a *spectator* field during inflation. Namely, it does not interact with any other field, including the inflaton, and it does not acquire a vacuum expectation value, therefore it does not drive inflation. Because it does not acquire an expectation value it does not contribute to *linear* isocurvature perturbations that source long-wavelength metric perturbations[92, 48, 20]. See section (5.6) for a discussion on *non-linear* entropy perturbations.

ii:) The inflationary stage is described by an exact de Sitter space-time, the ultralight field is in the Bunch-Davies vacuum state and we consider field fluctuations with superhorizon wavelengths at the end of inflation, since these are the wavelengths of cosmological relevance for structure formation.

iii:) We assume instantaneous reheating: namely we consider an instantaneous transition from the inflationary to a radiation dominated stage post-inflation. There is as yet an incomplete understanding of the non-equilibrium dynamics of reheating. Reheating dynamics depend crucially on various assumptions on couplings with the inflaton and/or other fields, and thermalization processes[9] in an expanding cosmology. The question of how the nearly $\simeq 100$ degrees of freedom of the Standard Model attain a state of local thermodynamic equilibrium after inflation and on what time scales is still unanswered. Most studies *model* the couplings and dynamics; therefore any model of reheating is at best tentative and very approximate. We bypass the inherent ambiguities and model dependence of the reheating dynamics, and assume *instantaneous* reheating after inflation to a radiation dominated (RD) era. The physical reason behind this assumption is that we are primarily concerned with wavevectors that have crossed the Hubble radius during inflation well before the transition to (RD) and are well outside the horizon during this transition, hence causally decoupled from microphysics. These modes feature very slow dynamics at the end of inflation, and

the assumption that they are frozen during the reheating time interval seems physically warranted (see further discussion in section (5.7)). We assume that both the scale factor and the Hubble rate are *continuous* across the transition. Along with the continuity of the mode functions and their time derivative across the transition (see below), this, in fact, entails the continuity of the energy density obtained from the energy momentum tensor (see below).

iv:) Unlike previous studies that invoked the adiabatic approximation, we study *non-adiabatic* cosmological production of (ULDM). This is a direct consequence of a very small mass and field fluctuations with superhorizon wavelengths after inflation.

v:) The (RD) era is dominated by a large number $\simeq 100$ of ultrarelativistic degrees of freedom justifying taking the space time metric during this era as a *background* and neglecting the contribution from the single scalar degree of freedom.

In comoving coordinates, the action for the real (ULDM) scalar field is given by

$$S = \int d^3x\, dt\, \sqrt{-g}\left\{\frac{1}{2}\dot{\phi}^2 - \frac{(\nabla\phi)^2}{2a^2} - \frac{1}{2}\left[m^2 + \xi\, R\right]\phi^2\right\} \tag{5.2.1}$$

where

$$R = 6\Big[\frac{\ddot{a}}{a} + \Big(\frac{\dot{a}}{a}\Big)^2\Big]\,, \tag{5.2.2}$$

is the Ricci scalar, (here the dot stands for derivatives with respect to comoving time t) and ξ is the coupling to gravity, with $\xi = 0, 1/6$ corresponding to minimal or conformal coupling, respectively, we will study both cases separately. We consider a spatially flat Friedmann-Robertson-Walker (FRW) cosmology in conformal time coordinate, with the metric given by

$$g_{\mu\nu} = a^2(\eta)\ \eta_{\mu\nu}\,, \tag{5.2.3}$$

where $\eta_{\mu\nu} = \mathrm{diag}(1, -1, -1, -1)$ is the flat Minkowski space-time metric.

Introducing the conformally rescaled fields

$$\phi(\vec{x}, t) = \frac{\chi(\vec{x}, \eta)}{a(\eta)}\,, \tag{5.2.4}$$

with

$$R = 6\,\frac{a''(\eta)}{a^3(\eta)}\,, \tag{5.2.5}$$

the primes now refer to derivatives with respect to conformal time. The action becomes (neglecting an irrelevant surface term that does not affect the equations of motion or energy momentum tensor),

$$S = \int d^3x\; d\eta\,\frac{1}{2}\left[\chi'^2 - (\nabla\chi)^2 - \mathcal{M}^2(\eta)\;\chi^2\right]\,, \tag{5.2.6}$$

where

$$\mathcal{M}^2(\eta) = m^2\,a^2(\eta) - \frac{a''(\eta)}{a(\eta)}\,(1-6\xi)\,. \tag{5.2.7}$$

The inflationary stage is described by a spatially flat de Sitter space time (thereby neglecting slow roll corrections) with a scale factor

$$a(\eta) = -\frac{1}{H_{dS}(\eta - 2\eta_R)}\,, \tag{5.2.8}$$

where H_{dS} is the Hubble constant during de Sitter and η_R is the (conformal) time at which the de Sitter stage transitions to the (RD) stage.

During the radiation dominated (RD) stage the scale factor is given by

$$a(\eta) = H_R\,\eta \tag{5.2.9}$$

with

$$H_R = H_0\,\sqrt{\Omega_R} \simeq 10^{-35}\,\mathrm{eV}\,, \tag{5.2.10}$$

and matter radiation equality occurs at

$$a_{eq} = \frac{\Omega_R}{\Omega_M} \simeq 1.66\;\times 10^{-4}\,. \tag{5.2.11}$$

We model the transition from de Sitter to (RD) at a (conformal) time η_R by requiring that the scale factor and the Hubble rate be continuous across the transition at η_R, assuming self-consistently that the transition occurs deep in the (RD) era so that $a(\eta_R) = H_R\,\eta_R \ll a_{eq}$. Continuity of the scale factor and Hubble rate at the instantaneous reheating time results in

that the energy density, namely the expectation value of T_0^0 is *continuous at the transition*. This important aspect is discussed further in section (5.5).

Using $H(\eta) = a'(\eta)/a^2(\eta)$, continuity of the scale factor and Hubble rate at η_R imply that

$$a_{dS}(\eta_R) = \frac{1}{H_{dS}\,\eta_R} = H_R\,\eta_R \quad ; \quad H_{dS} = \frac{1}{H_R\,\eta_R^2}\,, \tag{5.2.12}$$

yielding

$$\eta_R = \frac{1}{\sqrt{H_{dS}\,H_R}}\,. \tag{5.2.13}$$

The most recent constraints from Planck on the tensor-to-scalar ratio is[59]

$$H_{dS}/M_{Pl} < 2.5 \times 10^{-5} \;\; (95\%)\,\mathrm{CL}\,. \tag{5.2.14}$$

We take as a representative value $H_{dS} = 10^{13}\,\mathrm{GeV}$, from which it follows that

$$a_{dS}(\eta_R) = H_R\,\eta_R = \sqrt{\frac{H_R}{H_{dS}}} \simeq 10^{-28} \ll a_{eq}\,. \tag{5.2.15}$$

This scale corresponds to an approximate ambient radiation temperature after the transition from de Sitter to (RD)

$$T(\eta_R) \simeq \frac{T_0}{a_{RD}(\eta_R)} \simeq 10^{15}\,\mathrm{GeV} \tag{5.2.16}$$

where $T_0 \propto 10^{-4}\,\mathrm{eV}$ is the CMB temperature today.

We also define the mass of the (DM) particle in units of eV as

$$m_{ev} \equiv \frac{m}{(\mathrm{eV})}\,, \tag{5.2.17}$$

which for ultra-light (DM) particles we define as $m_{ev} \ll 1$.

5.3 "In-Out" States, Adiabatic Mode Functions, and Particle States

5.3.1 Asymptotic "In-Out" States

The quantization of the real (ULDM) scalar field in a finite comoving volume V proceeds by writing

$$\chi(\vec{x},\eta) = \frac{1}{\sqrt{V}} \sum_{\vec{k}} \left[a_{\vec{k}}\, g_k(\eta)\, e^{-i\vec{k}\cdot\vec{x}} + a^\dagger_{\vec{k}}\, g^*_k(\eta)\, e^{i\vec{k}\cdot\vec{x}} \right], \tag{5.3.1}$$

where $\vec{k}$ are comoving wave vectors. The mode functions $g_k(\eta)$ are solutions of the equations of motion

$$g''_k(\eta) + \left[k^2 + m^2\, a^2(\eta) - \frac{a''(\eta)}{a(\eta)}\,(1-6\xi) \right] g_k(\eta) = 0\,, \tag{5.3.2}$$

and are normalized to obey the Wronskian condition

$$g'_k(\eta)\, g^*_k(\eta) - g_k(\eta)\, g'^*_k(\eta) = -i \tag{5.3.3}$$

so that $a_{\vec{k}}, a^\dagger_{\vec{k}}$ obey canonical commutation relations.

A familiar interpretation of the mode equation follows by writing (5.3.2) as

$$-\frac{d^2}{d\eta^2}\, g_k(\eta) + V(\eta) g_k(\eta) = k^2 g_k(\eta) \;\;;\;\; V(\eta) = -m^2 a^2(\eta) + (1-6\xi)\,\frac{a''(\eta)}{a(\eta)}\,, \tag{5.3.4}$$

namely a Schroedinger equation for a wave function g_k with a potential $V(\eta)$ and "energy" k^2. The potential $V(\eta)$ and/or its derivative are discontinuous at the transition η_R; however $g_k(\eta)$ and $g'_k(\eta)$ are continuous at η_R. Defining

$$g_k(\eta) = \begin{cases} g^<_k(\eta) \;\;;\;\; \text{for} \;\;;\;\; \eta < \eta_R \\ g^>_k(\eta) \;\;;\;\; \text{for} \;\;;\;\; \eta > \eta_R \end{cases}, \tag{5.3.5}$$

the matching conditions are

$$\begin{aligned} g^<_k(\eta_R) &= g^>_k(\eta_R) \\ \frac{d}{d\eta} g^<_k(\eta)\Big|_{\eta_R} &= \frac{d}{d\eta} g^>_k(\eta)\Big|_{\eta_R}\,. \end{aligned} \tag{5.3.6}$$

As is discussed below (see section (5.5)), these continuity conditions on the mode functions, along with the continuity of the scale factor and Hubble rate at the transition ensures that the energy density is *continuous* at the transition from inflation to (RD).

5.3.1.1 Inflationary Stage We consider that the (ULDM) scalar is in the Bunch-Davies vacuum state during the inflationary stage, which corresponds to the mode functions $g_k(\eta)$ fulfilling the boundary condition

$$g_k(\eta) \quad \xrightarrow[\eta\to-\infty]{} \quad \frac{e^{-ik\eta}}{\sqrt{2k}}\,, \tag{5.3.7}$$

and the Bunch-Davies vacuum state $|0\rangle$ is such that

$$a_{\vec{k}}|0\rangle = 0 \;\forall \vec{k}\,. \tag{5.3.8}$$

We refer to this vacuum state as the *in* vacuum.

We will consider both cases: conformal coupling (CC) $\xi = 1/6$ and minimal coupling (MC) $\xi = 0$.

During the de Sitter stage ($\eta < \eta_R$), with the scale factor given by eqn. (5.2.8), the mode equation becomes

$$\frac{d^2}{d\tau^2}\, g_k^<(\tau) + \left[k^2 - \frac{\nu^2 - 1/4}{\tau^2}\right] g_k^<(\tau) = 0\,, \tag{5.3.9}$$

where

$$\tau = \eta - 2\eta_R \;\;;\;\; \nu^2 = \left\{ \begin{array}{c} \frac{9}{4} - \frac{m^2}{H_{dS}^2} \;\; \text{for} \;\; \xi = 0 \;\; (MC) \\ \frac{1}{4} - \frac{m^2}{H_{dS}^2} \;\; \text{for} \;\; \xi = 1/6 \;\; (CC) \end{array} \right\}. \tag{5.3.10}$$

The solution with the boundary condition (5.3.7) is given by

$$g_k^<(\tau) = \frac{1}{2}\sqrt{-\pi\tau}\; e^{i\frac{\pi}{2}(\nu+1/2)}\, H_\nu^{(1)}(-k\tau) \tag{5.3.11}$$

where $H_\nu^{(1)}$ is a Bessel function. We note that with $H_{dS} \simeq 10^{13}\,\text{GeV}$ it follows that $m/H_{dS} \simeq m_{ev}\,10^{-22} \ll 10^{-22}$ and can be safely ignored in the expression for ν. Therefore, neglecting the mass of the (ULDM) scalar, we find

$$g_k^<(\tau) = \left\{ \begin{array}{c} \frac{e^{-ik\tau}}{\sqrt{2k}}\left[1 - \frac{i}{k\tau}\right] \;\; \text{for} \;\; \xi = 0 \;\; (MC) \\ \frac{e^{-ik\tau}}{\sqrt{2k}} \;\; \text{for} \;\; \xi = 1/6 \;\; (CC) \end{array} \right\}. \tag{5.3.12}$$

With $H_{dS} \simeq 10^{13}\,\text{GeV}$ we find that $\eta_R \simeq 10^6\,\text{eV}^{-1} \simeq 0.2\,\text{meters}$. In what follows we will consider that all the modes of cosmological interest are *well outside* the Hubble radius at the end of inflation, namely

$$k\,\eta_R \ll 1\,, \tag{5.3.13}$$

for the value of H_{dS} assumed above, with $\eta_R \simeq 10^6\,(\mathrm{eV})^{-1}$ the superhorizon condition (5.3.13) corresponds to comoving wavevectors $k \ll \mu\mathrm{eV}$ or comoving wavelengths $\gg 1$ meters, obviously including *all* astrophysically relevant scales.

The "*in*" state is the Bunch-Davies vacuum defined by equation (5.3.8) and the mode functions (5.3.12) during the inflation stage, taken to be de Sitter space-time, thereby neglecting small slow-roll corrections.

5.3.1.2 Radiation Dominated Era During the radiation era for $\eta > \eta_R$, with $a(\eta) = H_R\eta$ we set $a'' = 0$, and the mode equation (5.3.2) becomes

$$\frac{d^2}{d\eta^2} g_k^>(\eta) + \left[k^2 + m^2\, H_R^2\, \eta^2\right] g_k^>(\eta) = 0\,, \tag{5.3.14}$$

the general solutions of which are linear combinations of parabolic cylinder functions[2, 152, 21, 145]. As "out" boundary conditions, we impose that such a combination should describe asymptotically positive frequency "particle" states and their hermitian conjugate. This identification relies on a WKB form of the asymptotic mode functions.

Let us consider a particular solution of (5.3.14) of the WKB form

$$f_k(\eta) = \frac{e^{-i\int_{\eta_R}^{\eta} W_k(\eta')\,d\eta'}}{\sqrt{2\,W_k(\eta)}}\,. \tag{5.3.15}$$

Upon inserting this ansatze in the mode equation (5.3.14) one finds that $W_k(\eta)$ obeys

$$W_k^2(\eta) = \omega_k^2(\eta) - \frac{1}{2}\left[\frac{W_k''(\eta)}{W_k(\eta)} - \frac{3}{2}\left(\frac{W_k'(\eta)}{W_k(\eta)}\right)^2\right], \tag{5.3.16}$$

where

$$\omega_k^2(\eta) = k^2 + m^2\, H_R^2\, \eta^2\,. \tag{5.3.17}$$

When $\omega_k(\eta)$ is a slowly-varying function of time the WKB eqn. (5.3.16) may be solved in a consistent *adiabatic expansion* in terms of derivatives of $\omega_k(\eta)$ with respect to η divided by appropriate powers of the frequency, namely

$$W_k^2(\eta) = \omega_k^2(\eta)\left[1 - \frac{1}{2}\,\frac{\omega_k''(\eta)}{\omega_k^3(\eta)} + \frac{3}{4}\left(\frac{\omega_k'(\eta)}{\omega_k^2(\eta)}\right)^2 + \cdots\right]. \tag{5.3.18}$$

We refer to terms that feature n-derivatives of $\omega_k(\eta)$ as of n-th adiabatic order. During the time interval of rapid variations of the frequencies the concept of particle is ambiguous, but at long time the frequencies evolve slowly and the concept of particle becomes clear.

We want to identify "particles" (dark matter "particles") near the time of matter radiation equality, so that entering in the matter dominated era we can extract the energy density and pressure (energy momentum tensor) associated with dark matter *particles*. Therefore, we seek to clearly define the concept of particles near matter-radiation equality namely $a(\eta) \simeq a_{eq} \simeq 10^{-4}$.

The condition of adiabatic expansion relies on the ratio

$$\frac{\omega_k^{'}(\eta)}{\omega_k^2(\eta)} \ll 1\,. \tag{5.3.19}$$

An upper bound on this ratio is obtained in the very long wavelength (superhorizon) limit, taking $\omega_k(\eta) = m\,a(\eta)$, in an (RD) cosmology leads to the condition

$$\frac{a'(\eta)}{m\,a^2(\eta)} = \frac{H_R}{m\,a^2(\eta)} \ll 1 \Longrightarrow a(\eta) \gg \frac{10^{-17}}{\sqrt{m_{ev}}}\,. \tag{5.3.20}$$

Therefore, even for $m_{ev} \simeq 1$ corresponding to to $a(\eta) \simeq 10^{-17}$ there is a long period of *non-adiabatic* evolution since the end of inflation $a(\eta_R) \simeq 10^{-29} \ll 10^{-17}/\sqrt{m_{ev}}$, during which the $\omega_k(\eta)$ varies *rapidly*. However, even for an ultra-light particle with $m_{ev} \simeq 10^{-22}$ yielding a much longer period of non-adiabatic evolution, the adiabatic condition is fulfilled well before matter-radiation equality. The adiabaticity condition becomes less stringent for non-vanishing wavevectors with $k \gg m\,a(\eta)$.

In conclusion, the evolution of the mode functions becomes adiabatic well before matter radiation equality. During the adiabatic regime the WKB mode function (5.3.15) asymptotically becomes

$$f_k(\eta) \to \frac{e^{-i\,\int^\eta\,\omega_k(\eta')\,d\eta'}}{\sqrt{2\,\omega_k(\eta)}}\,, \tag{5.3.21}$$

we refer to the mode functions with this asymptotic boundary condition as "out" particle states which obey the Wronskian condition

$$f_k^{'}(\eta)\,f_k^{*}(\eta) - f_k(\eta)\,f_k^{'*}(\eta) = -i\,. \tag{5.3.22}$$

The definition of these mode functions as describing particle states merits discussion. Our space time is *not* Minkowski space time; dark energy entails that the cosmology describing our space time is nearly de Sitter (if dark energy is in the form of a cosmological constant), and Minkowski space time is a local approximation valid on scales much smaller than the Hubble scale. The conformal and (local) comoving energy are related by

$$\omega_k(\eta) = \sqrt{k^2 + m^2 a^2(\eta)} = a(\eta)\, E_k(\eta)\,, \tag{5.3.23}$$

with

$$E_k(\eta) = \sqrt{k_{ph}^2(\eta) + m^2} \quad ; \quad k_{ph}(\eta) \equiv \frac{k^2}{a^2(\eta)}\,, \tag{5.3.24}$$

where $k_{ph}(\eta)$ is the physical momentum.

Consider the asymptotic phase of the mode function $f_k(\eta)$ given by eqn. (5.3.21), using the relations (5.3.23, 5.3.24) and $a(\eta)\, d\eta = dt$ with t being cosmic time, it follows that

$$\int_{\eta_0}^{\eta} \omega_k(\eta')\, d\eta' = \int_{t_0}^{t} E_k(t')\, dt'\,. \tag{5.3.25}$$

Expanding around the lower limit and integrating we find

$$\int_{t_0}^{t} E_k(t')\, dt' = E_k(t_0)\,(t - t_0)\left[1 - \frac{1}{2}\,\beta_k^2(t_0)\, H(t_0)\,(t - t_0) + \cdots\right], \tag{5.3.26}$$

where

$$\beta_k(t_0) = \frac{k_{ph}(t_0)}{E_k(t_0)} \quad ; \quad H(t_0) = \frac{\dot{a}(t_0)}{a(t_0)}\,, \tag{5.3.27}$$

with $H(t_0)$ the Hubble expansion rate at t_0. Therefore it is clear that the phase is associated with particle states over a time scale $t - t_0 \ll 1/H(t_0) \simeq 13\,\mathrm{Gyr}$. Thus on these time scales Minkowski space-time particle states are a valid description. This, of course is just a consequence of the equivalence principle.

The general solution of equation (5.3.14) is

$$g_k^{>}(\eta) = A_k\, f_k(\eta) + B_k\, f_k^*(\eta)\,, \tag{5.3.28}$$

where $f_k(\eta)$ are the solutions of the mode equation (5.3.14) with asymptotic boundary conditions (5.3.21) and A_k and B_k are Bogoliubov coefficients. Since $g_k^{>}(\eta)$ obeys the Wronskian condition (5.3.3) and so does $f_k(\eta)$, it follows that the Bogoliubov coefficients obey

$$|A_k|^2 - |B_k|^2 = 1\,. \tag{5.3.29}$$

Using the Wronskian condition (5.3.22) and the matching condition (5.3.6), we find that the Bogoliubov coefficients are determined from the following relations,

$$\begin{aligned} A_k &= i\Big[g_k^{'<}(\eta_R)\, f_k^*(\eta_R) - g_k^{<}(\eta_R)\, f_k^{'*}(\eta_R)\Big] \\ B_k &= -i\Big[g_k^{'<}(\eta_R)\, f_k(\eta_R) - g_k^{<}(\eta_R)\, f_k^{'}(\eta_R)\Big]\,. \end{aligned} \tag{5.3.30}$$

Since the mode functions $g_k^{<}(\eta)$ also fulfill the Wronskian condition (5.3.3), it is straightforward to confirm the identity (5.3.29).

For $\eta > \eta_R$ the field expansion (5.3.1) yields

$$\chi(\vec{x},\eta) = \frac{1}{\sqrt{V}}\sum_{\vec{k}}\Big[a_{\vec{k}}\, g_k^{>}(\eta)\, e^{-i\vec{k}\cdot\vec{x}} + a_{\vec{k}}^\dagger\, g_k^{*>}(\eta)\, e^{i\vec{k}\cdot\vec{x}}\Big] = \frac{1}{\sqrt{V}}\sum_{\vec{k}}\Big[b_{\vec{k}}\, f_k(\eta)\, e^{-i\vec{k}\cdot\vec{x}} + b_{\vec{k}}^\dagger\, f_k^*(\eta)\, e^{i\vec{k}\cdot\vec{x}}\Big]\,, \tag{5.3.31}$$

where

$$b_{\vec{k}} = a_k\, A_k + a_{-\vec{k}}^\dagger\, B_k^* \;\;;\;\; b_{\vec{k}}^\dagger = a_{\vec{k}}^\dagger\, A_k^* + a_{-\vec{k}}\, B_k\,. \tag{5.3.32}$$

We refer to $b_{\vec{k}}, b_{\vec{k}}^\dagger$ as the annihilation and creation operators of *out particle* states respectively. They obey canonical quantization conditions as a consequence of the relation (5.3.29). In the Heisenberg picture the field operators evolve in time but the states do not. The vacuum state $|0\rangle$ is the Bunch-Davies vacuum state (5.3.8) in which the number of *out*-particles is given by

$$\mathcal{N}_k = \langle 0|b_{\vec{k}}^\dagger b_{\vec{k}}|0\rangle = |B_k|^2\,. \tag{5.3.33}$$

We identify $\mathcal{N}_k$ with the number of dark matter particles produced *asymptotically* from cosmic expansion. Only in the asymptotic adiabatic regime can $\mathcal{N}_k$ be associated with the number of *particles*. This point will be discussed further in section (5.7).

It remains to obtain the solutions $f_k(\eta)$ of the mode equations (5.3.14) with asymptotic "out" boundary condition (5.3.21) describing asymptotic particle states.

It is convenient to introduce the dimensionless variables

$$x = \sqrt{2mH_R}\,\eta \;\;;\;\; \alpha = -\frac{k^2}{2mH_R}\,, \tag{5.3.34}$$

in terms of which the equation (5.3.14) is identified with Weber's equation[2, 152, 21, 145]

$$\frac{d^2}{dx^2}\,g(x) + \Big[\frac{x^2}{4} - \alpha\Big]g(x) = 0 \tag{5.3.35}$$

whose real solutions are Weber's parabolic cylinder functions[152, 2, 21, 145]:

$$W[\alpha;\pm x] = \frac{1}{2^{3/4}}\left[\sqrt{\frac{G_1}{G_3}}\;Y_1(\alpha;x) \mp \sqrt{\frac{2\,G_3}{G_1}}\;Y_2(\alpha;x)\right], \tag{5.3.36}$$

where

$$G_1 = \left|\Gamma\Big(\frac{1}{4} + i\frac{\alpha}{2}\Big)\right| \;\;;\;\; G_3 = \left|\Gamma\Big(\frac{3}{4} + i\frac{\alpha}{2}\Big)\right| \tag{5.3.37}$$

and[2, 152]

$$Y_1(\alpha;x) \;=\; 1 + \alpha\,\frac{x^2}{2!} + \big(\alpha^2 - \frac{1}{2}\big)\,\frac{x^4}{4!} + \cdots \tag{5.3.38}$$

$$Y_2(\alpha;x) \;=\; x\Big[1 + \alpha\,\frac{x^2}{3!} + \big(\alpha^2 - \frac{3}{2}\big)\,\frac{x^4}{5!} + \cdots\Big]\,. \tag{5.3.39}$$

With these real solutions we construct the complex solution that satisfies the Wronskian condition (5.3.22) and features the asymptotic "out-state" behavior (5.3.21) with $\omega_k^2(\eta) = \frac{x^2}{4} - \alpha$. It is straightforward to confirm that such a solution is given by (see appendix (C.1))

$$f_k(\eta) = \frac{1}{(8mH_R)^{1/4}}\left[\frac{1}{\sqrt{\kappa}}\,W[\alpha;x] - i\sqrt{\kappa}\,W[\alpha;-x]\right] \;\;;\;\; \kappa = \sqrt{1 + e^{-2\pi|\alpha|}} - e^{-\pi|\alpha|}\,. \tag{5.3.40}$$

It is shown in appendix (C.1) that these solutions do indeed satisfy the asymptotic "out" boundary condition (5.3.21) and fulfill the Wronskian condition (5.3.22).

The Bogoliubov coefficients are obtained from eqns. (5.3.30), where the mode functions during the de Sitter era $g_k^<(\eta)$ are given by eqn. (5.3.12) (with $\tau = \eta - 2\eta_R$).

For $\eta_R = 1/\sqrt{H_{dS}\,H_R}$ (see eqn. (5.2.13)) it follows that

$$x(\eta_R) = \sqrt{\frac{2m}{H_{dS}}} \simeq \sqrt{2\,m_{ev}}\;10^{-11} \;\;;\;\; -\alpha\,x^2(\eta_R) = (k\,\eta_R)^2 \ll 1\,, \tag{5.3.41}$$

therefore for $\eta \simeq \eta_R$ we can set $Y_1(x) \simeq 1; Y_2(x) \simeq x$ in order to obtain the Bogoliubov coefficients from equation (5.3.30).

We note that the condition $x(\eta) \ll 1$ implies that

$$\frac{1}{m\, H_R\, \eta^2} = \frac{a'(\eta)}{m\, a^2(\eta)} \gg 1\,. \tag{5.3.42}$$

Therefore, comparing with the condition for adiabaticity (5.3.20) we see that the mode functions after the transition are strongly non-adiabatic.

The regime of *non-adiabatic* evolution is where particle production is most effective (see discussion in section (5.7)). Furthermore, particle production is enhanced at *longer wavelengths* because these modes feature the strongest departure from adiabaticity.

We emphasize that while we assume an instantaneous transition from the inflationary to the (RD) stage, the scale factor, the Hubble rate, the mode functions and their (conformal) time derivatives are all *continuous* across the transition and this continuity implies a continuous process of particle production. As a consequence of these continuity conditions the transition *does not* induce a burst of particle production, nor is there any discontinuity in the production dynamics. This important aspect will be highlighted again in sections (5.4) and (5.5) below in more detail.

5.3.2 Minimal Coupling

We begin by studying the case of minimal coupling (MC), namely $\xi = 0$. The mode functions during the inflationary (de Sitter) era are given by (5.3.12) for (MC) and during (RD) the general solution of the mode equations is given by (5.3.28) in terms of the solutions (5.3.40) with *out* (particle) boundary conditions.

For the minimally coupled case (MC) we find from eqn. (5.3.12)

$$g_k^<(\eta_R) = \frac{e^{ik\eta_R}}{\sqrt{2k}}\left[1 + \frac{i}{k\,\eta_R}\right] \tag{5.3.43}$$

$$\frac{d}{d\eta} g_k^<(\eta)\Big|_{\eta_R} = -ik\,\frac{e^{ik\eta_R}}{\sqrt{2k}}\left[1 + \frac{i}{k\,\eta_R} - \frac{1}{(k\,\eta_R)^2}\right]. \tag{5.3.44}$$

Since $k\eta_R \ll 1$ we keep the leading order terms in the superhorizon limit $k\,\eta_R \to 0$ writing

$$g_k^<(\eta_R) = \frac{i}{\sqrt{2k}\,\delta} \tag{5.3.45}$$

$$\frac{d}{d\eta} g_k^<(\eta)\Big|_{\eta_R} = \frac{i\sqrt{k}}{\sqrt{2}\,\delta^2} \;\; ; \;\; \delta = k\,\eta_R\,. \tag{5.3.46}$$

From eqn. (5.3.41) we find

$$f_k(\eta_R) = \frac{1}{(8mH_R)^{1/4}} \left[\frac{1}{\sqrt{\kappa}} - i\sqrt{\kappa}\right] W[\alpha;0] \tag{5.3.47}$$

$$\frac{d\,f_k(\eta)}{d\eta}\Big|_{\eta_R} = \frac{\sqrt{2\,m\,H_R}}{(8mH_R)^{1/4}} \left[\frac{1}{\sqrt{\kappa}} + i\sqrt{\kappa}\right] W'[\alpha;0]\,, \tag{5.3.48}$$

with

$$W'[a,0] = -\frac{1}{2}\,W[a,0]\,. \tag{5.3.49}$$

Using these results with the matching conditions (5.3.30) yield the Bogoliubov coefficients,

$$A_k = \frac{i}{4\,\delta}\left\{\sqrt{\kappa}\left(R_k - \frac{2}{R_k\,\delta}\right) + \frac{i}{\sqrt{\kappa}}\left(R_k + \frac{2}{R_k\,\delta}\right)\right\}, \tag{5.3.50}$$

$$B_k = \frac{i}{4\,\delta}\left\{\sqrt{\kappa}\left(R_k - \frac{2}{R_k\,\delta}\right) - \frac{i}{\sqrt{\kappa}}\left(R_k + \frac{2}{R_k\,\delta}\right)\right\} \tag{5.3.51}$$

where

$$R_k = \frac{2^{3/4}}{|\alpha|^{1/4}} \left|\frac{\Gamma\left(\frac{3}{4} - i\frac{|\alpha|}{2}\right)}{\Gamma\left(\frac{1}{4} - i\frac{|\alpha|}{2}\right)}\right|^{1/2}. \tag{5.3.52}$$

Therefore, the distribution function of produced particles is given by

$$\mathcal{N}_k = |B_k|^2 = \frac{1}{4R_k^2\,\delta^4}\left[\kappa\left(\frac{R_k^2\delta}{2} - 1\right)^2 + \frac{1}{\kappa}\left(\frac{R_k^2\,\delta}{2} + 1\right)^2\right]. \tag{5.3.53}$$

It is convenient to extract the relevant scales, hence define

$$\sqrt{|\alpha|} = \frac{k}{\sqrt{2mH_R}} \equiv z\,, \tag{5.3.54}$$

in terms of which it follows that

$$\delta = k\,\eta_R = z\,\sqrt{\frac{2m}{H_{dS}}}\,, \tag{5.3.55}$$

yielding

$$
\begin{aligned}
R_k^2\,\delta &= 2^{3/2}\left|\frac{\Gamma\left(\frac{3}{4}-i\frac{z^2}{2}\right)}{\Gamma\left(\frac{1}{4}-i\frac{z^2}{2}\right)}\right|\sqrt{\frac{2m}{H_{dS}}} \\
\frac{1}{R_k^2\,\delta^4} &= \frac{1}{z^3}\left(\frac{H_{dS}}{m}\right)^2\frac{1}{8\sqrt{2}}\left|\frac{\Gamma\left(\frac{1}{4}-i\frac{z^2}{2}\right)}{\Gamma\left(\frac{3}{4}-i\frac{z^2}{2}\right)}\right|,
\end{aligned}
\tag{5.3.56}
$$

with

$$
\frac{H_{dS}}{m}=\frac{1}{m_{ev}}\left[\frac{H_{dS}}{10^{13}\,(\mathrm{GeV})}\right]\;10^{22}\,. \tag{5.3.57}
$$

Using Stirling's approximation we find that the asymptotic behavior of the ratio of Gamma functions in eqn.(5.3.56) is given by

$$
\left|\frac{\Gamma\left(\frac{1}{4}-i\frac{z^2}{2}\right)}{\Gamma\left(\frac{3}{4}-i\frac{z^2}{2}\right)}\right|\;\overrightarrow{z\to\infty}\;\frac{\sqrt{2}}{z}\,. \tag{5.3.58}
$$

We focus on wavelengths that are superhorizon at the end of inflation, namely $k\eta_R \ll 1$ which results in the following condition

$$
k\eta_R = z\sqrt{\frac{2m}{H_{dS}}}\ll 1\,. \tag{5.3.59}
$$

For large z the product

$$
R_k^2\,\delta\to 2\,z\sqrt{\frac{2m}{H_{dS}}}=2\,k\,\eta_R\,, \tag{5.3.60}
$$

therefore in the regime of validity of the superhorizon approximation $k\,\eta_R\ll 1$, the product $R_k^2\,\delta\ll 1$ and can be safely neglected. Hence we can approximate the distribution function as

$$
\mathcal{N}_k\simeq\frac{1}{16\sqrt{2}}\;\left(\frac{H_{dS}}{m}\right)^2\frac{D(z)}{z^3}\,. \tag{5.3.61}
$$

where

$$
D(z)=\sqrt{1+e^{-2\pi z^2}}\;\left|\frac{\Gamma\left(\frac{1}{4}-i\frac{z^2}{2}\right)}{\Gamma\left(\frac{3}{4}-i\frac{z^2}{2}\right)}\right|. \tag{5.3.62}
$$

Figs. (19, 20) display $D(z)$ and $zD(z)/\sqrt{2}$ vs z respectively.

The number of produced particles $\mathcal{N}_k$ is strongly peaked at low momentum $\mathcal{N}_k\propto 1/k^3$. This infrared enhancement and the factor H_{dS}^2 are both remnants of the infrared behavior of

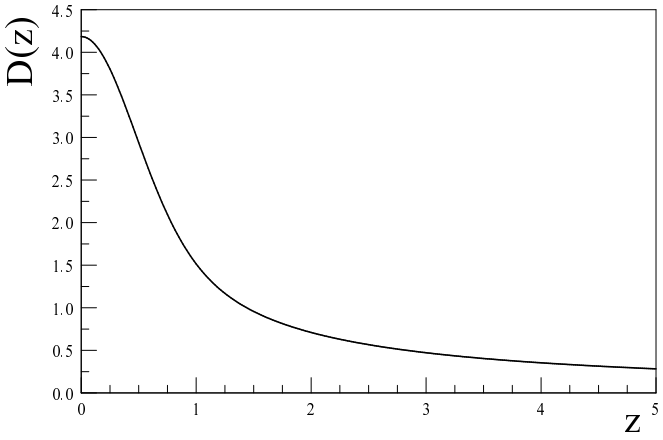

Figure 19: The function D(z) vs. z.

light minimally coupled scalars during the de Sitter era. Because $D(z) \to \sqrt{2}/z$ for $z \gg 1$ it follows that for large comoving wavevectors $\mathcal{N}_k \to 1/k^4$. The small and large momentum limits of the distribution function are summarized as follows:

$$\mathcal{N}_k \propto \begin{cases} 1/k^3 & ; \quad k \ll \sqrt{2mH_R} \\ 1/k^4 & ; \quad k \gg \sqrt{2mH_R} \end{cases} . \tag{5.3.63}$$

5.3.3 Conformal Coupling

Massless particles conformally coupled to gravity are not affected by the cosmological expansion. Therefore, we expect that very light particles with conformal coupling will not be substantially produced. However, in order to fully compare with the minimally coupled case, we study the production in the conformal case and focus on establishing the main aspects of the difference.

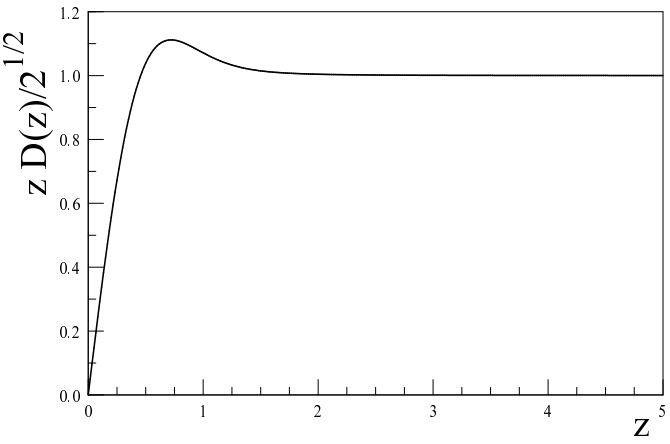

Figure 20: The function $\frac{z}{\sqrt{2}}\,D(z)$ vs. z displaying the asymptotic behavior (5.3.58).

For conformal coupling the mode functions during the inflationary stage are given by (5.3.12) for $\xi = 1/6$. With $k\eta_R \ll 1$ we find

$$g_k^<(\eta_R) = \frac{1}{\sqrt{2k}} \tag{5.3.64}$$

$$\frac{d}{d\eta} g_k^<(\eta)\Big|_{\eta_R} = \frac{-i\sqrt{k}}{\sqrt{2}}\,. \tag{5.3.65}$$

During the (RD) era the mode functions are given by (5.3.28) with $f_k(\eta)$ given by (5.3.40). The Bogoliubov coefficients are found in the same manner as for the minimal coupling by equating the functions and $\eta-$ derivatives at $\eta = \eta_R$.

We find

$$A_k = \frac{1}{4}\left\{ \left(\sqrt{\kappa}\,R_k + \frac{2}{\sqrt{\kappa}\,R_k}\right) + i\left(\frac{R_k}{\sqrt{\kappa}} + \frac{2\sqrt{\kappa}}{R_k}\right)\right\}, \tag{5.3.66}$$

$$B_k = \frac{1}{4}\left\{ \left(\sqrt{\kappa}\,R_k - \frac{2}{\sqrt{\kappa}\,R_k}\right) - i\left(\frac{R_k}{\sqrt{\kappa}} - \frac{2\sqrt{\kappa}}{R_k}\right)\right\}, \tag{5.3.67}$$

where κ and R_k is given by (5.3.40,5.3.52) respectively. It is straightforward to confirm the identity (5.3.29). A comparison with the Bogoliubov coefficients of the minimally coupled case, (5.3.50,5.3.51) reveals that A_k, B_k for minimal coupling feature the denominators with $\delta = k\,\eta_R \ll 1$. These denominators are a direct consequence of the infrared enhancement of the mode functions for nearly massless minimally coupled scalar fields in de Sitter space time, as evident in eqns. (5.3.12) and (5.3.43,5.3.44).

The distribution function of produced particles is

$$\mathcal{N}_k = |B_k|^2 = \frac{1}{8}\left\{\sqrt{1+e^{-2\pi|\alpha|}}\left(R_k^2 + \frac{4}{R_k^2}\right) - 4\right\}. \tag{5.3.68}$$

Using the asymptotic properties of the Gamma functions, we find that $\mathcal{N}_k \to 1/(32\alpha^2)^2 \propto 1/k^8$ for $k \to \infty$ and as $k \to 0$

$$\mathcal{N}_k \propto \frac{1}{\sqrt{|\alpha|}} \propto \frac{1}{k} \tag{5.3.69}$$

therefore particles are produced primarily with very small momentum $k \ll \sqrt{m\,H_R}$.

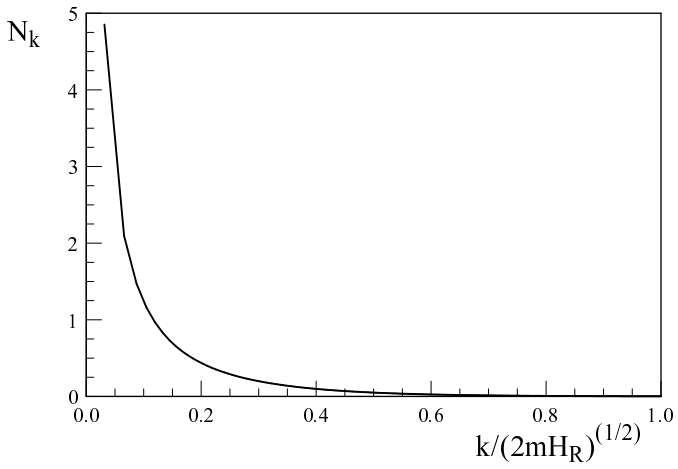

Figure 21: $\mathcal{N}_k$ vs. $z = \sqrt{|\alpha|} = \frac{k}{\sqrt{2mH_R}}$ for conformal coupling.

The distribution function $\mathcal{N}_k$ is solely a function of $z = k/\sqrt{2mH_R}$, fig. (21) displays N_k vs. $z = |\alpha|^{1/2} = k/\sqrt{2mH_R}$. It is then convenient to define the distribution function

$$\mathcal{N}(z) \equiv \mathcal{N}_k \,, \tag{5.3.70}$$

$\mathcal{N}(z)$ is peaked at low momentum and vanishes fast for $z > 1$, for example $\mathcal{N}(z = 1) \simeq 10^{-3}; \mathcal{N}(z = 10) \simeq 10^{-7}$. As a corollary, the particles are produced non-relativistically at the time of matter-radiation equality, since

$$\frac{k}{m\, a_{eq}} \lesssim \sqrt{\frac{2H_R}{m\, a_{eq}^2}} \simeq \frac{10^{-13}}{\sqrt{m_{ev}}} \,, \tag{5.3.71}$$

hence, even for $m_{ev} \simeq 10^{-22}$ it follows that $k/m\, a_{eq} \lesssim 10^{-2}$. Therefore for $m \gtrsim 10^{-22}\,\text{eV}$ the produced particles are non-relativistic at all times after matter-radiation equality.

Although the distribution function is peaked at low momentum, there is a striking difference between the minimal and conformal coupling cases. In the (MC) case $\mathcal{N}_k \simeq 1/k^3$ whereas for (CC) $\mathcal{N}_k \simeq 1/k$ as $k \to 0$. This difference can be traced to the difference in mode functions during the inflationary stage as displayed by eqn. (5.3.12), because during the (RD) era $a'' = 0$ and the mode equation and mode functions are the same for (MC) and (CC). During the inflationary stage $a'' \neq 0$ and minimally coupled fields with masses $m \ll H_{dS}$ feature an infrared enhancement, which propagates through the matching conditions into the Bogoliubov coefficients.

Note that unlike the (MC) case, in the (CC) case the Bogoliubov coefficients A_k, B_k do *not* depend on the scale of inflation H_{dS}, this is also a consequence of the infrared enhancement of (MC) light fields during inflation, encoded in the factors $1/k\eta$ in the (MC) mode functions.

During the (RD) era both minimally and conformally coupled fields obey the same equations of motion because $a'' = 0$ in (RD), hence the mode functions $f_k(\eta)$ are obviously the same in both cases. The difference in behavior for $\eta > \eta_R$ emerges from the different matching conditions with the mode functions during inflation. This leads us to conclude that most of the difference in particle production between these cases is a consequence of the evolution during the inflationary stage.

5.4 Non-Adiabatic Particle Production

In the expansion of the field in terms of the exact mode functions (5.3.1) the annihilation and creation operators $a_{\vec{k}}, a^{\dagger}_{\vec{k}}$ are time independent. Following [153, 156, 28, 84, 99, 64] we can introduce *time* dependent operators by expanding in the basis of adiabatic "out" particle states. Introduce the zeroth-order adiabatic modes

$$\widetilde{f}_k(\eta) = \frac{e^{-i\int^{\eta}\omega_k(\eta')\,d\eta'}}{\sqrt{2\,\omega_k(\eta)}} \quad ; \quad \omega_k(\eta) = \sqrt{k^2 + m^2\,a^2(\eta)}\,, \tag{5.4.1}$$

and expand the *exact* mode functions $g_k(\eta)$ as

$$g_k(\eta) = \widetilde{A}_k(\eta)\,\widetilde{f}_k(\eta) + \widetilde{B}_k(\eta)\,\widetilde{f}^{*}_k(\eta) \tag{5.4.2}$$

and the $\eta-$ derivative (canonical momentum)[153, 156, 99, 64]

$$g'_k(\eta) = Q_k(\eta)\,\widetilde{A}_k(\eta)\,\widetilde{f}_k(\eta) + Q^{*}_k(\eta)\,\widetilde{B}_k(\eta)\,\widetilde{f}^{*}_k(\eta)\,. \tag{5.4.3}$$

With

$$Q_k(\eta) = -i\omega_k(\eta) + V_k(\eta)\,, \tag{5.4.4}$$

with $V_k(\eta)$ a *real function* it follows that the Wronskian condition (5.3.3) yields

$$|\widetilde{A}_k(\eta)|^2 - |\widetilde{B}_k(\eta)|^2 = 1\,. \tag{5.4.5}$$

Inserting the ansatz (5.4.2,5.4.3) into the mode equations yields the coupled equations of motion for the coefficients $\widetilde{A}_k(\eta), \widetilde{B}_k(\eta)$, obtained in references [99, 64]. The relations (5.4.2,5.4.3) can be inverted to yield the coefficients[99]

$$\widetilde{A}_k(\eta) = i\,\widetilde{f}^{*}_k(\eta)\Big[g'_k(\eta) - Q^{*}_k(\eta)\,g_k(\eta)\Big] \tag{5.4.6}$$

$$\widetilde{B}_k(\eta) = -i\,\widetilde{f}_k(\eta)\Big[g'_k(\eta) - Q_k(\eta)\,g_k(\eta)\Big]\,. \tag{5.4.7}$$

Different choices of the real functions $V_k(\eta)$ yield different dynamics for coefficients $\widetilde{A}_k(\eta)$, $\widetilde{B}_k(\eta)$ [99, 64]. Taking, for example $V_k(\eta) = 0$ corresponds to the lowest (zeroth) adiabatic order, another choice, $V_k(\eta) = \omega'_k(\eta)/2\omega_k(\eta)$ yields a first adiabatic order correction [99, 64]. For both of these values, the continuity of $a(\eta), H(\eta), g_k(\eta), g'_k(\eta)$ across the inflation to (RD)

transition implies the continuity of the coefficients $\widetilde{A}_k(\eta), \widetilde{B}_k(\eta)$. Namely particle production is a continuous process across the transition, and *not* a consequence of the assumption of instantaneous reheating.

The difference in the η- dependence of the coefficients $\widetilde{A}, \widetilde{B}$ for these two choices has been studied in ref.[64]. Introducing the expansion (5.4.2) into (5.3.1) yields

$$a_{\vec{k}}\, g_k(\eta) + a^{\dagger}_{-\vec{k}}\, g^*_k(\eta) = c_{\vec{k}}(\eta)\, \widetilde{f}_k(\eta) + c^{\dagger}_{-\vec{k}}(\eta)\, \widetilde{f}^*_k(\eta)\,, \tag{5.4.8}$$

where

$$c_{\vec{k}}(\eta) = a_{\vec{k}}\, \widetilde{A}_k(\eta) + a^{\dagger}_{-\vec{k}}\, \widetilde{B}^*_k(\eta) \;\; ; \;\; c^{\dagger}_{\vec{k}}(\eta) = a^{\dagger}_{\vec{k}}\, \widetilde{A}^*_k(\eta) + a_{-\vec{k}}\, \widetilde{B}_k(\eta)\,. \tag{5.4.9}$$

Therefore the number of *adiabatic* particles at a given time η is

$$\widetilde{\mathcal{N}}_k(\eta) = \langle 0|c^{\dagger}_{\vec{k}}(\eta)\, c_{\vec{k}}(\eta)|0\rangle = |\widetilde{B}_k(\eta)|^2\,. \tag{5.4.10}$$

We now *choose* to expand in the basis of the zeroth-order adiabatic "out" particle states, by setting $V_k(\eta) = 0$. Note that if $g_k(\eta)$ coincides exactly with the adiabatic mode function $\widetilde{f}_k(\eta)$ then $\widetilde{A}_k(\eta) = 1; \widetilde{B}_k(\eta) = 0$ and there is no particle production.

During the inflationary stage with $a(\eta) = 1/H_{dS}(\eta - 2\eta_R)$ and $\eta < \eta_R$, the mode functions $g_k(\eta)$ are $g^<_k(\eta)$ given by (5.3.12). As $\eta \to -\infty$ ($\eta \ll \eta_R$) these approach the adiabatic mode functions $\widetilde{f}_k(\eta)$, hence it is straightforward to find that

$$\widetilde{A}_k(\eta) \to 1 \;\; ; \;\; \widetilde{B}_k(\eta) \to 0\,, \tag{5.4.11}$$

yielding as $\eta \to -\infty$

$$\widetilde{\mathcal{N}}_k(\eta \to -\infty) = 0\,, \tag{5.4.12}$$

namely the initial vacuum state. For super-horizon wavelengths, $k\eta \ll 1$, the exact mode functions for minimal coupling (MC) in eqn. (5.3.12) differ drastically from the adiabatic ones leading to non-adiabatic particle production when the wavelengths cross the horizon during the inflationary stage.

During the (RD) stage, for $\eta > \eta_R$, the mode functions are $g^>_k(\eta)$ given by (5.3.28) where $f_k(\eta)$ are solutions of Weber's equations with "out" boundary conditions (5.3.21). At early times after the transition $\eta \gtrsim \eta_R$, the Weber functions $f_k(\eta)$ differ drastically from

$\widetilde{f}_k(\eta)$, however, asymptotically at long time $f_k(\eta)$ coincide with $\widetilde{f}_k(\eta)$ because of the "out" boundary conditions (5.3.21). Therefore, for $\eta \gg \eta_R$ at asymptotically long time during (RD), it is also straightforward to show that

$$\widetilde{A}_k(\eta) \to A_k + \mathcal{O}\big(\omega_k'/\omega_k^2\big) \;\; ; \;\; \widetilde{B}_k(\eta) \to B_k + \mathcal{O}\big(\omega_k'/\omega_k^2\big)\,, \tag{5.4.13}$$

hence the interpolating time dependent number of particles yields asymptotically during (RD)

$$\widetilde{\mathcal{N}}_k(\eta \gg \eta_R) = |B_k|^2 = \mathcal{N}_k\,. \tag{5.4.14}$$

This analysis highlights that the "out" particles are produced during the time regimes where the exact mode functions depart from the adiabatic ones. During inflation particle production is substantially enhanced after horizon crossing in the minimally coupled case, and continues non-adiabatically into the (RD) era during the regime of non-adiabatic evolution (5.3.20). As clearly discussed in ref.[64], different choices of the real function $V_k(\eta)$ yield *different* time dependence of the interpolating particle number during the non-adiabatic stages, precisely when particles are produced. Nevertheless, the *asymptotic* number of particles coincide with $\mathcal{N}_k$ for *any* definitions of V_k that involve a higher adiabatic ratio[64]. For example, choosing $V_k(\eta) = \omega_k'(\eta)/2\omega_k^2(\eta)$ as in ref.[99], the asymptotic in and out behavior as $\eta \to -\infty$ and $\eta \gg \eta_R$ remain the same because the adiabatic ratio vanishes in the asymptotic limits. Therefore, whereas the definition of particles and the evolution of the time dependent interpolating particle number depends on the particular choice of basis vectors (adiabatic order) and the real function $V_k(\eta)$, the *aymptotic* (out) particle number $\mathcal{N}_k$ is *independent* of such choice.

During inflation, for a minimally coupled light scalar field the mode functions are *not* adiabatic after the corresponding wavelength becomes superhorizon, namely as $k\eta \ll 1$ as evidenced by the exact mode functions for the (MC) case given by eqn. (5.3.12). As we have stated above, during the (RD) era after inflation, the Weber mode functions are also non-adiabatic after the transition for superhorizon wavelengths. The production of "out" particles occurs primarily during the non-adiabatic evolution and is *continuous* across the transition from inflation to (RD) domination. As discussed above, this is a consequence of the

continuity of scale factor, Hubble rate, mode functions and their conformal time derivative across the transition.

For a conformally coupled (CC) light particle, and with $m/H_{dS} \ll 1$ the mode function in the inflationary era, given by eqn. (5.3.12) (CC), does not differ substantially from $\widetilde{f}_k(\eta)$, hence there is very little production during the inflationary era, unlike the minimally coupled case. Hence we expect, that the (CC) case will yield a much smaller abundance, an expectation that is confirmed by the analysis of the energy momentum tensor below. Furthermore, during (RD) both minimally and conformally coupled fields obey the same equations of motion, while the corresponding mode functions are drastically different during inflation. Therefore, the difference in the evolution for $\eta > \eta_R$ between these cases is imprinted from the inflationary stage through the matching conditions.

While there is a quantitative difference in the dynamics for different choices of $V_k(\eta)$, the above statements remain true for any choice consistent with the adiabatic expansion, as demonstrated in the study of ref.[64]. Furthermore, regardless of the precise definition of an interpolating time dependent particle number, ultimately what is needed to understand the production of dark matter and its cosmological impact is the energy momentum tensor associated with the (ULDM) field.

5.5 The Energy Momentum Tensor: Renormalization and Abundance

The energy momentum tensor for the real scalar field $\phi(x)$ with generic coupling to gravity is given by

$$\begin{aligned} T_{\mu\nu} &= (1-2\xi)\,\phi_{,\mu}\phi_{,\nu} - \frac{1}{2}\,(1-4\xi) g^{\alpha\beta}\,\phi_{,\alpha}\phi_{,\beta}\,g_{\mu\nu} - 2\xi\,\phi\,\phi_{;\mu;\nu} + \frac{1}{2}\,(1-6\xi) m^2\,\phi^2\,g_{\mu\nu} \\ &+ \frac{\xi}{2}\,g_{\mu\nu}\phi\,\Box\phi - \xi\left[R_{\mu\nu} - \frac{1}{2}\,(1-6\xi)\,R g_{\mu\nu}\right]\phi^2\,. \end{aligned} \tag{5.5.1}$$

Writing $\phi(x)$ in terms of the conformally rescaled field $\chi(x)$ as in eqn. (5.2.4) and with the mode expansion (5.3.1) the expectation value of the energy momentum tensor in the

Bunch-Davies vacuum state defined by eqn. (5.3.8) in the spatially flat FRW cosmology is given by[1]

$$\begin{aligned}\langle 0|T^0{}_0|0\rangle = \rho(\eta) &= \frac{1}{4\pi^2\, a^4(\eta)}\int_0^\infty k^2 dk\left\{|g_k^{'}(\eta)|^2+\omega_k^2(\eta)\,|g_k(\eta)|^2\right. \\ &- \left.(1-6\xi)\left[\frac{a'}{a}\left(g_k(\eta)g_k^{'*}(\eta)+g_k^{'}(\eta)g_k^*(\eta)-\frac{a'}{a}|g_k(\eta)|^2\right)\right\}, \quad (5.5.2)\end{aligned}$$

$$\begin{aligned}\langle 0|T^\mu{}_\mu|0\rangle &= \rho(\eta)-3P(\eta)=\frac{1}{2\pi^2\, a^4(\eta)}\int_0^\infty k^2 dk\left\{m^2\, a^2(\eta)\,|g_k(\eta)|^2\right. \\ &- (1-6\xi)\left[|g_k^{'}(\eta)|^2-\omega_k^2(\eta)\,|g_k(\eta)|^2-\frac{a'(\eta)}{a(\eta)}\left(g_k(\eta)g_k^{'*}(\eta)+g_k^{'}(\eta)g_k^*(\eta)\right)\right. \\ &- \left.\left.\left(\frac{a''(\eta)}{a(\eta)}-\left(\frac{a'(\eta)}{a(\eta)}\right)^2\right)|g_k(\eta)|^2+(1-6\xi)\,|g_k(\eta)|^2\,\frac{a''(\eta)}{a(\eta)}\right]\right\}, \quad (5.5.3)\end{aligned}$$

where $\rho(\eta), P(\eta)$ are the energy density and pressure respectively. Using the mode equations (5.3.2) it is straightforward to show the covariant conservation of $\langle 0|T^\mu{}_\nu|0\rangle$. We note that the continuity of the scale factor, the Hubble rate and the mode functions and their conformal time derivatives at the inflation-(RD) transition at η_R guarantees the continuity of the energy density $\langle 0|T^0{}_0|0\rangle$ as is evident from eqn. (5.5.2). Hence particle production is *not* a consequence of the approximation of a sudden transition but rather a consequence of the non-adiabatic evolution, as emphasized previously.

The instantaneous reheating approximation, with the continuity of mode functions, scale factor and Hubble rate across the transition, cannot yield a continuity in a''. The reason for this is physically clear: the expectation value of the energy momentum tensor *of the background* in the homogeneous and isotropic Bunch-Davies vacuum is of the ideal fluid form $\langle 0|T^\mu{}_\nu|0\rangle = \mathrm{diag}(\rho, -P, -P, -P)$ with $\langle 0|T^\mu{}_\mu|0\rangle = \rho - 3P$. The Ricci scalar $R = 6a''/a^3 \propto \langle 0|T^\mu{}_\mu|0\rangle = \rho - 3P$, during the inflationary stage the equation of state is $P = -\rho$ yielding $\langle 0|T^\mu{}_\mu|0\rangle \neq 0$ whereas in an (RD) era $P = \rho/3$ and $\langle 0|T^\mu{}_\mu|0\rangle = 0$ hence a vanishing Ricci scalar[2]. Therefore instantaneous reheating implies a discontinuity in the Ricci scalar, hence a''. For the scalar (DM) particle $\langle 0|T^\mu{}_\mu|0\rangle$ given by (5.5.3) depends explicitly on a'',

[1]We take the infinite volume limit with $\frac{1}{V}\sum_{\vec{k}} \to \int \frac{d^3k}{(2\pi)^3}$.

[2]This neglects the conformal anomaly[47, 10].

therefore, while the energy density is continuous, the pressure features a discontinuity as a consequence of the change in the background equation of state for instantaneous reheating.

During the inflationary stage $\eta < \eta_R$ the mode functions are $g_k^<(\tau)$ given by (5.3.11) corresponding to the "in" Bunch-Davies vacuum state. Therefore during this stage the energy density is simply the *zero point energy density* associated with the Bunch-Davies vacuum.

For $\eta > \eta_R$, the mode functions in (5.5.2,5.5.3) are $g_k(\eta) = g_k^>(\eta) = A_k\, f_k(\eta) + B_k\, f_k^*(\eta)$, with the Bogoliubov coefficients given by eqns. (5.3.30) obeying the relation (5.3.29). We now write $\langle 0|T^\mu_\nu|0\rangle$ in terms of the mode functions $f_k(\eta)$ describing the asymptotic particle states with "out" boundary conditions. Since we are interested in the energy momentum tensor near matter radiation equality we average over rapidly varying phases in the interference terms of the form ff, f^*f^* (and derivatives). We find

$$\begin{aligned}\langle 0|T^0{}_0|0\rangle = \rho(\eta) &= \frac{1}{4\pi^2\, a^4(\eta)} \int_0^\infty k^2 dk \left(1 + 2\,\mathcal{N}_k\right) \Big\{ |f_k^{'}(\eta)|^2 + \omega_k^2(\eta)\, |f_k(\eta)|^2 \\ &- (1-6\xi)\left[\frac{a'}{a}\left(f_k(\eta) f_k^{'*}(\eta) + f_k^{'}(\eta) f_k^*(\eta) - \frac{a'}{a}|f_k(\eta)|^2\right)\right]\Big\}, \quad (5.5.4)\end{aligned}$$

$$\begin{aligned}\langle 0|T^\mu{}_\mu|0\rangle &= \frac{1}{2\pi^2\, a^4(\eta)} \int_0^\infty k^2 dk \left(1 + 2\,\mathcal{N}_k\right) \Big\{ m^2\, a^2(\eta)\, |f_k(\eta)|^2 \\ &- (1-6\xi)\left[|f_k^{'}(\eta)|^2 - \omega_k^2(\eta)\, |f_k(\eta)|^2 - \frac{a'(\eta)}{a(\eta)}\left(f_k(\eta) f_k^{'*}(\eta) + f_k^{'}(\eta) f_k^*(\eta)\right)\right. \\ &- \left.\left(\frac{a''(\eta)}{a(\eta)} - \left(\frac{a'(\eta)}{a(\eta)}\right)^2\right)|f_k(\eta)|^2 + (1-6\xi)\,|f_k(\eta)|^2\,\frac{a''(\eta)}{a(\eta)}\right]\Big\}, \quad (5.5.5)\end{aligned}$$

where $\mathcal{N}_k = |B_k|^2$ and used the relation (5.3.29). The next step consists of expanding $W_k(\eta)$ defining the WKB form of the mode functions (5.3.15) in the adiabatic expansion (5.3.18). We follow the steps in ref.[47, 10, 99] and expand the expectation values of the energy momentum tensor up to fourth order in the adiabatic expansion, with the result

$$\rho(\eta) = \rho^{(0)}(\eta) + \rho^{(2)}(\eta) + \rho^{(4)}(\eta) + \cdots \quad (5.5.6)$$

$$\langle 0|T^\mu{}_\mu|0\rangle = \mathcal{T}^{(0)}(\eta) + \mathcal{T}^{(2)}(\eta) + \mathcal{T}^{(4)}(\eta) + \cdots \quad (5.5.7)$$

where the superscripts refer to the order in the adiabatic expansion. The respective contributions are similar to the results of ref.([47, 10]) but with the extra factor $1 + 2\mathcal{N}_k$ in the integrand.

Of particular interest for this study are the zeroth adiabatic order energy density and pressure, which are given by

$$\rho^{(0)}(\eta) = \frac{1}{4\pi^2\, a^4(\eta)} \int_0^\infty k^2\, [1 + 2\mathcal{N}_k]\, \omega_k(\eta)\, dk\,, \tag{5.5.8}$$

$$\mathcal{T}^{(0)}(\eta) = \frac{1}{4\pi^2\, a^4(\eta)} \int_0^\infty k^2\, [1 + 2\mathcal{N}_k]\, \frac{m^2\, a^2(\eta)}{\omega_k(\eta)}\, dk\,, \tag{5.5.9}$$

yielding

$$P^{(0)}(\eta) = \frac{1}{3}\left[\rho^{(0)}(\eta) - \mathcal{T}^{(0)}(\eta)\right] = \frac{1}{12\pi^2\, a^4(\eta)} \int_0^\infty [1 + 2\mathcal{N}_k]\, \frac{k^4}{\omega_k(\eta)}\, dk\,. \tag{5.5.10}$$

The energy momentum tensor features ultraviolet divergences that must be regularized and renormalized. This is explicit at zeroth adiabatic order given by eqns. (5.5.8,5.5.9), the higher order adiabatic corrections can be found in ref.[47, 10] by multiplying the integrand in momentum by the factor $1 + 2\mathcal{N}_k$. Appendix (C.2) shows some second order adiabatic contributions that yield ultraviolet divergences in $\langle T^\mu_\nu \rangle$ for $\mathcal{N}_k = 0$. These adiabatic terms feature inverse powers of ω_k as befits the adiabatic expansion, in particular $1/\omega_k; 1/\omega_k^3$ which yield quadratic and logarithmic ultraviolet divergences.

For the minimally coupled case $\mathcal{N}_k \propto k^{-4}$ at large momenta (see eqn. (5.3.63)) . Therefore the terms with $\mathcal{N}_k$ for the higher adiabatic orders do not contribute to the ultraviolet divergences. Consider for example the second adiabatic corrections $\rho^{(2)}$, explicitly given in appendix (C.2), as compared to the zeroth order contribution during the radiation dominated area near matter radiation equality (5.5.8) it is suppressed by a factor

$$\propto \left(\frac{a'}{ma}\right)^2 \simeq \left(\frac{H_R}{m\, a_{eq}}\right)^2 \simeq \left(\frac{10^{-31}}{m_{ev}}\right)^2, \tag{5.5.11}$$

with much larger suppression factors for the terms of higher adiabatic order. The same argument holds for $\mathcal{T}^{(2)}$, for which several contributions are explicitly given in appendix (C.2).

Renormalization:

The ultraviolet divergences in the energy momentum tensor must be regularized and renormalized. For $\mathcal{N}_k = 0$ such a program is well established and has been thoroughly studied and implemented in refs.[28, 157, 89, 108, 47, 10, 99, 27]. As discussed in detail in these references, the ultraviolet divergences are absorbed into renormalizations of the cosmological constant, Newton's constant G and into the geometric tensors $H^{(1,2)}_{\mu\nu}$ which result from the variational derivative of a gravitational action that includes higher curvature terms $\propto R^2, R^{\mu\nu}R_{\mu\nu}$. These higher curvature terms are added in the action multiplied by counterterms, which are then required to cancel the coefficients of the geometric tensors in such a way that the renormalized action is the Einstein-Hilbert action.

Since our focus is to study the contribution from particle production, namely $\mathcal{N}_k \neq 0$ we absorb the *full* energy momentum tensor for $\mathcal{N}_k = 0$ into these renormalizations, this is tantamount to subtracting the *zero point or vacuum energy density* during the inflation and radiation eras. After this subtraction and renormalization, only the terms proportional to $\mathcal{N}_k$ in (5.5.8) and (5.5.7) are considered.

Since, as shown explicitly in eqn. (5.3.63) $\mathcal{N}_k \propto 1/k^4$ as $k \to \infty$ for the minimally coupled case, the corrections of second adiabatic order and higher *do not feature* ultraviolet divergences, and are suppressed by factors of order $10^{-62}/m^2_{ev}$ near matter-radiation equality. Hence, we keep solely the contribution of zeroth adiabatic order from particle production. After renormalization and to leading adiabatic order we find the contributions to the energy density and pressure from particle production to be given by

$$\rho^{(pp)}(\eta) = \frac{1}{2\pi^2\, a^4(\eta)} \int_0^\infty k^2\, \mathcal{N}_k\, \omega_k(\eta)\, dk\,, \tag{5.5.12}$$

$$P^{(pp)}(\eta) = \frac{1}{2\pi^2\, a^4(\eta)} \int_0^\infty \frac{1}{3}\, k\, v_k(\eta)\, \mathcal{N}_k\, k^2 dk \quad ; \quad v_k(\eta) = \frac{k}{\omega_k(\eta)}\,. \tag{5.5.13}$$

This result is noteworthy: the density and pressure are *exactly* the diagonal components of a *kinetic* energy momentum tensor describing a (perfect) fluid. Note that the integrals are over comoving momentum, in terms of the physical (local) energy $E_k(\eta) = \sqrt{k^2_{ph}(\eta) + m^2}$ and physical momenta $k_{ph}(\eta) = k/a(\eta)$ these expressions can be written as

$$\rho^{(pp)}(\eta) = \frac{1}{2\pi^2}\int_0^\infty \mathcal{F}\big[a(\eta)\,k_{ph}\big]\,E_k(\eta)\,k_{ph}^2\,dk_{ph}\,, \tag{5.5.14}$$

$$P^{(pp)}(\eta) = \frac{1}{2\pi^2}\int_0^\infty \frac{1}{3}\,k_{ph}\,\frac{k_{ph}}{E_k(\eta)}\,\mathcal{F}\big[a(\eta)\,k_{ph}\big]\,k_{ph}^2 dk_{ph}\,, \tag{5.5.15}$$

where

$$\mathcal{F}\big[a(\eta)\,k_{ph}\big] \equiv \mathcal{N}_k\,, \tag{5.5.16}$$

is a *frozen*, i.e. a time independent distribution function of produced particles. It is straightforward to show covariant conservation, namely

$$\dot{\rho}^{(pp)}(t) + 3\,\frac{\dot{a}(t)}{a(t)}\,\Big(\rho^{(pp)}(t) + P^{(pp)}(t)\Big) = 0\,. \tag{5.5.17}$$

We highlight this result: *the usual fluid-kinetic energy momentum tensor emerges as the leading order (zeroth order) in the adiabatic expansion after subtracting the "vacuum" contribution which is absorbed in the renormalization of the cosmological and Newton's constant, and cancel counterterms that multiply higher curvature terms in the action.* The full expectation value of the energy momentum tensor during the non-adiabatic stage *cannot* be written in the kinetic form in terms of the distribution function; such simplification is *only* available during adiabatic evolution.

As discussed above, in the minimally coupled case the distribution function $\mathcal{N}_k \propto 1/k^4$ in the large k limit, therefore both, the energy density (5.5.12) and pressure (5.5.13) at zeroth adiabatic order feature *a priori* ultraviolet logarithmic divergences. However, these divergences are actually beyond the realm of validity of *two* of our main approximations, **i:)** superhorizon wavelengths at the end of inflation, namely $k\eta_R \ll 1$. As discussed in section (5.3), taking the upper bound on the scale of inflation this condition implies that $k \ll \mu$eV, this is hardly an ultraviolet large cutoff in momentum. Therefore, in principle and for consistency, the momentum integrals must be cutoff at this scale, thus the "divergences" associated with particle production are not physical. **ii:)** as discussed in detail in section (5.7) the assumption of instantaneous reheating will definitely not be warranted for sub-horizon wavelengths, and the distribution function for these (large) wavevectors (with $k \gg \mu$eV) *may* differ drastically from that of the wavevectors that are super-Hubble at the end of inflation.

Hence, consistency with our main assumptions imply that the contributions from particle production to the energy momentum tensor must be cut-off at a comoving momentum scale $\simeq \sqrt{H_R\, H_{dS}} \simeq \mu$eV for $H_{dS} \simeq 10^{13}\,$GeV, which corresponds to wavelengths longer than a meter.

Therefore, we regularize the integrals featuring $\mathcal{N}_k$ by introducing a comoving upper momentum cutoff $k_{max} \lesssim 1/\eta_R = \sqrt{H_R\, H_{dS}}$. Because the distribution function $\mathcal{N}_k$ is enhanced at low momentum we also include a *lower momentum cutoff* $k_{min} \simeq H_0$ corresponding to horizon-sized wavelengths *today*. Hence the energy density and pressure from particle production are given by

$$\rho^{(pp)}(\eta) = \frac{1}{2\pi^2\, a^4(\eta)} \int_{k_{min}}^{k_{max}} \mathcal{N}_k\, \omega_k(\eta)\, k^2\, dk\,, \,, \tag{5.5.18}$$

$$P^{(pp)}(\eta) = \frac{1}{6\pi^2\, a^4(\eta)} \int_{k_{min}}^{k_{max}} \mathcal{N}_k \frac{k^2}{\omega_k(\eta)}\; k^2 dk\,. \tag{5.5.19}$$

The abundance $\Omega(a)$ and the equation of state $w(a)$ are, respectively,

$$\Omega(a) = \frac{\rho^{(pp)}(\eta)}{\rho_c} \quad ; \quad \rho_c = \frac{3\, H_0^2}{8\pi\, G} \simeq 0.4\, \times 10^{-10}\, (\text{eV})^4\,, \tag{5.5.20}$$

$$w(a) = \frac{P^{(pp)}(\eta)}{\rho^{(pp)}(\eta)}\,. \tag{5.5.21}$$

5.5.1 Minimal Coupling

For the minimal coupling case $\mathcal{N}_k$ is given by eqn. (5.3.61) in terms of the variable z defined by eqn. (5.3.54), in this case we find the abundance (5.5.20)

$$\Omega(a) = \frac{m}{\rho_c\, a^3(\eta)} \left(\frac{H_{dS}}{m}\right)^2 \Big(m\, H_R\Big)^{3/2} \frac{1}{16\,\pi^2} \int_{z_m}^{z_M} D(z) \left[\frac{z^2}{a^2(\eta)} \Big(\frac{2H_R}{m}\Big) + 1\right]^{1/2} \frac{dz}{z}\,. \tag{5.5.22}$$

The minimum z_m provides an infrared cutoff, with $k_{min} \simeq H_0$, it follows that $z_m = \frac{H_0}{\sqrt{2mH_R}}$. Values of comoving momentum $k \gg m$ inside the integral of the distribution function yield contributions that redshift as $1/a^4(\eta)$ hence contributing to the radiation component. The

matter contribution for $a(\eta) \gtrsim a_{eq}$ is extracted from contributions to the integrals from comoving momenta $k \lesssim m\, a_{eq}$, hence we introduce an upper cutoff $z_M \leq m a_{eq}/\sqrt{2mH_R}$. Therefore for $a(\eta) > a_{eq}$ we find the contribution to the (DM) abundance

$$\Omega(a) \simeq 0.5\, \frac{\sqrt{m_{ev}}}{a^3(\eta)}\, \Big[\frac{H_{dS}}{10^{13}\,\mathrm{GeV}}\Big]^2\, \int_{z_m}^{z_M} \frac{D(z)}{z}\; dz \equiv \frac{\Omega_{pp}}{a^3(\eta)}\,. \tag{5.5.23}$$

Taking as the maximum comoving wavevector $k \simeq m\, a_{eq}$ and the minimum $k \simeq H_0$ it follows that $z_M \simeq \sqrt{m_{ev}} \times 10^{13} \gg 1$ and $z_m \simeq H_0/\sqrt{2\, m\, H_R} \simeq 10^{-16}/\sqrt{m_{ev}} \ll 1$, hence $D(z_M) \simeq 10^{-13}/\sqrt{m_{ev}} \ll 1$ and $D(z_m) \simeq \sqrt{2}\,\frac{\Gamma(\frac{1}{4})}{\Gamma(\frac{3}{4})}$. Upon integration by parts the integral in (5.5.23) is given by

$$\int_{z_m}^{z_M} \frac{D(z)}{z}\; dz \simeq -\sqrt{2}\,\frac{\Gamma(\frac{1}{4})}{\Gamma(\frac{3}{4})}\, \ln\Big[\frac{H_0}{\sqrt{2\, m\, H_R}}\Big] - \underbrace{\int_0^{\infty} \ln(z) \frac{d\, D(z)}{dz}\; dz}_{\simeq 0.6}\,, \tag{5.5.24}$$

where in the second term (integral) we have taken $z_m \to 0; z_M \to \infty$ because the integrand vanishes fast at both limits, and the remaining integral is carried out numerically. Therefore to leading order we find

$$\Omega(a) = \frac{\Omega_{pp}}{a^3(\eta)} \;\; ; \;\; \Omega_{pp} = 2.09\, \sqrt{m_{ev}}\, \Big[\frac{H_{dS}}{10^{13}\,\mathrm{GeV}}\Big]^2\, \ln\Big[\frac{\sqrt{2\, m\, H_R}}{H_0}\Big]\,. \tag{5.5.25}$$

For a given value of m_{ev} this equation yields the contribution to the dark matter abundance as a function of m_{ev} and the *only* uncertain cosmological parameter H_{dS}. Requiring that the abundance $\Omega_{pp} = \Omega_{DM} = 0.25$ gives the dependence of the mass that yields the correct abundance on H_{dS}, namely

$$\sqrt{m_{ev}}\, \Big[\ln\big[\sqrt{m_{ev}}\big] + 36\Big] = 0.12 \left[\frac{10^{13}\mathrm{GeV}}{H_{dS}}\right]^2\,. \tag{5.5.26}$$

For $H_{dS} \simeq 10^{13}\,\mathrm{GeV}$ we find that the correct (DM) abundance yields the value

$$m \simeq 1.5 \times 10^{-5}\,\mathrm{eV}\,. \tag{5.5.27}$$

The super-horizon approximation $k\,\eta_R \ll 1$ entails a maximum value of the mass for which the approximations involved are consistent. We have set the maximum value of the momentum integral as $k_M \simeq m\, a_{eq}$ so as to capture all the values of momenta that contribute to the (non-relativistic) matter contribution. For this upper limit to be consistent with the

superhorizon approximation it follows that the mass of the (ULDM) particle is constrained by the upper limit

$$m\, a_{eq}\, \eta_R \lesssim 1 \Rightarrow m \lesssim 0.02 \left[\frac{H_{dS}}{10^{13}\text{GeV}}\right]^{1/2} \text{eV}\,. \tag{5.5.28}$$

Fig. (22) displays $\ln\left[\frac{\Omega_{pp}}{\Omega DM}\right]$ with $\Omega_{DM} = 0.25$ vs. $\ln[m_{ev}]$ for $H_{dS} = 10^{13}\,\text{GeV}$.

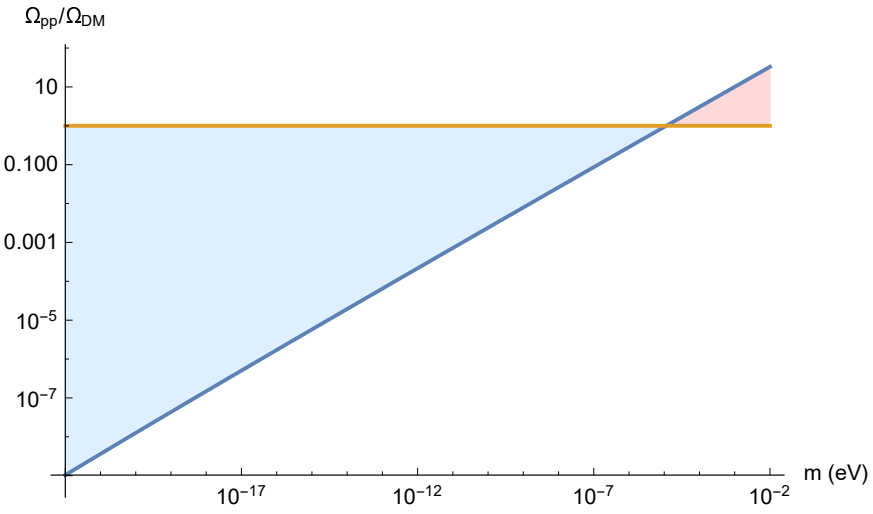

Figure 22: $\ln\left[\frac{\Omega_{pp}}{\Omega_{DM}}\right]$ vs. $\ln[m_{ev}]$ for $H_{dS} = 10^{13}\,\text{GeV}$. The blue-shaded region corresponds to under abundance and the red-shaded to overabundance (colors online).

The pressure and equation of state are given by eqns. (5.5.19,5.5.21) respectively. For the non-relativistic component describing a matter dominated "fluid" we take $\omega_k(\eta) = m\, a(\eta)$ in the integrands. The remaining integrals are similarly obtained with the above cutoffs. The equation of state parameter is given by

$$w(a) = \frac{2}{3}\frac{H_R}{m\, a^2(\eta)}\,\frac{\int_{z_m}^{z_M} D(z)\, z\, dz}{\int_{z_m}^{z_M} \frac{D(z)}{z}\, dz}\,, \tag{5.5.29}$$

taking $z_M = ma_{eq}/\sqrt{2mH_R}$ and $z_m \simeq H_0/\sqrt{2mH_R}$ we find

$$w(a) \simeq \frac{2\,\Gamma(3/4)}{3\,\Gamma(1/4)}\,\frac{\left(\frac{H_R}{2ma_{eq}^2}\right)^{1/2}}{\ln\left[\frac{\sqrt{2mH_R}}{H_0}\right]}\left(\frac{a_{eq}}{a(\eta)}\right)^2. \tag{5.5.30}$$

Taking the value of the mass as given by (5.5.27) with $H_{dS} \simeq 10^{13}\,\mathrm{GeV}$ we find

$$w(a_{eq}) \simeq 2.5 \times 10^{-14}\,. \tag{5.5.31}$$

For a non-relativistic species we find

$$\langle V^2(\eta)\rangle = \frac{\int \mathcal{N}_k \,\frac{k^2}{m^2 a^2(\eta)}\, k^2 dk}{\int \mathcal{N}_k\, k^2 dk} \equiv 3\frac{P(\eta)}{\rho(\eta)} = 3\, w(a)\,. \tag{5.5.32}$$

Therefore, indeed this is a very cold dark matter candidate despite being so light. The main reason is that the distribution function strongly peaks at small values of momentum. The redshift behavior of $w(a)$ is that expected for a non-relativistic component.

Free streaming length:

The comoving free streaming wave-vector is defined in analogy with the Jeans wavevector in the fluid description of perturbations, namely[39]

$$k^2_{fs}(\eta) = \frac{4\pi\, G\, \rho_m(\eta)}{\langle V^2(\eta)\rangle}\, a^2(\eta) = \frac{3}{2}\,\frac{H_0^2\,\Omega_m}{\langle V^2_{eq}\rangle\, a^2_{eq}}\, a(\eta)\,, \tag{5.5.33}$$

where $\langle V^2(\eta)\rangle$ is given by eqn. (5.5.32), which we have written as

$$\langle V^2(\eta)\rangle = \langle V^2_{eq}\rangle \left(\frac{a_{eq}}{a(\eta)}\right)^2. \tag{5.5.34}$$

As shown in ref.[39] the cutoff scale in the power spectrum is the comoving free streaming length

$$\lambda_{fs} \equiv \frac{2\pi}{k_{fs}(a_{eq})} = 2\pi\left[\frac{2\,\langle V^2_{eq}\rangle\, a_{eq}}{3\,\Omega_M}\right]^{1/2} d_H\,, \tag{5.5.35}$$

where $d_H = 1/H_0 = 3\,\mathrm{Gpc}/h$ is the Hubble distance. This definition differs from the usual definition of the comoving free streaming distance l_{fs} during matter domination by factors of $\mathcal{O}(1)$:

$$l_{fs} = \int_{\eta_{eq}}^{\eta_0} \sqrt{\langle V^2(\eta)\rangle}\, d\eta = \sqrt{\langle V^2_{eq}\rangle}\; a_{eq} \int_{\eta_{eq}}^{\eta_0} \frac{d\eta}{a(\eta)}\,. \tag{5.5.36}$$

During the matter dominated era it follows that

$$d\eta = \frac{1}{H_0\,\sqrt{\Omega_M}}\,\frac{da}{a^{1/2}}\,, \tag{5.5.37}$$

hence the free streaming distance from matter-radiation equality until $a_0 \simeq \mathcal{O}(1)$ is given by

$$l_{fs} = 2\left[\frac{\langle V_{eq}^2\rangle\, a_{eq}}{\Omega_M}\right]^{1/2} d_H\,. \tag{5.5.38}$$

Using the results (5.5.31,5.5.32)) corresponding to $H_{dS} \simeq 10^{13}\,\mathrm{GeV}$, we find

$$\lambda_{fs} \simeq l_{fs} \simeq 70\,\mathrm{pc}\,. \tag{5.5.39}$$

This is the cutoff scale in the matter power spectrum; thus we see that even for a very light (DM) candidate with $m \simeq 10^{-5}\,\mathrm{eV}$ the cosmological production yields a very *cold* species with a rather small free streaming length comparable to that of heavy weakly interacting massive particles.

5.5.2 Conformal Coupling

For the case of conformal coupling, the distribution function $\mathcal{N}_k$ that enters in the abundance and equation of state (5.5.18-5.5.21) is given by (5.3.68). The integral for the density, eqn. (5.5.18), cannot be obtained in closed form. However, $\mathcal{N}_k$ is solely a function of $z = k/\sqrt{2mH_R}$ and localized in the region $0 \leq z \leq 1$ as discussed in section (5.3.3) and displayed in fig. (21). Furthermore for $a(\eta) \simeq a_{eq}$ this region of comoving momenta correspond to non-relativistic particles and we can safely replace $\omega_k(\eta) \simeq m\, a(\eta)$ inside the integrand in (5.5.18), yielding (near matter radiation equality)

$$\rho^{(pp)}(\eta) = \frac{m}{a^3(\eta)}\int \mathcal{N}_k\, k^2\, \frac{dk}{2\pi^2}\,, \tag{5.5.40}$$

therefore the low momentum peak of the distribution function entails that the density redshifts as non-relativistic matter.

Changing variables to z and writing $\mathcal{N}_k \equiv \mathcal{N}(z)$, we find

$$\rho^{(pp)}(\eta) = \frac{1}{2\pi^2}\frac{m^4}{a^3(\eta)}\left[\frac{2\,H_R}{m}\right]^{3/2}\int_0^{z_M} \mathcal{N}(z)\, z^2\, dz\,, \tag{5.5.41}$$

where $z_M \lesssim m\, a_{eq}/\sqrt{2mH_R}$ and the lower limit can be taken to zero because the integrand does not feature an infrared divergence.

The remaining integral is rapidly convergent and is carried out numerically with an upper limit $z \simeq 20$ (with $\mathcal{N}(20) \simeq 10^{-20}$), for which the integral yields the value $\simeq 0.01$. Hence we find the abundance

$$\Omega(a) \simeq 1.3 \times \frac{1}{a^3(\eta)} \left[\frac{m}{(\mathrm{eV})}\right]^4 \left[\frac{2H_R}{m}\right]^{3/2} \times 10^7 \simeq \frac{(m_{ev})^{5/2}}{a^3(\eta)} \times 10^{-46}\,. \tag{5.5.42}$$

Thus, even for $m \simeq (\mathrm{eV})$ the dark matter abundance for conformally coupled particles is negligible. This is in qualitative agreement with our expectations of very small abundance in this case, but implementing the framework described in the previous section allowed us to obtain a quantitative understanding of the abundance in this case.

The main differences with the minimally coupled case can be traced back to the factors $\delta = k\eta_R$ in eqns. (5.3.50,5.3.50). These are a result of the behavior $\propto 1/(k\eta_R)$ of the (MC) mode functions during the inflationary stage (see eqn. (5.3.12), a hallmark of the infrared enhancement of correlations of nearly massless particles minimally coupled to gravity in de Sitter space time. These factors result in the infrared enhancement $\mathcal{N}_k \propto 1/k^3$ and the factor H_{dS}^2 for the (MC) case vs. $\mathcal{N}_k \propto 1/k$ for the (CC) case.

5.6 On Entropy Perturbations

Adiabatic and entropy perturbations from inflation have been thoroughly studied in refs.[92, 48, 20], and we refer the readers to these for details. In ref.[92, 48] the case of two fields is studied in detail; this is the case that is most relevant for our discussion: one of the fields is the inflaton, the other is the (ULDM) field with action given by (5.2.1). While the inflaton field develops an expectation value that drives the inflationary stage, the (ULDM) *does not* acquire an expectation value, and is taken to be in its Bunch-Davies vacuum state. In ref.[92] "adiabatic" and "entropy" fields are obtained from the *fluctuations* of the two fields around their expectation value, by introducing a "mixing" angle that depends explicitly on the time derivative of the *expectation values* of both fields. The "adiabatic" field represents a fluctuation along the background trajectory, while the "entropy" field is the orthogonal combination in terms of the "mixing" angle. We identify the (ULDM) field with the second

(χ)-field in ref.[92]. Since in our case this field *does not* acquire an expectation value, it follows that the "mixing" angle vanishes identically. In this case, the inflaton fluctuations are the "adiabatic" field and the (ULDM) field is identified with the "entropy" field. Therefore, considering perturbations *linear in the fluctuations*, the vanishing of the mixing angle implies that the entropy perturbation *does not* source the long-wavelength evolution of the comoving curvature perturbation, nor is there any cross correlation between the adiabatic and entropy perturbations (see for example eqns.(47,48,52,55) and comment below eqn. (50) in ref.[92]).

Ref.[56] focused on superheavy dark matter, and following on previous study in ref.[140] recognized that in the case in which the dark matter field does *not* acquire an expectation value the treatment of isocurvature perturbations must be modified substantially. The authors of ref.[56] also recognized that when the superheavy dark matter field does not acquire an expectation value (background) there is no mixing between the fluctuations of this and the inflaton field to linear order[3].

The treatment advocated in ref.[56] *defines* the energy density perturbation of the dark matter field as

$$\delta\rho^{(dm)}(\vec{x}) = \frac{:T_{00}^{(dm)}(\vec{x}): - \langle :T_{00}^{(dm)}(\vec{x}): \rangle}{\rho^{(dm)}} \tag{5.6.1}$$

$$\rho^{(dm)} = \langle :T_{00}^{(dm)}(\vec{x}): \rangle \,, \tag{5.6.2}$$

where normal ordering is referred to the Bogoliubov rotated vacuum state (see ref.[56] for details), and identifies the power spectrum of entropy perturbations from the spatial Fourier transform of the connected correlation function, namely

$$\int \frac{d^3r}{(2\pi)^3}\, e^{i\vec{k}\cdot\vec{r}}\, \langle \delta\rho^{(dm)}(\vec{x})\; \delta\rho^{(dm)}(\vec{x}+\vec{r}) \rangle \propto \mathcal{P}^{(dm)}(k)\,. \tag{5.6.3}$$

In free field theory the connected correlator in eqn. (5.6.3) is a one loop diagram.

In ref.[56] the expectation value $\rho^{(dm)}$ depends explicitly on the Bogoliubov coefficient β associated with particle production during inflation, and *vanishes identically* when this coefficient vanishes, which is the case in our study.

The above definitions *do not* apply to our case since during the inflationary stage the quantum state in our treatment is the Bunch-Davies vacuum state and consequently, the

[3]See the discussion prior to eqn. (87) in ref.[56].

energy momentum tensor during this stage describes the *zero point* energy density of this vacuum state. There is no Bogoliubov coefficient β and as per the result eqn. (90) in ref.[56] the energy density $\rho^{(dm)}$ given by (5.6.2) *vanishes identically*. Furthermore, as discussed in section (5.5) we have renormalized the energy momentum tensor by subtracting the full contribution from the *zero point energy density* during inflation and the radiation eras. Therefore the definition (5.6.1) cannot be applicable to our study.

There is another important caveat in the interpretation of entropy perturbations advocated in ref.[56]: as we discussed in detail in section (5.5) the expectation value of the energy momentum tensor features quartic, quadratic and logarithmic divergences and requires subtractions up to fourth adiabatic order to be renormalized. These aspects had already been addressed in references[47, 153, 156, 10, 108]. The various divergences are absorbed into renormalizations of the cosmological and Newton constants, but also in higher curvature counterterms in the bare action (corresponding to the tensors $H^{(1.2)}_{\mu\nu}$ [47]).

Different regularizations (subtractions) yield different finite contributions to the energy density, therefore the finite contribution to the expectation value yielding $\rho^{(dm)}$ is not uniquely defined and depends on the subtraction scheme. As discussed in section (5.5) we substract the *full zero point energy* all throughout the evolution. In fact this procedure subtracts completely the zero point contribution during inflation and radiation eras, hence in our case $\rho^{(dm)}$ *vanishes identically* during inflation after renormalization. This is the usual procedure in semiclassical gravity, for example during inflation only the background (expectation value) contribution is considered and in radiation domination only the finite temperature (kinetic) contributions to the energy momentum tensor are considered. Furthermore, there are several other caveats associated with the definition of the power spectrum (5.6.3) proposed in ref.[56] (see eqn. (96) in ref.[56]): **i:)** it is straightforward to show that the kinetic term contribution to the energy momentum tensor yields an ultraviolet divergence with the *fifth power* of an ultraviolet cutoff to $\mathcal{P}^{(dm)}(k)$. In ref.[56] this divergence in the kinetic contribution is not manifest because this contribution is evaluated near the end of inflation when the mode functions are dominated by the superhorizon contributions and the integrals have been cutoff in the ultraviolet, with an upper momentum $a_e H_e$. But the leading ultraviolet divergences are similar to those in Minkowski space time and dominate the earlier

dynamics. **ii:)** even for the mass term contribution of the energy momentum tensor, the one-loop connected diagram that yields $\mathcal{P}^{(dm)}(k)$ still features a linear ultraviolet divergence, which was neglected in ref.[56] because it is multiplied by a function of time that becomes vanishingly small near the end of inflation. **iii:)** unlike the renormalization of the energy momentum tensor whose subtractions are absorbed systematically into the parameters of the total action (including higher curvature terms), there is no natural manner to absorb the divergences in the power spectrum (5.6.3). In ref.[56] all the divergent integrals are cutoff at wavevectors $\simeq a_e\, H_e$, namely those that cross the horizon at the end of inflation. However, a complete treatment should include a proper renormalization of the divergences and the zero point energy. In our study, the fact that during inflation the *full* energy density is the zero point corresponding to the Bunch-Davies vacuum makes the framework to describe non-linear entropy perturbations advocated in ref.[56] not applicable to our case. Some of these caveats have been recognized in ref.[56][4].

Entropy perturbations post-inflation:

The discussion above has focused on the generation of entropy perturbations *during inflation* and the applicability of the framework introduced in ref.[56]. However, the important aspect is the impact of entropy (isocurvature) perturbations upon the (CMB). In the usual approach to cosmological perturbations, adiabatic and isocurvature perturbations during inflation provide the initial conditions of the respective perturbations upon horizon re-entry during the radiation (or matter) dominated era. As discussed in detail in refs.[20, 48], the initial conditions of isorcurvature perturbations are determined by the set of transfer functions discussed in ref.[48]. These, in turn, are proportional to the "mixing" (or correlation) angle associated with the expectation value of the entropy field (see for example eqns. (44, 45) in [20]), which in our case *vanishes identically*. Furthermore, the framework introduced in ref.[56] does not apply to our case as discussed above. Therefore, for the case that we study, the initial conditions for isocurvature perturbations during the radiation dominated era *cannot* be determined in the inflationary stage. As discussed above, the energy momentum tensor during inflation describes the vacuum zero point energy and is completely subtracted out by renormalization. In the post-inflationary stage it features three contributions: the

[4]See for example the comments after eqn. (86) in ref.[56].

vacuum contribution is subtracted out in the renormalization procedure, the interference term is rapidly oscillating in the adiabatic regime and therefore its expectation value averages out on short time scales, and the contribution from particle production, which in the adiabatic regime features the kinetic fluid form. It is this latter term that is the relevant one (after renormalization) to understand dark matter perturbations, the distribution function is completely determined by the Bogoliubov coefficient $|B_k|^2$. The influence of isocurvature perturbations on the (CMB) is a result of solving the system of Einstein-Boltzmann equations for *linear* cosmological perturbations, in which $|B_k|^2$ is the distribution function of the *unperturbed* (DM) component, and ρ_{pp} (5.5.18) describes the *background density*. This set of Einstein- Boltzmann equations must be appended with initial conditions, which are determined from the respective super-horizon perturbations at the end of inflation. From the above discussion, it is clear that in the case that we study, the proper initial conditions for isocurvature perturbations remain to be understood at a deeper level.

The corollary of this discussion is that a proper definition of the power spectrum of entropy perturbations in the case when the fields do *not* acquire expectation values remains to be understood at a deeper level. The caveats associated with the renormalization of the energy momentum tensor along with its correlations remain to be clarified in a consistent and unambiguous manner. These include a proper account of the fact that there is no natural manner to renormalize the divergences in a power spectrum obtained from the connected correlation function of the energy momentum tensor. These remain even when the zero point contribution to the energy density is completely subtracted. The contribution of zero point energy correlations to non-linear perturbations merits deeper scrutiny, *since even the fluctuations of the inflaton yield zero point contributions to the energy density and all other fields that are either produced or excited post-inflation presumably also contribute to the zero point energy density during inflation.* A satisfactory resolution of these important issues, necessary to quantify reliably the impact of *non-linear* entropy perturbations is still lacking, and is clearly well beyond the scope of this study.

5.7 Discussion and Caveats

On reheating:

Reheating dynamics, namely the non-equilibrium processes that lead to a (RD) dominated era after the inflationary stage are still being vigorously studied. Most studies of reheating necessarily input particular forms for the inflaton potential and model the couplings of (standard model) particles to the inflaton and/or other degrees of freedom thereby yielding model dependent descriptions with widely different time scales depending on unknown couplings and masses[9].

One of our main assumptions is that the transition from the inflationary stage to the (RD) dominated stage is instantaneous. The main physical reason behind this approximation is that we focus on wavelengths that are superhorizon at the end of inflation. The dynamics of the mode functions for these wave-vectors is on long time scales, hence insensitive to the reheating dynamics occurring on much shorter time scales. Furthermore, in principle, wavelengths larger than the particle horizon are causally disconnected from the causal microphysical processes of thermalization. While this assumption *seems* physically reasonable, it must be tested quantitatively. However, this requires studying a particular model of reheating dynamics. While conclusions of a particular model will not be universally valid, perhaps a simple model that dynamically and *continuously* interpolates (with continuous scale factor and Hubble rate) between a near de Sitter inflationary stage and a post-inflation (RD) stage would illuminate the validity of the instantaneous approximation. Most likely such study would require a substantial numerical effort to solve the mode equations during the transition and matching to the solutions in the subsequent (RD) era. Clearly such study is beyond the scope of this article but merits further attention.

Inflationary particle production:

During the (RD) era the equations of motion are the same for (MC) and (CC) fields because $a''(\eta) = 0$. However, during inflation the equations of motion for the two cases are very different, yielding the drastically different solutions given by eqn. (5.3.12). Whereas the mode functions for the (CC) case are "close" to the adiabatic mode functions, those of the (MC) depart substantially when the wavelength becomes superhorizon $k\eta \ll 1$. This

difference is imprinted on the evolution of the mode functions for $\eta > \eta_R$ through the matching conditions (continuity of function and derivative at η_R). The results from the (CC) case confirm negligible particle production in this case, this leads us to conclude that the largest contribution to particle production in the (MC) case occurs during the inflationary stage. This conclusion is bolstered by the analysis of section (5.4), where it is shown that the (MC) mode functions depart substantially from the adiabatic ones for superhorizon modes thus resulting in substantial particle production, whereas those for the (CC) case are similar to the adiabatic ones with little particle production.

Bose Einstein condensate vs. distribution function:

We have shown that for minimally coupled ultra-light particles the *distribution function* peaks at *very low* comoving momentum with $\mathcal{N}_k \propto 1/k^3$. As discussed in the previous section the distribution function of the produced particles "inherits" the infrared enhancement of the mode functions of minimally coupled ultra-light particles during the inflationary era (taken to be a de Sitter space-time). This enhancement, however, does *not* imply Bose Einstein condensation, particle number of the real scalar field is not conserved, and the field does not acquire a vacuum expectation value. Namely, there is no off-diagonal long range order and no expectation value that would break a $U(1)$ symmetry both of which are typically associated with Bose-Einstein condensation. The description of this (ULDM) is in terms of the contributions to the energy momentum tensor. This is very different from the phenomenological Schroedinger-Poisson equation advocated for "fuzzy" dark matter[109, 110, 111] which relies on a "many-body" Schroedinger-like wave function for a classical order parameter field akin to the Gross-Pitaevskii equation (non-linear Schroedinger equation) for a superfluid. In many body physics such equation is typically obtained from a variational derivative of the expectation value of a many-body Hamiltonian in a coherent state[130].

Self-consistency and backreaction:

We have taken the cosmological expansion as a (RD) background, neglecting the contribution of the (ULDM) to the radiation component. Such contribution is obtained from the momentum region with $k \gg m\, a_{eq}$ in the integrals for the density and pressure. In principle this contribution modifies the ulrarelativistic content of the plasma contributing a term that redshifts like radiation $\propto 1/a^4(\eta)$ and, in principle, should be treated self-consistently.

However, we consider that the (RD) era is dominated by the $\simeq 100$ ultrarelativistic degrees of freedom of the standard model (and possibly beyond), therefore the contribution of one extra degree of freedom, can be neglected as a first approximation.

Lower bound on abundance:

Including possible interactions with either the inflaton or other fields within or beyond the standard model entails *additional* production mechanisms for a very long lived (DM) particle. Production from reheating or from other mechanisms only *increases* the abundance, and loss mechanisms, such as decay, will occur on time scales comparable to or larger than the Hubble time today. Therefore, this study yields a *baseline* for the production of ultra-light dark matter particles; any other production mechanism will increase the abundance. This is an important corollary of our study: this simplest of models describing the darkest of dark matter (only gravitational interactions) yields an abundance from non-adiabatic particle production which must be accounted for in any model of (ULDM) particles featuring interactions. Thus the abundance resulting from this mechanism is a lower bound to the abundance of *any interacting* species of long-lived (ULDM), and applies, for example to axion-like candidates.

Similarities and differences with vector dark matter production:

The production of a massive vector boson during inflation has been recently studied in ref.[94]. The authors show that the longitudinal component behaves similarly to a massive, minimally coupled scalar field, whereas the transverse components are conformally coupled to gravity. Remarkably, in this reference it is found that the abundance of the longitudinal component is very similar to the result eqn. (5.5.25) above (up to logarithmic contributions). While the equivalence between the longitudinal component and a massive, minimally coupled scalar field is, perhaps expected, the origin of the similarity in the abundance is by no means clear to us.

In particular we match the mode functions with "in" (Bunch-Davies vacuum) boundary conditions during inflation to the *exact* mode equations in the radiation dominated era with "out" boundary conditions determined by the positive adiabatic frequencies at long time near matter radiation equality, with the matching conditions described in section (5.3). Furthermore we obtain the full energy momentum tensor, confirm covariant conservation and

identify the particle production contribution after the proper renormalization and well into the adiabatic regime when the renormalized energy momentum tensor attains the kinetic form in terms of the distribution function. Finally, the total matter density is obtained from the integral of this distribution function, which again is extracted during the adiabatic regime. While perhaps all of these aspects are somehow included in the scaling argument in ref.[94], we have not been able to find the proper equivalence between our treatment and the framework of ref.[94]. However, this aspect notwithstanding, the similarities between the abundance in both results is remarkable.

Caveats:

The result (5.5.26) implies that for a very low inflation scale, namely with $H_{dS} \ll 10^{13}\,\mathrm{GeV}$ and for a fixed, given mass m_{ev} the (ULDM) gravitationally produced yields a much smaller abundance. Or, equivalently, the value of the mass that yields the correct (DM) abundance increases substantially, whereas consistency of the approach requires the upper bound given by (5.5.28). Since there is a large uncertainty on the scale of inflation, to be resolved by a clear measurement of primordial gravitational waves (or the tensor-to-scalar ratio), it is possible that a very low scale would lead to a revision of the assumption on instantaneous reheating. Furthermore, the only direct observational evidence of a (RD) era is from Big Bang Nucleosynthesis via the primordial abundance of light elements; this scale, however, corresponds to a few MeV. Thus it is possible that the reheating temperature is as low as a few MeV[101]. If this were the case, a very large discrepancy between the scale of inflation and the reheating temperature cannot be accommodated within the instantaneous reheating approximation because modes that are superhorizon during inflation may re-enter during the dynamical evolution between the end of inflation and the (RD) stage, thus modifying the final distribution function even for long wavelengths. Such large discrepancy will require a fundamental understanding of the cosmological evolution *between* the two eras suggesting that there may be a long epoch after the end of inflation that is *not* described by a (RD) cosmology. This scenario would invalidate one of our main assumptions and require a completely different approach to describing cosmological production, and at the fundamental level, a complete revision of assumptions on post-inflationary cosmology.

5.8 Conclusions

We have studied the non-adiabatic cosmological production of ultra-light dark matter particles under a minimal set of assumptions: a single ultra-light real scalar field that *only* interacts with gravity and no other field, it is a spectator field in its Bunch-Davies vacuum state during inflation, it does not contribute to the inflationary dynamics nor to any linear metric perturbation (such as isocurvature). We focus on superhorizon wavelengths after inflation, since these are the cosmologically relevant scales for structure formation, and assume an instantaneous reheating into a (RD) cosmology. The cases of minimal and conformal coupling to gravity are analyzed separately. The mode equations in either case are solved *exactly* both in the inflationary and the (RD) eras with a continuous matching of scale factor, Hubble rate, mode functions and conformal time derivative at the transition. These continuity conditions imply the continuity of the energy density across the transition. The "out" particle states are carefully defined in terms of the zeroth-order adiabatic states at asymptotically long time after the transition, these states are *locally* identified with particle states as in Minkowski space-time. The matching conditions at the transition between inflation and (RD) yield the Bogoliubov coefficients from which we obtain the *distribution function* of produced particles. We establish a correspondence with a (conformal) time dependent particle number by introducing an adiabatic basis of "out" particle states and show explicitly that particle production is a direct consequence of *non-adiabatic* cosmological evolution during inflation and well into the (RD) era. We show that for a mass $10^{-22}\,\mathrm{eV} \lesssim m$ cosmological evolution becomes *adiabatic* well before matter-radiation equality. The number of produced particles *only* depends on cosmological parameters. Whereas a conformally coupled light scalar particle is produced with negligible abundance, there is substantial production for minimally coupled light particles with masses much smaller than the Hubble scale during inflation. The distribution function of minimally coupled light fields feature an infrared enhancement "inherited" from the inflationary stage yielding a behavior $\mathcal{N}_k \propto 1/k^3$ at small comoving wavevectors. We obtain the full energy momentum tensor for the (ULDM) from which we obtain the energy density and pressure near matter-radiation equality after renormalization, which is performed by subtracting the zero point energy density during inflation and ra-

diation domination. An important result is that the fully renormalized energy momentum tensor coincides with the fluid-kinetic one at zeroth-order in the adiabatic expansion. The abundance and equation of state depend solely on the mass and cosmological parameters, in particular the scale of inflation for the minimally coupled case. The main results of this study are the following, for a minimally coupled (ULDM): the ratio of the abundance of produced particles Ω_{pp} to Ω_{DM} is given by

$$\frac{\Omega_{pp}}{\Omega_{DM}} = 8.36 \left\{ \sqrt{m_{ev}} \left[\ln \left[\sqrt{m_{ev}} \right] + 36 \right] \right\} \left[\frac{H_{dS}}{10^{13}\text{GeV}} \right]^2$$

where $m_{ev} = m/(eV)$ and H_{dS} the Hubble scale during inflation. For the upper bound on the scale of inflation from Planck[59] $H_{dS} \simeq 10^{13}\,\text{GeV}$, we find that the produced particles saturate the (DM) abundance for

$$m \simeq 1.5 \times 10^{-5}\,\text{eV}\,.$$

For this value of the mass we find the equation of state parameter at matter-radiation equality

$$w(a_{eq}) \simeq 2.5 \times 10^{-14}\,,$$

and a free streaming length (cutoff scale of the matter power spectrum)

$$\lambda_{fs} \simeq 70\,\text{pc}\,. \tag{5.8.1}$$

Therefore the produced particles while very light are a *cold* dark matter candidate with a free streaming length comparable to that of weakly interacting massive particles.

This is the simplest model for the darkest of (ULDM) since this particle only features gravitational interactions. As such, the results for the abundance provide a *lower bound* and a baseline for the abundance of any (ULDM) candidate with a lifetime equal to or longer than $1/H_0$. Interactions with degrees of freedom of the standard model or beyond that leads to particle production will only *increase* the abundance. This lower bound applies to axion-like particles and must be accounted for in the (DM) contribution of *any* (ULDM) candidate. A study of cosmological production of fermionic degrees of freedom will be reported elsewhere[103].

We have also discussed the caveats associated with a proper treatment of isocurvature perturbations in the case when the (ULDM) (entropy) field does not acquire an expectation value, suggesting that a deeper understanding of this case is needed for a reliable estimate of isocurvature perturbations from the (ULDM) field. We note that such an analysis has not been done even for the inflaton fluctuations.

6.0 Gravitational Production of Nearly-thermal Fermionic Dark Matter

6.1 Introduction

While the cosmological and astrophysical evidence for, and necessity of, Dark Matter (DM) is compelling, it is abundantly clear that a particle physics candidate must be sought in extensions beyond the Standard Model. A multi decade effort for direct detection of various possible candidates has not yet led to the identification of a (DM) particle[25, 26, 117, 142, 58]. A theoretical challenge in proposing a suitable particle physics candidate is to identify a production mechanism that yields the correct abundance and equation of state to satisfy the cosmological and astrophysical constraints and whose lifetime is of the order of, or larger than, the age of the Universe.

Particle production as a consequence of cosmological expansion is a remarkable phenomenon that was studied in pioneering work in refs.[153, 84, 96, 97, 28, 87, 158, 149]. An important aspect of this production mechanism is that it is naturally a consequence of the dynamical gravitational background, and if the particle only interacts with gravity and no other degrees of freedom, its abundance is determined solely by the particle mass, its coupling to gravity, and cosmological parameters, independent of hypothetical couplings beyond the Standard Model.

Gravitational production has been studied for various candidates and different cosmological backgrounds: heavy particles produced during inflation[55, 52, 54, 124, 125], via inflaton oscillations[173, 77, 76], reheating[102, 132], or via cosmological expansion during an era with a particular equation of state[135], and more recently ultralight bosonic particles cosmologically produced during inflation and a post-inflation radiation era[105].

The study of cosmological production of a fermionic species has received far less attention. Early work[85, 13] addressed this important cosmological production channel within the context of standard cosmology, which was later extended to various inflationary scenarios[143, 53, 6, 78, 124, 125, 126].

In this article we focus on studying in detail the cosmological production of a fermionic

species that only interacts with gravity, setting up initial conditions during a de Sitter inflationary era and matching onto a post-inflation radiation dominated (RD) era, with important differences from previous studies [53]:

i:) We consider the non-adiabatic gravitational production of a fermionic degree of freedom throughout the inflationary and post-inflationary radiation dominated era until matter-radiation equality. The fermion mass m is taken to be much smaller than the Hubble scale during inflation, but is otherwise arbitrary. We solve *exactly* the Dirac equation during inflation and radiation domination with the proper boundary conditions, and match the solutions at the transition from inflation to radiation domination (RD).

ii:) This fermionic degree of freedom does *not* couple to the inflaton or any other field, it only interacts gravitationally, and is in its Bunch-Davies vacuum state during inflation, which is taken to be described by a de Sitter space-time.

iii:) We focus on super-Hubble wavelengths at the end of inflation, since these are the cosmologically relevant scales. Since these modes are outside the particle horizon and describe slow dynamics causally disconnected from sub-horizon microphysics, we assume a rapid transition from de Sitter inflation on to a radiation dominated stage. We obtain *exactly* the distribution function of the produced particles, and establish consistently that the superhorizon modes at the end of inflation yield the largest contribution to the final abundance and equation of state.

iv:) We *do not* invoke the adiabatic approximation to obtain a particle number. Instead, we obtain the full energy momentum tensor, and its expectation value in the "in" Bunch-Davies vacuum state. We discuss in detail its renormalization and unambiguously extract the contribution from particle production near matter radiation equality. We show that the asymptotic regime becomes adiabatic well before matter radiation equality and show that in this adiabatic regime the renormalized energy momentum tensor features the kinetic-fluid form after subtraction of the zero point contribution.

Summary of main results:

We consider one fermionic species in a cosmological background from de Sitter inflation followed by a radiation dominated (RD) era. This fermion has a mass m much smaller than the Hubble scale during inflation, H_{dS}, and does not couple to any other field. We focus

on wavelengths that are much larger than the particle horizon at the end of inflation; these modes describe slow evolution and are causally decoupled from the microphysics thereby justifying the assumption of a rapid transition from the de Sitter inflationary stage to a radiation dominated (RD) era. The fermionic field is in its Bunch-Davies vacuum state during inflation. The mode functions for the spinor solutions of the Dirac equation are found *exactly* during inflation and (RD) with proper asymptotic boundary conditions, and matched continuously across the transition. We consider space-time as a *background*: during inflation cosmological dynamics is dominated by the inflaton, and during (RD) by the $\gtrsim 100$ degrees of freedom of the standard model (and beyond). Thus the (DM) contribution is negligible during these eras until near matter radiation equality. We *do not* introduce an interpolating number operator based on some adiabatic approximation; instead we obtain the exact energy momentum tensor valid during and post-inflation. We discuss in detail its renormalization and extract the contribution from particle production near matter radiation equality, when the adiabatic approximation is valid. In this regime we find that the particle production contribution to the energy momentum tensor is of the kinetic fluid form with a distribution function of the produced particles $|B_k|^2 = \frac{1}{2}\left[1-(1-e^{-\frac{k^2}{2mT_H}})^{1/2}\right]$ with k the comoving wavevector and an *emergent* temperature $T_H = \frac{H_0}{2\pi}\sqrt{\Omega_R} \simeq 10^{-36}\,\mathrm{eV}$, with H_0, Ω_R the Hubble expansion rate and radiation fraction today. This distribution function is remarkably similar to a Maxwell-Boltzmann distribution for a non-relativistic particle in thermal equilibrium at temperature T_H and vanishing chemical potential. The energy density near matter-radiation equality is given by $\rho_{pp} \simeq m(mT_H)^{3/2}/a^3$, with an abundance $\frac{\Omega_{pp}}{\Omega_{DM}} \simeq \left(\frac{m}{10^8\,\mathrm{GeV}}\right)^{5/2}$ and equation of state $w(a) \simeq \left(\frac{T_H}{m\,a^2}\right)$. We confirm, self-consistently, that the contribution to the abundance and equation of state is completely dominated by wavevectors that were well outside the horizon at the end of inflation. We discuss subtle aspects of isocurvature perturbations. A comparison between fermionic and bosonic fields conformally coupled to gravity is also discussed.

This article is organized as follows: in section (4.2) we introduce the model and main assumptions. In section (6.3) we obtain the *exact* fermionic spinors with "in" and "out" boundary conditions during inflation and (RD) respectively, matching them at the end of inflation, and obtain the Bogoliubov coefficients. In section (6.4) we obtain the full energy

momentum tensor, discuss in detail its renormalization and show explicitly that in the adiabatic regime the contribution from particle production features the kinetic-fluid form, with a distribution function determined by the Bogoliubov coefficients. This distribution function exhibits an "emergent" temperature and is remarkably similar to the Maxwell-Boltzmann distribution function for a non-relativistic degree of freedom thermalized at this temperature. In this section we determine the (DM) abundance from this fermionic species and its equation of state parameter w. In section (6.5) we discuss important and subtle issues associated with isocurvature perturbations in the case under study. Section (6.6) presents a discussion of various aspects and comparison with previous work and the bosonic case. Section (6.7) summarizes our results and conclusions. Several appendices provide various technical details.

6.2 The Model

We consider a free Dirac fermion of mass m as a dark matter candidate (generalization to Majorana fermions is straightforward) and invoke the following main assumptions:

i:) It does not interact with any other field, including the inflaton or any other field that drives inflation. It only interacts gravitationally. It is light as compared to the Hubble scale during inflation H_{dS}, and we focus on superhorizon wavelengths at the end of inflation, since these are the most relevant for structure formation. The small dimensionless parameters $\varepsilon = \sqrt{m/H_{dS}} \ll 1$ and $k\eta_R \ll 1$ with η_R the horizon scale at the end of inflation, furnish two small parameters that allow for an exact solution of Bogoliubov coefficients (see below).

ii:) The inflationary stage is described by an exact de Sitter space-time, thereby neglecting slow roll corrections, and the fermion field is in its Bunch-Davies vacuum state during this stage.

iii:) We assume instantaneous reheating: namely we consider an instantaneous transition from the inflationary to a radiation dominated stage post-inflation. There is as yet an incomplete understanding of the non-equilibrium dynamics of reheating. Reheating dynamics depend crucially on various assumptions regarding couplings with the inflaton and/or other

fields, and on thermalization processes in an expanding cosmology; see the review[9] for further references. The question of how the nearly $\simeq 100$ degrees of freedom of the Standard Model attain a state of local thermodynamic equilibrium after inflation and on what time scales is still unanswered. Most studies *model* the couplings and dynamics; therefore any model of reheating is at best tentative and very approximate. We bypass the inherent ambiguities and model dependence of the reheating dynamics, and assume *instantaneous* reheating after inflation to a radiation dominated (RD) era. The physical reason behind this assumption is that we are primarily concerned with wavevectors that have crossed the Hubble radius during inflation well before the transition to (RD) and are well outside the horizon during this transition; hence they are causally decoupled from the microphysics of reheating. These modes feature very slow dynamics at the end of inflation, and the assumption that they are nearly frozen during the reheating time interval seems physically warranted (see further discussion in section (6.6)). We assume that both the scale factor and the Hubble rate are *continuous* across the transition. Along with the continuity of fermion wave functions across the transition, this, in fact, entails the continuity of the energy momentum tensor. These aspects will be discussed in detail below.

iv:) Unlike previous studies that invoked the adiabatic approximation, we study *non-adiabatic* cosmological production. This is a direct consequence of a very small mass compared to the Hubble scale during inflation and field fluctuations with superhorizon wavelengths after inflation.

v:) Inflation is generically driven by a scalar field whose expectation value dominates the energy momentum tensor that sources gravity. The (RD) era is dominated by a large number $\gtrsim 100$ of ultrarelativistic degrees of freedom, therefore neglecting the back reaction of the (DM) degree of freedom is justified. Therefore, we take the space time metric during these eras as a *background*.

In comoving coordinates, the action is given by

$$S = \int d^3x\, dt\, \sqrt{-g}\, \overline{\Psi}\Big[i\, \gamma^\mu\, \mathcal{D}_\mu - m \Big] \Psi\, . \tag{6.2.1}$$

For Majorana fermions the action is multiplied by a factor 1/2 (see appendix (D.1)).

Introducing the vierbein field $e^{\mu}_{a}(x)$ defined as

$$g^{\mu\,\nu}(x) = e^{\mu}_{a}(x)\; e^{\nu}_{b}(x)\; \eta^{ab}\;,$$

where $\eta_{ab} = \mathrm{diag}(1,-1,-1,-1)$ is the Minkowski space-time metric, the curved space time Dirac gamma- matrices $\gamma^{\mu}(x)$ are given by

$$\gamma^{\mu}(x) = \gamma^{a} e^{\mu}_{a}(x) \quad , \quad \{\gamma^{\mu}(x), \gamma^{\nu}(x)\} = 2\; g^{\mu\nu}(x)\;, \tag{6.2.2}$$

where the γ^{a} are the Minkowski space time Dirac matrices, chosen to be in the standard Dirac representation. The fermion covariant derivative $\mathcal{D}_{\mu}$ is given in terms of the spin connection by[191, 50, 158, 28]

$$\mathcal{D}_{\mu} = \partial_{\mu} + \frac{1}{8}\,[\gamma^{c}, \gamma^{d}]\; e^{\nu}_{c}\;\left(\partial_{\mu} e_{d\nu} - \Gamma^{\lambda}_{\mu\nu}\; e_{d\lambda}\right)\;, \tag{6.2.3}$$

where $\Gamma^{\lambda}_{\mu\nu}$ are the usual Christoffel symbols.

For a spatially flat Friedmann-Robertson-Walker cosmology in conformal time $d\eta = dt/a(t)$, the metric becomes

$$g_{\mu\nu} = a^{2}(\eta)\; \eta_{\mu\nu}\,, \tag{6.2.4}$$

and the vierbeins e^{μ}_{a} are given by

$$e^{\mu}_{a} = a^{-1}(\eta)\; \delta^{\mu}_{a} \;\; ; \;\; e^{a}_{\mu} = a(\eta)\; \delta^{a}_{\mu}\,. \tag{6.2.5}$$

The fermionic part of the action in conformal coordinates now becomes

$$S_{f} = \int d^{3}x\, d\eta\, a^{4}(\eta)\, \overline{\Psi}(\vec{x},\eta)\left[i\frac{\gamma^{0}}{a(\eta)}\left(\frac{d}{d\eta} + 3\frac{a^{'}(\eta)}{2a(\eta)}\right) + i\,\frac{\gamma^{i}}{a(\eta)}\nabla_{i} - m\right]\Psi(\vec{x},\eta)\,. \tag{6.2.6}$$

The Dirac Lagrangian density in conformal time simplifies to

$$\sqrt{-g}\;\overline{\Psi}\Big(i\;\gamma^{\mu}\;\mathcal{D}_{\mu}\Psi - m\Big)\Psi = \left(a^{3/2}(\eta)\,\overline{\Psi}(\vec{x},\eta)\right)\;\Big[i\;\partial\!\!\!/ - m\;a(\eta)\Big]\left(a^{3/2}(\eta)\,\Psi(\vec{x},\eta)\right), \tag{6.2.7}$$

where $i\partial\!\!\!/ = \gamma^{a}\partial_{a}$ is the usual Dirac differential operator in Minkowski space-time in terms of flat space time γ^{a} matrices. Introducing the conformally rescaled fields

$$a^{\frac{3}{2}}(\eta)\,\Psi(\vec{x},t) = \psi(\vec{x},\eta)\,, \tag{6.2.8}$$

the action becomes

$$S = \int d^3x\, d\eta\, \overline{\psi}\, \Big[i\, \not{\partial} - M(\eta) \Big] \psi \,, \tag{6.2.9}$$

with

$$M(\eta) = m\, a(\eta) \,. \tag{6.2.10}$$

The Dirac equation for the conformally rescaled fermi field becomes

$$\Big[i\, \not{\partial} - M(\eta) \Big] \psi = 0 \,. \tag{6.2.11}$$

We consider Dirac fermions (Majorana fermions are a straightforward generalization), and expand $\psi(\vec{x},\eta)$ in a comoving volume V as

$$\psi(\vec{x},\eta) = \frac{1}{\sqrt{V}} \sum_{\vec{k},s} \Big[b_{\vec{k},s}\, U_s(\vec{k},\eta) + d^\dagger_{-\vec{k},s}\, V_s(-\vec{k},\eta) \Big]\, e^{i\vec{k}\cdot\vec{x}} \,, \tag{6.2.12}$$

and the spinor mode functions U, V obey the Dirac equations

$$\Big[i\, \gamma^0\, \partial_\eta - \vec{\gamma}\cdot\vec{k} - M(\eta) \Big] U_s(\vec{k},\eta) = 0 \tag{6.2.13}$$

$$\Big[i\, \gamma^0\, \partial_\eta - \vec{\gamma}\cdot\vec{k} - M(\eta) \Big] V_s(-\vec{k},\eta) = 0 \,. \tag{6.2.14}$$

Multiplying the above equations both by γ^0 we find that

$$\frac{d}{d\eta}\Big(U^\dagger_s(\vec{k},\eta)\, U_s(\vec{k},\eta) \Big) = 0 \;\; ; \;\; \frac{d}{d\eta}\Big(V^\dagger_s(-\vec{k},\eta)\, V_s(-\vec{k},\eta) \Big) = 0 \;\; ; \;\; \frac{d}{d\eta}\Big(U^\dagger_s(\vec{k},\eta)\, V_s(-\vec{k},\eta) \Big) = 0 \,. \tag{6.2.15}$$

We choose to work with the standard Dirac representation of the (Minkowski) γ^a matrices.

It proves convenient to write

$$U_s(\vec{k},\eta) \;=\; \Big[i\, \gamma^0\, \partial_\eta - \vec{\gamma}\cdot\vec{k} + M(\eta) \Big] f_k(\eta)\, u_s \tag{6.2.16}$$

$$V_s(-\vec{k},\eta) \;=\; \Big[i\, \gamma^0\, \partial_\eta - \vec{\gamma}\cdot\vec{k} + M(\eta) \Big] g_k(\eta)\, v_s \tag{6.2.17}$$

with $u_s\,,\, v_s$ being constant spinors obeying

$$\gamma^0\, u_s = u_s \qquad , \qquad \gamma^0\, v_s = -v_s \,. \tag{6.2.18}$$

We choose the spinors $u_s\,;\,v_s$ as

$$u_s = \begin{pmatrix} \xi_s \\ 0 \end{pmatrix} \quad ; \quad v_s = \begin{pmatrix} 0 \\ \xi_s \end{pmatrix} , \tag{6.2.19}$$

where the two component spinors ξ_s are chosen to be helicity eigenstates, namely

$$\vec{\sigma}\cdot\vec{k} = s\,k\,\xi_s \quad ; \quad s = \pm 1\,. \tag{6.2.20}$$

Inserting the ansatz (6.2.16,6.2.17) into the Dirac equations (6.2.13,6.2.14) we find that the mode functions $f_k(\eta); g_k(\eta)$ obey the following equations of motion

$$\left[\frac{d^2}{d\eta^2} + k^2 + M^2(\eta) - i\,M'(\eta)\right] f_k(\eta) \;=\; 0\,, \tag{6.2.21}$$

$$\left[\frac{d^2}{d\eta^2} + k^2 + M^2(\eta) + i\,M'(\eta)\right] g_k(\eta) \;=\; 0\,. \tag{6.2.22}$$

where primes stand for derivatives with respect to η.

We will adopt "in" boundary conditions for wave vectors deep inside the Hubble radius during inflation, so that as $-k\eta \to \infty$

$$f_k(\eta) \;\to\; e^{-ik\eta} \quad ; \quad g_k(\eta) \;\to\; e^{ik\eta}\,. \tag{6.2.23}$$

With these boundary conditions, it follows from equations (6.2.21,6.2.22) that

$$g_k(\eta) = f_k^*(\eta)\,. \tag{6.2.24}$$

Finally, the spinor solutions with "in" boundary conditions are

$$U_s(\vec{k},\eta) = N \begin{pmatrix} \mathcal{F}_k(\eta)\,\xi_s \\ k\,f_k(\eta)\,s\,\xi_s \end{pmatrix} , \tag{6.2.25}$$

$$V_s(-\vec{k},\eta) = N \begin{pmatrix} -k\,f_k^*(\eta)\,s\,\xi_s \\ \mathcal{F}_k^*(\eta)\,\xi_s \end{pmatrix} , \tag{6.2.26}$$

where we introduced

$$\mathcal{F}_k(\eta) = i f_k'(\eta) + M(\eta) f_k(\eta)\,, \tag{6.2.27}$$

and N is a (constant) normalization factor.

The spinor solutions are normalized as follows

$$U_s^\dagger(\vec{k},\eta)\, U_{s'}(\vec{k},\eta) = \delta_{s,s'} \quad ; \quad V_s^\dagger(-\vec{k},\eta)\, V_{s'}(-\vec{k},\eta) = \delta_{s,s'}\,, \tag{6.2.28}$$

yielding

$$|N|^2\Big[\mathcal{F}_k^*(\eta)\,\mathcal{F}_k(\eta) + k^2 f_k^*(\eta)\, f_k(\eta)\Big] = 1\,. \tag{6.2.29}$$

With these normalization conditions the operators $b_{\vec{k},s}, d_{\vec{k},s}$ in the field expansion (6.2.12) obey the usual canonical anticommutation relations.

Furthermore, it is straightforward to confirm that

$$U_s^\dagger(\vec{k},\eta)\, V_{s'}(-\vec{k},\eta) = 0\,. \tag{6.2.30}$$

The spinors U_s, V_s furnish a complete set of four independent solutions of the Dirac equation.

The inflationary stage is described by a spatially flat de Sitter space time (thereby neglecting slow roll corrections) with a scale factor

$$a(\eta) = -\frac{1}{H_{dS}(\eta - 2\eta_R)}\,, \tag{6.2.31}$$

where H_{dS} is the Hubble constant during de Sitter and η_R is the (conformal) time at which the de Sitter stage transitions to the (RD) stage.

During the (RD) stage

$$H(\eta) = \frac{1}{a^2(\eta)}\frac{da(\eta)}{d\eta} = 1.66\sqrt{g}\,\frac{T_0^2}{M_{Pl}\, a^2(\eta)}\,, \tag{6.2.32}$$

where g is the effective number of ultrarelativistic degrees of freedom, which varies in time as different particles become non-relativistic. We take $g = 2$ corresponding to radiation today. As discussed in detail in section (5.7) by taking $g = 2$ we obtain a *lower bound* on the (DM) abundance and equation of state, differing by a factor of $\mathcal{O}(1)$ from the abundance if the (RD) era is dominated only by standard model degrees of freedom.

With this approximation the scale factor is given by

$$a(\eta) = H_R\,\eta\,, \tag{6.2.33}$$

with

$$H_R = H_0 \sqrt{\Omega_R} \simeq 10^{-35}\,\mathrm{eV}\,, \tag{6.2.34}$$

and matter radiation equality occurs at

$$a_{eq} = \frac{\Omega_R}{\Omega_M} \simeq 1.66\ \times 10^{-4}\,. \tag{6.2.35}$$

The result (4.2.36) corresponds to the value of the fraction density Ω_R *today*, thereby neglecting the change in the number of degrees of freedom contributing to the radiation density fraction. If there are g effective ultrarelativistic degrees of freedom, eqn. (4.2.36) must be multiplied by $\sqrt{g/2}$. However, as discussed in detail in section (5.7) accounting for ultrarelativistic degrees of freedom of the standard model at the time of the transition between inflation and (RD) modifies the final abundance by a factor of $\mathcal{O}(1)$.

We model the transition from de Sitter to (RD) at a (conformal) time η_R by requiring that the scale factor and the Hubble rate be continuous across the transition at η_R, assuming self-consistently that the transition occurs deep in the (RD) era so that $a(\eta_R) = H_R\,\eta_R \ll a_{eq}$.

Using $H(\eta) = a'(\eta)/a^2(\eta)$, continuity of the scale factor and Hubble rate at η_R imply that

$$a_{dS}(\eta_R) = \frac{1}{H_{dS}\,\eta_R} = H_R\,\eta_R \quad ; \quad H_{dS} = \frac{1}{H_R\,\eta_R^2}\,, \tag{6.2.36}$$

yielding

$$\eta_R = \frac{1}{\sqrt{H_{dS}\,H_R}}\,. \tag{6.2.37}$$

The most recent constraints from Planck[59] on the tensor-to-scalar ratio yields

$$H_{dS}/M_{Pl} < 2.5 \times 10^{-5} \quad (95\%)\,\mathrm{CL}\,. \tag{6.2.38}$$

We take as a representative value $H_{dS} = 10^{13}\,\mathrm{GeV}$, from which it follows that

$$a_{dS}(\eta_R) = H_R\,\eta_R = \sqrt{\frac{H_R}{H_{dS}}} \simeq 10^{-28} \ll a_{eq}\,. \tag{6.2.39}$$

This scale corresponds to an approximate ambient radiation temperature after the transition from de Sitter to (RD)

$$T(\eta_R) \simeq \frac{T_0}{a_{RD}(\eta_R)} \simeq 10^{15}\,\mathrm{GeV} \tag{6.2.40}$$

where $T_0 \propto 10^{-4}\,\mathrm{eV}$ is the CMB temperature today.

We focus on the case when the fermion is "light" as compared to the scale of inflation, namely $m \ll H_{dS}$, but otherwise arbitrary, and introduce the dimensionless ratio

$$\varepsilon = \sqrt{\frac{m}{H_{dS}}} \ll 1\,, \tag{6.2.41}$$

which will play an important role in the analysis.

6.2.1 Matching Conditions

Defining $\psi^{<}(\vec{x},\eta)$ and $\psi^{>}(\vec{x},\eta)$ the fermion field for $\eta < \eta_R$ and $\eta > \eta_R$ respectively, and because the Dirac equation (6.2.11) is first order in time the Dirac field is continuous across the transition, the matching condition is

$$\psi^{<}(\vec{x},\eta_R) = \psi^{>}(\vec{x},\eta_R)\,. \tag{6.2.42}$$

This continuity condition along with the continuity of the scale factor and Hubble rate at η_R results in that the energy density, namely the expectation value of T^0_0 is *continuous at the transition*. This important aspect is discussed further in section (6.4).

Introducing the Dirac spinors during the inflationary ($\eta < \eta_R$) and radiation-dominated ($\eta > \eta_R$) dominated stages as $U^{<}$, $V^{<}$ and $U^{>}$, $V^{>}$ respectively, it follows from the matching condition (6.2.42) that

$$U^{<}_s(\vec{k},\eta_R) = U^{>}_s(\vec{k},\eta_R)\,, \tag{6.2.43}$$

$$V^{<}_s(-\vec{k},\eta_R) = V^{>}_s(-\vec{k},\eta_R)\,. \tag{6.2.44}$$

6.2.2 Adiabatic vs. Non-adiabatic Evolution, Asymptotic "Out" Particle States

Our goal is to solve *exactly* the mode equations during the inflationary and (RD) stages and implement the matching conditions (6.2.42,6.2.43,6.2.44). During inflation the mode equations are solved with the "in" boundary conditions (6.2.23) corresponding to the fermi fields being in the Bunch-Davies vacuum state (see next section). We now need to determine the boundary conditions on the mode functions during (RD).

Let us consider solving the mode equation (6.2.21) in a Wentzel-Kramers-Brillouin (WKB) adiabatic expansion, writing

$$f_k(\eta) = e^{-i\int^\eta \Omega_k(\eta')\,d\eta'}\,, \tag{6.2.45}$$

we find that $\Omega_k(\eta)$ obeys

$$\Omega_k^2(\eta) + i\,\Omega_k'(\eta) - \omega_k^2(\eta) + iM'(\eta) = 0 \;\;;\;\; \omega_k^2(\eta) = k^2 + M^2(\eta)\,. \tag{6.2.46}$$

Expanding $\Omega_k(\eta) = \Omega_k^{(0)}(\eta) + \Omega_k^{(1)}(\eta) + \cdots$ where the superscript implies order in a derivative adiabatic expansion, we find up to first order (see Appendix (D.4))

$$\Omega_k(\eta) = \omega_k(\eta)\left[1 - i\frac{\omega_k'(\eta)}{2\,\omega_k^2(\eta)} - i\frac{M'(\eta)}{2\,\omega_k^2(\eta)} + \cdots\right], \tag{6.2.47}$$

where the dots stand for terms with higher order derivatives with respect to η. We refer to terms with n-derivatives as $n-th$ order adiabatic. We note that the term $M'(\eta)$ in the mode equation (6.2.21) is formally first order adiabatic, as is manifest in eqn. (6.2.47). This adiabatic expansion is reliable and useful provided that terms of higher adiabatic order are smaller order by order. To assess the reliability, consider the first order corrections displayed in (6.2.47), and writing them as follows

$$\frac{M'(\eta)}{\omega_k^2(\eta)} = \frac{H(\eta)}{m}\,\frac{1}{\gamma_k^2(\eta)} \;\;;\;\; \frac{\omega_k'(\eta)}{\omega_k^2(\eta)} = \frac{H(\eta)}{m}\,\frac{1}{\gamma_k^3(\eta)}\,, \tag{6.2.48}$$

where $H(\eta), \gamma_k(\eta)$ are the Hubble expansion rate and local Lorentz factor respectively, namely

$$H(\eta) = \frac{a'(\eta)}{a^2(\eta)} \;\;;\;\; \gamma_k(\eta) = \left[1 + \Big(\frac{k}{m\,a(\eta)}\Big)^2\right]^{1/2}. \tag{6.2.49}$$

During inflation and for superhorizon wavelengths, it follows that

$$\frac{M'(\eta)}{\omega_k^2(\eta)} \simeq \frac{\omega_k'(\eta)}{\omega_k^2(\eta)} \simeq \frac{H_{dS}}{m} \simeq \frac{1}{\varepsilon} \gg 1\,. \tag{6.2.50}$$

Therefore, the adiabatic approximation *fails* during the inflationary stage for superhorizon wavelengths and $m \ll H_{dS}$.

During the (RD) era and for very long-wavelength modes,

$$\frac{M'(\eta)}{\omega_k^2(\eta)} \simeq \frac{\omega_k'(\eta)}{\omega_k^2(\eta)} \simeq \frac{H_R}{m\,a^2(\eta)}\,, \tag{6.2.51}$$

therefore the adiabatic expansion becomes reliable for

$$a(\eta) \gg \frac{10^{-17}}{\sqrt{m/(\mathrm{eV})}}\,. \tag{6.2.52}$$

Even for m as small as $10^{-22}\,\mathrm{eV}$ the adiabatic expansion becomes reliable prior to matter radiation equality. We anticipate that the most interesting range for fermionic (DM) is $m \gg \mathrm{GeV}$ (see section (6.4) below), hence the adiabatic approximation becomes very reliable for $a(\eta) \gg 10^{-22}$. Two important points follow from this analysis: **i:)** during inflation and in the early stages of (RD) following the transition from inflation, the adiabatic approximation is not reliable in the range $10^{-28} \lesssim a(\eta) \lesssim 10^{-22}$, **ii:)** *near* matter radiation equality ($a_{eq} \simeq 10^{-4}$) the adiabatic approximation to *zeroth* order is very reliable. Therefore, the mode functions both during inflation and the early stages after the transition to (RD) must be found *exactly*, and the asymptotic "out" boundary conditions for these modes during (RD) can be reliably defined in the asymptotic adiabatic regime. Appendix (D.4) provides more technical details on the nature of the adiabatic expansion for Fermi fields.

In summary: we do *not* invoke the adiabatic approximation during inflation or the early stages after the transition to (RD), solving exactly for the mode functions during these stages. However, we *do* invoke it to determine the asymptotic "out" boundary conditions on the mode functions and spinors during the (RD) era. We refer to the solutions of eqn. (6.2.21) for the mode functions $f_k(\eta)$ during the (RD) era obeying the asymptotic "out" boundary conditions just prior to a_{eq}, as asymptotic "out" *particle* states.

$$f_k(\eta) \quad \rightarrow \quad e^{-i\int^\eta \omega_k(\eta')\,d\eta'} = e^{-i\int^t E_k(t')\,dt'}\,, \tag{6.2.53}$$

where in comoving time

$$E_k(t) = \sqrt{k_{ph}^2(t) + m^2} \;\; ; \;\; k_{ph}(t) = k/a(\eta(t))\,. \tag{6.2.54}$$

In the next section we will solve *exactly* for the mode functions $f_k(\eta)$ and the spinor solutions of the Dirac equation both during inflation and radiation domination with the "in" and "out" (particle) asymptotic boundary conditions,

$$f_k(\eta) \;\; \xrightarrow[-k\eta\to\infty]{} \;\; e^{-ik\eta} \;\; \text{IN} \;\; \text{(inflation)}\,, \tag{6.2.55}$$

$$f_k(\eta) \;\; \xrightarrow[a(\eta)\simeq a_{eq}]{} \;\; e^{-i\int^\eta \omega_k(\eta')\,d\eta'} \;\; \text{OUT} \;\; \text{(RD)}\,, \tag{6.2.56}$$

identifying the solutions with this "out" boundary conditions as describing particle states. The mode functions $g_k(\eta) = f_k^*(\eta)$ and the corresponding spinors are associated with the anti-particle "out" states. We then match the respective solutions at $\eta = \eta_R$ via the matching conditions (6.2.43,6.2.44).

6.3 Exact Solutions

6.3.1 Inflationary Stage

We consider that the inflationary stage is described by an exact de Sitter space time with scale factor given by eqn. (6.2.31) and that the fermionic degrees of freedom are in the Bunch-Davies vacuum state during inflation. This implies that consistently with (6.2.23) the solutions $U_s(\vec{k},\eta); V_s(-\vec{k},\eta)$ obey the "in" boundary conditions

$$U_s(\vec{k},\eta) \to e^{-ik\eta} \;;\; V_s(\vec{k},\eta) \to e^{ik\eta}\,, \tag{6.3.1}$$

for wavevectors deep inside the Hubble radius $-k\eta \to \infty$, given by (6.2.25,6.2.26) along with

$$b_{\vec{k},s}|0\rangle = 0 \;\; ; \;\; d_{-\vec{k},s}|0\rangle = 0\,, \tag{6.3.2}$$

The equations (6.2.21,6.2.22) for the mode functions becomes

$$\left[\frac{d^2}{d\tau^2} + k^2 - \frac{\nu^2 - 1/4}{\tau^2}\right] f_k(\tau) = 0 \;\; ; \;\; \tau = \eta - \eta_R \;\; ; \;\; \nu = \frac{1}{2} - i\,\varepsilon^2 \,. \tag{6.3.3}$$

in terms of the dimensionless ratio (6.2.41). The solution with "in" boundary conditions (6.2.55), namely $f_k(\eta) \to e^{-ik\eta}$ for sub-Hubble modes, is given by

$$f_k(\tau) = \sqrt{-\frac{\pi k\tau}{2}}\; e^{i\pi(\nu+1/2)/2}\; H^{(1)}_\nu(-k\tau) \;\; ; \;\; g_k(\tau) = f^*_k(\tau)\,, \tag{6.3.4}$$

where $H^{(1)}_\nu$ is a Hankel function.

Therefore with Bunch-Davies boundary conditions, the spinors $U^<(\vec{k},\eta)$; $V^<(-\vec{k}\eta)$ are given by the expressions (6.2.25,6.2.26) with $f_k(\eta)$ given by (6.3.4). In the superhorizon limit the solution (6.3.4) behaves as

$$f_k(\tau) \propto \big[-k\tau\big]^{i\varepsilon^2}\,, \tag{6.3.5}$$

therefore unlike the case of bosonic degrees of freedom, these mode functions are *not* enhanced for superhorizon wavelengths with the modulus remaining $\mathcal{O}(1)$. Furthermore, as it will become clear below, the relevant dimensionless comoving momentum is (see below) $q = k/\sqrt{mH_R}$ from which it follows that at the end of inflation $k\eta_R = q\,\varepsilon \ll 1$. It will be shown below (see section (6.4)) that the abundance of produced (DM) particles is dominated by the region $q \simeq 1$ hence the phase in (6.3.5) is very slowly varying at the end of inflation for the relevant modes.

6.3.2 Radiation Dominated Stage

We define the mode functions during (RD) as $h_k(\eta)$ to distinguish them from the solutions during the inflationary era. These obey the mode equations

$$\left[\frac{d^2}{d\eta^2} + \omega^2_k(\eta) - i\,mH_R\right] h_k(\eta) = 0 \;\; ; \;\; \omega^2_k(\eta) = k^2 + m^2 H^2_R \eta^2\,. \tag{6.3.6}$$

During the (RD) stage we introduce the spinors $\mathcal{U},\mathcal{V}$ that describe asymptotic particle and anti-particle "out" states at long time respectively. These are solutions of the Dirac

equation during the (RD) era satisfying the asymptotic "out" boundary conditions (6.2.56) yielding

$$\mathcal{U}(\vec{k},\eta) \to\propto e^{-i\int^{\eta}\omega_k(\eta')\,d\eta'} \;\;;\;\; \mathcal{V}(\vec{k},\eta) \to\propto e^{i\int^{\eta}\omega_k(\eta')\,d\eta'}\,. \tag{6.3.7}$$

This "out" boundary condition corresponds to the mode functions $h_k(\eta)$ solutions of (6.3.6) with the asymptotic behavior (6.2.56), namely

$$h_k(\eta) \to e^{-i\int^{\eta}\omega_k(\eta')\,d\eta'}\,. \tag{6.3.8}$$

With these boundary conditions we find that these particle-antiparticle spinors are given by

$$\mathcal{U}_s(\vec{k},\eta) = \widetilde{N}\begin{pmatrix} \mathcal{H}_k(\eta)\,\xi_s \\ k\,h_k(\eta)\,s\,\xi_s \end{pmatrix}, \tag{6.3.9}$$

$$\mathcal{V}_s(-\vec{k},\eta) = \widetilde{N}\begin{pmatrix} -k\,h_k^*(\eta)\,s\,\xi_s \\ \mathcal{H}_k^*(\eta)\,\xi_s \end{pmatrix}, \tag{6.3.10}$$

where we have introduced

$$\mathcal{H}_k(\eta) = ih_k'(\eta) + M(\eta)h_k(\eta)\,, \tag{6.3.11}$$

and $\widetilde{N}$ is a (constant) normalization factor chosen so that

$$\mathcal{U}_s^{\dagger}(\vec{k},\eta)\,\mathcal{U}_{s'}(\vec{k},\eta) = \delta_{s,s'} \;\;;\;\; \mathcal{V}_s^{\dagger}(-\vec{k},\eta)\,\mathcal{V}_{s'}(-\vec{k},\eta) = \delta_{s,s'}\,, \tag{6.3.12}$$

yielding

$$|\widetilde{N}|^2\Big[\mathcal{H}_k^*(\eta)\mathcal{H}_k(\eta) + k^2 h_k^*(\eta)h_k(\eta)\Big] = 1\,. \tag{6.3.13}$$

Again, it is straightforward to confirm that

$$\mathcal{U}_s^{\dagger}(\vec{k},\eta)\,\mathcal{V}_{s'}(-\vec{k},\eta) = 0\,. \tag{6.3.14}$$

These form a complete set of four solutions of the Dirac equation ($s = \pm 1$) during (RD). It is convenient to introduce the following dimensionless combinations,

$$z = \sqrt{mH_R}\;\eta \;\;;\;\; q = \frac{k}{\sqrt{mH_R}} \;\;;\;\; \lambda = q^2 - i \tag{6.3.15}$$

in terms of which eqn. (6.3.6) becomes

$$\frac{d^2}{dz^2}h_k(z) + (z^2+\lambda)h_k(z) = 0\,, \tag{6.3.16}$$

the solutions of which are the parabolic cylinder functions[93, 2, 152, 21, 145]

$$D_\alpha[\sqrt{2}e^{i\pi/4}z] \;\;;\;\; D_\alpha[\sqrt{2}e^{3i\pi/4}z] \;\;;\;\; \alpha = -\frac{1}{2} - i\frac{\lambda}{2} = -1 - i\,\frac{q^2}{2}\,. \tag{6.3.17}$$

The solution that fulfills the "out" boundary condition (6.3.8) (see appendix A) is given by

$$h_k(\eta) = D_\alpha[\sqrt{2}e^{i\pi/4}z]\,. \tag{6.3.18}$$

The general solution for the spinor wave functions $U^>, V^>$ during the (RD) era are linear combinations of the four independent solutions (6.3.9,6.3.10). In principle, with four independent solutions during inflation matching onto four independent solutions during (RD) there would be a 4×4 matrix of Bogoliubov coefficients, however, because helicity is conserved, the linear combinations are given by

$$U_s^>(\vec{k},\eta) = A_{k,s}\,\mathcal{U}_s(\vec{k},\eta) + B_{k,s}\,\mathcal{V}_s(-\vec{k},\eta) \tag{6.3.19}$$

$$V_s^>(-\vec{k},\eta) = C_{k,s}\;\mathcal{V}_s(-\vec{k},\eta) + D_{k,s}\,\mathcal{U}_s(\vec{k},\eta)\,. \tag{6.3.20}$$

The Bogoliubov coefficients $A_{k,s}\cdots D_{k,s}$ are obtained from the matching conditions (6.2.43, 6.2.44) and the relations (6.3.12,6.3.14). We find

$$A_{k,s} = \mathcal{U}_s^\dagger(\vec{k},\eta_R)U_s^<(\vec{k},\eta_R) = N\widetilde{N}\Big[\mathcal{H}_k^*\,\mathcal{F}_k + k^2 h_k^* f_k\Big]_{\eta=\eta_R} \tag{6.3.21}$$

$$B_{k,s} = \mathcal{V}_s^\dagger(-\vec{k},\eta_R)U_s^<(\vec{k},\eta_R) = N\widetilde{N}\,s\,\Big[-kh_k\mathcal{F}_k + kf_k\mathcal{H}_k\Big]_{\eta=\eta_R} \tag{6.3.22}$$

$$C_{k,s} = \mathcal{V}_s^\dagger(-\vec{k},\eta_R)V_s^<(-\vec{k},\eta_R) = N\widetilde{N}\Big[k^2 h_k f_k^* + \mathcal{H}_k\,\mathcal{F}_k^*\Big]_{\eta=\eta_R} \tag{6.3.23}$$

$$D_{k,s} = \mathcal{U}_s^\dagger(\vec{k},\eta_R)V_s^<(-\vec{k},\eta_R) = N\widetilde{N}\,s\,\Big[-kf_k^*\mathcal{H}_k^* + kh_k^*\mathcal{F}_k^*\Big]_{\eta=\eta_R}\,. \tag{6.3.24}$$

From these relations we find the important corollary

$$D_{k,s} = -B_{k,s}^* \;\;;\;\; C_{k,s} = A_{k,s}^*\,, \tag{6.3.25}$$

which guarantees the orthogonality

$$U_s^{>\dagger}(\vec{k},\eta)V_s^{>}(-\vec{k},\eta) = 0\,. \tag{6.3.26}$$

Furthermore the normalization conditions (6.2.28,6.2.30,6.3.12,6.3.14) yield the following relations between Bogoliubov coefficients

$$|A_{k,s}|^2 + |B_{k,s}|^2 = |C_{k,s}|^2 + |D_{k,s}|^2 = 1\,, \tag{6.3.27}$$

which can be confirmed straightforwardly from the expressions (6.3.21-6.3.24) and the normalization conditions.

During the (RD) era, with $U_s \equiv U_s^{>}; V_s \equiv V_s^{>}$ with $U^{>}, V^{>}$ given by (6.3.19,6.3.20) the field expansion (6.2.12) becomes

$$\psi(\vec{x},\eta) = \frac{1}{\sqrt{V}}\sum_{\vec{k},s}\left[\widetilde{b}_{\vec{k},s}\,\mathcal{U}_s(\vec{k},\eta) + \widetilde{d}^{\dagger}_{-\vec{k},s}\,\mathcal{V}_s(-\vec{k},\eta)\right]\,e^{i\vec{k}\cdot\vec{x}}\,, \tag{6.3.28}$$

where

$$\widetilde{b}_{\vec{k},s} = b_{\vec{k},s}A_k + d^{\dagger}_{-\vec{k},s}D_{k,s} \tag{6.3.29}$$

$$\widetilde{d}^{\dagger}_{-\vec{k},s} = d^{\dagger}_{-\vec{k},s}C_{k,s} + b_{\vec{k},s}B_{k,s}\,. \tag{6.3.30}$$

The relations (6.3.27, 6.3.25) entail that the new operators $\widetilde{b}, \widetilde{d}$ obey the canonical anti-commutation relations. The operators $\widetilde{b}$ and $\widetilde{d}$ create asymptotic particle and antiparticle states respectively. In particular we find that the number of asymptotic "out" particle and antiparticle states in the Bunch-Davies vacuum state (6.3.2) are given by

$$\langle 0|\widetilde{b}^{\dagger}_{\vec{k},s}\widetilde{b}_{\vec{k},s}|0\rangle = |D_{k,s}|^2 = \langle 0|\widetilde{d}^{\dagger}_{-\vec{k},s}\widetilde{d}_{-\vec{k},s}|0\rangle = |B_{k,s}|^2\,. \tag{6.3.31}$$

We identify $|B_{k,s}|^2$ with the *distribution function of produced particles.* The relation (6.3.27) implies that

$$|B_{k,s}|^2 \leq 1\,, \tag{6.3.32}$$

for each polarization s, consistent with Pauli exclusion.

6.3.3 Bogoliubov Coefficients

The Bogoliubov coefficients are obtained from the relations (6.3.21-6.3.24) where the scalar products of spinors are evaluated at the transition time $\eta = \eta_R$. For light fermions with $m/H_{dS} \ll 1$ ($\varepsilon \ll 1$) these can be greatly simplified with the following approximations:

i:) During the inflationary era and taking $\nu = 1/2$ for $\varepsilon \ll 1$ in the solutions (6.3.4)) yields

$$f_k(\eta_R) = e^{ik\eta_R} \simeq 1\,, \tag{6.3.33}$$

where we have considered modes that are super-Hubble at the transition time, namely $|k\eta_R| \ll 1$. Furthermore, with

$$M(\eta_R) = \frac{mH_R}{\sqrt{H_R H_{dS}}} = \varepsilon\,\sqrt{mH_R}\,, \tag{6.3.34}$$

the normalization constant N in the spinors (6.2.25,6.2.26) is obtained by normalizing the spinors at $\eta = \eta_R$. In terms of the dimensionless ratio $q = k/\sqrt{mH_R}$ to lowest order in ε at $\eta = \eta_R$ these spinors are given by

$$U_s^<(\vec{k},\eta_R) = \frac{1}{\sqrt{2q(q+\varepsilon)}}\begin{pmatrix}(q+\varepsilon)\,\xi_s\\ q\,s\,\xi_s\end{pmatrix} \tag{6.3.35}$$

$$V_s^<(-\vec{k},\eta_R) = \frac{1}{\sqrt{2q(q+\varepsilon)}}\begin{pmatrix}q\,s\,\xi_s\\ (q+\varepsilon)\,\xi_s\end{pmatrix}\,. \tag{6.3.36}$$

ii:) During radiation domination, it follows from the definitions (6.3.15) that at the transition time,

$$z_R = \sqrt{\frac{mH_R}{H_R H_{dS}}} = \varepsilon \ll 1\,, \tag{6.3.37}$$

and for $z \ll 1$ the parabolic cylinder functions feature an expansion in z_R and $q\,z_R = k\eta_R \ll 1$ (see appendix (D.2)) for superhorizon wavevectors. Therefore we can safely approximate $z_R = 0$ in the argument of the parabolic cylinder functions yielding the following identities,

$$h_k(\eta_R) \;=\; \frac{\sqrt{\pi/2}\;\;2^{-iq^2/4}}{\Gamma[1+i\frac{q^2}{4}]}\,, \tag{6.3.38}$$

$$h'_k(\eta_R) \;=\; -\frac{\sqrt{2\pi}\,e^{i\pi/4}2^{-iq^2/4}\,\sqrt{mH_R}}{\Gamma[\frac{1}{2}+i\frac{q^2}{4}]}\,. \tag{6.3.39}$$

iii:) The result $|B_{k,s}|^2 \leq 1$ implies that there are no infrared divergences in the distribution function of particles, and in integrals, the small k region is suppressed by phase space. Furthermore, we anticipate, and prove below self-consistently, that in typical integrals involving $|B_{k,s}|^2$ the most relevant region is $k \simeq \sqrt{mH_R}$, namely $q \simeq 1$ (see below). Therefore, consistently with neglecting the $\mathcal{O}(\varepsilon)$ terms in (6.3.38,6.3.39) we set $\varepsilon \to 0$ in the spinors (6.3.35,6.3.36). With these results, the normalization constant $\widetilde{N}$ is obtained from the normalization conditions (6.3.12) at $\eta = \eta_R$, it is given by (see appendix (D.3))

$$\widetilde{N} = \frac{e^{-\pi q^2/8}}{\sqrt{2mH_R}}\,. \tag{6.3.40}$$

With the approximations discussed above, and from the result (6.3.22) we find

$$|B_{k,s}|^2 = \frac{1}{2}\left[1 - \widetilde{N}\, q\, \sqrt{mH_R}\left(\mathcal{H}_k^*(\eta_R)\, h_k(\eta_R) + \mathcal{H}_k(\eta_R)\, h_k^*(\eta_R)\right)\right]. \tag{6.3.41}$$

The calculation of the second term in the bracket is discussed in detail in appendix (D.3) with the result,

$$|B_{k,s}|^2 = \frac{1}{2}\left[1 - \left(1 - e^{-\pi q^2}\right)^{1/2}\right], \tag{6.3.42}$$

yielding the behaviour

$$|B_{k,s}|^2 \;\xrightarrow[k\to 0]{}\; \frac{1}{2} \;\;;\;\; |B_{k,s}|^2 \;\xrightarrow[k\gg\sqrt{mH_R}]{}\; \frac{1}{4}\, e^{-\frac{2\pi\, k^2}{2mH_R}} \equiv \frac{1}{4}|B_{mb}(k)|^2\,. \tag{6.3.43}$$

The long-wavelength limit agrees with ref.[53]. Remarkably, up to the prefactor 1/4, for $k \gtrsim \sqrt{mH_R}$ the Bogoliugov coefficient yields a Maxwell-Boltzmann distribution function ($|B_{mb}(k)|^2$) for a non-relativistic particle at an "emergent" temperature

$$T_H = \frac{H_R}{2\pi} \simeq 10^{-36}\,\mathrm{eV}\,, \tag{6.3.44}$$

and vanishing chemical potential in agreement with the result (6.3.31) which indicates that the number of produced particles equals that of anti-particles. Figs. (23; 24) display $|B(q)|^2$ and $q^2|B(q)|^2$ vs. q respectively.

Writing the *distribution function* as

$$|B_{k,s}|^2 = \frac{1}{2}\Big[1 - \big(1 - e^{-\frac{k^2}{2mT_H}}\big)^{1/2}\Big] \tag{6.3.45}$$

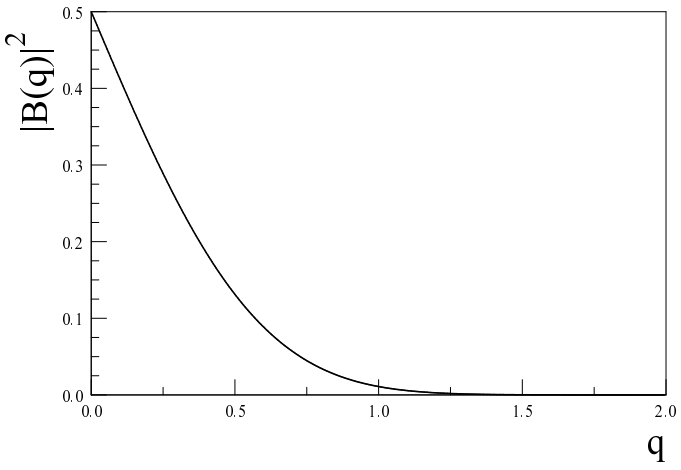

Figure 23: The distribution function of produced particles $|B_{k,s}|^2 \equiv |B(q)|^2$ vs $q = k/\sqrt{mH_R}$.

makes manifest the striking similarity with a Maxwell-Boltzmann distribution function of a non-relativistic particle in thermal equilibrium at temperature T_H and vanishing chemical potential, up to an overall normalization. Clearly the similarity does not hold for the longest wavelengths, which however are suppressed by the phase space factor, but for $\frac{k^2}{2m} \gtrsim T_H$ the difference is small. Fig. (25) compares $K^2|B_{k,s}|^2$ to $\frac{K^2}{4}|B_{mb}(k)|^2 \equiv \frac{K^2}{4}e^{-K^2}$ vs. $K = \frac{k}{\sqrt{2mT_H}}$. The maximum difference is $\lesssim 10\,\%$, and occurs at low momenta.

An important note is that the distribution function is localized in the region $q \simeq 1$, namely in the range of momenta $k \simeq \sqrt{mH_R}$, for which $k\eta_R \lesssim \sqrt{\frac{mH_R}{H_{dS}H_R}} \lesssim \varepsilon \ll 1$. Therefore, the largest contribution to the distribution function, hence the abundance and equation of state, is from wavelengths that are well outside the horizon at the end of inflation. This analysis confirms self-consistently the validity of one of the main assumptions, namely that of focusing on superhorizon wavelengths at the end of inflation.

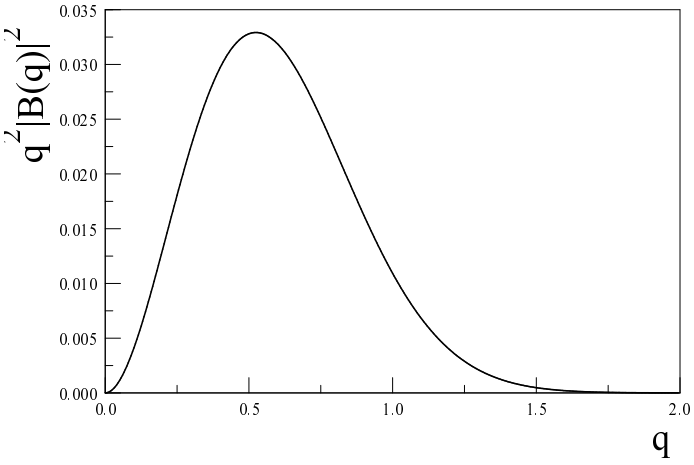

Figure 24: The integrand for the total abundance $q^2|B_{k,s}|^2$ vs $q = k/\sqrt{mH_R}$. The abundance is dominated by typical momenta $k \simeq \sqrt{mH_R}$.

6.4 Energy Momentum Tensor: Renormalization and Asymptotics

6.4.1 Energy Density and Pressure

The energy momemtum tensor for Dirac fields is given by [158]

$$T^{\mu\nu} = \frac{i}{2}\Big(\overline{\Psi}\gamma^{\mu}\overset{\leftrightarrow}{\mathcal{D}^{\nu}}\Psi\Big) + \mu \leftrightarrow \nu \tag{6.4.1}$$

The expectation value of the energy momentum tensor in the Bunch-Davies vacuum state is given by

$$\langle 0|T^{\mu}_{\nu}|0\rangle = \mathrm{diag}\big(\rho(\eta), -P(\eta), -P(\eta), -P(\eta)\big)\,. \tag{6.4.2}$$

In terms of conformal time and the conformally rescaled fields (6.2.8) The energy density ρ and pressure P are given by

$$\rho(\eta) = \langle 0|T^{0}_{0}|0\rangle = \frac{i}{2a^4(\eta)}\,\langle 0|\Big(\psi^{\dagger}(\vec{x},\eta)\frac{d}{d\eta}\,\psi(\vec{x},\eta) - \frac{d}{d\eta}\,\psi^{\dagger}(\vec{x},\eta)\,\psi(\vec{x},\eta)\Big)|0\rangle\,, \tag{6.4.3}$$

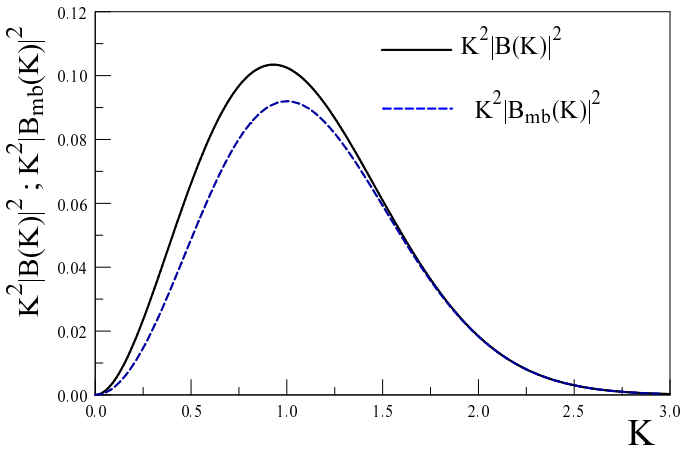

Figure 25: The distributions $K^2|B_{k,s}|^2$ and $\frac{K^2}{4}|B_{mb}(k)|^2 = \frac{K^2}{4}\,e^{-K^2}$ vs $K = k/\sqrt{2mT_H}$. The near agreement in the region of momenta $k \simeq \sqrt{2mT_H}$, which dominates the integrals, entails a near thermal abundance.

$$P(\eta) = -\frac{1}{3}\sum_j \langle 0|T^j_j|0\rangle = \frac{-i}{6a^4(\eta)}\,\langle 0|\Big(\psi^\dagger(\vec{x},\eta)\,\vec{\alpha}\cdot\vec{\nabla}\,\psi(\vec{x},\eta) - \vec{\nabla}\psi^\dagger(\vec{x},\eta)\cdot\vec{\alpha}\,\psi(\vec{x},\eta)\Big)|0\rangle\,, \tag{6.4.4}$$

where $\vec{\alpha} = \gamma^0\,\vec{\gamma}$ and the expectation value is in the Bunch-Davies vacuum state. With the field expansion (6.2.12) we find

$$\rho(\eta) = \frac{i}{2a^4(\eta)}\,\int_0^\infty \sum_s \left[V_s^\dagger(-\vec{k},\eta)\,\frac{d}{d\eta}V_s(-\vec{k},\eta) - \frac{d}{d\eta}V^\dagger{}_s(-\vec{k},\eta)\,V_s(-\vec{k},\eta)\right]\frac{d^3k}{(2\pi)^3}\,, \tag{6.4.5}$$

$$P(\eta) = \frac{1}{3\,a^4(\eta)}\,\int_0^\infty \sum_s V_s^\dagger(-\vec{k},\eta)\,\vec{\alpha}\cdot\vec{k}\,V_s(-\vec{k},\eta)\,\frac{d^3k}{(2\pi)^3}\,. \tag{6.4.6}$$

Using the Dirac equation, it is straightforward to confirm covariant energy conservation, and also that $\rho(\eta)$ can be written as

$$\rho(\eta) = \frac{1}{a^4(\eta)} \int_0^\infty \sum_s V_s^\dagger(-\vec{k},\eta) \left[\vec{\alpha}\cdot\vec{k} + \gamma^0 M(\eta)\right] V_s(-\vec{k},\eta) \frac{d^3k}{(2\pi)^3}\,, \tag{6.4.7}$$

yielding

$$\langle 0|T^\mu_\mu|0\rangle = \frac{m}{a^3(\eta)} \int_0^\infty \sum_s \overline{V}_s(-\vec{k},\eta)\, V_s(-\vec{k},\eta) \frac{d^3k}{(2\pi)^3}\,. \tag{6.4.8}$$

Furthermore, the continuity of the scale factor and Hubble rate and the continuity condition (6.2.42) ensure that the energy momentum tensor is *continuous* across the transition from inflation to radiation domination.

During the inflationary stage the V spinors are given by (6.2.26) with (6.3.4) and the energy momentum tensor yields the Bunch-Davies *vacuum* energy density and pressure, which will be fully subtracted in the renormalization of the energy momentum tensor (see below) .

During the (RD) stage the spinors $V_s \equiv V_s^>$ are given by (6.3.20) in terms of the Bogoliubov coefficients and the spinors $\mathcal{U},\mathcal{V}$ with particle and anti-particle "out" boundary conditions. Both the energy density and pressure feature *three* distinct terms:

$$\rho(\eta) = \rho_{vac}(\eta) + \rho_{int}(\eta) + \rho_{pp}(\eta) \tag{6.4.9}$$

$$P(\eta) = P_{vac}(\eta) + P_{int}(\eta) + P_{pp}(\eta)\,, \tag{6.4.10}$$

where

$$\rho_{vac} = \frac{1}{a^4(\eta)} \int \sum_{s=\pm1} \left[\mathcal{V}_s^\dagger(-\vec{k},\eta)\,\Sigma(\vec{k},\eta)\,\mathcal{V}_s(-\vec{k},\eta)\right] \frac{d^3k}{(2\pi)^3}\,, \tag{6.4.11}$$

$$\rho_{int} = -\frac{1}{a^4(\eta)} \int \sum_{s=\pm1} \left[A_{k,s}\, B^*_{k,s}\, \mathcal{V}_s^\dagger(-\vec{k},\eta)\,\Sigma(\vec{k},\eta)\,\mathcal{U}_s(\vec{k},\eta) + h.c.\right] \frac{d^3k}{(2\pi)^3}\,, \tag{6.4.12}$$

$$\rho_{pp} = \frac{1}{a^4(\eta)} \int \sum_{s=\pm1} |B_{k,s}|^2 \left[\mathcal{U}_s^\dagger(\vec{k},\eta)\,\Sigma(\vec{k},\eta)\,\mathcal{U}_s(\vec{k},\eta) - \mathcal{V}_s^\dagger(-\vec{k},\eta)\,\Sigma(\vec{k},\eta)\,\mathcal{V}_s(-\vec{k},\eta)\right] \frac{d^3k}{(2\pi)^3}\,, \tag{6.4.13}$$

where

$$\Sigma(\vec{k},\eta) = \vec{\alpha}\cdot\vec{k} + \gamma^0 M(\eta)\,, \tag{6.4.14}$$

is the conformal time instantaneous Dirac Hamiltonian, and

$$P_{vac} = \frac{1}{3a^4(\eta)}\int \sum_{s=\pm 1}\Big[\mathcal{V}_s^\dagger(-\vec{k},\eta)\,\vec{\alpha}\cdot\vec{k}\;\mathcal{V}_s(-\vec{k},\eta)\Big]\frac{d^3k}{(2\pi)^3}\,, \tag{6.4.15}$$

$$P_{int} = -\frac{1}{3a^4(\eta)}\int \sum_{s=\pm 1}\Big[A_{k,s}\,B^*_{k,s}\,\mathcal{V}_s^\dagger(-\vec{k},\eta)\,\vec{\alpha}\cdot\vec{k}\,\mathcal{U}_s(\vec{k},\eta) + h.c.\Big]\frac{d^3k}{(2\pi)^3}\,, \tag{6.4.16}$$

$$P_{pp} = \frac{1}{3a^4(\eta)}\int \sum_{s=\pm 1}|B_{k,s}|^2\Big[\mathcal{U}_s^\dagger(\vec{k},\eta)\,\vec{\alpha}\cdot\vec{k}\,\mathcal{U}_s(\vec{k},\eta) - \mathcal{V}_s^\dagger(-\vec{k},\eta)\,\vec{\alpha}\cdot\vec{k}\,\mathcal{V}_s(-\vec{k},\eta)\Big]\frac{d^3k}{(2\pi)^3}\,, \tag{6.4.17}$$

where we have used the identities (6.3.25,6.3.27).

The terms ρ_{vac}, P_{vac} are the *vacuum* contributions during (RD); that this is the case should be clear from the fact that the spinors $\mathcal{V}$ are the solutions during (RD) with "out" boundary conditions associated with asymptotic anti-particle states.

The terms ρ_{int}, P_{int} describe the interference between positive and negative (asymptotic) energy solutions akin to the phenomenon of *Zitterbewegung*, and the last terms ρ_{pp}, P_{pp} describe the contributions from particle production with $|B_{k,s}|^2$ being identified as the *distribution function* of the produced particles.

Renormalization:

The expectation value of the energy momentum tensor in a gravitational background features ultraviolet divergences that must be renormalized. The renormalization program has been thoroughly studied in refs.[47, 157, 89, 108, 107, 10, 27, 99, 28, 158], and extended for spin 1/2 degrees of freedom in refs.[68, 81, 19, 90, 63, 129, 128].

The *vacuum terms*, namely those for $B_{k,s} = 0$, feature quartic, quadratic and logarithmic ultraviolet divergences that are renormalized by *subtractions*. The program to renormalize these divergences is well established and has been implemented in refs.[28, 158, 157, 89, 108, 107, 47, 10, 99, 27, 68, 81, 19, 90, 63, 129, 128]. As discussed in detail in these references, the ultraviolet divergences are absorbed into renormalizations of the cosmological constant, Newton's constant G, and into the geometric tensors $H^{(1,2)}_{\mu\nu}$ which result from the variational

derivative with respect to the metric of a gravitational action that includes higher curvature terms $\propto R^2, R^{\mu\nu}R_{\mu\nu}\cdots$. These higher curvature terms are added in the action multiplied by counterterms, which are then required to cancel the coefficients of the geometric tensors in such a way that the renormalized action is the Einstein-Hilbert action. The subtractions necessary to renormalize the (expectation value) of the energy momentum tensor, not only include the ultraviolet divergent terms but depending on the renormalization prescription may also subtract *finite* terms. Therefore, *the finite renormalized energy momentum tensor is not unique* and depends on the renormalization prescription.

Since $|B_{k,s}|$ is exponentially suppressed at large momentum, the interference and particle production contributions in the (RD) era are *ultraviolet finite*, and originate, distinctly in the particle production mechanism, whereas the *vacuum* terms both during (RD) and inflation feature the ultraviolet divergences and are independent of particle production as these are, simply, the zero point contributions. We renormalize the theory by *completely subtracting the vacuum contribution to the energy momentum tensor, both during inflation and the (RD) stage.*

6.4.2 Asymptotics: Kinetic Fluid Form of T^{μ}_{ν}, (DM) Abundance and Equation of State

After subtraction of the vacuum terms, the renormalized $\langle 0|T^{\mu}_{\nu}|0\rangle$ *vanishes identically during inflation* and features only the particle production terms proportional to the Bogoliubov coefficient B_k during (RD). In this latter era, the cosmological dynamics is dominated by the thermalized relativistic degrees of freedom of the standard model (and possibly beyond). Hence, the contribution of the (DM) degree of freedom can be neglected until it begins to dominate near matter radiation equality. As discussed in section (6.2.2) the adiabatic approximation becomes reliable well before matter radiation equality for masses $m \gg 10^{-22}\,\mathrm{eV}$.

In the adiabatic regime the exact solution of the mode equation (6.3.6) for the spinors $\mathcal{U}, \mathcal{V}$ evolves into the WKB adiabatic solution (6.3.8) as discussed in section (6.3.2) and described in detail in appendix (D.4).

Therefore, we can study the contribution of the energy momentum tensor in this regime

by implementing the adiabatic expansion of the mode functions discussed in (6.2.2) and appendix (D.4). We will show self-consistently below that the mass range of interest for (DM) abundance is certainly of the order of several GeV making the adiabatic approximation very reliable for $a(\eta) \gg 10^{-22}$ *well before* matter-radiation equality.

The solution to leading adiabatic order (zeroth order) with "out" boundary conditions (6.3.6) is given by (see Appendix (D.4))

$$h_k(\eta) \propto e^{-i\int^\eta \omega_k(\eta')\,d\eta'} \quad ; \quad \omega_k(\eta) = \sqrt{k^2 + m^2 H_R^2 \eta^2}\,, \tag{6.4.18}$$

in terms of which, the zeroth order normalized spinor solutions are given by (we suppress the conformal time argument for ease of notation)

$$\mathcal{U}_s(\vec{k},\eta) = \frac{e^{-i\int^\eta \omega_k(\eta')\,d\eta'}}{\sqrt{2\omega_k(\omega_k+M)}} \begin{pmatrix} (\omega_k + M)\,\xi_s \\ k\,s\,\xi_s \end{pmatrix}, \tag{6.4.19}$$

$$\mathcal{V}_s(-\vec{k},\eta) = \frac{e^{i\int^\eta \omega_k(\eta')\,d\eta'}}{\sqrt{2\omega_k(\omega_k+M)}} \begin{pmatrix} -k\,s\,\xi_s \\ (\omega_k + M)\,\xi_s \end{pmatrix}. \tag{6.4.20}$$

These spinors are eigenstates of the instantaneous conformal time Dirac Hamiltonian $\vec{\alpha}\cdot\vec{k} + \gamma^0\,M(\eta)$ with eigenvalues $\pm\omega_k(\eta)$ respectively.

The spinors $U^>, V^>$ are given in terms of these by the relations (6.3.19,6.3.20), and the Bogoliubov coefficients are obtained in the previous section. For masses as large as a few GeV these solutions are an excellent approximation for $a(\eta) \gg 10^{-22} \gg a_{eq} \simeq 10^{-4}$, with corrections $\ll \mathcal{O}(10^{-54})$ (see appendix (D.4)).

In appendix (D.4) we find up to second adiabatic order (see eqns. (D.4.18, D.4.19)),

$$V^\dagger(-\vec{k},\eta)\,\Sigma(\vec{k},\eta)\,V(-\vec{k},\eta) = -U^\dagger(-\vec{k},\eta)\,\Sigma(\vec{k},\eta)\,U(-\vec{k},\eta) = -\omega\left[1 - \frac{1}{8}\left(\frac{a'}{ma^2}\right)^2\left(\frac{k}{\gamma^2\,\omega}\right)^2\right], \tag{6.4.21}$$

$$\begin{aligned} V^\dagger(-\vec{k},\eta)\,\vec{\alpha}\cdot\vec{k}\,V(-\vec{k},\eta) &= -U^\dagger(\vec{k},\eta)\,\vec{\alpha}\cdot\vec{k}\,U(\vec{k},\eta) = -\frac{k^2}{\omega_k}\Bigg\{1 - \frac{1}{8\,\gamma^4}\left(\frac{a'}{ma^2}\right)^2 \\ &\times \quad (1+\frac{1}{\gamma})\Big[1 - \frac{1}{\gamma} + 2(1+\frac{1}{\gamma})\left(\frac{\gamma-2}{(1+\gamma)^2}\right)\Big]\Bigg\} \end{aligned} \tag{6.4.22}$$

where $\gamma \equiv \sqrt{1+(k/ma)^2}$ is the local Lorentz factor. The second terms inside the brackets are proportional to $\left(\frac{a'}{ma^2}\right)^2 \simeq 10^{-54}/(m/\mathrm{eV})^2$ near matter radiation equality, and can be safely neglected. Therefore near matter radiation equality it is justified to keep only the leading (zeroth) order term in the adiabatic expansion for the spinors.

The leading adiabatic order spinors (6.4.19,6.4.20) imply that the inteference terms feature the oscillatory factors

$$e^{\pm 2i\int^\eta \omega_k(\eta')\,d\eta'} = e^{\pm 2i\int^t E_k(t')\,dt'} \quad ; \quad E_k(t) = \sqrt{k_p^2(t)+m^2}\ ;\ k_p(t) = \frac{k}{a(\eta(t))}\,, \tag{6.4.23}$$

therefore, the interference terms average out by dephasing on (comoving) time scales $\lesssim 1/m$.

Using the leading order spinors (6.4.19,6.4.20) in the adiabatic regime during (RD) and the relations (6.3.25,6.3.27) among Bogoliubov coefficients, and, neglecting the interference terms by averaging over their rapid oscillations [1], we find

$$\rho(\eta) = \underbrace{-\frac{2}{2\pi^2 a^4(\eta)}\int_0^\infty k^2 dk\,\omega_k(\eta)}_{\textit{zero point energy density}} + \underbrace{\frac{4}{2\pi^2 a^4(\eta)}\int_0^\infty k^2 dk\,|B_{k,s}|^2\,\omega_k(\eta)}_{\textit{particle production}}\,, \tag{6.4.24}$$

$$P(\eta) = \underbrace{-\frac{2}{6\pi^2 a^4(\eta)}\int_0^\infty k^2 dk\,\frac{k^2}{\omega_k(\eta)}}_{\textit{zero point pressure}} + \underbrace{\frac{4}{6\pi^2 a^4(\eta)}\int_0^\infty k^2 dk\,|B_{k,s}|^2\,\frac{k^2}{\omega_k(\eta)}}_{\textit{particle production}}\,. \tag{6.4.25}$$

The zero point energy density and pressure coincide with those obtained in [68]. It is straightforward to show covariant conservation of energy:

$$\dot\rho + 3\,\frac{\dot a}{a}(P+\rho) = 0\,, \tag{6.4.26}$$

where the dot stands for derivative with respect to comoving time t. *This identity holds separately for the vacuum and the particle production components.* We have purposely kept the vacuum terms to highlight the ultraviolet divergence. For example for the vacuum contribution to the energy density, expanding $\omega_k(\eta) \simeq k + M^2(\eta)/2k - 3M^4(\eta)/8k^3 + \cdots$

[1] It turns out that at zeroth adiabatic order the interference terms ρ_{int} vanish identically for each helicity separately, but not for P_{int}.

displays the quartic, quadratic and logarithmic divergences ubiquitous in the energy momentum tensor. Considering higher order adiabatic contributions to $\rho_{vac}; P_{vac}$ it is found that these feature ultraviolet divergences up to quartic adiabatic order[68, 81, 90, 63, 129, 128], therefore the *vacuum* contribution to the energy momentum tensor must be subtracted up to fourth adiabatic order. However, because $|B_{k,s}|^2$ falls off exponentially at large momenta the contribution from particle production is *ultraviolet finite*.

We renormalize the energy momentum tensor by *fully subtracting the zero point, vacuum contributions to all orders in the adiabatic expansion*. See discussion on this point in section (6.6). Because covariant conservation (6.4.26) holds separately for both the zero point and particle production contributions, the subtraction of the zero point contribution does not affect covariant conservation of the particle production term.

Remarkably, the contribution from particle production is identified with the kinetic form of the energy density and pressure, where $|B_{k,s}|^2$ is the distribution function. The factors 4 in the numerator of the contribution from particle production of (6.4.24,6.4.25) arise from two polarizations and particle and antiparticle states, namely four degrees of freedom.

The contributions from particle production are obtained by changing variables to $k = q\sqrt{mH_R}$. The Bogoliubov coefficient $|B_{k,s}|^2$ is solely a function of q and is exponentially suppressed for $q > 1$; the product $q^2|B_{k,s}|^2$ peaks at $q \simeq 0.6$ and drops-off exponentially. This behavior is displayed in figs. (23,24). Writing

$$\omega_k(\eta) = m\, a(\eta)\Big[1 + \frac{q^2}{a^2(\eta)}\,\frac{H_R}{m}\Big]^{1/2} \tag{6.4.27}$$

near matter radiation equality $a \simeq 10^{-4}$ and with $H_R/m \simeq 10^{-35}(\text{eV})/m$ and $q \simeq 1$ it follows that we can safely approximate $\omega_k(\eta) \simeq ma(\eta)$ for $m \geq 10^{-29}\,\text{eV}$, implying that this is a non-relativistic species. Furthermore, consistently with the approximation of superhorizon modes, the momentum integrals in (6.4.24,6.4.25) must be cutoff at a scale $k_c \simeq 1/\eta_R = \sqrt{H_R H_{dS}}$, in terms of the variable q this implies a cutoff $q_c \simeq \sqrt{H_{dS}/m} = 1/\varepsilon \gg 1$, however, because $|B_{k,s}|^2$ is exponentially suppressed for $q > 1$ the upper limit can be safely taken to infinity. Therefore, the particle production contributions to the energy density and pressure

are given in terms of the "emergent" temperature T_H by

$$\rho_{pp}(\eta) = \frac{4\sqrt{2}\,m}{\sqrt{\pi}\,a^3(\eta)}\left[mT_H\right]^{3/2}\underbrace{\int_0^\infty q^2\,|B(q)|^2\,dq}_{0.023}\,, \tag{6.4.28}$$

$$P_{pp}(\eta) = \frac{8\sqrt{2\pi}}{3\,m\,a^5(\eta)}\left[mT_H\right]^{5/2}\underbrace{\int_0^\infty q^4\,|B(q)|^2\,dq}_{0.01}\,. \tag{6.4.29}$$

If $|B(q)|^2$ in the integrands of (6.4.28,6.4.29) is replaced by $\frac{1}{4}\,e^{-\frac{k^2}{2mT_H}}$ we find the numerical values in these expressions to be $0.02\,,\,0.0095$ respectively. This similarity has a remarkable consequence: noticing that the pre-factor $1/4$ that multiplies the Maxwell-Boltzmann distribution in the asymptotic limit of $|B(q)|^2$ in (6.3.43) cancels the factor 4 in the particle-production contributions to (6.4.24,6.4.25) leads us to conclude that the abundance and the equation of state differ only by $\simeq 10\%$ from those obtained with a Maxwell-Boltzmann distribution function for a *single non-relativistic degree of freedom at temperature T_H and vanishing chemical potential* consistent with particles and antiparticles being produced with equal abundance.

Since the energy density redshifts as matter, we obtain (with $\rho_c = 3H_0^2/8\pi G \simeq 0.4\,\times 10^{-10}\,(\mathrm{eV})^4$, and $\Omega_{dm} \simeq 0.25$)

$$\frac{\Omega_{pp}}{\Omega_{dm}} = a^3(\eta)\,\frac{\rho_{pp}(\eta)}{0.25\,\rho_c} \simeq \left(\frac{m}{3\,.10^8\,\mathrm{GeV}}\right)^{5/2}. \tag{6.4.30}$$

The equation of state parameter is given by

$$w(a) = \frac{P_{pp}(\eta)}{\rho_{pp}(\eta)} \simeq \frac{2\pi}{6\,a^2(\eta)}\left(\frac{T_H}{m}\right). \tag{6.4.31}$$

These results differs by $\lesssim 10\%$ from those obtained for a single a non-relativistic degree of freedom with a Maxwell-Boltzmann distribution function with a temperature $T_H = H_R/2\pi$ since for non-relativistic particles $w \simeq < v^2 > /3$ where $< v^2 >$ is the velocity dispersion.

These results suggest that this *nearly thermal* fermionic species with $m \simeq 10^8\,\mathrm{GeV}$ can be produced with the correct dark matter abundance and features the equation of state of cold dark matter. Such value of the mass is consistent with our main approximation $m/H_{dS} \ll 1$ and the upper bound from Planck for $10^8\,\mathrm{GeV} \ll H_{dS} \lesssim 10^{13}\,\mathrm{GeV}$.

We also note the following *consistency aspects*:

i:) range of momenta: The integrals for the abundance and pressure are dominated by the range $q \simeq 1$, namely, momenta $k \simeq \sqrt{mH_R}$. Therefore for momenta in this range it follows that $k\eta_R \simeq \sqrt{m/H_{dS}} = \varepsilon \ll 1$ for the values of m that saturate the dark matter abundance and H_{dS} in the above range. Therefore the integrals are dominated by wavelengths that are superhorizon at the end of inflation, *consistently with one of our main approximations*.

ii:) neglect of $\mathcal{O}(\varepsilon)$ terms: In the calculation of the Bogoliubov coefficients we have neglected $\mathcal{O}(\varepsilon)$ terms both in the spinors and the functions $\mathcal{F}, \mathcal{H}$. Since the integrals are dominated by the region $q \simeq 1 \gg \varepsilon$ and is suppressed at small momenta by phase space $\propto q^2$, neglecting these terms is warranted. Including these terms yields corrections of $\mathcal{O}(\varepsilon)$.

6.5 Isocurvature Perturbations

6.5.1 During Inflation

In the case of bosonic theories, adiabatic and entropy perturbations from inflation have been studied in refs.[92, 48, 20] in the case where the bosonic fields associated with curvature and entropy perturbations both acquire expectation values. Adiabatic and isocurvature perturbations result from linear combinations of fluctuations of the different bosonic fields around their respective expectation values. The case in which *only* the inflaton field acquires an expectation value was addressed in ref.[56] within the context of (bosonic) superheavy dark matter produced during the inflationary era. This study recognized that in the case in which the dark matter field does *not* acquire an expectation value the treatment of isocurvature perturbations must be modified substantially. In particular, in absence of an expectation value for the entropy field there is no mixing between the fluctuations of this and the inflaton field and no cross correlations between adiabatic and isocurvature perturbations to linear order. Several subtleties on the interpretation of isocurvature perturbations in the bosonic case have been discussed in ref.[104].

A similar situation arises in the case of fermionic fields since these cannot acquire an expectation value. Fermionic isocurvature fluctuations were studied in ref.[57] within a model that couples fermions to another scalar field via a Yukawa coupling. Although the comoving isocurvature perturbations are defined by the following correlation function of the (DM) energy momentum tensor

$$\int \frac{d^3r}{(2\pi)^3}\, e^{i\vec{k}\cdot\vec{r}}\, \langle \delta(\vec{x})\; \delta(\vec{x}+\vec{r})\rangle \propto \mathcal{P}^{(dm)}(k)\,, \tag{6.5.1}$$

where

$$\delta(\vec{x}) = \frac{T^{(dm)}_{00}(\vec{x}) - \langle 0|T^{(dm)}_{00}(\vec{x})|0\rangle}{\rho^{(dm)}} \tag{6.5.2}$$

$$\rho^{(dm)} = \langle 0|T^{(dm)}_{00}(\vec{x})|0\rangle\,, \tag{6.5.3}$$

the authors of ref.([57]) only consider the correlations involving the composite operator $m\overline{\psi}\,\psi$ and take $\rho^{(dm)} \equiv m\langle\overline{\psi}\,\psi\rangle$.

The case that we study here departs from the model studied in ([57]) in several crucial aspects: **i:)** we do not consider *any* coupling of the fermionic fields to any other bosonic field, **ii:)** the fermion field in our case is in the Bunch-Davies vacuum state. As we discussed in detail in the previous section, we renormalize the energy momentum tensor by *completely subtracting the vacuum contribution*, hence during inflation the *renormalized* $\rho^{(dm)} = 0$. Therefore, the (DM) energy density perturbation (6.5.3) cannot even be defined in the case that we study here.

As discussed in section (6.4) and in more detail in refs.[28, 157, 89, 108, 107, 47, 10, 99, 27, 68, 81, 19, 90, 129] the expectation value of the energy momentum tensor features quartic, quadratic and logarithmic divergences, these are renormalized by *subtractions* absorbed in the counterterms in the gravitational action described in section (6.4). The *finite* part of $\langle 0|T_{\mu\nu}|0\rangle$ is not unique and depends on the renormalization prescription. When the field acquires an expectation value (background) the identification of $\rho^{(dm)}$ as that from the background energy momentum tensor, and δ as the contribution to the energy momentum tensor *linear in the fluctuations of the field* are unambiguous. However, in absence of a background expectation value, the energy momentum tensor is at least quadratic in the fluctuations and

its renormalization yields a finite part that depends on the renormalization procedure. In this scenario $\rho^{(dm)}$ and $\delta\rho$ are not uniquely defined. Because we subtract the full expectation value of the energy momentum tensor in the Bunch-Davies vacuum state, it follows that $\rho^{(dm)} = 0$ during inflation in our renormalization scheme.

Therefore, neither the analysis of ref.([56]) nor that of ref.([57]) which specifically considers fermionic degrees of freedom, applies to the case that we study here.

6.5.2 Post Inflation

The discussion above has focused on the generation of entropy perturbations *during inflation* and the applicability of the framework introduced in ref.[56, 57]. However, the relevant aspect is how entropy (isocurvature) perturbations affect the temperature power spectrum of the (CMB). In the usual approach to cosmological perturbations, adiabatic and isocurvature perturbations during inflation provide the initial conditions of the respective perturbations upon horizon re-entry during the radiation (or matter) dominated era. As discussed in detail in refs.[20, 48], the initial conditions of isorcurvature perturbations are determined by the set of transfer functions discussed in ref.[48]. These, in turn, are proportional to the "mixing" (or correlation) angle which is determined by the expectation value of the entropy field, and *vanishes identically* in the fermionic case.

Furthermore, as we discussed above the framework introduced in ref.[57] cannot be applied directly to the case that we study because the renormalization procedure that we follow subtracts the full expectation value of the energy momentum tensor in the Bunch-Davies vacuum during inflation. Therefore the background density vanishes identically in our case. This directly implies that the initial conditions for isocurvature perturbations during the radiation dominated era *cannot* be determined during the inflationary stage. In the radiation era the energy density and pressure feature three contributions: the vacuum contribution is subtracted out in the renormalization procedure, the interference term is rapidly oscillating in the adiabatic regime (for the energy density it vanishes at the leading adiabatic order) and therefore its expectation value averages out on short time scales, and the contribution from particle production, which in the adiabatic regime features the kinetic fluid form. It is this

latter term that is the relevant one (after renormalization) to understand dark matter perturbations, the distribution function is completely determined by the Bogoliubov coefficient $|B_k|^2$. The influence of isocurvature perturbations on the (CMB) is a result of solving the system of Einstein-Boltzmann equations for *linear* cosmological perturbations, in which $|B_k|^2$ is the distribution function of the *unperturbed* (DM) component, and ρ_{pp} (6.4.24) describes the *background density*. This set of Einstein- Boltzmann equations must be appended with initial conditions, which are determined from the respective super-horizon perturbations at the end of inflation. From the above discussion, it is clear that in the case of fermions, the proper initial conditions for isocurvature perturbations remain to be understood.

The corollary of this discussion is that a proper definition of the power spectrum of entropy perturbations in the case when the fields do *not* acquire expectation values remains to be understood at a deeper level. The caveats associated with the renormalization of the energy momentum tensor along with its correlations remain to be clarified in a consistent and unambiguous manner. These include a proper account of the fact that there is no natural manner to renormalize the divergences in a power spectrum obtained from the connected correlation function of the energy momentum tensor. These remain even when the zero point contribution to the energy density is completely subtracted. The contribution of zero point energy correlations to non-linear perturbations merits deeper scrutiny, *since even the fluctuations of the inflaton yield zero point contributions to the energy density and all other fields that are either produced or excited post-inflation presumably also contribute to the zero point energy density during inflation.* A satisfactory resolution of these important issues, necessary to quantify reliably the impact of *non-linear* entropy perturbations is still lacking, and is clearly well beyond the scope of this study.

6.6 Discussion

On reheating:

The non-equilibrium reheating dynamics leading to a (RD) dominated era after inflation, is still a subject of much research. Reheating dynamics is not universal, as a large body of

studies show, depending on particular forms for the inflaton potential and the couplings of particles within and beyond the standard model to the inflaton and/or other degrees of freedom, thereby yielding model dependent descriptions with widely different time scales depending on generally unknown couplings and masses. See ref.[9] for a review.

One of our main assumptions is to focus on wavelengths that are superhorizon at the end of inflation. Two aspects of this assumption justify one of our main approximations, that of instantaneous reheating: the dynamics of the mode functions for these wave-vectors is on long time scales, hence insensitive to the reheating dynamics occurring on much shorter time scales. Furthermore, in principle, wavelengths larger than the particle horizon are causally disconnected from the microphysical processes of thermalization. While this assumption *seems* physically reasonable, it must be tested quantitatively. This requires studying a particular model of reheating dynamics, which however, would yield conclusions that would not be universally valid. Perhaps a simple model that dynamically and *continuously* interpolates (with continuous scale factor and Hubble rate) between a near de Sitter inflationary stage and a post-inflation (RD) stage would illuminate the validity of the instantaneous approximation. Such study would, undoubtedly, require a substantial numerical effort to solve the mode equations during the transition and matching to the solutions in the subsequent (RD) era. Clearly such a study is beyond the scope of this article but merits further attention.

Radiation density vs number of degrees of freedom:

During (RD) the Hubble rate is proportional to $\sqrt{g}$ with g the effective number of ultrarelativistic degrees of freedom. In our analysis we took Ω_R to be the radiation component today, corresponding to 2. Therefore the value of H_R (6.2.34) and consequently of T_H in (6.4.28,6.4.28) scales as $\sqrt{g/2}$. For a fixed value of the mass m the ratio (6.4.30) is multiplied by a factor $(g/2)^{3/4}$. If we assume only standard model degrees of freedom being thermalized after reheating, $g \simeq 100$, in turn this implies that the numerator in the bracket of (6.4.30) is replaced by $m \to \quad \simeq 3\,m$. Hence the value of the mass that saturates the (DM) abundance is replaced by $m \simeq 10^8\,\mathrm{GeV}$, a simple rescaling by a factor $\mathcal{O}(1)$. Therefore, just taking the radiation fraction to be today's value yields a lower bound on the abundance and *upper bound on the mass* that saturates the (DM) abundance. In any extension beyond the standard model g will be larger, this implies that the ratio (6.4.30) must be multiplied by

$(\frac{g}{2})^{3/4}$ and the equation of state $w \to w\sqrt{g/2}$. The main conclusions remain the same with only a quantitative change: in the case of the standard model with $g \simeq 100$, by a factor of $\mathcal{O}(1)$ in the mass bound and abundance, and a factor $\simeq 10$ in the equation of state, which, however will still describe cold dark matter.

When are particles produced?

This question does not have a unique answer. As discussed in refs.[99, 64] a *time dependent* number operator for produced particles depends on the basis to define these particles. Different definitions or basis correspond to including higher adiabatic orders. While all these definitions yield the same number of particles *asymptotically at long time* when the adiabatic approximation becomes reliable, they differ in the production dynamics during the non-adiabatic stages. This fact has been discussed in detail in ref.[104] and illustrated with various examples in ref.[64]. We emphasize that we do *not* introduce a number operator associated with a particular definition, instead we study the full energy momentum tensor and unambiguously extract the contribution of produced *particles* asymptotically when the adiabatic approximation is very reliable. During the non-adiabatic stages at the end of inflation and early (RD) era, different definitions will yield very different dynamics. Furthermore, as emphasized above, the continuity of the solutions of the Dirac equation, along with the continuity of the scale factor and Hubble rate at the transition from inflation to (RD) ensure that the energy momentum tensor is *continuous* across the transition. Therefore there is no "burst" of particle production at the transition.

Renormalization:

We have emphasized that the renormalization scheme that we implement subtracts completely the zero point contribution both during inflation and in (RD). Such scheme is, in fact, completely consistent with the usual working assumptions in (semiclassical) cosmology during and after inflation. For example, in the case of the inflaton, the background contribution to the energy momentum tensor is separated and assumed to drive inflation, the linearized perturbation of the energy momentum tensor around the background sources linear metric perturbations, but the quadratic and higher terms in the fluctuations are generically *neglected*. However, these terms feature the ultraviolet divergences that must be renormalized; in not including this contribution in Einstein's equations, it is effectively completely

subtracted out. Furthermore, if the standard model degrees of freedom are truly fundamental, they all contribute to the energy momentum tensor during inflation as well, when, presumably, all of these fields are in their (Bunch-Davies) vacuum state and their contribution amounts to zero point energy density and pressure. Not including their contribution in the dynamics of the geometry is tantamount to subtracting completely their contribution to the energy momentum tensor. In the (RD) era, the energy density of particles in thermal equilibrium is the expectation value of the Hamiltonian in the thermal density matrix and features the zero temperature zero point energy, which is ultraviolet divergent and is subtracted out. Therefore, the renormalization scheme that we adopt is consistent with the usual subtraction of zero point energies in cosmology.

Comparison to previous work:

In refs. [53, 126] the gravitational production of fermions was studied. Our independent analysis agrees with some of these results while also presenting crucial differences. Regarding points of agreement: 1.) The long wavelength limit of the Bogoliubov coefficient $|B_{k,s}|^2 \to 1/2$ as $k \to 0$ is consistent with the Pauli blocking term in Fermi-Dirac distribution and confirms a similar limit in ref.[53]. 2.) For $m \ll H_{dS}$, we find that the final abundance does not feature any dependence on the inflationary stage in agreement with the results of ref.[53]. Moreover we find that this abundance has an overall dependence on the mass scale of the fermion species consistent with the result of [126]. 3.) The abundance we obtain saturates the necessary dark matter energy density at the same mass scale as obtained in [53, 126]. We note that this is likely a consequence of m and H_R (the Hubble scale during RD) being the only relevant scales in the $m \ll H_{dS}$ scenario.

However, we also recognize important differences in our results from the literature: 1.) For large k, our distribution given by (6.3.45) is in stark contrast to the behavior shown in fig. (1) of [53] (see $m \ll H_{dS}$ case). The authors quote a power law $|B_{k,s}|^2 \simeq k^{-4}$ for large k regarding modes which are super-horizon at the end of inflation. This disagrees with our description of Maxwell-Boltzmann-like exponential behavior for these same modes. We do not understand the origin of this important difference. 2.) The matching conditions employed in [53] for enforcing continuity of the mode functions from inflation to RD are quite distinct from our procedure. We perform an in-out calculation, analytically solving the equations of

motion for the mode functions in the $m \ll H_{dS}$ limit. While the solution in the inflationary regime is fixed by our initial condition (BD vacuum, in-state), the solution in RD regime must be the *general solution* constructed out of a linearly-independent combination of solutions. Each *particular solution* of this linear combination smoothly, asymptotically matches onto our adiabatic, out-states (i.e. our particle and anti-particle states with associated u-type and v-type spinors.) Thus our matching condition leads to (6.3.19,6.3.20) where a u-type spinor in inflation is a linear combination of u-type and v-type spinors in RD. In [53], the u-type spinors of inflation are matched with solely u-type spinors during RD. We believe this important difference is a result of the authors in [53] using a time-dependent particle number which we *do not* resort to for reasons discussed above. 3.) Neither [53] nor [126] obtain the energy density or pressure. Given their result of $|B|^2 \propto 1/k^4$ these quantities would depend logarithmically on H_{dS} as discussed above. 4.) In [53], the authors introduce an upper bound on the mass of the dark fermion candidate for their calculation to be consistent. When this upper bound is imposed the produced particle abundance becomes negligible and cannot saturate the necessary dark matter abundance. Conversely, in our calculation we do not find any upper bound more restrictive than $m \ll H_{dS}$ making our result (6.4.30) robust and general. To be clear, we have shown self-consistently, that only the low momentum, superhorizon modes contribute to the abundance and equation of state; therefore, our instantaneous reheating approximation is well-justified and our results are insensitive to any reheating model-dependent parameters.

Fermions vs Bosons:

Ref. [104] studied the cosmological particle production of scalar particles both minimally (MC) and conformally (CC) coupled to gravity focusing on ultralight dark matter candidates ($m \ll H_{dS}$) under the same assumption of an instantaneous transition to the (RD) era. Thus we can now compare the results of that study with the analysis conducted here. The result for the abundance in the bosonic (CC) case given by eqn. (V.42) in ref.[104] is remarkably similar to the fermionic abundance (6.4.30) after the proper rescaling of the energy units. However, the similarity of the results conceals very important differences between the bosonic and fermionic cases.

First we highlight the differences in the produced particle distribution (focusing on the

asymptotic regimes) using equations (6.3.43) and (III.63, III.69 from [104]):

$$k \ll \sqrt{mH_R}:$$
$$N_{k,s} \simeq \frac{1}{2} \text{ (Fermions)} \quad N_k \propto \frac{1}{k} \text{ (CC)} \quad N_k \propto \frac{1}{k^3} \text{ (MC)}$$

$$k \gg \sqrt{mH_R}:$$
$$N_{k,s} \simeq e^{-\frac{k^2}{2mT_H}} \text{ (Fermions)} \quad N_k \propto \frac{1}{k^8} \text{ (CC)} \quad N_k \propto \frac{1}{k^4} \text{ (MC)}$$

In all three cases the distribution function is peaked at low co-moving wave vectors. However, in the fermion case it is bound by Pauli blocking at very low momentum reaching the maximum value 1/2 and is *exponentially* suppressed for large momenta by the thermal factor, while in the bosonic case the distribution function diverges as a power law in the infrared and falls off with a different power law at large momentum. The distribution functions for the bosonic (CC) and the fermionic case are displayed in Fig. (26)).

For minimally coupled bosons extracting the matter-like contribution to the energy density (the component which redshifts as $1/a^3(\eta)$) requires introducing an upper integration bound ($k \lesssim ma_{eq}$). When combined with the stipulation of superhorizon modes at the end of inflation ($k\eta_R \ll 1$), this results in an upper mass bound $m \lesssim \frac{1}{a_{eq}\eta_R} \simeq 0.01\,\text{eV}$ for ultralight, non-adiabatic particle production. One *does not obtain* this bound in the case of fermions as the exponential suppression of the distribution function permits one to integrate over all momenta self-consistently as discussed above. Thus, one can consider non-adiabatic particle production of TeV-scale fermions (or even higher) with only $m \ll H_{dS}$ required.

The comparison between fermions and conformally coupled bosons is more apt as both cases obey the same de Sitter mode equation for superhorizon modes (for $m \ll H_{dS}$) (6.3.3). This is unsurprising since in either case there is no direct coupling between the scalar curvature and the quantum fields. However, despite these similarities with conformally coupled bosons, the fermion mode functions *do not* feature an infrared enhancement (compare (6.3.33) with (III.12) of [104]) unlike those of either bosonic case. This discrepancy is a consequence of the normalization of the fermion spinors, and ultimately the canonical anti-commutation relations and Pauli blocking, and explains the differences in the low momentum

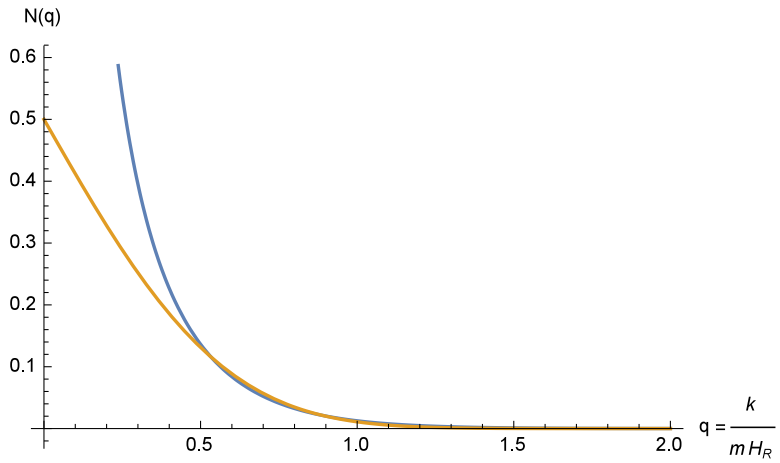

Figure 26: The produced particle distributions N(q) where $q = \frac{k}{mH_R}$ for conformally coupled bosons (blue) and fermions (gold). (Colors available online.)

behavior of the distribution functions (see Fig. (26)). These differences in the distribution function are not a just a formal issue, the *moments* of the distribution function will be very different. These moments enter in the Boltzmann hierarchy for the coupled radiation-matter-gravitational perturbations during the (RD) era prior to matter radiation equality. Therefore, despite the similarity in the abundance between the bosonic (CC) and fermionic cases, we expect substantial modifications in the transfer functions obtained from Boltzmann codes from the two very different distribution functions. These aspects remain to be studied further, however they are beyond the scope of this article.

On thermality:

A noteworthy aspect of our result is a near thermal distribution of produced particles with the distribution function (6.3.45). It yields a near thermal abundance and equation of state very similar to that of one non-relativitistic degree of freedom with a Maxwell-Boltzmann distribution at the "emergent temperature" T_H. The surprising emergence of this temperature is unexpected because an (RD) cosmology does not feature an event horizon, hence this temperature cannot be identified with Gibbons-Hawking radiation[91]. Aspects of thermality in the distribution of particles produced via cosmological expansion were also

revealed in early work in refs.[13, 51] in very different cosmological settings. Ref.[13] studied cosmological production in a radiation dominated cosmology *including and extending the singularity*, the authors find a distribution of particles that is also non-relativistic with en effective temperature (see also [28] section 3.5). A similar conclusion was reached in ref.[51] that studied cosmological particle production in a path-integral framework but with a different cosmological model with scale factor $\propto t$ (t being comoving time), and an effective temperature that is $\propto a(t)$. Our results apply to a very different situation since we consider fermion fields, initial "in" conditions during inflation, and match onto (RD). Furthermore, the "emergent temperature" that we find, T_H, is independent of time. Therefore, while the results of the early references [13, 51] suggest a general "thermality" aspect of the distribution of produced particles, the relationship to our results, if any, and the physical origin of the near thermal spectrum is not clear to us.

Pair annihilation into gravitons:

Because we are considering that the dark matter candidate only couples to gravity, the process of particle anti-particle pairs annihilating into gravitons could lead to a depletion of the (DM) abundance. Fundamentally, to understand the dynamics of this process one would set up a Boltzmann-like equation with a loss term determined by the annihilation process, assuming a negligible abundance of gravitons one can, in principle, neglect the inverse process. Such an equation would feature the six-dimensional momentum integrals of the distribution functions for the annihilating pairs multiplied by the transition probability obtained from the time evolution via the interaction picture. For the case of annihilation into gravitons, writing the metric as $g_{\mu\nu} = \overline{g}_{\mu\nu} - \frac{h_{\mu\nu}}{M_{Pl}}$ with $\overline{g}_{\mu\nu}$ being the background metric and $h_{\mu\nu}$ the canonically normalized quantum fluctuations of the gravitational field, the coupling to gravitons is given by

$$\frac{h_{\mu\nu}}{M_{Pl}}\, T^{\mu\nu}\,. \tag{6.6.1}$$

This is the interaction vertex that is required in the interaction picture to obtain the transition probability. The usual implementation of S-matrix theory taking the long time limit to obtain the transition probability (per unit time) is unreliable for the following conceptual and technical reasons.

In transverse-traceless gauge, the graviton field is expanded into canonical creation and

annihilation operators for each polarization $(+, \times)$ and mode functions solutions of the Klein-Gordon equation for a massless field minimally coupled to gravity. Conceptually the notion of particles is physically unambiguous only in the asymptotic long time regime. Using the basis of fermion "out" states entails that during the *non-adiabatic* regime, during which most of the particle production takes place, the mode functions for these states are the parabolic cylinder functions, not the usual Minkowski type exponentials $e^{\pm i\omega t}$. The mode functions for gravitons during (RD) are actually of the form $e^{\pm ik\eta}/a(\eta)$, and while spatial momentum is conserved (in a spatially flat metric with three space-like Killing vectors) energy is *not* conserved. Taking the infinite time limit in the transition amplitudes as is implicit in an S-matrix calculation, is obviously unreliable in a rapidly expanding cosmological setting. Therefore a calculation even to lowest order is very different from that in Minkowski space time and confronts daunting technical challenges, that to the best or our knowledge have not yet been discussed, much less worked out in the literature. For example, even during the adiabatic regime the correct assessment of particle decay in an expanding cosmology is technically challenging as can be gleaned from the work in refs. [105, 36] with results which are generally very different from those expected in Minkowski space time. A similar calculation for annihilation has not been carried out in the literature even in the adiabatic regime.

Therefore, in light of these conceptual and technical challenges it should be clear that a reliable quantitative assessment of the influence of pair annihilation in the expanding cosmology is well outside the main scope of this article and must await the development of new techniques. Here we can at best provide a very preliminary and rough estimate for the depletion from pair annihilation into two gravitons at second order in the interaction based on a Minkowski intuition and the main scales involved. Assuming (without warrant) that Minkowski-like dynamics provides a useful guide, the main ingredients in this argument are the following: i) there are initially no gravitons so that the inverse process does not occur (this by itself is a major assumption since gravitons are produced during and post inflation), ii) the strength of the vertex (for the spatial components) (6.6.1) is determined by the typical momentum in the distribution functions $\simeq \sqrt{mH_R}$, and the typical energy scale $\simeq m$, which we take as the main scale for the fermionic degrees of freedom. Therefore

the effective coupling in this vertex is $\simeq m/M_{pl} \simeq 10^{-10}$ for $m \simeq 10^8\,\mathrm{GeV}$ which saturates the bound for (DM) abundance (6.4.30). The intermediate state yields a fermion propagator with a typical scale $1/m$, the comoving number density is $n \simeq (mH_R)^{3/2}$ and the probability for pair annihilation is $\propto n^2$. Thus we are led to conclude that on dimensional grounds, and within the assumption of the validity of a Minkowski space-time estimate, at second order in the vertex

$$\frac{\delta n}{\delta t} \simeq \frac{n^2}{m^2}\left(\frac{m}{M_{Pl}}\right)^4, \tag{6.6.2}$$

integrating this expression during a time interval $\Delta t \simeq 1/H_R$ yielding a total depletion $\Delta n = \delta n/H_R \delta t$, we find

$$\frac{\Delta n}{n} \simeq \left(\frac{H_R}{m}\right)^{1/2}\left(\frac{m}{M_{Pl}}\right)^4 \simeq 10^{-65}\,. \tag{6.6.3}$$

Therefore, this assessment suggests that pair annihilation into gravitons will not affect the abundance. However this result should be interpreted as a guide with all of the caveats discussed above, a more detailed assessment with new methods that can describe consistently the time evolution of annihilation during the non-adiabatic regime is needed. Such method should not rely on the usual S-matrix approximations of taking the long time limit with manifest energy conservation and should input the correct mode functions. The program to develop these new methods and applying them consistently to the calculation of pair annihilation is well beyond the scope of this article and merits a detailed study.

6.7 Conclusions and Further Questions

We have studied the gravitational production of fermionic dark matter during inflation and radiation domination under a minimal set of assumptions: i) its mass m is much smaller than the Hubble scale during inflation, described as de Sitter space time, ii) only interact gravitationally, iii) fermions are in the Bunch-Davies vacuum state during inflation, iv) focus on wavelengths that are well outside the Hubble radius at the end of inflation, v) a rapid transition from inflation to (RD).

We solve exactly the Dirac equation during inflation and radiation domination with "in" and "out" boundary conditions and match the solutions at the transition. Particle-antiparticle pairs are produced non-adiabatically with a distribution function $|B(k)|^2 = \frac{1}{2}\left[1-\left(1-e^{-\frac{k^2}{2mT_H}}\right)^{1/2}\right]$ exhibiting an *emergent temperature* $T_H = H_0\sqrt{\Omega_R}/2\pi \simeq 10^{-36}\,\mathrm{eV}$ with H_0, Ω_R the Hubble expansion rate and radiation fraction today respectively. This distribution function is remarkably similar to a Maxwell-Boltzmann distribution for a non-relativistic species with vanishing chemical potential, in agreement with the fact that particles and antiparticles are produced with the same distribution.

With the exact solution we obtain the full energy momentum tensor, discuss in detail its renormalization and extract unambiguously the contribution from particle production near matter radiation equality. We show that after renormalization this contribution features the kinetic-fluid form with $|B(k)|^2$ as the distribution function. We obtain the energy density ρ_{pp}, pressure P_{pp} and equation of state parameter $w(a)$ of the produced particles factor a

$$\begin{aligned}
\rho_{pp} &= 0.074\,\frac{m}{a^3}\left[m\,T_H\right]^{3/2} \\
P_{pp} &= 0.067\,\frac{\left[m\,T_H\right]^{5/2}}{m\,a^5} \\
w(a) &= \frac{P_{pp}}{\rho_{pp}} \simeq \left[\frac{T_H}{m\,a^2}\right],
\end{aligned}$$

where a is the scale factor. Remarkably these correspond to a *nearly thermal* non-relativistic species in equilibrium at temperature T_H and vanishing chemical potential, with the equation of state function related to the velocity dispersion for this species as $w(a) \simeq \langle V^2\rangle/3$. The departure from an *exactly* thermal non-relativistic single species with a Maxwell-Boltzmann distribution at temperature T_H is $\lesssim 10\%$. The reason behind this small discrepancy is the behavior of $|B(k)|^2$ as $k \to 0$.

The ratio of the abundance of produced particles to the dark matter abundance is given by

$$\frac{\Omega_{pp}}{\Omega_{dm}} = \left(\frac{m}{3\,.10^8\,\mathrm{GeV}}\right)^{5/2}. \tag{6.7.1}$$

Therefore, a fermionic particle with mass $\simeq 10^8\,\mathrm{GeV}$ can be produced gravitationally, with the correct dark matter abundance and constitutes cold dark matter.

The integrals yielding ρ_{pp}, P_{pp} are dominated by wavevectors $k \lesssim \sqrt{2mT_H}$ and these correspond to wavelengths that are well outside the Hubble radius at the end of inflation, confirming self-consistently the validity of the main approximation of focusing solely on these wavevectors for the matching conditions from inflation to (RD).

We discuss important aspects of renormalization during both the inflationary and (RD) era which imply subtle uncertainties associated with an unambiguous determination of isocurvature perturbations from gravitationally produced fermions. These uncertainties are not only a characteristic of fermionic degrees of freedom, but apply generally to fields that do *not* acquire an expectation value during inflation and whose energy momentum tensor feature ultraviolet divergences of the zero point contributions that must be renormalized by proper subtractions. These subtractions depend on the particular renormalization scheme, therefore the finite part of the energy density and pressure arising from the renormalization of the zero point contributions would be scheme dependent. Our procedure is to subtract completely the zero point contributions, and we argue that this procedure is implicitly implemented in all treatments of inflationary dynamics. However, the corollary of this subtraction is that the initial conditions for isocurvature perturbations during radiation or matter domination *cannot* be defined during the inflationary epoch. The resolution of these aspects remains a subject of further study.

The origin of thermality in the distribution function is also an aspect that merits further understanding, since it cannot be identified with a Gibbons-Hawking temperature because an (RD) cosmology does not feature an event horizon.

7.0 Conclusions

It is a remarkable fact that the physics of elementary particle interactions, which describes nature at the smallest scales, plays an important role in understanding the evolution of the entire Universe. Our present understanding of cosmology indicates that the Universe evolved from an extremely compact, high temperature initial state. After a brief period of inflation-driven exponential expansion, processes described by the Standard Model of particle physics were responsible for producing the observed primordial abundances of light elements and the cosmic microwave background radiation. The success of these predictions, complemented by astronomical observations of distant galaxies has lead to a paradigmatic cosmological model, ΛCDM. However, the nature of the dark matter and energy which together comprise the majority of the Universe's present energy content remains elusive. Additionally, the mechanism responsible for the observed asymmetric abundance of matter over anti-matter is also unknown. Particle physics models have been the most popular candidate explanations for these cosmological quandaries. Yet, most of these models, particularly in the case of dark matter and baryogenesis, neglect the effects of the expanding spacetime on the evolution of quantum fields, instead leveraging static, Minkowski spacetime descriptions.

The overarching goal of this thesis was to develop and employ a consistent, quantum field theoretic treatment of the dynamics of particles inhabiting the expanding early universe. After quantifying and understanding the effects of this expansion, this novel phenomenology was applied to provide new insights regarding the open questions of particle cosmology, with an emphasis on theories of dark matter. To facilitate this goal, the canonical process of particle decay, albeit in the post-inflationary cosmological epoch, was studied in chapters 3 and 4. Implications for dark matter and baryogenesis were also discussed. In chapters 5 and 6, the process of non-adiabatic, gravitational/cosmological particle production was investigated as a dark matter production mechanism . Here we summarize the main findings of these two projects.

7.1 Cosmological Particle Decay

The goal of this project was to obtain the decay law for a massive scalar particle produced in the early universe. This particle is described as an excited state of a field quantized in FRW spacetime. The main assumptions and methods of the analysis are as follows:

- Conformal Time: The FRW metric is conformal to the Minkowski metric. Working in conformal time $d\eta = \frac{dt}{a(t)}$ is more convenient for many calculations ($a(\eta)$ is the scale factor).
- Adiabaticity: The equations of motion for even free scalar fields quantized in FRW spacetime are difficult to solve. Exact solutions only exist for separate stages of cosmology (e.g. Matter Domination) or for model expansion histories. We instead focus on obtaining approximate solutions using the adiabatic expansion [28]. This expansion is valid for as $\delta = \frac{H(t)}{\gamma_k^2(t)E_k(t)} \ll 1$ Where γ_k, H, and E_k are the Lorentz factor (measured by a comoving observer), Hubble parameter, and local energy of the quanta respectively. We obtain approximation solutions to 0th adiabatic order in our analysis.
- Radiation Domination: We restrict ourselves primarily to the cosmological epoch of radiation domination (RD) where most of the interesting particle physics processes occur. However our methods can be extended to matter domination (MD) as well, in principle. Additionally, in RD, the scale factor depends linearly on conformal time which simplifies several calculations, $a(\eta) = H_0\sqrt{\Omega_R}\,\eta$ where H_0 and Ω_R are the Hubble Parameter and present day energy density of radiation.
- Finite Time Evolution of States: Since the usual S-matrix approaches are in general invalid for FRW spacetime, we obtain the decay law using a non-perturbative formalism ubiquitous in quantum optics. In this method the state kets are expanded in the complete set of 0th order adiabatic particle states ($|\psi\rangle = \sum_n C_n(\eta)|n\rangle$), and the interaction picture Schrodinger equation ($i\partial_\eta|\psi(\eta)\rangle = H_I|\psi(\eta)\rangle$) is used to carry out the time evolution yielding coupled differential equations. By choosing the field to be initially in a single particle state ($C_A(\eta_i) = 1$), the decay law and rate can be obtained analytically and are

given by

$$|C_A(\eta)|^2 = e^{-\int_{\eta_i}^{\eta}\Gamma_A(\eta')d\eta'}\,|C_A(\eta_i)|^2 \;\;;\;\; \Gamma_A(\eta) = 2\int_{\eta_i}^{\eta} d\eta_1\,\mathrm{Re}\left[\Sigma_A(\eta,\eta_1)\right]. \tag{7.1.1}$$

where $|C_A(\eta)|^2$ is the survival probability of the initial state.

$$\Sigma_A(\eta;\eta') = \sum_{\kappa}\langle A|H_I(\eta)|\kappa\rangle\langle\kappa|H_I(\eta')|A\rangle \tag{7.1.2}$$

is known as the *self-energy*, with H_I being the interaction Hamiltonian of the theory, and is summed over momenta. Note the lack of the infinite time limit.

7.1.1 Massive Scalar to Scalar Decay

The analysis presented in chapter 3 studied the decay of a massive scalar field, $\phi_1 = \frac{\chi_1}{a(\eta)}$, coupled to a second scalar field with the following interaction Lagrangian density

$$\mathcal{L}_I = -\lambda a(\eta)\,\chi_1\chi_2^2 \tag{7.1.3}$$

The field operators are of course quantized in FRW spacetime, and the methods and assumptions stated previously are employed. The principle findings can be summarized as follows:

- The survival probability of the decaying parent particle is obtained and may be written as an effective time-dependent decay rate $P(t) = e^{-\tilde{\Gamma}_k(t)t}$. The effective rate is characterized by a timescale t_{nr}. For $t \ll t_{nr}$ the decaying particle is relativistic and

$$P(t) = e^{-\frac{1}{3}\Gamma_0 t_{nr}(\frac{t}{t_{nr}})^{\frac{3}{2}}}\;; \tag{7.1.4}$$

  while for $t \gg t_{nr}$ the decaying particle is non-relativistic and

$$P(t) = (\frac{t}{t_{nr}})^{\frac{\Gamma_0 t_{nr}}{2}}\,e^{-\Gamma_0 t}\,. \tag{7.1.5}$$

  In both regimes, Γ_0 refers to the usual Minkowski spacetime decay rate at rest. Generically speaking, the decay of the particle is *slowed* by the expanding spacetime. The reason for this delayed decay is the cosmic redshifting of the particle's local Lorentz factor. Thus, particles "born" with a large local Lorentz factor live longer in an expanding FRW spacetime.

- The expansion of spacetime introduces a new energy uncertainty associated with and determined by the particle horizon ($\frac{1}{H(t)}$). This effect is encapsulated in a result we call the *Cosmological Fermi's Golden Rule*. A distinct consequence of this new energy uncertainty is the relaxing of decay thresholds, permitting the decay to daughter particles *heavier* than the parent. These channels close as the expansion proceeds, and the usual kinematic thresholds seen in laboratory experiments today obtain.

7.1.2 Massive Scalar to Fermion Decay

In chapter 4 we extended the above results to the study of a more physical model: the decay of a Higgs like scalar (ϕ) with Yukawa couplings to fermions (Ψ).

$$\mathcal{L}_{\mathcal{I}} = -Y\chi\bar{\psi}\psi\,;\;\; \chi = \phi\, a(\eta)\,;\;\; \psi = a^{\frac{3}{2}}(\eta)\Psi \tag{7.1.6}$$

Unlike in the previous study, this model is *renormalizable* theory (the self-energy is divergent) which complicates the calculation tremendously. Therefore, in order to simplify the analysis we consider massless fermion daughters. This assumption is well warranted for a heavy Higgs-like scalar within or beyond the Standard Model decaying to any charged lepton or quark (except the top.)

The study of cosmic particle decay into fermionic channels introduces a novel physics phenomenon related to the renormalization: the formation and subsequent decay of a *quasi-particle* state (i.e. a state dressed by fermion/anti-fermion pairs.) We implement a renormalization procedure which permits one to separate the dynamics of dressed-state formation from the decay dynamics since these two processes are *separated by a large time scale*. The key step is the introduction of a renormalization time scale (t_b) which is larger than the dressing time scale yet smaller than the lifetime of the particle. The time dependent decay function is evaluated at this t_b and then subtracted from the general result yielding a finite decay function ($\tilde{\Gamma}(t) - \tilde{\Gamma}(t_b) = \tilde{\Gamma}_S(t;t_b)$). The survival probability of the quasiparticle state (defined at time, t_b) is then given by this new finite decay function

$$P_r(t) = e^{-\tilde{\Gamma}_S(t;t_b)}\, P_r(t_b) \tag{7.1.7}$$

The renormalized survival probability then obeys a dynamical renormalization group equation $\frac{\partial}{\partial t_b} P_r(t) = 0$ and is ultraviolet finite.

Using this dynamical renormalization scheme in conjunction with the methods and assumptions discussed previously we obtain the following results:

- The survival probability of the parent particle is obtained and characterized by a timescale, t_{nr} as in the scalar to scalar case. During the regime $t_b \ll t \ll t_{nr}$, the decaying particle is relativistic, and the survival probability is

$$P(t) = e^{-\frac{2}{3}\Gamma_0 t_{nr}(\frac{t}{t_{nr}})^{\frac{3}{2}}} \tag{7.1.8}$$

  and nearly identical to the decay to scalars case. Again Γ_0 is the usual Minkowski spacetime decay rate at rest.
- However, for $t \gg t_{nr}$ (and t_b) cosmic redshift has rendered the decaying particle non-relativistic, and its survival probability is given by

$$P(t) = [\frac{t}{t_{nr}}]^{(\frac{-Y^2}{8\pi^2})}\, e^{\frac{Y^2}{8\pi^2}(t/t_{nr})^{\frac{1}{4}}}\, [\frac{t}{t_{nr}}]^{\frac{\Gamma_0 t_{nr}}{2}}\, e^{-\Gamma_0(t-t_{nr})} P(t_{nr})\,. \tag{7.1.9}$$

  The power of $\frac{t}{t_{nr}}$ with anomalous dimension and the stretched exponential with power 1/4 are remnants of the formation of a quasiparticle state encoded into the decay function by cosmic redshift. These factors are the prominent difference between the bosonic daughter particles case studied previously. Their presence is a result of the confluence of a renormalizable theory in an expanding spacetime. Specifically, in an expanding spacetime, even at leading adiabatic order, the particle state frequencies (ω_k) are *time-dependent* unlike in Minkowski spacetime. This time-dependence allows "memory" of the transient dynamics associated with the formation of a dressed state to persist and imprint on the decay law.
- In the case of very long lived particles ($Y \lll 1$), we can place an upper bound on the survival probability of a Higgs like scalar produced in the early universe and decaying well into matter domination or beyond. The result is

$$P(z) \geq e^{\frac{-\Gamma_0}{H_0}\Upsilon(z,z_b)}\, P(z_b)\,. \tag{7.1.10}$$

Here the survival probability has been written as a function of redshift, z with z_b being the renormalization scale redshift. The function Υ has the following form

$$\Upsilon(z, z_b) = \int_{\frac{1}{z_b}}^{\frac{1}{1+z}} \frac{da}{\sqrt{a_{nr}^2 + a^2}\sqrt{\Omega_M a^{-3} + \Omega_R a^{-4} + \Omega_\Lambda}} \,. \tag{7.1.11}$$

This function depends only on cosmological parameters and the value of the scale factor at which the decaying particle transitions to being non-relativistic (a_{nr}).

In studying the decay of particles produced in the early universe, while consistently treating the expanding spacetime, two important conclusions can be inferred from these results:

1.) Using decay rates computed in Minkowski spacetime as a measure of decay dynamics is at best an approximation, but in general is problematic since it *underestimates* the lifetime and misses the various temporal behaviors of the survival probability.

2.) Minkowski spacetime inspired approaches are quite handicapped in cosmological settings, for while they are sufficient for describing weakly coupled particles decaying at rest at late times in the expansion history, they clearly miss non-equilibrium dynamics manifest in renormalizable theories. Such dynamics can, in principle, effect baryogenesis, leptogenesis, and other early universe quantum kinetic processes. In particular, the usual result of *detailed balance* in quantum kinetics in Minkowski spacetime results from the consideration of decay and inverse decay processes and as direct consequence of energy conservation. The lack of energy conservation, and the modification of the decay laws in FRW spacetime motivate a future investigation of detailed balance in cosmology, a result which is usually assumed in the physics of the early universe.

7.2 Cosmological Particle Production

The goal of this second project was to study the cosmological particle production of a dark matter field coupled only to gravity. Such a generic and conservative model can, in a sense, be considered the simplest possible dark matter candidate. The particle production is the result of the highly non-adiabatic evolution of the field during even the post-inflationary epoch of the cosmic expansion. The main assumptions of this investigation follow:

- Spectator light field during inflation: We consider the dark matter to be described by quantum field, quantized in FRW spacetime, that does not couple to any other degrees of freedom beyond gravity. It does *not* acquire an expectation value and therefore does not contribute to perturbations in the metric. The particle mass of the field is light compared to the scale of inflation $\frac{m}{H_{dS}} \ll 1$
- Low momentum modes in Bunch-Davies vacuum: We consider the inflationary stage to be exactly de Sitter spacetime. The dark matter field is assumed to be in the Bunch-Davies vacuum state (the ground state seen by a comoving observer.) We focus on field fluctuations with long wavelengths ($\sim$ 1m $\ll \lambda \ll \frac{1}{H_0}$) which include all astrophysical scales. Such modes have the property that they are outside the particle horizon of the Universe at the onset of reheating.
- Instantaneous reheating: We consider an instantaneous, smooth transition from the inflationary stage to the radiation dominated epoch occurring at a conformal time η_R. This allows us to avoid reheating model-dependent conclusions and is consistent with our attention on superhorizon modes which evolve very slowly post-inflation (while outside the horizon) compared to the reheating time-scale.
- Non-adiabaticity: We consider particle production coming from non-adiabatic evolution. For small masses and low momentum modes, the adiabatic condition $\frac{\omega_k'}{\omega_k^2} \ll 1$, (where ω_k is the comoving mode frequency) is violated even during the RD epoch.
- No Backreaction: The RD epoch is dominated by a large number ($\sim$ 100) of Standard Model degrees of freedom which are insensitive to our DM. We therefore neglect any contribution from our single field to the radiation component of the energy density in this phase. Consequently, the spacetime metric is regarded as a true background upon which our field is quantized.

With these assumptions in place we then proceed to compute the particle production in 5 steps. 1.) Solve the equations of motion for the scalar field during inflation exactly, choosing Bunch-Davies initial conditions as previously described. 2.) Solve exactly the equations of motion during RD, obtaining a general solution which, while distinct, asymptotically approaches the adiabatic mode functions in the long time limit. These adiabatic mode functions are identified as particle states which match the free field theory states of Minkowski

spacetime. 3.) Match the inflationary and RD solutions at conformal time η_R enforcing a smooth transition. The matching coefficients, are Bogoliubov coefficients, and yield the amount of particle production. 4.) Compute the energy momentum tensor of our dark matter field. By the onset of the matter dominated epoch, our modes are now well described by the adiabatic approximation. We therefore proceed according to [10] and expand the vacuum expectation values of the tensor to fourth order in the adiabatic expansion before performing a renormalization of the tensor, fully subtracting away the zero-point energy. 5.) Focusing on the dominant, leading order term, we identify the contribution to the energy density and pressure coming from the particle production, compute the relic abudance Ω_{pp} and compare it to the observed dark matter abundance Ω_{DM}.

7.2.1 Scalar Dark Matter

In chapter 5, we studied the cosmological particle production of ultralight scalar dark matter ($m \ll 1\,\mathrm{eV}$) in the early universe. At such a small mass scale, the field exhibits non-adiabatic evolution until the scale factor, $a \gg 10^{-17}$, so there is a long window for this evolution even after the end of inflation $a \simeq 10^{-29}$. We considered both conformal and minimal couplings to the scalar curvature. Using the previously discussed assumptions and procedure, the following results are obtained:

- For both conformal coupling ($\xi = 1/6$) and minimal coupling ($\xi = 0$) the produced particle distribution $\mathcal{N}_k$ is peaked at low comoving momentum (k)

$$k \ll \sqrt{mH_R}: \qquad N_k \propto \frac{1}{k} \ \text{(CC)} \quad N_k \propto \frac{1}{k^3} \ \text{(MC)} \tag{7.2.1}$$

$$k \gg \sqrt{mH_R}: \qquad N_k \propto \frac{1}{k^8} \ \text{(CC)} \quad N_k \propto \frac{1}{k^4} \ \text{(MC)} \tag{7.2.2}$$

  but the minimally coupled case features a significant infrared enhancement, a relic from their inflationary mode function behavior.

- Obtaining the matter-like contribution to the produced particle energy density (the component which redshifts as $1/a^3(\eta)$) requires introducing an upper integration bound ($k \lesssim ma_{eq}$). In combination with requirement of superhorizon modes at the end of inflation, this results in an upper mass bound $m \lesssim \frac{1}{a_{eq}\eta_R} \simeq 0.01\,\text{eV}$ for ultralight, non-adiabatic particle production.
- For conformally coupled scalars, the produced dark matter abundance is negligible in the mass range of interest. For the minimally coupled case, the produced abundance is significant,

$$\frac{\Omega_{pp}}{\Omega_{DM}} = 8.36\left\{\sqrt{m_{ev}}\left[\ln\left[\sqrt{m_{ev}}\right]+36\right]\right\}\left[\frac{H_{dS}}{10^{13}\text{GeV}}\right]^2 \tag{7.2.3}$$

  where m_{ev} is the particle mass in eV and H_{dS} is the scale of inflation. Thus, the abundance depends only on cosmological parameters and the particle mass. The required dark matter abundance is saturated by a minimally coupled scalar with mass $m \simeq 1.5\times10^{-5}\,\text{eV}$. For this mass, we also obtain the equation of state parameter (at matter-radiation equality) and the free streaming length which are $w(a_{eq}) \simeq 2.5\times10^{-14}$ and $\lambda_{fs} \sim 70\,\text{pc}$ respectively. Accordingly, the produced ultralight bosons are still very cold and have a free streaming length comparable to weakly interacting massive particles.

7.2.2 Fermionic Dark Matter

In chapter 6, the process of cosmological particle production was investigated with a fermionic dark matter field subject to the same main assumptions as in the previously studied bosonic case. Fermions require the introduction of spinors which obey orthonormality relations. These relations are used, in tandem with the assumptions and 5 step method discussed previously, to yield the following results:

- Non-adiabatic production of particle-antiparticle pairs yields the distribution function,

$$\mathcal{N}_k = \frac{1}{2}\left[1-\left(1-e^{-\frac{k^2}{2mT_H}}\right)^{1/2}\right] \tag{7.2.4}$$

  possessing an *emergent temperature* $T_H = H_0\sqrt{\Omega_R}/2\pi \simeq 10^{-36}\,\text{eV}$ with H_0, Ω_R being the Hubble expansion rate and radiation fraction of today respectively.

- The temporal equation of motion for the fermion fields (for $m \ll H_{dS}$) during inflation is the same as that for conformally coupled scalars. This is expected, since both types of quantum fields feature no direct dependence on the scalar curvature in their equations of motion. However, despite this similarity, the distribution function for the fermions does not possess the power law scaling seen in the conformally coupled bosonic distribution function, in either limit.
- In the low momentum limit, $k \ll (m\,H_0\,\sqrt{\Omega_R})^{1/2}$ the distribution is maximized at the constant $\mathcal{N}_k \simeq 1/2$. Like the bosonic case, the distribution is largest at low comoving momentum. However, the fermion case is effected by Pauli blocking, a direct consequence of the anticommutation relations enjoyed by the fermion creation/annihilation operators, which produces an upper bound and the distinct low momentum behavior.
- The distribution function, in the large momentum limit $k \gg (m\,H_0\,\sqrt{\Omega_R})^{1/2}$, is highly similar to a Maxwell-Boltzmann distribution for a non-relativistic species albeit with vanishing chemical potential,

$$\mathcal{N}_k \simeq e^{-\frac{k^2}{2mT_H}}\,. \tag{7.2.5}$$

  The absence of a chemical potential is indicative of the fact that the particles and antiparticles are produced with the same distribution.
- Because of the exponential suppression of the distribution function, one can integrate the distribution over all momenta, when extracting the matter-like contribution to the produced particle energy density. Therefore, contrary to the bosonic case, an upper mass bound (beyond $m \ll H_{dS}$) is *not* introduced; this permits the production of much heavier quanta while still considering superhorizon modes. The resulting energy density, pressure, and equation of state parameter are

$$\rho_{pp} = 0.074\,\frac{m}{a^3}\left[m\,T_H\right]^{3/2} \tag{7.2.6}$$

$$P_{pp} = 0.067\,\frac{\left[m\,T_H\right]^{5/2}}{m\,a^5} \tag{7.2.7}$$

$$w(a) = \frac{P_{pp}}{\rho_{pp}} \simeq \left[\frac{T_H}{m\,a^2}\right], \tag{7.2.8}$$

  which surprisingly nearly correspond to a non-relativistic species in thermal equilibrium at temperature T_H with vanishing chemical potential. The discrepancy with the results as

obtained from non-relativistic Maxwell-Boltzmann distribution at the same temperature is $\lesssim 10\%$ as consequence of the low momentum behavior in the fermionic produced particle distribution.

- The produced particle abundance as compared with observed dark matter abundance is

$$\frac{\Omega_{pp}}{\Omega_{dm}} = \left(\frac{m}{3\,.10^8\,\mathrm{GeV}}\right)^{5/2}. \tag{7.2.9}$$

such that dark fermions of mass $\simeq 10^8\,\mathrm{GeV}$ can be produced purely through gravitational interactions, with the correct abundance and a cold equation of state ($w(a_{eq}) \simeq 10^{-49}$).

The results of these studies of purely gravitational particle production, as a direct consequence of protracted non-adiabatic evolution, imply four important conclusions:

1.) Provided the particles are ultralight compared to the scale of inflation $m \ll H_{dS}$, non-adiabatic production is a competition between the mass of the particle and the scale factor range for which non-adiabatic evolution is observed. Increasing the particle mass closes this window earlier, but each produced particle contributes more to the matter energy density. In all studied cases, the particle mass is the more important parameter, and increasing the mass always increases the produced abundance Ω_{pp}. Thus in general a wide mass range admits of non-adiabatic gravitational production. However in the bosonic case, the form of the distribution, in combination with the considering of exclusively superhorizon modes at the end of inflation, imposes a cutoff on the particle mass at $m \lesssim 0.1\,\mathrm{eV}$. Considering heavier bosons violates the assumptions of the calculation.

2.) The assumptions for which these calculation hold are mild. In all cases the distribution is peaked for precisely post-inflation superhorizon modes, exhibiting self-consistency in the calculation. Moreover these calculations focus on the *darkest* of matter, namely particles with purely gravitational interactions. Including interactions with the inflaton, or other fields in the Standard Model or beyond, will introduce additional production mechanisms for a stable (on Hubble scales) dark matter candidate. These production mechanisms will *increase the abundance*. Therefore, crucially, the abundances calculated above represent a baseline for dark matter production. *Any* dark matter model featuring interactions must account for this production mechanism, and hence these abundances represent a generic lower bound for *any interacting species* of long-lived dark matter. In the bosonic case, the

salient mass range for non-adiabatic production is comparable to that of axion-like particle dark matter (ALPs). Since ALP models necessarily entail some production mechanism, the phenomenology of gravitational production in conjunction with that mechanism, should be investigated and in principle can constrain the model's parameter space.

3.) For the minimally-coupled bosons, the produced particle abundance was directly sensitive to the scale of inflation. This is a consequence of their equation of motion during the inflationary phase. Accordingly, the detection of minimally coupled dark bosons would in principle represent a probe of the Hubble parameter during inflation, which is presently unknown and is only tightly bound from above.

4.) For fermions, a nearly thermal distribution function was produced via this mechanism. This is surprising since the initial field configuration is in its vacuum state which is zero entropy. However, the final abundance corresponds to a high entropy, thermal distribution with an *emergent* temperature set by present day cosmological parameters. The origin of this thermality is unclear. This temperature cannot be interpreted as a Gibbons-Hawking temperature (as, for example, in the case of a black hole), since the radiation dominated cosmological epoch has a *finite* particle horizon, and therefore *does not* have an event horizon. This aspect merits further study.

Appendix A Supplement for Scalar Decay Products

A.1 Particle Decay in Minkowski Spacetime

In order to understand more clearly the decay law in cosmology, it proves convenient to study the decay of a massive particle into two particles in Minkowski space time implementing the Wigner-Weisskopf method.

Integrating in momentum first: massless daughters:

This is achieved from the expression (3.7.3) by simply taking

$$\eta \to t \;\; ; \;\; a(\eta) \to 1 \;\; , \;\; g_k^{(1)}(\eta) \to \frac{e^{-iE_k\,t}}{\sqrt{2E_k}} \;\; ; \;\; g_k^{(2)}(\eta) \to \frac{e^{-ik\,t}}{\sqrt{2k}}\,, \tag{A.1.1}$$

with $E_k = \sqrt{k^2+m^2}$, leading to

$$\Sigma_k(t-t') = \frac{\lambda^2}{E_k}\int \frac{d^3p}{(2\pi)^3}\;\; \frac{e^{i(E_k-p-q)(t-t')}}{2p\,2q} \;\; ; \;\; q = |\vec{k}-\vec{p}|\,. \tag{A.1.2}$$

The integral over p can be done by writing $d^3p = p^2dp\,d(\cos(\theta))$ and changing variables from $\cos(\theta)$ to $q = \sqrt{k^2+p^2-2kp\cos(\theta)}$ with $d(\cos(\theta))/q = -dq/k\,p$, and introducing a convergence factor $t-t' \to (t-t'-i\epsilon)$ with $\epsilon \to 0^+$. We find

$$\Sigma_k(t-t') = \frac{-i\,\lambda^2}{16\pi^2\,E_k}\;\frac{e^{i(E_k-k)(t-t')}}{(t-t'-i\epsilon)} = \frac{\lambda^2}{16\pi^2\,E_k}\;e^{i(E_k-k)(t-t')}\left[-i\,\mathcal{P}\left(\frac{1}{t-t'}\right)+\pi\,\delta(t-t')\right], \tag{A.1.3}$$

and

$$\mathrm{Re}\Sigma_k(t-t') = \frac{\lambda^2}{16\pi^2\,E_k}\left\{\pi\,\delta(t-t')+\frac{\sin\left[(E_k-k)(t-t')\right]}{(t-t')}\right\}. \tag{A.1.4}$$

This expression yields a *time dependent* decay rate $\Gamma(t)$ given by

$$\Gamma(t) = 2\int_0^t \mathrm{Re}\Sigma_k(t-t')\,dt' = \frac{\lambda^2}{8\pi\,E_k}\,\frac{1}{2}\Big[1+\frac{2}{\pi}\,Si[(E_k-k)t]\Big]\,, \tag{A.1.5}$$

where $Si[x]$ is the sine-integral function with asymptotic limit $Si[x] \to \pi/2$ for $x \to \infty$. The time scale to reach the asymptotic behavior

$$t_{asy} \propto \frac{1}{E_k-k}\,, \tag{A.1.6}$$

therefore the approach to asymptotia and to the full width takes a much longer time for an ultrarelativistic particle with $t_{asy} \propto 2k/m^2$, whereas it is much shorter in the non-relativistic case $t_{asy} \propto 1/m$. In S-matrix theory in Minkowski space time one takes $t \to \infty$, and obviously in this limit the $Si-$ function reaches its asymptotic value, therefore the time dependence of the rate cannot be gleaned.

Integrating in time first: massive particles and Fermi's Golden rule:

Let us consider now the full dispersion relations for the daughter particles, calling E_k that of the parent decaying particle and $\omega_p = \sqrt{p^2 + m_2^2}$ that of the daughter. From (3.6.7) and (3.6.21), we need

$$\mathcal{E}_k[t;t] = \int_0^t \Sigma_k(t-t')\, dt' \quad ; \quad \Gamma_k(t) = 2\,\mathrm{Re}\mathcal{E}_k[t,t]\,. \tag{A.1.7}$$

We find

$$\Gamma_k(t) = \frac{2\,\lambda^2}{E_k} \int \frac{d^3p}{(2\pi)^3} \quad \frac{\sin\big[(E_k - \omega_p - \omega_q)\,t\big]}{2\omega_p\, 2\omega_q \big[(E_k - \omega_p - \omega_q)\big]} \quad ; \quad q = |\vec{k} - \vec{p}|\,, \tag{A.1.8}$$

the asymptotic long time limit

$$\frac{\sin\big[(E_k - \omega_p - \omega_q)\,t\big]}{\big[(E_k - \omega_p - \omega_q)\big]} \quad \xrightarrow[t\to\infty]{} \quad \pi\,\delta\big(E_k - \omega_p - \omega_q\big)\,, \tag{A.1.9}$$

yields

$$\Gamma_k(t) \;\xrightarrow[t\to\infty]{}\; \frac{\lambda^2}{E_k} \int \frac{d^3p}{(2\pi)^3\, 2\omega_p\, 2\omega_q} \;(2\pi)\,\delta\big(E_k - \omega_p - \omega_q\big)\,, \tag{A.1.10}$$

this is simply Fermi's Golden rule which yields the standard result for the decay rate

$$\Gamma_k = \frac{\lambda^2}{8\pi\, E_k}\left[1 - \frac{4\,m_2^2}{E_k^2 - k^2}\right]^{1/2} \Theta(E_k^2 - k^2 - 4\,m_2^2)\,. \tag{A.1.11}$$

Although $E_k^2 - k^2 = m_1^2$ we have left the result in the form shown to make use of it in the cosmological case and to highlight the threshold.

Before taking the limit $t \to \infty$ the real time rate (A.1.8) can be conveniently written in a dispersive form, namely

$$\Gamma_k(t) = \int_{-\infty}^{\infty} \rho(k_0, k)\, \frac{\sin\big[(k_0 - E_k)\,t\big]}{\big[\pi\,(k_0 - E_k)\big]}\, dk_0 \tag{A.1.12}$$

with the spectral density

$$\rho(k_0,k)=\frac{\lambda^2}{E_k}\int\frac{d^3p}{(2\pi)^3}\;\;\frac{(2\pi)\,\delta(k_0-\omega_p-\omega_q)}{2\omega_p\,2\omega_q}\;\;;\;\;q=|\vec{k}-\vec{p}|\,, \tag{A.1.13}$$

which, following the steps leading up to (A.1.11) is given by

$$\rho(k_0,k)=\frac{\lambda^2}{8\pi\,E_k}\left[1-\frac{4\,m_2^2}{k_0^2-k^2}\right]^{1/2}\Theta(k_0^2-k^2-4\,m_2^2)\,\Theta(k_0)\,. \tag{A.1.14}$$

The case of massless daughter's particles $m_2=0$ is particularly simple, yielding

$$\Gamma_k(t)=\frac{\lambda^2}{8\pi^2\,E_k}\int_{-(E_k-k)t}^{\infty}\frac{\sin(x)}{x}\;dx=\frac{\lambda^2}{8\pi\,E_k}\,\frac{1}{2}\Big[1+\frac{2}{\pi}Si[(E_k-k)t]\Big]\,. \tag{A.1.15}$$

This expression of course agrees with eqn. (A.1.5) and clarifies the emergence of a prompt term given by $\delta(t-t')$ in (A.1.3) and the "rising" term, namely the Si function that reaches its asymptotic value $\pi/2$ over a time scale $\approx 1/(E_k-k)$, by integrating in time first.

Using the result (3.6.4) adapted to Minkowski space time, with the state $|\kappa\rangle=|1^{(2)}_{\vec{p}},1^{(2)}_{\vec{q}}\rangle$ the amplitude for daughter particles becomes

$$C_{\vec{p},\vec{k}}(t)=-i\langle 1^{(2)}_{\vec{p}}1^{(2)}_{\vec{q}}|H_I|1^{(2)}_{\vec{k}}\rangle\int_0^t e^{-i\left(E_k-\omega_p-\omega_q\right)t'}\,e^{-\Gamma_k t'/2}\,dt' \tag{A.1.16}$$

with the probability given by

$$|C_{\vec{p},\vec{k}}(t)|^2=\frac{\lambda^2}{2\,\omega^{(1)}_k\,\omega^{(2)}_p\,\omega^{(2)}_q\,V}\,\frac{\left|1-e^{-\Gamma_k t/2}\,e^{-i\left(E_k-\omega_p-\omega_q\right)t}\right|^2}{\left[(E_k-\omega_p-\omega_q)^2+\frac{\Gamma_k^2}{4}\right]}\;\;;\;\;\vec{q}=\vec{k}-\vec{p}. \tag{A.1.17}$$

A.2 First Order Adiabatic Correction for Massive Daughters

There are two contributions of first adiabatic order in the time integrals up to η of equation (3.7.2): 1) keeping the quadratic term $(\eta - \eta')^2$ multiplied by derivatives of the frequencies in the exponential (see eqn. (3.7.27)). With the substitution $\tau = \omega_k^{(1)}(\eta)\,(\eta - \eta')$ this term is proportional to τ^2, and 2) in the first order expansion of the scale factor and the frequencies obtained from the expression (3.7.24), this term is proportional to τ. Both terms are of first adiabatic order, hence are multiplied by $H(t)/E_k(t) \equiv 1/z$ where we have taken the frequency of the parent particle as reference frequency. The contributions to the integral (here we set $\eta_i = 0$)

$$\int_0^\eta \Sigma_k(\eta, \eta')\, d\eta'$$

are of the form

$$\frac{1}{z}\int_0^z (a\,\tau + i\,b\,\tau^2)\, e^{i\left[1-\frac{\omega_p^{(2)}(\eta)}{\omega_k^{(1)}(\eta)}-\frac{\omega_q^{(2)}(\eta)}{\omega_k^{(1)}(\eta)}\right]\tau}\, d\tau$$

where a, b are z-independent coefficients but depend on the momenta. Introducing the dispersive form of the momentum integrals as in equation (3.7.50) and introducing

$$\epsilon = \frac{k_0 - E_k^{(1)}}{E_k^{(1)}}\,, \tag{A.2.1}$$

we find the following contributions to the corrections to $\mathrm{Re}\Sigma_k$:

$$\mathrm{Re}\int_0^z \tau e^{i\epsilon\tau} d\tau = f_1(\epsilon, z) = \frac{d}{d\epsilon}\Big[\frac{(1-\cos(\epsilon\, z)}{\epsilon}\Big] \tag{A.2.2}$$

$$\mathrm{Re}\int_0^z i\,\tau^2 e^{i\epsilon\tau} d\tau = f_2(\epsilon, z) = \frac{d^2}{d\epsilon^2}\Big[\frac{(1-\cos(\epsilon\, z)}{\epsilon}\Big]\,. \tag{A.2.3}$$

Changing integration variables from k_0 to ϵ in the dispersive form and writing the spectral density $\rho(k_0, k) \equiv \rho(\epsilon)$ to simplify notation the corrections to the rate $\Gamma_k(\eta)$ to first adiabatic order are determined by the following integrals

$$I_{1,2}(z) = \frac{1}{z}\int_{-\infty}^{\infty} \rho(\epsilon) f_{1,2}(\epsilon, z)\, d\epsilon\,, \tag{A.2.4}$$

for comparison, in terms of the same variables, the zeroth order adiabatic term is given by

$$I_0(z) = \int_{-\infty}^{\infty} \rho(\epsilon) \frac{\sin(\epsilon z)}{\epsilon} \, d\epsilon \, . \tag{A.2.5}$$

The function $f_0(\epsilon, z)$ is the usual function of Fermi's Golden Rule: for large z it is sharply localized near $\epsilon \simeq 0$ with total area $= \pi$, it becomes a delta function in the large z limit, probing the region $\epsilon \simeq 0$ of the spectral density. The function $f_1(\epsilon, z)$ is even in ϵ and for large z is also localized near $\epsilon \simeq 0$ but in this limit it becomes the *difference* of delta functions multiplied by z plus subdominant terms. Because this function is a total derivative the total integral area is independent of z and vanishes in the integration domain $-\infty < \epsilon < \infty$. If m_1 is above the threshold the total integral does not vanish but becomes independent of z and small as $z \to \infty$, thus we expect $I_1(z)$ to fall off rapidly with z. Finally, the function $f_2(\epsilon, z)$ is odd in ϵ and for large z is also localized near $\epsilon \simeq 0$ but vanishing at $\epsilon = 0$ and rapidly varying in this region, averaging out the integral over the spectral density. Thus we also expect that $I_2(z)$ falls off with z with nearly zero average because of being odd in ϵ. Figures (27, 28) display I_0, I_1, I_2 for a representative set of parameters. The main features are confirmed by a comprehensive numerical study for a wide range of parameters for $m_1 > 2m_2$ (above threshold). If m_1 is below the two particle threshold, the spectral density vanishes in the region of support of the functions f_1, f_2 thereby yielding rapidly vanishing integrals for large z. We have confirmed numerically that both I_1, I_2 vanish very rapidly as a function of z in this case, remaining perturbatively small when compared to I_0. Therefore this study confirms that the first order adiabatic corrections are indeed subleading as compared to the leading (zeroth) order contribution for large $z = E_k(t)/H(t)$.

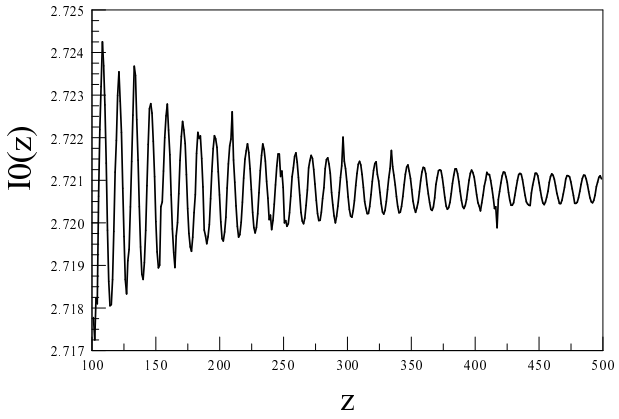

Figure 27: The integral $I_0(z)$ vs. z, for $m_2/m_1 = 0.25$, $k = 0$.

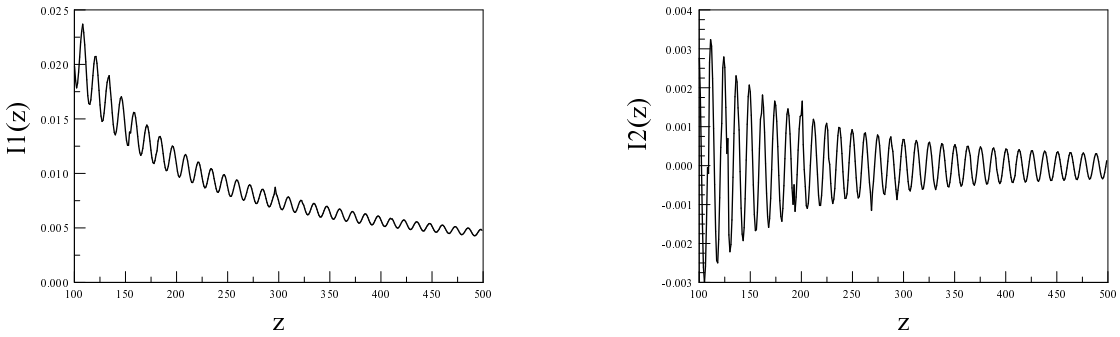

Figure 28: The integrals $I_1(z), I_2(z)$ vs. z, for $m_2/m_1 = 0.25$, $k = 0$.

Appendix B Supplement for Fermion Decay Products

B.1 Projectors

Introducing the notation

$$\Omega_k(\eta) \equiv \sqrt{\omega_k^{\psi}(\eta) + M_f(\eta)} \;\; ; \;\; \omega_k^{\psi}(\eta) = \sqrt{k^2 + M_f^2(\eta)}\,, \tag{B.1.1}$$

with the zeroth-adiabatic order spinors (4.2.60,4.2.61), the projector operators are given by equations (4.2.62). We find

$$\Lambda_{\vec{k}}^{+}(\eta,\eta') = \begin{pmatrix} \Omega_k(\eta)\Omega_k(\eta')\,\mathbb{I} & -\vec{\sigma}\cdot\vec{k}\,\frac{\Omega_k(\eta)}{\Omega_k(\eta')} \\ \vec{\sigma}\cdot\vec{k}\,\frac{\Omega_k(\eta')}{\Omega_k(\eta)} & -\frac{k^2}{\Omega_k(\eta)\Omega_k(\eta')}\,\mathbb{I} \end{pmatrix}, \tag{B.1.2}$$

$$\Lambda_{\vec{k}}^{-}(\eta',\eta) = \begin{pmatrix} \frac{k^2}{\Omega_k(\eta)\Omega_k(\eta')}\,\mathbb{I} & -\vec{\sigma}\cdot\vec{k}\,\frac{\Omega_k(\eta)}{\Omega_k(\eta')} \\ \vec{\sigma}\cdot\vec{k}\,\frac{\Omega_k(\eta')}{\Omega_k(\eta)} & -\Omega_k(\eta)\Omega_k(\eta')\,\mathbb{I} \end{pmatrix}, \tag{B.1.3}$$

where $\mathbb{I}$ is the 2×2 identity matrix. These expressions can be written more compactly introducing the following functions (suppressing the momentum and conformal time arguments),

$$\lambda_0 = \frac{1}{2}\Big(\Omega_k(\eta)\Omega_k(\eta') + \frac{k^2}{\Omega_k(\eta)\Omega_k(\eta')}\Big) \tag{B.1.4}$$

$$\lambda_1 = \frac{1}{2}\Big(\frac{\Omega_k(\eta)}{\Omega_k(\eta')} + \frac{\Omega_k(\eta')}{\Omega_k(\eta)}\Big) \tag{B.1.5}$$

$$\lambda_2 = \frac{1}{2}\Big(\frac{\Omega_k(\eta)}{\Omega_k(\eta')} - \frac{\Omega_k(\eta')}{\Omega_k(\eta)}\Big) \tag{B.1.6}$$

$$\lambda_3 = \frac{1}{2}\Big(\Omega_k(\eta)\Omega_k(\eta') - \frac{k^2}{\Omega_k(\eta)\Omega_k(\eta')}\Big)\,, \tag{B.1.7}$$

as

$$\Lambda_{\vec{k}}^{+}(\eta,\eta') = \gamma^0\,\lambda_0 - \vec{\gamma}\cdot\vec{k}\,\lambda_1 + \vec{\gamma}\cdot\vec{k}\,\gamma^0\,\lambda_2 + \lambda_3 \tag{B.1.8}$$

$$\Lambda_{\vec{k}}^{-}(\eta',\eta) = \gamma^0\,\lambda_0 - \vec{\gamma}\cdot\vec{k}\,\lambda_1 + \vec{\gamma}\cdot\vec{k}\,\gamma^0\,\lambda_2 - \lambda_3\,. \tag{B.1.9}$$

Two relevant cases:

1:) Equal time, $\eta = \eta'$,

$$\begin{aligned}\Lambda^{+}_{\vec{k}}(\eta,\eta) &= \gamma^0\omega^{\psi}_k(\eta) - \vec{\gamma}\cdot\vec{k} + M_f(\eta) \\ &= a(t)\Big[\not{K}(t) + m_f\Big] \;\; ; \;\; K_\mu(t) = (E^{\psi}_k(t), -\vec{k}_p(t))\,, \end{aligned} \tag{B.1.10}$$

$$\begin{aligned}\Lambda^{-}_{\vec{k}}(\eta,\eta) &= \gamma^0\omega^{\psi}_k(\eta) - \vec{\gamma}\cdot\vec{k} - M_f(\eta) \\ &= a(t)\Big[\not{K}(t) - m_f\Big]\,. \end{aligned} \tag{B.1.11}$$

2:) Massless fermions,

$$\Lambda^{+}_{\vec{k}} = \Lambda^{-}_{\vec{k}} = \gamma^0 k - \vec{\gamma}\cdot\vec{k}\,. \tag{B.1.12}$$

B.2 Minkowski Space-time: $m_\psi = 0$

The Minkowski space-time limit is obtained by replacing $\eta \to t$ and the frequencies are time independent. The self-energy in this case becomes[32]

$$\Sigma_\chi(k,t,t') = \frac{Y^2}{16\pi^2}\,\frac{e^{i\omega^{\phi}_k(t-t')}}{\omega^{\phi}_k}\int dk_0\rho(k_0,k)e^{-ik_0(t-t')} \;\; ; \;\; \rho(k_0,k) = (k_0^2-k^2)\,\Theta(k_0-k)\,. \tag{B.2.1}$$

Replacing $k_0^2 \to -d^2/dt'^2$, and introducing a convergence factor $\epsilon \to 0^+$ yields

$$\Sigma_\chi(k,t,t') = -i\frac{Y^2}{16\pi^2}\;\frac{e^{i\omega^{\phi}_k\,(t-t')}}{\omega^{\phi}_k}\left[\frac{d^2}{dt'^2} + k^2\right]\left[\frac{e^{-i\Lambda(t-t'-i\epsilon)} - e^{-ik(t-t'-i\epsilon)}}{(t-t'-i\epsilon)}\right], \tag{B.2.2}$$

and the decay function

$$\int_0^t \Gamma_k(t')\,dt' = 2\int_0^t\left\{\int_0^{t'}\mathrm{Re}\Big[\Sigma_\chi(k,t',t'')\Big]dt''\right\}dt'\,. \tag{B.2.3}$$

Integrating by parts twice the derivative term in (B.2.2) we find

$$\int_0^t \Gamma^{\phi}_k(t')\,dt' = \frac{Y^2}{8\pi^2\,\omega^{\phi}_k}\Big[T_1(\Lambda,k,t) + T_2(\Lambda,k,t) + T_3(k,t)\Big]\,, \tag{B.2.4}$$

where

$$T_1(\Lambda,k,t)=\frac{1}{\epsilon}\Big(e^{(\omega_k^\phi-k)\epsilon}-e^{(\omega_k^\phi-\Lambda)\epsilon}\Big)-\frac{\sin\Big((\Lambda-\omega_k^\phi)t\Big)}{t}-\frac{\sin\Big((\omega_k^\phi-k)t\Big)}{t}\,, \tag{B.2.5}$$

$$T_2(\Lambda,k,t)=2\,\omega_k^\phi\int_0^t\left[\frac{1-\cos\Big((\Lambda-\omega_k^\phi)t'\Big)}{t'}-\frac{1-\cos\Big((k-\omega_k^\phi)t'\Big)}{t'}\right]dt' \tag{B.2.6}$$

$$T_3(k,t)=m_\phi^2\int_0^t\left[Si\Big((\Lambda-\omega_k^\phi)\,t'\Big)+Si\Big((\omega_k^\phi-k)\,t'\Big)\right]dt'\,, \tag{B.2.7}$$

where $Si(t)=\int_0^t\sin(x)/x dx$. Taking $\epsilon\to 0^+$ and keeping Λ large but finite yields

$$T_1(\Lambda,k,t)=(\Lambda-k)\left[1-\frac{\sin\Big((\Lambda-\omega_k^\phi)\,t\Big)}{(\Lambda-k)\,t}-\frac{\sin\Big((\omega_k^\phi-k)\,t\Big)}{(\Lambda-k)\,t}\right], \tag{B.2.8}$$

$$T_2(\Lambda,k,t)=2\,\omega_k^\phi\left[\ln\Big(\frac{\Lambda-\omega_k^\phi}{\omega_k^\phi-k}\Big)-Ci\big[(\Lambda-\omega_k^\phi)\,t\big]+Ci\big[(\omega_k^\phi-k)\,t\big]\right], \tag{B.2.9}$$

and

$$\begin{aligned}T_3(k,t)=\;& m_\phi^2\Bigg\{t\Big[Si\big[(\Lambda-\omega_k^\phi)\,t\big]+Si\big[(\omega_k^\phi-k)\,t\big]\Big]-\frac{\Big[1-\cos\big[(\Lambda-\omega_k^\phi)\,t\big]\Big]}{(\Lambda-\omega_k^\phi)}\\&-\frac{\Big[1-\cos\big[(\omega_k^\phi-k)\,t\big]\Big]}{(\omega_k^\phi-k)}\Bigg\},\end{aligned} \tag{B.2.10}$$

where for $\Lambda t\to\infty$ it follows that $Si\big[(\Lambda-\omega_k^\phi)\,t\big]\to\pi/2$, and $Ci\big[(\Lambda-\omega_k^\phi)\,t\big]\to 0$. Taking the limit $\Lambda\to\infty$ yields

$$\begin{aligned}\int_0^t\Gamma_k^\phi(t')dt' \;&=\; \frac{Y^2}{8\pi^2\,\omega_k^\phi}\Bigg\{\Lambda-k+2\,\omega_k^\phi\ln\left[\frac{\Lambda}{\omega_k^\phi-k}\right]+m_\phi^2\,t\Big[\frac{\pi}{2}+Si\big[(\omega_k^\phi-k)\,t\big]\Big]\\&+\;Ci\big[(\omega_k^\phi-k)\,t\big]-\frac{\Big[1-\cos\big[(\omega_k^\phi-k)\,t\big]\Big]}{(\omega_k^\phi-k)}+\mathcal{O}(1/t)\Bigg\}.\end{aligned} \tag{B.2.11}$$

This is exactly the same result as obtained in ref.[32] integrating in k_0 first.

B.3 Useful Identities

In this appendix we gather some useful identities valid during the radiation dominated stage (see also appendix (B.4)).

$$\begin{aligned}\omega(\eta) &= \left[k^2 + m^2\, H_R^2\, \eta^2\right]^{1/2} = \left[k^2 + m^2\, H_R^2\, \eta_i^2 + m^2\, H_R^2\, (\eta^2 - \eta_i^2)\right]^{1/2} \equiv \frac{\omega_i}{\gamma_i}\left[\gamma_i^2 - 1 + \frac{\eta^2}{\eta_i^2}\right]^{1/2} \\ \omega_i &= \omega(\eta_i) \;\; ; \;\; \gamma_i = \gamma(\eta_i)\,. \end{aligned} \tag{B.3.1}$$

The local Lorentz factor in conformal time is given by

$$\begin{aligned}\gamma(\eta) &= \left[\frac{(\gamma_i^2 - 1)}{\left(\frac{\eta}{\eta_i}\right)^2} + 1\right]^{1/2} = \left[\frac{k^2}{m^2\, H_R^2\, \eta^2} + 1\right]^{1/2} \equiv \left[\frac{\eta_{nr}^2}{\eta^2} + 1\right]^{1/2} = \left(\frac{\eta_i}{\eta}\right)\left[\gamma_i^2 - 1 + \frac{\eta^2}{\eta_i^2}\right]^{1/2} \\ \gamma_i^2 &= 1 + \frac{\eta_{nr}^2}{\eta_i^2} \;\; ; \;\; \eta_{nr} = \frac{k}{m\, H_R} = \eta_i\, \sqrt{\gamma_i^2 - 1}\,, \end{aligned} \tag{B.3.2}$$

yielding the identity

$$\gamma^2(\eta) - 1 = \left(\frac{\eta_i}{\eta}\right)^2 (\gamma_i^2 - 1)\,. \tag{B.3.3}$$

The relationship with comoving time t is obtained via eqn. (4.2.39), namely

$$\gamma(\eta(t)) = \left[\frac{(\gamma_i^2 - 1)}{\left(\frac{t}{t_i}\right)} + 1\right]^{1/2} \equiv \left[\frac{t_{nr}}{t} + 1\right]^{1/2}. \tag{B.3.4}$$

The conformal and comoving time scales $\eta_{nr}\,, t_{nr}$ respectively, determine the scale at which the decaying particle transitions from relativistic with $\gamma(\eta) \gg 1$ for $\eta \ll \eta_{nr}$ or $t \ll t_{nr}$ to non-relativistic with $\gamma(\eta) \simeq 1$ for $\eta \geq \eta_{nr}$ or $t \geq t_{nr}$. In terms of η, η_i we find,

$$\omega(\eta)\, \eta = \frac{\omega_i\, \eta_i}{\gamma_i}\left(\frac{\eta}{\eta_i}\right)\left[\gamma_i^2 - 1 + \frac{\eta^2}{\eta_i^2}\right]^{1/2}. \tag{B.3.5}$$

B.4 Analysis of I_2: Eqn. (4.4.7)

Consider the first term in I_2 eqn. (4.4.7),

$$I_{2,a}(\Lambda,k,\eta)=\int_{\eta_i}^{\eta}\left[\sqrt{\frac{\omega_k^\phi(\eta')}{\omega_k^\phi(\eta_i)}}+\sqrt{\frac{\omega_k^\phi(\eta_i)}{\omega_k^\phi(\eta')}}\right]\times\left[\frac{1-\cos\Big(\int_{\eta_i}^{\eta'}\big(\omega_k^\phi(\eta_1)-\Lambda\big)d\eta_1\Big)}{\eta'-\eta_i}\right]d\eta'\,, \quad \text{(B.4.1)}$$

For $\Lambda\gg k,m_\phi$ the argument of the cosine becomes simply $\Lambda\,(\eta'-\eta_i)$. Define $x=\Lambda\,(\eta'-\eta_i)$, and change integration variable to x, with $x_f=\Lambda\,(\eta-\eta_i)$, yielding

$$I_{2,a}(\Lambda,k,\eta)=\int_0^{x_f}\left[\sqrt{\frac{\omega_k^\phi(\eta_i+x/\Lambda)}{\omega_k^\phi(\eta_i)}}+\sqrt{\frac{\omega_k^\phi(\eta_i)}{\omega_k^\phi(\eta_i+x/\Lambda)}}\right]\times\left[\frac{1-\cos(x)}{x}\right]dx\,. \quad \text{(B.4.2)}$$

In the limit $\Lambda\to\infty$ we find

$$I_{2,a}\to 2\big[\,\ln(x_f)+\gamma_E-Ci(x_f)\big] \quad \text{(B.4.3)}$$

where $\gamma_E=0.577\cdots$ is Euler's constant and for $x_f\gg 1$ we find $Ci(x_f)=\sin(x_f)/x_f+\cdots$. We confirmed the result (B.4.3) numerically. Therefore for $\Lambda\gg k,m_\phi,1/(\eta-\eta_i)$ we find

$$I_{2,a}=2\,\ln\big[\Lambda\,e^{\gamma_E}\,(\eta-\eta_i)\big]\,. \quad \text{(B.4.4)}$$

Let us now consider

$$I_{2,b}(k,\eta)=-\int_{\eta_i}^{\eta}\left[\sqrt{\frac{\omega_k^\phi(\eta')}{\omega_k^\phi(\eta_i)}}+\sqrt{\frac{\omega_k^\phi(\eta_i)}{\omega_k^\phi(\eta')}}\right]\times\left[\frac{1-\cos\Big(\int_{\eta_i}^{\eta'}\big(\omega_k^\phi(\eta_1)-k\big)d\eta_1\Big)}{\eta'-\eta_i}\right]d\eta'\,. \quad \text{(B.4.5)}$$

Using the identities obtained in appendix (B.3) for a radiation dominated cosmology, we write

$$\begin{aligned}\omega_k^\phi(\eta) &= \sqrt{k^2+m_\phi^2H_R^2\,\eta^2}=\left\{k^2+m_\phi^2H_R^2\,\eta_i^2+m_\phi^2H_R^2\,\eta_i^2\Big[\Big(1+\frac{\eta-\eta_i}{\eta_i}\Big)^2-1\Big]\right\}^{1/2}\\ &= \omega_i\,W[\xi]\,, \end{aligned} \quad \text{(B.4.6)}$$

where we introduced the definitions

$$W[\xi]=\frac{1}{\gamma_i}\left[\gamma_i^2-1+(1+\xi)^2\right]^{1/2}, \quad \text{(B.4.7)}$$

$$\omega_i \equiv \omega_k^{\phi}(\eta_i) \;\; ; \;\; \xi = \left(\frac{\eta}{\eta_i} - 1\right) \;\; ; \;\; \gamma_i = \frac{\omega_i}{m_\phi \, H_R \, \eta_i} \equiv \frac{E_k^{\phi}(t_i)}{m_\phi} \,, \tag{B.4.8}$$

and γ_i is the local Lorentz factor at time η_i.

In terms of these variables we find

$$\begin{aligned} J[\xi'] \equiv \int_{\eta_i}^{\eta'} \left[\omega_k^{\phi}(\eta_1) - k\right] d\eta_1 &= \frac{\omega_i \, \eta_i}{2} \left\{ \big(1+\xi'\big) W[\xi'] - 1 - 2\,\frac{\xi'}{\gamma_i}\,\sqrt{\gamma_i^2 - 1} \right. \\ &+ \left. \frac{\big(\gamma_i^2 - 1\big)}{\gamma_i} \, \ln\left[\frac{\gamma_i \, W[\xi'] + 1 + \xi'}{1+\gamma_i}\right] \right\}. \end{aligned} \tag{B.4.9}$$

We note that the fulfillment of the adiabatic condition at all times implies that

$$\omega_i \, \eta_i = \frac{E_k^{\phi}(\eta_i)}{H(\eta_i)} \gg 1 \,. \tag{B.4.10}$$

For $\xi' \ll 1$ it is straightforward to find that $J[\xi']$ features the expansion

$$J[\xi'] = \omega_i \, \eta_i \, \xi' \left[1 - \sqrt{1 - \frac{1}{\gamma_i^2}} + \frac{1}{2}\,\frac{\xi'}{\gamma_i^2} + \cdots\right]. \tag{B.4.11}$$

In terms of these variables we find that the subtracted integral $I_{2b}(k,\eta,\eta_b)$ defined by eqn. (4.5.4) is given by

$$I_{2,b}[k,\eta,\eta_b] = -\int_{\xi_b}^{\xi} \left[\sqrt{W[\xi']} + \frac{1}{\sqrt{W[\xi']}}\right] \left[\frac{1 - \cos[J(\xi')]}{\xi'}\right] d\xi' \,. \tag{B.4.12}$$

Consider the two contributions to this function,

$$F_1(\xi) = \int_{\xi_b}^{\xi} \left[\sqrt{W[\xi']} + \frac{1}{\sqrt{W[\xi']}}\right] \frac{d\xi'}{\xi'} \tag{B.4.13}$$

$$F_2(\xi) = \int_{\xi_b}^{\xi} \left[\sqrt{W[\xi']} + \frac{1}{\sqrt{W[\xi']}}\right] \frac{\cos[J(\xi')]}{\xi'} \, d\xi' \,. \tag{B.4.14}$$

During the time scale when $J(\xi') \ll 1$ the term $\cos[J(\xi')] \simeq 1$ therefore $F_2(\xi) \simeq F_1(\xi)$ and $I_{2b} \simeq 0$. Figures (29, 30) display $F_{1,2}(\xi)$ for $\omega_i \eta_i = 100$ and $\gamma_i = 2, 10$ respectively for $\xi_b = 1/\omega_i \eta_i$. $F_2(\xi)$ grows up to a maximum at ξ_m at which $J(\xi_m) = \pi/2$ and begins damped oscillations reaching a plateau. During the rise-time up to the maximum $F_2(\xi) \simeq F_1(\xi)$ thereby yielding $I_{2b}(k,\eta,\eta_b) \simeq 0$ during the interval $\xi_b \leq \xi \lesssim \xi_m$.

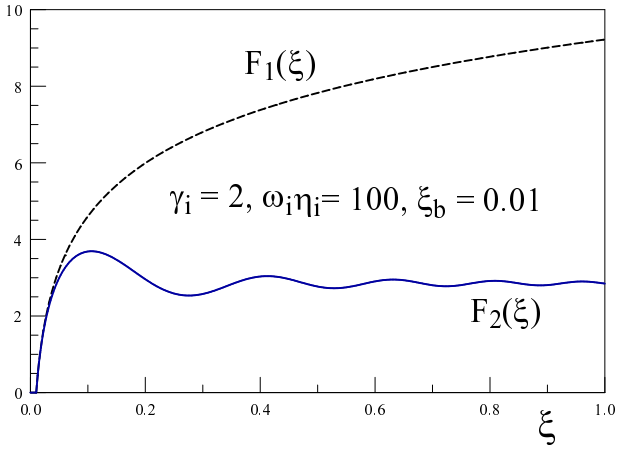

Figure 29: The contributions $F_1(\xi), F_2(\xi)$, for $\xi_b = 0.01, \gamma_i = 2, \omega_i\eta_i = 100$.

Although in general the value of ξ_m must be obtained numerically, for $\omega_i\eta_i \gg 1$ there are two limits that afford an analytic estimate: **a:)** for $\omega_i\eta_i \gg 1$ and $\gamma_i \simeq 1$, we assume, self consistently that $\xi_m \ll 1$, therefore from eqn. (B.4.11) we obtain

$$\xi_m \simeq \frac{\pi}{2}\left\{\omega_i\eta_i\left[1-\sqrt{1-\frac{1}{\gamma_i^2}}\right]\right\}^{-1} \quad \text{for} \quad \gamma_i \simeq 1\,, \tag{B.4.15}$$

this expression confirms the assumption that $\xi_m \ll 1$ for $\gamma_i \simeq 1$. **b:)** for $\gamma_i \gg 1$, it is convenient to carry out the integral (B.4.9) by expanding $\omega_k^\phi(\eta_1) \simeq k + m_\phi^2\, C^2(\eta_1)/k + \cdots$ and keeping the leading order term, we find

$$\xi_m \simeq \left\{\left[1+\frac{3\,\pi\gamma_i^2}{\omega_i\,\eta_i}\right]^{\frac{1}{3}} - 1\right\} \quad \text{for} \quad \gamma_i \gg 1\,. \tag{B.4.16}$$

This latter expression is fairly accurate even for $\gamma_i \simeq 2, 3$. We have confirmed numerically the validity of these approximate values of the maxima of $F_2(\xi)$ (see figures (29,30)). In both cases we find that for $\omega_i\eta_i \gg 1$ the value at the maxima fulfill $\xi_m/\gamma_i \ll 1$. In summary, we

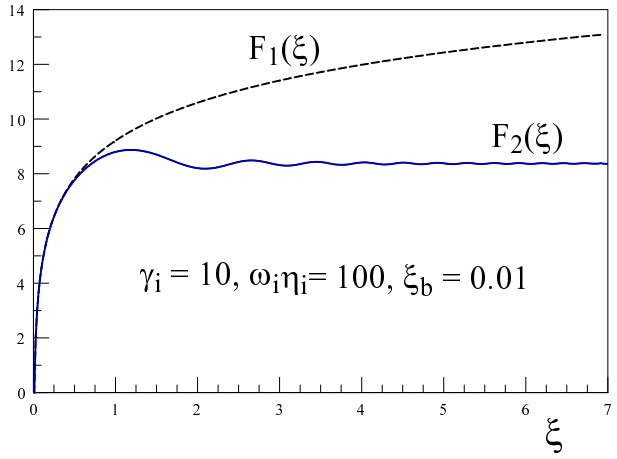

Figure 30: The contributions $F_1(\xi), F_2(\xi)$, for $\xi_b = 0.01, \gamma_i = 10, \omega_i\eta_i = 100$.

find that during the time interval $\xi_b < \xi < \xi_m$ $F_1(\xi) \simeq F_2(\xi) \simeq 2\ln[\xi/\xi_b]$ and $I_{2b}[k,\eta,\eta_b] \simeq 0$. For $\xi > \xi_m$ the contribution $F_2(\xi) \simeq F_2(\xi_m) \simeq 2\ln[\xi_m/\xi_b]$ remaining constant while $F_1(\xi)$ increases monotonically. The above analysis shows that for $\omega_i\eta_i \gg 1$ it follows that $\xi_m \ll \gamma_i$ in the whole range of γ_i, therefore during the interval $\xi_m < \xi < \gamma_i$ and $W[\xi'] \simeq 1$, hence

$$F_1(\xi) \simeq F_1(\xi_m) + 2\,\ln\left[\frac{\xi}{\xi_m}\right] \quad ; \quad \xi_m < \xi < \gamma_i\,, \tag{B.4.17}$$

with $F_1(\xi_m) \simeq F_2(\xi_m) \simeq 2\ln[\xi_m/\xi_b]$. For $\xi \gg \gamma_i$ the function $\sqrt{W[\xi]} + \frac{1}{\sqrt{W[\xi]}} \geq 2$ as shown in fig. (31) hence $F_1[\xi] > 2\,\ln[\xi]$, with asymptotic behavior

$$F_1[\xi] \simeq 2\ln\left[\frac{\gamma_i}{\xi_b}\right] + 2\sqrt{\frac{\xi}{\gamma_i}} \quad ; \quad \text{for } \xi \gg \gamma_i\,. \tag{B.4.18}$$

The behavior of $F_{1,2}$ in the ultrarelativistic case $\gamma_i \gg 1$ is summarized as follows:

$$\begin{aligned} F_1[\xi] &\simeq F_2[\xi] \simeq 2\ln\left[\frac{\xi}{\xi_b}\right] \quad \text{for} \quad \xi_b \lesssim \xi \lesssim \xi_m\,, \\ F_1[\xi] &\simeq 2\ln\left[\frac{\xi}{\xi_b}\right] \;\; ; \;\; F_2[\xi] \simeq 2\ln\left[\frac{\xi_m}{\xi_b}\right] \quad \text{for} \quad \xi_m \lesssim \xi \lesssim \gamma_i\,, \\ F_1[\xi] &\simeq 2\ln\left[\frac{\gamma_i}{\xi_b}\right] + 2\sqrt{\frac{\xi}{\gamma_i}} \;\; ; \;\; F_2[\xi] \simeq 2\ln\left[\frac{\xi_m}{\xi_b}\right] \quad \text{for} \quad \xi \gg \gamma_i\,. \end{aligned} \tag{B.4.19}$$

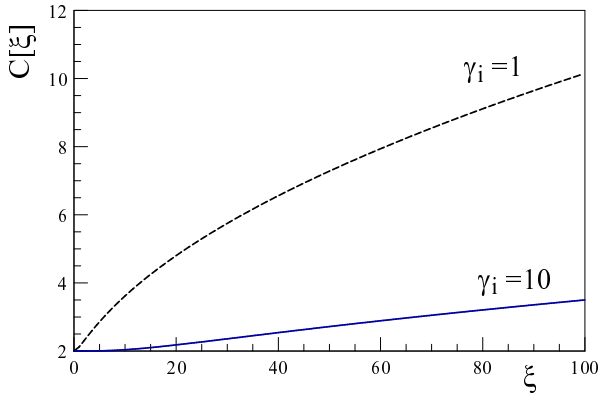

Figure 31: The function $C[\xi] = W^{1/2}[\xi] + 1/W^{1/2}[\xi]$ vs ξ, for $\gamma_i = 1, 10$.

B.5 Analysis of $I_{3b}(k, \eta, \eta_b)$: Eqn. (4.4.8)

Let us now consider the following integral in I_{3b}, namely the second contribution to eqn. (4.4.8):

$$\mathcal{I}(\eta') = \int_{\eta_i}^{\eta'} \frac{C^2(\eta_1)}{\sqrt{\omega_k^\phi(\eta_1)}} \, \frac{\sin\left(\int_{\eta_1}^{\eta'} \left(\omega_k^\phi(\eta_2) - k\right) d\eta_2\right)}{\eta' - \eta_1} \, d\eta_1\,, \tag{B.5.1}$$

this integral is similar to the case of decay into bosonic particles studied in ref.[105].

Following the treatment in this reference we introduce the following definitions

$$\omega_k^\phi(\eta')\,\eta' = z(\eta') \gg 1\,, \tag{B.5.2}$$

along with

$$\omega_k^\phi(\eta')\,(\eta' - \eta_2) = x \;\;;\;\; \omega_k^\phi(\eta')\,(\eta' - \eta_1) = \tau\,. \tag{B.5.3}$$

In terms of these variables, it follows that

$$\omega_k^\phi(\eta_2) = \omega_k^\phi(\eta')\,R[x;z]\,, \tag{B.5.4}$$

with

$$R[x;z] = \left[1 - \frac{2x}{z\,\gamma^2} + \frac{x^2}{z^2\,\gamma^2}\right]^{1/2}, \tag{B.5.5}$$

where there is an implicit η' dependence in z and γ.

The argument of the sine function in (B.5.1) becomes

$$A(\tau,\eta') = \int_0^\tau R[x;z]\,dx - \frac{k\,\tau}{\omega_k^\phi(\eta')} = \tau\left[1 - \left(1 - \frac{1}{\gamma^2}\right)^{1/2}\right] + \delta_k(\tau;\eta')\,, \tag{B.5.6}$$

with

$$\delta(\tau;\eta') = \frac{z}{2}\left\{\left(1 - \frac{2\,\tau}{z}\right) - \left(1 - \frac{\tau}{z}\right)R[\tau;z] - \frac{(\gamma^2-1)}{\gamma}\,\ln\left[\frac{\gamma\,R[\tau;z] + \left(1 - \frac{\tau}{z}\right)}{1+\gamma}\right]\right\}, \tag{B.5.7}$$

where $z \equiv z(\eta')$; $\gamma \equiv \gamma_k(\eta')$. Writing

$$\frac{C^2(\eta_1)}{\sqrt{\omega_k^\phi(\eta_1)}} = \frac{C^2(\eta')}{\sqrt{\omega_k^\phi(\eta')}}\,P[\eta',\eta_1]\,, \tag{B.5.8}$$

and using (B.5.4) it is straightforward to find

$$P[\tau;\eta'] = \frac{\left[1 - \frac{\tau}{z}\right]^2}{\sqrt{R[\tau;z]}}\,. \tag{B.5.9}$$

We finally obtain

$$\mathcal{I}(\eta') = \frac{C^2(\eta')}{\sqrt{\omega_k^\phi(\eta')}}\int_0^{\widetilde{z}} \mathcal{P}[\tau;\eta']\;\;\frac{\sin[A(\tau,\eta')]}{\tau}\,d\tau\,, \tag{B.5.10}$$

where $\widetilde{z} = \omega_k^\phi(\eta')\,(\eta' - \eta_i)$. Gathering together this result with eqn. (4.4.13) for I_{3a} we find

$$I_3(k,\eta) = \frac{\pi}{2}\, m_\phi \int_{\eta_i}^{\eta} \frac{C(\eta')}{\gamma_k(\eta')}\Big[1 + \mathcal{S}(\eta')\Big]\, d\eta' \,, \tag{B.5.11}$$

where

$$\mathcal{S}(\eta') = \frac{2}{\pi}\int_0^{\widetilde{z}} P[\tau;\eta']\;\; \frac{\sin[A(\tau,\eta')]}{\tau}\, d\tau \;\;;\;\; \widetilde{z} = \omega_k^\phi(\eta')\,(\eta' - \eta_i)\,. \tag{B.5.12}$$

For $\eta' \gg \eta_i$ and $z(\eta') \gg 1$ the integral in (B.5.10) has an adiabatic expansion, for $\tau \ll z$ we find

$$\delta_k(\tau;\eta') = -\frac{\tau^2}{2\gamma^2\, z} + \cdots \,, \tag{B.5.13}$$

therefore δ_k is of adiabatic order one and higher, furthermore,

$$R[\tau;z] = 1 - \frac{\tau}{z\,\gamma^2} + \cdots \tag{B.5.14}$$

and to leading (zeroth) adiabatic order we can replace $\mathcal{P}[\tau;\eta'] = 1$. The τ integral in (B.5.10) is dominated by the region $\tau \simeq 0$, and the region for which $\tau \simeq z$ yields a contribution $\propto 1/z$, hence of first adiabatic order or smaller. Therefore to leading (zeroth) adiabatic order we neglect δ_k in (B.5.6) and replace $P \to 1$ in (B.5.10).

Although the variables (B.5.2,3.7.14) allow an explicit identification of the nature of the adiabatic expansion, the most suitable variables to merge the results for I_{3b} with those of the contributions from I_{2b} are those introduced in appendices (B.3) and (B.4). We now recast the results for I_{3b} in terms of these variables. Introducing

$$t = \frac{\eta' - \eta_1}{\eta_i} \;\;;\;\; y = \frac{\eta'}{\eta_i} = 1 + \xi' \,, \tag{B.5.15}$$

in terms of which we find using (B.3.1)

$$\omega_k^\phi(\eta') = \frac{\omega_i}{\gamma_i}\, f(y) \;\;;\;\; f(y) = \sqrt{\gamma_i^2 - 1 + y^2}\,. \tag{B.5.16}$$

Similarly, using (B.3.3) we obtain

$$\gamma_k(\eta') \equiv \gamma(y) = \sqrt{\frac{\big(\gamma_i^2 - 1\big)}{y^2} + 1} = \frac{f(y)}{y}\,, \tag{B.5.17}$$

and the variables z, τ introduced in eqns. (B.5.2)) and (3.7.14) respectively are given by

$$z(\eta') = \frac{\omega_i\,\eta_i}{\gamma_i}\,f(y)\,y \;\;;\;\; \tau = \frac{\omega_i\,\eta_i}{\gamma_i}\,f(y)\,t\,, \tag{B.5.18}$$

which fulfill the identity

$$\frac{z(\eta')}{\gamma_k(\eta')}\,(\gamma_k^2(\eta') - 1) = \frac{\omega_i\,\eta_i}{\gamma_i}\,(\gamma_i^2 - 1)\,. \tag{B.5.19}$$

Using these results we find

$$R[\tau, z] \equiv \mathcal{R}[t, y] = \frac{1}{\gamma(y)}\left[\frac{(\gamma_i^2 - 1)}{y^2} + \left(1 - \frac{t}{y}\right)^2\right]^{1/2}\,, \tag{B.5.20}$$

and the ratio (B.5.9) becomes

$$P[\tau, \eta'] \equiv \mathcal{P}[t, y] = \frac{\left(1 - \frac{t}{y}\right)^2}{\sqrt{\mathcal{R}[t, y]}}\,, \tag{B.5.21}$$

and $\delta(\tau, \eta')$ in eqn. (B.5.7) becomes

$$\begin{aligned}\delta(\tau, \eta') \equiv \quad \Delta[t, y] \quad &= \frac{\omega_i\,\eta_i}{\gamma_i}\left\{y\,f(y)\left[\left(1 - 2\frac{t}{y}\right) - \left(1 - \frac{t}{y}\right)\mathcal{R}[t, y]\right]\right. \\ (\gamma_i^2 - 1) \quad &\left. ln\left[\frac{\gamma(y)\,\mathcal{R}[t, y] + \left(1 - \frac{t}{y}\right)}{1 + \gamma(y)}\right]\right\}.\end{aligned} \tag{B.5.22}$$

Finally the function $A(\tau, \eta')$ given by eqn. (B.5.6), becomes

$$A(\tau, \eta') \equiv \mathcal{A}[t, y] = \mathcal{A}_0[t, y] + \Delta[t, y]\,, \tag{B.5.23}$$

with

$$\mathcal{A}_0[t, y] = \frac{\omega_i\,\eta_i}{\gamma_i}\,t\left[\sqrt{(\gamma_i^2 - 1) + y^2} - \sqrt{(\gamma_i^2 - 1)}\right], \tag{B.5.24}$$

and the integral (B.5.12) becomes

$$\mathcal{S}(\eta') = \frac{2}{\pi}\int_0^{\xi'} \mathcal{P}[t, y]\,\frac{\sin[\mathcal{A}(t, y)]}{t}\,dt \;\;;\;\; y = 1 + \xi'\;;\;\xi' = (\frac{\eta'}{\eta_i} - 1)\,. \tag{B.5.25}$$

We have argued above in this appendix that for $\omega_k^{\phi}(\eta')\,\eta' \gg 1$ the term $\delta \equiv \Delta$ is higher order in the adiabatic approximation and can be neglected, and that to leading order in this approximation we can set $P \equiv \mathcal{P} \to 1$. We now test this assertion numerically in terms of

the new variables. Since in the new variables the product $\omega_k^\phi(\eta')\,\eta' = \frac{\omega_i\,\eta_i}{\gamma_i}\,y\,f(y)$ it follows that $\omega_k^\phi(\eta')\,\eta' \gg 1$ at all times implies that $\omega_i\,\eta_i \gg 1$ which is precisely the statement of the validity of the adiabatic approximation at the initial time. Fig. (32) compares $\frac{\sin[\mathcal{A}_0[y,t]]}{t}$ and $\mathcal{P}[y,t]\,\frac{\sin[\mathcal{A}[y,t]]}{t}$ for $\gamma_i = 5, \omega_i\,\eta_i = 100, y = 10$, confirming the validity of the adiabatic approximation. We have explored a wide range of parameters with similar results.

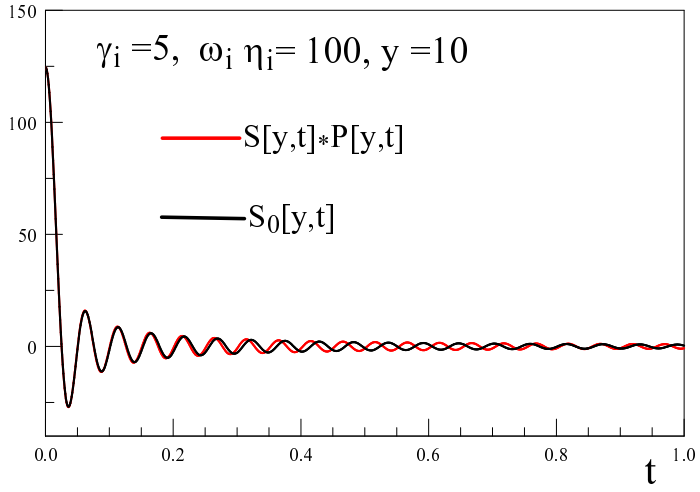

Figure 32: Comparison of $S_0[y,t] = \frac{\sin[\mathcal{A}_0[y,t]]}{t}$ and $S[y,t] \times \mathcal{P}[y,t]$ with $S[y,t] = \frac{\sin[\mathcal{A}[y,t]]}{t}$ for $\gamma_i = 5, \omega_i\,\eta_i = 100, y = 10$, confirming the validity of the adiabatic approximation.

Therefore to leading order in the adiabatic approximation we can replace the argument of the integral in (B.5.25) by $\frac{\sin[\mathcal{A}_0[y,t]]}{t}$, yielding to lowest adiabatic order

$$\mathcal{S}(\xi') = \frac{2}{\pi}\,Si\big[\alpha(\xi')\big] \quad ; \quad \alpha(\xi') = \frac{\omega_i\,\eta_i}{\gamma_i}\,\xi'\left[\sqrt{(\gamma_i^2-1)+(1+\xi')^2} - \sqrt{(\gamma_i^2-1)}\right], \qquad \text{(B.5.26)}$$

where $Si[x]$ is the sine-integral function, with $Si[x] \simeq x$ as $x \to 0$, reaches a maximum at $x = \pi$ and $Si[x] \to \pi/2$ for $x \gtrsim \pi$. The maximum of $\mathcal{S}(\xi)$ occurs when

$$\alpha(\xi) = \pi\,, \qquad \text{(B.5.27)}$$

beyond which $\mathcal{S}(\xi) \simeq 1$.

In particular for $\gamma_i = 1$ (the particle decaying at rest) and $\omega_i \eta_i \gg 1$, $\mathcal{S}(\xi')$ reaches a maximum at $\xi' = \xi_s \simeq \pi/\omega_i\eta_i + \mathcal{O}(1/(\omega_i\eta_i)^2)$ with $\mathcal{S}(\xi_s) \simeq 1$. In the opposite limit, for an ultrarelativistic particle with $\gamma_i \gg 1$ and $\omega_i\eta_i \gg 1$ we find self-consistently that $S(\xi')$ reaches a maximum at ξ_s with $\alpha(\xi_s) = \pi$, where ξ_s is a solution of

$$\xi_s\,(1+\xi_s)^2 = \frac{2\pi\,\gamma_i^2}{\omega_i\eta_i}\,. \tag{B.5.28}$$

For $2\pi\,\gamma_i^2/\omega_i\eta_i \ll 1$ we find

$$\xi_s \simeq \left[\frac{2\pi\,\gamma_i^2}{\omega_i\eta_i}\right] - \left[\frac{2\pi\,\gamma_i^2}{\omega_i\eta_i}\right]^2 + \cdots\,, \tag{B.5.29}$$

and for $2\pi\,\gamma_i^2/\omega_i\eta_i \gg 1$

$$\xi_s \simeq \left[\frac{2\pi\,\gamma_i^2}{\omega_i\eta_i}\right]^{\frac{1}{3}} - \frac{2}{3} + \cdots\,. \tag{B.5.30}$$

In both cases we find that $\frac{\xi_s}{\gamma_i} \ll 1$ whenever $\gamma_i \gg 1$. Fig. (33) displays the behavior of $\mathcal{S}(\xi)$ for $\omega_i = 100; \gamma_i = 2, 10$.

Using the relations derived in appendix (B.3) along with the identities $C(\eta') = C(\eta_i)\,(\eta'/\eta_i) = C(\eta_i)\,(1+\xi')$ and $m_\phi C(\eta_i) = \omega_i/\gamma_i$, it follows that $I_3(k,\eta)$ given by (B.5.11) can be written in terms of the same variables as I_2, namely $\xi = \eta/\eta_i - 1$ and $\eta_b = \eta_b/\eta_i - 1$. We find

$$I_3(k,\xi) = \frac{\pi}{2}\,\frac{\omega_i\eta_i}{\gamma_i}\,\int_{\xi_b}^{\xi}\frac{(1+\xi')^2\left[1+\mathcal{S}(\xi')\right]}{\sqrt{(\gamma_i^2-1)+(1+\xi')^2}}\,d\xi'\,. \tag{B.5.31}$$

The contribution from the term with $\mathcal{S}$ in the integrand must be done numerically, however, the first term can be done analytically, yielding

$$I_{3A}(k,\xi) = \frac{\pi}{4}\,\omega_i\eta_i\left\{(1+\xi)\,W[\xi] - 1 - \frac{(\gamma_i^2-1)}{\gamma_i}\,\ln\left[\frac{\gamma_i\,W[\xi]+(1+\xi)}{1+\gamma_i}\right]\right\}, \tag{B.5.32}$$

where we have set $\xi_b = 0$ to leading adiabatic order.

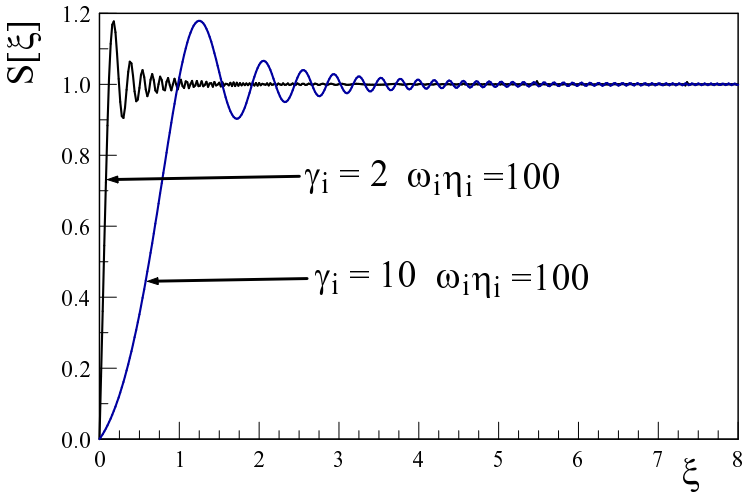

Figure 33: $S[y,t]$ for $\gamma_i = 2, 10$ and $\omega_i \eta_i = 100$.

The function $\mathcal{S}[\alpha(\xi)]$ has the following behavior for $\xi \ll \xi_s$ and $\xi \gg \xi_s$, corresponding to $\alpha(\xi) \ll \pi$ and $\alpha(\xi) \gg \pi$ respectively:

$$\mathcal{S}[\alpha(\xi)] \simeq \frac{2}{\pi}\left[\alpha - \frac{\alpha^3}{18} + \frac{\alpha^5}{600} + \cdots\right] \quad ; \quad \alpha \ll \pi \quad (\xi \ll \xi_s) \tag{B.5.33}$$

$$\mathcal{S}[\alpha(\xi)] \simeq \frac{2}{\pi}\left[1 - \frac{\cos[\alpha]}{\alpha} - \frac{\sin[\alpha]}{\alpha^2} + \cdots\right] \quad ; \quad \alpha \gg \pi \quad (\xi \gg \xi_s) \tag{B.5.34}$$

Appendix C Supplement for Scalar Particle Production

C.1 The Mode Functions (5.3.40) and WKB Asymptotics

The mode functions (5.3.40) can be written as

$$f_k(\eta) = \frac{|\mathcal{F}(x,\alpha)|}{(8mH_R)^{1/4}}\, e^{-i\varphi(x,\alpha)}\,, \tag{C.1.1}$$

with x, α defined in eqn. (5.3.34). For $|\alpha| \gg x^2$ the Weber function features the asymptotic behavior[2]

$$\begin{aligned} |\mathcal{F}(x,\alpha)| &= \frac{1}{|\alpha|^{1/4}}\left[1 - \frac{x^2}{16|\alpha|} + \cdots\right] = \frac{(2mH_R)^{1/4}}{\sqrt{k}}\left[1 - \frac{1}{4}\,m^2\,H_R^2\,\eta^2 + \cdots\right] \\ \varphi(x,\alpha) &= \frac{\pi}{4} + \sqrt{|\alpha|}\,x\left[1 + \frac{2\,x^2}{48\,|\alpha|} + \cdots\right] = \frac{\pi}{4} + k\,\eta\left[1 + \frac{m^2\,H_R^2\,\eta^2}{6\,k^2} + \cdots\right] \end{aligned} \tag{C.1.2}$$

And for $x^2 \gg |\alpha|$

$$\begin{aligned} |\mathcal{F}(x,\alpha)| &= \frac{\sqrt{2}}{\sqrt{x}}\left[1 - \frac{|\alpha|}{x^2} + \cdots\right] = \frac{\sqrt{2}}{(2mH_R)^{1/4}\,\sqrt{\eta}}\left[1 - \frac{k^2}{4\,m^2\,H_R^2\,\eta^2} + \cdots\right] \\ \varphi(x,\alpha) &= \frac{x^2}{4} + |\alpha|\,\ln(x) + \cdots = \frac{1}{2}mH_R\,\eta^2 + \frac{k^2}{2mH_R}\,\ln[\eta\,\sqrt{2mH_R}] + \cdots \end{aligned} \tag{C.1.3}$$

Up to an overall constant phase these expansions coincide with the expansions of

$$f_k(\eta) = \frac{e^{-i\int^\eta \omega_k(\eta')\,d\eta'}}{\sqrt{2\omega_k(\eta)}} \tag{C.1.4}$$

in both limits $k \gg m\,H_R\,\eta$ and $k \ll m\,H_R\,\eta$ respectively.

C.2 Second Order Adiabatic Contributions to $T_{\mu\nu}$

We gather the results of second adiabatic order for the expectation value of the energy momentum tensor (see [10, 47]).

$$\rho^{(2)}(\eta) = \Big[\frac{a'}{m\,a}\Big]^2 \frac{1}{4\pi^2\,a^4(\eta)} \int_0^\infty k^2 dk\, m \left(1 + 2\,\mathcal{N}_k\right) \Big[\frac{m^5\,a^4}{8\omega_k^5} + \frac{1}{2}\,(1-6\xi)\left(\frac{m}{\omega_k} + \frac{m^3 a^2}{\omega_k^3}\right)\Big]\,. \tag{C.2.1}$$

$$\begin{aligned}
\mathcal{T}^{(2)}(\eta) &= \frac{1}{4\pi^2\,a^4(\eta)} \int_0^\infty k^2 dk \left(1 + 2\,\mathcal{N}_k\right) \Bigg\{ \frac{m^6\,a^4}{4\,\omega_k^5} \left[\frac{a''}{m^2\,a} + \Big(\frac{a'}{m\,a}\Big)^2\right] \\
&- \frac{5\,m^8\,a^6}{8\,\omega_k^7}\Big(\frac{a'}{m\,a}\Big)^2 + (1-6\xi)\left[\frac{m^2}{\omega_k}\left(\frac{a''}{m^2\,a} - \Big(\frac{a'}{m\,a}\Big)^2\right)\right. \\
&+ \left.\frac{m^4 a^2}{2\,\omega_k^3}\left(2\frac{a''}{m^2\,a} - \Big(\frac{a}{m\,a}\Big)^2\right) - \frac{3\,m^6\,a^4}{\omega_k^5}\Big(\frac{a'}{m\,a}\Big)^2\right]\Bigg\}
\end{aligned} \tag{C.2.2}$$

The terms with $1/\omega_k; 1/\omega_k^3$ yield ultraviolet divergences for $\mathcal{N}_k = 0$, which are subtracted and absorbed into the renormalization counterterms as discussed in section (5.5), whereas the term proportional to $\mathcal{N}_k$ yields ultraviolet finite contributions because $\mathcal{N}_k \lesssim 1/k^4$ at large k. During the (RD) dominated era and near matter-radiation equality, these terms are suppressed by a factor

$$\simeq \Big(\frac{a'}{m\,a}\Big)^2 \simeq \frac{10^{-62}}{m_{ev}^2}\,, \tag{C.2.3}$$

with respect to the zeroth-adiabatic order contributions (5.5.9,5.5.10). A similar analysis confirms that the terms of fourth adiabatic order which feature $\mathcal{N}_k$ in the integrand are much further suppressed and can be safely neglected.

Appendix D Supplement for Fermion Particle Production

D.1 Majorana Fermions

In this appendix we gather the main features for the quantization of Majorana fermions. With the solutions of the Dirac equation obtained in section (4.2), we construct self-conjugate Majorana fermions as follows.

Introducing

$$w(k,\eta) = i\frac{f_k'(\eta)}{f_k(\eta)} + M(\eta) \tag{D.1.1}$$

where $' = d/d\eta$, the Dirac spinors are written as

$$U_\lambda(\vec{k},\eta) = N\, f_k(\eta) \begin{pmatrix} w(k,\eta)\,\chi_\lambda \\ \vec{\sigma}\cdot\vec{k}\,\chi_\lambda \end{pmatrix} \quad ; \quad \chi_1 = \begin{pmatrix} 1 \\ 0 \end{pmatrix} \; ; \; \chi_2 = \begin{pmatrix} 0 \\ 1 \end{pmatrix} , \tag{D.1.2}$$

and

$$V_\lambda(\vec{k},\eta) = N\, f_k^*(\eta) \begin{pmatrix} \vec{\sigma}\cdot\vec{k}\,\varphi_\lambda \\ w^*(k,\eta)\,\varphi_\lambda \end{pmatrix} \quad ; \quad \varphi_1 = \begin{pmatrix} 0 \\ 1 \end{pmatrix} \; ; \; \varphi_2 = -\begin{pmatrix} 1 \\ 0 \end{pmatrix} . \tag{D.1.3}$$

These spinors are normalized

$$U_\lambda^\dagger U_{\lambda'} = V_\lambda^\dagger V_{\lambda'} = \delta_{\lambda,\lambda'} , \tag{D.1.4}$$

yielding the same normalization factor as obtained in section (4.2), and fulfill the orthogonality condition

$$U_\lambda^\dagger(\vec{k},\eta) V_{\lambda'}(-\vec{k},\eta) = 0 \quad ; \quad \lambda,\lambda' = 1,2 . \tag{D.1.5}$$

It is straightforward to confirm that the U and V spinors (D.1.2, D.1.3) obey the charge conjugation relation

$$i\gamma^2 U_\lambda^*(\vec{k},\eta) = V_\lambda(\vec{k},\eta) \quad : \quad i\gamma^2 V_\lambda^*(\vec{k},\eta) = U_\lambda(\vec{k},\eta) \quad ; \quad \lambda = 1,2 . \tag{D.1.6}$$

In terms of these spinor solutions we can construct Majorana (charge self-conjugate) fields obeying[1]

$$\psi^c_M(\vec{x},\eta) = C(\overline{\psi}_M(\vec{x},\eta))^T = \psi_M(\vec{x},\eta) \;\; ; \;\; C = i\gamma^2\gamma^0 \tag{D.1.7}$$

and given by

$$\psi_M(\vec{x},\eta) = \frac{1}{\sqrt{V}} \sum_{\vec{k},\lambda} \left[b_{\vec{k},\lambda}\, U_\lambda(\vec{k},\eta)\, e^{i\vec{k}\cdot\vec{x}} + b^\dagger_{\vec{k},\lambda}\, V_\lambda(\vec{k},\eta)\, e^{-i\vec{k}\cdot\vec{x}} \right] . \tag{D.1.8}$$

In the case of Majorana fields the Lagrangian density, and the energy momentum tensor must be multiplied by a factor 1/2 since a Majorana field has half the number of degrees of freedom of the Dirac field. Furthermore, one can take linear combinations of the Weyl spinors $\chi_{1,2}; \varphi_{1,2}$ and construct helicity eigenstates. The steps leading to the final form of the abundance and equation of state are the same as for the Dirac case, with the only difference being a factor 2 instead of the factor 4 because for a Majorana field particles are the same as antiparticles, thereby halving the number of degrees of freedom.

D.2 Properties of the Solution (6.3.18)

During the (RD) stage the solution of the mode functions is given by (6.3.18) with z, α given by eqns. (6.3.15,6.3.17) respectively. Using the properties of the parabolic cylinder functions[2, 152, 21, 145] we find for $|z| \gg |\alpha|$

$$D_\alpha[\sqrt{2}e^{i\pi/4}\, z] \simeq e^{-i\frac{z^2}{2}} \left[\sqrt{2}e^{i\pi/4}\, z\right]^\alpha \left[1 + \cdots\right], \tag{D.2.1}$$

and for $|\alpha| \gg |z| \gg 1$

$$D_\alpha[\sqrt{2}e^{i\pi/4}\, z] \simeq \frac{e^{\pi q^2/8}}{\sqrt{2q^2}}\, e^{-izq} \left[1 + \cdots\right], \tag{D.2.2}$$

Up to an overall phase and normalization, these limits describe the asymptotic WKB solution (6.4.18) yielding the spinor solutions (6.4.19,6.4.20) valid in the adiabatic limit. Note that

[1] We set the Majorana phase to zero as it is not relevant for the discussion.

the term $e^{\pi q^2/8}$ cancels the normalization factor (6.3.40) in this limit, yielding the correct normalization of the spinors (6.4.19,6.4.20).

Since the matching condition is evaluated at η_R, in terms of the variable z it follows that $z_R = \sqrt{mH_R}/\sqrt{H_R H_{dS}} = \varepsilon \ll 1$. For $z \simeq 0$ we find

$$D_\alpha[\vartheta] = D_\alpha[0]\left[1+\frac{1}{2}(1+iq^2)\vartheta^2+\cdots\right] + \frac{d}{d\vartheta}D_\alpha[\vartheta]\Big|_{\vartheta=0}\vartheta\left[1+\frac{1}{12}(1+iq^2)\vartheta^2+\cdots\right]. \quad \text{(D.2.3)}$$

At the transition time $\eta = \eta_R$ it follows that

$$q^2 z_R^2 = \frac{k^2}{mH_R}\, mH_R\, \eta_R^2 = (k\eta_R)^2 \ll 1\,, \quad \text{(D.2.4)}$$

for superhorizon wavelengths at the end of inflation. Therefore, for $\varepsilon \ll 1$, and $k\eta_R \ll 1$ we can reliably approximate

$$D_\alpha(z_R) \simeq D_\alpha(0) \;\; ; \;\; \frac{d}{d\eta}D_\alpha(z)|_{z_R} \simeq \frac{d}{d\eta}D_\alpha(z)|_{z=0}\,. \quad \text{(D.2.5)}$$

D.3 Calculation of $|B_{k,s}|^2$

Neglecting terms of $\mathcal{O}(\varepsilon)$ the spinors $\mathcal{U}, \mathcal{V}$ are given by

$$\mathcal{U}_s(\vec{k},\eta) \simeq \widetilde{N}\begin{pmatrix} ih_k'\,\xi_s \\ k\,h_k\,s\,\xi_s \end{pmatrix}, \quad \text{(D.3.1)}$$

$$\mathcal{V}_s(-\vec{k},\eta) \simeq \widetilde{N}\begin{pmatrix} -k\,h_k^*\,s\,\xi_s \\ -ih_k^{*'}\,\xi_s \end{pmatrix}. \quad \text{(D.3.2)}$$

The normalization constant is determined by

$$|\widetilde{N}|^2\Big[|h_k'(\eta_R|^2 + k^2|h_k(\eta_R|^2\Big] = 1\,, \quad \text{(D.3.3)}$$

using the identities[2]

$$\left|\Gamma(\frac{1}{2}+i\frac{q^2}{4})\right|^2 = \frac{\pi}{\cosh[\pi q^2/4]} \;\; ; \;\; \left|\Gamma(1+i\frac{q^2}{4})\right|^2 = \frac{\pi(q^2/4)}{\sinh[\pi q^2/4)]}\,. \quad \text{(D.3.4)}$$

we find

$$|\widetilde{N}|^2 = \frac{e^{-\pi q^2/4}}{2mH_R}\,. \tag{D.3.5}$$

The final form of $|B_{k,s}|^2$ is given by eqn. (6.3.41), neglecting terms of $\mathcal{O}(\varepsilon)$ as discussed in section (6.3.3) we find

$$\mathcal{H}_k^*(\eta_R)\,h_k(\eta_R) + \mathcal{H}_k(\eta_R)\,h_k^*(\eta_R) = \frac{e^{i\pi/4}}{\Gamma(\frac{1}{2} - i\frac{q^2}{4})\,\Gamma(1 + i\frac{q^2}{4})} + \frac{e^{-i\pi/4}}{\Gamma(\frac{1}{2} + i\frac{q^2}{4})\,\Gamma(1 - i\frac{q^2}{4})}\,. \tag{D.3.6}$$

Using the doubling formula for Gamma functions[2, 21, 145], and defining $q^2/4 \equiv y$

$$\Gamma(1+iy)\,\Gamma(\frac{1}{2} - iy) = 2\sqrt{\pi}\,y\,e^{i\pi/2}\,e^{2iy\,ln(2)}\,\Gamma(-2iy)\frac{\Gamma(iy)}{\Gamma(-iy)}\,, \tag{D.3.7}$$

and writing

$$\Gamma(-2iy)\frac{\Gamma(iy)}{\Gamma(-iy)} = \Big|\Gamma(-2iy)\Big|\,e^{i\Phi(y)} \quad ; \quad \Big|\Gamma(-2iy)\Big| = \left[\frac{\pi}{2y\,\sinh[2\pi y]}\right]^{1/2}\,, \tag{D.3.8}$$

where

$$\Phi(y) = \mathrm{Im}\Big\{\,\ln[\Gamma(-2iy)] + \ln[\Gamma(iy)] - \ln[\Gamma(-iy)]\,\Big\}\,. \tag{D.3.9}$$

Using the identity[2, 21, 145]

$$\ln[\Gamma(z)] = \big(z - \frac{1}{2}\big)\,\ln(z) - z + \frac{1}{2}\ln(2\pi) + \int_0^\infty \left[\frac{1}{2} - \frac{1}{t} + \frac{1}{e^t - 1}\right]\frac{e^{-iz}}{t}\,dt\,, \tag{D.3.10}$$

we find

$$\Phi(y) = -\frac{\pi}{4} - 2y\ln(2)\,, \tag{D.3.11}$$

which, combined with the normalization factor (6.3.40) yields the final result (6.3.42).

D.4 Adiabatic Expansion for Fermi Fields

In this appendix we provide a discussion of the adiabatic approach to fermionic degrees of freedom which is alternative to the framework discussed in refs.[68, 81, 19, 90, 129], with the advantage that it yields more compact expressions for the energy density and pressure. We write generically the spinors as U, V with the understanding that during (RD) these are to be identified with the solutions $\mathcal{U}\,;\,\mathcal{V}$.

Consider the mode equation (we suppress the momentum label and conformal time arguments for ease of notation)

$$h^{''} + (\omega^2 - iM')h = 0 \tag{D.4.1}$$

and propose the solution

$$h(\eta) = e^{-i\int^{\eta}\Omega(\eta')\,d\eta'} \;\;;\;\; \Omega = \Omega_R + i\Omega_I\,. \tag{D.4.2}$$

Introducing this ansatz into the mode equation (D.4.1) yields

$$\Omega^2 + i\Omega' - \omega^2 + iM' = 0\,, \tag{D.4.3}$$

separating the real and imaginary parts yields the coupled system of equations

$$\Omega_R^2 - \Omega_I^2 - \Omega_I^{'} - \omega^2 = 0 \tag{D.4.4}$$

$$2\Omega_R\Omega_I + (\Omega_R^{'} + M') = 0 \;\;\Rightarrow\;\; \Omega_I = -\frac{(\Omega_R^{'} + M')}{2\Omega_R}\,. \tag{D.4.5}$$

The above equations can be solved in a consistent adiabatic expansion in derivatives of ω, M with respect to conformal time. A corollary of these equations is that Ω_R, Ω_I feature an adiabatic expansion *even* and *odd* in the number of derivatives (adiabatic order) respectively, with

$$\Omega_R^{(0)} = \omega\,;\,\Omega_I^{(0)} = 0\;\;;\;\;\Omega_R^{(1)} = 0\,;\,\Omega_I^{(1)} = -\frac{(\omega' + M')}{2\omega}\;\;;\;\;\Omega_R^{(2)} = \frac{(\Omega_I^{(1)})^2 + (\Omega_I^{(1)})'}{2\omega}\,;\,\Omega_I^{(2)} = 0\cdots\,. \tag{D.4.6}$$

To highlight the nature of the adiabatic expansion, consider the dimensionless ratio

$$\frac{\Omega_I^{(1)}}{\Omega_R^{(0)}} = -\frac{a'}{m\,a^2}\Big[\frac{1}{\gamma^2} + \frac{1}{\gamma^3}\Big] \tag{D.4.7}$$

$$\gamma = \sqrt{\frac{k^2}{m^2 a^2} + 1} \geq 1 \tag{D.4.8}$$

is the local Lorentz factor. The ratio (D.4.7) highlights that the adiabatic approximation becomes reliable for long wavelengths for $a'/ma^2 \ll 1$.

In the representation (D.4.2) it follows that the spinors can be written compactly as

$$U_s(\vec{k},\eta) = N\, e^{-i\int^\eta \omega_k(\eta')d\eta'} \begin{pmatrix} (\Omega + M)\,\xi_s \\ k\, s\, \xi_s \end{pmatrix}, \tag{D.4.9}$$

$$V_s(-\vec{k},\eta) = N\, e^{i\int^\eta \Omega_k^*(\eta')d\eta'} \begin{pmatrix} -k\, s\, \xi_s \\ (\Omega^* + M)\,\xi_s \end{pmatrix}, \tag{D.4.10}$$

with N a normalization constant. The orthogonality conditions $U_s^\dagger U_{s'} = 0, V_s^\dagger V_{s'} = 0$ for $s \neq s'$ and $U_s^\dagger\, V_{s'} = 0$ for all s, s' are evident. Furthermore, using the equations (D.4.4, D.4.5) it is straightforward to show that

$$\frac{d}{d\eta}\Big(U_s^\dagger\, U_s\Big) = 0 \;\;;\;\; \frac{d}{d\eta}\Big(V_s^\dagger\, V_s\Big) = 0\,, \tag{D.4.11}$$

therefore normalizing the spinors $U_s^\dagger U_{s'} = \delta_{s,s'} = V_s^\dagger V_{s'}$ it follows that

$$|N|^2\, e^{2\int^\eta \Omega_I(\eta')d\eta'} \Big[\Omega_R^2 + \Omega_I^2 + \omega^2 + 2M\Omega_R\Big] = 1\,. \tag{D.4.12}$$

Up to an overall constant phase this equation yields

$$N = \frac{e^{-\int^\eta \Omega_I(\eta')d\eta'}}{\Big[\Omega_R^2 + \Omega_I^2 + \omega^2 + 2M\Omega_R\Big]^{1/2}}\,. \tag{D.4.13}$$

Using this result, the general form of the normalized spinors is given by

$$U_s(\vec{k},\eta) = \frac{e^{-i\int^\eta \Omega_R(\eta')d\eta'}}{\Big[\Omega_R^2 + \Omega_I^2 + \omega^2 + 2M\Omega_R\Big]^{1/2}} \begin{pmatrix} (\Omega + M)\,\xi_s \\ k\, s\, \xi_s \end{pmatrix}, \tag{D.4.14}$$

$$V_s(-\vec{k},\eta) = \frac{e^{i\int^\eta \Omega_R(\eta')d\eta'}}{\Big[\Omega_R^2 + \Omega_I^2 + \omega^2 + 2M\Omega_R\Big]^{1/2}} \begin{pmatrix} -k\, s\, \xi_s \\ (\Omega^* + M)\,\xi_s \end{pmatrix}. \tag{D.4.15}$$

To leading (zeroth) adiabatic order with $\Omega_R = \omega, \Omega_I = 0$ we find the spinors given in eqns. (6.4.19,6.4.20).

It is straightforward to find the general result (for each polarization s) ($\Sigma = \alpha \cdot \vec{k} + \gamma^0 M$)

$$V^\dagger(-\vec{k},\eta)\,\Sigma(\vec{k},\eta)\,V(-\vec{k},\eta) = -U^\dagger(\vec{k},\eta)\,\Sigma(\vec{k},\eta)\,U(\vec{k},\eta) = -\frac{M(\Omega_R^2+\Omega_I^2+\omega^2)+2\omega^2\Omega_R}{\left[\Omega_R^2+\Omega_I^2+\omega^2+2M\Omega_R\right]}\,. \tag{D.4.16}$$

$$V^\dagger(-\vec{k},\eta)\,\vec{\alpha}\cdot\vec{k}\,V(-\vec{k},\eta) = -U^\dagger(\vec{k},\eta)\,\vec{\alpha}\cdot\vec{k}\,U(\vec{k},\eta) = -\frac{2k^2\left(\Omega_R+M\right)}{\left[\Omega_R^2+\Omega_I^2+\omega^2+2M\Omega_R\right]}\,. \tag{D.4.17}$$

These results imply that the adiabatic expansion for both energy density and pressure is *even* in adiabatic derivatives confirming some results in ref.[68].

Up to second order in the adiabatic expansion we find

$$V^\dagger(-\vec{k},\eta)\,\Sigma(\vec{k},\eta)\,V(-\vec{k},\eta) = -U^\dagger(\vec{k},\eta)\,\Sigma(\vec{k},\eta)\,U(\vec{k},\eta) = -\omega\left[1-\frac{1}{8}\left(\frac{a'}{ma^2}\right)^2\left(\frac{k}{\gamma^2\,\omega}\right)^2\right], \tag{D.4.18}$$

$$\begin{aligned} V^\dagger(-\vec{k},\eta)\,\vec{\alpha}\cdot\vec{k}\,V(-\vec{k},\eta) &= -U^\dagger(\vec{k},\eta)\,\vec{\alpha}\cdot\vec{k}\,U(\vec{k},\eta) = -\frac{k^2}{\omega_k}\Bigg\{1-\frac{1}{8\,\gamma^4}\left(\frac{a'}{ma^2}\right)^2 \\ &\times \quad (1+\frac{1}{\gamma})\Big[1-\frac{1}{\gamma}+2(1+\frac{1}{\gamma})\left(\frac{\gamma-2}{(1+\gamma)^2}\right)\Big]\Bigg\} \end{aligned} \tag{D.4.19}$$

where $\gamma \equiv \sqrt{1+(k/ma)^2}$ is the local Lorentz factor. These results agree with those in ref.[68].

For $a \simeq a_{eq} \simeq 10^{-4}$ it follows that

$$\left(\frac{a'}{ma^2}\right)^2 \simeq \frac{10^{-54}}{(m/\mathrm{eV})^2}\,. \tag{D.4.20}$$

At leading (zeroth) adiabatic order $\Omega_R = \omega; \Omega_I = 0$ the spinors are instantaneous eigenstates of the instantaneous conformal time Dirac Hamiltonian $\Sigma(\vec{k},\eta)$, namely,

$$\Sigma(\vec{k},\eta)\,U(\vec{k},\eta) = \omega\,U(\vec{k},\eta) \quad ; \quad \Sigma(\vec{k},\eta)\,V(\vec{k},\eta) = -\omega\,V(\vec{k},\eta)\,. \tag{D.4.21}$$

Consequently the interference terms ρ_{int} (6.4.12) vanish identically at zeroth adiabatic order, however, this is not the case for the interference terms in the pressure.

Bibliography

[1] L. Abbott and P. Sikivie. *Phys. Lett. B*, 120:133, 1983.

[2] M. Abramowitz and I. A. Stegun. *Handbook of Mathematical Functions*. Dover, NY, 1964.

[3] P. Ade, N. Aghanim, M. Arnaud, F. Arroja, M. Ashdown, J. Aumont, C. Baccigalupi, M. Ballardini, A. Banday, R. Barreiro, et al. *Astron.Astrophys.*, 594:A20, 2016.

[4] P. A. Ade, N. Aghanim, M. Arnaud, M. Ashdown, J. Aumont, C. Baccigalupi, A. Banday, R. Barreiro, J. Bartlett, N. Bartolo, et al. *Astron.Astrophys.*, 594:A13, 2016.

[5] P. A. R. Ade, N. Aghanim, C. Armitage-Caplan, M. Arnaud, M. Ashdown, F. Atrio-Barandela, J. Aumont, C. Baccigalupi, A. J. Banday, and et al. *Astronomy Astrophysics*, 571:A16, Oct 2014.

[6] P. Adshead and E. I. Sfakianakis. *JCAP*, 11:021, 2015.

[7] C. Alcock, R. A. Allsman, D. R. Alves, T. S. Axelrod, A. C. Becker, D. P. Bennett, K. H. Cook, N. Dalal, A. J. Drake, K. C. Freeman, and et al. *The Astrophysical Journal*, 542(1):281–307, Oct 2000.

[8] J. Alexander and collaborators.

[9] M. A. Amin, M. P. Hertzberg, D. I. Kaiser, and J. Karouby. *Int. J. of Mod. Phys.*, 24(1530003), 2015.

[10] P. Anderson and L. Parker. *Phys. Rev. D*, 36:2963, 1987.

[11] A. Arvanitaki, S. Dimopoulos, and K. V. Tilburg. *Phys. Rev. X*, 8:041001, 2018.

[12] B. Audren, J. Lesgourgues, G. Mangano, P. D. Serpico, and T. Tram. *JCAP*, 1412:028, 2014.

[13] J. Audretsch and G. Schafer. *Phys. Lett. A*, 66:459, 1978.

[14] J. Audretsch and P. Spangehl. *Class. Quantum Grav.*, 2:733, 1985.

[15] J. Audretsch and P. Spangehl. *Phys. Rev.*, 33:997, 1986.

[16] J. Audretsch and P. Spangehl. *Phys. Rev. D*, 35:2365, 1987.

[17] J. Baacke and C. Patzold. *Phys.Rev. D*, 62:084008, 2000.

[18] N. Banerjee and S. Mallik. *Phys. Rev. D*, 45:701, 1992.

[19] J. F. Barbero, A. Ferreiro, J. Navarro-Salas, and E. J. S. Villasenor. *Phys. Rev. D*, 98:025016, 2018.

[20] N. Bartolo, S. Matarrese, and A. Riotto. *Phys. Rev. D*, 64(12350):4, 2001.

[21] H. Bateman. *Higher Transcendental Functions, vol. II.* McGraw-Hill, N.Y, 1953.

[22] M. Battaglieri and collaborators.

[23] C. L. Bennett, D. Larson, J. L. Weiland, N. Jarosik, G. Hinshaw, N. Odegard, K. Smith, R. Hill, B. Gold, M. Halpern, et al. *Astrophys.J.Suppl.*, 208:20, 2013.

[24] J. Bernstein. *Kinetic Theory in the Early Universe.* Cambridge University Press, 1988.

[25] G. Bertone, D. Hooper, and J. Silk. *Physics Reports*, 405:279, 2005.

[26] G. Bertone and T. M. P. Tait. *Nature*, 562(7725):51–76, 2018.

[27] N. D. Birrell. *Proc. R. Soc. Lond., B*, 361(1707):513–526, 1978.

[28] N. D. Birrell and P. C. W. Davies. *Quantum fields in curved space time.* Cambridge University Press, 1982.

[29] N. D. Birrell and L. H. Ford. *Annals of Physics*, 122:1, 1979.

[30] G. Blackadder and S. M. Koushiappas. *Phys. Rev. D*, 93:023510, 2016.

[31] M. Boezio, P. Carlson, T. Francke, N. Weber, M. Suffert, M. Hof, W. Menn, M. Simon, S. Stephens, R. Bellotti, et al. *The Astrophysical Journal*, 518(1):457, 1999.

[32] D. Boyanovsky. *Annals of Physics*, 405:176, 2019.

[33] D. Boyanovsky and H. J. de Vega. *Phys. Rev. D*, 70:063508, 2004.

[34] D. Boyanovsky, H. J. de Vega, and N. G. Sanchez. *Phys. Rev. D*, 71:023509, 2005.

[35] D. Boyanovsky, H. J. de Vega, and N. G. Sanchez. *Phys. Rev. D*, 72:103006, 2005.

[36] D. Boyanovsky and N. Herring. *Phys. Rev. D*, 100(2):023531, 2019.

[37] D. Boyanovsky and R. Holman. *JHEP*, 47, 2011.

[38] D. Boyanovsky, P. Kumar, and R. Holman. *Phys. Rev. D*, 56, 1997.

[39] D. Boyanovsky and J. Wu. *Phys. Rev. D*, 83:043524, 2011.

[40] J. Bros, H. Epstein, and U. Moschella. *JCAP*, 0802:003, 2008.

[41] J. Bros, H. Epstein, and U. Moschella. *Annales Henri Poincare*, 11:611, 2010.

[42] W. Buchmuller, P. D. Bari, and M. Plumacher. *Annals of Physics*, 315:305, 2005.

[43] W. Buchmuller, V. Domcke, and K. Schmitz. *Phys. Lett. B*, 713:63–67, 2012.

[44] W. Buchmuller, R. D. Peccei, and T. Yanagida. *Ann. Rev. Nucl. Part. Sci.*, 55:311, 2005.

[45] M. R. Buckley and A. H. G. Peter. *Phys. Rept.*, 761:1, 2018.

[46] P. Bull, Y. Akrami, J. Adamek, T. Baker, E. Bellini, J. B. Jimenez, E. Bentivegna, S. Camera, S. Clesse, J. H. Davis, et al. *Physics of the Dark Universe*, 12:56–99, 2016.

[47] T. S. Bunch, P. Paanangaden, and L. Parker. *J. Phys. A: Math. Gen.*, 13:901, 1980.

[48] C. T. Byrnes and D. Wands. *Phys. Rev. D*, 74:043529, 2006.

[49] L. Canetti, M. Drewes, and M. Shaposhnikov. *New Journal of Physics*, 14(9):095012, 2012.

[50] M. A. Castagnino, L. Chimento, D. D. Harari, and C. Nunez. *J. Math. Phys.*, 25:360, 1984.

[51] D. M. Chitre and J. B. Hartle. *Phys. Rev. D*, 16:251, 1977.

[52] D. J. H. Chung, P. Crotty, E. W. Kolb, and A. Riotto. *Phys. Rev. D*, 64:043503, 2001.

[53] D. J. H. Chung, L. L. Everett, H. Yoo, and P. Zhou. *Phys. Lett. B*, 712:147, 2012.

[54] D. J. H. Chung, E. W. Kolb, and A. J. Long. *JHEP*, 2019(1):189, 2019.

[55] D. J. H. Chung, E. W. Kolb, and A. Riotto. *Phys. Rev. D*, 59:023501, 1999.

[56] D. J. H. Chung, E. W. Kolb, A. Riotto, and L. Senatore. *Phys. Rev. D*, 72:023511, 2005.

[57] D. J. H. Chung, H. Yoo, and P. Zhou. *Phys. Rev. D*, 91:043516, 2015.

[58] E. A. X. Collaboration). *Phys. Rev. Lett.*, 121(11130):2, 2018.

[59] P. collaboration.

[60] X. C. P.-I. Collaboration). *Phys. Rev. Lett.*, 119(18130):2, 2017.

[61] J. Collins. *arXiv preprint arXiv:1904.10923*, 2019.

[62] D. Curtin, R. Essig, S. Gori, and J. Shelton. *JHEP*, 2015(2):157, 2015.

[63] P. R. D. 93:044032, 2016.

[64] R. Dabrowski and G. V. Dunne. *Phys. Rev. D*, 90:025021, 2014.

[65] R. Dabrowski and G. V. Dunne. *Phys. Rev. D*, 94:065005, 2016.

[66] M. Davis, G. Efstathiou, C. S. Frenk, and S. D. White. *The Astrophysical Journal*, 292:371–394, 1985.

[67] A. del Rio, A. Ferreiro, J. Navarro-Salas, and F. Torrenti. *Phys. Rev. D*, 95:105003, 2017.

[68] A. del Rio, J. Navarro-Salas, and F. Torrenti. *Phys. Rev. D*, 90:084017, 2014.

[69] T. Dent, G. Lazarides, and R. R. de Austri. *Phys. Rev. D*, 69:075012, 2004.

[70] M. Dine and W. Fischler. *Phys. Lett.B*, 120:137, 1983.

[71] S. Dodelson. *Modern Cosmology*. Academic Press, 2003.

[72] M. DREWES. *International Journal of Modern Physics E*, 22(08):1330019, Aug 2013.

[73] A. Duncan. *Phys. Rev. D*, 17:964, 1978.

[74] R. Durrer. *Classical and Quantum Gravity*, 32, 06 2015.

[75] D. J. Eisenstein, I. Zehavi, D. W. Hogg, R. Scoccimarro, M. R. Blanton, R. C. Nichol, R. Scranton, H.-J. Seo, M. Tegmark, Z. Zheng, et al. *The Astrophysical Journal*, 633(2):560, 2005.

[76] Y. Ema, R. Jinno, K. Mukaida, and K. Nakayama. *Phys. Rev. D*, 94:063517, 2016.

[77] Y. Ema, K. Nakayama, and Y. Tang. *JHEP*, 2018(9):135, 2018.

[78] Y. Ema, K. Nakayama, and Y. Tang. *JHEP*, 07:060, 2019.

[79] S. Enomoto and N. Maekawa. *Phys. Rev. D*, 84(9):096007, 2011.

[80] J. L. Feng. *Ann. Rev. Astron. Astrophys.*, 48:495, 2010.

[81] A. Ferreiro, A. del Rio, J. Navarro-Salas, S. Pla, and F. Torrenti. *arXiv preprint arXiv:1904.00062*, 2017.

[82] B. D. Fields. *Annual Review of Nuclear and Particle Science*, 61:47–68, 2011.

[83] B. D. Fields, P. Molaro, and S. Sarkar. *arXiv preprint arXiv:1412.1408*, 2014.

[84] L. H. Ford. *Phys. Rev. D*, 35:2955, 1987.

[85] V. M. Frolov, S. G. Mamayev, and V. M. Mostepanenko. *Phys. Lett. A*, 55:389, 1976.

[86] S. A. Fulling. *General Relativity and Gravitation*, 10:807, 1979.

[87] S. A. Fulling. *Aspects of quantum field theory in curved space-time*. Cambridge University Press, 1989.

[88] S. A. Fulling and L. Parker. *Ann. Phys. (N. Y.)*, 87:176, 1974.

[89] S. A. Fulling, L. Parker, and B. L. Hu. *Phys. Rev. D*, 10:3905, 1974.

[90] S. Ghosh. *Phys. Rev. D*, 91:124075, 2015.

[91] G. W. Gibbons and S. W. Hawking. *Phys. Rev. D*, 15:2738, 1977.

[92] C. Gordon, D. Wands, B. A. Bassett, and R. Maartens. *Phys. Rev. D*, 63:023506, 2000.

[93] I. S. Gradshteyn and I. M. Ryzhik. *Table of Integrals, Series and Products*. Academic Press, New York, 1980.

[94] P. W. Graham, J. Mardon, and S. Rajendran. *Phys. Rev. D*, 93:10352, 2016.

[95] W. Greiner and J. Reinhardt. *Field Quantization*. Springer, 1996.

[96] A. A. Grib, S. G. Mamayev, and V. M. Mostepanenko. *Gen.Rel.and Grav.*, 7:535, 1976.

[97] A. A. Griv, B. A. Levitsky, and V. M. Mostepanenko. *Teor.Mat.Fiz.*, 19:59, 1974.

[98] A. H. Guth. *Physical Review D*, 23(2):347, 1981.

[99] S. Habib, C. Molina-Paris, and E. Mottola. *Phys. Rev. D*, 61:024010, 1999.

[100] L. J. Hall, K. Jedamzik, J. March-Russell, and S. M. West. *Journal of High Energy Physics*, 2010(3):80, 2010.

[101] T. Hasegawa, N. Hiroshima, K. Kohri, R. S. Hansen, and S. Hannestad. *JCAP*, 2019(12):012, 2019.

[102] S. Hashiba and J. Yokoyama. *Phys. Rev. D*, 99:043008, 2019.

[103] N. Herring and D. Boyanovsky. *Physical Review D*, 101(12), 2020.

[104] N. Herring, D. Boyanovsky, and A. Zentner. *Phys. Rev. D*, 101:083516, 2020.

[105] N. Herring, B. Pardo, D. Boyanovsky, and A. R. Zentner. *Phys. Rev. D*, 98:083503, 2018.

[106] M. P. Hertzberg, M. Tegmark, and F. Wilczek. *Phys. Rev. D*, 78:083507, 2008.

[107] B. L. Hu. *Phys. Rev. D*, 18:4460, 1978.

[108] B. L. Hu. *Phys. Lett. A*, 71:169, 1979.

[109] W. Hu. *Phys. Rev. Lett.*, 85:1158, 2000.

[110] W. Hu, R. Barkana, and A. Gruzinov. *Phys. Rev. Lett.*, 85:1158, 2000.

[111] L. Hui, J. Ostriker, S. Tremaine, and E. Witten. *Phys. Rev. D*, 95:043541, 2017.

[112] F. Iocco, G. Mangano, G. Miele, O. Pisanti, and P. D. Serpico. *Phys. Rept.*, 472(1-6):1–76, 2009.

[113] V. Irsic, M. Viel, M. G. Haehnelt, J. S. Bolton, and G. Becker. *Phys. Rev. Lett.*, 119:031302, 2017.

[114] H. Ishida, M. Kusakabe, and H. Okada. *Phys. Rev. D*, 90:083519, 2014.

[115] K. Jedamzik. *Phys. Rev. D*, 70:063524, 2004.

[116] K. Jedamzik. *Phys. Rev. D*, 74:103509, 2006.

[117] F. Kahlhoefer. *Int. J.Mod.Phys. A*, 32(17300):06, 2017.

[118] M. Kawasaki, K. Kohri, and T. Moroi. *Phys. Rev. D*, 71:083502, 2005.

[119] M. Kawasaki, K. Kohri, and T. Moroi. *Phys. Rev. B*, 625:7, 2005.

[120] W. H. Kinney. Tasi lectures on inflation, 2009.

[121] E. Kolb and M. S. Turner. *The Early Universe*. Avalon Publishing, 1994.

[122] E. W. Kolb, A. Riotto, and I. I. Tkachev. *Phys. Lett. B*, 423(3-4):348–354, 1998.

[123] E. W. Kolb and M. S. Turner. *Ann. Rev. Nucl. Part. Sci.*, 33:645, 1983.

[124] V. Kuzmin and I. Tkachev. *Phys. Rev. D*, 59(12):123006, 1999.

[125] V. A. Kuzmin and I. I. Tkachev. *JETP Lett.*, 68:271, 1998.

[126] V. A. Kuzmin and I. I. Tkachev. *Phys. Rept.*, 320:199, 1999.

[127] F. V. L. Covi, E. Roulet. *Phys. Lett. B*, 384:169, 1996.

[128] A. Landete, J. Navarro-Salas, and F. Torrenti. *Phys. Rev. D*, 88:061501, 2013.

[129] A. Landete, J. Navarro-Salas, and F. Torrenti. *Phys. Rev. D*, 89:044030, 2014.

[130] J. S. Langer. *Phys. Rev.*, 167:183, 1968.

[131] J. Lankinen, O. Kerppo, and I. Vilja. *Phys. Rev. D*, 101(6), Mar 2020.

[132] J. Lankinen, J. Malmi, and I. Vilja. *arXiv preprint arXiv:1904.05084*, 2019.

[133] J. Lankinen and I. Vilja. *Phys. Rev. D*, 96:105026, 2017.

[134] J. Lankinen and I. Vilja. *JCAP*, 2017(08):025, 2017.

[135] J. Lankinen and I. Vilja. *Phys. Rev. D*, 97:065004, 2018.

[136] J. Lee. *EPJ Web of Conferences*, 168:06005, 2018.

[137] L. Lello and D. Boyanovsky. *Phys. Rev. D*, 87:073017, 2013.

[138] L. Lello, D. Boyanovsky, and R. Holman. *JHEP*, 116, 2013.

[139] J. Lesgourgues. Tasi lectures on cosmological perturbations, 2013.

[140] A. R. Liddle and A. Mazumdar. *Phys. Rev. D*, 61(12350):7, 2000.

[141] A. Linde. *Particle Physics and Inflationary Cosmology*. Harwood Academic, London, 1990.

[142] D. S. A. (lux collaboration). *Phys. Rev. Lett.*, 118:021303, 2017.

[143] D. Lyth and D. Roberts. *Phys. Rev. D*, 57:7120, 1998.

[144] L. N. Machado, H. A. S. Costa, M. S. I. G. da Paz, and J. B. Araujo. *Phys. Rev. D*, 98:125009, 2018.

[145] W. Magnus, F. Oberhettinger, and R. P. Soni. *Formulas and Theorems for the Special Functions of Mathematical Physics*. Springer-Verlag, NY, 1966.

[146] M. Markevitch, A. Gonzalez, D. Clowe, A. Vikhlinin, W. Forman, C. Jones, S. Murray, and W. Tucker. *The Astrophysical Journal*, 606(2):819, 2004.

[147] D. J. E. Marsh. *Phys. Rept.*, 643:1–79, 2016.

[148] D. E. Morrissey and M. J. Ramsey-Musolf. *New Journal of Physics*, 14(12):125003, Dec 2012.

[149] V. Mukhanov and S. Winitzki. *Introduction to quantum effects in gravity*. Cambridge University Press, 2012.

[150] J. C. Niemeyer. *arXiv preprint arXiv:1912.07064*, 2019.

[151] M. Nori, R. Murgia, V. Irsic, M. Baldi, and M. Viel. *MNRAS*, 482:3227, 2019.

[152] F. W. Olver, D. W. Lozier, R. F. Boisvert, and C. W. Clark. *NIST Handbook of Mathematical Functions*. Cambridge Univ. Press, N.Y, 2010.

[153] L. Parker. *Phys. Rev. Lett.*, 21(562), 1968.

[154] L. Parker. *Phys. Rev. Lett.*, 183(1057), 1969.

[155] L. Parker. *Phys. Rev. D*, 3(346), 1971.

[156] L. Parker. *J. Phys. A*, 45:374023, 2012.

[157] L. Parker and S. A. Fulling. *Phys. Rev. D*, 9:341, 1974.

[158] L. Parker and D. Toms. *Quantum field theory in curved spacetime: quantized fields and gravity*. Cambridge University Press, 2009.

[159] C. Patrignani and others (Particle Data Group). *Chin. Phys. C*, 40:100001, 2016.

[160] D. H. Perkins. *Particle Astrophysics*. Oxford University Press, 2003.

[161] M. E. Peskin and D. V. Schroeder. *An Introduction to Quantum Field Theory*. Westview Press, 2016.

[162] N. K. Porayko and collaborators. *Phys. Rev. D*, 98(10200):2, 2018.

[163] M. Pospelov and J. Pradler. *Ann. Rev. Nucl. Part. Sci.*, 60:539, 2010.

[164] V. Poulin and P. D. Serpico. *Phys. Rev. Lett.*, 114:091101, 2015.

[165] V. Poulin and P. D. Serpico. *Phys. Rev. D*, 91:103007, 2015.

[166] V. Poulin, P. D. Serpico, and J. Lesgourgues. *JCAP*, 1608:036, 2016.

[167] A. G. Riess, A. V. Filippenko, P. Challis, A. Clocchiatti, A. Diercks, P. M. Garnavich, R. L. Gilliland, C. J. Hogan, S. Jha, R. P. Kirshner, et al. *AJ*, 116(3):1009, 1998.

[168] A. G. Riess, A. V. Filippenko, P. Challis, A. Clocchiatti, A. Diercks, P. M. Garnavich, R. L. Gilliland, C. J. Hogan, S. Jha, R. P. Kirshner, et al. *The Astronomical Journal*, 116(3):1009, 1998.

[169] A. G. Riess, L. Macri, S. Casertano, M. Sosey, H. Lampeitl, H. C. Ferguson, A. V. Filippenko, S. W. Jha, W. Li, R. Chornock, et al. *The Astrophysical Journal*, 699(1):539, 2009.

[170] A. Riotto. Inflation and the theory of cosmological perturbations, 2002.

[171] V. C. Rubin, W. K. Ford Jr, and N. Thonnard. *The Astrophysical Journal*, 225:L107–L111, 1978.

[172] L. Salvati, L. Pagano, M. Lattanzi, M.Gerbino, and A. Melchiorri. *JCAP*, 1608:022, 2016.

[173] J. M. Sanchez-Velazquez and J. A. R. Cembranos.

[174] S. Sarkar. *Reports on Progress in Physics*, 59:1493, 1998.

[175] B. E. Schaefer. *The Astrophysical Journal Letters*, 450(1):L5, 1995.

[176] M. O. Scully and M. S. Zubairy. *Quantum Optics*. Cambridge University Press, 1997.

[177] U. Seljak and M. Zaldarriaga. *The Astrophysical Journal*, 469:437, 1996.

[178] P. Sikivie. *Lect. Notes. Phys.*, 741:19, 2008.

[179] Y. Sofue and V. Rubin. *Annual Review of Astronomy and Astrophysics*, 39(1):137–174, 2001.

[180] D. N. Spergel, R. Bean, O. Dore, M. R. Nolta, C. L. Bennett, J. Dunkley, G. Hinshaw, N. Jarosik, E. Komatsu, L. Page, and et al. *The Astrophysical Journal Supplement Series*, 170(2):377–408, Jun 2007.

[181] D. N. Spergel, L. Verde, H. V. Peiris, E. Komatsu, M. Nolta, C. Bennett, M. Halpern, G. Hinshaw, N. Jarosik, A. Kogut, et al. *Astrophys.J.Suppl.*, 148:175, 2003.

[182] G. Steigman. *Ann. Rev. Nucl. Part. Sci.*, 57:463, 2007.

[183] M. Thomson. *Modern Particle Physics*. Cambridge University Press, 2013.

[184] P. Tisserand, L. Le Guillou, C. Afonso, J. N. Albert, J. Andersen, R. Ansari, Aubourg, P. Bareyre, J. P. Beaulieu, X. Charlot, and et al. *Astronomy Astrophysics*, 469(2):387–404, Apr 2007.

[185] M. Trodden. *Rev. of Mod. Phys.*, 71:1463, 1999.

[186] K. Vattis, S. M. Koushiappas, and A. Loeb. *arXiv preprint arXiv:1903.06220*, 2019.

[187] A. Wagner, G. Rybka, M. Hotz, L. J. Rosenberg, S. J. Asztalos, G. Carosi, C. Hagmann, D. Kinion, K. van Bibber, J. Hoskins, C. Martin, P. Sikivie, D. B. Tanner, R. Bradley, and J. Clarke. *Phys. Rev. Lett.*, 105(17180):1, 2010.

[188] M.-Y. Wang, R. A. C. Croft, A. H. G. Peter, A. R. Zentner, and C. W. Purcell. *Phys. Rev. D*, 88:123515, 2013.

[189] M.-Y. Wang, A. H. G. Peter, L. E. Strigari, A. Zentner, B. Arant, S. Garrison-Kimmel, and M. Rocha. *MNRAS*, 445:614, 2014.

[190] M.-Y. Wang and A. Zentner. *Phys.Rev. D*, 82:123507, 2010.

[191] S. Weinberg. *Gravitation and Cosmology: principles and applications of the general theory of relativity*. John Wiley, 1972.

[192] V. Weisskopf and E. Wigner. *Z. Phys.*, 63:54, 1930.

[193] S. Winitzki. *Phys. Rev. D*, 72:104011, 2005.

[194] Y. B. Zeldovich and A. A. Starobinsky. *Sov. Phys. JETP*, 34:1159, 1972.

[195] Y. B. Zeldovich and A. A. Starobinsky. *JETP letters*, 26:252, 1977.

[196] A. R. Zentner and T. P. Walker. *Phys. Rev. D*, 65(6):063506, 2002.